https://doi.org/10.35662/unine-thesis-3051

Université de Neuchâtel

Synthesis and functional characterization of secondary metabolites from nematodes

PhD thesis submitted to the Faculty of Sciences

Institute of Chemistry

University of Neuchatel

For the title of Doctor in Science

By

Célia Patricia Bergame

Dissertation Committee:

Prof. Stephan H. von Reuss, University of Neuchatel, Switzerland, Thesis director

Prof. Bruno Therrien, University of Neuchatel, Switzerland, Internal examinator

Prof. Frank Schroeder, BTI and Cornell University, USA, External examinator

Defended on the 7th of February 2023

unine
Université de Neuchâtel
Faculté des sciences

Rue Emile-Argand 11
CH-2000 Neuchâtel
doctorat.sciences@unine.ch

IMPRIMATUR POUR THESE DE DOCTORAT

La Faculté des sciences de l'Université de Neuchâtel autorise l'impression de la présente thèse soutenue par

Madame Célia BERGAME

Titre :

"Synthesis and functional characterization of secondary metabolites from nematodes"

sur le rapport des membres du jury composé comme suit :

- Prof. Stephan von Reuss, directeur de thèse, Université de Neuchâtel, Suisse
- Prof. tit. Bruno Therrien, Université de Neuchâtel, Suisse
- Prof. Frank C. Schroeder, BTI and Cornell University, USA

Neuchâtel, le 11 mai 2023

Le Doyen, Prof. R. Bshary

Acknowledgements

First and foremost, I would like to express my sincere gratitude for my supervisor, professor Stephan von Reuss, who guided, instructed and motivated me during these five years. The results presented in my thesis would be impossible without your supervision. Thank you for trusting me and giving me the opportunity to do this PhD in your research group at a time when I thought I would never be able to do a PhD. At the end of this journey I feel like, more than a great supervisor, I have also won a friend if I may call you that. Thank you for the M&M's, the funny conversation at night in the lab and please, try to reduce your Coca Cola intake.

I would also like to thank the members of my jury for their good advice and the quality of our conversation during the defense.

I will not forget to express my gratitude to Dr. Gaetan Glauser and Dr. Sylvain Sutour from the NPAC who helped me analyzing and purifying these molecules.

Then, I would like to thank the members of the bioanalytical chemistry group, Rocìo, Siva, Désirée and Hanna. Especially Rocìo with whom I started this PhD. Thank you for tolerating me and for helping me settling, along with Stephan, the lab and the TP.

I also want to thank the other members of the chemistry and the physic institute. I had a lot of fun preparing and doing the Halloween parties with you. I want to give a special thank you to Mathilde, Chrysanti and João with whom I build a strong and beautiful friendship.

Most importantly, none of this could have happened without my family and my closest friends who were the first to believe in me. Thank you Annie-Claude and Jean-Baptiste for cheering me up and for encouraging me. Thank you mom for always supporting me financially and emotionally and thank you dad for making me understand that a Bergame never gives up and for both of your love.

Table of Contents

Table of figure

Abstract

Nematodes are the most abundant group of animals on Earth and include free-living and parasitic species, which have successfully adapted to nearly all ecosystems. Nematodes excrete several different molecules into their environment for inter- and intraspecies communication. Recent studies have found that a group of small molecules called ascarosides regulate many aspects of their life history such as mating, lifespan, and development. The ascarosides are glycolipids of the 3,6-dideoxysugar L-ascarylose linked to fatty acid-like aglycones derived from the peroxisomal β-oxidation cycle and are highly conserved in nematodes. Small structural alterations of the side chain or the attachment of additional building blocks downstream of the β-oxidation cycle can dramatically alter the biological activity of the ascarosides, which forms the molecular basis of the species-specific "chemical language" of nematodes.

Using HPLC-MS/MS analytical techniques along with one- and two-dimensional NMR spectroscopy, four families of species-specific modular ascarosides were identified in nematodes from the Elegans group: the *ortho*-aminobenzoate ascarosides (abas) in *C. nigoni* and *C. tropicalis*, the urocanate ascarosides (ucas) in *C. nigoni*, *C. remanei* and *C. briggsae,* the 4-epimeric ascaroside (caen) in *C. nigoni*, and the oligomeric ascarosides in *C. tropicalis*.

This PhD thesis focused on the total synthesis of these novel species-specific ascarosides, in order to confirm their structure assignment and to determine their biological functions in nematodes. For this purpose, this study first focused on the synthesis of two different types of ascaroside building blocks, prepared from commercially available L-rhamnose. First, the 2,4-di-*O*-benzoyl ascarylose commonly used for the synthesis of basic ascarosides that only differ by the length and the terminal function of their side chain was prepared. Then, the orthogonally protected ascarylose, first introduce by Zhang *et al*. with the 4-*O*-*tert*-butyldiphenylsilyl-2-*O*-benzoyl ascarylose and that allows the regioselective formation of 4- or 2-modified ascaroside, was synthesized.

Given the importance of the ascarylose building block for the synthesis of ascarosides, different synthetic strategies were studied to develop a short and selective synthesis to obtain the ascarylose building blocks. The six step synthesis of the dibenzoyl ascarylose from Jeong *et al*. based on regioselective elimination of the 2,3,4-tri-*O*-benzoyl rhamnose was successfully shortened to four steps via Barton McCombie deoxygenation of the methyl-3-*O*-phenyloxythiocarbonyl rhamnoside while the seven steps synthesis of the orthogonally protected 4-*O*-*tert*-butyldiphenylsilyl-2-*O*-benzoyl ascarylose from Zhang *et al*. via regioselective sulfate ring opening of the methyl-2,3-(*O*-sulfate)-4-*O*-*tert*-butyldiphenylsilyl rhamnoside was reduced to six steps via regioselective opening of methyl-2,3-*O*-benzylidène rhamnoside. Moreover, the synthesis also provided access to a wide range of 4-modified ascarylose building blocks while Zhang's synthesis give only access to the 4-*O*-*tert*-

butyldiphenylsily-2-*O*-benzoyl ascarylose.

These building blocks were subsequently used to synthesize the 4-modified urocanate ascarosides and *ortho*-aminobenzoate ascarosides as well as the oligomeric ascarosides, while the 3,6-dideoxy-*lyxo*-hexose building block from the caenorhabdoside, was obtained via epoxide ring opening. In total ten novel species-specific ascaroside were synthesized. The (*E*)-configured urocanate ascarosides were synthesized in seven steps from the 4-*O*-*tert*-butyldiphenylsily-2-*O*-benzoyl ascarylose and there corresponding (*Z*)-isomers obtained by UV irradiation. The *ortho*-aminobenzoate ascarosides were also synthesized in seven steps from the 4-*O*-*tert*-butyldiphenylsilyl-2-*O*-benzoyl ascarylose. The oligomeric ascarosides were obtained by convergent synthesis from the 4-*O*-*tert*-butyldiphenylsily-2-*O*-benzoyl ascarylose and the 2,4-di-*O*-benzoyl ascarylose and the caenorhabdoside synthesized by glycosylation of the (7*R*,8*R*,2*E*)-*threo*-ethyl-7-benzoyloxy-8-hydroxy-2-nonenoate with the 3,6-dideooxy-*lyxo*-hexose.

Comparative analysis of HR-MS and NMR data of the synthetic and the natural compounds confirmed their structure assignment. Furthermore, the synthetic compounds were subsequently tested in behavioral assays. However, only the dimeric ascaroside showed significant retention activity in males of *C. tropicalis*. The identification of these novel species-specific ascarosides demonstrates that ascaroside signaling is more complex than previously anticipated and that nematodes have evolved to utilize the conserved basic ascarosides as scaffold from which they generate species-specific signaling molecules by the attachment of additional building blocks from diverse metabolic pathways, such as the amino acid metabolism, but also by oligomerization or epimerization of the ascarylose sugar.

The discovery of these modular ascarosides give some insights for the mechanism underlying the biosynthesis of species-specific ascaroside. Currently, limited information regarding the genes involved in the biosynthesis of these modular ascarosides is available. Therefore, additional investigation to decipher the mechanism of the biosynthesis of these ascarosides will be required in the future. Moreover, additional bioassays with maybe a focus on development or the formation of dauer worms will be required to find the biological functions of these highly specific modular ascaroside.

Keywords: Nematode, ascaroside, chemical communication, species-specificity, total synthesis.

Résumé

Les nématodes constituent le groupe animal le plus abondant sur Terre et comprennent des espèces libres ainsi que des parasites qui se sont adaptées avec succès à presque tous les écosystèmes. Les nématodes excrètent diverses molécules dans leur environnement pour communiquer avec leurs congénères ou avec d'autres espèces. De récentes études ont montré qu'une famille de petites molécules appelées ascarosides régule de nombreux aspects de leur vie tels que la reproduction, le cycle de vie ainsi que le développement. Ces ascarosides sont des glycolipides du 3,6-didésoxysucre L-ascarylose liés à des aglycones de type acide gras issus de la β-oxydation peroxisomale et sont hautement conservés chez les nématodes. De petites modifications structurelles de la chaîne latérale ou l'attachement de building blocks en aval de la β-oxydation peuvent considérablement modifier l'activité biologique de ces ascarosides. Elles constituent la base moléculaire du « langage chimique » des nématodes.

En utilisant des techniques analytiques telles que la HPLC-MS/MS ainsi que la spectroscopie RMN uni- et bidimensionnelle, quatre nouvelles familles d'ascarosides modulaires spécifiques à l'espèce ont été identifiées chez des nématodes du groupe *Elegans*: les *ortho*-aminobenzoate d'ascarosides (abas), les urocanates d'ascarosides (ucas), les 4-épimères d'ascarosides (caen) ainsi que les oligomères d'ascarosides.

Cette thèse de doctorat s'intéresse à la synthèse totale de ces nouveaux ascarosides afin, d'une part, de confirmer leur structure et d'autre part de déterminer leurs fonctions biologiques chez les nématodes. À cette fin, cette étude s'est d'abord concentrée sur la synthèse de deux types de building-blocks, tous deux préparés à partir du L-rhamnose disponible commercialement. Dans un premier temps, le 2,4-di-*O*-benzoyle ascarylose, couramment utilisée pour la synthèse d'ascarosides basiques qui ne diffèrent que par la longueur et le groupement fonctionnel terminal de leur chaîne latérale, a été synthétisé. Puis, l'ascarylose possédant des groupements protecteurs orthogonaux, dont l'ascarylose 4-*O*-*tert*-butyldiphenylsilyl-2-*O*-benzoyle ascarylose introduit pour la première fois par Zhang *et al.* et qui permet la formation régiosélective d'ascarosides modulaires modifié en position 4 ou 2-, a également été synthétisée.

Compte tenu de l'importance du noyau ascarylose pour la synthèse des ascarosides, différentes voies de synthèse ont été étudiées pour développer une synthèse courte et sélective permettant d'obtenir le building block d'ascarylose. Ainsi, la synthèse en six étapes du 2,4-di-*O*-benzoyle ascarylose de Jeong *et al.* basée sur l'élimination régiosélective du 2,3,4-tri-*O*-benzoyle rhamnose a été raccourcie par une synthèse en quatre étapes via désoxygénation de Barton McCombie du methyl-3-*O*-phenyloxythiocarbonyl rhmanoside, tandis que la synthèse en sept étapes du 4-*O*-*tert*-butyldiphenylsilyl-2-*O*-benzoyle ascarylose proposée par Zhang *et al.* via l'ouverture régiosélective du

methyl-2,3-(*O*-sulfate)-4-*O*-*tert*-butyldiphenylsilyl rhamnoside a été réduite à six étapes via l'ouverture régiosélective du methyl-2,3-*O*-benzylidène rhamnoside. En outre, cette dernière synthèse a également donné accès à un large éventail de building-block d'ascarylose protégé par divers groupements protecteurs en position 4 là où la voie de synthèse proposé par Zhang *et al*. ne permet que d'obtenir le 4-*O*-*tert*-butyldiphenylsilyl-2-*O*-benzoyle ascarylose. Ces building blocks ont ensuite été utilisés pour synthétiser les urocanates d'ascarosides, les ortho-aminobenzoate d'ascaroisdes ainsi que les oligomères d'ascarosides, tandis que le 3,6-didésoxy-*lyxo*-hexose du caenorhabdoside a été obtenu par ouverture d'époxyde.

Les (*E*)-urocanates d'ascarosides ont été synthétisés en sept étapes à partir du 4-*O*-*tert*-butyldiphenylsilyl-2-*O*-benzoyle ascarylose et leur isomères (*Z*) obtenus par irradiation UV. L'*ortho*-aminobenzoate d'ascarosides a été synthétisé en huit étapes également à partir du 4-*O*-*tert*-butyldiphenylsilyl-2-*O*-benzoyle ascarylose. Pour la synthèse des oligomères d'ascarosides, ceux-ci ont été obtenus à partir du 4-*O*-*tert*-butyldiphenylsilyl-2-*O*-benzoyle ascarylose et du 2,4-di-*O*-benzoyle ascarylose par synthèse convergente. Enfin, le caenorhabdoside a été obtenu par glycosylation du (7*R*,8*R*,2*E*)-threo-ethyl 7-benzoyloxy-8-hydroxy-2-nonenoate avec le 3,6-didésoxy-*lyxo*-hexose.

L'analyse comparative des spectres de masse et de la RMN des composés synthétiques et naturels a confirmé la structure de ces nouveaux ascarosides. Ces composés synthétiques ont ensuite été soumis à des tests biologiques. Toutefois, seul le dimer a montré une activité de rétention significative chez les mâles de *C. tropicalis.* Malgré l'absence d'activité biologique pour la plupart des composés, l'identification de ces nouveaux ascarosides démontre que la communication chimique via les ascarosides est plus complexe que prévu et que les nématodes ont évolué pour utiliser les ascarosides simples comme noyaux à partir desquels ils génèrent des molécules de signalisation spécifiques à l'espèce par attachement de groupement provenant de diverses voies métaboliques comme le métabolisme d'acides aminés, mais aussi par oligomérisation ou épimérisation du sucre ascarylose.

La découverte de ces ascarosides modulaires donne un aperçu du mécanisme de biosynthèse des ascarosides spécifiques. Actuellement, peu d'information concernant les gènes impliqués dans la biosynthèse de ces ascarosides modulaires sont disponibles. Par conséquent, des recherches supplémentaires pour comprendre le mécanisme de la biosynthèse de ces ascarosides seront nécessaires à l'avenir. De plus, des tests biologiques supplémentaires axés par exemple sur le développement ou la formation de vers dauer seront nécessaires pour trouver les fonctions biologiques de ces ascarosides modulaires hautement spécifiques.

Mots-clés : Nématode, ascaroside, communication chimique, spécificité, synthèse totale.

1. Introduction

1.1. Chemical ecology

All life-forms from bacteria to animals, emit mixtures of chemicals, which, once they are perceived by another organism, become a system of communication. Whether it is for mating, feeding or defense, chemical communication is conserved across all living organisms, from bacteria to humans, and every species develops its own language. Chemical ecology, a vast and highly interdisciplinary field, studies the role of these chemical interactions to gain a better understanding of the biological processes underlying inter- and intra-species interactions and their ecological significance.

"Pheromones" are chemical cues emitted by one individual and received by a second individual of the same species in which they trigger a specific physiological or behavioral reaction. This term was introduced in 1959 by Karlson and Lüscher[1] after the first pheromone, bombykol (**Figure 1.A**), had been described from the silk moth *Bombyx mori*[2]. Since then, thousands of pheromones have been identified, ranging from individual molecules like the rabbit mammary pheromone, 2-methyl-2-butenal (**Figure 1.B**)[3], to mixtures of chemicals like the Nasonov pheromone released by the worker bees, which comprises seven components, (*E*) and (*Z*)-citral, nerol, geraniol, nerolic acid, geranic acid, and (*E*,*E*)-farnesol (**Figure 1.C**)[4].

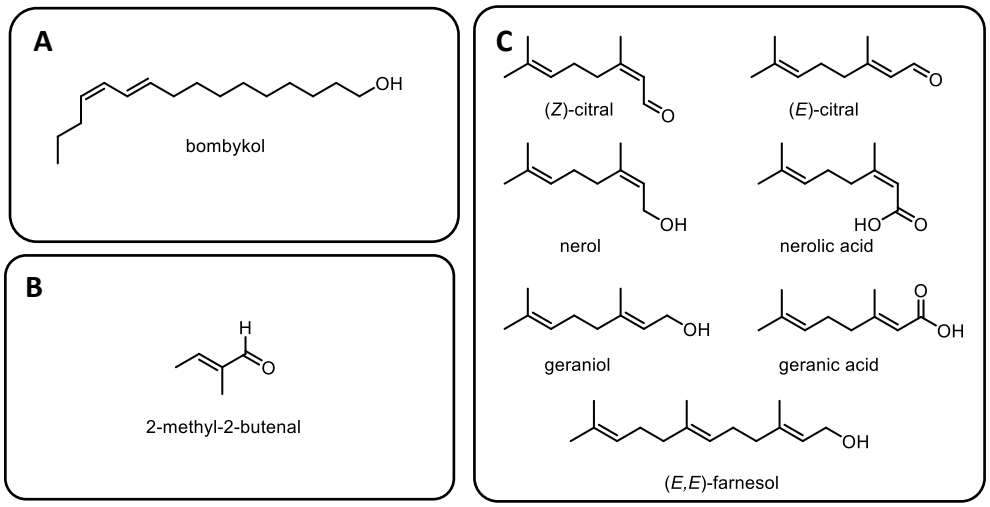

Figure 1 : Chemical structures of (A) the bombykol from the silk moth Bombyx mori. (B) the rabbit mammary pheromone 2-methyl-2-butenal. (C) the Nasonov pheromone from the worker bees.

1.2. The nematodes

The nematodes, or roundworms, are the most numerous but often un-recognized class of animals on Earth, due to their small size and their habit of hiding in soil and other substrates. Nevertheless, roundworms are ubiquitous in every ecosystem from marine to terrestrial environments where they interact with plants, insects or animals including humans. Many nematodes are free-living bacterial or

fungal feeders but some are parasites of plant and animals and are a threat for human health and agriculture. Indeed, plant parasitic nematodes are responsible for up to 12% of annual agricultural losses and gastrointestinal nematodes infect 3.5 billion people worldwide. On the other hand, the nematodes also contribute to the proper functioning of the soil ecosystem and serve as good bioindicators for soil quality[5]. One particular nematode from the Rhabditida group, the free-living bacterivorous *Caenorhabditis elegans*, was introduced by Sydney Brenner in 1963 as a model organism to study developmental biology and neurobiology. This self-fertilizing, hermaphroditic, and facultative outcrossing nematode is a cosmopolitan that feeds primarily on bacteria. Under favorable conditions, the life cycle of *C. elegans* includes six developmental stages starting from the egg stage followed by four larval stages (L1 - L4) until the egg-laying adult stage (**Figure 2**). However, under unfavorable conditions, like depletion of food, high population density, adverse temperature or accumulation of nematode pheromones, the L2 larvae will molt into an alternative, non-feeding, and highly stress resistant "L3d" larval stage called the dauer stage (from the German word for "enduring") with a dramatically increased lifespan of several months.

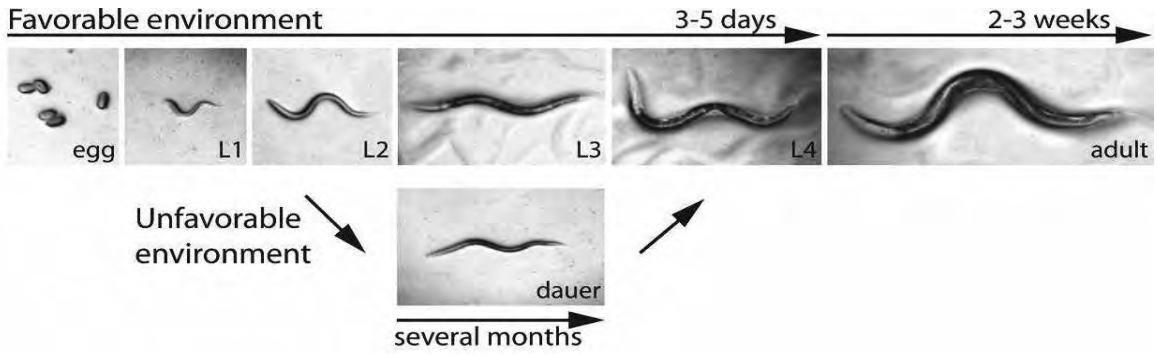

Figure 2 : Life cycle of the Caenorhabditis elegans.

Due to its short reproductive life cycle (3 days at 25 °C from egg to fertile adult), its body transparency, as well as its easy maintenance in laboratory culture, *C. elegans* has become a widely used model organism with which important discoveries have been made including genetic regulation of apoptosis (programed cell death)[6], RNA interference[7], and the identifications of genes implicated in the Alzheimer's disease[8]. At this stage *C. elegans* is certainly one of the most well understood organisms. However, in comparison with the great amount of information regarding *C. elegans* biology, its chemical ecology is still poorly understood. Recent studies found that *C. elegans* and other nematodes produce a group of small molecules called ascarosides by utilizing a strategy of modular assembly of diverse building blocks from primary metabolic pathways. These ascarosides induce a wide variety of biological responses[9] and have been found to be widely conserved among nematodes[10] with the *Caenorhabditis* spp.[11] and *Pristionchus* spp. being studied in most detail[12].

1.3. Ascarosides signaling

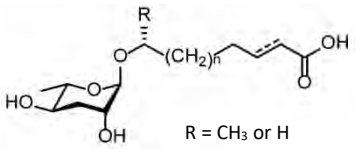

Figure 3: General structure of a basic ascaroside from nematodes.

The ascarosides are glycolipids of the 3,6-dideoxysugar L-ascarylose (3,6-dideoxy-L-*arabino*-hexose) linked via the α-anomeric position to a fatty-acid like side chain of various length and functionality, at either the ultimate (ω) or the penultimate (ω – 1) carbon of the side chain (**Figure 3**). Ascaroside-type glycolipids with very long chain aglycones were first isolated in 1912 by Flury from the intestinal parasitic roundworm *Ascaris lumbricoides* and represent what he described as an "unsaponifiable matter" of the worms lipids[13]. Forty years later, Fouquet elucidated the exact structure of these ascarosides[14]. These lipophilic molecules consist of very long aliphatic side chains that are glycosylated at the (ω – 1)-position with an α-L-ascarylose and are presumed to form a protective lipid layer within the ascaris eggs[15].

In 1982, Golden and Riddle found that an unidentified component accumulating in the nematode's culture medium is causing the formation of dauer larvae[16]. Few years after the discovery of the dauer inducing compound, Golden and Riddle also identified a dauer defective mutant, the *daf-22* mutant[17] that carries defects in a gene for the peroxisomal 3-ketoacyl-S-CoA thiolase. Using the wild type worm's pheromone extract, they were able to induce dauer formation in the *daf-22* mutant proving that the dauer pheromone is worm-derived and that the *daf-22* mutant cannot produce it. However, the molecular structure of the dauer inducing pheromone remained elusive for twenty years until research from several laboratories found that the *C. elegans* dauer pheromone consists in a mixture of multiple short chain ascarosides. In 2005, Jeong and coworkers were the first to isolate one of the components of the dauer pheromone by activity-guided fractionation of the *C. elegans* liquid culture extract[18]. It consists in an ascaroside carrying a seven-carbon fatty-acid-like aglycone, which they called daumone (later named ascr#1 by the Schroeder group[9b] and asc-C7 by the Butcher group[19], **Figure 4**). However, asc-C7 (**1**) exhibits only a weak dauer-inducing activity, suggesting that the dauer pheromone was a more complex mixture of ascarosides that potentially act synergistically. In the following years additional ascarosides with a stronger dauer-inducing activities were discovered such as asc-C6MK (ascr#2, **2**, **Figure 4**) bearing a six carbon aglycon with a methyl ketone moiety[19], asc-ΔC9 (ascr#3, **3**, **Figure 4**) with a nine-carbon α,β-unsaturated carboxylic acid side chain[19], and asc-ωC3 (ascr#5, **Figure 4**) with a (ω)-linked three carbon side-chain [20].

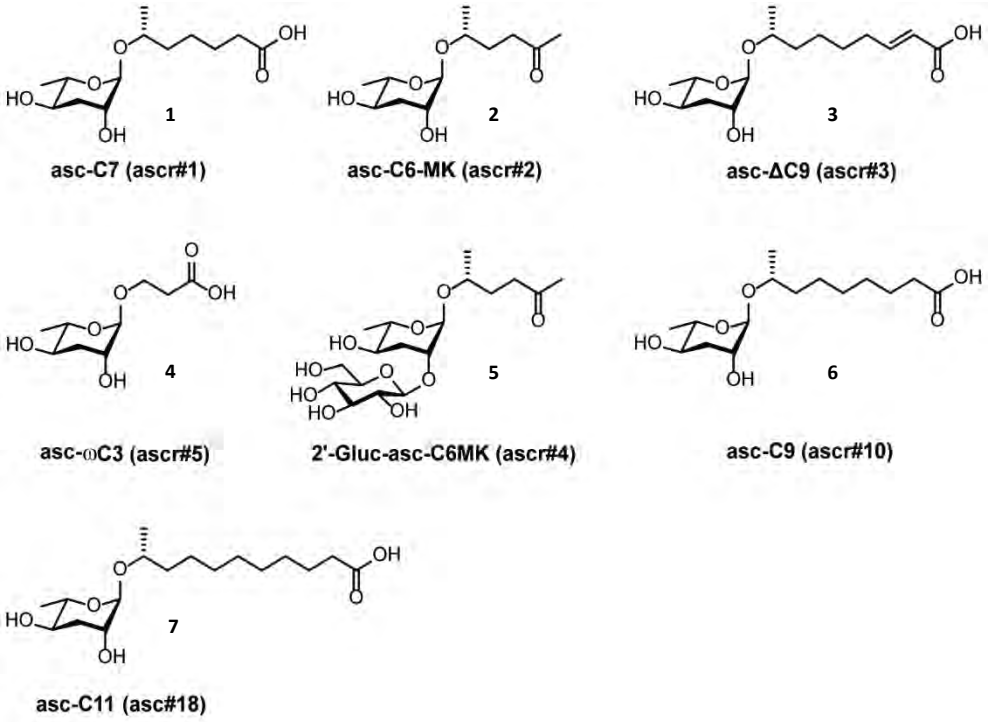

Figure 4: Ascarosides identified in *C. elegans*.

Following the discovery of these ascarosides it was later shown that these glycolipids are not only regulating developmental plasticity (entry and exit into the dauer stage), but are also inducing behavioral responses at concentration several orders of magnitude lower than those required to induce dauer formation (pico to femtomolar). Their functional characterization revealed that a synergistic blend of asc-C6MK (ascr#2, **2**, **Figure 4**), asc-ΔC9 (ascr#3, **3**, **Figure 4**) and the 2-*O*-glucoside 2'-Glu-asc-C6-MK (ascr#4, **4**, **Figure 4**) produced by hermaphrodites of *C. elegans* induces attraction of males while a mixture of asc-C6MK and asc-ΔC9 repels hermaphrodites[9b]. Further studies showed that small structural alterations result in dramatic changes in the bioactivity of the ascaroside[21]. For example, asc-C9 (ascr#10, **6**, **Figure 4**), with a saturated nine carbon side chain induces attraction of *C. elegans* hermaphrodites but the corresponding asc-ΔC9 (ascr#3, **3**, **Figure 4**) with an additional α,β-double bond acts as a repellent[22]. Ascarosides were also reported to be involved in cross-kingdom interactions[23]. For example, some nematophagous fungi have evolved to detect ascarosides and respond by formation of traps to catch and consumes nematodes[24] while various plants respond to asc-C11 (ascr#18, **7**, **Figure 4**) with an upregulation of their plant defenses, which repels plant parasitic nematodes[25].

1.4. Nomenclature of ascarosides

When the first ascarosides were identified they were named daumone 1, daumone 2 and daumone 3 by the Paik group[18] or ascaroside 1, ascaroside 2 and ascaroside 3 by the Clardy group[19] as no one at the time would have expected the diversity of ascarosides produced by nematodes. When it became apparent that ascarosides represent homologous series, these naming systems became unpractical. Therefore, a third naming system was introduced by Butcher[19] based on the length of the side chain of the ascarosides using the abbreviation "asc" followed by the side chain length. Thus, the ascaroside ascr#1, bearing a side chain with 7 carbons, would become asc-C7 and the ascr#10 with 9 carbons asc-C9.

In parallel, an additional naming system in collaboration with the Wormbase database was developed by the Schroeder group. The Small Molecule Identifier (SMIDs) consists of four lower case non-italicized letters referring to the general structural class of the compound, followed by a pound sign and a number. For example, the 7-carbon side chain ascaroside would be named ascr#1. The objective of the SMID system is to provide every nematode metabolite with a unique, simple, and searchable name. As this nomenclature does not provide an intuitive description of the structure of the modular ascarosides, the SMID system as well as the naming conventions originally implemented by the Butcher group (as depicted in **Figure 5**) are used for this work.

To name a modular ascaroside it is divided into four parts:

- The core which represents the ascaroside moiety attached to its side chain (asc),
- The fatty acid like aglycon (Cx)
- The head group for the additional attachment of building blocks on the sugar.
- The terminal group for additional modifications attached to the side chain.

The ascaroside building block is referred to as "asc" and the side chain length is represented by "Cx" where x is the number of carbons of the aglycon. Commonly, the side chain is (ω - 1)-linked to the ascarylose and when it is the case the oxygenated carbon is always (*R*)-configurated. Therefore, when the aglycon is (ω - 1)-linked to the ascarylose, neither the configuration nor the linkage will be mentioned whereas linkage of the side to the ascarylose at its ultimate carbon is mentioned as "ω" in front of "Cx" such as "asc-ωC3". When the side chain is bearing an α,β-unsaturation this is represented as "Δ" in front of "Cx" such as "asc-ΔC9". Alternative hydroxylation of the aglycone are indicated in front of "Cx" as "xHO" where x refers to the location of the hydroxy group. Additional building blocks linked to the sugar unit are mentioned, in front of the core, using a characteristic abbreviation (for example "IC" for indole-3-carbonyl) preceded by "2'-" or "4'-" depending on their position on the sugar unit. Since the terminal group of most of the ascarosides is a carboxylic acid, only non-carboxylic groups will be specified. For example, the methyl ketone aglycon in ascr#2 will be indicated as C6MK

(**Figure 5**).

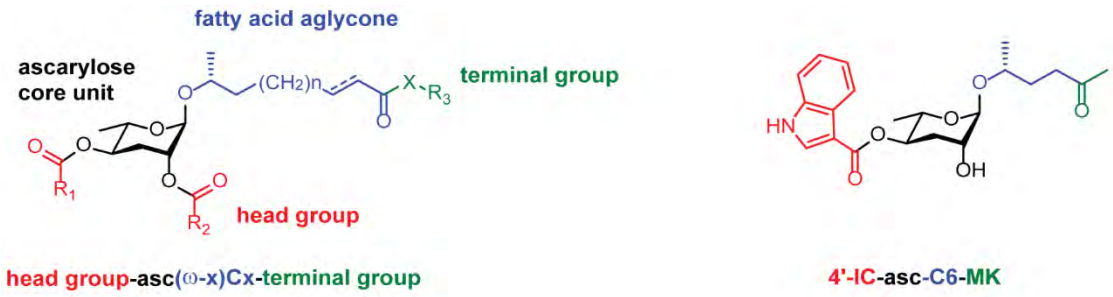

Figure 5 : Example of nomenclature for this work.

While Butcher's naming system provides a description of the molecular structure of the ascaroside, on the other hand, this system results in long and complex name which increases with the complexity of the ascaroside. The SMID system has the advantage of generating more concise trivial names which can be easily searchable in a database.

1.5. Analytical techniques for the detection of ascarosides

Initially, the discovery of ascarosides relied on activity-guided fractionation of the worm culture supernatant. However, the discovery that the ascarosides worked synergistically in dauer induction as well as mating[9b, 19-20], made the activity guided fractionation unsuitable for the identification of new ascarosides, since the separation of components would lead to the partial loss of activity as it was the case for the dauer inducing pheromone. Thus, in 2009, Pungaliya et al. developed an NMR spectroscopic methodology to identify new ascarosides[26]. Using differential analysis of 2D NMR spectroscopy (DANS), a spectroscopic method that compares the *dqf*-COSY spectra of wild-type and *daf-22* worms (**Figure 6.A**), they were able to identify several known ascarosides as well as new ascarosides including the seven carbon aglycon ascaroside asc-ΔC7 (ascr#7, **9**), the two diastereomeric ascarosides asc-C6-(*R*)-OH and asc-C6-(*S*)-OH (ascr#6.1, **10** and ascr#6.2, **11**) and the most potent dauer-inducing ascaroside asc-ΔC7-PABA (ascr#8, **12**) that bears a terminal *para*-amino benzoic acid (PABA) moiety linked via an amide bond (**Figure 6.B**)[26]. Furthermore, DANS also revealed a novel class of modular ascarosides that incorporates a tryptophan derived indole-3-carbonyl unit attached to the 4-position of the ascarylose moiety, like seen in 4'-IC-asc-ΔC9 (icas#3, **14**) or 4'-IC-asc-C5 (icas#9, **13**) first identified by Butcher et al. by activity-guided fractionation as a minor component of the dauer-inducing pheromone blend (**Figure 6.C**)[27]. Later, behavior studies revealed that 4'-IC-asc-C5 (**13**) and 4'-IC-asc-ΔC9 (**14**) are acting synergistically to induce aggregation and attraction of hermaphrodites at pico and femtomolar concentrations[28].

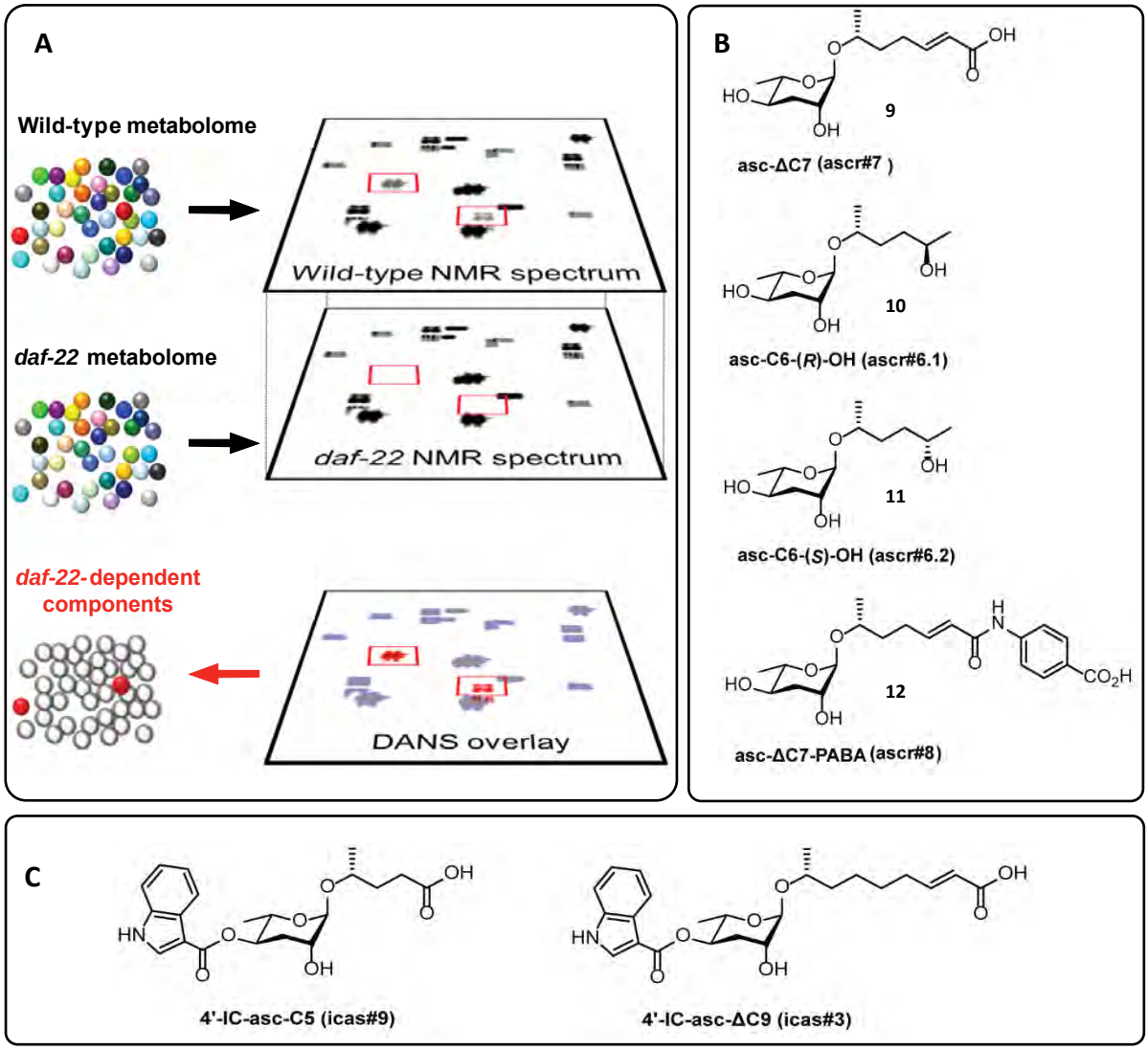

Figure 6: (A) Schematic representation of Differential Analysis via 2D-NMR spectroscopy (DANS). Comparison of wild-type NMR spectra with daf-22 mutant NMR spectra. (B) Ascaroside identified via DANS. (C) Indole ascarosides identified via DANS[26].

Since the ascarosides were inducing behavioral responses at picomolar concentration and given the low sensitivity of the NMR, the detection of ascarosides with mass spectrometric techniques, which are more sensitive than NMR spectroscopy, were considered. In 2012 von Reuss *et al*. developed a highly sensitive mass spectrometric technique that facilitates the detection of ascarosides in crude nematode exometabolomes[29]. This method is based on the observation that, upon negative-ion electrospray ionization (ESI^-), the ascarosides exhibit a specific fragment ion at *m/z* 73 ($[C_3H_5O_2]^-$) derived from the ascarylose unit (**Figure 7.C**). Screening for this specific fragment results in chromatograms that display signals corresponding to potential ascarosides, while masking most of the signals that are not related to ascarosides (**Figure 7.A & B**). The LC-MS/MS precursor ion screening for *m/z* 73 resulted in the characterization of several genes implicated in ascaroside biosynthesis, as well

as the detection of known and unidentified ascarosides, like the highly potent male attractant hbas#3 (PHBA-asc-ΔC9, **15**) and the mbas#3 (MB-asc-ΔC9, **16**) carrying a *para*-hydroxybenzoyl and a (*E*)-2-methyl-2-butenoyl moiety at the 4'-position of the sugar unit, respectively (**Figure 7.D**)[29]. Additionally, the sensitivity of the MS/MS precursor ion screening enabled to identify life stage and sex-specific ascarosides from only a few hand-picked *C. elegans* individuals[22, 30]. The LC-MS/MS screen is suitable for ascarosides that ionize well in negative electro spray ionization mode, however, the technique appears to be less sensitive in positive mode due to the large variety of additional adducts that is formed in ESI^+ mode[29].

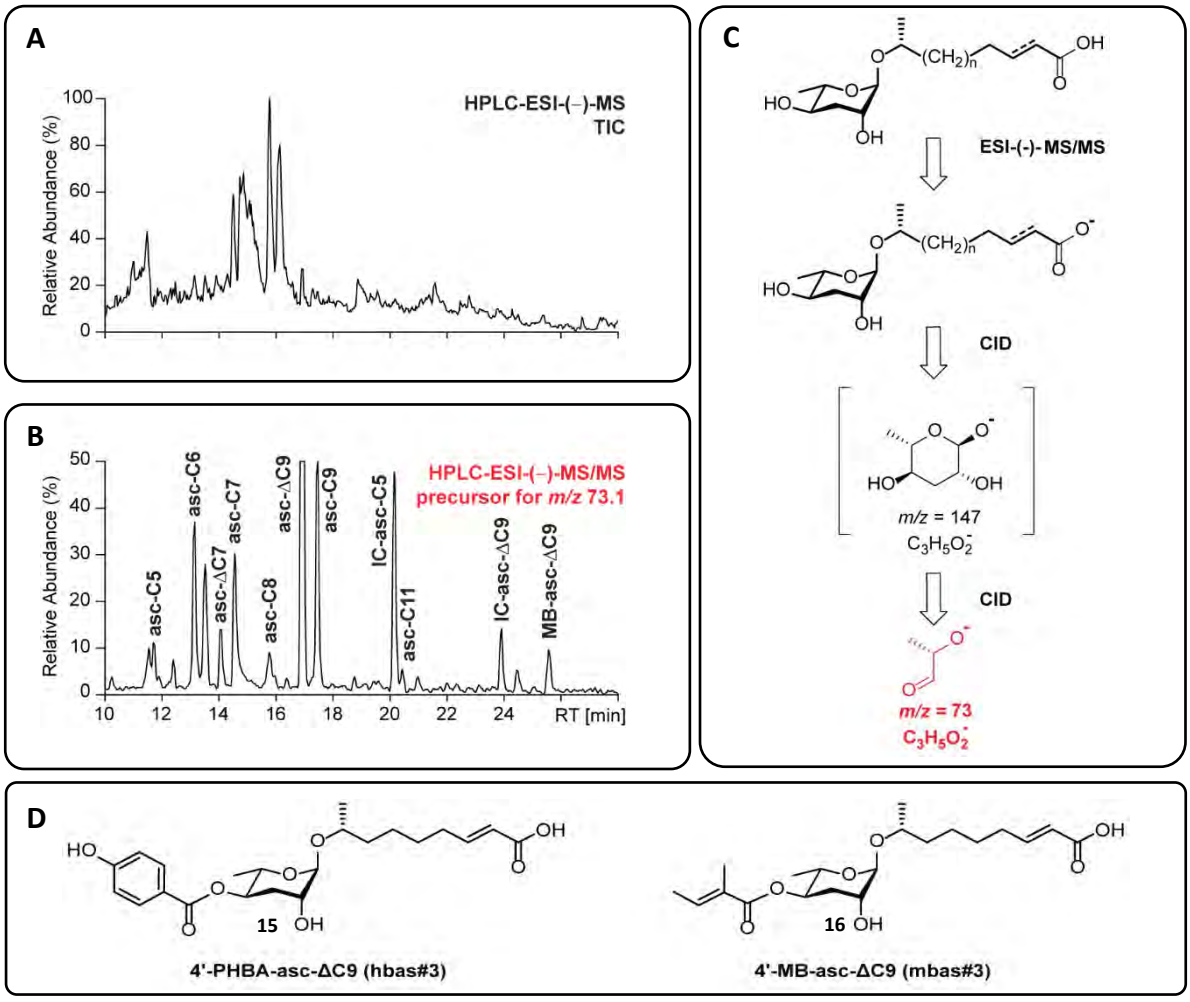

Figure 7: (A) LC-MS total ion chromatogram of C. elegans exometabolome. (B) HPLC-MS/MS precursor ion screen (m/z 73, $[C_3H_5O_2]^-$) of the *C. elegans* exometabolome. (C) Mass spectrometric fragmentations of ascaroside upon electrospray ionization. (D) *para*-hydroxybenzoyl (hbas#3) and (*E*)-2-methyl-2-butenoyl (mbas#3) ascarosides identified via HPLC-MS/MS precursor ion screening[29].

Von Reuss' group also developed a complementary method based on gas chromatography electron-ionization mass spectrometry of TMS-derivatized nematode exometabolomes (**Figure 8.A & B**)[11b]. Analysis of their mass spectra revealed three characteristic ascarylose-derived fragments, the

fragment K1 at *m/z* = 130.1 $[C_6H_{14}OSi]^{+\bullet}$ and the fragment A1 at *m/z* = 275.1 $[C_{12}H_{27}O_3Si_2]^+$ and the fragment A2 at *m/z* = 185.1 $[C_9H_{17}O_2Si]^+$. In addition, the technique also revealed two side-chain specific fragments, the fragment J1 at $[M - 173]^+$ along with the fragment J2 $[M - 291]^+$ (**Figure 8.C**). Using GC-MS ascaroside screening, they were able to identify all the basic ascarosides including asc-C6MK (ascr#2, **2**) that could not be detected by ESI^- MS/MS. Moreover, it also permitted the detection of new ascarosides like the hydroxylated ascarosides asc-7OH-ΔC9 (**17**), asc-7OH-C9 (**18**) and asc-9OH-ΔC9 (**19**, **Figure 8.D**) and the side chain derived fragments J1 and J2 facilitate the structure assignment of their aglycons[11a]. However, the GC-MS screening after TMS derivatization is limited to the detection of basic ascarosides as more complex compounds like the indole ascarosides are not volatile enough to be detected. Taken together, the GC and the LC-MS/MS screening are powerful complementary tools, which, along with NMR spectroscopy, enabled the description of several knew ascarosides.

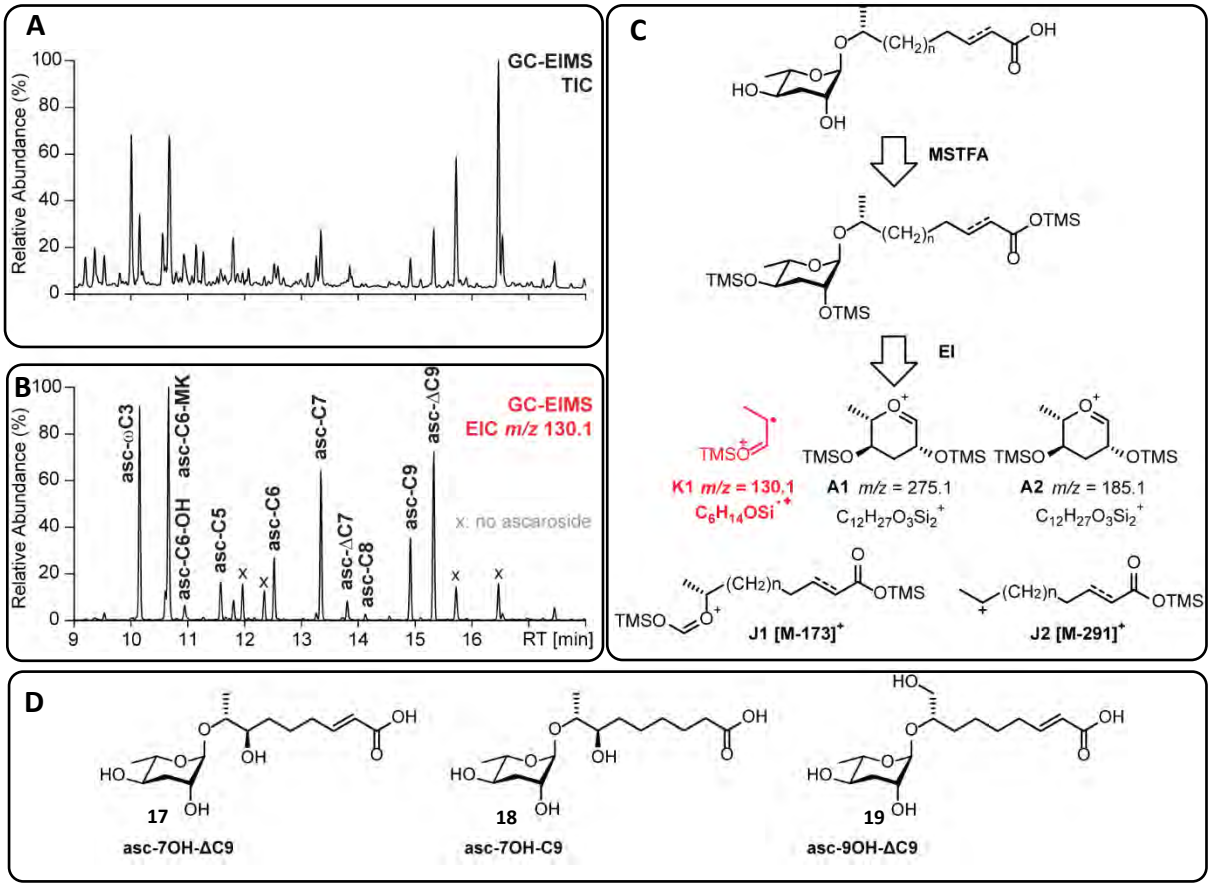

Figure 8: (A) GC-MC total ion chromatogram of the TMS-derivatized *C. elegans* exometabolome. (B) Extracted ion chromatogram (EIC) for the K1-fragment at *m/z* 130.1 $[C_6H_{14}OSi]^{+\bullet}$. (C) Mass spectrometric fragmentations upon electron impact. (D) Hydroxylated ascarosides identified via GC-EIMS screening of TMS-derivatized *C. nigoni*'s exometabolome[11a].

1.6. Species-specific ascarosides

The initial discovery of ascaroside-based signaling molecules in *C. elegans* suggested that other nematodes could also use ascarosides for chemical communication. The analysis of several representatives of free-living, parasitic and entomopathogenic nematodes by mass spectrometry confirmed that the production and the use of basic ascarosides as chemical signals is not unique to *C. elegans* and is widely conserved among the nematodes[10]. Given that different nematode species cohabitate in nature and excrete several partially overlapping ascarosides, the question appears as to how nematodes can maintain dedicated channels for intraspecies communication. Biological investigations showed that nematodes use the widely conserved basic ascarosides as scaffolds for the addition of building blocks derived from primary metabolism in order to generate a library of species-specific ascarosides. For example, one of the most basic species-specific modification, the (ω - 3)-hydroxylation of side chains, was first detected in the free living *Panagrellus redivivus*[19]. The male *P. redivivus* produces a dihydroxylated ascaroside, the asc-8OH-βOH-C11 (dhas#18, **20,** Figure 9) that attracts females[31].

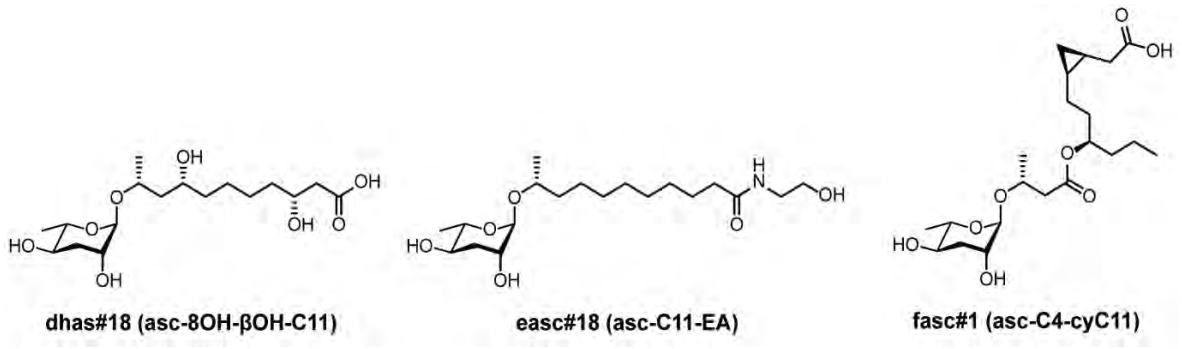

Figure 9: Structures of the dihydroxylated ascaroside, asc-8OH-βOH-C11 (dhas#18, 20)[31], the ethanolamide ascaroside asc-C11-EA (easc#18, 21)[32] and the cyclopropyl fatty acid ascaroside asc-C4-cyC11 (fasc#1, 22)[33] isolated in male *P. redivivus, H. bacteriophora* and female *C. remanei* respectively.

Another type of modification is the selective attachment of building blocks originating from diverse primary metabolic pathways like fatty acid, amino acid, carbohydrate, and nucleoside metabolism. For example, the ethanolamide ascaroside asc-C11-EA (easc#18, **21,** Figure 9) produced by the entomopathogenic *Heterorhabditis bacteriophora* induces the development of infective juveniles, a larval stage homologous to the dauer stage of *C. elegans*[32]. More recently the highly species-specific female produced male attractant asc-C4-*cy*C11 (fasc#1, **22,** Figure 9) has been identified in *Caenorhabditis remanei*[33], which integrates a cyclopropyl fatty-acid building block of bacterial origin. Furthermore, highly complex ascaroside assemblies were found in the necromenic *Pristionchus pacificus* including a homodimeric ascaroside 4'-(asc-C7)-asc-C7 (dasc#1, **23**) or the paratoside npar#1

(**24**) with an unsual 2'-epimeric ascaroside building block, that regulates mouth form dimorphism and dauer formation respectively[12b] (**Figure 10**).

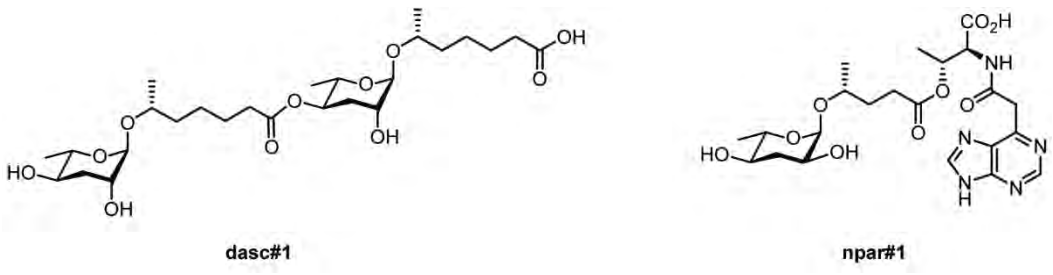

Figure 10 : Structures of the dimeric 4'-(asc-C7)-asc-C7 (dasc#1, 23) and the paratose derivative npar#1 (24) found in the necromenic nematode *P. pacificus*[12b].

1.7. Biosynthesis of ascarosides

Since the discovery of the ascarosides, the chemical biology behind these glycolipids has been investigated extensively with a focus on the biosynthesis of homologous side-chains and the attachment of additional building blocks on the ascarylose unit[29, 34].While the biosynthesis of ascarylose is well understood in bacteria[35], still little is known about its biosynthesis in nematodes. Feeding experiment with *E. coli K12* that lacks the ascarylose biosynthesis genes *ascB* (JW2686) and *ascF*[36] and the detection of ascarosides in the conditioned media supernatant of axenic nematode cultures[28] demonstrated that the L-ascarylose unit is worm derived. For the synthesis of the short-chain ascarosides, it has been demonstrated that the aglycones originate from the peroxisomal β-oxidation cycle, a four-step process that shortens very long chain fatty acids (as well as ascarosides) iteratively by two carbons. In 1985, following the discovery of the *daf-22* mutant, Golden and Riddle concluded that the *daf-22* gene was necessary for dauer pheromone production. Shortly after the identification of the components of the dauer pheromone, Srinivasan *et al.* confirmed the importance of this gene for the production of ascarosides[9b]. The following year, Butcher *et al.* showed that *daf-22* encodes a homologue of the peroxisomal 3-ketoacyl-CoA thiolase that catalyzes the final step in peroxisomal fatty acid β-oxidation[34a] and analysis of the *dhs-28* mutant metabolome indicated that *dhs-28*, which encodes a homologue of a *(R)*-selective β-hydroxyacyl-CoA dehydrogenase domain of human MFE-2, is involved in ascaroside biosynthesis[34a, 36]. Subsequent studies revealed the remaining genes that participate in the peroxisomal β-oxidation cycle of very long chain ascarosides including the acyl-CoA oxidases genes *acox-1*[34b], *acox-2* and *acox-3*[34c], as well as the enoyl-CoA hydratase *maoc-1*[29]. The function of *acox-1*, *maoc-1*, *dhs-28* and *daf-22* were subsequently clarified by comparative LC-MS analysis of *C. elegans* wildtype and the peroxisomal β-oxidation mutant[29]. MS/MS precursor ion screening revealed that the acyl-CoA oxidase participate in the first step of the

peroxisomal β-oxidation cycle by introducing an α,β-unsaturation to the fatty acid side chain. Additional studies from Zhang *et al*. demonstrated that the three acyl-CoA oxidases (ACOX-1, ACOX-2 and ACOX-3) exhibit differential preferences for ascaroside-CoA esters of different length and functionality[34b]. Then, the peroxisomal 2-enoyl-CoA hydratase MAOC-1 hydrates the double bond and the resulting (3*R*)-hyroxyacyl intermediate is oxydized by the 3-hydroxyacyl-CoA dehydrogenase DHS-28. The resulting 3-ketoacyl-CoA ascarosides are substrates for the 3-ketoacyl-CoA thiolase DAF-22, which cleaves an acetyl-S-CoA unit to furnish an acyl-S-CoA ascaroside that is shortened by two carbons and could enter the β-oxidation cycle again.

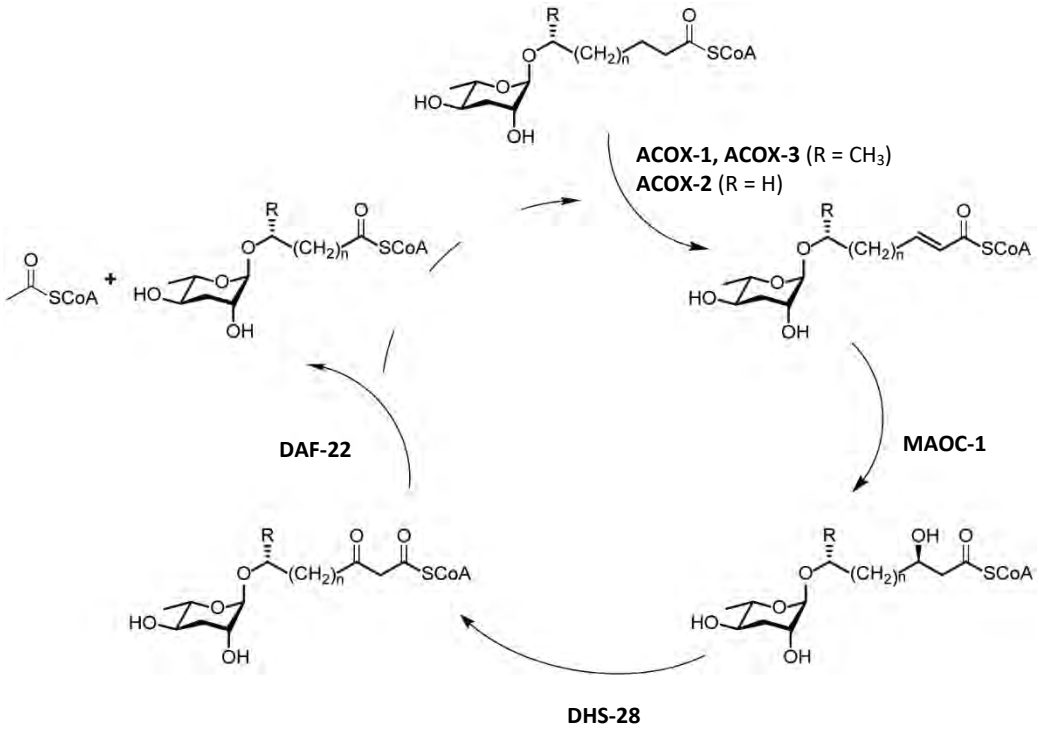

Figure 11: Highly conserved peroxisomal β-oxidation cycle from which originate short chain ascarosides.

While the production of short and medium-chain ascarosides from very long chain ascarosides is well explained via the peroxisomal β-oxidation cycle, the mechanism behind the production of modular ascarosides via attachment of additional building blocks to the sugar unit or the side chain remains less understood. Biosynthetic studies suggested that the additional building blocks attached to the ascaroside core structure originate from primary metabolisms. The incorporation of deuterium-labelled tryptophan by axenic cultures of *C. elegans* confirmed that the indole-3-carbonyl (**27**) units of indole ascarosides originate from L-tryptophan (**25**), whereas the 4-hydroxybenzoyl (**31**) and tigloyl (**33**) head groups of hbas and mbas ascarosides are likely derived from L-tyrosine (**30**) and L-isoleucine (**32**), respectively[29] (Figure 12). Moreover, the analysis of the exometabolome of mutant worms that lack the production of tyramine and octopamine did not show any traces of succinylated tyramine

ascaroside (tsas) or succinylated octopamine ascarosides (osas) without affecting the production of the other ascarosides[30].

Recently, a large family of carboxylic ester hydrolases (CEST) enzymes localized in the lysosomal related organelles (LRO) have been identified as being responsible for the selective attachment of the indole-3-carbonyl and octopamine succinyl group to the ascarylose unit of medium chain ascarosides[34f, 37]. Furthermore, isotope feeding experiments have also revealed that the ACS-7 enzyme, also located in the LRO, activates the side chain of 4'-IC-asc-C9 (**14**) and 4'-OS-asc-C9 to be further shortened via the peroxisomal β-oxidation cycle[34e, f, 38]. Based on these data, a model for the biosynthesis of medium and short-chain modular ascarosides can be proposed in which CEST enzymes mediate the attachment of building block on medium-chain ascarosides downstream of the peroxisomal β-oxidation cycle (**Figure 12**) which, upon activation by ACS-7 can be further shortened in the peroxisomal β-oxidation cycle.

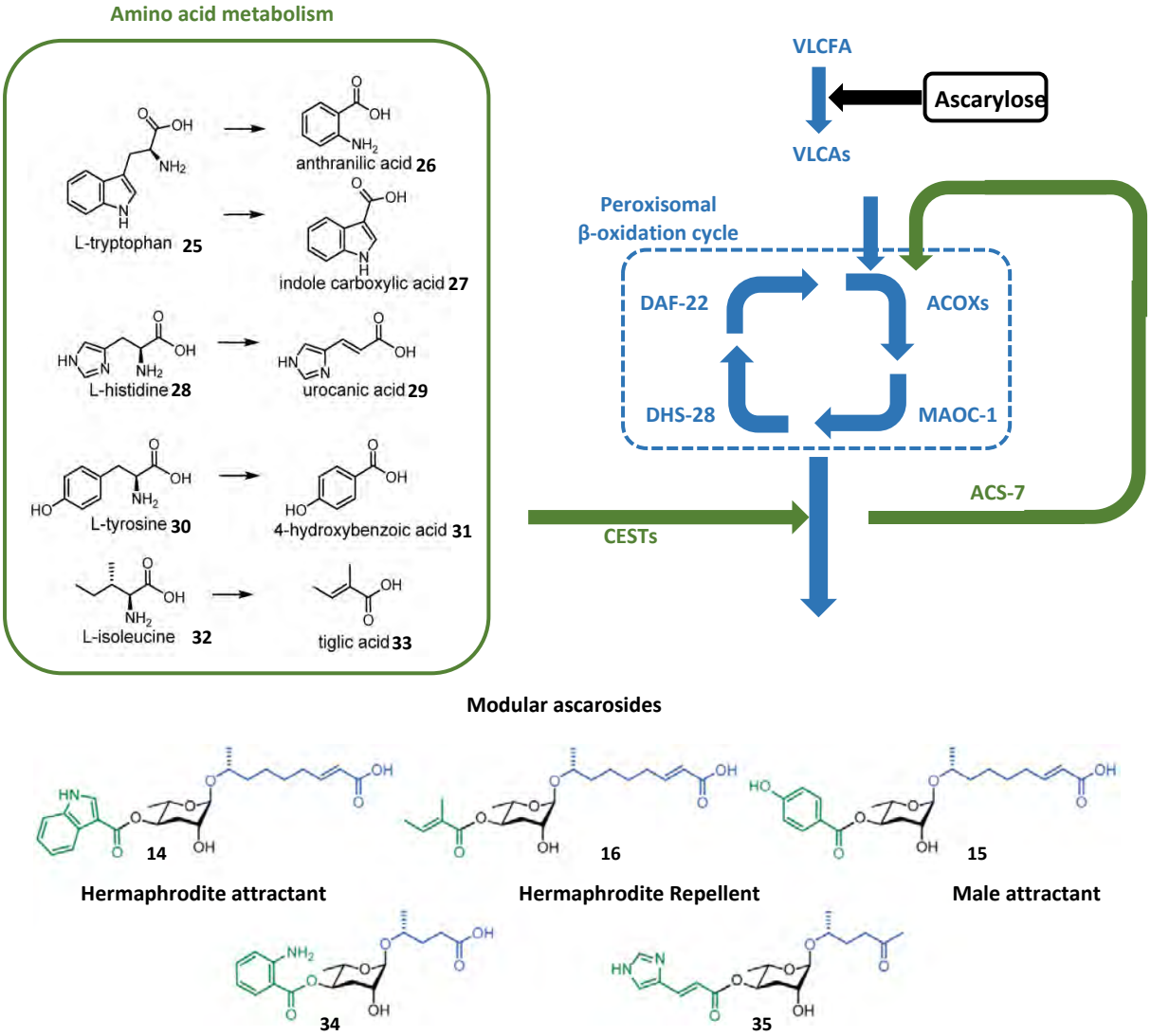

Figure 12 : Model for the biosynthesis of modular ascarosides (VLCFA: very long chain fatty acid, VLCA: very long chain ascaroside).

1.8. Aim of the PhD thesis

The ascarosides, a family of modular metabolites based on the 3,6-dideoxy ascarylose, constitute an important group of nematodes signaling molecules that regulate a wide diversity of biological functions, ranging from developmental plasticity to sex-specific behavior. Recent investigations have revealed that a large number of nematodes can produce and sense ascarosides, therefore raising the question of how nematodes can maintain intra-species communications.

Over the last decade, the development of sensitive analytical techniques like selective mass spectrometric techniques or NMR spectroscopy has enabled the identification of more than hundred ascarosides structures from the crude exometabolomes of several nematode species. These analytical tools have also highlighted the presence of highly species-specific ascarosides derived from the widely conserved basic ascarosides by the attachment of additional building blocks from diverse metabolic pathways. These results suggest that roundworms use basic ascarosides as a scaffold to generate a more diversified family of species-specific ascarosides.

Using the highly sensitive HPLC-MS/MS precursor ion screening of crude nematode exometabolomes combined with classical chromatographic fractionation and most sensitive ^{1}H detected *dqf*-COSY NMR spectroscopy, four new classes of species-specific ascarosides in closely related *Caenorhabditis* species (**Figure 13**) were identified by C. Dong[39]:

- The photochromic 4'-linked ascarosides 4'-UC-asc-ΔC9 (ucas#3, **37-38**) and 4'-UC-asc-C6MK (ucas#2, **35 & 36**) bearing an urocanic acid moiety derived from L-histidine and were identified in *C. nigoni* , *C. remanei*, and *C. briggsae*,
- The 4'-linked 4'-AB-asc-C5 (abas#9, **34**) bearing a 4'-anthranilic acid derived from L-tryptophan and were identified in *C. nigoni* and *C. tropicalis*,
- The 2'-linked homo-oligomers of the asc-C5 (**40-43**) were identified in *C. tropicalis*,
- The 2'-epimeric ascaroside cae-7OH-ΔC9 (caen#1, **39**) was identified in *C. nigoni*.

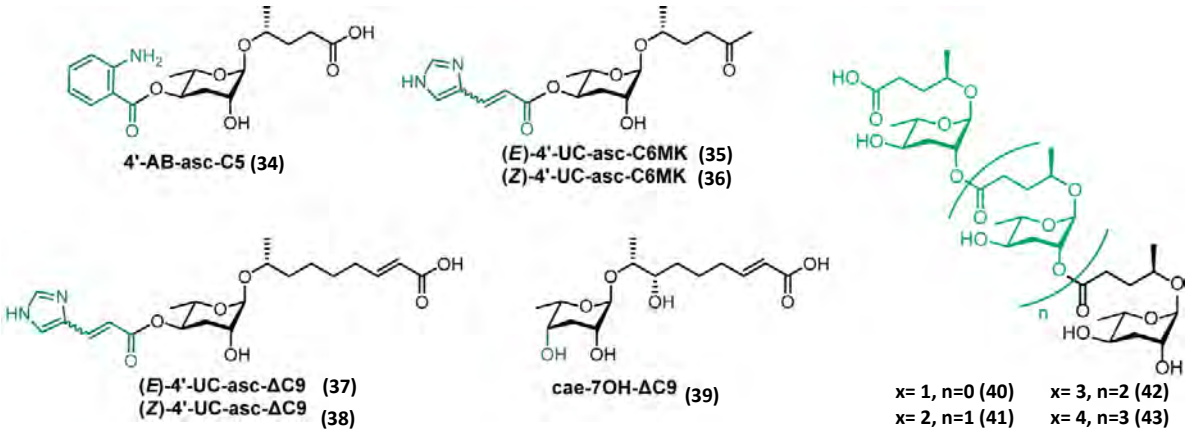

Figure 13: Structures of ascarosides from *C. nigoni, C. remanei* and *C. tropicalis* identified by C. Dong and synthesized for this project.

However, these novel ascarosides were isolated in quantities too small to unambiguously establish their structural assignment or their purity was too small to decipher their biological functions. In the case of the asc-C5 oligomers, structure assignment was based solely on MS/MS data. Therefore, these compounds needed to be synthesized in order to confirm their structure assignment and to provide pure material suitable for a functional characterization in various bioassays.

Consequently, this PhD thesis focuses on the total synthesis of these highly species-specific ascarosides identified in the gonochoristic *C. nigoni* and *C. remanei* and in the hermaphroditic *C. tropicalis*, and the assessment of their biological functions. Moreover, given the importance of the L-ascarylose building block for the synthesis of modular and basic ascarosides in general, the first part of this PhD project focuses on strategies to access useful ascarylose building blocks from the commercially available L-rhamnose. Zhang *et al.* has recently described an orthogonally protected ascarylose building block that facilitates the specific synthesis of 4- or 2-modified ascarosides[40] in contrast to the 2,4-dibenzoylascarylose utilized by Jeong[18] and others, which does not permit the regioselective attachment of additional building blocks on the sugar core. However, the synthesis of this orthogonally protected ascarylose building block involves a long synthetic pathway. Therefore, a shorter and more versatile alternative based on the work of Florent *et al.*[41] was developed. Furthermore, shorter strategies to access 2,4-dibenzoylascarylose for the synthesis of basic ascarosides were explored.

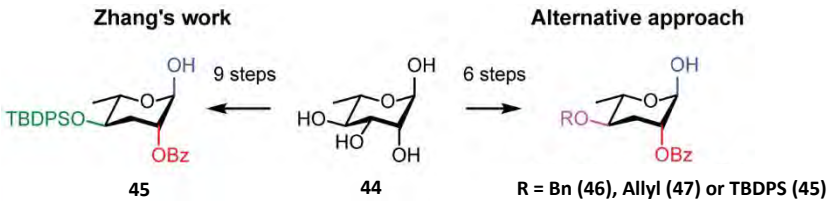

Figure 14 : The two different synthetic strategies for the synthesis of orthogonally protected ascarylose.

Using the different L-ascarylose building blocks the novel modular ascarosides were synthesized and their identity with the natural products was unambiguously established by comparison of their NMR and LC-MS data. After confirmation of the structure assignments, the nematode response to these ascarosides was evaluated using holding assays.

2. Synthesis of the L-ascarylose building blocks

The deoxysugars are an important class of naturally occurring carbohydrates that play important roles in diverse biological processes like intercellular communications and biological activity of many antibiotics[42]. Among them, the 3,6-dideoxyhexoses are common in the O-specific side chain of lipopolysaccharides of Gram-negative bacteria[42a, 43] where they act as antigenic determinants. To this date, of the eight possible enantiomers, six had been identified in nature (**Figure 15**) : D-abequose (**51**) from *Salmonella abortus equi*[44], D-tyvelose (**49**) from *Salmonella typhi*[45], D-paratose (**53**) from *Salmonella paratyphi*[46] and L-colitose (**50**) from *Salmonella enterica O35*[46b] while L-ascarylose (**48**), also detected in *Yersinia pseudotuberculosis*, was first found in the eggs of the parasitic nematode *Ascaris lumbricoides* and L-paratose (**52**) in the *Pristonchius pacificus* exometabolome[12b].

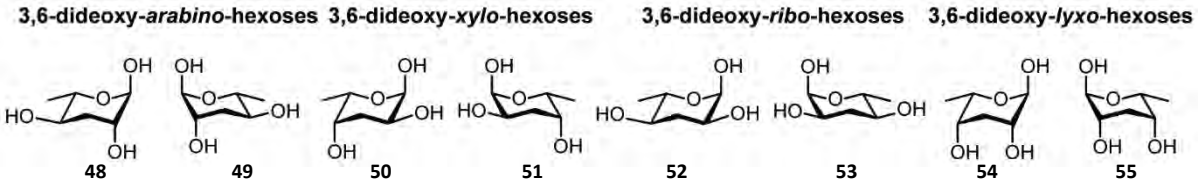

Figure 15 : Eight possible isomers of 3,6-dideoxyaldohexose.

Because of their considerable biological significance, there has been a wide interest in the synthesis of the 3,6-dideoxysugars[42a, 47].For the ascarylose sugar, a number of multi-step synthesis have been reported, usually following a traditional protection/deprotection pathway from the commercially available L-rhamnose[41, 47c, 48] but also more recently from smaller achiral precursors via a C-C bond forming strategy[49] (**Figure 16**).

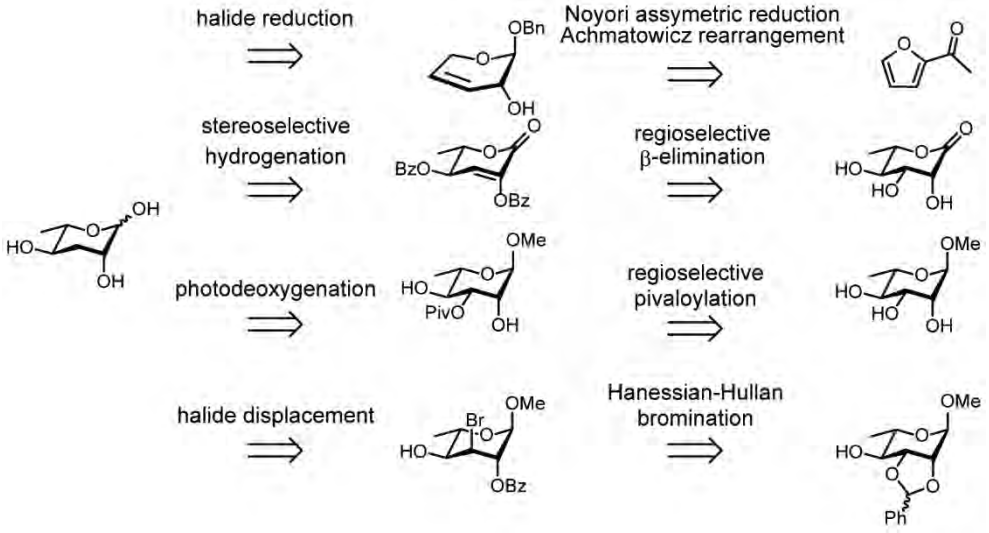

Figure 16 : Some of the different reported strategies to access the ascarylose sugar.

In 1977, Florent *et al*. described the conversion of L-rhamnose into the 3,6-dideoxysugar ascarylose[41]. The reaction proceeded via the lithium aluminum hydride reduction of the 1-*O*-methyl-2-*O*-benzoyl-3-bromo-3,6-dideoxy-altro-hexose **58** generated via benzylidene ring opening under Hanessian-Hullar conditions. The resulting 1-*O*-methyl-ascaroside was then hydrolyzed under acidic conditions to give the L-ascarylose sugar **48**.

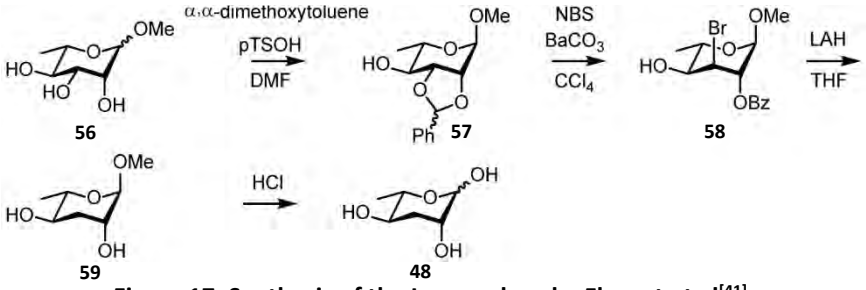

Figure 17: Synthesis of the L-ascarylose by Florent et al[41].

Alternatively, Varela *et al*. provided another synthesis of **48** from the L-rhamno-1,5-lactone **60** generated by oxidation of L-rhamnose with bromine[48, 50]. The C3-deoxygenation was accomplished by stereoselective hydrogenation of the 2-enolactone **61**, obtained by benzoylation under conditions that favor β-elimination. In this synthesis Varela *et al*. introduced the 2,4-di-*O*-benzoyl ascarylose **63**, which was later used by Jeong *et al.* in the first synthesis of asc-C7 (ascr#1, daumone 1, **1**)[18].

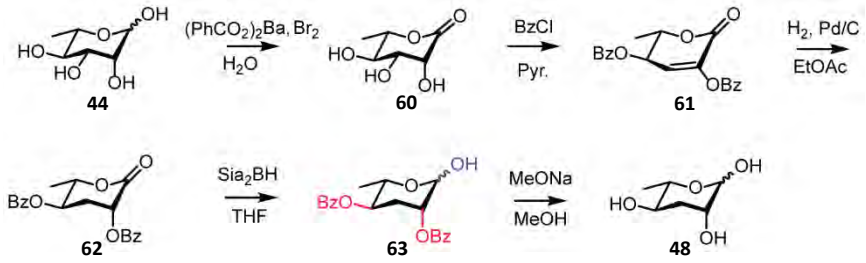

Figure 18: Synthesis of the L-ascarylose by Varela et al. [48].

Until recently, most of the ascarosides were synthesized from the 2,4-di-*O*-benzoyl ascarylose building block **63**, which allows the synthesis of α-configured basic ascarosides with high selectivity due to the anchimeric assistance provided by the benzoyl ester at the 2-position[18, 27, 51]. However, since the discovery of modular ascarosides that incorporate additional moieties attached to the sugar unit, orthogonally protected ascarylose building blocks are highly desired. Traditionally the synthesis of modular ascarosides from **63** always resulted in the formation of a mixture of 4- and 2- substituted ascarosides, as well as 2,4-disubstituted ascarosides, which required tedious chromatographic separation and diminished the yield of the reaction[9b, c, 10]. Therefore, efforts were made to synthesize an orthogonally protected ascarylose building block that facilitates the selective synthesis of modular

ascarosides[40, 52]. This chapter reports on the different synthetic strategies currently used to synthesize 2,4-di-*O*-benzoyl- and orthogonally protected ascarylose building blocks.

2.1. Synthesis of 2,4-di-*O*-benzoyl ascarylose

2.1.1. Via stereoselective hydrogenation

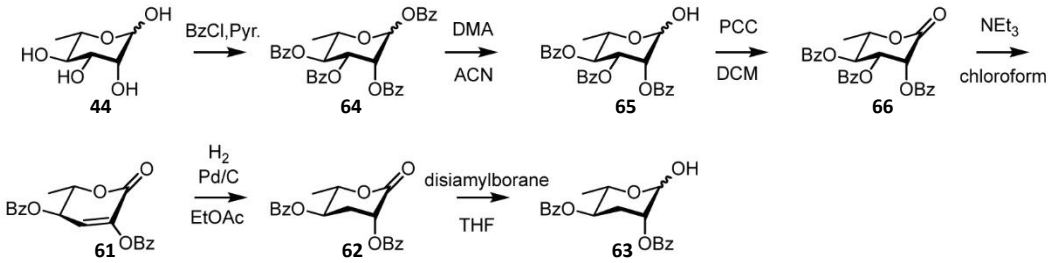

Figure 19: Jeong's synthesis of L-2,4-di-*O*-benzoyl ascarylose[18].

An improved synthesis of the 2,4-di-*O*-benzoyl-ascarylose **63** used to synthesize simple ascarosides was utilized by Jeong *et al.* **Figure 19**[18] based on the work of Varela *et al*[48]. This synthetic strategy was also employed in this project to generate basic ascarosides like the starter unit of the oligomeric asc-C5 (**Chapter 6**). The ascarylose building block was obtained in six steps from the commercially available L-rhamnose (**44**) with an overall yield of 13% via stereoselective hydrogenation of 2,4-di-*O*-benzoyl-2-enol-lactone (**61**) prepared by oxidation of 2,3,4-tri-*O*-benzoyl-ascarylose **65** followed by a regioselective β-elimination of the 3-*O*-benzoyl group. First, the L-rhamnose (**44**) was fully benzoylated under basic condition with benzoyl chloride to give a 1/1 mixture of α- and β-isomers **64**. Then, the anomeric position was selectively deprotected using dimethylamine to afford compound **65**, which was oxidized to the lactone **66**. **66** was converted to the enol-lactone **61** in excellent yield (94%) by base-catalyzed β-elimination of the 3-*O*-benzoyl group using an excess of triethylamine in chloroform.

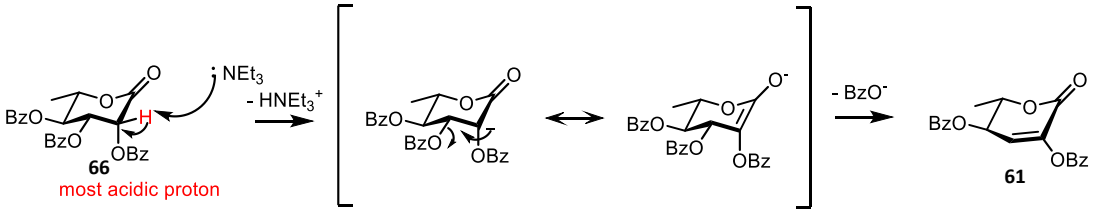

Figure 20: Regioselective β-elimination of the 2,3,4-tri-O-benzoyl lactone 66.

The reaction proceeds via an $E1_cB$ mechanism, in which the carbanion initially generated at the 2-position is stabilized by resonance thus inducing selectively a β-elimination of the 3-*O*-benzoyl group

(**Figure 20**)[48, 63]. No additional elimination products were isolated. Subsequently, the eno-lactone was stereo-selectively hydrogenated to the dibenzoyl lactone **62**. The high stereoselectivity of the hydrogenation may be due to the distorted chair conformation adopted by the α, β-unsaturated lactone **61** . The conformation of **61** was confirmed by ^{1}H NMR. The coupling constant $^{3}J_{4,3}$= 4.8 Hz between the 4- and the 3-position suggested a dihedral angle of circa 45° according to Garbisch equations[64]. Similarly, the coupling constant $^{3}J_{4,5}$= 4.6 Hz between the 4- and the 5-position was more consistent with a quasi-diequatorial interaction. This hypothesis was further supported by the long-range coupling between the 3- and the 5-position ($^{4}J_{3,5}$= 0.8 Hz) suggesting a W-arrangement between the two protons.

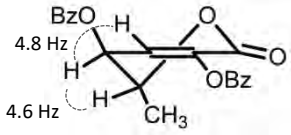

Figure 21 . Conformation of the 2,4-di-*O*-benzoyl-2-enol-lactone 61.

In this conformation, the steric hindrance exerted by the quasi-axial methyl group at the 5-position [65] would prevent the binding to the catalyst from underneath the sugar (**Figure 22**), therefore generating preferentially the 2,4-di-*O*-benzoyl-3,6-dideoxy-*arabino*-hexono-1,5-lactone **62** (ratio of 7/1). **62** was finally reduced selectively with *in situ* generated disiamylborane to afford the 2,4-di-*O*-benzoyl ascarylose **63**[66].

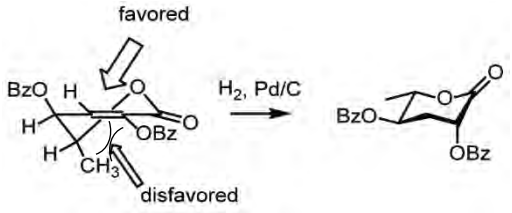

Figure 22: Regioselective hydrogenation of the eno-lactone 62.

2.1.2. Via regioselective functionalization

Recently, Curtis *et al.* has reported a shorter synthesis for **63**[67] in which methyl-L-rhamnoside **56** is tosylated at the 3-position by organotin-catalyzed regioselective tosylation[68] followed by nucleophilic substitution (**Figure 24**) based on Martinelli's work[69].

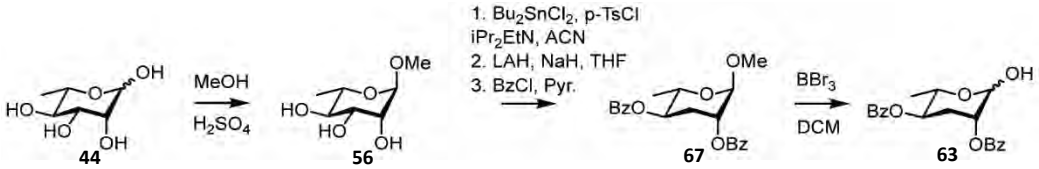

Figure 23: Curtis synthesis of the 2,4-di-*O*-benzoyl ascarylose[67].

In this procedure, the methyl rhamnoside **56** reacts with dibutyltinchloride and tosyl chloride under basic conditions to afford selectively the 1-*O*-methyl-3-*O*-tosyl-ascaroside. The regioselectivity for the cleavage of the equatorial 3-position in the organotin-mediated protection is enhanced by the stereoelectronic effects of the methyl rhamnoside **56**. For cis-diols, the transition state with the equatorial SnO bond is higher in energy than the transition state with the axial SnO bond which leads to the formation of the anion at the 3-position, which attacks the electrophilic tosyl chloride (**Figure 24**)[69-70].

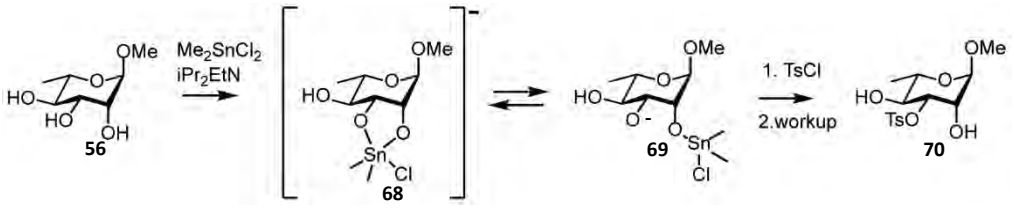

Figure 24: Organotin catalyzed selective protection of the 3-position.

Next, the resulting 1-*O*-methyl-3-*O*-tosyl-ascaroside (**70**) is converted to the 1-*O*-methyl-2,4-di-*O*-benzoyl-ascaroside **67** upon treatment with sodium hydride (NaH) and lithium aluminum hydride (LAH) followed by benzoylation with benzoyl chloride in pyridine. Subsequent demethylation with boron tribromide provided the 2,4-di-*O*-benzoyl-ascarylose **63** (**Figure 23**). This new synthetic strategy provides the desired ascarylose building block with high selectivity in 45% yield. However, the reductive desulfonylation of **70** often leads to the formation of **74** via the ring contraction of the 1-*O*-methyl-3-*O*-tosyl-rhamnoside (**Figure 25**)[71].

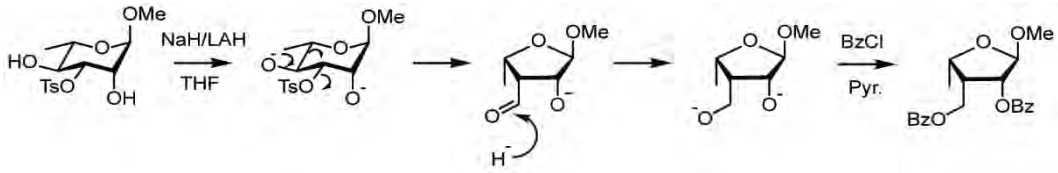

Figure 25: Product from the rearrangement of the 1-*O*-methyl-3-*O*-tosyl-rhamnoside.

Alternatively, Muramatsu et al. developed an organotin catalyzed regioselective thionylation for non-protected sugars that utilizes the selective transformation of the 3-position of the methyl-L-rhamnose **56**[68]. The resulting 1-*O*-methyl-3-*O*-phenyloxythiocarbonyl-rhamnoside (**75**) could subsequently be reduced to the corresponding ascarylose via Barton McCombie deoxygenation. Using Muramatsu's procedure, the 2,4-di-*O*-benzoyl ascarylose (**63**) could be obtained in four steps from L-rhamnose with an overall yield of 18% as described in **Figure 26.** The methyl-rhamnoside was converted to the 1-*O*-methyl-3-*O*-phenyloxythiocarbonyl-rhamnoside **75** in 82% yield by regioselective thionylation, and

then converted to the 1-*O*-methyl-2,4-di-*O*-benzoyl-ascaroside **67** via Barton McCombie deoxygenation with tritbutyltin hydride and azobisisobutyronitrile (AIBN) followed by dibenzoylation with pyridine in one step with an overall yield of 49%. Subsequent demethylation with boron tribromide would yield the dibenzoyl ascarylose.

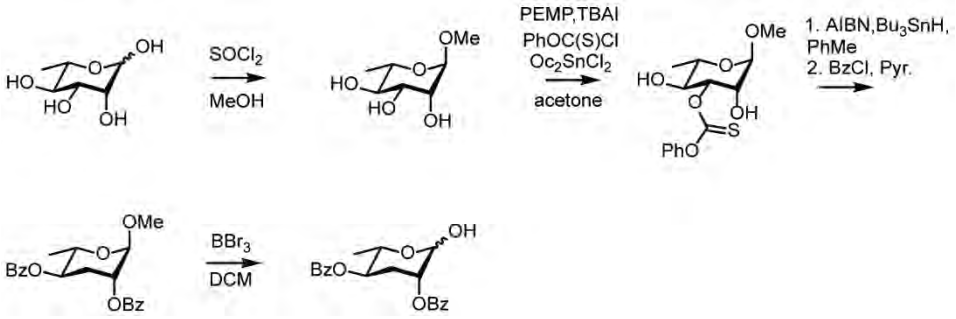

Figure 26: Synthesis of the 2,4-di-*O*-benzoyl ascarylose via Muramatsu strategy[68].

The Muramatsu and Curtis strategies significantly improved the synthesis of the 2,4-di-benzoyl ascarylose building block. However, these strategies are ill-suited for the selective attachment of additional moiety to either the 2- or the 4-position.

2.2. Synthesis of orthogonally protected ascaryloses

2.2.1. Via sulfate ring opening

In 2017, Zhang et al introduced a novel orthogonally protected ascaroside building block, the 2-*O*-benzoyl-4-*O*-*tert*-butyldiphenylsilyl-ascarylose **45**[40], obtained in seven steps with an overall yield of 33% via an S_N2 reductive opening of a cyclic sulfate derived from L-rhamnose **44**[47d, 72]. This building block provides an easier access to 4- and 2-substituted ascarosides. For example, 4'-IC-asc-C5 (icas#9, **13**, **Figure 6**) was synthesized in 15% of yield from the 2-*O*-Bz-4-*O*-TBDPS-ascarylose **45** instead of 9.5% of yield from the 2,4-di-*O*-benzoyl ascarylose **63**[27]. The orthogonally protected ascarylose was used in this work for the synthesis of the modular ascarosides **34-38** (**Chapter 3 & 4**) and to build the oligomeric ascarosides **40-43** (**Chapter 6**).

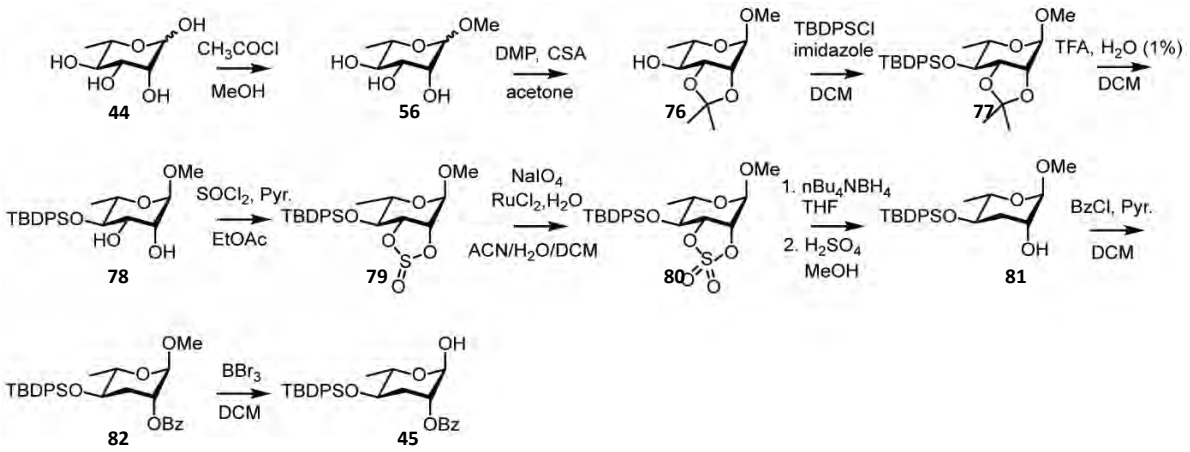

Figure 27 : Synthesis of 2-O-Bz-4-*O*-TBPDS-ascarylose[40].

The 2-*O*-benzoyl-4-*O*-*tert*-butyldiphenylsilyl-ascarylose **45** was synthesized in 9 steps with an overall yield of 12% (**Figure 27**) according to the literature[40]. The anomeric position was methylated via acid catalyzed Fischer glycosylation in methanol to give the 1-*O*-methyl-rhamnoside **56** as a 7:1 mixture of the α- and the β-isomer[73], which was treated with 2,2-dimethoxypropane to afford the 1-*O*-methyl-2,3-*O*-isopropylidene-rhamnoside **76**. Next, the authors reported the formation of the 1-*O*-methyl-4-*O*-TBDPS-rhamnoside **78** in 99% by treatment of **76** with *tert*-butyldiphenylsilyl chloride in *N,N*-dimethylformamide[40]. However, this procedure only provided a 1/1 mixture of 1-*O*-methyl-4-*O*-*tert*-butyldiphenylsilyl-rhamnoside **78** and 1-*O*-methyl-rhamnoside **56** after flash column chromatography. Therefore, the 1-*O*-methyl-4-*O*-TBDPS-rhamnoside **78** was prepared in two steps by TBDPS protection of **76** followed by deacetonation with trifluoroacetic acid (TFA)[74]. Treatment of **78** with thionyl chloride then gave a diastereomeric mixture of cyclic sulfites **79**, which, upon ruthenate catalyzed oxidation, gave the cyclic sulfate **80**.

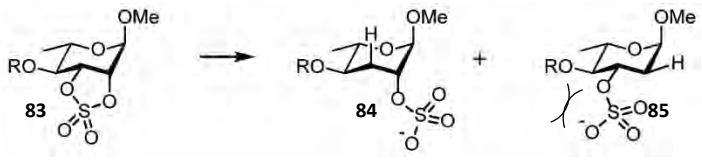

Figure 28: The selective cleavage of the cyclic sulfate is influenced by the nature of the protecting group at 4-position.

The deoxygenation of compound **80** by tetrabutylammonium borohydride followed by the hydrolysis of the sulfate group with sulfuric acid subsequently provided the diaxial (3-deoxy) and the diequatorial (2-deoxy) product with a ratio of respectively 12 to 1 following the Fürst-Plattner rule[75]. Moreover, the regioselectivity for the desired 3-deoxy product was also influenced by the nature of the protecting group at the 4-position (**Figure 28**), most likely due to steric and polar interactions between the

generated sulfate anion and the protecting group. When the bulky TBDPS group was replaced with the smaller TBDMS group, a diminution of regioselectivity was observed during the nucleophilic substitution (**Figure 29**). Lower regioselectivity was also described in the literature with the 4-*O*-PMB ascaroside[40]. The resulting ascaroside **81** was subsequently benzoylated under basic conditions and the anomeric position demethylated with boron tribromide to afford the ascarylose **50** as a 4 to 1 mixture of the α:β anomers.

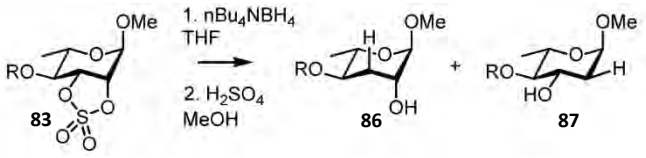

R	86	87
TBDPS	12	1
TBDMS	2	1
PMB[40]	6	1

Figure 29 : Selectivity for the reductive cyclic sulfate opening depends on the protecting group at the 4-position.

The 2-*O*-Bz-4-*O*-TBDPS-ascarylose building block **45** allowed the synthesis of the species-specific ascarosides for this project with good yield. However, this synthetic pathway is limited by a large number of synthetic steps, expensive reagents and a lack of versatility regarding the nature of the protecting group at the 4-position.

2.2.2. Via benzylidene ring opening

To improve the synthesis of the orthogonally protected ascarylose unit and to extend the synthesis to building blocks with a different protecting group at the 4-position, Florent's approach[41] was explored. When Florent et al. synthesized ascarylose via benzylidene ring opening (**Figure 17**), they obtained 1-*O*-methyl-2-*O*-benzoyl-3-bromo-3,6-dideoxy-*altro*-hexose **58** with the 2-position already protected as a benzoyl ester, which is crucial in order to obtain high α-selectivity during the glycosylation step. The 3-bromo intermediate **58** was easily reducible by catalytic hydrogenation under alkaline condition to furnish the 1-*O*-methyl-2-*O*-benzoyl-ascaroside **88** as described by Bundle et al (**Figure 30**)[53]. However, Florent's synthesis utilized carbon tetrachloride, an ozone depleting solvent[54], for the Hanessian-Hullar bromination, which needed to be substituted.

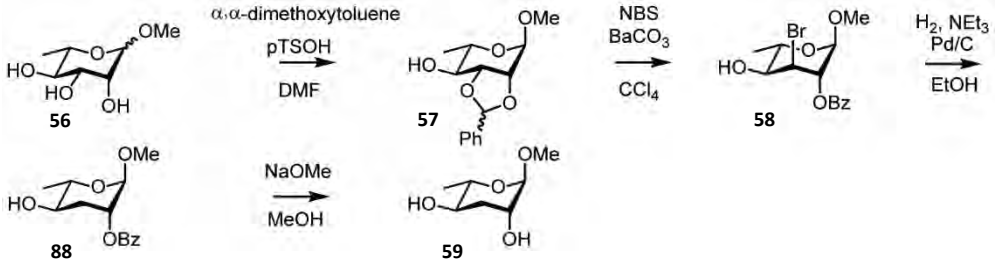

Figure 30: Synthesis of the 1-*O*-methyl-ascarylose by Bundle et al [53].

Nowadays, acetonitrile has proven to be a suitable solvent for bromination reactions with *N*-bromosuccinimide[55] and therefore can be used instead of carbon tetrachloride for the synthesis of the 1-*O*-methyl-2-*O*-benzoyl-3-bromo-3,6-dideoxy-*altro*-hexose **58**. After reduction of **58**, the resulting 1-*O*-methyl-2-*O*-benzoyl-ascaroside building block **88** provides an easy access to a wide range of 4-protected methyl ascarosides without affecting the selectivity of the deoxygenation (**Figure 30**).

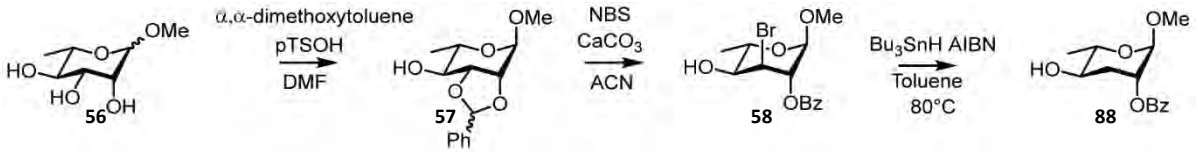

Figure 31: A versatile synthesis of orthogonally protected ascarylose based on Florent's work.

The 1-*O*-methyl-2-*O*-benzoyl-ascaroside **88** was synthesized in three steps via *trans* benzylidene ring opening from the 1-*O*-methyl-α-L-rhamnoside (**56**) (**Figure 31**). The 1-*O*-methyl-2,3-*O*-benzylidene rhamnoside **57** was obtained by acetalization of the 2- and the 3-position of **56** with α,α-dimethoxytoluene to give **57** as a 1 : 1 diastereomeric mixture of benzylidene acetals. Then, the *N*-bromosuccinimide mediated regio-selective fragmentation of the benzylidene acetals **57** gave the 1-*O*-methyl-2-*O*-benzoyl-3-bromo-3,6-dideoxy-*altro*-hexose **58**. The reaction proceeds via a Wohl-Ziegler bromination (**Figure 32**) by abstraction of a hydrogen radical from the acetal to form a bromoacetal **90**. Upon the departure of the bromine, a cyclic carbocation **91** is formed, which will subsequently be opened by a bromine anion via an S_N2 pathway characterized by the inversion of configuration at the 3-position (**Figure 32**).

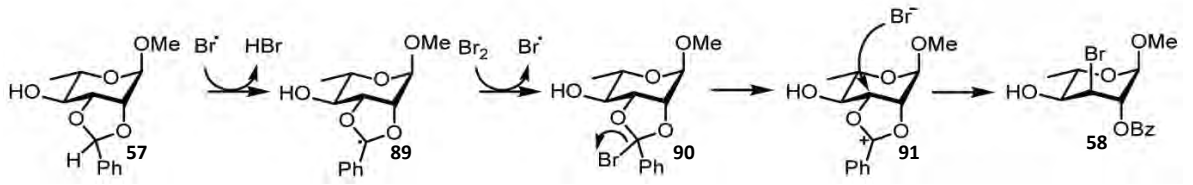

Figure 32 : Mechanism of the Hanessian-Hullar reaction.

In contrast to the original procedure the barium carbonate was replaced with calcium carbonate[56] without affecting the yield of the reactions. Next, to debrominate the intermediate **58** without hydrolyzing the benzoyl ester, three different approaches from the literature were considered (**Figure 33**): radical dehalogenation with tributyltin hydride (method A)[47b], reduction with nickel borohydride generated *in situ* from nickel chloride and sodium borohydride (method B)[47b] and catalytic hydrogenation with palladium under basic conditions (method C) [53].

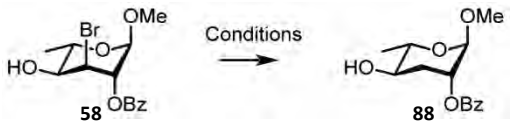

Method	Conditions	Yield (%)
A	Bu_3SnH, AIBN in toluene, 80 °C	92
B	$NaBH_4$, $NiCl_2$,$6H_2O$ in EtOH	77
C	H_2 Pd/C, NEt_3 in EtOH	79

Figure 33 : The different conditions tested for the debromination of 88.

The three methods afforded the methyl 2-*O*-benzoyl-ascaroside **88** with good to excellent yields (**Figure 37**). However, the radical dehalogenation with tributyltin hydride[47b] provided cleaner product in higher yield (92%) after column chromatography and did not require any specific work-up.

To demonstrate the versality of this alternative strategy, five methyl ascarosides bearing different protecting group at the 4-position were synthesized: the 2-*O*-benzoyl-4-*O*-*tert*-butyldiphenylsilyl-ascarylose (**83**), the 2-*O*-benzoyl-4-*O*-benzyl-ascarylose (**92**), the 2-*O*-benzoyl-4-*O*-allyl-ascarylose (**93**), the 2-*O*-benzoyl-4-*O*-(4-methoxybenzyl)-ascarylose (**94**) and the 2-*O*-benzoyl-4-*O*-tert-butyldimethylsilyl-ascarylose (**95**). These five different methyl ascarosides were synthesized in good yield as summarized in **Figure 34**.

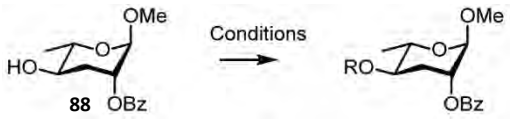

R	Conditions	Product	Yield (%)
TBDPS	TBDPSCl, imidazole, DCM	**82**	89
Bn[57]	Dudley's reagent, MgO, $PhCF_3$	**92**	82
Allyl[58]	*O*-Allyl-2,2,2-TCA, triflic acid, DCM/cyclohexane	**93**	67
PMB[59]	PMB-*O*-lepidine, CSA, DCM	**94**	79
TBDMS	TBDMSCl, Pyr., DCM	**95**	91

Figure 34 : Conditions for the different protection of the 4-position of 1-*O*-methyl-2-*O*-benzoyl-ascaroside.

Next, the 1-*O*-methyl-2-*O*-benzoyl-4-*O*-*tert*-butyldiphenylsilyl-ascaroside **82** was deprotected with boron tribromide as described in the previous section. However, the use of boron tribromide to demethylate the 1-*O*-methyl-2-*O*-benzoyl-4-*O*-benzyl-ascaroside **92** resulted in the loss of the benzyl ether instead of the methyl ether as benzylic and allylic ethers are more reactive to boron tribromide than alkyl ethers[60]. Therefore, the 1-*O*-methyl-2-*O*-benzoyl-4-*O*-benzyl-ascaroside **92** and the 1-*O*-methyl-2-*O*-benzoyl-4-*O*-allyl-ascaroside **93** were deprotected by acidic hydrolysis, with concentrated hydrochloric acid in acetic acid, in 78% and 86% of yield, respectively. The attempt to synthesize the 2-*O*-benzoyl-4-*O*-(4-methoxybenzyl)-ascarylose was unsuccessful because the PMB protecting group was too sensitive towards acidic conditions and was cleaved prior to the anomeric methyl ether during

BBr_3 methylation. The same results were obtained for the 2-*O*-benzoyl-4-*O*-(*tert*-butyldimethylsilyl)-ascarylose.

Furthermore, another interesting synthesis of orthogonally protected ascarylose was recently reported by Ning et al.[52]. This new approach uses a combination of selective orthogonal protection and Barton McCombie deoxygenation to synthesize in five steps a protected *p*-thiocresol-ascaroside building block **100** (**Figure 35**) instead of the usual protected ascarylose[52]. The synthesis proceeded by a one-pot acetylation/thionylation reaction to give the 1-*p*-thiocresol-2,3,4-*O*-triacetyl-rhamnoside **96** (**Figure 36**)[61], which, upon alkaline hydrolysis with triethylamine, gives the rhamnoside **97**. Next, a one-pot orthoester formation/benzylation/regioselective hydrolysis furnished the 1-*p*-thiocresol-2-*O*-acetyl-4-*O*-benzyl-rhamnoside **98**[62], which, after thiocarbonylation of the 3-position followed by Barton McCombie deoxygenation, provides the 1-*p*-thiocresol-2-*O*-acetyl-4-*O*-benzyl-ascaroside building block **100**.

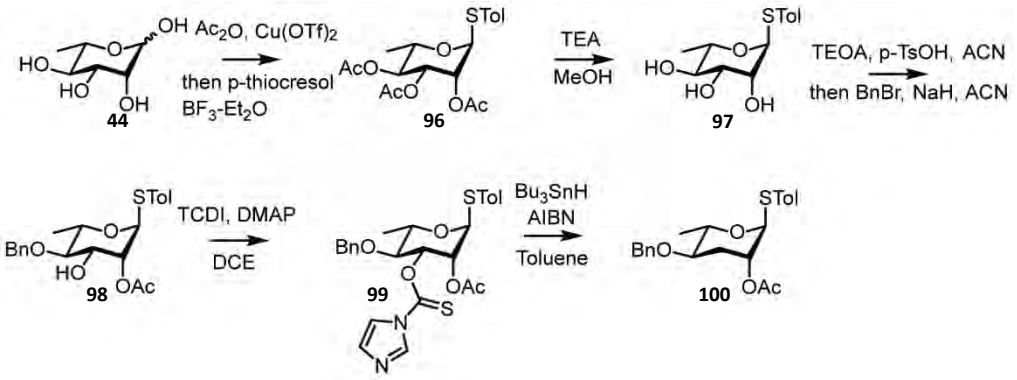

Figure 35 : Ning's synthesis of 1-*p*-thiocresol-2-*O*-acetyl-4-*O*-benzyl-ascarylose 100[52].

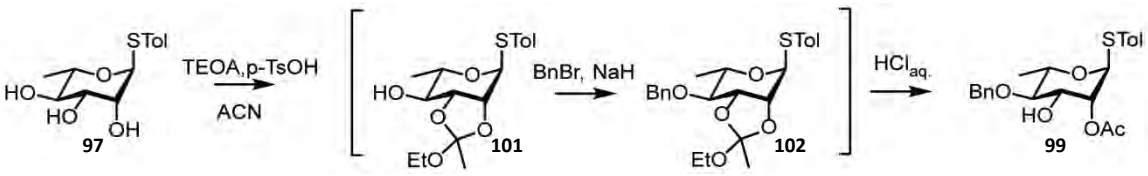

Figure 36 : One-pot orthoester formation/benzylation[61].

This strategy represents the first synthesis of ascarosides via a *p*-thiocresol protected ascaroside building block and represent a good alternative to the two-step Schmidt glycosylation via trichloroacetimidates or the BF_3 catalyzed glycosylation commonly utilized. The authors reported similar yields and selectivities for the glycosylation of standard side chains as procedures based on the 2,4-di-*O*-benzoyl ascarylose **63** or the 2-*O*-benzoyl-4-*O*-*tert*-butyldiphenylsilyl-ascarylose **45** building blocks[52].

2.3. Conclusion

Four different ascarylose building blocks were synthesized: the 2,4-di-*O*-benzoyl ascarylose **63** for the synthesis of basic ascarosides and three 4-*O*-protected 2-*O*-benzoyl-ascaryloses (**45**-**47**) for the synthesis of modular ascarosides. Different methods to synthesize these building blocks from L-rhamnose were utilized (**Figure 37** & **Figure 38**).

The 2,4-di-*O*-benzoyl-ascarylose was synthesized in six steps as described by Jeong *et al.*[18] with an overall yield of 13%. A shorter alternative based on regioselective tin catalyzed protection/Barton Mc Combie deoxygenation of methyl rhamnose was also explored. The new synthetic route provided the dibenzoyl ascarylose in four steps with an overall yield of 18% (**Figure 37**).

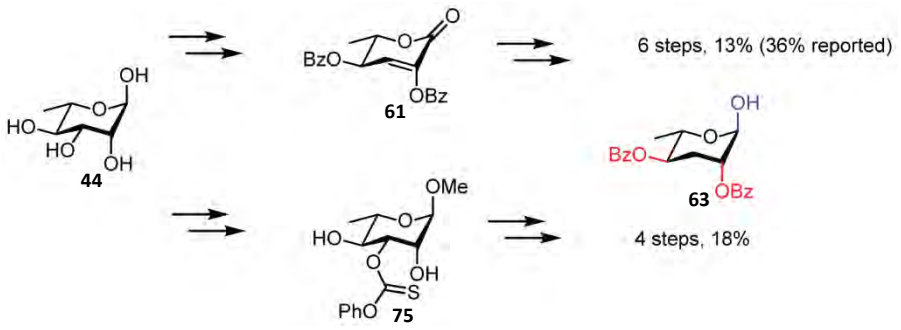

Figure 37 : Different strategies toward the synthesis of the 2,4-di-*O*-benzoyl ascarylose building block 63.

The 2-*O*-benzoy-4-*O*-tert-butyldiphenylsilyl-ascarylose was obtained via sulfate ring opening in nine steps with an overall yield of 12% instead of seven steps as reported by Zhang *et al*.[40] (**Figure 38**). A shorter and more versatile synthesis of orthogonally protected ascarylose building blocks via benzylidene ring opening was developed. This alternative synthesis is based on Hanessian-Hullard benzylidene ring opening and provided the 2-*O*-benzoyl-4-*O*-*tert*-butyldiphenylsilyl-ascarylose (**45**) in six steps with an overall yield of 40% (**Figure 38**). Additionally, the 4-*O*-allyl- (**47**) and 4-*O*-benzyl- (**46**) 2-*O*-benzoyl-ascarylose building blocks could be readily obtained via this new pathway with an overall yield of 33% and 38%, respectively (**Figure 38**). Taken together, these results demonstrate the versatility of the benzylidene route as it provides orthogonally protected ascarosides with high selectivity and good yield and is not limited to the sole synthesis of the 4-*O*-TBDPS protected ascarylose building block.

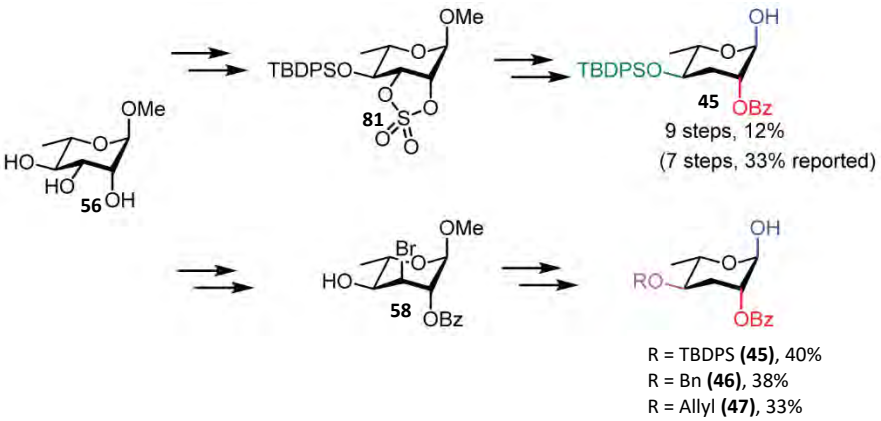

Figure 38 : Different strategies toward the synthesis of orthogonally protected ascarylose building blocks.

3. The urocanic acid ascarosides (ucas)

3.1. Identification of urocanic acid ascarosides

Using the HPLC-ESI-(-)-MS/MS precursor ion screen for *m/z* = 73, a new class of modular ascarosides was detected in the *C. remanei* exometabolome by C. Dong[39]. The most dominating representative exhibits a *m/z* of 421.1982 $[M - H]^-$ for a molecular formula of $C_{21}H_{30}N_2O_7$ with the unusual presence of two nitrogen atoms. The presence of the fragment ion at *m/z* = 301.1657 $[C_{15}H_{25}O_6]^-$ upon HPLC-ESI-(-)-HR-MS/MS suggests the presence of an asc-ΔC9 (**3**) derivative (**Figure 39.A & C**). Moreover, the analysis of the MS/MS fragmentation of the target compound on HPLC-ESI-(+)-HR-MS/MS showed a fragment with a *m/z* of 251.1026 for a molecular formula of $[C_{12}H_{31}N_2O_4]^+$ from the loss of the side chain and a second fragment with a m/z of 139.0502 for a molecular formula of $[C_6H_7N_2O_2]^+$ from the loss of the ascarylose unit, thus, suggesting a urocanic acid moiety attached to the ascaroside (**Figure 39.B & C**).

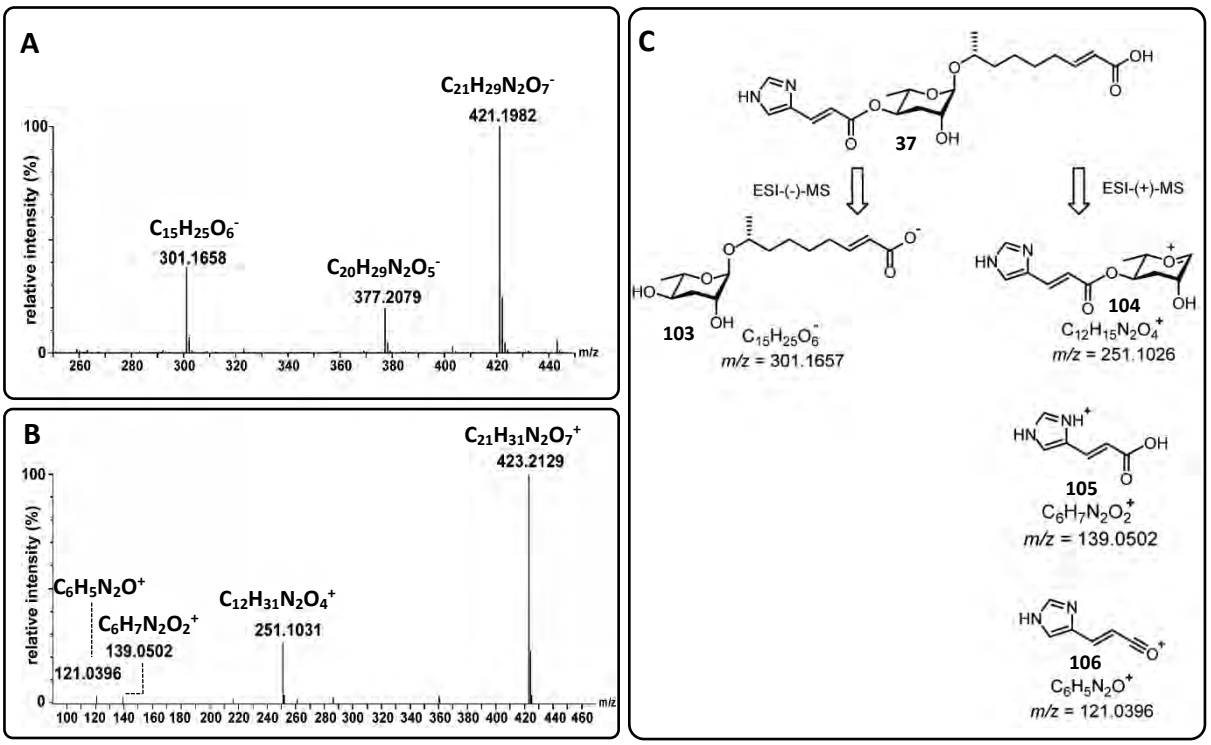

Figure 39: HPLC-ESI-HR-MS/MS spectrum of 4'-UC-asc-ΔC9 (37) from *C. remanei* in (A) negative and (B) positive mode. (C) MS/MS fragmentation of 4'-UC-asc-ΔC9 (37).

The compound was isolated by Dong from the *C. remanei* exometabolome extract using a combination of reverse phase C18 SPE fractionation and semipreparative HPLC and further characterized by one and two-dimensional NMR (**Figure S1 & S2**) and HR-MS/MS (**Figure 39.A & B**)[39]. The ^{1}H NMR and *dqf*-COSY spectra confirmed the presence of a ΔC9 side chain (two vinylic proton at δ_H= 5.84 ppm (*d*, $^3J_{2,3}$ = 15.5 Hz) and 6.82 ppm (*ddd* $^3J_{3,2}$ = 15.5 Hz, $^3J_{3,4a}$ = 6.8 Hz, $^3J_{3,4b}$ = 7.0 Hz) (**Figure 40.A & B**) and the

additional doublet corresponding to a methyl group at δ_H=1.15 ppm ($^3J_{9,8}$ = 6.1 Hz, **Figure 40.B**) indicated that the side chain is (ω-1)-linked to the ascarylose moiety. Moreover, the presence of four sets of ^{1}H NMR signals at δ_H= 6.43, 7.60, 7.79 and 7.44 ppm confirmed the presence of an urocanic acid group attached to the asc-ΔC9 and the coupling constant between the two vinylic protons ($^3J_{1'',2''}$= 15.9 Hz) indicated a (*E*)-configured urocanate (**Figure 40**). Furthermore, the downfield shift of the proton with *ddd* multiplicity at δ_H= 4.95 ppm, characteristic for the 4'-position, indicated that the urocanate unit is attached at the 4'-position of the asc-ΔC9 (**Figure 40.A & B**).

A

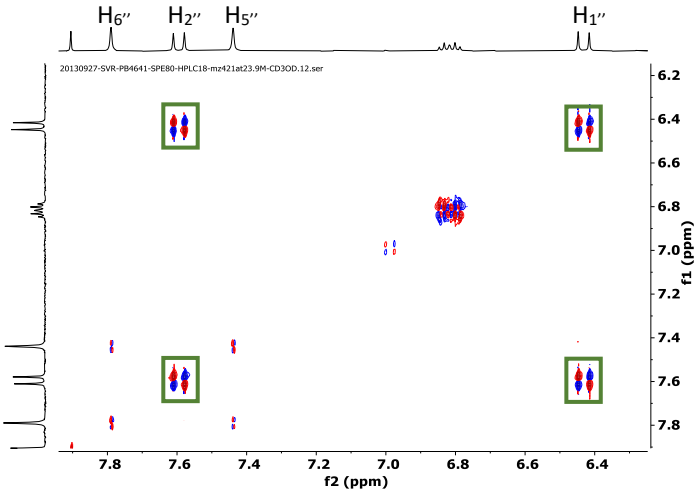

B

H	isolated 4'-UC-asc-ΔC9[39]
1'	4.71 *br.s*
2'	3.74 *br.s* (2.2)
3'ax	1.89 *ddd* (12.9, 11.6, 6.9)
3'eq	2.10 *ddd* (12.9, 6.8, 4.8)
4'	4.95 *ddd* (11.6, 9.4, 4.8)
5'	3.91 *dq* (9.4, 6.3)
6'	1.16 *d* (6.3)
1	-
2	5.84 *d* (15.5)
3	6.82 *ddd* (15.5, 6.8, 7.0)
4a	2.22 *m* (6.9)
4b	2.25 *m* (6.7)
5	1.52 *m*
6	1.53 *m*
7	1.58 *m*
8	3.82 *m*
9	1.15 *d* (6.1)
1''	-
2''	6.43 *d* (15.9)
3''	7.60 *dd* (15.9, 1.6)
4''	-
5''	7.79 *dd* (1.9, 1.6)
6''	7.44 *s*

C

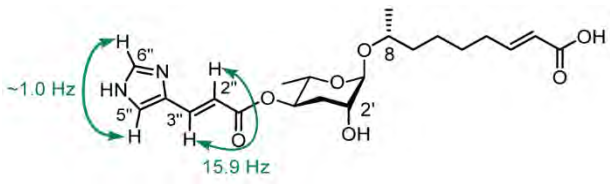

Figure 40: (A) Section of the 400 MHz *dqf*-COSY spectrum of (*E*)-4'-UC-asc-ΔC9 (37) isolated from the *C. remanei*'s exometabolome (B) 400 MHz ^{1}H NMR data of the isolated (*E*)-4'-UC-asc-ΔC9 (37) (in CD_3OD) [39]. (C) Structure of (*E*)-4'-UC-asc-ΔC9.

Targeted ESI-(+)-MS/MS screening of nematode exometabolome extracts using the specific fragment *m/z* 251.1026 revealed that 4'-UC-asc-ΔC9 (ucas#3, **37**) is part of a homologous series of urocanic acid substituted ascarosides. Moreover, the targeted ESI-(+)-MS/MS screen of sixteen *Caenorhabditis* species showed that these urocanic acid ascarosides are species-specific with only five *Caenorhabditis* species producing urocanate ascarosides (**Figure 41.C**) [39]. Trace quantities were also detected in the model organism *C. elegans*. The extracted ion chromatogram also showed that the profiles of urocanate ascarosides is highly species-specific. While the composition of urocanate derivatives in *C. brenneri* PB2801, *C. remanei* PB4641, and *C. wallacei* JU1904 is dominated by 4'-UC-asc-ΔC9 (**37**) and

4’-UC-asc-C9 (ucas#10, **101**), the hermaphroditic *C. briggsae* AF16 produces predominantly 4’-UC-asc-C6MK (ucas#2, **35**).

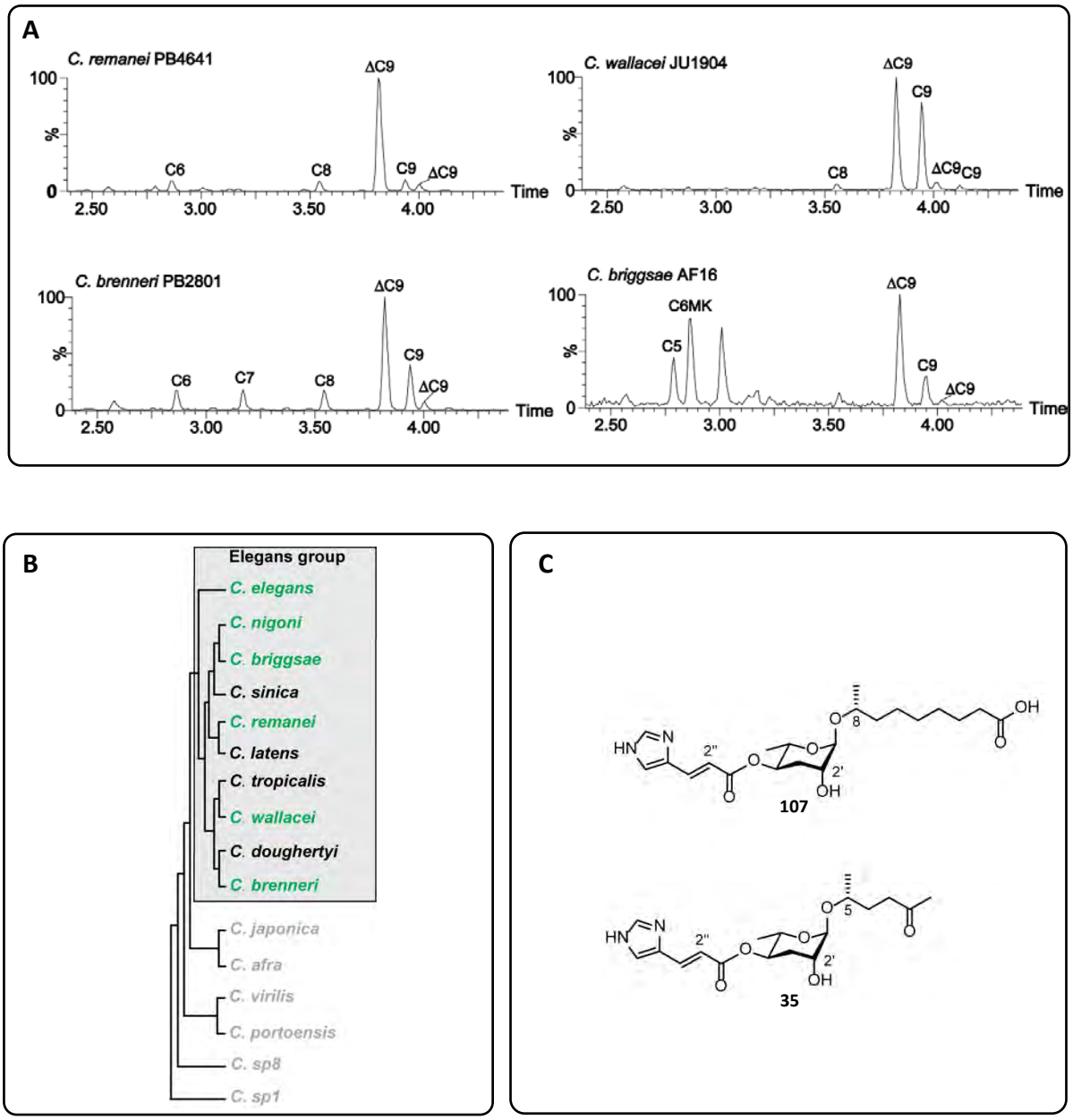

Figure 41: (A) ESI-(+)-MS/MS screen of the *C. remanei, C. wallacei, C. brenneri* and *C. briggsae* metabolome for m/z 251.1026 $[C_{12}H_{15}N_2O_4]^+$. (B) Phylogenetic tree of analyzed Caenorhabditis species. The nematode species producing urocanic ascarosides are marked in green. (C) Structure of 4’-UC-asc-C9 (107) and 4’-UC-asc-C6MK (35).

Furthermore, the HPLC-MS chromatograms of enriched nematode metabolome fractions measured in both positive and negative mode showed that each urocanate ascaroside is accompanied by an additional compound with a distinct retention time and the same molecular formula suggesting the

presence of isomers. The isomeric compound of 4'-UC-asc-ΔC9 (**37**) was enriched from the *C. remanei* exometabolome extract and the fraction containing the additional compound analyzed by NMR spectroscopy (**Figure S3 & S4**). Like the *E*-urocanate substituted 4'-UC-asc-ΔC9 (**37**), the ^{1}H NMR and the *dqf*-COSY spectra showed the presence of an *E*-configured asc-ΔC9 coupled to an urocanate unit at the 4'-position. However, the olefinic protons of the urocanate unit exhibited a coupling constant of *J* = 12.8 Hz, instead of *J* = 15.9 Hz for the (*E*)-4'-UC-asc-ΔC9, which is consistent with a (*Z*)-configured double bond, suggesting that the additional compound represents the (*Z*)-isomeric (*Z*)-4'-UC-asc-ΔC9 (**38**) (**Figure 42**, **Figure S4 & S5**).

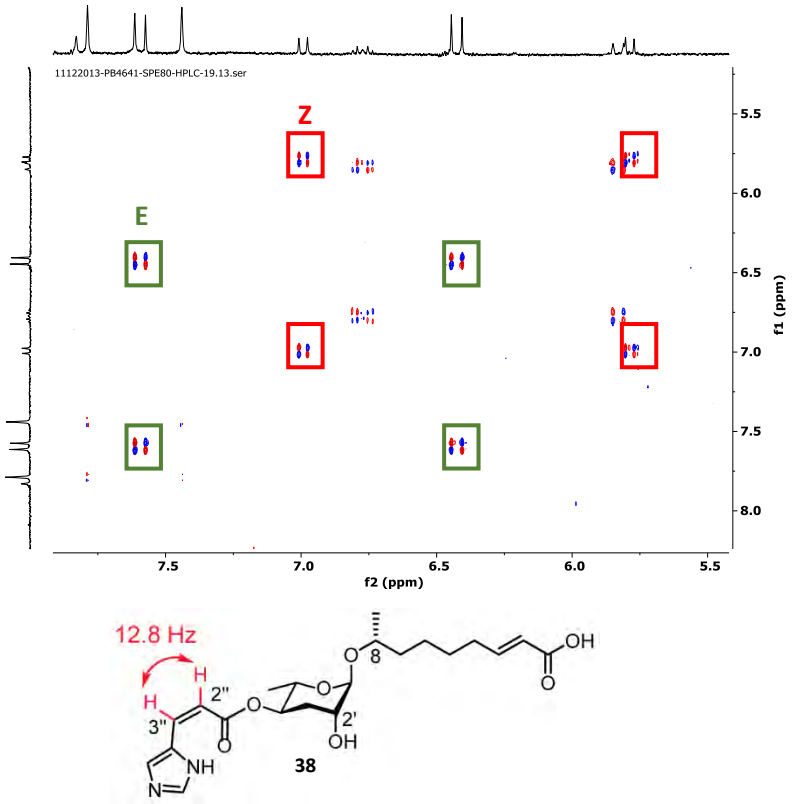

Figure 42: Section of the 400 MHz *dqf*-COSY spectrum of a mixture of (*E*)-4'-UC-asc-ΔC9 (37) and (*Z*)-4'-UC-asc-ΔC9 (38) enriched from the *C. remanei* exometabolome.

To confirm the structure assignment of these new ascarosides and to study their biological activities, the (*E*) and (*Z*)-isomers of two representative examples, the dominating 4'-UC-asc-ΔC9 (ucas#3, **37**) and 4'-UC-asc-C6MK (ucas#2, **35**) were synthesized.

3.2. Synthesis of 4'-UC-asc-ΔC9 (ucas#3) and 4'-UC-asc-C6MK (ucas#2)

Due to the photochromic properties of the urocanic acid and its related esters[76], reaction involving urocanic acid ascarosides had to be performed in an environment protected against UV light. Even if test reactions performed at night under laboratory illumination did not induce photoisomerization,

reaction were carried out in amber glass vials as it does efficiently protect from UV irradiation[77]. Moreover, due to the presence of the α/β-unsaturated carbonyl groups on both the aglycone and the urocanic acid, all types of protecting groups requiring cleavage by alkaline hydrolysis or hydrogenation had to be excluded. Therefore, a protecting group strategy that employs the 4-methoxybenzyl (PMB) moiety, easily cleavable under acidic conditions with trifluoroacetic acid or by mild oxidation with 2,3-dichloro-5,6-dicyanobenzoquinone (DDQ), was employed. Following the procedure previously described for the synthesis of 4'-MB-asc-ΔC9 (mbas#3, **16**)[40], (*R*)-octen-2-ol (**110**) was prepared by organocuprate-catalyzed ring opening of (*R*)-(+)-propylene oxide (**108**) using 6-bromo-1-hexene[18, 21] (**Figure 43**). The aglycone (**110**) was then glycosylated using Schmidt glycosylation[78] with the 4'-*O*-TBDPS-2'-*O*-benzoyl-ascarylose building block **45** in 67% yield. Next, the terminal alkenyl was further elongated via cross metathesis with ethyl acrylate and Grubbs 2nd generation catalyst to afford exclusively the thermodynamic product 2'-*O*-Bz-4'-*O*-TBDPS-asc-(*E*)-ΔC9-OEt **112**. Cleavage of both the ethyl and benzoyl ester under basic conditions with lithium hydroxide solution provided the 4'-*O*-TBDPS-asc-ΔC9 **113** which should subsequently be converted to the 2'-*O*-PMB-4'-*O*-TBDPS-asc-ΔC9-*O*-PMB ester (**114**) by reaction with 4-methoxybenzyl-trichloroacetimidate catalyzed by boron trifluoride as described by Zhang *et al.* in 2017[40] (**Figure 44**). Unfortunately, most of the starting material decomposed under these conditions and the small amount of resulting di-*O*-PMB protected ascaroside and PMB ester ascaroside was accompanied with PMB-related impurities (PMB-trichloro acetamide and uncharacterized material from the degradation of the PMB-trichloroacetimidate), which, despite repeated purification by flash column chromatography, could not be separated from the desired reaction product.

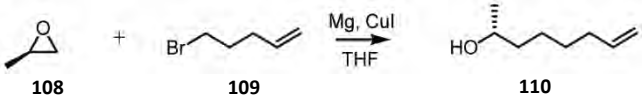

Figure 43: Synthesis of the (*R*)-octen-2-ol

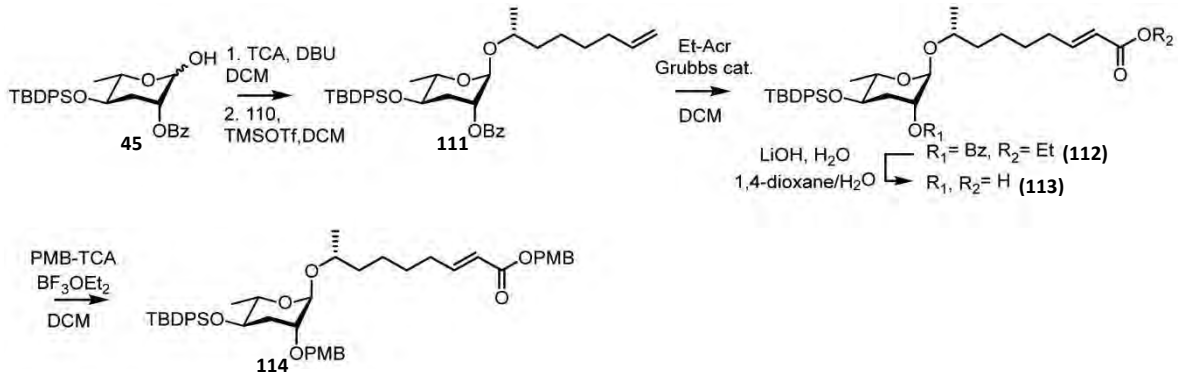

Figure 44: Synthesis of 2'-*O*-PMB-4'-*O*-TBDPS-asc-ΔC9-*O*-PMB ester (114).

Since the conditions for the PMB etherification with PMB-TCA were too harsh, the di-*O*-PMB ascaroside **114** was synthesized with Dudley's 2-(4-methoxybenzyloxy)-4-methylquinoline (PMB-*O*-lepidine, **115**)[57, 79] (**Figure 45** & **Figure 47**). The use of this reagent offers several advantages in comparison to PMB-TCA: 1) PMB-*O*-lepidine is a shelf stable reagent, 2) the lepidine by-product **116** could be easily removed by silica gel chromatography and 3) the reaction could be performed under neutral conditions by activation with methyl triflate. Unfortunately, no product was detected upon activation of **115** with methyl triflate as described by Dudley. However, when the PMB-*O*-lepidine was activated with a catalytic amount of camphorsulfonic acid[59] the reaction provided pure (7*R*)-octenyl 2'-*O*-PMB-4'-*O*-TBDPS-ascaroside **123** in 42% of yield without any deterioration of the starting material (**Figure 47**).

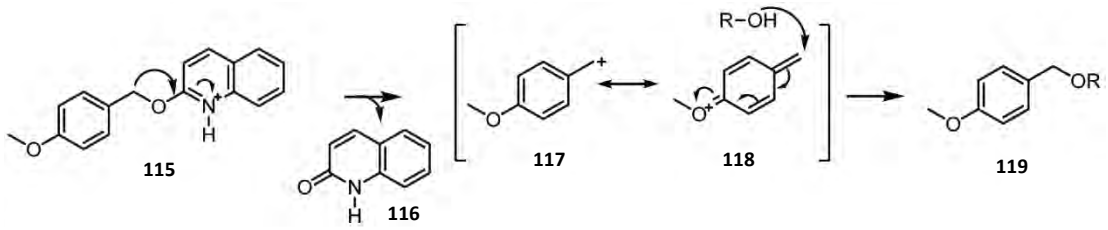

Figure 45 : Mechanism of the PMB-etherification with Dudley's reagent under acidic conditions.

Next, the 4'-*O*-TBDPS substituted ascaroside (**121**) was desilylated with tetrabutylammonium fluoride to afford the intermediate **124** in 69% yield. Then, the terminal alkenyl was elongated by cross metathesis with Grubbs 2nd generation catalyst and 4-methoxybenzyl acrylate (**121**) (prepared from the commercially available acrylic acid (**120**) and 4-methoxybenzyl chloride under basic conditions with potassium carbonate (**Figure 46**) [80]. The resulting 2'-*O*-PMB-asc-ΔC9-*O*-PMB ester **125** previously described by Zhang *et al.*[40] was linked to *N*-Boc-protected urocanic acid via Steglich esterification catalyzed with DMAP using 1-ethyl-3-(3-dimethylaminopropyl)carbodiimide hydrochloride as coupling reagent to provide the fully protected ascaroside **126**. Subsequent acid catalyzed hydrolysis using trifluoroacetic acid afforded the 4'-UC-asc-ΔC9 (ucas#3, **37**) in 62% yield. Alternatively, **37** was also prepared via the 2'-*O*-PMB-asc-ΔC9 *O*-*tert*-butyl ester (**127**), obtained from cross metathesis of the ascaroside **123** and the commercially available *tert*-butyl acrylate (**Figure 48**). However, the *tert*-butyl ester appeared to be quite resistant towards TFA-mediated deprotection, as 18% of the *tert*-butyl ester intermediate could still be recovered even after 24 h of reaction with six equivalents of TFA (**Figure 47**).

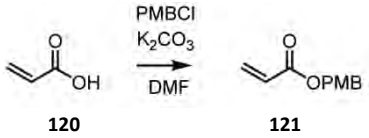

Figure 46: Synthesis of the 4-methoxybenzyl-acrylate[80].

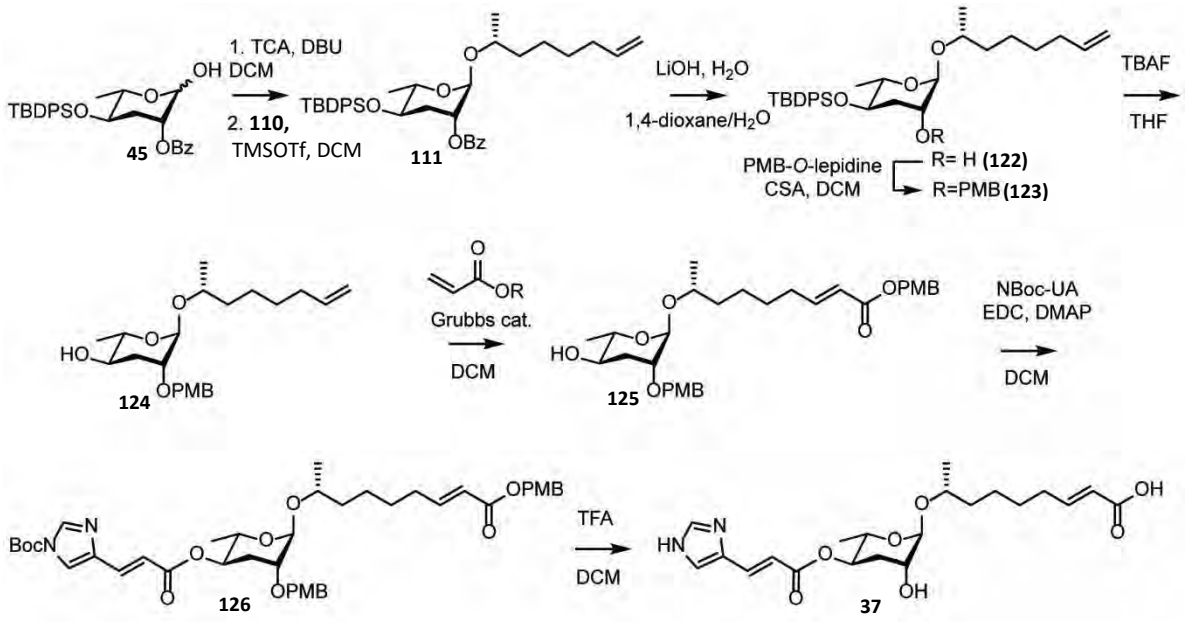

Figure 47: Synthesis of (*E*)-4'-UA-asc-ΔC9 (37) using PMB-*O*-lepidine for the 2-OH protection.

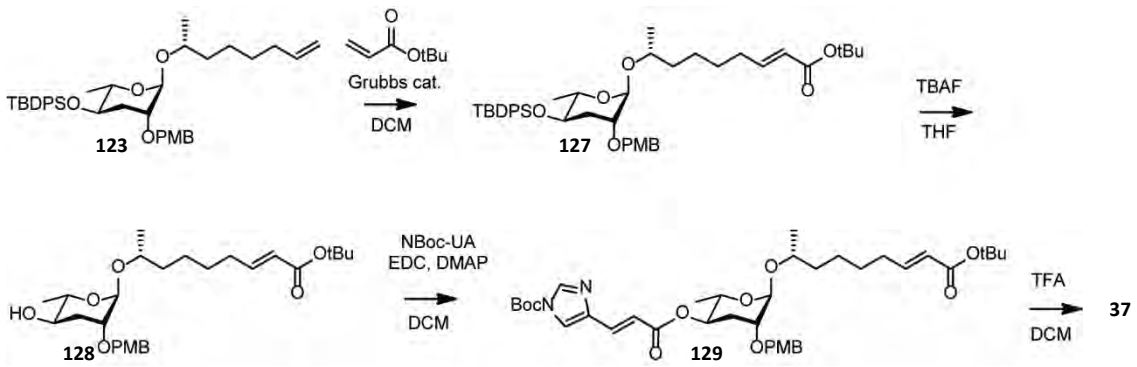

Figure 48 : Synthesis of (*E*)-4'-UA-asc-ΔC9 (37) with tert-butyl acrylate.

In order to synthesize 4'-UA-asc-C6MK (ucas#2, **35**), the commercially available (*2R*,*5R*)-2,5-hexanediol was glycosylated with the 4'-*O*-TBDPS-2'-*O*-Bz-ascarylose building block **45** (**Figure 49**). Next, the free hydroxyl group of the aglycon was oxidized to the corresponding methyl ketone **131** with pyridinium chlorochromate. After alkaline hydrolysis of the 2'-*O*-benzoyl group with lithium hydroxide solution, the 2'-*O*-position was protected as a PMB-ether by camphorsulfonic catalyzed PMB-etherification using Dudley's PMB-*O*-lepidine reagent to give the fully protected 2'-*O*-PMB-4'-*O*-

TBDPS-asc-C6MK **133**. Subsequent desilylation of the 4'-*O*-position with TBAF provided the 2'-*O*-PMB-asc-C6MK **134** in 51% yield, which yielded 94% of the fully protected urocanic acid ascaroside **135** upon DMAP catalyzed Steglich esterification with dicyclohexylcarbodiimide and *N*-Boc-protected urocanic acid. The desired 4'-UC-asc-C6MK (**35**) was finally obtained in 42% yield after TFA-mediated deprotection of **135** (**Figure 49**).

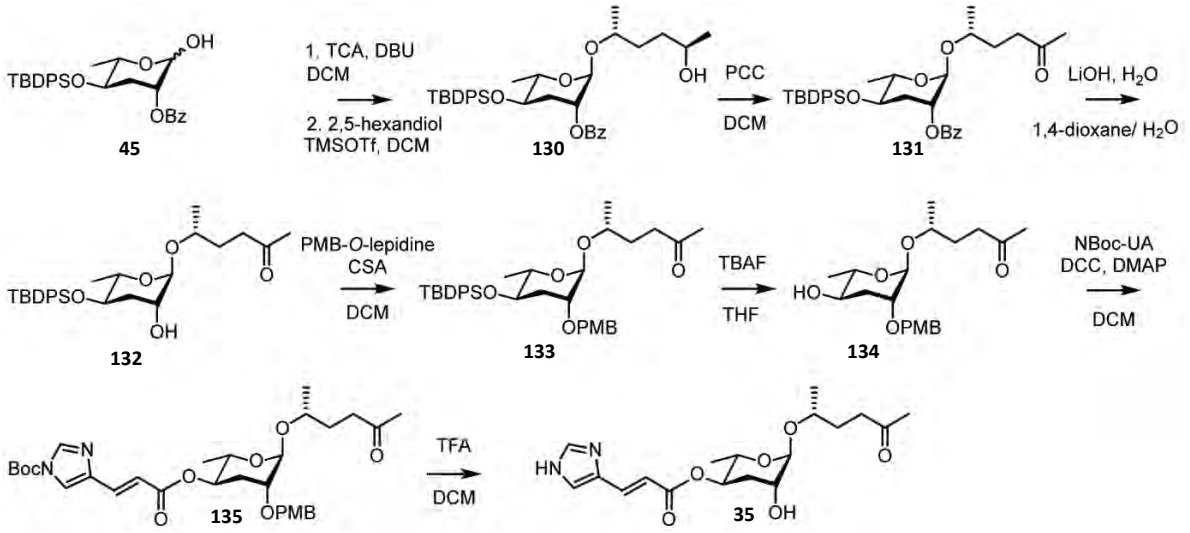

Figure 49: Synthesis of 4'-UA-asc-C6MK 35.

Next, the (*E*)-configured 4'-UC-asc-ΔC9 and the 4'-UC-asc-C6MK were converted to their corresponding (*Z*)-isomers by photoisomerization. (*E*)-Urocanic acid is one of the main UV absorbing components of the human epidermis[81]and its (*Z*)-isomer has been associated to an immunosuppressive effect, photocarcinogenesis and skin aging[82]. Therefore, the photochemical properties of urocanic acid have been widely investigated[83]. This research has shown that urocanic acid has an unusual wavelength-dependent photobehavior. The maximum production of (*Z*)-urocanic acid is obtained when the molecule is irradiated at the red edge of the absorption spectrum (around 10 to 12 nm above its maximum absorption band) but is drastically reduced when approaching the absorption maximum[83a, b]. However, ester derivatives of urocanic acid have shown the opposite behavior with a maximum (*E*) to (*Z*) photoconversion rate obtained at shorter wavelengths[84] [76b]. One of the hypotheses to explain this wavelength dependency is the presence of tautomers that absorb in different spectral regions. The analysis of the UV spectrum of the two (*E*)-configured urocanic acid ascarosides and their corresponding (*Z*)-isomer shows similar UV absorption profile (**Figure 50**). Both (E)-urocanic acid ascarosides display an absorption maximum at around 270 nm (**Figure 50**) in the UV-B region while their corresponding (*Z*)-isomer exhibited a bathochromic shift of 2 to 3 nm. Therefore,

higher (*E*) to (*Z*) conversion would be expected at wavelength under 270 nm according to previous studies[76b].

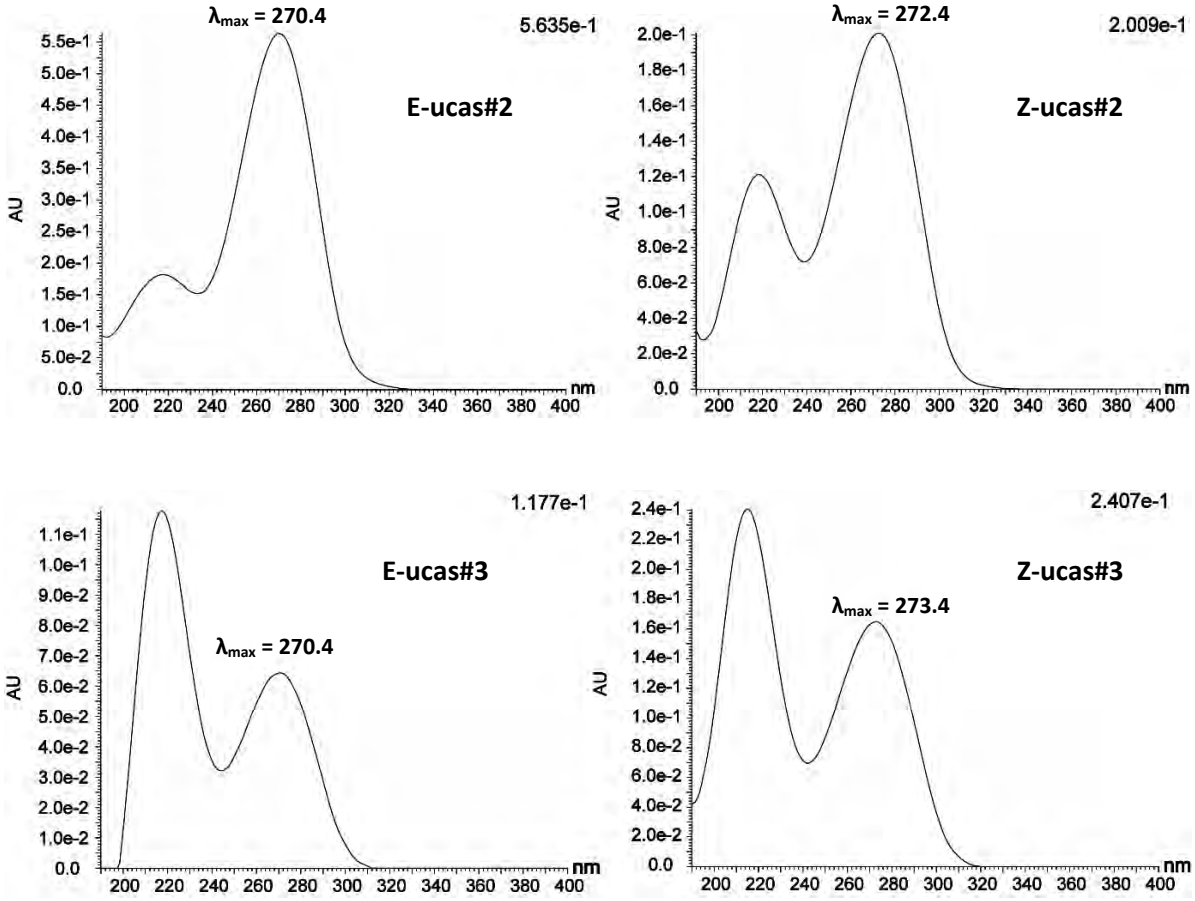

Figure 50 : UV-absorption spectra of (*E*)- and (*Z*)-4'-UC-asc-ΔC9 and (*E*)- and (*Z*)-4'-UC-asc-C6MK.

Different UV-sources were tested for the conversion of (*E*)-4'-UC-asc-ΔC9 (**37**) and (*E*)-4'-UC-asc-C6MK (**35**) to their corresponding (*Z*)-isomers **38** and **36**, respectively. Each compound in deuterated methanol was irradiated for 50 min an NMR quartz tube with either a UVC (λ_{max} = 254 nm) or a UVB lamp (λ_{max} = 306 nm). Moreover, the effect of sun light irradiation on (*E*)-4'-UC-asc-C6MK (**35**) was also explored. The reactions were monitored by ^{1}H NMR spectroscopy, which demonstrated that the total amount of urocanic acid ascarosides during the experiments remained constant, thus indicating that the UV irradiation is not inducing substantial decay or other side reactions to form alternative products.

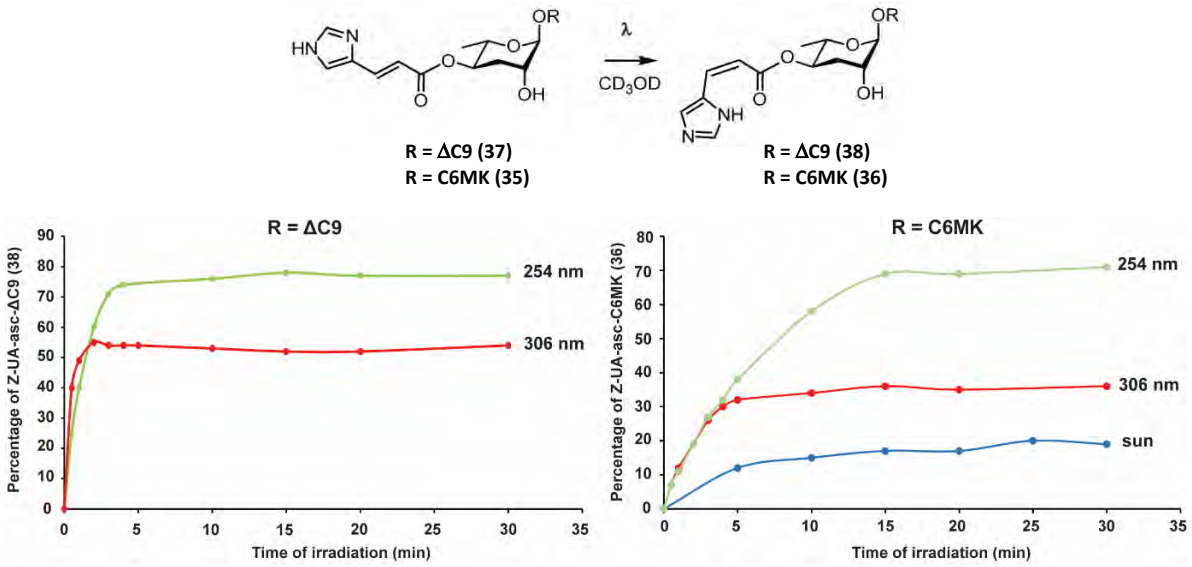

Figure 51: Kinetic of the photoconversion of (E)-4'-UC-asc-ΔC9 (37) and (E)-4'-UC-asc-C6MK (35) after irradiation with UVC, UVB or sun light (29/12/2020, 11h, 3°C).

As shown in **Figure 51**, the photostationary equilibrium states for 4'-UC-asc-ΔC9 irradiated with the 254 nm lamp (UVC) had a composition of 75% of (*Z*) and 25% of (*E*), while only 52% of (*Z*) and 48% of (*E*) were obtained with the 306 nm lamp (UVB). For 4'-UC-asc-C6MK the photostationary equilibrium contained 71% of the (*Z*)-isomer with the 254 nm lamp and only 35% with the 306 nm lamp. Only 20% of the (*E*)-4'-UC-asc-C6MK could be converted to the corresponding (*Z*)-isomer via irradiation with sun light (**Figure 51**) most likely due to the UV-C being absorbed by the stratospheric ozone layer. No isomerization was observed when the samples were exposed to the sunlight behind a window that filters UV-light.

The resulting (*E*/*Z*)-mixtures were stored in the freezer at -20 °C for five days and subsequently reanalyzed by ^{1}H NMR, which did not show any change in (*E*/*Z*)-ratios. Additionally, no (Z) to (*E*) conversion was observed when the mixture was stored for one day at room temperature, nor when the sample was manipulated under laboratory light at night. In conclusion, these experiments demonstrate that the urocanic acid ascarosides can be efficiently isomerized from the (*E*) to the (*Z*)-isomers using UV irradiation under laboratory conditions as well as sunlight under ecologically relevant conditions.

3.3. Confirmation of structure assignments

To confirm the structure assignment of the (*E*) and the (*Z*)-configured urocanic ascarosides, ^{1}H NMR and the chromatographic retention time of the synthetic material and the isolated urocanate ascarosides were compared (**Figure 52, Figure 53, Figure S5**). For the 4'-UC-asc-ΔC9 (ucas#3, **37**), the 1H NMR from the natural and the synthetic sample showed identical chemical shifts and coupling

constants except for the chemical shift of the vinylic proton 3-H from the side chain, which is highly pH dependent[85]. In addition, the comparison of the LC-MS retention time confirmed that both samples are identical. Similarly, the corresponding (*Z*)-isomer presented identical chemical shifts and LC-MS retention times as the natural product enriched from *C. remanei*. Furthermore, the 4'-UC-asc-C6MK (ucas#2, **35**) that dominates in *C. briggsae* AF16 (**Figure 41**) but has not yet been enriched was shown to be identical to the synthetic material by comparison of LC-HR-MS/MS data (**Figure 53**

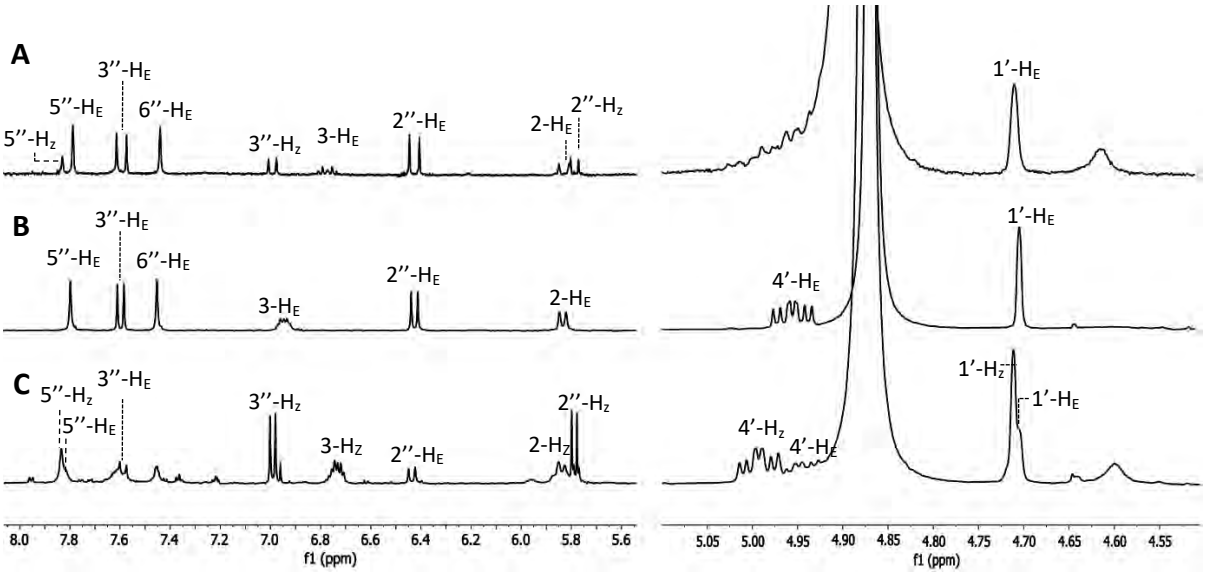

Figure 52 : Comparison of ^{1}H NMR spectra of (A) the enriched mixture of (*Z*) and (*E*)- 4'-UC-asc-ΔC9 (38 & 37) (B) the synthetic (*E*)-4'-UC-asc-ΔC9 (37) and (C) the crude synthetic mixture of (*Z*) and (*E*)- 4'-UC-asc-ΔC9 (38 & 37).

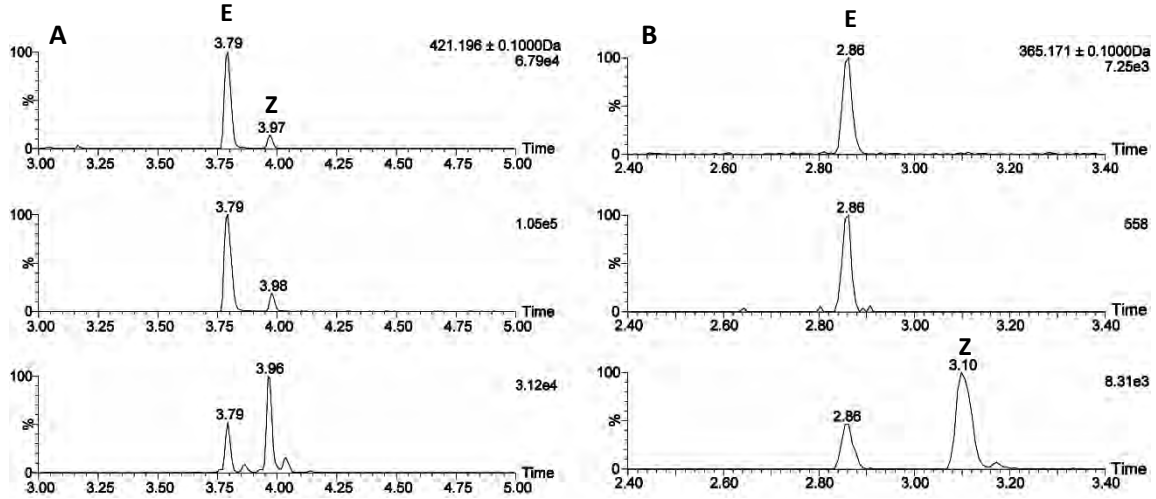

Figure 53 : Comparison of the ion chromatograms of the isolated and synthetic (A) 4'-UC-asc-ΔC9 (37) and (B) 4'-UC-asc-C6MK (35) before and after irradiation with the UV-C lamp.

3.4. Functional characterization

A sex-specific comparative ESI-(-)-HR-MS analysis of the exometabolomes obtained from the gonochoristic *C. remanei* or *C. nigoni* revealed that urocanic acid ascarosides like ucas#3 **40** are exclusively produced by males (**Figure S6**). These results suggested that urocanate ascaroside might act as a female attractant. Consequently, holding assay that quantify the dwelling time of a worm in a defined scoring region conditioned with either 1 µl of urocanic acid ascaroside solution in water or 1 µl of aqueous methanol solution were performed using female *C. remanei* PB4641 and *C. nigoni* JU1422 with 1 µM to 100 pM of (*E*)-4'-UC-asc-ΔC9 (**37**). As shown in **Figure 54**, *C. remanei* females were not retained by (*E)*-4'-UC-asc-ΔC9 (**37**) at any of the concentrations tested. *C. nigoni* females were only retained by the highest concentration of (*E*)-4'-UC-asc-ΔC9 (**37**) (**Figure 54**). The hermaphroditic *C. briggsae* AF16 was also tested in holding assays with 4'-UC-asc-C6MK (**35**). Both the (*E*) and the (*Z*)-somer were tested individually on *C. briggsae* and did not exhibit any retention activity (**Figure 55**). These results indicate that the urocanate ascarosides **37** and **35** might not serve as a sex-specific chemoattractants but, might exhibit other biological functions. Furthermore, considering the complex blend of urocanate ascarosides produced by the worms, potential synergism between the compounds could also account for the lack of activity of 4'-UC-asc-ΔC9 (**37**) and 4'-UC-asc-C6MK (**35**) in the holding assays.

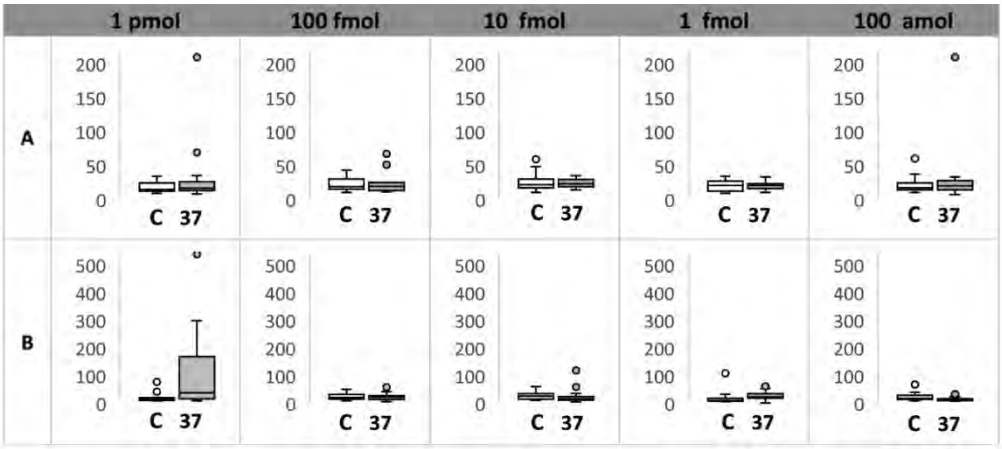

Figure 54 : Holding assays on female (A) *C. remanei* (PB4641) (B) *C. nigoni* (JU1422) for 1 pmol to 100 amol of (*E*)-4'-UC-asc-ΔC9 (37).

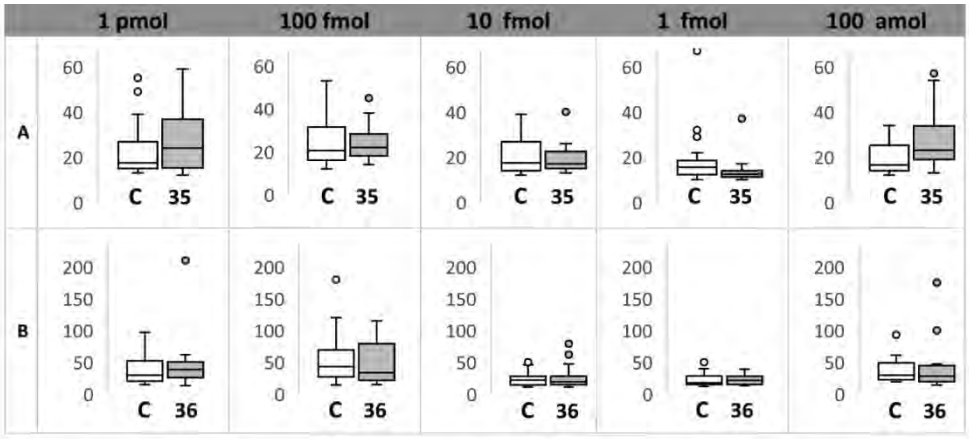

Figure 55 : Holding assays on hermaphrodite *C. briggsae* (AF16) 1 pmol to 100 amol of (A) (*E*)-4'-UC-asc-C6MK (35) and (B) (*Z*)-4'-UC-asc-C6MK (36).

The results from the irradiation with the different UV-source showed that the urocanate ascarosides are highly sensitive to UV and sun irradiation. Therefore, a potential photoprotective function of urocanate ascarosides could be considered. Following this hypothesis, the worms could excrete the urocanate ascarosides into their environment to sense UV-light by detecting the ratio of (*E*)/(*Z*)-urocanate ascaroside derivative. Thus, a potential avoidance for the (*Z*)-isomer could be expected. To answer this question the (*Z*)-4'-UC-asc-C6MK should next be tested in a quadrant assay that quantifies the preference or avoidance of the worm for a region conditioned with either the test compound or a control solution.

3.5. Biogenesis

Having confirmed the molecular structure assignment of the urocanate ascarosides, the biosynthesis of these new ascarosides was investigated. Since previous experiments suggested an amino acid origin for some of the additional building blocks of the modular ascarosides, as exemplified with indole-3-carbonyl ascaroside (icas) that integrate an indole-3-carboxylic acid unit derived from L-tryptophan metabolism, it was therefore suggested that the urocanate ascarosides (ucas) originate from L-histidine metabolism. To confirm the origin of the urocanate moiety and the mechanism underlying its biosynthesis, feeding experiments with stable isotopes as well as comparative analysis of wild-type and mutants *C. elegans* metabolomes were performed. These experiments focus on the production of 4'-UC-asc-C9 (**107**) and 4'-UC-asc-ΔC9 (**37**), the most dominating urocanate ascaroside compounds in *C. elegans*.

To determine the biosynthetic origin of the urocanic acid unit, starvation experiments with *C. brenneri* PB2801 (from Costa Rica) and *C. wallacei* JU1904 (from Indonesia) were performed. First, the exometabolomes of starved and well-fed *C. brenneri* PB2801 and *C. wallacei* JU1904 were analyzed by

ESI-(-)-MS/MS. Comparative analysis indicated that depletion of food abolishes the production of urocanic acid ascarosides. As depicted in **Figure 56** and **Figure 57** well-fed worms produce 4'-UA-asc-C9 (**107**) and 4'-UA-asc-ΔC9 (**37**) and, starved worms produce considerably less urocanate ascarosides, whereas the biosynthesis of their putative precursors, asc-C9 (**4**, **Figure 4**) and asc-ΔC9 (**3**, **Figure 4**) are not affected by starvation. These results suggest that the urocanic acid unit is derived from L-histidine originating from the bacterial food source.

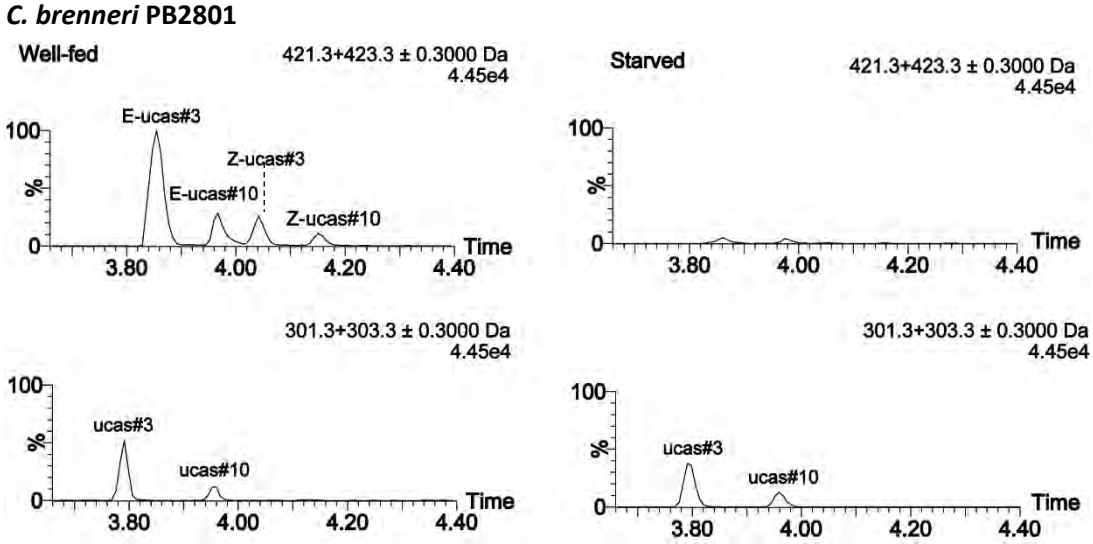

Figure 56 : Production of 4'-UA-asc-C9 (ucas#10, 107) and 4'-UA-asc-ΔC9 (ucas#3, 37) and their hypothetical precursor asc-C9 (ucas#10, 6) and asc-ΔC9 (ucas#9, 3) in well fed and starved *C. brenneri*.

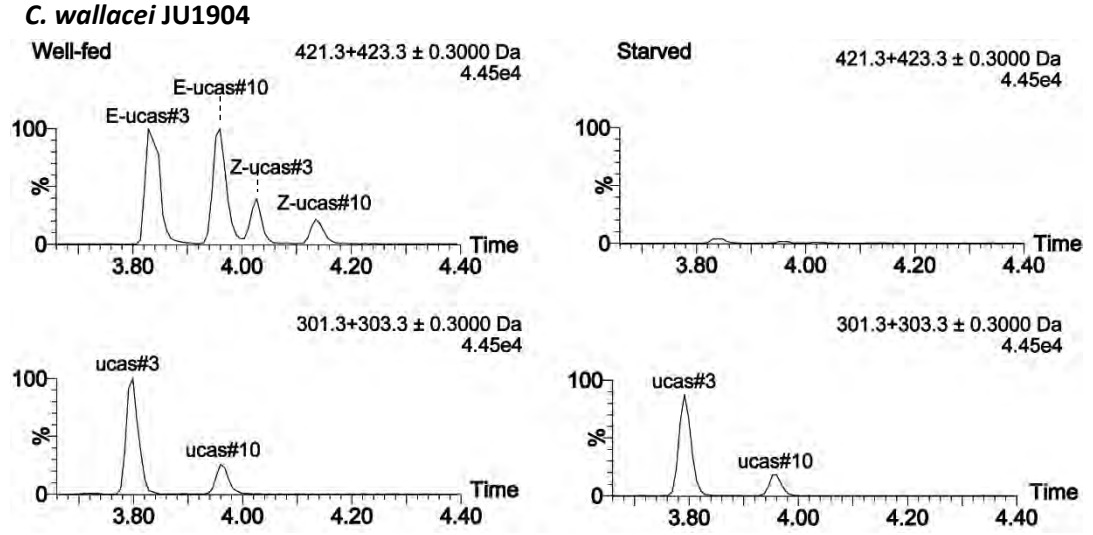

Figure 57 : Production of 4'-UA-asc-C9 (ucas#10, 107) and 4'-UA-asc-ΔC9 (ucas#3, 37) and their hypothetical precursor asc-C9 (ucas#10, 6) and asc-ΔC9 (ucas#9, 3) in well fed and starved *C. wallacei*.

In order to unambiguously decipher the biosynthetic origin of the urocanate unit, *C. wallacei* JU1904 was fed with a 1:1 mixture of [U-^{13}C]-labeled and natural abundance *E. coli* BL21(DE3) for 7 days. The worms' exometabolomes were analyzed by mass spectrometry using electrospray ionization in positive mode (**Figure 58** & **Figure 59**). Upon ^{13}C enrichment the MS/MS fragmentation pattern of **37** and **107** showed two sets of peaks of equal intensity with *m/z* = 121.0396 and 127.0607 for [$C_6H_5N_2O^+$] and *m/z* 139.0502 and 145.0713 for [$C_6H_7N_2O_2^+$], corresponding to the unlabeled and the [U-^{13}C]-labelled urocanic acid moiety, respectively. The observed Δ*m/z* value of 6 Da corresponds to the total number of carbons in the fragment **105** (**Figure 39**. **C**), therefore proving that the urocanic acid unit is entirely derived from bacterial histidine. Furthermore, the fragment **104** (**Figure 39**. **C**) at *m/z* 251.1026 [$C_{12}H_{15}N_2O_4^+$] for the urocanate substituted ascarylose fragment derived from the loss of the aglycone in ESI-(+) appeared as a broad peak showing a bimodal distribution of ^{13}C isotopomers with two maxima at 254 Da and 260 Da. The lower mass half of these signals correspond to fragments containing an unlabeled urocanic acid unit, whereas the higher mass half of these signals corresponds to fragments that contain [U-$^{13}C_6$]-labeled urocanic acid unit, while the bell shape distribution indicates a *de novo* synthesis of the ascarylose unit from dietary metabolites[86] by the worm as previously suggested by Joo *et al*[36]. Similarly, a broad Gaussian type distribution was observed for the molecular ion signals, which is the result of the overlapping of two gaussian distributions that originate from the *de novo* synthesis of the ascarylose unit, along with de novo biosynthesis of the aglycone part via very long chain fatty acids.

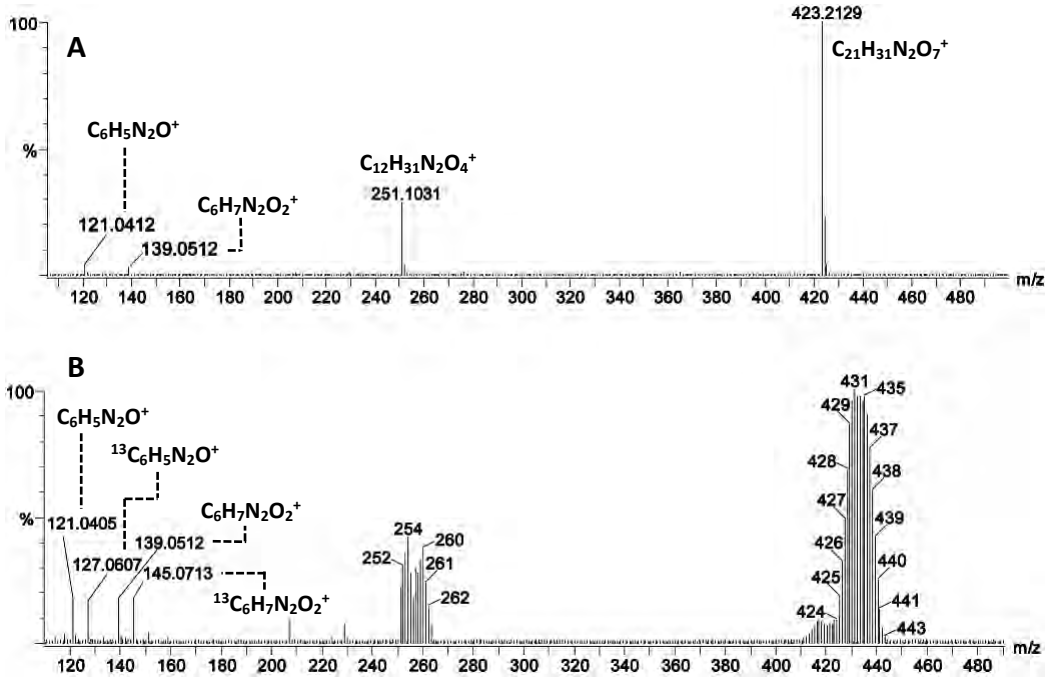

Figure 58 : ESI-HR-MS/MS spectra of 4'-UA-asc-ΔC9 (40) from *C. wallacei* fed with *E.coli* OP50 (A) and C. wallacei fed with ^{13}C enriched *E. coli* BL21(DE3) (B).

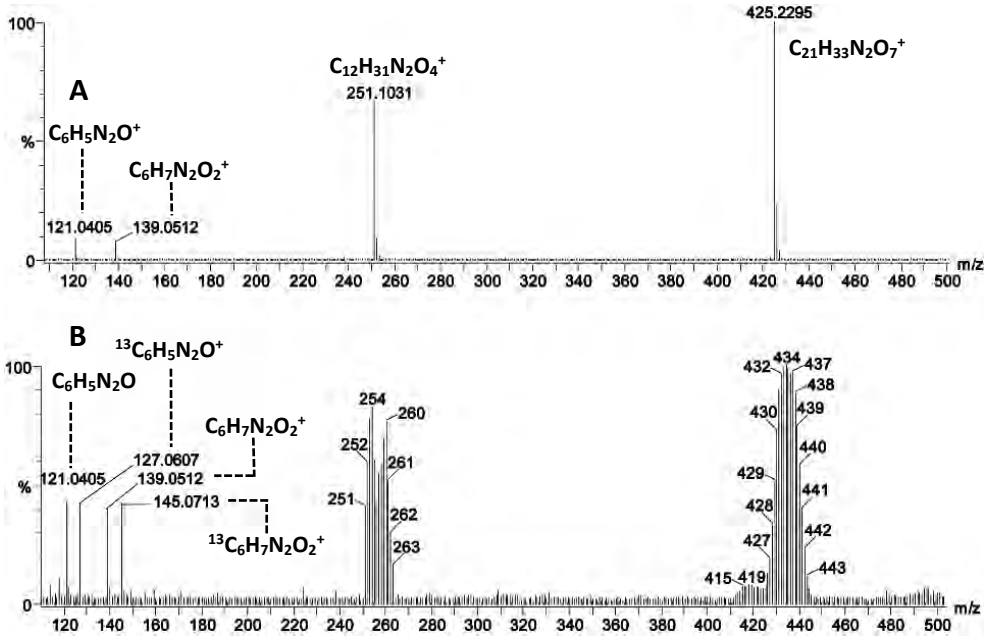

Figure 59 : ESI-HR-MS/MS spectra of 4'-UA-asc-C9 (107) from C. wallacei fed with E.coli OP50 (A) and C. wallacei fed with ^{13}C enriched *E. coli* BL21(DE3) (B).

Taken together, these experiments indicate that the urocanic acid moiety of the urocanate ascarosides (ucas) originates from food derived precursors. Next, the biosynthetic origin of the urocanic acid moiety was investigated. Since modular ascarosides commonly integrate building blocks derived from amino acid metabolism, the urocanic acid moiety was hypothesized to be derived from L-histidine metabolism. To prove this hypothesis, the HPLC-HR-MS/MS chromatograms of the exometabolome of two wild-type strains of *C. elegans* (N2 and AB1) were compared with those of two histidine ammonium lyase (histidase) mutants, *haly*-1(am130) and *haly*-1(am 132)that carry defects in the enzyme catalyzing the desamination of L-histidine to (*E*)-urocanic acid and one urocanase mutant, *uroc-1*(gk324463) that lacks the enzymes catalyzing the degradation of urocanic acid. As depicted in **Figure 60**, both wild-type strains produce comparable amount of 4'-UC-asc-ΔC9 (**37**) while the histidase mutants *haly*-1(am130) and *haly*-1(am 132) produce significantly less 4'-UC-asc-ΔC9 (**37**). In contrast, increased levels of urocanate ascaroside were detected in the urocanase mutant *uroc*-1 (gk324463).

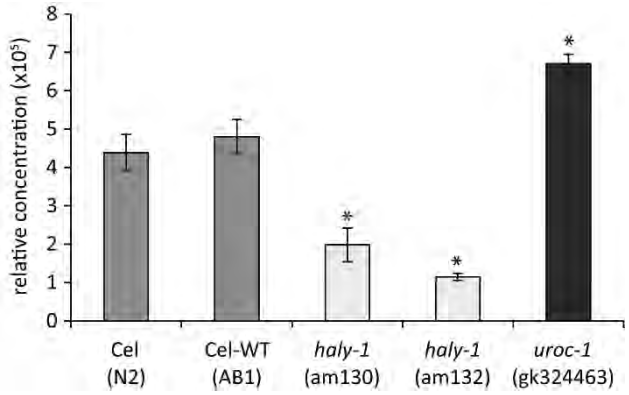

Figure 60 : Production of 4'-UC-asc-ΔC9 in the exometabolome of two wild-type strains of *C. elegans* (N2 and AB1), the histidase mutants haly-1(am130) and haly-1(am132), and the urocanase mutant uroc-1 (gk324463).

These results confirm that the urocanic acid moiety is a product of the degradation of *E. coli* derived L-histidine catalyzed by *C. elegans haly-1*, whereas a lack of *uroc-1* results in increased production of the urocanate ascarosides due to accumulation of urocanic acid.

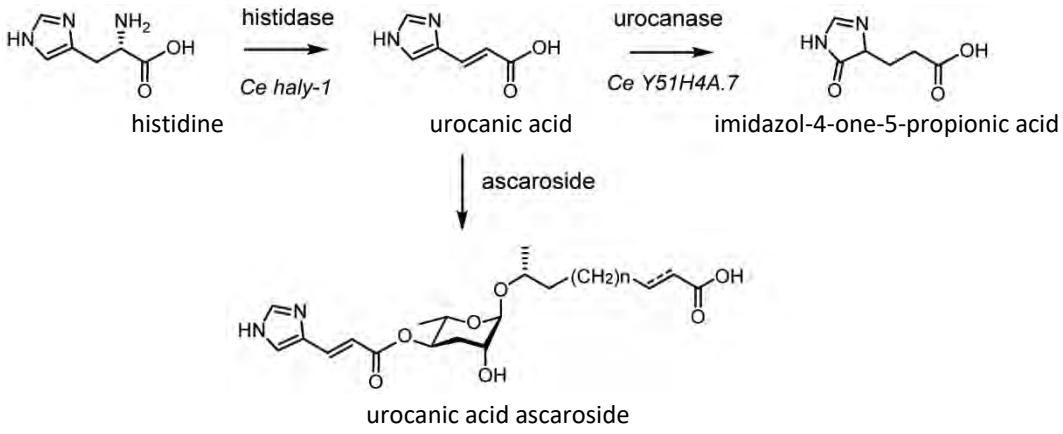

Figure 61 : Biosynthesis of the urocanic acid ascarosides.

3.6. Conclusion

A new class of photo switchable ascarosides that integrate an urocanic acid moiety attached at the 4'-position was identified from male *C. remanei* using a combination of one and two-dimensional NMR spectroscopy along with HR-MS/MS. The comparative analysis of several *Caenorhabditis* species revealed that urocanate ascaroside signals species-specific for nematodes of the *Elegans* group. (*E*)-4'-UA-asc-ΔC9 (ucas#3, **37**) represents the dominating urocanate ascaroside in most species, while *C. briggsae* produces predominatly (*E*)-4'-UA-asc-C6MK (ucas#2, **35**). Along with the (*E*)-configured urocanate ascarosides, smaller amounts of the corresponding (*Z*)-isomers were also detected. The structure assignments of the prominent (*E*)-4'-UA-asc-ΔC9 (**37**) and the (*E*)-4'-UA-asc-C6MK (**35**) as well as their corresponding (*Z*)-isomers were unambiguously established by total synthesis using the

orthogonally protected ascarylose building block **45** that facilitates the synthesis of 2- and 4-linked modular ascarosides, followed by comparison of the NMR spectra and the LC-MS chromatograms of the natural and the synthetic products. Biosynthetic investigations revealed that the urocanate moiety is derived from bacterial L-histidine, and that the enzymes *haly-1* and *uroc-1* are responsible for the conversion of histidine to urocanic acid and its degradation, respectively. The urocanate ascarosides represent the first class of modular ascarosides that integrate a building block from L-histidine metabolism and the first ascaroside that can isomerize by absorption of UV light. Due to its occurrence in males *C. remanei* and others *Caenorhabditis* species, the urocanate ascarosides were initially hypothesized to function as a female attractant. However, holding assays with female *C. nigoni* JU1422 and *C. remanei* PB4641 did not show any significant retention effect. Similarly, no significant holding activity was detected with the hermaphroditic *C. briggsae* AF16. Additional experiments will be required to decipher the biological activity of the urocanate ascarosides.

4. The *ortho*-aminobenzoate ascarosides (abas)

4.1. Identification of *ortho*-aminobenzoate ascarosides

The new class of homologous anthranilic acid ascarosides was identified from the exometabolome of *C. nigoni* JU1422 (from India) by C. Dong[39]. In contrast to many other modular ascarosides that have been identified in recent years, the aminobenzoate ascarosides do not give the characteristic MS/MS fragment ion at *m/z* 73 ($[C_3H_5O_2]^-$) and were only detected upon systematic ^{1}H NMR analysis of exometabolome fractions. Using a combination of chromatography on RP-C18 and semi-preparative HPLC, approximately 100 µg of 4'-AB-asc-C5 (abas#9, **34**) was isolated from 1.6 L of the *C. nigoni* liquid culture supernatant. The ESI-(-)-HR-MS/MS spectrum of the isolated compound indicated a molecular formula of $C_{18}H_{23}NO_7$ with a mass of 366.1554 Da. Analysis of the ESI-(+)-HR-MS/MS fragmentation showed a fragment ion with m/z 250.1054 (**137**) corresponding to the molecular formula $[C_{13}H_{16}NO_4]^+$ from the loss of the C5 side chain as well as an aminobenzoate fragment ion at *m/z* 120.0444 $[C_7H_6NO]^+$ (**139**) from the loss of the ascaroside unit **Figure 62**. The ESI-(-)-HR-MS/MS analysis furnished a specific fragment of m/z 192.0666 (**138**) for a molecular formula of $[C_{10}H_{10}NO_3]^-$ corresponding to the ascaroside-specific fragment *m/z* 73 ($[C_3H_5O_2]^-$) substituted with an aminobenzoate moiety which has not yet been observed for 4'-substituted ascaroside (**Figure 62**).

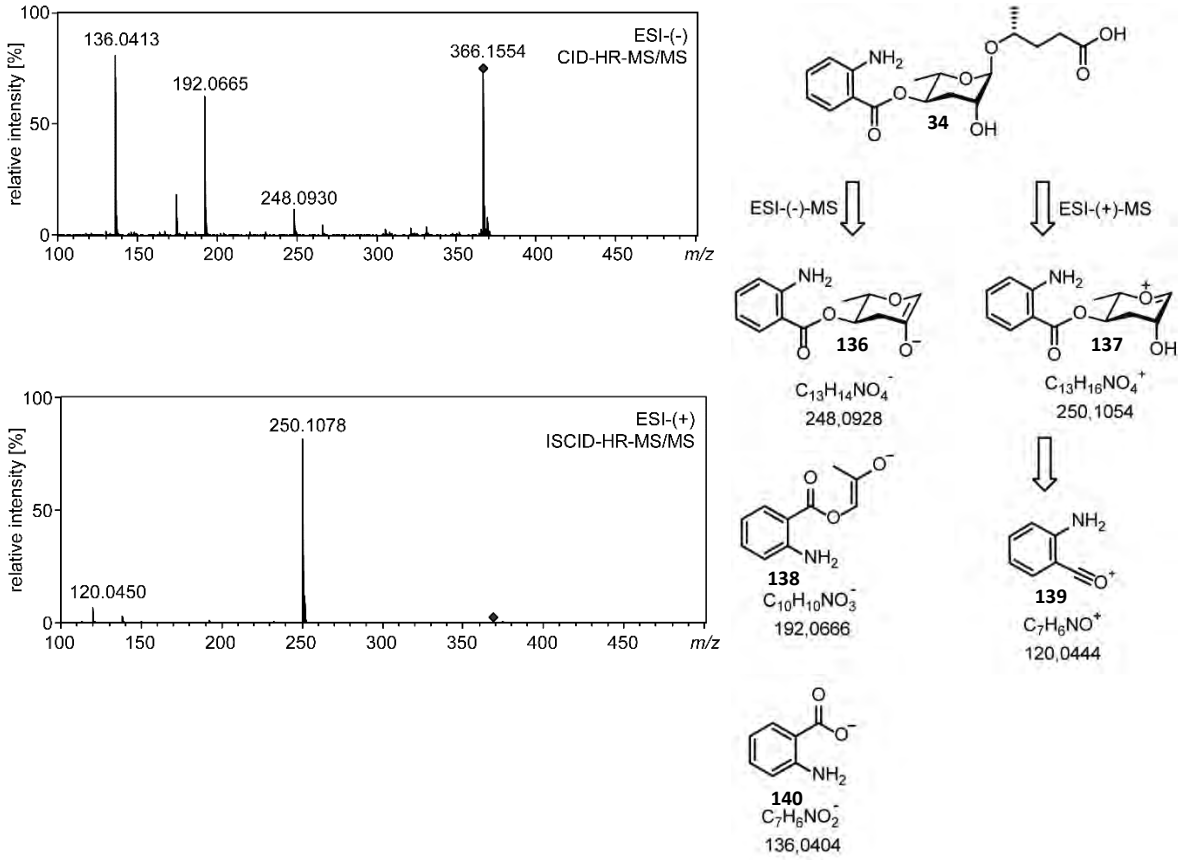

Figure 62: ESI-HR-MS/MS spectra of 4'-AB-asc-C5 (34) from *C. nigoni* and MS/MS fragmentation of abas derivatives.

Since the mass spectrometric data could unambiguously establish the position of the aminobenzoic group on the sugar moiety nor the substitution pattern of the aminobenzoic acid group, the target compound was isolated by RP-C18 chromatography and further characterized by one- and two-dimension NMR. The inspection of ^{1}H NMR and the *dqf*-COSY spectra showed the presence of an aminobenzoate moiety attached to an asc-C5 unit. The shifted 4'-position (δ_H= 5.07 ppm) of the ascarylose sugar indicated that the ascaroside is 4'-substituted by the aminobenzoyl group (**Figure 63.B**), while the multiplicities of the four distinct signals corresponding to the aromatic methine protons is consistent with an *ortho*-substituted amino-benzoic acid corresponding to the anthranilic acid group (**Figure 63.A & B**).

A

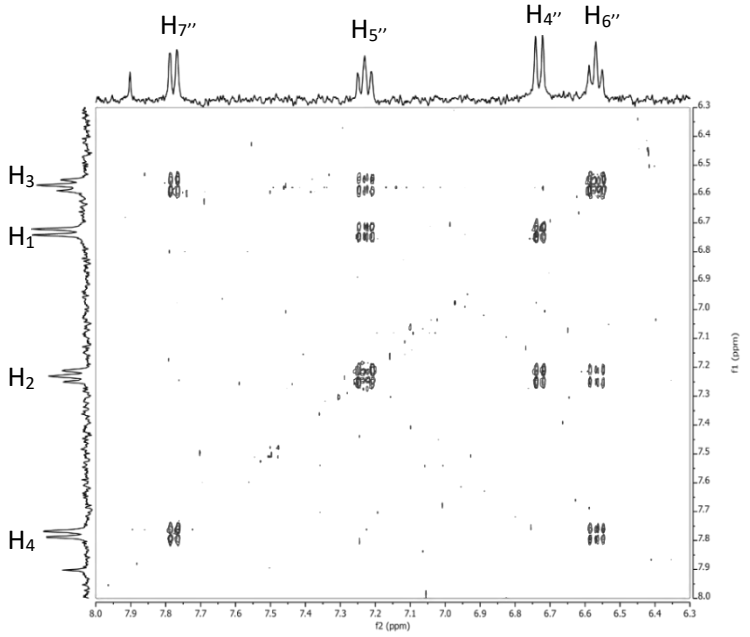

B

H	isolated 4'-AB-asc-C5 (34)
1'	4.74 br.s
2'	3.77 br.s
3'ax	1.98 ddd (13.8, 11.0, 2.97)
3'eq	2.18 ddd (4.8, 2.76)
4'	5.07 ddd
5'	4.04 dq
6'	1.20 d (6.7)
1	-
2_a	2.42 m
2_b	2.33 m
3	1.90-1.84 m
4	3.87 m
5	1.18 d (6.2)
1''	-
2''	-
3''	-
4''	6.73 d
5''	7.23 dd
6''	6.57 dd
7''	7.78 d
8''	-

C

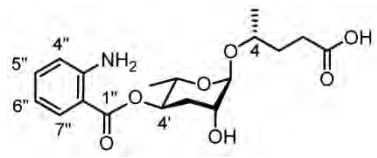

Figure 63: Section of the *dqf*-COSY spectra of 4'-AB-asc-C5 (abas#9, 34). (B) 400 MHz ^{1}H NMR data of the isolated 4'-AB-asc-C5 (in CD_3OD)[39]. (C) Structure of 4'-AB-asc-C5 (34).

Targeted ESI-(+)-MS/MS screening of fourteen *Caenorhabditis* species for the fragment ion at *m/z* 250.1054 ($[C_{13}H_{16}NO_4]^+$) highlighted a homologous series of anthranilic acid ascarosides that are produced by only two members of the Elegans group: the gonochoristic *C. nigoni* and the hermaphroditic *C. tropicalis* (**Figure 64.A**), which are not particularly closely related. Both species

produce a different blend of anthranilic acid ascarosides. While *C. nigoni* produces a broad range of anthranilic acid ascarosides from C5 to C11, *C. tropicalis* produces predominantly short chain anthranilic acid ascarosides (C5 to C8). Since the 4'-AB-asc-C5 was predominant in both species this compound was synthesized as a representative to confirm the molecular structure of anthranilic acid ascarosides and to investigate their biological activities.

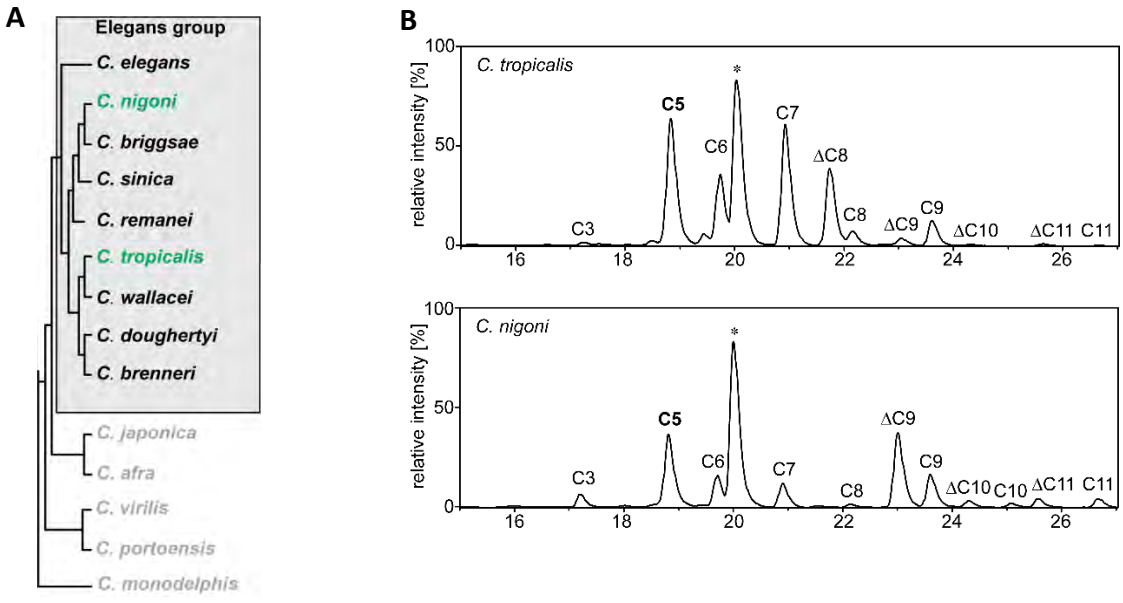

Figure 64: (A) Distribution of 4'-AB-asc-C5 (34) among Caenorhabditis species of the *Elegans* group. (B) ESI-(+)-MS/MS screen of the *C. nigoni* and *C. tropicalis* metabolome for m/z 250.1074 $[C_{13}H_{16}NO_4]^+$.

4.2. Synthesis of 4'-AB-asc-C5 (abas#9)

Two approaches were considered to generate the (4*R*)-hydroxypentanoic acid aglycone of 4'-AB-asc-C5. The first approach involved the oxidation of (*R*)-5-hexen-2-ol to the corresponding carboxylic acid as described by Zhang *et al*. for the synthesis of 4'-IC-asc-C5 (**13**) (**Figure 65**)[40] while the second approach was based on cross metathesis of a (3*R*)-1-butenyl ascaroside with benzyl acrylate (**Figure 68**).

Following the procedure described in the literature, (*R*)-5-hexen-2-ol was glycosylated with the 2'-*O*-Bz-4'-*O*-TBDPS-ascarylose building block **45** via the trichloroacetimidate route[78]. Next, the terminal alkene group was converted to the corresponding carboxylic acid (**142**) by oxidation with sodium periodate catalyzed with ruthenium (III) chloride in 71% of yield. The resulting 2'-*O*-Bz-4'-*O*-TBDPS-asc-C5 (**142**) was debenzoylated at the 2'-position by alkaline hydrolysis with lithium hydroxide solution to afford 4'-*O*-TBDPS-asc-C5 **143**, which was converted to the 2'-*O*-Bn-4'-*O*-TBDPS-asc-C5 *O*-benzyl ester **144** with benzyl bromide and sodium hydride. Next, the 4'-position of **142** was desilylated with TBAF and the resulting free 4'-hydroxy position of **145** was linked to the *N*-Cbz-protected

anthranilic acid by DMAP catalyzed Steglich esterification with 1-ethyl-3-(3-dimethylaminopropyl)carbodiimide hydrochloride to afford the fully protected aminobenzoate ascaroside **146** that was subsequently converted to the 4'-AB-asc-C5 (**34**) by palladium catalyzed hydrogenation in methanol.

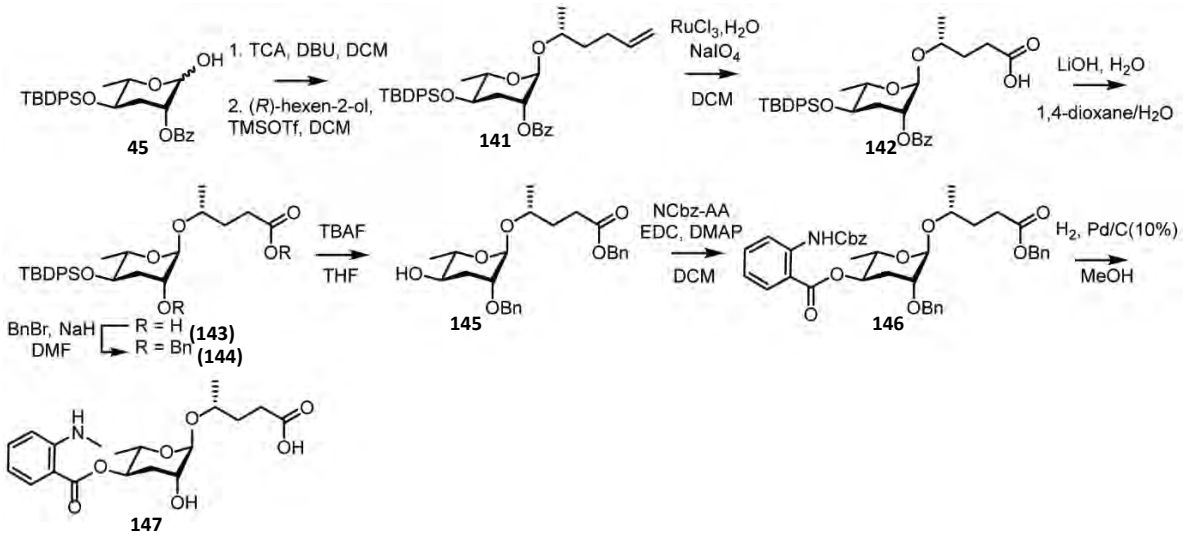

Figure 65: Attempted synthesis of 4'-AB-asc-C5.

Unfortunately, the comparison of the ^{1}H NMR of the resulting product with the isolated 4'-AB-asc-C5 (**34**) from *C. nigoni* did not match. Both compounds presented similar signals for the ascarylose unit and the aglycone (

Table 1**, Figure S7**) however, the chemical shifts of the aromatic protons of the anthranilic acid as well as the methyl group of the ascarylose moiety for the side product did not match with the corresponding signals of the isolated compound. Moreover, the synthetic material presented an additional deshielded singlet that accounts for three protons. Since the HR-MS/MS spectrum indicated a *m/z* of 380.1709 with a molecular formula of $C_{19}H_{27}NO_7$, combined with the signals in the ^{1}H NMR, the dominating product was identified as the *N*-methylated derivative of 4'-AB-asc-C5 **147**. The formation of **147** results from the presence of methanol as the solvent for the hydrogenation reaction, which leads to what is called the "borrowing hydrogen catalysis" or the "hydrogen auto transfer process" (**Figure 66**)[87]. During the deprotection of the anthranilic acid, the methanol present in the reaction was activated by the palladium to give formaldehyde. The resulting aldehyde then underwent condensation with the deprotected amino group of the anthranilic ester to afford the phenyl imine, which was subsequently reduced by hydrogenation to the methylamine product **147**.

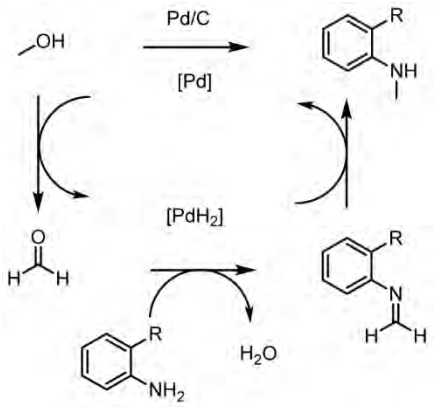

Figure 66: The borrowing hydrogen catalysis.

While the oxidation of terminal alkenes (**Figure 65**) provides an easy access to 4'-substituted-asc-C5 derivatives, it is less suitable for the synthesis of 2'-substituted ascarosides. Moreover, it does not provide a 2'-OH-ascaroside building block with the 4'-position and the acyl group orthogonally protected. Since 2-linked asc-C5 derivatives are commonly encountered among nematode ascarosides and this project also required an orthogonally protected 2'-OH-ascaroside building block, a different synthetic strategy was developed that permits the synthesis of both 4'- and 2'-substituted modular asc-C5 derivatives (**Figure 67**).

For this purpose, the (3*R*)-1-butenyl 2'-*O*-Bz-4'-*O*-TBDPS-ascaroside building block **148** was generated (**Figure 68**). The use of the (*R*)-buten-2-ol for the side chain permits the selective protection of either the 4- or the 2-position without altering the side chain, which can later be elongated to the five-carbon side chain of asc-C5 as well as the 6-carbon sidechains of C6MK and C6-OH via Grubbs metathesis.

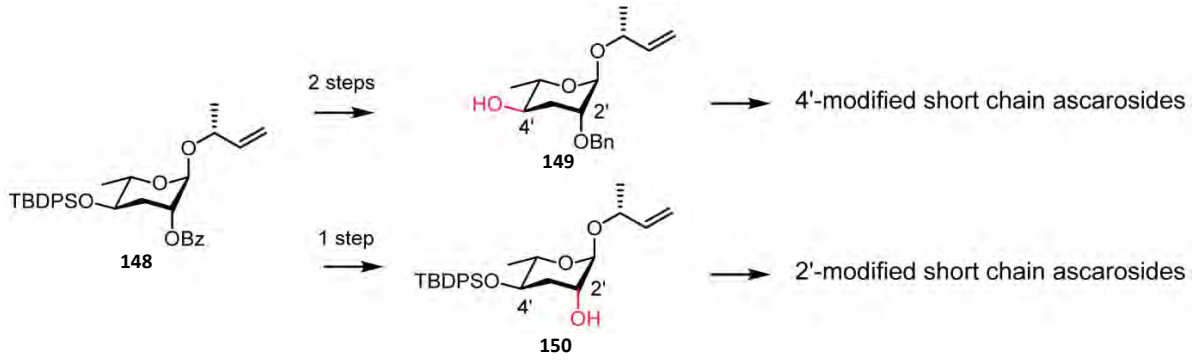

Figure 67 : The (3*R*)-1-butenyl-2'-*O*-Bz-4'-*O*-TBDPS-ascaroside building block 148 give access to 4'-and 2'-modified ascarosides.

For this alternative pathway the commercially available (*R*)-3-butyn-2-ol was glycosylated with the 2'-*O*-Bz-4'-*O*-TBDPS-ascarylose building block **45** via the trichloroacetimidate route[87b, c]. The terminal alkyne was selectively reduced to the corresponding terminal alkene **148** by catalytic hydrogenation with Lindlar's catalyst[88]. Alkaline hydrolysis of the 2'-*O*-benzoyl ester with lithium hydroxide solution

furnished the alkenyl ascaroside **150**. Next, the free 2'-hydroxyl group of **152** was protected as a *O*-benzyl ether with benzyl bromide and sodium hydride, and the 4'-position was desilylated with tetrabutylammonium fluoride. Cross metathesis of **149** with benzyl acrylate and Grubbs 2nd generation catalyst provided the *E*-configured 2'-*O*-Bn-asc-ΔC5-*O*-benzyl ester **153** in 65% yield. The resulting **153** was coupled to *N*-Cbz-protected anthranilic acid via DMAP catalyzed Steglich esterification with dicyclohexylcarbodiimide to afford the fully protected anthranilic acid ascaroside **154** in 35% yield. Next, a short hydrogenation with palladium on activated charcoal resulted in the reduction of the double bond and cleavage of the *O*-benzyl ether and *N*-carboxybenzyl protecting groups to furnish the 4'-AB-asc-C5 **34** in 41% yield along with *N*-methylated 4'-(*N*-methyl-AB)-asc-C5 **147** in 21% yield that could be separated by semipreparative HPLC.

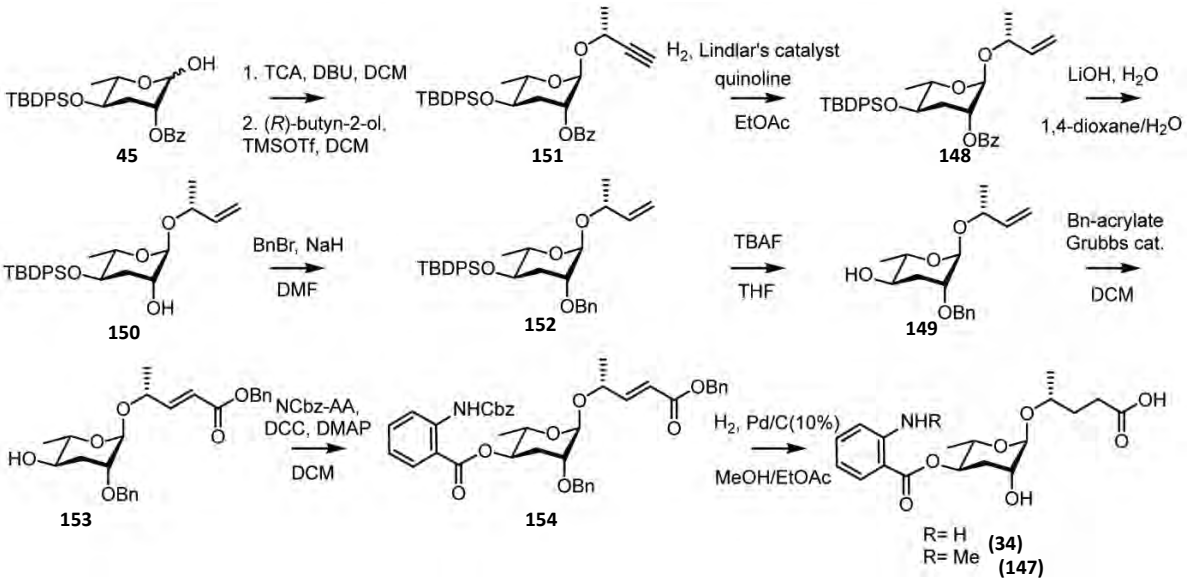

Figure 68: Synthesis of 4'-AB-asc-C5 via cross metathesis.

4.3. Confirmation of structure assignments

To confirm the structure assignment of 4'-AB-asc-C5 (abas#9, **34**) from *C. nigoni,* the ^{1}H NMR spectra as well as the chromatographic retention times of the natural and the synthetic compound were compared. The LC retention time of the natural 4'-AB-asc-C5 (**34**) was identical to those of the synthetic compound as shown by coinjection of a 1:1 mixture of natural and synthetic product (**Figure S8**). However, initially, the ^{1}H NMR spectra of the synthetic 4'-AB-asc-C5 (**34**) did not fully match those of the isolated natural product (**figure S9**,

Table 1). Indeed, the protons of the alpha-methylene group appeared as a single multiplet for the synthetic 4'-AB-asc-C5 (**34**), while the isolated 4'-AB-asc-C5 (**34**) exhibited two distinct multiplets for

the diastereotopic protons (**Figure 69**). Furthermore, the oxymethine proton (4-H) of the aglycone appeared less shifted in the isolated abas#9 (**34**) than in the synthetic one (**Figure 69**). These differences might possibly be explained by the differences in pH for both samples, which affects the dissociation of the carboxylic acid group and therefore influences the chemical shifts of the adjacent protons.

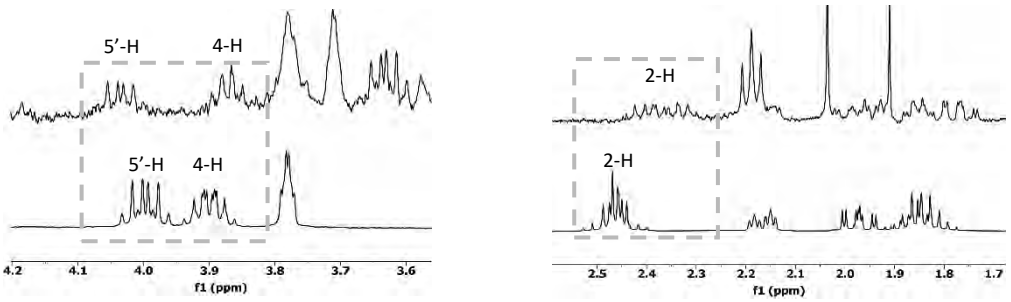

Figure 69 : Comparison of ^{1}H NMR spectra of the 1:1 mixture of natural asc-C7 (1) and 4'-AB-asc-C5 (34) and the synthetic 4'-AB-asc-C5 (34) in CD_3OD.

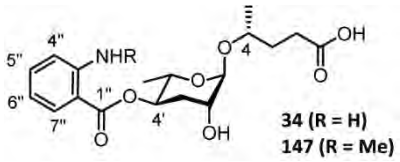

	isolated 4'-AB-asc-C5 (34)	synthetic 4'-AB-asc-C5 (34)	synthetic 4'-(*N*-Me-AB)-asc-C5 (147)
1'	4.74 br.s	4.74 br.s	4.74 br.s
2'	3.77 br.s	3.78 dd (3.9, 3.1)	3.78 dd (3.8, 3.0)
3'ax	1.98 ddd (13.8, 11.0, 2.97)	1.97 ddd (13.5, 11.1, 3.2)	1.97 ddd (12.9, 11.1, 3.0)
3'eq	2.18 ddd (4.8, 2.76)	2.17 ddd (13.5, 4.8, 3.9)	2.15 ddd (12.9, 4.7, 3.8)
4'	5.07 ddd	5.07 ddd (11.1, 9.7, 4.8)	5.06 ddd (11.1, 9.6, 4.7)
5'	4.04 dq	4.00 dq (9.7, 6.4)	4.00 dq (9.6, 6.2)
6'	1.20 d (6.7)	1.19 d (6.4)	1.184 d (6.2)
1	-	-	-
2_a	2.42 m	2.55-2.39 m	2.53-2.39 m
2_b	2.33 m		
3	1.90-1.84 m	1.93-1.77 m	1.93-1.78 m
4	3.87 m	3.90 m	3.90 m
5	1.18 d (6.2)	1.18 d (6.1)	1.18 d (6.1)
1''	-	-	-
2''	-	-	-
3''	-	-	-
4''	6.73 d	6.74 dd (8.4, 1.2)	6.71 d (8.6)
5''	7.23 dd	7.23 ddd (8.2, 7.1, 1.8)	7.38 ddd (8.6, 7.1, 1.7)
6''	6.57 dd	6.57 ddd (8.2, 7.1, 1.2)	6.57 dd (8.1, 7.1)
7''	7.78 d	7.77 dd (8.2, 1.8)	7.85 dd (8.1, 1.7)
8''	-	-	2.90 s

Table 1: 400 MHz ^{1}H NMR data of the isolated and the synthetic 4'-AA-asc-C5 (34) from *C. nigoni* and the synthetic 4'-(N-Me-AB)-asc-C5 (147) (in CD_3OD).

To confirm this hypothesis, an ^{1}H NMR of a mixture of the synthetic and the natural compound (3:1) was acquired by adding a small volume of the concentrated synthetic compound to the solution of the isolated material. When the synthetic 4'-AB-asc-C5 was measured under exactly identical conditions as the natural 4'-AB-asc-C5 isolated from *C. nigoni*, its ^{1}H NMR chemical shifts and H,H-coupling constants matched those of the natural product. The 5'-position of the ascarylose unit and the oxymethine proton (4-H) of the aglycone exhibit identical chemical shifts with the natural product (4.00 ppm and 5.07ppm) while the two diastereotopic protons of the aglycon at the 2-position exhibit two distinct multiplets at 2.42 ppm and 2.33 ppm as observed for the natural product. The chemical shifts of the aromatic signals from the aminobenzoate moiety were not affected. This indicates that the chemical shifts of the aminobenzoate ascaroside are influenced by the conditions of the sample (pH, salt content) and thereby confirms the results from the LC-MS analysis by demonstrating that the natural and synthetic 4'-AB-asc-C5 are identical.

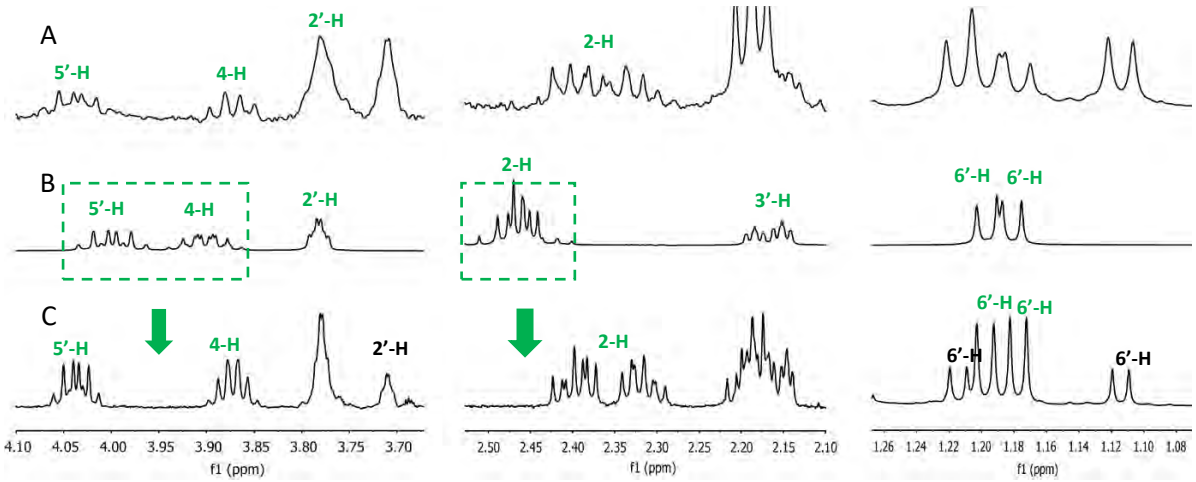

Figure 70 : Comparison of NMR spectra: (A) mixture of natural 4'-AB-asc-C5 (34) (green) and asc-C7 (black) from *C. nigoni* (measured at 400 MHz). (B) synthetic 4'-AB-asc-C5 (34) (measured at 400 MHz). (C) mixture of natural and synthetic (1/3) 4'-AB-asc-C5 (34) (measured at 600 MHz).

4.4. Functional characterization

The potential activity of 4'-AB-asc-C5 (abas#9, **34**) on nematode behavior was characterized in holding assays for amounts ranging from 10 pmol to 100 amol using gonochrostic *C. nigoni* JU1422 and hermaphroditic *C. tropicalis* JU1373. Since anthranilic acid ascarosides were detected in both male and female *C. nigoni* JU1422, the compound was tested on both sexes.

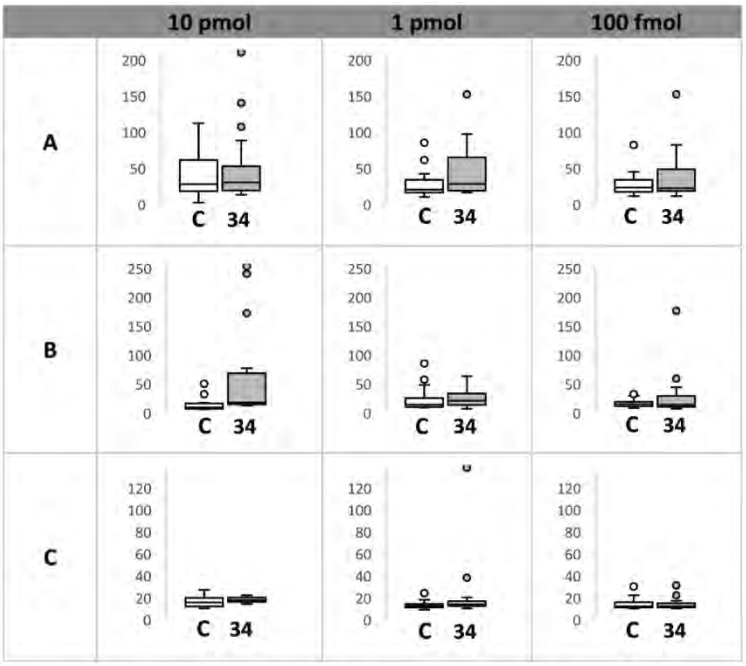

Figure 71 : Holding assays with 10 pmol to 100 fmol 4'AB-asc-C5 for female (A) and male (B) *C.nigoni* and hermaphroditic *C.tropicalis* (C).

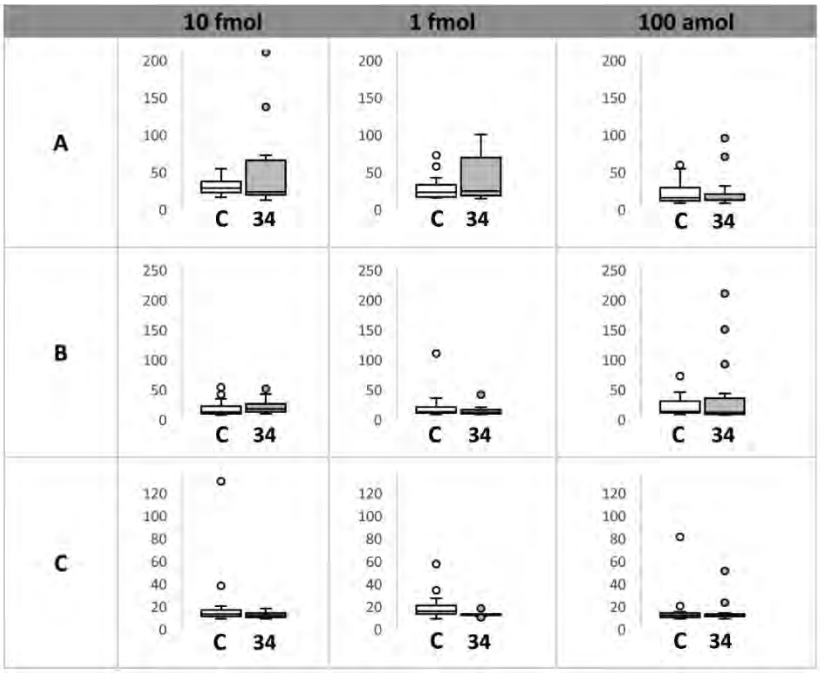

Figure 72 : Holding assays with 10 fmol to 100 amol 4'AB-asc-C5 for female (A) and male (B) *C.nigoni* and hermaphroditic *C.tropicalis* (C).

As depicted in **Figure 71** and **Figure 72** the hermaphroditic *C. tropicalis* did not respond to 4'-AB-asc-C5 (**34**) at any of the concentrations tested. Similarly, none of the female or male *C. nigoni* were retained by ecologically relevant amounts of anthranilic acid ascaroside. Male *C. nigoni* were retained by 10 pmol of 4'-AB-asc-C5 (**34**) (**Figure 71**), amounts that are considerably higher than those observed

in high density cultures, which might indicate that the worms can sense the compound, although they are not particularly attracted to it.

As mentioned previously for the urocanate ascarosides the lack of bioactivity in the holding assay can be a consequence of synergism between various aminobenzoate ascarosides since both *C. nigoni* and *C. tropicalis* produce mixtures of aminobenzoate ascarosides with different chain lengths. In addition, aminobenzoate ascarosides might react in synergism with other basic or modular ascarosides present in the *C. nigoni* or *C. tropicalis* exometabolome. Furthermore, the aminobenzoate ascarosides might regulate other biological functions that cannot be determined by holding assays. Recently, large quantities of aminobenzoate derivatives have been shown to be accumulated in the *C. elegans* gut granule including aminobenzoate glucoside (angl#1, **156**, **Figure 73**), which have been linked to the propagation of a blue fluorescent wave upon *C. elegans* death, but their exact physiological role is still unclear[89]. Moreover, the anthranilic acid moiety was also found in the satellite model organism *Pristionchus pacificus* as part of a pentamodular ascaroside pasa#9 (**157**, **Figure 73**), which acts as a dauer inducing pheromone[90]. Aminobenzoate ascarosides from *C. nigoni* and *C. tropicalis* might modulate biological responses other than behavior, and additional experiments are required to establish their biological function(s).

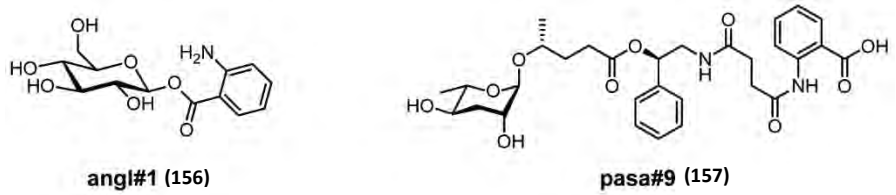

Figure 73 : Structure of the aminobenzoate glucoside angl#1 (156) and the pentamodular ascaroside pasa#9 (157).

The biogenesis of anthranilic acid (**26**) is well known and proceeds by the conversion of L-tryptophan (**25**) to the corresponding L-formyl kynurenine (**158**) by tryptophan 2,3-dioxygenase (TDO-2), which is then converted to kynurenine (**159**) by kynurenine formamidase and subsequently converted to the anthranilic acid (**26**) by kynureninase (FLU-2) (**Figure 74**). The corresponding genes have been identified in *Caenorhabditis* genomes[89b, 91].

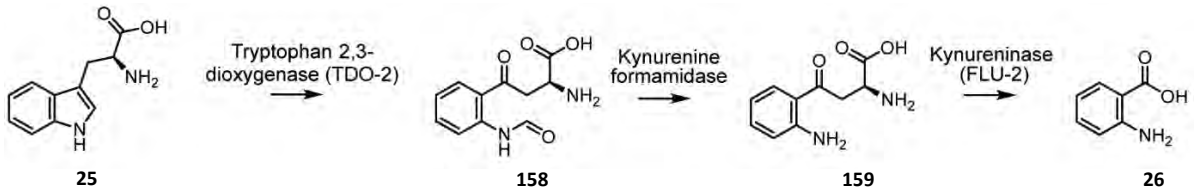

Figure 74 : Biosynthesis of anthranilic acid via the kynurenine pathway.

4.5. Conclusion

A new class of highly species-specific aminobenzoate ascarosides produced by *C. nigoni* and *C. tropicalis* was identified. The structure of the dominating component 4'-AB-asc-C5 (abas#9, **34**) carrying an anthranilic acid moiety at the 4'-position of the ascarylose unit was confirmed by total synthesis from L-rhamnose. 4'-AB-asc-C5 (**34**) was first synthesized via oxidation of the (*R*)-5-hexen-2-ol aglycone followed by attachment to the N-Cbz-protected anthranilic acid by Steglich esterification to give the fully protected aminobenzoate ascaroside **146**, which, after hydrogenation should have provided the 4'-AB-asc-C5 (**34**). However, the hydrogenation did not yield the expected product but instead the 4'-(*N*-methyl-AB)-asc-C5 **147** due to the palladium catalyzed oxidation of methanol to the more reactive formaldehyde. In a second attempt, the 4'-AB-asc-C5 **34** was synthesized via cross metathesis of (*R*)-3-buten-2-ol side chain with benzyl acrylate and subsequent hydrogenation in a mixture of ethyl acetate and methanol. Despite the different signals in ^{1}H NMR for the side chain in the natural and the synthetic 4'-AB-asc-C5 (**34**), the structure assignment of the target compound was finally confirmed by analyzing the NMR of the mixture of the natural and the synthetic product, which, together with comparative LC-MS analysis, confirms the molecular structure of **34** isolated from *C. nigoni*.

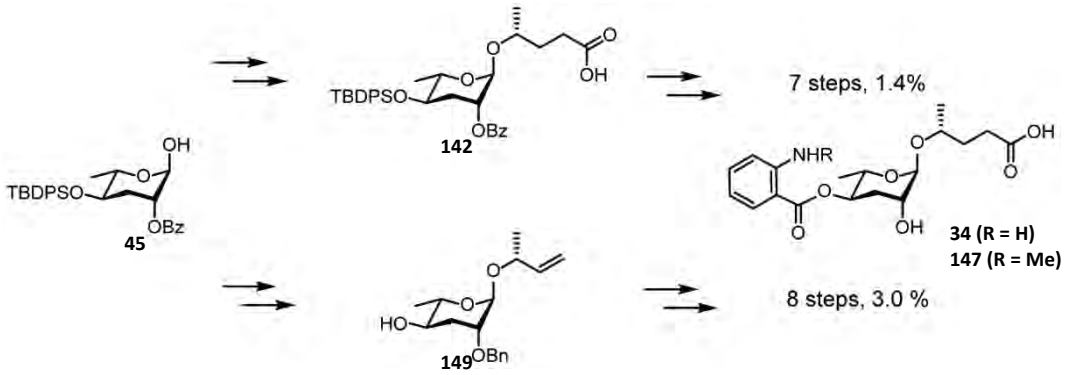

Figure 75 : Two different pathways for the synthesis of 4'-AB-asc-C5 (34).

Although their biological functions were not elucidated, the aminobenzoate ascarosides translate the availability of L-tryptophan, an essential amino acid for nematodes, into a species-specific signal and shows the importance of this food derived amino acid in nematode chemical communication. In fact, there are two families of modular ascarosides that are directly dependent on the availability of L-tryptophan: icas and abas via the indole-3-carboxylate and the kynurenine pathway, respectively.

5. The caenorhabdoside cae-7OH-ΔC9 (caen#1)

Almost all nematode signaling molecules identified so far are glycosides based on the 3,6-dideoxyhexose L-ascarylose. Since the discovery of the first dauer pheromone, hundreds of ascarosides have been identified from diverse nematode species, and all are based on the L-ascarylose sugar. An unexpected exception is the identification of the paratosides, which are 2-epimeric ascarosides produced by *Pristionchus pacificus*[12b] that regulate dauer formation. Recently, using a combination of GC-EIMS screening of the TMS-derivatized *C. nigoni* exometabolome and HPLC-ESI-(-)-MS/MS precursor ion screening, Dong et al. described a new series of species-specific hydroxylated ascarosides including asc-7OH-ΔC9 (**17**)[11a], the structures of which were confirmed by total synthesis. Along with this series of hydroxylated ascarosides, HPLC-MS analysis suggested the presence of one additional hydroxylated glycoside, cae-7OH-ΔC9 (caen#1, **39**, **Figure 76.B**)[92] that carries an unprecedented 4-*epi*-ascarylose *lyxo* configuration. Comparative MS analysis of twelve *Caenorhabditis* species revealed that glycosides based on the 3,6-dideoxy-*lyxo*-hexose, as well as side chain hydroxylated ascarosides, are highly specific for *C. nigoni*, although they were also detected in *C. afra,* a distantly related species (**Figure 76**).

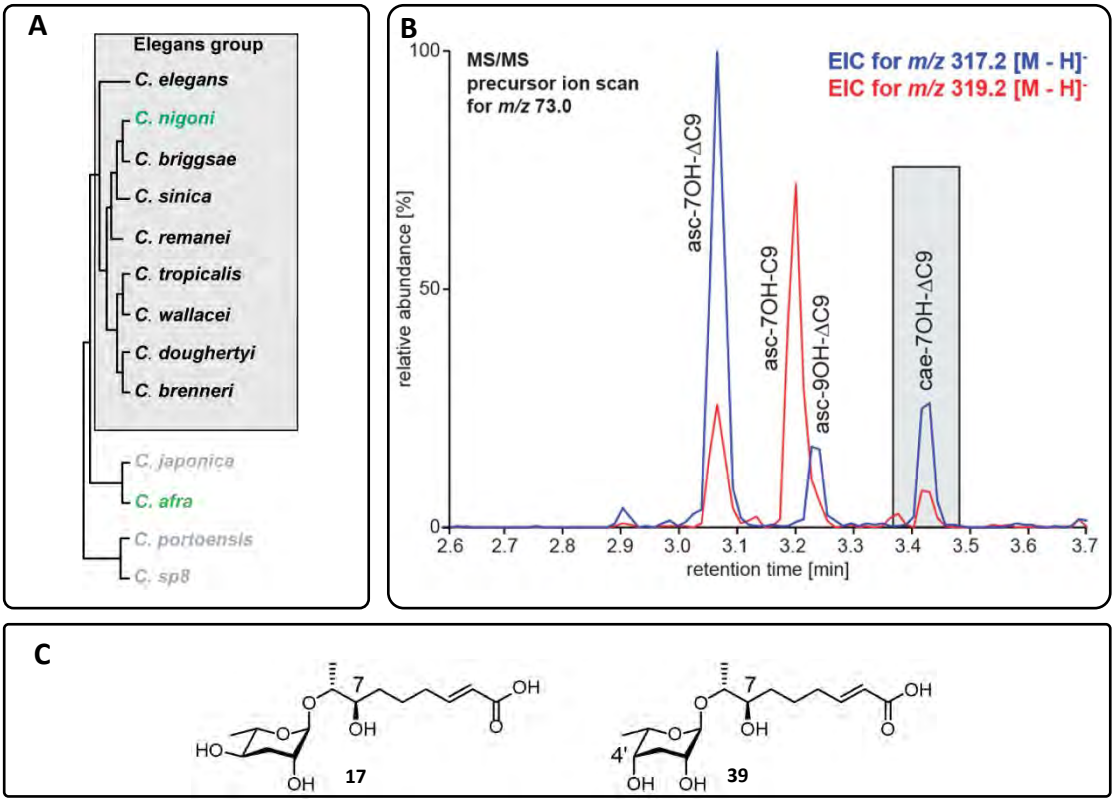

Figure 76. A. Phylogenetic tree of analyzed *Caenorhabditis* species. The nematode species producing cae-7OH-ΔC9 (39) are marked in green; B. Detection of hydroxylated ascarosides in the *C. nigoni* exometabolome using the HPLC-ESI-(–)-MS/MS precursor ion screen[92]; C. Structure of asc-7OH-ΔC9 (17) and cae-7OH-ΔC9 (39) identified in the *C. nigoni* exometabolome[11a].

5.1. Identification of cae-7OH-ΔC9

The target compound was isolated from the *C. nigoni* exometabolome extract as a 1 : 1 mixture with coeluting asc-C7 (ascr#1, **1**) using a combination of reverse phase C18 chromatography and semipreparative RP-C18-HPLC. The analysis of the HR-MS spectra indicated that this new compound has the molecular formula $C_{15}H_{26}O_7$ (found *m/z* 317.1603 $[M - H]^-$) identical to the asc-7OH-ΔC9 (**17**)[11a], while the analysis of the HR-MS/MS spectra showed evidence for an hydroxynonenoic acid aglycone (**Figure 77**) due to the presence of the fragment ion at *m/z* 187.0980 $[C_9H_{15}O_4]^-$ (**161**) from the loss of the sugar unit.

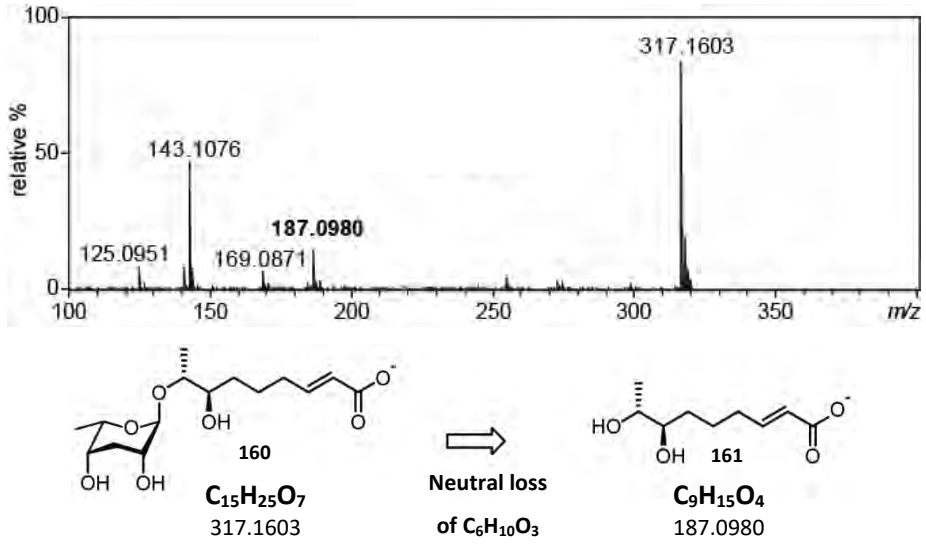

Figure 77. ESI-(-)-HR-MS/MS spectrum of cae-7'OH-ΔC9 (39) from *C. nigoni*[92].

By comparing the NMR data of the enriched fraction with those of asc-C7 (**1**, **Figure 4**) the NMR signals for the new compound (**Figure S10 & Figure S11**) were deduced. The analysis of the one- and two-dimensional ^{1}H NMR spectra showed a H,H-coupling correlation between a terminal methyl at 1.15 ppm (*d*, $^3J_{8,9}$ = 6.3 Hz) and an oxymethine at 3.75 ppm (*dq*, $^3J_{8,9}$ = 6.3 Hz, $^3J_{7,8}$ = 3.9 Hz). The *dqf*-COSY also displayed a correlation between the oxymethine and another hydroxymethine proton at 3.52 ppm (*m*), which suggested that the aglycone was (ω - 1) linked to the ascarylose and (ω - 2)-hydroxylated like the asc-7OH-ΔC9 (**17**) (**Figure 78**, **Figure S12 & Figure S13**). Furthermore, the vinylic proton 2-H appeared at 5.82 ppm as a doublet ($^3J_{2,3}$ = 15.6 Hz) from the trans coupling interaction with the vinylic proton 3-H at 6.91 ppm. Only the H-3 showed a correlation with both a vinylic and an aliphatic proton ($^3J_{3,2}$ = 15.6 Hz, $^3J_{3,4}$ = 7.0 Hz), which confirmed that the target compound carries an α,β-unsaturated ΔC9 side chain. Then, to establish the configuration of the (ω-2)-hydroxymethine group, the NMR spectra of the natural product was compared with those of the previously synthesized standards of *erythro* and *threo*-asc-7OH-ΔC9 (**162** and **17**)[11a]. The 7-H and 8-H of **39** exhibit similar

chemical shifts and coupling constants ($^3J_{7,8}$ = 3.9 Hz) as the *threo*-asc-7OH-ΔC9 (**17**), thus suggesting a *threo*-configuration for the (ω-2)-hydroxylated aglycone (**Figure 78**, **Figure S14**)[11a].

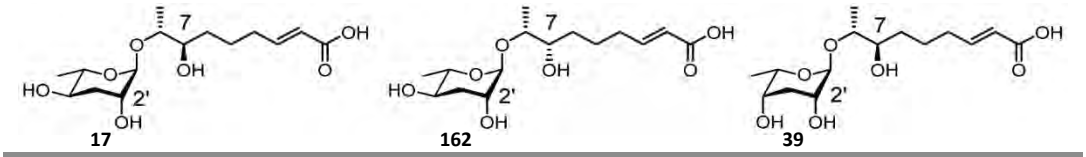

	***threo*-asc-7OH-ΔC9[11a] (17)**	***erythreo*-asc-7OH-ΔC9[11a] (162)**	**cae-7OH-ΔC9 (39)**
1'	4.65 s	4.66 s	4.78 s
2'	3.75 br.s	3.75 br.s	3.58 br.s
3'ax	1.80 ddd (13.1, 11.0, 3.0)	1.80 ddd (13.1, 11.1, 3.0)	2.06 dt (14.3, 3.1)
3'eq	1.95 dt (13.1, 3.8)	1.95 (13.3, 3.7)	1.93 ddt (14.3, 1.0, 3.5)
4'	3.52 ddd (11.3, 9.3, 4.3)	3.52 m	3.57 br.s
5'	3.64 dq (9.3, 6.2)	3.63 dq (9.5, 6.2)	3.99 dq (6.6, 1.0)
6'	1.22 d (6.2)	1.22 d (6.2)	1.18 d (6.6)
1	-	-	-
2	5.82 d (15.6)	5.82 d (15.5)	5.82 dt (15.6, 1.5)
3	6.95 dt (15.6, 7.0)	6.96 dt (15.5, 7.1)	6.91 dt (15.6, 7.0)
4	2.27 m	2.27 m	2.26 m
5	1.54-1.68 m	1.65 m	1.70 m
5			1.62-1.45 m
6	1.48-1.62 m	1.54 m	1.62-1.45 m
6		1.43 m	
7	3.53 m	3.53 m	3.52 m
8	3.74 dq (3.9, 6.2)	3.66 m	3.75 qd (6.3, 4.1)
9	1.14 d (6.2)	1.15 d (6.2)	1.15 d (6.3)

Figure 78. 400 MHz ^{1}H NMR data of the synthetic *threo* (17) and *erythreo* asc-7OH-ΔC9 (162) and isolated cae-7OH-ΔC9 (39) from *C. nigoni* (in CD_3OD)[92].

Since the LC-MS and the NMR spectra showed that asc-7OH-ΔC9 (**17**) and cae-7OH-ΔC9 (**39**) are two different compounds, we reevaluated the stereochemistry of the 3,6-dideoxyhexose sugar based on chemical shifts and coupling constants (**Figure 79**). This dideoxy sugar is characterized by a quartet multiplicity for H-5 with a coupling constant of $^3J_{5,6}$ = 6.7 Hz, instead of a *dq* signal with $^3J_{5',4'}$ = 9.3 Hz and $^3J_{5',6'}$ = 6.3 Hz commonly observed for the ascarylose unit, indicating a small vicinal coupling between 5'-H and 4'-H. Moreover, both diastereotopic 3'-H protons exhibit a small vicinal coupling constant (^3J = 3.5 Hz and ^3J = 3.1 Hz) with both 4'-H and 2'-H, which, for 3'$_{eq}$-H was consistent with a gauche interaction with 4'-H but for 3'$_{ax}$-H did not correspond to an antiperiplanar-relationship commonly seen for the ascarylose (**Figure 79**). Therefore, these results indicated that the target compound cae-7OH-ΔC9 (**39**) is composed of a 3,6-dideox-*lyxo*-hexose unit linked to a (ω - 2)-hydroxylated α,β-unsaturated nonenoic acid aglycone. This represent the first description of a natural 3,6-dideoxyhexose with a *lyxo*-configuration and due to its occurrence in only two *Caenorhabditis* species, *C. nigoni* and *C. afra*, this novel sugar called caenorhabdose.

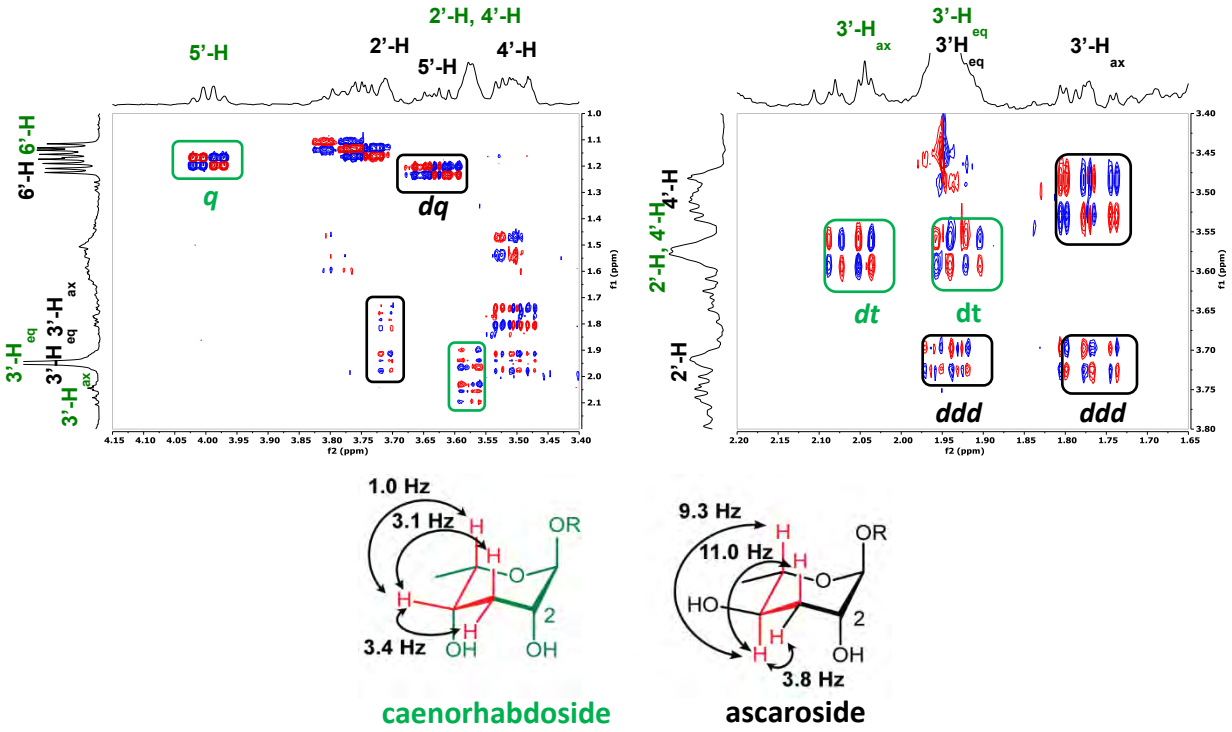

Figure 79. Sections of the 400 MHz *dqf*-COSY of a cae-7OH-ΔC9 (39) and asc-C7 (1) mixture isolated from the *C. nigoni* exometabolome.

5.2. Synthesis of cae-7OH-ΔC9

In order to synthesize the 3,6-dideoxy-*lyxo*-hexose building block from commercially available L-rhamnose, a synthetic pathway that permits the inversion of the configuration at the 4-position of the sugar as well as the deoxygenation of the 3-position was required. A number of examples using epoxides as intermediates for the synthesis of deoxysugars have been described by Baer et al[93]. Among them, the authors describe the synthesis of the 1-*O*-methyl-3,6-dideoxy-*lyxo*-hexose via hydride mediated epoxide ring opening of the 3,4-anhydro-1-*O*-methyl-6-dideoxy-*lyxo*-hexopyranoside[93b]. The deoxygenation of **168** was achieved via intramolecular nucleophilic substitution according to Zunk's procedure[94]. By combining Zunk and Baer's synthetic pathways, the L-2,4-di-*O*-benzoyl-caenorhabdose **170** was prepared in 1% yield over 8 steps as depicted in **Figure 80**. First, L-rhamnose (**45**) was converted to an α/β mixture of the 1-*O*-benzyl-rhamnosides **163**, which were later separated after conversion of the 2,3-positions to the corresponding isopropylidene ketal **164**. After formation of the triflate ester **165**, the isopropylidene ketal was hydrolyzed under acidic conditions to give the triflate **166** in moderate yields (33 - 59%), due to partial decomposition of **166** during column chromatography. Attempts to improve the yield by replacing the triflate with a tosylate group were unsuccessful as the subsequent hydrolysis of the 1-*O*-benzyl-2,3-isopropylidene-4-*O*-tosyl-rhamnoside **171** gave only 40% of the 1-*O*-benzyl-4-*O*-tosyl-rhamnoside **172** but generated about 20%

of the 1-*O*-benzyl-rhamnoside **163** (**Figure 81**).

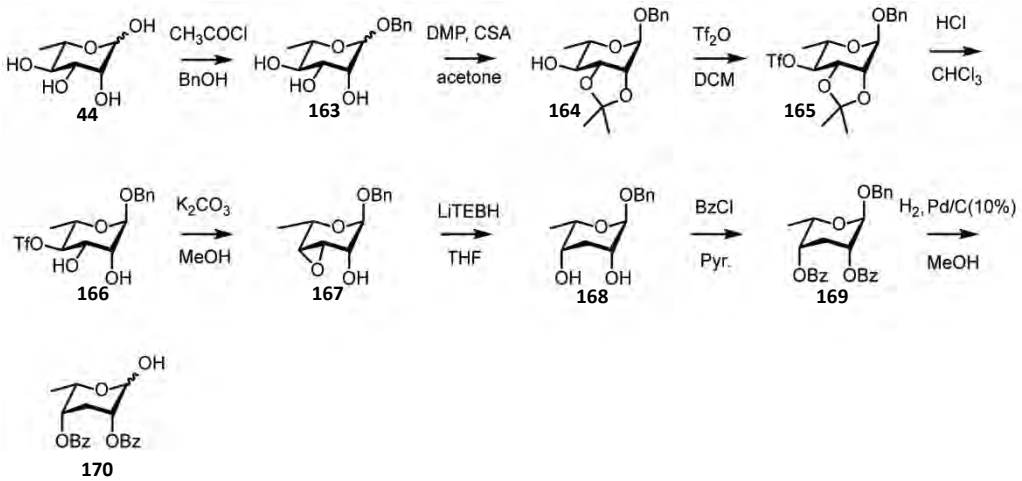

Figure 80. Synthesis of the caenorhabdose 170.

Figure 81. Product of the hydrolysis of the tosyl-rhamnoside 171.

The 1-*O*-benzyl-4-*O*-triflate-rhamnoside **166** was cyclized by nucleophilic substitution of the triflate under basic conditions to give the oxirane **167**. Then, the reductive ring opening of **167** furnished the expected Fürst Plattner product **168** [75], along with minor quantities of the 1-*O*-benzyl-4,6-dideoxy-L-*lyxo*-hexopyranoside **173** with a ratio of 28 to 1, respectively. The regioselectivity is explained by the stability of the chair conformation of the transition state upon attack on the 3-position in contrast to the twisted boat conformation required upon attack on the 4-position (**Figure 82**). Cuccarese et al. reported a procedure for the epoxide ring opening using LAH, but this method yielded only 20% of **168** instead of 81% reported in the literature[95]. The use of a stronger reducing agent, the lithium triethylborohydride (LiTEBH) as described by Baer et al[93b], provided **168** in 75% yield. The stereochemistry of the resulting 1-*O*-benzyl-3,6-dideoxy-*lyxo*-hexose (**168**) was confirmed by NMR. The small coupling constant between H-5 and H-4 for the major α-anomer ($^3J_{4,5}$ = 1.3 Hz) was consistent with a dihedral angle of about 60° between the two protons.

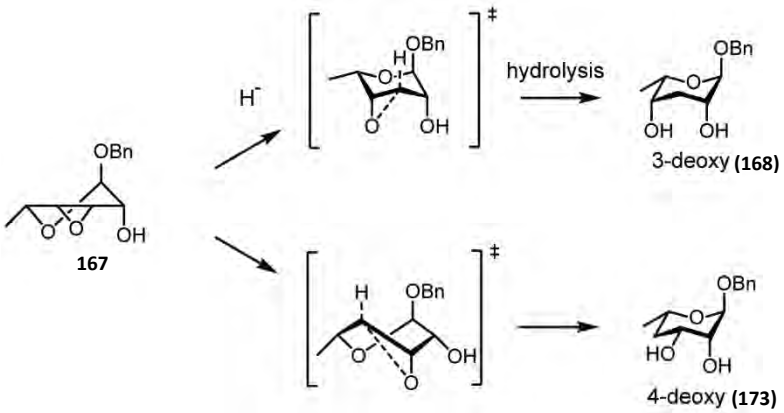

Figure 82. Different pathway for the epoxide opening of 167.

168 was finally 2,4-dibenzoylated to the diester **169** and the anomeric position deprotected via palladium catalyzed hydrogenation to furnish the L-2,4-di-*O*-benzoyl-3,6-dideoxy-*lyxo*-hexose (**170**) as a 7:3 mixture of the α- and the β-isomers.

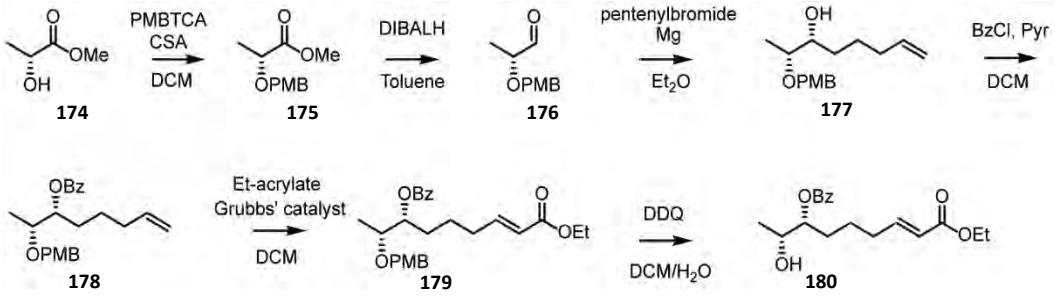

Figure 83. Synthesis of (7R,8R,2E)-*threo*-ethyl-7-benzoyloxy-8-hydroxy-2-nonenoate (180).

The aglycone was synthesized in 9.5% yield over six steps starting from the commercially available (+)-(*R*)-methyl-D-lactate via a Cram chelate controlled nucleophilic addition[96] to introduce the stereocenter at C-7 as previously described by Dong *et al.* (**Figure 83**)[11a]. First, the (+)-(*R*)-methyl-D-lactate **174** was protected as a PMB ether **175** and reduced to the corresponding aldehyde **176** with DIBALH. Then, the PMB-aldehyde **176** reacted with 4-pentenyl magnesium bromide to furnish the *threo*-configured 2-*O*-PMB-3-hydroxy-oct-7-ene **177** in 55% of yield with a diasteromeric excess of *de* > 92%. The preference towards the formation of the 7,8-*syn*-diol is based on the Cram-chelate complex depicted in **Figure 84** that favors addition from the sterically less hindered side.

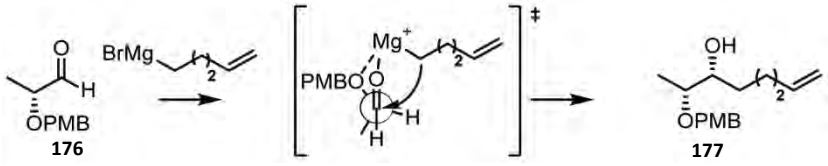

Figure 84: Stereoselective synthesis of the aglycone 175 via asymmetric induction to provide the *syn* alcohol 177 as the major product.

After benzoylation of **177**, cross-metathesis of **178** with ethyl acrylate using Grubbs 2nd generation catalyst provided only the thermodynamically preferred (*E*)-configured nonenoate ester **179** in 89% yield, which was converted to the final aglycone **180** upon selective oxidative cleavage of the PMB ether with 2,3-dichloro-5,6-dicyano-*p*-benzoquinone. Glycosylation of the aglycone **180** with the L-2,4-di-*O*-benzoyl-3,6-dideoxy-*lyxo*-hexose **170** via the trichloroacetimidate route[78] followed by alkaline hydrolysis furnished the target compound, cae-7OH-ΔC9 **39** with an overall yield of 15%.

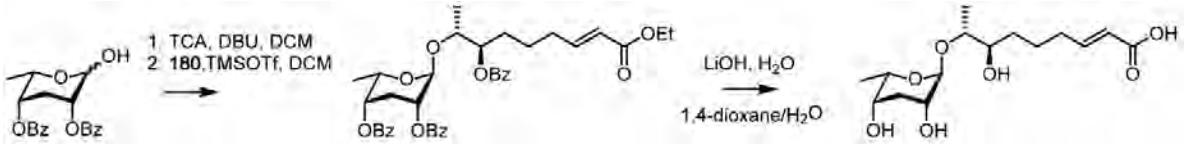

170 **181** **39**

Figure 85. Synthesis of cae-7OH-ΔC9 (39) via Schmidt glycosylation.

5.3. Confirmation of structure assignment

To confirm the *lyxo*-configuration of cae-7OH-ΔC9 from *C. nigoni*, the ^{1}H NMR spectra of synthetic cae-7OH-ΔC9 was compared with those of the 1:1 mixture of asc-C7 and cae-7OH-ΔC9 (**Figure 86**, **Figure S15**. Both natural cae-7OH-ΔC9 and the synthetic sample exhibit identical chemical shifts and multiplicities, especially for the 5- and the 4-position of the 3,6-dideoxysugar (**Figure 86**), which confirms the *lyxo*-configuration of the sugar unit. Similarly, the ^{1}H NMR signals for the side chain are the same for both samples. Only the vinylic proton 3-H displayed an upfield chemical shift compared to the natural product, which is due to the differences in pH values for both samples[85]. Moreover, both compounds exhibited identical retention times and molecular masses upon LC-MS analysis (**Figure S16**), which confirms the structure assignment of cae-7OH-ΔC9 identified in *C. nigoni.*

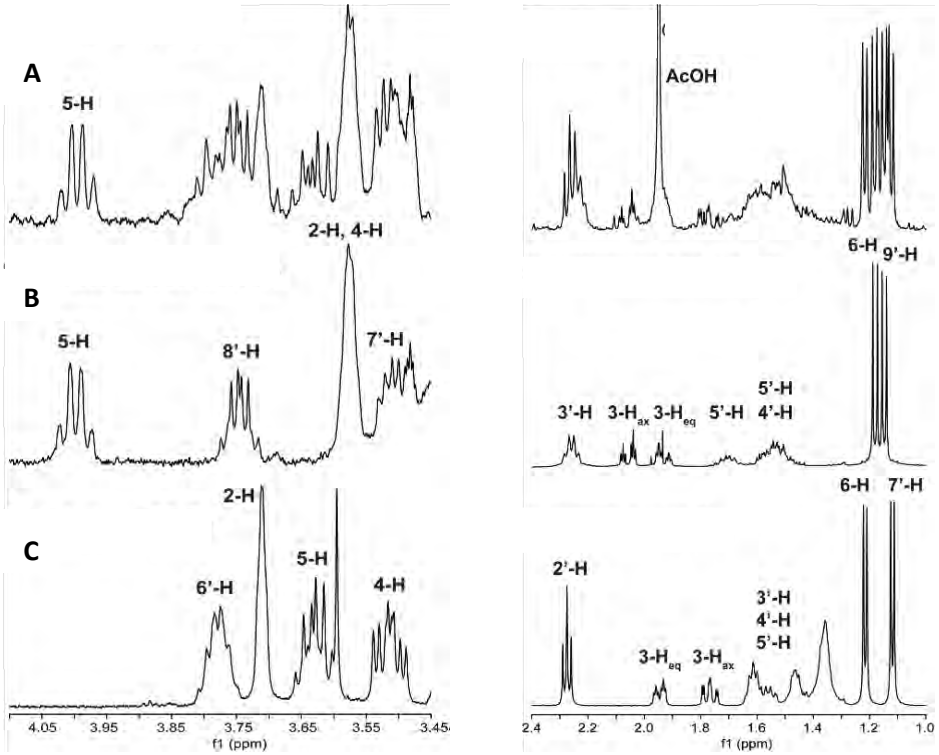

Figure 86. Comparison of ^{1}H NMR spectra of (A) the 1:1 mixture of natural asc-C7 (1) and cae-7OH-ΔC9 (39) and (B) the synthetic cae-7OH-ΔC9 (39) and (C) synthetic asc-C7 (1) in CD_3OD[92].

5.4. Biogenesis

Until the identification of the caenorhabdoside (39) from the nematode *C. nigoni*, only 3,6-dideoxy sugars with *arabino*, *xylo* or *ribo* configuration have been identified in natural products (

Figure 15). The caenorhabdoside 39 represents the first example of a natural compound carrying a 3,6-dideoxy-*lyxo*-hexoses. Therefore, the mechanism underlying the biosynthesis of the caenorhabdose building block is of particular interest. While the biosynthesis of L-ascarylose in bacteria is well known [35, 97] the detailed mechanism behind the biosynthesis of L-ascarylose in nematodes remains enigmatic. It has been reported that the nematodes are producing the sugar moiety endogenously and some studies are in favor for a de novo synthesis of the ascarylose[28, 36]. Additionally, the lack of several genes responsible for the production of ascarylose in bacteria suggests that the biosynthetic pathway to generate ascarylose in nematodes is significantly different from the pathway in bacteria[35b, 98].

Due to the high specificity of the caenorhabdose building block for the 7OH-ΔC9 side chain, the 3,6-dideoxy-*lyxo*-hexose was hypothesized to originate directly from the corresponding ascaroside. The careful analysis of the LC-MS data of the enriched SPE fractions of the *C. nigoni* exometabolome did not show any evidence for precursor molecules of caenorhabdoside cae-7OH-ΔC9 (**39**). No long chain caenorhabdoside precursors, and, despite the abundance of asc-ΔC9 (**3**) as the putative precursor of

asc-7OH-ΔC9 (**17**)[11a], no evidence for the 4-epimeric asc-ΔC9 was observed (**Figure S17**). Moreover, no additional hydroxylated ascaroside (7OH-C9 or 9OH-ΔC9) bearing a 4'-epimerization was detected (**Figure S17**). Taken together, these results demonstrate that the 4'-epimerization is highly specific for the 7OH-ΔC9 aglycone and that it most likely occurs downstream of the conserved peroxisomal β-oxidation cycle and species-specific side-chain hydroxylation as depicted in **Figure 87**. Similarly, LC-MS analysis of the *P. pacificus daf-22* mutant has not been reported to reveal any long chain L-paratoside precursors[99], which suggests that, like the caenorhabdoside cae-7OH-ΔC9 (**39**), the paratoside par-C5 (**183**) most likely originates from the corresponding asc-C5 (**182**) via the epimerization of the 2-position downstream of the β-oxidation cycle (**Figure 87**). However, unlike the cae-7OH-ΔC9 (**39**), the presence of paratoside-based modular metabolites such as npar#1 (**24**) suggests that the epimerization in *P. pacificus* might precede the modular attachment of additional building block.

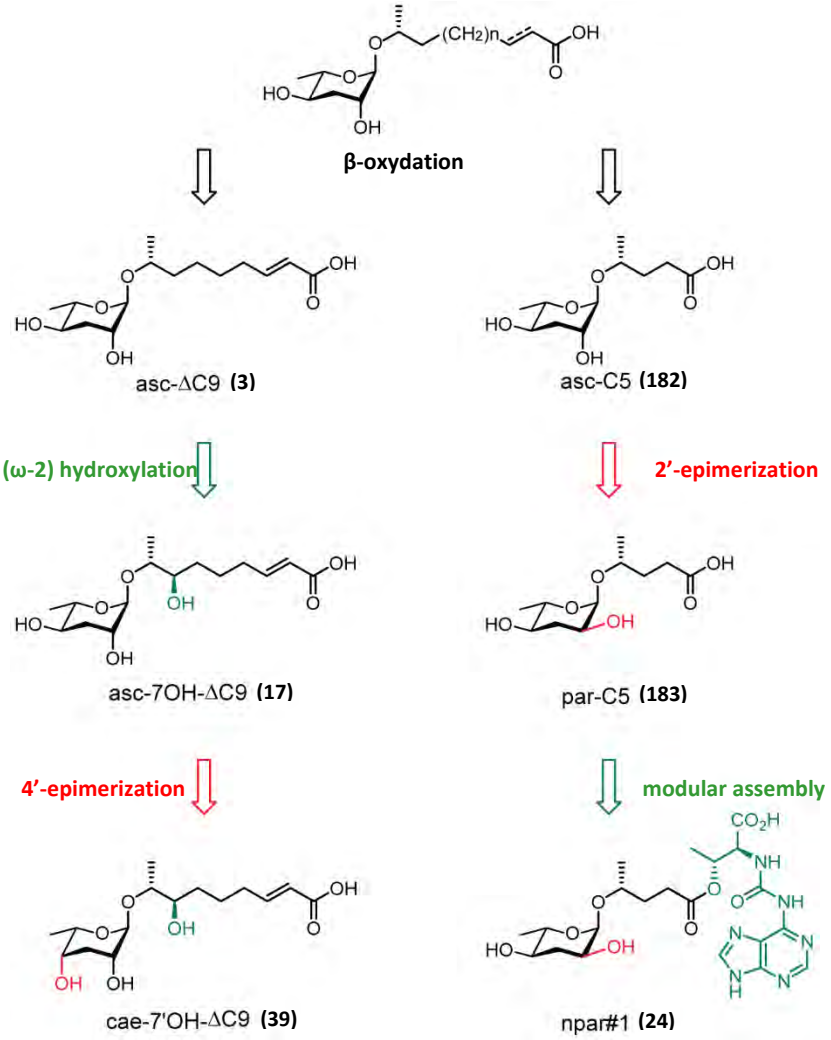

Figure 87. Postulated biosynthesis of highly species-specific signaling molecules in the nematodes *C. nigoni* and *P. pacificus* based on epimerization of the L-ascarylose building block downstream of the β-oxidation cycle.

5.5. Conclusion

A novel epimeric ascaroside-type glycolipid with an unprecedent *lyxo*-configuration was identified two more distantly related species of the *Caenorhabditis* genius, *C. nigoni* and *C. afra*. The structure assignment of the novel 3,6-dideoxy-*lyxo*-glycoside was unambiguously established by a 16 steps convergent synthesis from the commercially available L-rhamnose and methyl-D-lactate. The 3,6-dideoxy-*lyxo*-hexose (caenorhabdose) core **54** of cae-7OH-ΔC9 (**39**) was successfully synthesized by converting L-rhamnose to its corresponding epoxide **167** by nucleophilic substitution followed by deoxygenation the 3-position by regioselective epoxide ring opening. The aglycon was obtained via the Cram-chelate complex-mediated nucleophilic addition of the 2-benzyloxy aldehyde **176** to afford the *threo* alcohol intermediate **177**, which subsequently provided the *threo*-configured side chain **180**. The comparison of the analytic data for the synthetic cae-7OH-ΔC9 (**39**) and the enriched natural product from *C. nigoni* unambiguously established the structure assignment of this novel ascaroside.

The discovery of the cae-7OH-ΔC9 in nematodes represents the first identification of a natural product carrying a 3,6-dideoxy-*lyxo*-hexose. While the biosynthesis of the ascarylose unit in nematodes remains enigmatic, the biosynthesis of the caenorhabdose was hypothesized to derive from the ascarylose unit based on the high specificity of the sugar for the 7OH-ΔC9 chain. The enzymes capable of catalyzing the epimerization of nonactivated sugars in bacteria and their biosynthetic pathways are well understood[100] but the enzyme responsible for the 4-epimerization of the ascarylose remains to be identified. The results from the MS screening allowed us to propose a model for the biosynthesis of this 4-epimeric ascaroside-type glycolipid in *C. nigoni.* The LC-MS data, which do not show evidence for any non-hydroxylated short or long chain caenorhabdoside precursor, suggest that the epimerization might occur at the very end of the biosynthetic pathway.

The caenorhabdoside did not elicit any biological activity during holding bioassays with male or female *C. nigoni* JU1422, either individually or in combination with asc-7OH-ΔC9 (**17**). Additional bioassays are required in order to decipher its potential bioactivity. Nevertheless, the identification of highly specific-specific epimeric ascaroside-type glycolipids in *C. nigoni, C. afra* and *P. pacificus* demonstrates how nematode can utilize epimerization of the sugar moiety as an additional mechanism to generate species-specific signaling components.

6. Oligomeric Ascarosides

The large structural and functional diversity of nematode ascaroside signals arises from diverse modifications of basic ascarosides. These modifications include side-chain modifications, modular attachment of additional building block (**Chapter 3 & 4**) or epimerization of the ascarylose unit (**Chapter 5**) and are highly species-specific.

In 2012, Bose et al. provided the first evidence for the presence of a homodimeric ascaroside called dasc#1 in which two asc-C7 molecules are connected via an ester bond and the 4-position of the ascarylose sugar (abbreviated 4'-(asc-C7)-asc-C7, **23**, **Figure *10***), a metabolite that controls mouth form dimorphism in *Pristionchus pacificus*[12b]. Later, some highly specific male attractants 4'-(asc-C4)-asc-C5 (**185**) in *C. remanei* and 2'-(asc-C6)-asc-C5 (dasc#6, **184**) from *C. nigoni* (**Figure 88.C**) were identified and it was shown that additional species-specific homo and heterodimeric ascarosides are prominent in *Caenorhabditis* spp.[12a] (**Figure 88.A & B**) and *Pristionchus* spp.[101], which demonstrates that dimerization of conserved ascaroside building blocks is an important mechanism used by nematodes to generate species-specific signaling molecules.

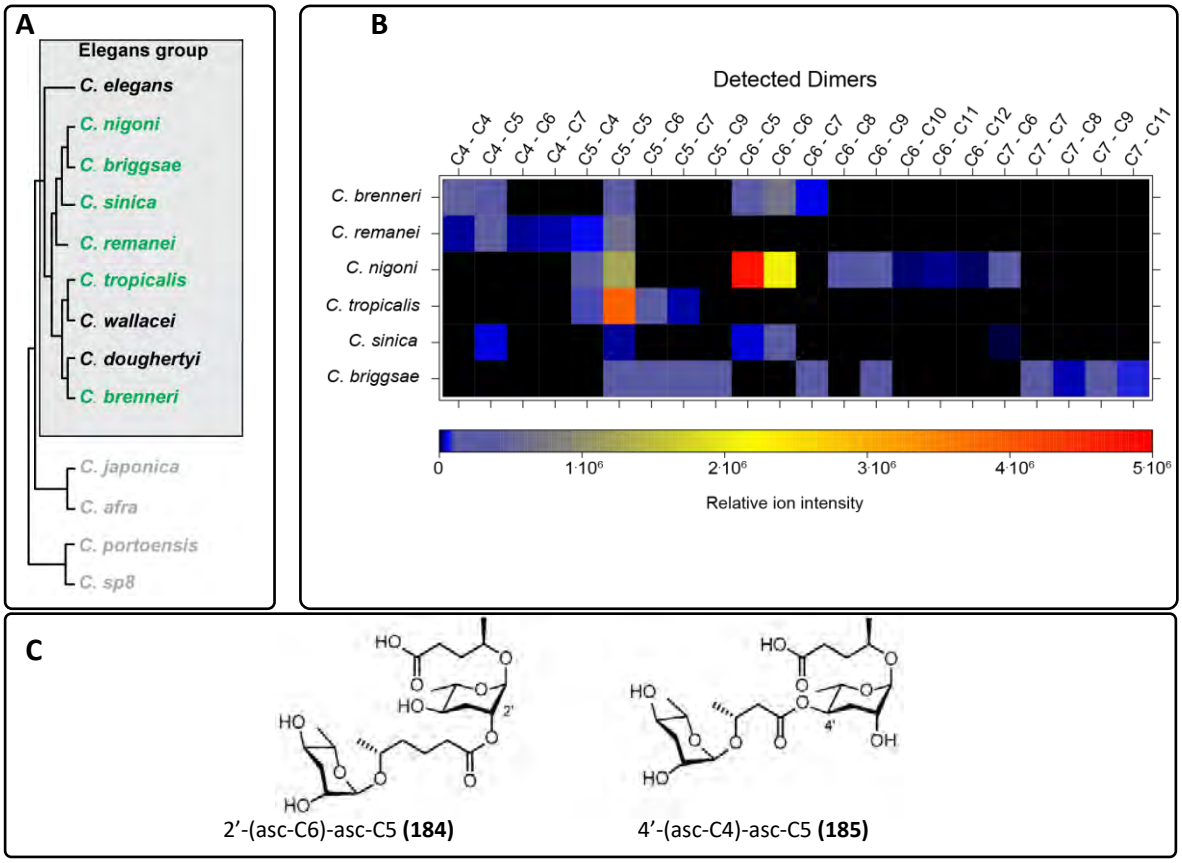

Figure 88 : (A) Phylogenetic tree of analyzed *Caenorhabditis* species. The nematode species producing dimeric ascaroside are marked in green. (B) Relative ion abundance of dimeric ascarosides produced by *Caenorhabditis* species[102]. (C) Chemical structures of 2'-(asc-C6)-asc-C5 (184, dasc#6) from *C. nigoni* and 4'-(asc-C4)-asc-C5 (185) from *C. remanei*.

The molecular structures of the dimeric ascarosides were elucidated by a combination of NMR spectroscopic and MS spectrometric techniques. The analysis of the LC-ESI-(+)-MS/MS fragmentation of this new class of ascarosides highlighted two characteristic fragments corresponding to the loss of the terminal side chain (the aglycone) and the cleavage of the ester bond, which facilitate the assignment of monomeric units and their order of assembly. Furthermore, the *dqf*-COSY spectrum, when available, can differentiate 2- and 4- linked dimers. For example, the LC-ESI-(+)-MS/MS spectrum of 4'-(asc-C4)-asc-C5 (**185**) from *C. remanei* shows a fragment with *m/z* of 347.1718 ($[C_{16}H_{27}O_8]^+$, **189**) from the loss of the C5 side chain therefore revealing the head and the terminal ascaroside as being (asc-C4)-asc-C5, respectively. Subsequent analysis of the *dqf*-COSY spectrum showed a deshielded 4-position, indicating that the dimer represents the 4-linked 4'-(asc-C4)-asc-C5 (**185**)[12a].

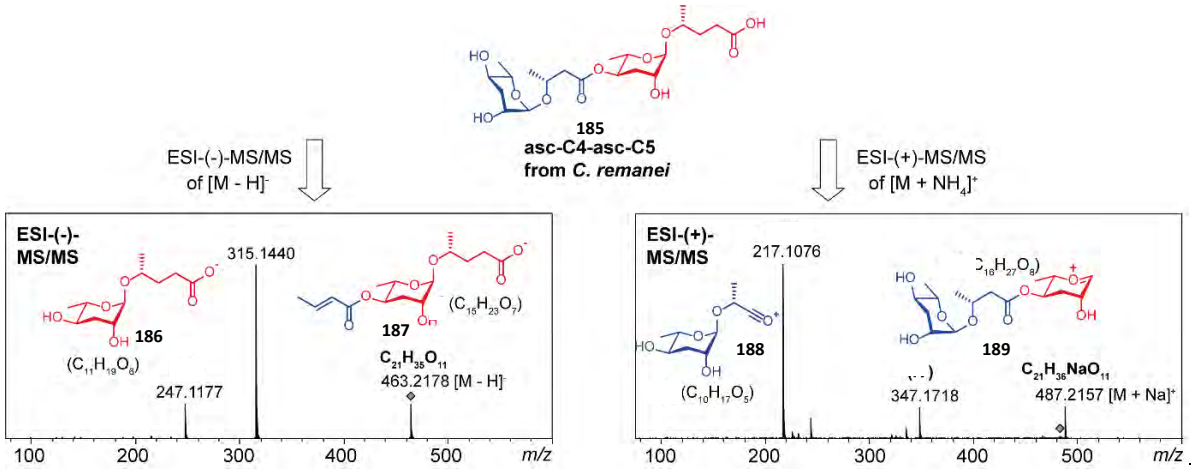

Figure 89 : HPLC-ESI-HR-MS/MS spectra of 4'-(asc-C4)-asc-C5 from *C. remanei*[12a].

6.1. Identification of the pentameric series of asc-C5

While some *Caenorhabditis* species like *C. nigoni* or *C. briggsae* produce a complex blend of homo and heterodimeric ascarosides[12a], the HPLC-HR-MS analysis of the *C. tropicalis* exometabolome indicated an asc-C5 based dimer and several derivatives (**Figure 88)**. Above all, *C. tropicalis* was found to produce considerable amounts of the homodimeric (asc-C5)-asc-C5 (**40**), the structure of which was elucidated by analysis of the ESI-(+)-MS/MS spectrum (**Figure 91**) that presented fragments from the loss of the terminal C5 side chain (**192**) and an additional fragment corresponding to the oxonium ion (**191**) from the cleavage of the ester bond as described previously (**Figure 91**).

Screening ESI-(-)-MS/MS chromatograms for *m/z* 477.2341 ($[C_{27}H_{37}O_{11}]^-$), the fragment ion corresponding to the dimeric (asc-C5)-asc-C5, revealed a homologous series of additional oligomeric ascaroside derivatives with the general molecular formula $C_{11n}H_{18n+2}O_{5n+1}$ with n representing the number of monomer units in the oligomer (**Figure 91**).

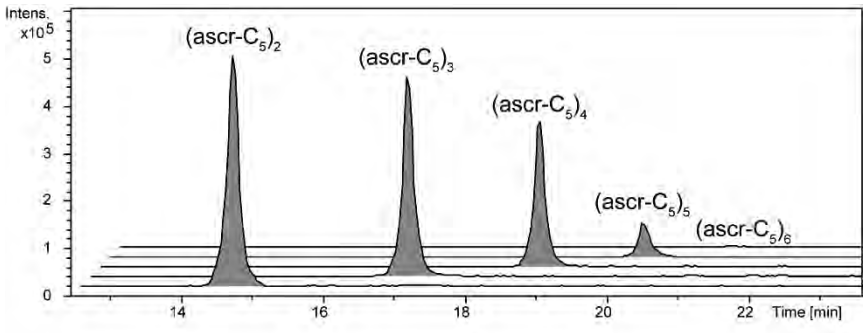

Figure 90 : HR-MS ion traces of the oligomeric ascaroside in *C. tropicalis* exometabolome.

The analysis of the ESI-(+)-MS/MS fragmentation pattern of the different oligomers showed the presence of fragments from successive loss of a terminal C5 side chain (**192**) and fragments from successive cleavage of the ester bond (**191**). Moreover, all the fragments identified in the smaller oligomers could be detected in the MS/MS spectra of the larger oligomers (**Figure 91**). Taken together, these results suggest a series of linear homo-oligomers of the asc-C5 building block, rather than a branched oligomer. After defining the architecture of the oligomer, one needed to determine its exact linkage. Unfortunately, the mass spectrometric data do not permit to conclude whether the oligomers are 2- or 4-linked. However, the oligomers could be hypothesized to originate from the dimeric asc-C5 by iterative addition of additional asc-C5 units via a yet unknown enzyme catalyzed biosynthetic pathway. Based on this hypothesis, we concluded that the entire series of asc-C5 oligomers should have the same linkage, which could be determined based on the structure of the (asc-C5)-asc-C5 dimer. Thus, the exact linkage of the dimeric asc-C5 was investigated.

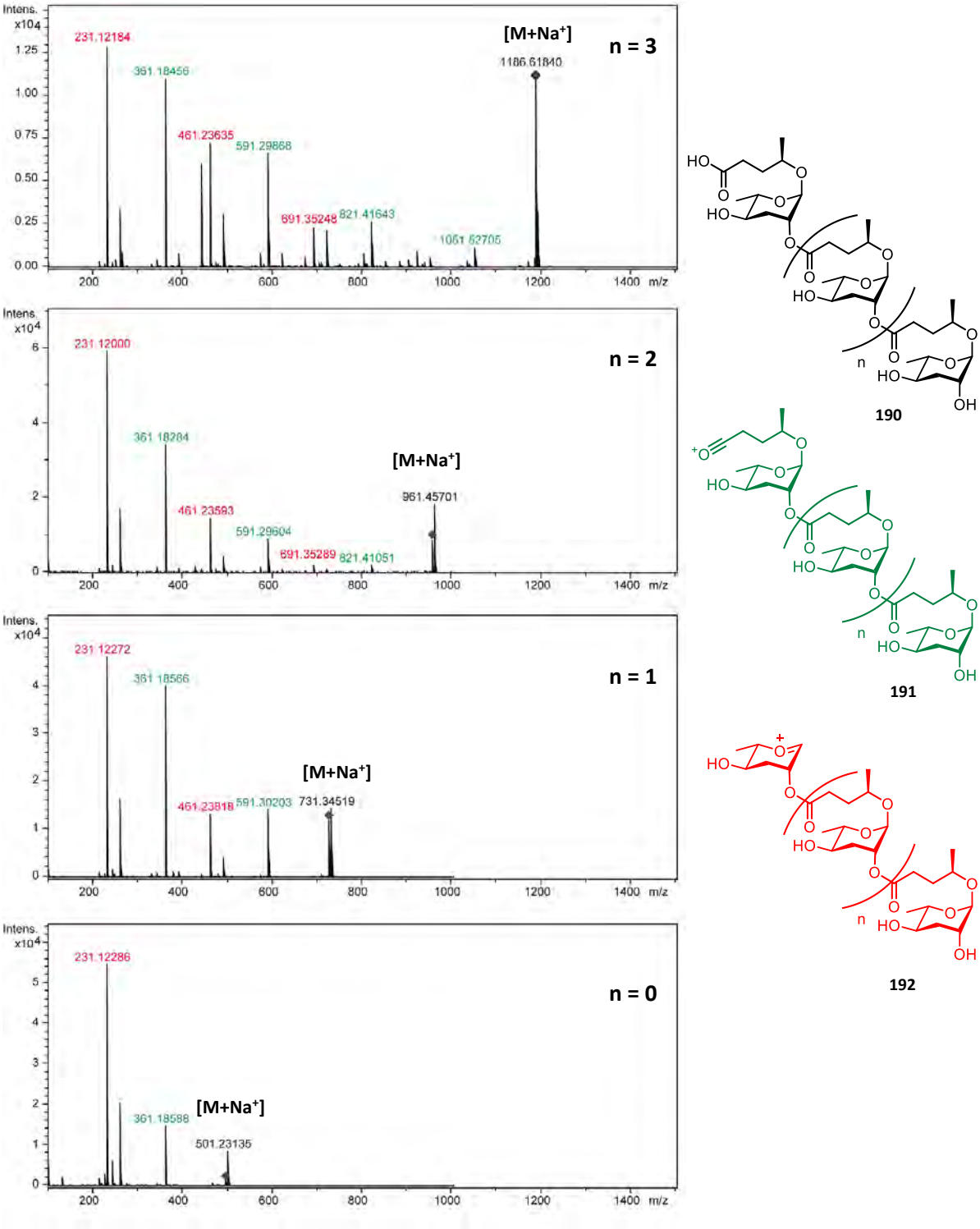

Figure 91: (A) HPLC-ESI-(+)-HR-MS/MS spectra of the asc-C5 oligomers. (B) Proposed chemical structure of the asc-C5 oligomers (in black) from *C. tropicalis* and the structure of the fragments (red and green) observed in ESI-(+)-HR-MS/MS spectra.

Since the available amounts of (asc-C5)-asc-C5 from *C. tropicalis* were not sufficient to isolate enough material for ^{1}H NMR analysis, its structure was determined by comparison of the HPLC-MS retention

times of the target compound from *C. tropicalis* with those of the 2- and 4-linked dimeric asc-C5 identified from other *Caenorhabditis* species. Two dimeric asc-C5 showing different LC-MS retention times were previously identified in *C. nigoni* and *C. remanei* (**Figure 93**). The *dqf*-COSY spectra of an enriched fraction from *C. nigoni* suggested a 2'-(asc-C5)-asc-C5 (**40**, dasc#4, **Figure 92**) and therefore suggested that *C. remanei* is producing the 4'-(asc-C5)-asc-C5 (**193**, dasc#5, **Figure 92.B**). This hypothesis was further supported by the analysis of the *dqf*-COSY spectra, which revealed that *C. nigoni* produces mainly 2-linked dimers, like 2'-(asc-C5)-asc-C5 (**40**, dasc#4) and 2'-(asc-C6)-asc-C5 (**184**, dasc#6), whereas *C. remanei* produces 4-linked dimers such as 4'-(asc-C4)-asc-C5 (**185**)[12a].

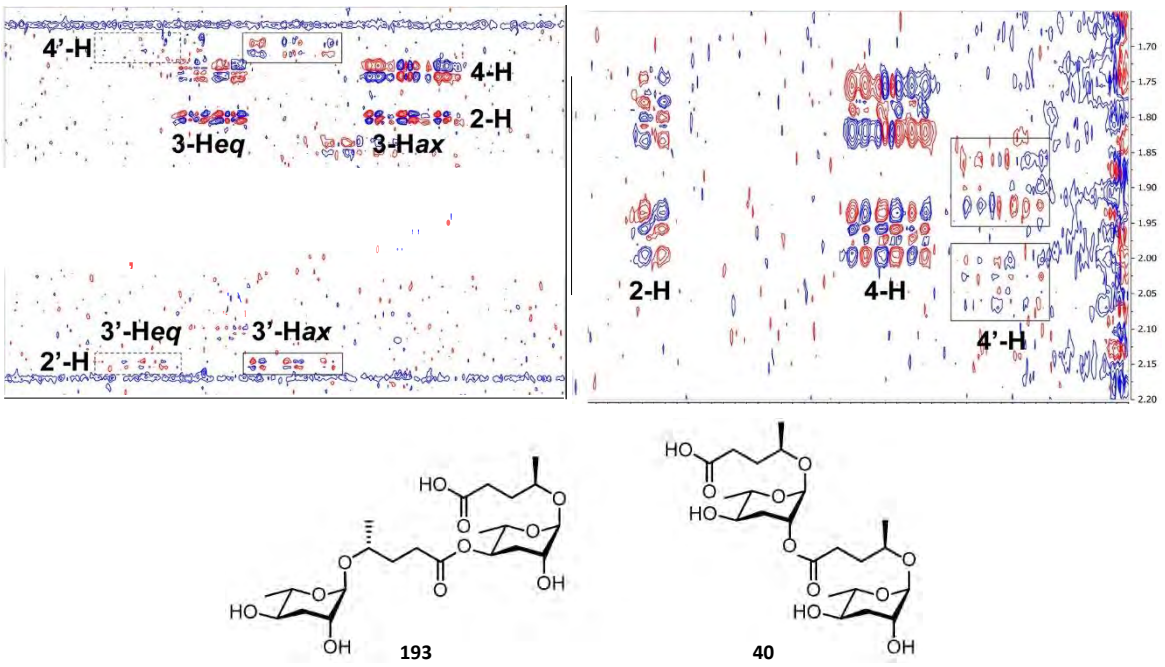

Figure 92 : (A) Sections of the 400 MHz *dqf*-COSY spectra (in CD_3OD) of 2'-(asc-C5)-asc-C5 (40) from *C. nigoni*[12a]. (B) Chemical structure of 2'-(asc-C5)-asc-C5 (40) and 4'-(asc-C5)-asc-C5 (193) from *C. nigoni* and *C. remanei*.

Next, the (asc-C5)-asc-C5 from *C. tropicalis* was compared with the 2'-(asc-C5)-asc-C5 (**40**) and 4'-(asc-C5)-asc-C5 (**195**) from *C. nigoni* and *C. remanei*, respectively (**Figure 93**). The identical retention times of the target compound and the homodimer from *C. nigoni* indicated that *C. tropicalis* is exclusively producing the 2'-(asc-C5)-asc-C5 (**40**) and therefore suggested that the homologous series of complex asc-C5 oligomers is also 2'-linked. In order to corroborate this hypothesis, the 2-linked asc-C5 oligomers were prepared via total synthesis.

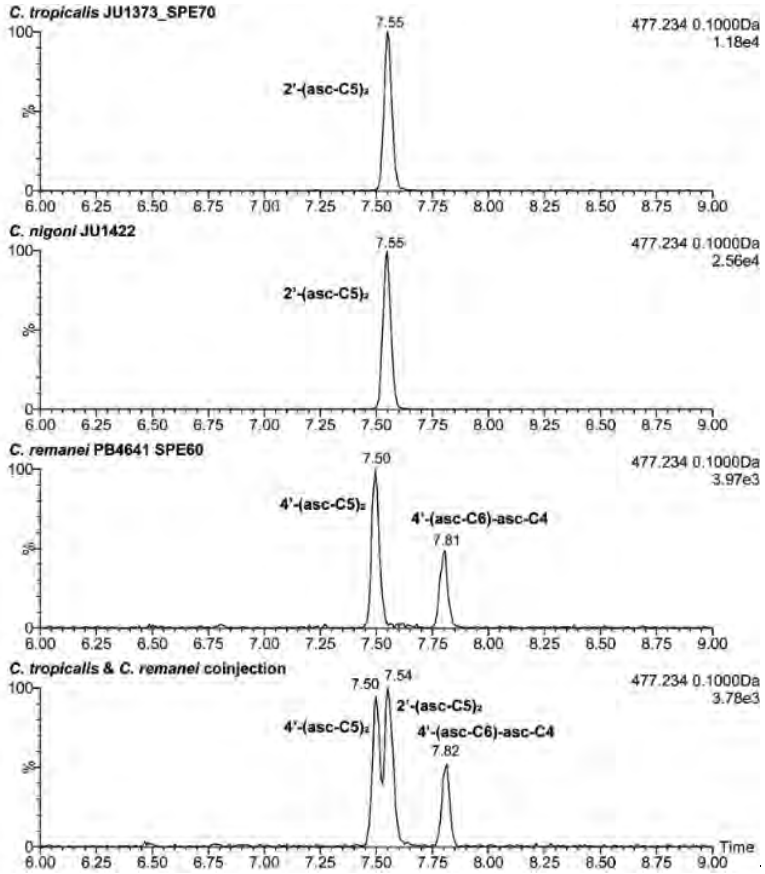

Figure 93: Comparative HPLC-HR-MS/MS analysis of (A) isolated 2'-(asc-C5)-asc-C5 (40) in *C. tropicalis* (B) isolated 2'-(asc-C5)-asc-C5 (40) in *C. nigoni* (C) isolated 4'-(asc-C5)-asc-C5 (193) in *C. remanei* and (D) coinjection of 2'-(asc-C5)-asc-C5 (40) and 4'-(asc-C5)-asc-C5 (193) in *C. tropicalis* and *C. remanei.*

6.2. Synthesis of the homologous series of asc-C5 oligomers

6.2.1. Synthesis via nonselective assembly of monomers

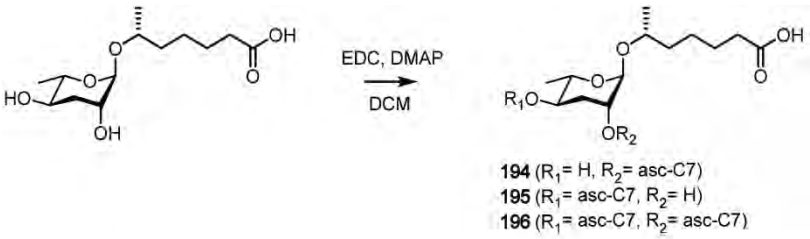

Figure 94: Bose's synthesis of 4'-(asc-C7)- asc-C7.

Initially, Bose et al. synthesized dasc#1 (**23**) via Steglich esterification of the asc-C7 (**1**) monomer (**Figure 94**)[12b]. The non-selective reaction afforded a complex mixture of ascaroside dimers and oligomers from which the desired 4'-(asc-C7)-asc-C7 (**23,** dasc#1) was isolated. Yields were small and, therefore, this approach was not suitable for the synthesis of higher order oligomers. In a first attempt

to generate a mixture of the asc-C5 oligomer series, the 4'-protected 4'-*O*-TBDPS-asc-C5 **143** was treated with DCC and DMAP (**Figure 95**). The resulting reaction mixture would subsequently be desilylated and purified by semi-preparative HPLC.

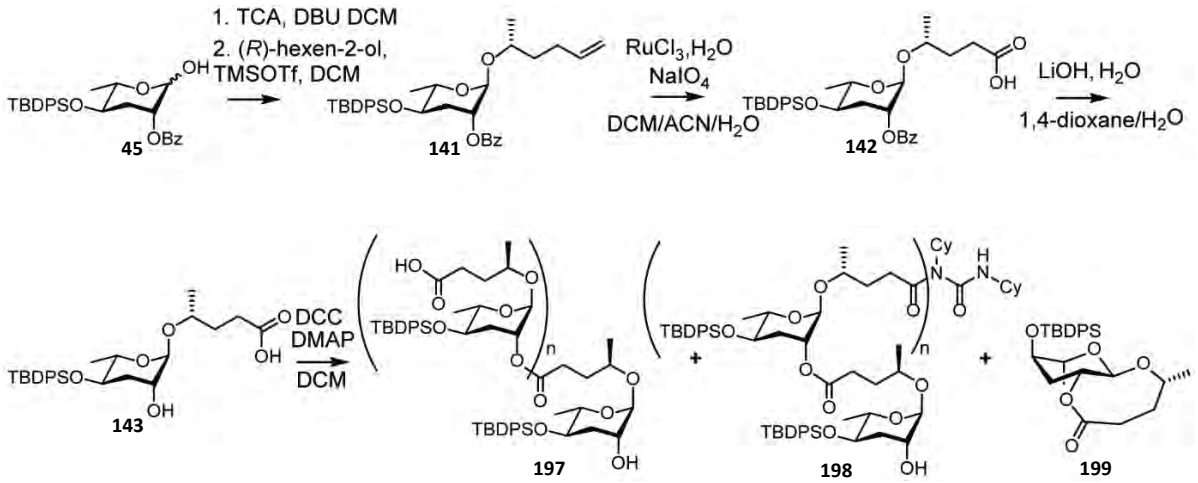

Figure 95: One-pot synthesis of the TBDPS-protected oligomeric ascarosides.

The 4-*O*-TBDPS-asc-C5 **143** was synthesized in three steps from orthogonally protected 2-*O*-Bz-4-*O*-TBDPS-ascarylose **45** as shown in **Figure 95**[40]. The (*R*)-5-hexen-2-ol was glycosylated via the trichloroacetimidate route[78] with the ascaroside building block **45** .Next, the terminal alkene was converted to the corresponding carboxylic acid **142** using ruthenate catalyzed oxidation followed by alkaline 2-*O*-debenzoylation to provide the 4-protected building block **143**. Monomeric **143** was then treated with DCC and DMAP to afford 12% of the intramolecular cyclization product of 4-*O*-TBDPS-asc-C5 (**199**) along with 13% of a mixture of dimeric and trimeric asc-C5 derivatives **197** and a mixture of *N*-acylureas **198** (n = 0 - 3).

Considering the limited yields, each oligomer was generated individually via a more selective protecting group strategy that would allow specific coupling between the acyl group and the 2'-position of two individual monomeric asc-C5 building blocks specifically protected at the 4'-position and at the acyl side chain. For this purpose, two ascaroside building blocks were synthesized: the starter unit with both the 2'- and 4'-positions protected and the aglycon as an unprotected acyl group, and the extender unit with the 4'-position and the acyl group of the aglycon protected for selective ester coupling via the free 2'-hydroxy position. Moreover, two different deprotection strategies were studied for this synthesis, an orthogonal and a chemoselective deprotection strategy.

6.2.2. Synthesis via the silyl ether route

The first synthetic strategy that has been investigated utilizes silyl ethers as protecting groups for the ascarylose unit and an α,β-unsaturated benzyl ester for the aglycon. The starter unit, the 2',4'-di-*O*-TBS-asc-C5 **202**, was synthesized in four steps from 2,4-di-*O*-benzoyl-ascarylose **63** with an overall yield of 27% (**Figure 96**). (*R*)-5-hexene-2-ol was glycosylated with 2,4-di-*O*-benzoyl-ascarylose **63** via Schmidt glycosylation to afford **200**. Deprotection of the 2'- and the 4'- position under basic conditions followed by TBS protection afforded the 2',4'-di-O-TBS-protected intermediate **201**, which, upon ruthenate catalyzed oxidation, afforded the 2',4'-di-*O*-TBS-asc-C5 **202**. Next, the extender unit, the 4'-*O*-TBDPS-asc-ΔC5-OBn (**203**) was synthesized in four steps from 2-*O*-benzoyl-4-*O*-TBDPS-ascarylose **45** (**Figure 96.B**). After glycosylation of (*R*)-3-butyn-2-ol with **45** , followed by selective catalytic hydrogenation, **148** was 2-debenzoylated and the resulting alkenyl ascaroside **150** was subjected to cross metathesis with benzyl acrylate using Grubb's 2nd generation catalyst to give the extender unit **203** with an overall yield of 34%.

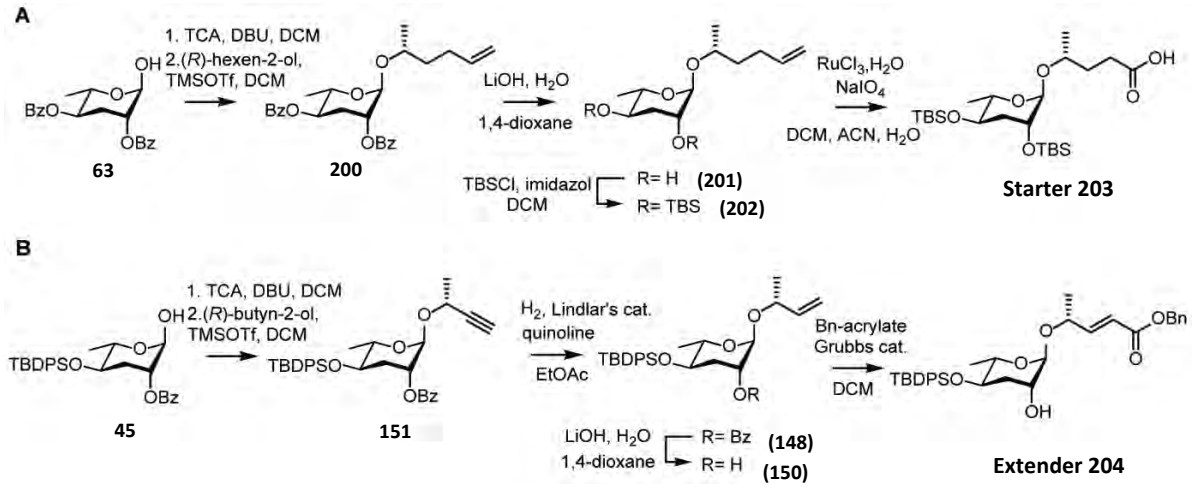

Figure 96 : Synthesis of (A) the starter 203 and (B) the extender 204.

To generate oligomeric ascarosides the extender **204** and the starter **203** units were coupled via Steglich esterification using EDC and DMAP to give the fully protected dimer **205** in 65% yield. Subsequently the protected dimer **205** was hydrogenated with palladium to provide 2'-(2,4-di-*O*-TBDMS-asc-C5)-4'-*O*-TBDPS-asc-C5 (**224**), which served as the new starter and was reacted with an additional extender **204** to give the trimer **206**. Repeated rounds of palladium catalyzed hydrogenation followed by Steglich coupling with **204** catalyzed by EDC and DMAP provided the fully protected tetramer and pentamer, respectively (**Figure 97**).

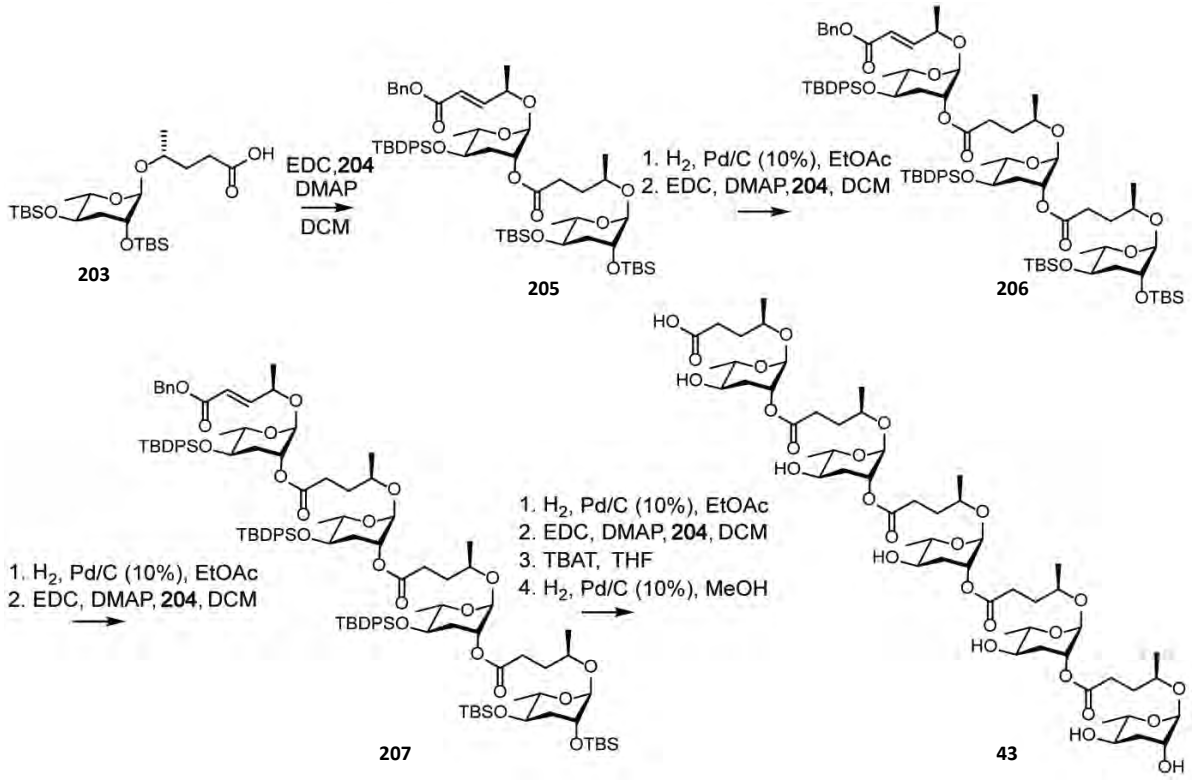

Figure 97: Synthesis of the pentamer 43 via the *O*-TBDPS protecting group strategy.

Having synthesized the four fully protected oligomers, they were first *O*-desilylated and then *O*-debenzyated. Previous attempts to deprotect silyl ethers of dimeric ascarosides with tetrabutyl ammonium fluoride (TBAF) resulted in the partial decomposition of the reaction products due to the strong basicity of the fluoride source, especially in the presence of traces of water. Dong et al. reported the deprotection of silyl ethers of dimeric ascarosides with Olah's reagent (HF/pyridine) in excess pyridine with yield ranging from 30 to 49% after 10 days of reaction[12a] but this alternative was not further explored. Instead, two anhydrous fluoride sources, the tetrabutylammonium difluorotriphenylsilicate (TBAT)[103] and the tris(dimethylamino)sulfonium difluorotrimethylsilicate (TASF)[104] (**Figure 98**) were tested to deprotect the hydroxy groups.

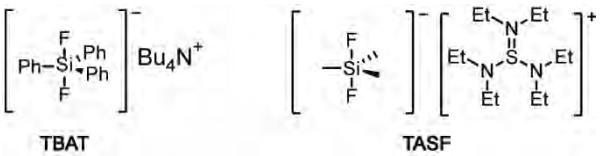

Figure 98 : Structure of the tetrabutylammonium difluorotriphenylsilicate (TBAT) and the tris(dimethylamino)sulfonium difluorotrimethylsilicate (TASF).

The silyl ether-protected dimer **205** was deprotected with 5 equivalents of the fluoride reagent per silyl ether group at room temperature for 7 days. Only the experiment with TBAT furnished complete

consumption of the starting material according to TLC. After 7 days, the desilylation with TASF furnished the 2'-(2,4-di-*O*-TBS-asc-C5)-asc-ΔC5-OBn (**208**) as the major product (indicating that TBDPS is more easily cleaved) along with traces of mono-TBS dimers (**209** and **210**) and starting material (**205**), while the deprotection with TBAT provided the 2'-(2-*O*-TBS-asc-C5)-asc-ΔC5-OBn (**209**) as the major product along with traces of the desired 2'-(asc-C5)-asc-ΔC5-OBn and 2'-(4-*O*-TBS-asc-C5)-asc-C5-ΔOBn (**210**) (**Figure 99**). Therefore, the deprotection with TASF was no longer investigated.

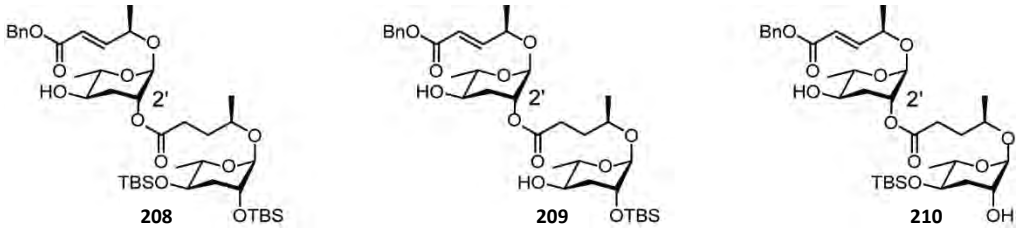

Figure 99 : Intermediates from the silyl ether deprotection with TBAT or TASF.

After 9 days of reaction, the deprotection with TBAT afforded the 2'-(asc-ΔC5)-asc-C5-OBn (**205**) in 91% of yield. To prevent the decomposition of the final product, the reaction mixture was quenched with acetic acid to furnish a mixture of ammonium acetate salt and dimer, that could be easily purified by flash column chromatography. Using this procedure, the four oligomers were deprotected with good yield (65 - 91%). Final catalytic hydrogenation provided the fully deprotected series of asc-C5 oligomers with yields ranging from 51 to 79%.

6.2.3. Synthesis via chemoselective deprotection

Aiming to prevent the fluoride based desilylation altogether, a second synthetic approach that took advantage of the higher reactivity of benzyl ester compared to benzyl ethers during hydrogenolysis as reported in the literature[105]. This selectivity was also noticed during the final deprotection of 4'-AB-asc-C5 (**34**). In 1992 Bajwa et al. reported a catalytic transfer hydrogenation with 1,4-cyclohexadiene (1,4-CHD) as hydrogen donor that selectively deprotects *O*-benzyl ester even in the presence of *O*-benzyl ethers[106]. Therefore, to synthesize the oligomers, the fully benzylated analogs of the starter unit, the 2',4'-di-*O*-Bn-asc-C5 **217**, and the extender unit, 4'-*O*-Bn-asc-ΔC5-OBn **214,** were used. To demonstrate the utility of this method, the trimeric ascaroside **41** was synthesized.

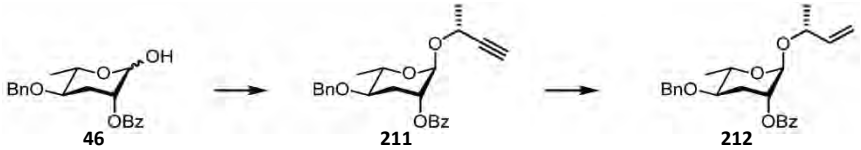

Figure 100 : Synthesis of 210 from the 2-*O*-benzoyl-4-*O*-benzyl-ascarylose (46).

To obtain the starter unit **217** and the extender unit **214** the intermediate (3*R*)-butenyl 2'-*O*-benzoyl-4'-*O*-benzyl-ascaroside **212** was synthesized in two steps (**Figure 100**) from the 2-*O*-benzoyl-4-*O*-benzyl-ascarylose (**46**) described in **chapter 2.2.2**. The (*R*)-3-butyn-2-ol was glycosylated with the ascarylose building block **46** and the resulting ascaroside **211** reduced to the corresponding terminal alkene **212** via selective catalytic hydrogenation with Lindlar's catalyst.

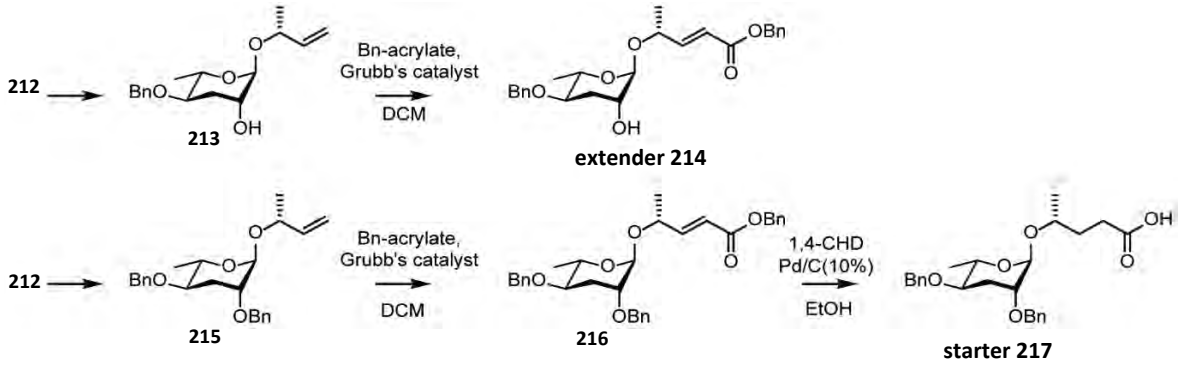

Figure 101 : Synthesis of the benzylated starter 217 and the benzylated extender 214.

The extender 4'-*O*-Bn-asc-ΔC5-OBn **214** was obtained by alkaline hydrolysis of **212** followed by cross-metathesis with benzyl acrylate (**Figure 101**). Next, the (3*R*)-butenyl 2',4'-di-*O*-benzyl ascaroside (**215**) was synthesized via a one-pot debenzoylation/benzylation of the intermediate **212** and subsequently coupled with benzyl acrylate via cross metathesis using Grubbs 2nd generation catalyst. As a proof of concept, the resulting 2',4'-di-*O*-Bn-asc-ΔC5-OBn **216** was selectively deprotected by hydrogenation with 1,4-cyclohexadiene under different reaction conditions listed below (**Figure 102**). The *O*-benzyl ester was easily cleaved by 1,4-CHD and the reaction did not produce any of the fully deprotected asc-C5 nor a significant amount of 2'-*O*-Bn-asc-C5 (**218**), despite the excessive amounts of 1,4-CHD and long reaction time.

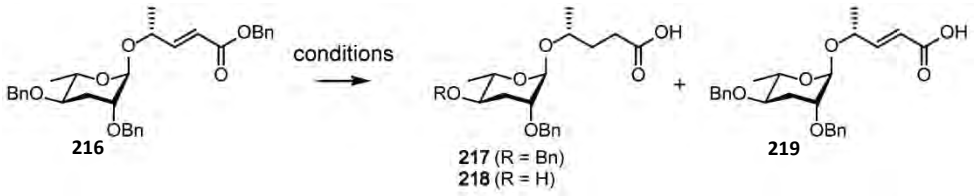

starting material	reagent	t (h)	217 (%)	218(%)	219 (%)
216	1,4-cyclohexadiene (19 eq)	24	74	-	26
217/219 : 10/3	1,4-cyclohexadiene (19 eq)	18	93	7	-
216	1,4-cyclohexadiene (111 eq)	11	80	20	-

Figure 102 : Conditions tested for the chemioselective deprotection of the side chain.

To generate ascaroside oligomers, the 2',4'-di-*O*-Bn-asc-C5 starter unit (**217**) was linked to the 4'-*O*-Bn-asc-ΔC5-OBn extender unit (**214**) using Steglich esterification to afford the fully protected dimeric ascaroside **220**. Next, the *O*-benzyl ester group of **220** was selectively deprotected in 76% of yield to give the dimer **227**, which upon Steglich esterification provided the fully protected asc-C5 trimer **223**. The selective hydrogenation of the fully benzylated trimer **223** with 1,4-CHD provided the free acyl trimer **221** in good yield (78%), demonstrating the usefulness of this approach for the synthesis of oligomeric ascarosides. Palladium catalyzed hydrogenation of **221** furnished the free asc-C5 trimer **41** in 75% of yield, identical to the natural product according to the LC-MS (**Figure 104**) from *C. tropicalis*.

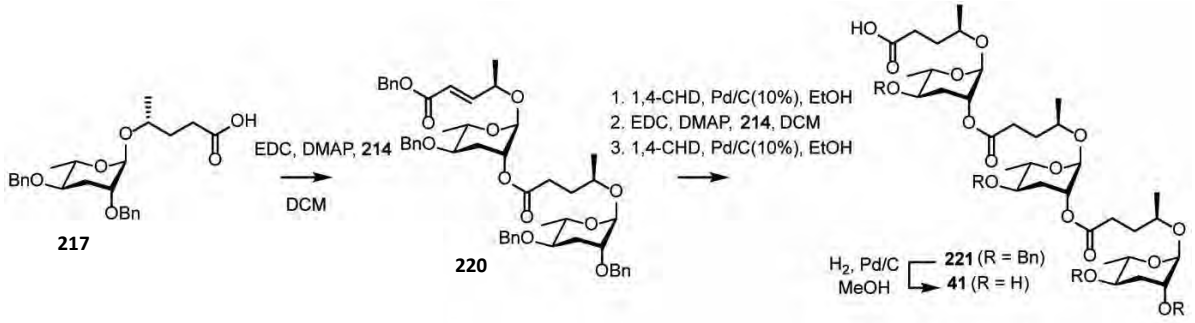

Figure 103 : Synthesis of the trimer 41 via chemoselective deprotection.

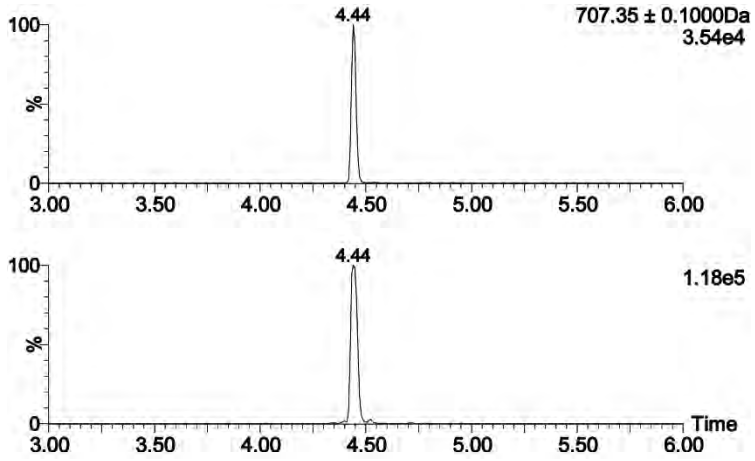

Figure 104 : Comparison of retention time of the synthetic trimer obtained by chemoselective hydrogenation and the natural trimer detected in *C. tropicalis.*

6.3. Confirmation of structure assignment

The structure assignments of the asc-C5 oligomers were finally confirmed by comparison of the LC-MS chromatogram of a mixture of the four synthetic oligomers with those of the natural oligomers enriched from *C. tropicalis*. As shown in **Figure 105**, the retention times of all the four synthetic compounds match with those of the natural products, which confirms the linkage via the 2-position for these natural homo-oligomers. Moreover, the ESI-(-)-HR-MS/MS spectra of each oligomer showed

the same fragmentation pattern for the isolated and the synthetic materials (**Figure S18-S21**). Furthermore, comparison of the NMR data for the natural 2'-(asc-C5)-asc-C5 (**40,** dasc#4) and the 4'-(asc-C5)-asc-C5 (**193**, dasc#5) isolated by Dong et al. from *Pristionchus* species[101] with the synthetic 2'-(asc-C5)-asc-C5 (**40**) from *C. tropicalis* further confirmed the structure assignment of these natural products (**Figure 106**).

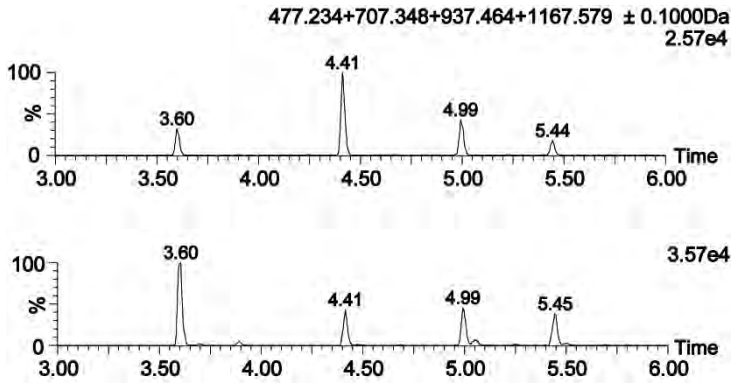

Figure 105 : Comparison of retention time of the four synthetic and natural oligomers detected in *C. tropicalis.*

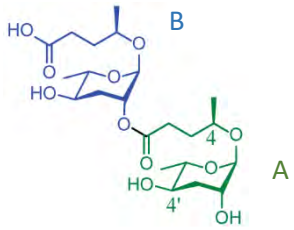

Position		Synthetic 2'-(asc-C5)-asc-C5 (40)		Isolated 2'-(asc-C5)-asc-C5 (40)[101]		Isolated 4'-(asc-C5)-asc-C5 (193)[101]	
		^{1}H	^{13}C	^{1}H	^{13}C	^{1}H	^{13}C
sugar A	1'	4.65 *br.s*	97.0	4.65 *br.s*	97.0	4.65 *br.s*	97.1
	2'	3.71 *dd* (3.8, 3.1)	69.6	3.72 *br.s* (2.5)	69.6	3.72 *br.s* (2.6)	69.5
	3'ax	1.76 *ddd* (13.3, 11.5, 3.1)	35.6	1.76 *ddd* (13.1, 3.1)	35.7	1.77 *ddd* (13.3, 3.2)	35.7
	3'eq	1.95 *ddd* (13.3, 4.6, 3.8)		1.96 *ddd* (13.1, 4.7)		1.95 *ddd* (13.3, 4.8)	
	4'	3.51 *ddd* (11.5, 9.5, 4.6)	68.0	3.51 *ddd* (11.0, 4.0)	68.0	3.51 *ddd* (11.4, 3.9)	68.2
	5'	3.57 *dq* (9.7, 6.2)	71.2	3.57 *dq* (9.3)	71.1	3.58 *dq* (9.6)	71.1
	6'	1.22 *d* (6.2)	17.7	1.23 *d* (6.2)	17.7	1.22 *d* (6.2)	17.8
sugar B	1'	4.72 *br.s*	94.1	4.72 *br.s*	94.1	4.69 *s*	97.0
	2'	4.79 *dd* (3.7, 3.1)	72.5	4.79 *br.s* (2.1)	72.6	3.72 *br.s* (2.6)	69.2
	3'ax	1.89 *ddd* (13.4, 11.5, 3.1)	33.2	1.88 *ddd* (13.6, 3.1)	33.1	1.87 *ddd* (13.1, 3.0)	32.8
	3'eq	2.01 *ddd* (13.4, 4.6, 3.7)		2.02 *ddd* (13.6, 4.8)		2.04 *ddd* (13.1, 4.9)	
	4'	3.38 *ddd* (11.5, 9.5, 4.6)	68.3	3.40 *ddd* (11.1, 4.0)	68.4	4.86 *ddd* (11.2, 4.1)	71.2
	5'	3.70 *dq* (9.5, 6.6)	70.6	3.69 *dq* (9.4)	70.8	3.89 *dq* (10.0)	67.9
	6'	1.22 *d* (6.6)	17.7	1.22 *d* (6.2)	17.9	1.15 *d* (6.4)	18.5
chain A	1	-	172.7	-	172.8	-	174.3
	2a	2.54-2.45 *m*	31.0	2.50 *m*	31.1	2.43 *m*	31.3
	2b					2.47 *m*	
	3	1.89-1.76 *m*	32.0	1.84 *m*	33.0	1.80 *m*	35.0
	4	3.85 *m*	70.9	3.85 *m*	71.1	3.82 *m*	71.1
	5	1.15 *d* (6.3)	18.7	1.16 *d* (6.1)	18.8	1.15 *d* (6.3)	18.1
chain B	1	-	179.8	-	180.1	-	181.5
	2a	2.36 *dt* (14.4, 8.1)	34.2	2.33	33.1	2.24 *m*	34.7
	2b	2.28 *dt* (14.4, 7.8)		2.38		2.35 *m*	
	3	1.84-1.80 *m*	33.5	1.83	34.1	1.82 *m*	34.1
	4	3.81 *m*	72.2	3.82	72.1	3.82	71.7
	5	1.14 d (6.3)	18.7	1.15	18.7	1.15 d (6.3)	18.1

Figure 106 : NMR data in CD_3OD of 2'-(asc-C5)-asc-C5 (40, dasc#4) and 4'-(asc-C5)-asc-C5 (193, dasc#5) detected in *Pristionchus* species[101] and the synthetic dasc#4 identified in *C. tropicalis*.

The assignment of NMR signals for the more complex oligomer was performed using one- and two-dimensionnal NMR spectroscopy (**table S5-S7**). The head monomeric unit was easily identified with both the 2-position (δ_H = 3.72 ppm) and the 4-position (δ_H = 3.51 ppm) having chemical shifts similar to the head unit of the dimer (**Figure 106**, sugar A) while the ester-linked 2-position exhibits deshielded peaks at around 4.79 ppm (**Figure 107**). The terminal monomeric unit in the tetramer and the pentamer could be distinguished from the internal monomers as two (for the tetramer) or three (for the pentamer) sugar units were displaying identical chemical shift for the 4-position (δ_H = 3.42 ppm), while an additional sugar, supposedly the terminal monomer, exhibits a distinct chemical shift for the 4-position (δ_H = 3.38 ppm). This hypothesis was supported by the chemical shift of the 4-position for

the terminal monomer in 2'-(asc-C5)-asc-C5 **40** (**Figure 106**) which is identical to the chemical shift of the (proposed) terminal monomer in the tetramer and the pentamer.

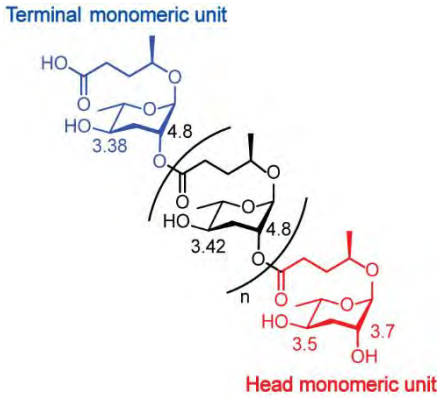

Figure 107 : Chemical shift of the 2'-H and 4'-H relative to the sugar unit.

Similarly, the α-protons next to the carbonyl group of one aglycon exhibit signals for two diastereotopic protons at approximatively 2.35 and 2.26 ppm (*dt*, $^{2}J_{2,2}$ = 14 Hz and $^{3}J_{2',3'}$ = 8 Hz) instead of one multiplet for 2 protons seen on the other aglycons. A similar phenomenon was observed for 2'-(asc-C5)-asc-C5 (**40,** dasc#4), 4'-AB-asc-C5 (abas#9, **34**) and the 2',4'-di-*O*-TBS-asc-C5 (**202**), which also bears a saturated C5 sidechain. Therefore, this signal was assigned to the terminal aglycon. Next, the head aglycon was distinguished from the internal aglycons by comparison of the signal for the methyl group protons. As described for the sugar units, the head aglycon showed a distinct doublet for one methyl group at around 1.15 ppm, while the internal aglycons displayed one doublet at around 1.16 ppm that accounts for more than one methyl group in the case of the tetramer and pentamer ($^{3}J_{5',4'}$ = ~ 6 Hz for 3, 6 or 9 H depending on the oligomer).

6.4. Functional characterization

Since the previous study from Dong et al. reports that only male *C. remanei* and *C. nigoni* respond to their conspecific dimeric ascarosides[12a], male progeny was generated within the predominantly hermaphroditic *C. tropicalis* to perform bioassays on both, hermaphrodites and males. As the previous study also reported that dimerization was highly species-specific, and since the nematodes only respond to their own dimeric ascarosides it was therefore interesting to see if the dimer could also induce activity on different strains of *C. tropicalis*. Thus, the oligomers were tested on two different strains of *C. tropicalis* (JU1373 from La Réunion and JU1428 from French Guyana) using holding assays to quantify nematode retention.

For this purpose, approximately five males observed on crowded plates were picked and mated with one hermaphroditic *C. tropicalis* from each strain. Upon outcrossing a sex ratio of circa 1:1 (male:

hermaphrodite) was observed for the strain JU1428. Unfortunately, outcrossing in the strain JU1373 resulted in sick worms and was unsuitable to generate healthy male offspring. Therefore, for the strain JU1373 only the hermaphrodites could be tested.

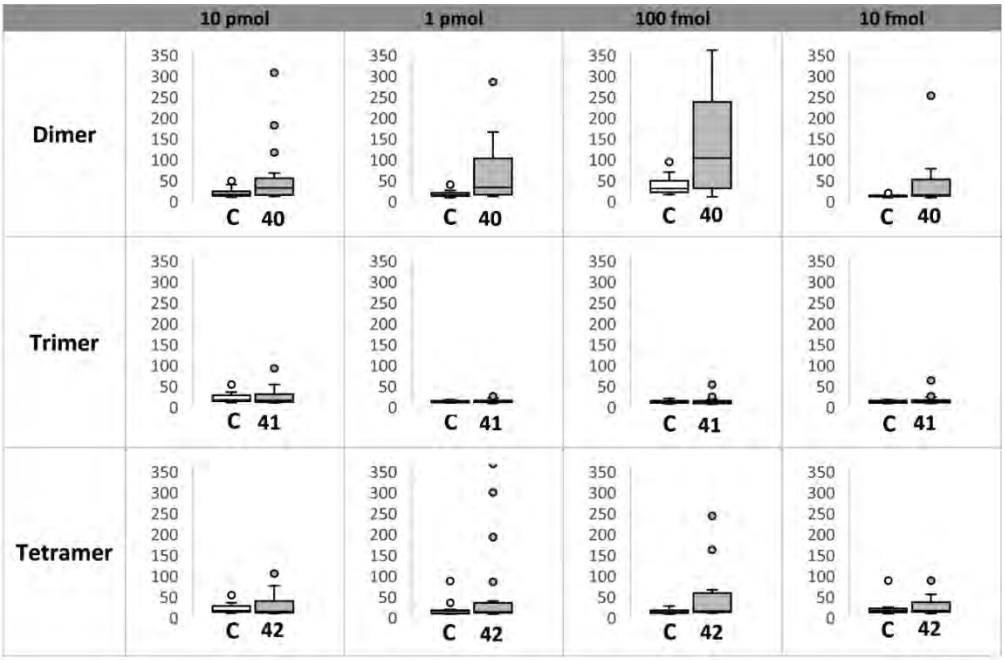

Figure 108 : Holding assays on male C. *tropicalis (JU1428)* for 10 pmol to 10 fmol of oligomers.

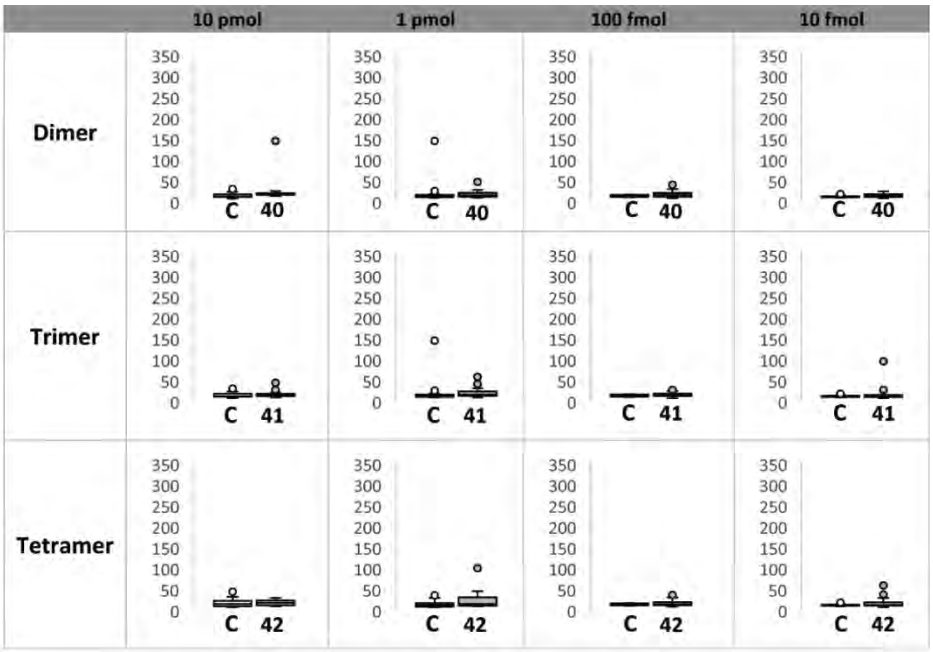

Figure 109 :Holding assays on hermaphrodite C. *tropicalis (JU1428)* for 10 pmol to 10 fmol of oligomers.

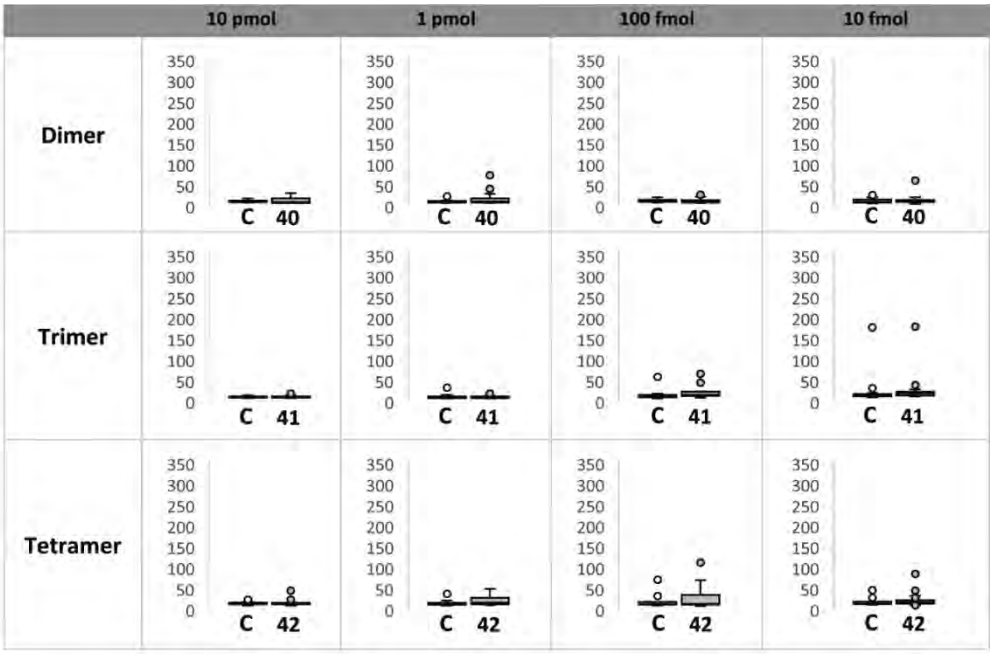

Figure 110 : Holding assays on hermaphrodite C. *tropicalis (JU1373)* for 10 pmol to 10 fmol of oligomers.

The dimeric ascaroside 2'-(asc-C5)-asc-C5 (**40**, dasc#4) showed similar retention of *C. tropicalis* males as were previously observed with 4'-(asc-C4)-asc-C5 (**193**, dasc#5) in *C. remanei* males as well as 2'-(asc-C6)-asc-C5 (**185**, dasc#6) and 2'-(asc-C6)-asc-C6 (dasc#8) for *C. nigoni* males[12a] [12a]. None of the *C. tropicalis* hermaphrodites (strain JU1428 and JU1373) responded to the dimeric ascaroside, while male *C. tropicalis* JU1428 were retained by 100 fmol of 2'-(asc-C5)-asc-C5, which shows that nematodes use dimerization of conserved ascarosides to generate sex-specific and species-specific chemoattractants.

None of the trimeric (**41**) or tetrameric (**42**) asc-C5 elicited a response at any of the concentrations tested which indicates that the attachment of additional monomeric units to the 2'-(asc-C5)-asc-C5 (**41**) attractant results in the loss of holding activity and therefore suggests that the dimer and higher oligomers (the trimer and the tetramer) might serve different biological functions in *C. tropicalis*. The change of biological activity upon structural modification is common in ascaroside signaling and many examples are known in which the incorporation of additional building blocks to basic ascarosides results in a different response by the nematodes. Thus, it can be speculated that the addition of monomeric units to the 2'-(asc-C5)-asc-C5 (**41**) might induce alternative responses (like aggregation or repulsion that cannot be detected with the holding assay) or that these oligomeric structures affect developmental plasticity as described for 4'-(asc-C7)-asc-C7 (**23,** dasc#1) in *P. pacificus*[12b]. Furthermore, the asc-C5 oligomers were tested in relatively high concentrations, which can also affect the nematode's response. Since the oligomeric ascarosides in *C. tropicalis* were identified in rather small concentrations, it could be worth to (re)-test the trimer and the tetramer in even smaller

concentrations.

Moreover, male *C. nigoni*, in which only traces of 2'-(asc-C5)-asc-C5 (**41**) were detected (along with dominating 2'-(asc-C6)-asc-C6, did not respond to this dimer during the holding assays, which confirms that nematodes responses to dimeric ascarosides are highly species-specific since each species produces a specific blend of homo and/or heterodimers and responds to their own dimeric ascarosides.

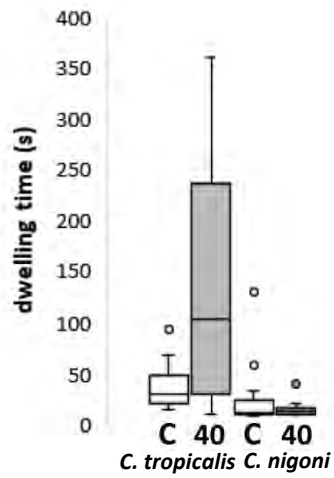

Figure 111 : Comparison of male *C. tropicalis* (JU1428) and *C. nigoni* (JU1422) response to 100 fmol of 2'-(asc-C5)-asc-C5 (40).

6.5. Conclusion

The combination of HR-MS/MS and NMR techniques permitted the identification of a novel class of oligomeric ascarosides, represented by the pentameric asc-C5 (**43**) in *C. tropicalis*. The total synthesis of the five homo oligomers was achieved via an orthogonal protecting group strategy. This approach provided the oligomeric asc-C5 with 47, 25 and 6.6% overall yield from the disilylated starter (**201**). Furthermore, a chemoselective approach was developed using fully *O*-benzylated extender and starter. This method afforded the trimeric asc-C5 **41** in five steps with an overall yield of 10%, which can be reduced to four steps by hydrogenation of the fully benzylated trimeric ascaroside therefore proving the efficiency of this method. The comparison of HPLC-MS retention times between the natural and the synthetic samples confirmed the 2'-linked linear structures of the oligomers detected in *C. tropicalis.*

The bioactivity of the oligomers was tested in holding assays, which confirmed that the dimerization of ascarosides provides highly sex- and species-specific signaling molecules, since only *C. tropicalis* males were retained by 2'-(asc-C5)-asc-C5 (**40**), while neither males of *C. nigoni*, nor the hermaphroditic *C. tropicalis* were affected thus confirming previous observations for species-specific

responses to conspecific ascaroside dimers by *C. remanei* and *C. nigoni*[12a].

The results from the bioassays of the trimeric and the tetrameric asc-C5 **41** and **42** indicated that the attachment of additional monomeric asc-C5 unit to the male attracting dimers results in the loss of the retention activity.

The dimerization of basic monomeric ascarosides is prominent among the *Elegans* group. While basic ascarosides, the building blocks of the dimeric structures, are most widely conserved within *Caenorhabditis* species, only specific monomers are converted to homo or heterodimeric ascarosides depending on the species. High species specificity was also noticed for the linkage of the oligomers, since *C. nigoni* and *C. tropicalis* show a preference for 2'-linked oligomers, while *C. remanei* produces mainly 4'-linked dimers, which suggest that the biosynthesis of these compounds is tightly controlled and proceeds via dedicated enzymes. The identification of species-specific asc-C5 oligomers in *C. tropicalis* is an indication that nematodes use the tightly controlled oligomerization of widely conserved building blocks as another methodology to generate a highly species-specific chemical language.

Dimerization of basic ascaroside is also present outside of the *Caenorhabditis* genus suggesting ancient origin for the dimerization pathway. Along with dasc#1 which, was first discovered in *P. pacificus*[12b], a large family of dimeric ascarosides with yet uncharacterized functions were identified in most of the *Pristionchus* species[101] by Dong *et al*. High species specificity for the structure of the dimers was also noticed among *Pristionchus* species. However, oligomerization toward pentameric ascarosides has so far been exclusively observed in *C. tropicalis*.

7. Conclusion & Outlook

For many decades, the molecular structure of nematode pheromones remained elusive. The recent development of sophisticated analytical tools has enabled the identification of ascaroside based glycolipids from crude nematodes exometabolome and therefore provided a better comprehension of chemical communication in nematodes. Analytical screens on different species of nematodes inside and outside of the *Caenorhabditis* genus have shown that ascaroside signaling is highly conserved, therefore raising the question of how nematodes can maintain species-specificity in their chemical communication. Using highly sensitive mass spectrometric screens combined with one and two-dimensional ^{1}H NMR spectroscopy on a collection of *Caenorhabditis* species closely related to the model organism *C. elegans*, four classes of novel species-specific ascarosides were identified. The total synthesis of these novel ascarosides, as well as their analytical and biological characterization were described in this PhD thesis.

Given the importance of the ascarylose building block to generate ascaroside structures, this PhD first investigated different approaches for a short and efficient synthetic route to generate useful ascarylose building blocks. At first, an improvement for the synthesis of 2,4-di-*O*-benzoyl-ascarylose building block **63** was achieved based on Barton McCombie deoxygenation of 1-*O*-methyl-3-*O*-phenyloxythiocarbonyl-rhamnoside **75**, which was synthesized by tin catalyzed regioselective functionalization. This synthetic route provided the dibenzoyl ascarylose building block **63** in four steps with an overall yield of 18%, while Jeong's strategy[18] derived from Varela's work[48] provided the dibenzoyl ascarylose building block **63** in 13% of yield over six steps. However, the new synthetic route requires additional improvement regarding the overall yield of the deoxygenation/dibenzoylation step. Next, an alternative strategy toward Zhang's synthesis of the 2-*O*-Bz-4-*O*-TBDPS-ascarylose building block **45** was developed. An alternative procedure based on the benzylidene ring opening provided the orthogonally protected ascarylose building block in five steps with an overall yield of 40%, whereas Zhang's strategy based on regioselective cyclic sulfate ring opening provided the 2-*O*-Bz-4-*O*-TBDPS-ascarylose building block **45** in 33% of yield over seven steps. Moreover, the benzylidene ring strategy is not limited to the sole synthesis of 2-*O*-Bz-4-*O*-TBDPS-ascarylose **45** but also provides access to a diverse range of 4-*O*-protected ascarylose building blocks. Nevertheless, even shorter alternatives for the two step benzylidene ring opening/debromination reaction should be investigated in the future.

Next, the 4-modified ascarosides were synthesized from the orthogonally protected 2-*O*-Bz-4-*O*-TBDPS-ascarylose building blocks (**45**). The asc-C6MK (ascr#2, **35**) and asc-ΔC9 (ascr#3,**37**) units for the photoswitchable urocanate ascarosides (ucas) were generated following existing procedures[84] [76b]. The protected asc-C6MK (**135**) was synthesized by glycosylation of the commercially available

(*2R*,*5R*)-2,5-hexanediol with the orthogonally protected ascarylose building block **45** followed by oxidation of the secondary alcohol to the corresponding ketone while the side chain of 4'-UA-asc-ΔC9 (**37**) was synthesized by glycosylation of (*R*)-octen-2-ol **110**, obtained by organocuprate-catalyzed ring opening of (*R*)-(+)-propylene oxide **108** with 6-bromo-1-hexene **109**, followed by Grubbs metathesis. The ascaroside building blocks (**125** & **134**) were subsequently coupled to the Boc-protected urocanic acid via Steglich esterification. Both ucas compounds were synthesized via a PMB protecting group strategy. In case the carboxylic group could be easily protected as a PMB ester, the 2-position of the ascarylose building block required the use of Dudley's reagent to be protected as a PMB ether because the standard conditions to synthesize PMB ethers were too harsh. Next, the (*E*)-configured urocanate ascarosides (ucas) were converted to their corresponding (*Z*)-isomers by UV-irradiation in deuterated methanol. The (*Z*)-isomer could be easily obtained by sunlight (20% for 4'-UA-asc-C6MK, **35**) and UV-B irradiation (52% for 4'-UC-asc-ΔC9 , **37** and 35% for 4'-UA-asc-C6MK , **35**) nevertheless, the maximum conversion rate was obtained with an UV-C lamp (75% for 4'-UC-asc-ΔC9 , **37** and 71% for 4'-UA-asc-C6MK, **35**).

The *ortho*-aminobenzoate ascaroside 4-AB-asc-C5 (abas#9, **34**) was synthesized using two different methods. The first method involved the glycosylation of (*R*)-5-hexen-2-ol with the orthogonally protected ascarylose building block (**45**) followed by oxidation of the terminal alkene as described in literature. An alternative method involved the glycosylation of commercially available (*R*)-3-butyn-2-ol with the orthogonally protected ascarylose building block (**45**) followed by selective hydrogenation and Grubbs metathesis between the corresponding alkene (**149**) and an acrylate ester. Unexpectedly, the final hydrogenation to remove the Bn protecting groups provided, instead of the target compound, the *N*-methylated analogue **147** due to the "borrowing hydrogen transfer" from the methanol used as the solvent for the reaction. This problem could be circumvented by exchanging the methanol for ethyl acetate.

Furthermore, the synthesis of the 3,6-dideoxy-*lyxo*-hexose building block (**165**) for cae-7OH-ΔC9 (**39**) was done via regioselective epoxide ring opening of the 3,4-anhydro-1-*O*-methyl-6-dideoxy-*lyxo*-hexopyranoside (**162**) obtained by intramolecular nucleophilic substitution of 1-*O*-benzyl-4-*O*-triflate-rhamnoside (**161**) under alkaline conditions. In parallel, the aglycone was synthesized in high diastereoselectivity via Cram chelate complex mediated allylation of the 2-benzyloxy aldehyde **171** to afford the *threo*-allylic alcohol intermediate **172** which was elongated by Grubbs metathesis. Glycosylation of the side chain to the 3,6-dideoxy-*lyxo*-hexose building block (**165**) followed by alkaline deprotection then provided the desired compound, which represents the first natural product featuring a 3,6-dideoxy-*lyxo*-hexose moiety.

The 2-substituted oligomeric ascarosides were synthesized by successive coupling of the orthogonally

protected 4'-*O*-TBDPS-asc-ΔC5-*O*-Bn ester (**204**) to 2',4'-di-*O*-TBS-asc-C5 (**203**), synthesized from 2,4-di-*O*-benzoyl-ascarylose (**63**) and 2-*O*-Bz-4-*O*-TBDPS-ascarylose (**45**) respectively, followed by O-debenzylation of the side chain of the coupling product upon hydrogenation. Since the use of TBAF for silyl ether deprotection induced the decomposition of the final products in previous attempts, an alternative fluoride reagent was used for the desilylation step. Using TBAT under optimized conditions, the silyl ether protected oligomeric asc-C5 could be deprotected in high yield without any loss of material from ester cleavage. Final hydrogenation then provided the homologous series of asc-C5 oligomers, including the dimer (**40**), trimer (**41**), tetramer (**42**), and pentamer (**43**). Alternatively, a chemoselective benzyl ester deprotection pathway to obtain the oligomeric compounds was also studied using 4'-*O*-Bn-asc-ΔC5 *O*-Bn ester (**214**) and 2',4'-di-*O*-Bn-asc-C5 (**217**) as coupling partner. In this second method, the dimeric intermediate **220** was deprotected with 1,4-cyclohexadiene to the desired benzyl ether protected dimer with a free carboxylic acid moiety with high yield (76%), which was subsequently coupled to an additional unit of 4'-*O*-Bn-asc-ΔC5 *O*-Bn ester (**214**). Selective benzyl ester deprotection was also achieved in good yield for the benzylated asc-C5 trimer (**223**) demonstrating the usefulness of this methodology for the synthesis of oligomeric ascarosides.

After establishing the exact structures of the novel ascarosides by NMR and HPLC-HR-MS, the potential biological activities of the target compounds were investigated. These bioassays were limited to behavioral responses using retention assays with amounts varying from 100 amol to 10 pmol depending on the molecule. Only the dimeric asc-C5 (**40**) elicited significant retention activities in male *C. tropicalis*, which are in accordance with previous results for other dimeric ascarosides. Given the wide range of biological functions linked to ascaroside signaling, the results from the retention assays alone do not permit to conclude on the biological activity of these novel ascarosides. Furthermore, the complexity of ascaroside blends released by nematodes and the potential for synergistic activities makes it difficult to elucidate their potential biological functions. Additional investigations will be required to unravel the biological function of these new ascarosides.

Nevertheless, the identification of these novel components revealed that ascaroside diversity is more complex than previously anticipated and provides new insights into the mechanisms that govern the biosynthesis of species-specific modular ascarosides. The results demonstrate how nematodes have evolved to utilize the conserved basic ascarosides as building blocks from which they generate species-specific signaling molecules by integrating diverse additional metabolic pathways. The identification of the urocanate ascarosides (ucas) and *o*-aminobenzoate ascarosides (abas) represents additional examples for the integration of amino acid derived building blocks for the assembly of modular ascarosides. Along with the indole ascarosides (icas) [27-28] the *o*-aminobenzoate ascarosides (abas) represent a second group of modular ascarosides that integrate L-tryptophan metabolism into

chemical signaling, whereas the urocanate ascarosides (ucas) represent the first example for the integration of L-histidine metabolism in ascaroside signaling. Additionally, the discovery of the 4-epimeric cae-7OH-ΔC9 along with the pentameric asc-C5 revealed that nematodes could also use additional metabolic pathways like the epimerization of the sugar unit as well as oligomerization of conserved ascaroside building blocks downstream of the β-oxidation cycle to generate additional structural complexity in their chemical language.

So far, limited information regarding the genes involved in the biosynthesis of these new ascarosides are available. Considering the recent discovery of the carboxylesterase (*cest*) enzymes involved in the synthesis of modular ascarosides in lysosome related organelles (LROs) of the model organism *C. elegans*, parallel investigations in the closely related species will be required in order to fully understand the biomechanistic mechanisms that control the biosynthesis of species-specific ascarosides and thereby provide dedicated channels for species-specific communication in nematodes.

8. Experimental section

8.1. General information

Chemicals and reagents

Unless stated otherwise, all commercial reagents and solvents were used as received without any additional purification. Analytic grade solvents from Fisher chemical were used and dry solvents were purchased over molecular sieves from Acros Organics. Flash column chromatography was carried out on silica gel 60 (230-400 mesh) from Roth. Thin layer chromatography (TLC) were done on 0.20 mm silica gel 60 F_{254} on alumina backed plates from Macherey-Nagel and compounds were visualized using UV light (254 nm) and/or by staining with thymol solution (1.0 g thymol, 5 ml conc. H_2SO_4 in 100 ml EtOH), ninhydrin solution (0.1 g ninhydrin, 0.5 ml acetic acid in 100 ml acetone), p-anisaldehyde solution (6.0 g p-anisaldehyde, 1 ml H_2SO_4 in 100 ml EtOH) or permanganate solution (3.0 g $KMnO_4$, 20.0 g K_2CO_3, 5 ml 1 M NaOH in 300 ml of H_2O) followed by heating.

UV spectroscopy

UV spectra were acquired with an Acquity PDA eλ detector. Photoisomerization were conducted in a dark chamber and the compounds were irradiated with a 254 nm SterilAir® UVC9 lamp or with a 306 nm Ushio® UV-B lamp.

NMR spectroscopy

NMR spectra were recorded in $CDCl_3$ or CD_3OD at 600 MHz for ^1H and 150 MHz for ^{13}C or at 400 MHz for ^1H and 100 MHz for ^{13}C at room temperature on a Bruker AV Neo 600 spectrometer or a Bruker Avance III HD 400, respectively. Chemical shifts (δ) are reported in part per million (ppm) and NMR data are reported as follows: chemical shift (multiplicity [singlet (s), double (d), triplet (t), quartet (q) and multiplet (m)], coupling constant [Hz], integral). Residual solvent signals with ^1H at 7.26 ppm and ^{13}C at 77.16 ppm for $CDCl_3$ or ^1H at 3.31 ppm and ^{13}C at 49.05 ppm for CD_3OD were used as internal standards. Two-dimensional homonuclear double quantum filtered (*dqf*)-COSY spectra were recorded using phase cycling for coherence selection. Spectra were zero-filled prior to Fourier transformation, phased manually, and baseline corrected using the MNova v14 (Mestrelab Research) software. Structure assignments of new compounds are based on ^1H NMR, ^{13}C NMR, *dqf*-COSY, HSQC and HMBC when data from HSQC were not sufficient.

Mass spectrometry

HPLC-ESI-HR-MS/MS analysis of natural products was performed using a UHPLC-quadrupole time-of-flight mass spectrometry (QTOFMS) using Acquity UPLC coupled to a Synapt G2 MS (Waters) equipped

with an electrospray ionization (ESI) unit operated in positive or negative mode. Data were analyzed with the MassLynx 4.1 software (Waters).

Semi-preparative HPLC

Final synthetic products were separated with a semi-preparative Waters Breeze HPLC system (1525 binary HPLC pump with a 2487 dual wavelength absorbance detector) equipped with a reverse-phase XTerra MS C18 OBD column (19 × 150 mm, 5 µm) coupled with a Gilson FC 203B fraction collector then concentrated with a SpeedVac at 35 °C 24 h.

Bioassays

Wild-type Caenorhabditis isolates of *C. afra* JU1286 (Ghana), *C. brenneri* PB2801 (Costa Rica), *C. briggsae* AF16 (India), *C. nigoni* JU1422 (India), *C. remanei* PB4641 (United States), *C. tropicalis* JU1373 (La Réunion) and JU1428 (French Guyana) were obtained from the *Caenorhabditis elegans* Genetics Center (CGC). All nematodes were kept on solidified nematode growth medium (NGM agar) seeded with *Escherichia coli* OP50 and cultivated at 23 °C. *E. Coli* was obtained from the *Caenorhabditis* Genetics Center (CGC) at the University of Minnesota and cultivated on LB agar. Male nematodes were generated for the androdioecious *C. tropicalis* (JU1428) by growing on crowded plates and then transferring around ten spontaneously formed males and one hermaphrodite on a new NGM agar plate seeded with *E. coli* OP50. Male progeny was maintained by continuous mating of males and hermaphrodites.

Holding assays

Nematode preference for environments conditioned with modular ascarosides was measured using a holding assay. Circular scoring region were marked on a 6 cm peptone free NGM agar plate. The scoring regions were then conditioned with either 1 µl of 10% aqueous methanol (v/v, as solvent control) or with 1 µl of a solution of ascarosides and let to dry for 5 min. Non-starving young adult nematodes from non-crowded NGM agar plates seeded with E. coli OP50 were sorted by sex and transferred on an empty peptone-free NGM agar plate and let to crawl for approximately 15 min. Then, individual worms were placed into the center of the circular scoring region and the time required for the nematode to leave the scoring region was recorded with a timer. Once no part of the nematode was in the scoring region, the timer was stopped. A total number of 20 worms per condition were analyzed.

Attraction assays

Nematode feeding preference for environments conditioned with 4'-AB-asc-C5 (**34**) was measured using an attraction assay. On a 6 cm peptone-free NGM agar plate, two circular scoring regions of circa 9 mm diameter were marked. Next, 1 µl of 10% aqueous methanol (*v/v*, as solvent control) was placed in the center of one scoring region onto the agar and 1 µl of 10 nM solutions of *ortho*-aminobenzoate ascaroside in 10% aqueous methanol (*v/v*) was placed in the center of the second scoring areas onto the agar and left to dry for 5 minutes. Non-starving young adult nematodes from non-crowded NGM agar plates seeded with E. coli OP50 were sorted by sex and transferred on an empty peptone-free NGM agar plate and let to crawl for approximately 15 min. Then, ten worms were placed in two locations equidistant from the product and the control spot. The number of worms at both locations were determined after 30 min. The experiment was repeated ten times.

8.2. Synthesis of 2,4-di-*O*-benzoyl-ascarylose

1,2,3,4-tetra-*O*-benzoyl-6-deoxy- α-L-*arabino*-hexose (64).

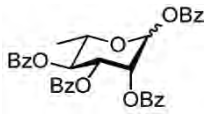

A solution of *L*-rhamnose monohydrate (**44**) (10 g, 45.69 mmol) in dry pyridine (133 ml) was treated with benzoyl chloride (39 mL, 260.42 mmol) at 0 °C. The solution was kept for 1.5 h at 0 °C and afterwards the solution was warmed to room temperature and stirred for 4 h at room temperature. The reaction was quenched with water (40 ml) and then extracted with dichloromethane (200 ml). The organic phase was washed with a 3 M hydrochloric acid solution (3 x 500 ml) and with a saturated aqueous solution of $NaHCO_3$ (200 ml), then dried over anhydrous $MgSO_4$. The solution was concentrated under reduced pressure to give **64** (21,31 g, 36.71 mmol, 80% yield, α/β mixture: 1/1), which was used without any further purification.

^{1}H NMR (600 MHz, $CDCl_3$) of the α/β mixture: δ (ppm) 8.21-8.16 (*m*, 4H), 8.14-8.11 (*m*, 2H), 8.01-7.96 (*m*, 4H), 7.95-7.92 (*m*, 2H), 7.86-7.81 (*m*, 4H), 7.68 (*tt*, *J* = 7.5 Hz, *J* = 1.3 Hz, 1H), 7.65 (*tt*, *J* = 7.5 Hz, *J* = 1.3 Hz, 1H), 7.64 (*tt*, *J* = 7.4 Hz, *J* = 1.3 Hz, 1H), 7.59-7.50 (*m*, 9H), 7.47-7.42 (*m*, 2H), 7.42-7.38 (*m*, 4H), 7.37-7.33 (*m*, 2H), 7.31-7.26 (*m*, 4H), 6.54 (*d*, *J* = 1.9 Hz, 1H), 6.34 (*d*, *J* = 1.2 Hz, 1H), 6.07 (*dd*, *J* = 2.9 Hz, *J* = 1.2 Hz, 1H), 5.98 (*dd*, *J* = 10.2 Hz, *J* = 3.5 Hz, 1H), 5.86 (*dd*, *J* = 3.5 Hz, *J* = 1.9 Hz, 1H), 5.79 (*dd*, *J* = 10.2 Hz, *J* = 10.0 Hz, 1H), 5.75-5.71 (*m*, 2H), 4.35 (*dq*, *J* = 10.0 Hz, *J* = 6.2 Hz, 1H), 4.09 (*m*, 1H), 1.48 (*d*, *J* = 6.1 Hz, 3H), 1.40 (*d*, *J* = 6.2 Hz, 3H). NMR identical to data reported in literature[18].

2,3,4-tri-*O*-benzoyl-6-deoxy-α-L-*arabino*-hexose (65).

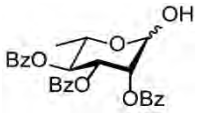

A solution of 1,2,3,4-tetra-*O*-benzoyl-L-rhamnopyranose (**64**) (21.31 g, 36.71 mmol) in acetonitrile (25 mL) was treated with a 2 M dimethylamine solution in tetrahydrofuran (30 mL, 60.6 mmol) at room temperature. The reaction was stirred for 16 h then concentrated under reduced pressure. The residue was purified by flash column chromatography using 20% ethyl acetate in toluene *(v/v)* as eluent to give **65** (12.9 g, 27.1 mmol, 74% yield, α/β mixture: 8/1).

^{1}H NMR (600 MHz, $CDCl_3$) for the dominating α-anomer: δ (ppm) 8.12-8.09 (*m*, 2H), 8.00-7.96 (*m*, 2H), 7.85-7.81 (*m*, 2H), 7.61 (*tt*, *J* = 7.4 Hz, 1.3 Hz, 1H), 7.54-7.47 (*m*, 3H), 7.44-7.36 (*m*, 3H), 5.91 (*dd*, *J* = 10.1 Hz, *J* = 3.4 Hz, 1H), 5.70 (*dd*, *J* = 3.4 Hz, *J* = 1.7 Hz, 1H), 5.69 (*dd*, *J* = 10.1 Hz, *J* = 9.7 Hz, 1H), 5.45 (*br. s*, 1H), 4.45 (*dq*, *J* = 9.7 Hz, *J* = 6.2 Hz, 1H), 1.37 (*d*, *J* = 6.2 Hz, 3H).NMR identical to data reported in literature[18].

2,3,4-tri-*O*-benzoyl-6-deoxy-α-L-*arabino*-hexono-1,5-lactone (66).

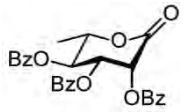

Under N_2 atmosphere, a mixture of pyridinium chlorochromate (16.8 g, 77.9 mmol) and dried molecular sieves (4 Å, 13.0 g) in dichloromethane (110 ml) was stirred for 1 h at 0 °C. Then a solution of 2,3,4-tri-O-benzoyl-L-rhamnopyranose (**65**) (9.3 mg, 19.6 mmol) in dichloromethane (110 ml) was added and the resulting mixture was stirred for 24 h at room temperature. Diethyl ether (200 ml) was added and the solution was filtered through silica gel. The filtrate was concentrated under reduced pressure and the residue purified by flash column chromatography using 6% ethyl acetate in toluene *(v/v)* as an eluent to give **66** (5.3 g, 11.2 mmol, 57% yield).

^{1}H NMR (600 MHz, $CDCl_3$): δ (ppm) 8.10-8.07 (*m*, 4H), 7.97-7.94 (*m*, 2H), 7.66-7.61 (*m*, 2H), 7.54 (*tt*, *J* = 7.5 Hz, *J* = 1.3Hz, 1H), 7.52-7.47 (*m*, 4H), 7.38-7.34 (*m*, 2H), 6.22 (*d*, *J* = 3.9 Hz, 1H), 6.00 (*dd*, *J* = 3.9 Hz, *J* = 1.7 Hz, 1H), 5.33 (*dd*, *J* = 8.3 Hz, *J* = 1.7 Hz, 1H), 4.85 (*dq*, *J* = 8.2 Hz, *J* = 6.2 Hz, 1H), 1.63 (*d*, *J* = 6.4 Hz, 3H). NMR identical to data reported in literature[18].

2,4-di-*O*-benzoyl-3,6-dideoxy-L-*erythro*-hex-2-enono-1,5-lactone (61).

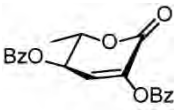

A solution of 2,3,4-tri-O-benzoyl-L-rhamnono-1,5-lactone (**66**) (1.6 g, 3.3 mmol) in chloroform (162 ml) was treated with NEt_3 (40 ml) under N_2 and stirred for 2 days at room temperature. The reaction mixture was extracted with 2 M hydrochloric acid solution, washed with water and dried over anhydrous Na_2SO_4. The mixture was concentrated in vacuum to give **61** (1.1 g, 3.1 mmol, 94% yield). The product was used without further purification.

^{1}H NMR (600 MHz, $CDCl_3$): δ (ppm) 8.14-8.11 (*m*, 2H), 8.08-8.05 (*m*, 2H), 7.66-7.60 (*m*, 2H), 7.51-7.46 (*m*, 4H), 6.71 (*d*, *J* = 4.8 Hz, 1H), 5.70 (*dd*, *J* = 4.8 Hz, *J* = 4.6 Hz, 1H), 4.96 (*qd*, *J* = 6.7 Hz, *J* = 4.6 Hz, 1H), 1.65 (*d*, *J* = 6.7 Hz, 3H). NMR identical to data reported in literature[18].

2,4-di-*O*-benzoyl-3,6-dideoxy- α-L-*arabino*-hexono-1,5-lactone (62).

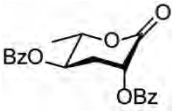

Under N_2 atmosphere, a solution of **61** (311 mg, 0.88 mmol) in ethyl acetate (3 ml) was added to a suspension of 10% palladium on activated charcoal (100 mg) in ethyl acetate (2 ml). The solution was flushed with hydrogen (1 atm) and stirred for 14 h, the mixture was filtered over a thin layer of silica and the catalyst rinsed with ethyl acetate. The filtrate was concentrated under reduced pressure and the residue purified by flash column chromatography on silica gel using 8% ethyl acetate in toluene *(v/v)* as eluent to afford **62** (159 mg, 0.44 mmol, 51% yield) as a colorless oil.

^{1}H NMR (600 MHz, $CDCl_3$): δ (ppm) 8.11-8.09 (*m*, 2H), 8.08-8.05 (*m*, 2H), 7.63 (*tt*, *J* = 7.5 Hz, 1.3 Hz, 1H), 7.60 (*tt*, *J* = 7.5 Hz, 1.3 Hz, 1H), 7.52-7.45 (*m*, 4H), 5.90 (*dd*, *J* = 12.1 Hz, *J* = 7.5 Hz, 1H), 5.28 (*dd*, *J* = 6.2 Hz, *J* = 3.6 Hz, 1H), 4.82 (*dq*, *J* = 6.1 Hz, *J* = 6.5 Hz, 1H), 2.71 (*ddd*, *J* = 14.1, *J* = 12.1, *J* = 6.1 Hz, 1H), 2.58 (*ddd*, *J* = 14.2 Hz, *J* = 7.5 Hz, *J* = 3.6 Hz, 1H), 1.59 (*d*, *J* = 6.5 Hz, 3H). NMR identical to data reported in literature[18].

2,4-di-*O*-benzoyl-3,6-dideoxy- α-L-*arabino*-hexose (63).

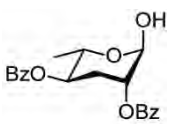

A pre-cooled solution of 1M borane tetrahydrofuran complex (2.1 ml, 2.1 mmol) at 0 °C was treated slowly with a solution of 2-methyl-2-butene (509 µl, 4.3 mmol) in dry tetrahydrofuran (1.6 ml). After 2 h a solution of 2,4-di-*O*-benzoyl-3,6-dideoxy-L-*arabino*-hexono-lactone (**62**) (270 mg, 0.77 mmol) in

dry tetrahydrofuran (17 ml) was added and the solution was stirred for 21 h. at room temperature. water (170 µl) was added and the reaction was stirred for further 30 min at room temperature. The mixture was cooled to 0 °C and treated with a solution of 35% H_2O_2 (650 µl) and the solution was adjusted to pH 7-8 by addition of concentrated sodium hydroxide solution (850 µl). The mixture was concentrated under reduced pressure then purified by flash column chromatography using 35% ethyl acetate in hexane *(v/v)* as eluent to give the 2,4-di-*O*-benzoyl-ascarylose **63** (220 mg, 0.62 mmol, 81% yield, α/β mixture 4/1) as a colorless oil.

^{1}H NMR (600 MHz, $CDCl_3$) for the dominating α-anomer: δ (ppm) 8.13 – 8.09 (*m*, 2H), 8.06 – 8.03 (*m*, 2H), 7.61 – 7.56 (*m*, 2H), 7.51 – 7.43 (*m*, 4H), 5.28 (*br.s*, 1H), 5.25 (*dd*, *J* = 3.4 Hz, 3.2 Hz, 1H), 5.20 (*ddd*, *J* = 11.2, *J* = 9.6, *J* = 4.6 Hz, 1H), 4.33 (*dq*, *J* = 9.6 Hz, *J* = 6.3 Hz, 1H), 2.44 (*ddd*, *J* = 13.7 Hz, *J* = 4.6 Hz, *J* = 3.4 Hz, 1.0 Hz, 1H), 2.29 (*ddd*, *J* = 13.7 Hz, *J* = 11.2 Hz, *J* = 3.2 Hz, 1H), 1.30 (*d*, *J* = 6.3 Hz, 3H), **^{13}C NMR**(150 MHz, $CDCl_3$): δ (ppm) 166.0, 165.8, 133.5, 133.4, 130.0, 129.8, 128.6, 91.2, 70.9, 70.7, 67.0, 29.2, 18.1.

1-*O*-methyl-6-deoxy-α-L-*arabino*-hexose (56).

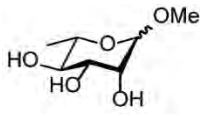

Under N_2 atmosphere, a solution of L-Rhamnose **44** (15.0 g, 91 mmol) in methanol (230 ml) was treated with acetyl chloride (25.5 ml, 364.5 mmol) and the mixture was refluxed overnight. After completion of the reaction, the mixture was cooled to room temperature and saturated aqueous $NaHCO_3$ solution was added to the solution. The mixture was filtered, concentrated under reduced pressure and the resulting residue purified through a silica plug using 10% methanol in dichloromethane *(v/v)* as eluent to afford **56** (14.8 g, 83.1 mmol, 91% yield, α/β: 7/1) as a yellow oil.

^{1}H NMR (400 MHz, CD_3OD): δ (ppm) 4.55 (*d*, *J* = 1.6 Hz, 1H), 3.78 (*dd*, *J* = 3.5 Hz, *J* = 1.7 Hz, 1H), 3.60 (*dd*, *J* = 9.5, *J* = 3.5 Hz, 1H), 3.53 (*dq*, *J* = 9.5 Hz, *J* = 6.2 Hz, 1H), 3.35 (*dd*, *J* = 9.5 Hz, *J* = 9.5 Hz, 1H) 3.34 (*s*, 1H), 1.27 (*d*, *J* = 6.2 Hz, 3H). NMR identical to data reported in literature[73].

1-*O*-methyl-3-*O*-phenoxythiocarbonyl-6-deoxy-α-L-*arabino*-hexose (75).

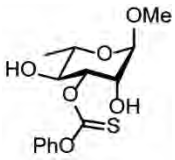

In a brown vial, the L-methyl-rhamnose **56** (50 mg, 0.28 mmol) in acetone (2.8 ml) was treated with di-n-octyldichlorotin (11.5mg, 0.028 mmol), at room temperature. After stirring for 10 min, the mixture was cooled to 0 °C and treated with tetrabutylammonium iodide (10 mg, 0.028 mmol), phenyl

chlorothionoformate (49 µl) and 1,2,2,6,6-pentamethylpiperidine (76 µl, 0.42 mmol). After stirring at 0 °C for 3h, the solution was quenched with a saturated solution of NH_4Cl (1 ml). The extracted organic phase was washed with water (1 ml) and brine (1 ml), dried with Na_2SO_4 and concentrated under reduced pressure. The resulting residue was purified by flash column chromatography with a gradient of 20 to 35% ethyl acetate in hexane *(v/v)* to afford **75** (72 mg, 0.22 mmol, 82%).

^{1}H NMR (600 MHz, $CDCl_3$): δ (ppm) 7.43 (t, J = 7.9 Hz, 2H), 7.31 (t, J = 7.5 Hz, 1H), 7.13 (d, J = 8.2 Hz, 2H), 5.56 (dd, J = 9.7 Hz, J = 3.1 Hz, 1H), 4.73 (br.s, 1H), 4.35 (br.s, 1H), 3.90 (dd, J = 9.7 Hz, J = 9.7 Hz, 1H), 3.80 (dq, J = 9.7 Hz, J = 6.1 Hz, 1H), 3.42 (s, 3H), 2.35-2.26 (m, 2H), 1.40 (d, J = 6.1 Hz, 3H), **^{13}C NMR**(150 MHz, $CDCl_3$): δ (ppm) 195.0, 153.5, 129.3, 126.9, 122.0, 100.8, 84.4, 71.3, 68.7, 68.5, 55.2, 17.7.

1-*O*-methyl-2,4-di-*O*-benzoyl-3,6-dideoxy- α-L-*arabino*-hexose (67).

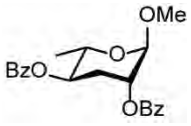

Under N_2 atmosphere, a solution of **56** (30 mg, 0.095 mmol) in toluene (3 ml) was treated with tri-n-butyltin hydride (40 µl, 0.15 mmol), and 2,2'-azobis(2-methylpropionitrile) (3 mg, 0.02 mmol). After stirring for 20 min at 80 °C, the mixture was cooled to room temperature and concentrated under reduced pressure. The residue was treated with dry pyridine (200 µl, 2.4 mmol) and benzoyl chloride (40 µL, 0.27 mmol) at 0 °C. After stirring for 24 h, the solution was treated with saturated aqueous $NaHCO_3$ solution (1 ml), extracted with hexane (3 x 1 ml), dried with Na_2SO_4 and concentrated under reduced pressure. The residue was purified by flash column chromatography on silica gel using a gradient of 0 to 10% of ethyl acetate in hexane *(v/v)* as eluent to afford **67** (15 mg, 0.040 mmol, 42% yield, α/β mixture) as a colorless oil.

^{1}H NMR (600 MHz, $CDCl_3$): δ (ppm) 8.13-8.10 (m, 2H), 8.05-8.02 (m, 2H), 7.61-7.56 (m, 2H), 7.50-7.43 (m, 4H), 5.21 (m, 1H), 5.19 (ddd, J = 11.1 Hz, J = 9.6 Hz, J = 4.7 Hz), 4.74 (br.s, 1H), 4.07 (dq, J = 9.6 Hz, J = 6.3 Hz, 1H), 3.48 (s, 3H), 2.42 (ddd, J = 13.7 Hz, J = 4.7 Hz, J = 3.1 Hz, 1H), 2.20 (ddd, J = 13.7 Hz, J = 11.3 Hz, J = 3.2 Hz, 1H), 1.32 (d, J = 6.3 Hz, 3H). NMR identical to data reported in literature[67].

8.3. Synthesis of 2-*O*-benzoy-4-*O*-*tert*-butyldiphenylsilyl-ascarylose

1-*O*-methyl-6-deoxy-2,3-(*O*-isopropylidene)-α-L-*arabino*-hexose (76).

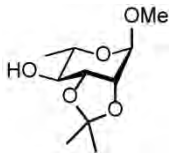

Under N_2 atmosphere, a solution of **56** (14.8 g, 83.1 mmol) in dry acetone (300 ml) was treated with camphor-10-sulfonic acid (202 mg, 0.87 mmol) followed by 2,2-dimethoxypropane (57.8 ml, 465 mmol). After stirring overnight at room temperature, the mixture was neutralized with 1 M solution of sodium hydroxide (90 ml) then concentrated under reduced pressure. The residue was dissolved in dichloromethane (200 ml), the organic phase washed with water (2 x 100 ml) and brine (100 ml) then concentrated under reduced pressure. The resulting residue was purified by flash column chromatography on silica gel using 35% ethyl acetate in hexane *(v/v)* as eluent to afford **76** (14.0 g, 64.1 mmol, 77% yield) as a yellow oil.

^{1}H NMR (400 MHz, $CDCl_3$): δ (ppm) 4.83 (*br.s*, 1 H), 4.14-4.08 (*m*, 1H), 4.05 (*dd*, *J* = 7.1 Hz, *J* = 5.8 Hz, 1H), 3.62 (*dq*, *J* = 9.2 Hz, *J* = 6.3 Hz, 1H), 3.37 (*s*, 3H), 3.37 (*dd*, *J* = 9.5 Hz, *J* = 7.2 Hz, 1H), 1.51 (*s*, 3H), 1.34 (*s*, 3H), 1.29 (*d*, *J* =6.4 Hz, 3H). NMR identical to data reported in literature[40].

1-*O*-methyl-6-deoxy-2,3-*O*-(isopropylidene)-4-*O*-*tert*-butyldiphenylsilyl-α-L- *arabino*-hexose (77).

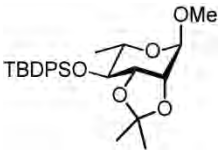

A solution of **76** (14.0 g, 64.1 mmol) in dichloromethane (152 ml) was treated with *tert*-butyldiphenylchlorosilane (25 ml, 96 mmol) and imidazole (8.8 g, 128 mmol). After stirring overnight at room temperature, the mixture was filtered and the filtrate concentrated under reduced pressure. The resulting residue was purified by flash column chromatography on silica gel using 20% ethyl acetate in hexane *(v/v)* as eluent to afford **77** (27.6 g, 60.4 mmol, 94% yield) as a yellow oil.

^{1}H NMR (400 MHz, $CDCl_3$): δ (ppm) 7.75 – 7.70 (*m*, 2H), 7.69 – 7.65 (*m*, 2H), 7.44 – 7.32 (*m*, 6H), 4.75 (*br.s*, 1H), 4.19 (*dd*, *J* = 6.9 Hz, *J* = 5.8 Hz, 1H), 4.06 (*dd*, *J* = 5.8 Hz, *J* = 0.8 Hz, 1H), 3.67 (*dqd*, *J* = 9.6 Hz, *J* = 6.3 Hz, *J* = 0.6 Hz, 1H), 3.38 (*dd*, *J* = 9.6 Hz, *J* = 6.9 Hz, 1H), 3.36 (*s*, 3H), 1.23 (*s*, 3H), 1.09 (*s*, 3H), 1.07 (*s*, 9H), 1.05 (*d*, *J* = 6.3 Hz, 3H). NMR identical to data reported in literature[40].

1-*O*-methyl-6-deoxy-4- *O*-*tert*-butyldiphenylsilyl-α-L-*arabino*-hexose (78).

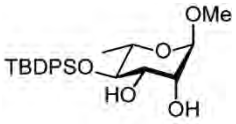

A solution of **77** (27.6 g, 60.4 mmol) in dichloromethane (600 ml) was treated with a solution of trifluoroacetic acid (3.1 ml, 40 mmol) containing 1% of water. After stirring overnight, the mixture was concentrated under reduced pressure and the residue purified by flash column chromatography on silica gel using a gradient of 10 to 50% of ethyl acetate in hexane *(v/v)* as eluent to afford **78** (14.5 g, 34.8 mmol, 58% yield) as a colorless oil.

^{1}H NMR (400 MHz, $CDCl_3$): δ (ppm) 7.77-7.73 (*m*, 2H), 7.72-7.66 (*m*, 2H), 7.48-7.38 (*m*, 6H), 4.59 (*br.s*, 1H), 3.83 (*dd*, *J* = 8.5 Hz, *J* = 3.6 Hz, 1H), 3.78 (*dd*, *J* = 3.5 Hz, *J* = 1.6 Hz, 1H), 3.74 (*dq*, *J* = 9.2 Hz, *J* = 6.3 Hz, 1H), 3.54 (*dd*, *J* = 9.2 Hz, *J* = 8.5 Hz, 1H), 3.38 (*s*, 3H), 1.26 (*d*, *J* = 6.3 Hz, 3H), 1.07 (*s*, 9H). NMR identical to data reported in literature[40].

1-*O*-methyl-6-deoxy-2,3-(*O*-sulfite)-4-*O*-*tert*-butyldiphenylsilyl-α-L-*arabino*-hexose (79).

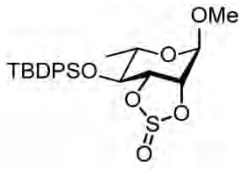

A solution of **78** (14.5 g, 34.8 mmol) in ethyl acetate (185 ml) was treated with pyridine (5.63 ml, 69.6 mmol). The mixture was cooled to 0 °C then thionyl chloride (3.8 ml, 52.2 mmol) was added. After stirring for 30 min, ethyl acetate was added to the mixture (100 ml). The organic phase was washed with water (3 x 100 ml), dried with Na_2SO_4 and concentrated under reduced pressure. The resulting residue was purified by flash column chromatography on silica gel using 35% ethyl acetate in hexane *(v/v)* as eluent to give **79** (15.64 g, 33,8 mmol, 97% yield) as a yellow oil.

^{1}HNMR (400 MHz, $CDCl_3$): δ (ppm) 7.72-7.65 (*m*, 4H), 7.47- 7.34 (*m*, 6H), 4.91 (*dd*, *J* = 7.6 Hz, *J* = 5.5 Hz, 1H), 4.92 (*br.s*, 1H), 4.73 (*dd*, *J* = 5.5 Hz, *J* = 0.9 Hz, 1H), 3.75 (*dq*, *J* = 9.7 Hz, *J* = 6.3 Hz, 1H), 3.40 (*s*, 3H), 3.14 (*dd*, *J* = 9.6 Hz, *J* = 7.6 Hz, 1H), 1.12 (*d*, *J* = 6.3 Hz, 3H), 1.06 (*s*, 9H). NMR identical to data reported in literature[40].

1-*O*-methyl-6-deoxy-2,3-(*O*-sulfate)-4-*O*-*tert*-butyldiphenylsilyl-α-L-*arabino*-hexose (80).

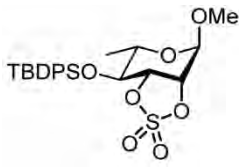

A vigorously stirred solution of **79** (15.6 g, 33.8 mmol) in dichloromethane (110 ml), acetonitrile (110 ml) and water (96 ml) was treated with ruthenium (III) chloride hydrate (348 mg, 1.6 mmol) in water (14 ml) followed by sodium periodate (37.4 g). After 20 min of stirring, water (100 ml) was added to the mixture and the aqueous phase was extracted with dichloromethane (3 x 100 ml). The organic phase was dried with Na_2SO_4 and concentrated under reduced pressure. The resulting residue was purified by flash column chromatography on silica gel using a gradient of 10 to 35% ethyl acetate *(v/v)* in hexane as eluent to afford **80** (11.3 g, 23.6 mmol, 70% yield) as an oil.

^{1}H NMR (400 MHz, $CDCl_3$): δ (ppm) 7.70-7.65 (*m*, 4H), 7.47-7.36 (*m*, 6H), 4.96 (*dd*, *J* = 7.3 Hz, *J* = 5.4 Hz, 1H), 4.90 (*dd*, *J* = 5.4 Hz, *J* = 0.9 Hz, 1H), 4.85 (*br.s*, 1H), 3.81 (*dd*, *J* = 9.6 Hz, *J* = 7.3 Hz, 1H), 3.73 (*dq*, *J* = 9.7, *J* = 6.1 Hz, 1H), 3.38 (*s*, 3H), 1.05 (*s*, 9H), 1.02 (*d*, *J* = 6.1 Hz, 3H). NMR identical to data reported in literature[40].

1-*O*-methyl-4-*O*-*tert*-butyldiphenylsilyl 3,6-dideoxy-α-L-*arabino*-hexose (81).

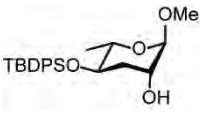

A solution of **80** (11.3 g, 23.6 mmol) in tetrahydrofuran (110 ml) was stirred at 55 °C then, tetrabutylammonium borohydride (12.1 g, 47.2 mmol) was added to the mixture. After stirring for 5 h, the mixture was cooled to 0 °C and quenched with acetone (10 ml). Concentrated sulfuric acid (4.4 ml) was added to the mixture and the resulting mixture stirred for 1 h then methanol (4.4 ml) was added. After stirring for 3 h, ethyl acetate (2 x 100 ml) was added to the mixture followed by saturated aqueous $NaHCO_3$ solution (100 ml). The organic phase was extracted then washed with water, dried with Na_2SO_4 and concentrated under reduced pressure. The resulting residue was purified by flash column chromatography on silica gel using 20% ethyl acetate in hexane *(v/v)* as eluent to afford **81** (6.99 g, 17.4 mmol 74% yield).

^{1}H NMR (400 MHz, $CDCl_3$): δ (ppm) 7.72-7.64 (*m*, 4H), 7.46-7.34 (*m*, 6H), 4.37 (*br.s*, 1H), 3.74 (*dq*, *J* = 8.9 Hz, *J* = 6.3 Hz, 1H), 3.70-3.66 (*m*, 1H), 3.64 (*ddd*, *J* = 10.7 Hz, *J* = 9.1 Hz, *J* = 4.7 Hz, 1H), 3.38 (*s*, 3H), 1.86 (*ddd*, *J* = 13.5, *J* = 10.7 Hz, *J* = 3.1 Hz, 1H), 1.78 (*ddd*, *J* = 13.5 Hz, *J* = 4.7Hz, *J* = 3.5 Hz, 1H), 1.19 (*d*, *J* = 6.2 Hz, 3H), 1.06 (*s*, 9H). NMR identical to data reported in literature[40].

1-*O*-methyl-2-*O*-benzoyl-4-*O*-*tert*-butyldiphenylsilyl 3,6-dideoxy-α-L-*arabino*-hexose (82).

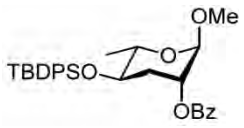

- **From 1-*O*-methyl-4-*O*-*tert*-butyldiphenylsilyl 3,6-dideoxy-α-L-*arabino*-hexose (81).**

A solution of **81** (7.0 g, 17.4 mmol) in pyridine (310 ml) at 0 °C was treated dropwise with benzoyl chloride (5.7 ml, 52.2 mmol). After stirring for 1 h, water (200 ml) was added to the mixture and the organic phase extracted with hexane (3 x 100 ml), dried with Na_2SO_4 and concentrated under reduced pressure. The resulting residue was purified by flash column chromatography on silica gel using 20% ethyl acetate in hexane *(v/v)* as eluent to afford **82** (7.2 g, 14.3 mmol, 81% yield) as a white solid.

- **From 1-*O*-methyl-2-*O*-benzoyl 3,6-dideoxy-α-L-*arabino*-hexose (88).**

A solution of **88** (5 mg, 18.8 µmol) in dichloromethane (500 µl) was treated with imidazole (2.6 mg, 37.6 µmol) and *tert*-butyldiphenylchlorosilane (10 µl, 37.6 µmol). After stirring for 19 h, the mixture was filtered and concentrated under reduced pressure. The resulting residue was purified by flash column chromatography on silica gel using 20% ethyl acetate in hexane *(v/v)* as eluent to afford **82** (8.5 mg, 16.8 µmol, 89 % yield) as a white solid.

^{1}H NMR (400 MHz, $CDCl_3$): δ (ppm) 7.77-7.71 (*m*, 2H), 7.70-7.63 (*m*, 4H), 7.58-7.53 (*m*, 1H), 7.42-7.35 (*m*, 3H), 7.35-7.28 (*m*, 5H), 4.96-4.92 (*m*, 1H), 4.54 (*br.s*, 1H), 3.84 (*dq*, *J* = 9.2, *J* = 6.3 Hz, 1H), 3.66 (*ddd*, *J* = 11.1 Hz, *J* = 9.2 Hz, *J* = 4.4 Hz, 1H), 3.41 (*s*, 3H), 2.03 (*ddd*, *J* = 13.6, *J* = 11.2, *J* = 3.0 Hz, 1H), 1.87 (*ddd*, *J* = 13.6 Hz, *J* = 4.4 Hz, *J* = 3.2 Hz, 1H), 1.29 (*d*, *J* = 6.2 Hz, 1H), 1.05 (*s*, 9H). NMR identical to data reported in literature[40].

2-*O*-benzoyl-4-*O*-*tert*-butyldiphenylsilyl-3,6-dideoxy-α-L-*arabino*-hexose (45).

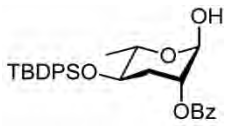

Under N_2 atmosphere, a solution of **82** (7.2 g, 14.3 mmol) in dichloromethane (170 ml) at -78 °C was treated dropwise with 1 M boron tribromide solution in dichloromethane (11.7 ml, 28.1 mmol). After stirring for 3 h the mixture was quenched with saturated aqueous $NaHCO_3$ solution (50 ml) and the mixture was extracted with ethyl acetate, dried with Na_2SO_4 and concentrated under reduced pressure. The resulting residue was purified by flash column chromatography on silica gel using 20% ethyl acetate in hexane *(v/v)* as eluent to afford **45** (5.24 g, 10.7 mmol, 76% yield, α/β mixture 4/1) as a yellow oil.

^{1}H NMR (400 MHz, $CDCl_3$) for the dominating α-anomer: δ (ppm) 7.77-7.64 (*m*, 7H), 7.45-7.23 (*m*, 8H),

5.08 (*br.s*, 1H), 5.00-4.97 (*m*, 1H), 4.09 (*dq*, *J* = 8.9 Hz, *J* = 6.2 Hz, 1H), 3.68 (*ddd*, *J* = 11.4 Hz, *J* = 8.9 Hz, *J* = 4.4 Hz, 1H), 2.13 (*ddd*, *J* = 13.8 Hz, *J* = 11.4 Hz, *J* = 3.0 Hz, 1H), 1.89 (*dt*, *J* = 13.8 Hz, *J* = 3.9 Hz, 1H), 1.27 (*d*, *J* = 6.2 Hz, 3H), 1.06 (*s*, 9H). NMR identical to data reported in literature[40].

8.4. Synthesis of 2-*O*-benzoyl-4-*O*-benzyl-ascarylose

1-*O*-methyl-6-deoxy-2,3-(*O*-benzylidene)-α-L-*arabino*-hexose (57).

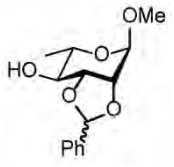

A solution of **56** (3.0 g, 16.8 mmol) in dimethylformamide (11 ml) was treated with α,α-dimethoxytoluene (3 ml, 20.2 mmol) and *para*-toluenesulfonic acid and the mixture was stirred at 60 °C under reduced pressure (20 mbar) in the rotary evaporator overnight. After completion of the reaction, the mixture was neutralized with saturated aqueous $NaHCO_3$ solution (10 ml), extracted with dichloromethane (2 x 20 ml), dried with Na_2SO_4 and concentrated under reduced pressure. The resulting residue was purified by flash column chromatography using 35% ethyl acetate in hexane *(v/v)* as eluent to afford a 1/1 diastereosiomeric mixture of **57** (3.2 g, 12.0 mmol, 72 % yield) as a colorless oil.

^{1}H NMR (600 MHz, $CDCl_3$): δ (ppm) 7.53-7.50 (*m*, 2H), 7.45-7.43 (*m*, 2H), 7.41-7.34 (*m*, 6H), 6.16 (*s*, 1H), 5.91 (*s*, 1H), 4.98 (*br.s*, 1H), 4.92 (*br.s*, 1H), 4.38 (*dd*, *J* = 7.2 Hz, *J* = 2.8 Hz, 1H), 4.24 (*dd*, *J* = 6.5 Hz, *J* = 2.9 Hz, 1H), 4.21(*dd*, *J* = 2.9 Hz, *J* = 1.1 Hz, 1H), 4.11 (*dd*, *J* = 2.8 Hz, *J* = 1.2 Hz, 1H), 3.74 (*qd*, *J* = 9.3 Hz, *J* = 6.4 Hz, 1H), 3.71 (*qd*, *J* = 8.8 Hz, *J* = 6.3 Hz, 1H), 3.56 (*ddd*, *J* = 9.3 Hz, *J* = 7.2 Hz, *J* = 4.2 Hz, 1H), 3.46 (*ddd*, *J* = 8.8 Hz, *J* = 6.5 Hz, *J* = 4.9 Hz, 1H), 3.42 (*s*, 3H), 3.39 (*s*, 3H), 2.40 (*d*, *J* = 4.2 Hz, 1H), 2.34 (*d*, *J* = 4.9 Hz, 1H), 1.36 (*d*, *J* = 6.3 Hz, 3H), 1.31 (*d*, *J* = 6.4 Hz, 3H), **^{13}C NMR**(150 MHz, $CDCl_3$): δ (ppm) 138.7, 137.2, 129.6, 129.4, 128.62, 128.59, 126.8, 126.2, 104.3, 103.2, 98.3,98.2, 79.7, 78.2, 77.9, 75.5, 74.5, 72.1, 66.3, 65.5, 55.19, 55.18, 17.8, 17.6, **HRMS** (ESI-TOF) m/z $(M + Na)^+$ calcd for $C_{14}H_{18}O_5Na$ 289.1052, found 289.1049, ∆ppm -1.

1-*O*-methyl-2-*O*-benzoyl-3-bromo-3,6-dideoxy-*altro*-hexose (58)

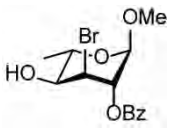

Under N_2 atmosphere, a solution of **57** (2.0 g, 7.5 mmol) in dry acetonitrile (100 ml) was treated with oven dried calcium carbonate (900 mg, 9 mmol) and *N*-bromosuccinimide (1.55 g, 8.7 mmol). After refluxing for 1 h the mixture was cooled to room temperature, filtered and the filtrate diluted with

dichloromethane (50 ml). The organic phase was washed with water (2 x 20 ml), dried with Na_2SO_4 and concentrated under reduced pressure. The resulting residue was purified by flash column chromatography using 35% of ethyl acetate in hexane *(v/v)* as eluent to afford **58** (2.3 g, 6.6 mmol, 89% yield) as a yellow oil.

^{1}H NMR (600 MHz, $CDCl_3$): δ (ppm) 8.04 (*dd*, *J* = 8.3 Hz, *J* = 1.8 Hz, 2H), 7.60 (*tt, J* = 7.6 Hz, *J* = 1.8 Hz, 1H), 7.47 (*dd*, *J* = 8.3 Hz, *J* = 7.6 Hz, 2H), 5.52 (*dd*, *J* = 3.6 Hz, *J* = 1.6 Hz, 1H), 4.72 (*br.s*, 1H), 4.54 (*dd*, *J* = 4.4 Hz, *J* = 3.6 Hz, 1H), 4.05 (*dq*, *J* = 8.9 Hz, *J* = 6.4 Hz, 1H), 3.59 (*dd*, *J* = 8.9 Hz, *J* = 4.4 Hz, 1H), 3.44 (*s*, 3H), 1.39 (*d*, *J* = 6.4 Hz, 3H), **^{13}C NMR**(150 MHz, $CDCl_3$): δ (ppm) 165.0, 133.8, 130.0, 128.7, 99.2, 73.2, 69.8, 65.9, 55.7, 52.7, 17.3, **HRMS** (ESI-TOF) m/z (M + Na)$^+$ calcd for $C_{14}H_{17}BrNaO_5$ 367.0157, found 367.0146, Δppm -3.0.

1-*O*-methyl-2-*O*-benzoyl 3,6-dideoxy-α-L-*arabino*-hexose (88).

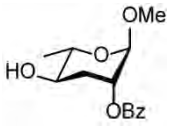

- **Via radical dehalogenation**

Under N_2 atmosphere, a solution of **58** (400 mg, 1.2 mmol) in dry toluene (17 ml) was treated with tri-*n*-butyltin hydride (600 µl, 2.3 mmol), and 2,2'-azobis(2-methylpropionitrile) (30 mg, 0.18 mmol). After stirring for 2 h at 80 °C, the mixture was cooled to room temperature and concentrated under reduced pressure. The resulting residue was purified by flash column chromatography using 35 % ethyl acetate in hexane *(v/v)* as eluent to afford **88** (300 mg, 1.1 mmol, 92% yield) as a yellow oil.

- **Via catalytic hydrogenation**

A solution of **58** (10 mg, 29 µmol) in ethanol (1 ml) was treated with palladium on charcoal (5 mg). After stirring under hydrogen atmosphere (1 atm) for 13 h the mixture was filtered over a cotton plug and the catalyst rinsed with ethanol. The filtrate was washed with water (2 x 1 ml), dried with Na_2SO_4 then concentrated under reduced pressure. The resulting residue was purified by flash column chromatography using 35 % ethyl acetate in hexane *(v/v)* as eluent to afford **88** (6 mg, 23 µmol, 79% yield) as a yellow oil.

- **Via reduction with nickel borohydride**

A solution of **58** (40 mg, 116 µmol) in ethanol (10 ml) was slowly treated with sodium borohydride (26 mg, 650 µmol) and nickel chloride hexahydrate (59 mg, 260 µmol). After stirring the solution at room temperature for 25 min the mixture was concentrated under reduced pressure. The resulting residue

was purified by flash column chromatography using 20% ethyl acetate in hexane *(v/v)* s eluent to afford **88** (23.9 mg, 89.8 µmol, 77% yield).

^{1}H NMR (600 MHz, $CDCl_3$): δ (ppm) 8.04 (*dd*, *J* = 8.3 Hz, 1.6 Hz, 2H), 7.57 (*tt*, *J* = 7.5 Hz, *J* = 1.6 Hz, 1H), 7.45 (*dd*, *J* = 8.3 Hz, *J* = 7.5 Hz, 2H), 5.17 (*ddd*, *J* = 3.2 Hz, *J* = 3.2 Hz, *J* = 1.6 Hz, 1H), 4.66 (*br.s*, 1H), 3.72-3.66 (*m*, 2H), 3.42 (*s*, 3H), 2.23 (*ddd*, *J* = 13.3 Hz, *J* = 4.0 Hz, *J* = 3.2 Hz, 1H), 1.99 (*ddd*, *J* = 13.3 Hz, *J* = 10.8 Hz, *J* = 3.2 Hz, 1H), 1.35 (s, 3H), **^{13}C NMR**(150 MHz, $CDCl_3$): δ (ppm) 165.8, 133.4, 129.9, 128.6, 97.5, 71.1, 69.4, 68.5, 55.0, 32.9, 17.9, **HRMS** (ESI-TOF) m/z $(M + Na)^+$ calcd for $C_{14}H_{18}O_5Na$ 289.1052 found 289.1052 Δppm 0.

1-*O*-methyl-2-*O*-benzoyl-4-*O*-benzyl 3,6-dideoxy-α-L-*arabino*-hexose (92).

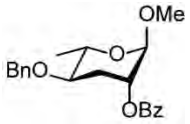

A solution of **88** (300 mg, 1.13 mmol) in α,α,α-benzotrifluoride (2.3 ml) was treated with 2-benzyloxy-1-methylpyridinium triflate (779 mg, 2.26 mmol) and magnesium oxide (91 mg, 2.26 mmol). After stirring the solution for 14 h at 83 °C, the mixture was cooled to room temperature and filtered . The solid was washed with dichloromethane (5 ml) and the filtrate concentrated under reduced pressure. The resulting residue was purified by flash column chromatography using 20% ethyl acetate in hexane (*v/v*) as eluent to afford **92** (330 mg, 0.93 mmol, 82%) as a yellow oil.

^{1}H NMR (600 MHz, $CDCl_3$): δ (ppm) 8.04 (*dd*, *J* = 8.0 Hz, *J* = 2.7 Hz, 2H), 7.60 (*tt*, *J* = 7.6 Hz, *J* = 2.7 Hz, 1H), 7.47 (*dd*, *J* = 8.0 Hz, *J* = 7.6 Hz, 2H), 7.35-7.27 (*m*, 5H), 5.19 (*ddd*, *J* = 3.4 Hz, *J* = 3.1 Hz, *J* = 1.4 Hz, 1H), 4.68 (*br.s*, 1H), 4.65 (*d*, *J* = 11.2 Hz, 1H), 4.51 (*d*, *J* = 11.2 Hz, 1H), 3.85 (*dq*, *J* = 9.0 Hz, *J* = 6.2 Hz, 1H), 3.49 (*ddd*, *J* = 11.4 Hz, *J* = 9.0 Hz, *J* = 6.4 Hz, 1H), 3.43 (*s*, 1H), 2.37 (*ddd*, *J* = 13.7 Hz, *J* = 6.4 Hz, *J* = 3.1 Hz, 1H), 2.02 (*ddd*, *J* = 13.7 Hz, *J* = 11.4 Hz, *J* = 3.4 Hz, 1H), 1.37 (*d*, *J* = 6.2 Hz, 3H), **^{13}C NMR**(150 MHz, $CDCl_3$): δ (ppm) 165.7, 138.4, 138.2, 133.3, 129.9, 128.51, 128.49, 128.0, 97.4, 75.0, 71.2, 71.0, 68.0, 54.8, 29.6, 18.3, **HRMS** (ESI-TOF) m/z $(M + Na)^+$ calcd for $C_{21}H_{24}O_5$ 379.1521, found 379.1504, Δppm -4.5.

2-*O*-benzoyl-4-*O*-benzyl 3,6-dideoxy-α-L-*arabino*-hexose (46).

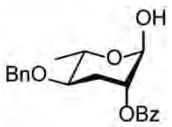

A solution of **92** (170 mg, 0.48 mmol) in acetic acid (6.8 ml) was treated with a 3 M solution of hydrochloric acid (630 µl, 1.89 mmol). After stirring the solution for 2 h at 80 °C, the mixture was cooled to room temperature, quenched with $NaHCO_3$ (180 mg) and concentrated under reduced

pressure. The resulting residue was purified by flash column chromatography using 20% ethyl acetate in hexane (v/v) as eluent to afford **46** (129 mg, 0.38 mmol, 78%, α/β mixture 3/1) as a yellow oil.

^{1}H NMR (600 MHz, $CDCl_3$) for the dominating α-anomer: δ (ppm) 8.01 (*dd*, *J* = 8.6 Hz, *J* = 2.8 Hz, 2H), 7.59 (*tt*, *J* = 7.7 Hz, *J* = 2.8 Hz, 1H), 7.46 (*dd*, *J* = 8.6 Hz, *J* = 7.7 Hz, 2H), 5.20 (*dd*, J = 3.2 Hz, *J* = 3.1 Hz, 1H), 5.19 (*br.s*, 1H), 4.65 (*d*, J = 11.4 Hz, 1H), 4.50 (*d*, J = 11.4 Hz, 1H), 4.09 (*dq*, J = 8.7 Hz, *J* = 6.5 Hz, 1H), 3.48 (*ddd*, J = 11.2 Hz, *J* = 8.7 Hz, *J* = 4.4 Hz, 1H), 2.34 (*ddd*, J = 13.8 Hz, *J* = 4.4 Hz, *J* = 3.2 Hz, 1H), 2.09 (*ddd*, J = 13.8 Hz, *J* = 11.2 Hz, *J* = 3.1 Hz, 1H), 1.33 (*d*, J = 6.5 Hz, 3H), **^{13}C NMR**(150 MHz, $CDCl_3$): δ (ppm) 165.8, 138.2, 133.4, 129.9, 128.6, 128.1, 91.2, 75.1, 71.3, 71.2, 68.3, 29.0, 18.3, **HRMS** (ESI-TOF) m/z $(M + Na)^+$ calcd for $C_{20}H_{22}O_5Na$ 365.1365, found 365.1356, Δppm -2.5, $(M_2 + Na)^+$ calcd for $C_{40}H_{44}O_{10}Na$ 707.2832, found 707.2830, Δppm -0.3.

8.5. Synthesis of 2-*O*-benzoyl-4-*O*-allyl-ascarylose

1-*O*-methyl-2-*O*-benzoyl-4-*O*-allyl 3,6-dideoxy-α-L-*arabino*-hexose (93).

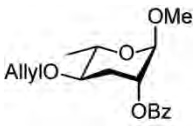

A solution of **88** (20 mg, 75 μmol) in dichloromethane (313 μl) and cyclohexane (626 μl) was treated with *O*-allyl 2,2,2-trichloroacetimidate (38.3 μl, 188 μmol) followed by trifluoromethanesulfonic acid (5 μl). After stirring the solution for 20 h, the mixture was filtered, the filtrate neutralized with saturated aqueous $NaHCO_3$ solution (50 μl), dried with Na_2SO_4 and concentrated under reduced pressure. The resulting residue was purified by flash column chromatography using 20% ethyl acetate in hexane as eluent to afford **93** (15 mg, 50 μmol, 67%) as a colorless oil.

^{1}H NMR (600 MHz, $CDCl_3$): δ (ppm) 8.05 (*dd*, *J* = 8.3 Hz, *J* = 1.5 Hz, 2H), 7.58 (*tt*, *J* = 7.4 Hz, *J* = 1.5 Hz, 1H), 7.46 (*dd*, *J* = 8.3 Hz, *J* = 7.4 Hz, 2H), 5.89 (*dddd*, *J* = 17.2 Hz, *J* = 10.4 Hz, *J* = 5.8 Hz, *J* = 5.6 Hz, 1H), 5.26 (*dddd*, *J* = 17.2 Hz, *J* = 1.7 Hz, *J* = 1.4 Hz, *J* = 1.2 Hz, 1H), 5.1627 (*ddd*, *J* = 3.1 Hz, *J* = 2.7 Hz, *J* = 1.5 Hz, 1H), 5.1589 (*dddd*, *J* = 10.4 Hz, *J* = 1.7 Hz, *J* = 1.1 Hz, *J* = 1.0 Hz, 1H), 4.64 (*br.s*, 1H), 4.10 (*dddd*, *J* = 12.4 Hz, *J* = 5.8 Hz, *J* = 1.2 Hz, *J* = 1.1 Hz, 1H), 3.96 (*dddd*, *J* = 12.4 Hz, *J* = 5.8 Hz, *J* = 1.4 Hz, *J* = 1.0 Hz, 1H), 3.78 (*dq*, *J* = 9.3 Hz, *J* = 6.2 Hz, 1H), 3.41 (*s*, 3H), 3.39 (*dddd*, *J* = 11.2 Hz, *J* = 9.3 Hz, *J* = 4.7 Hz, 1H), 2.30 (*ddd*, *J* = 14.1 Hz, *J* = 4.7 Hz, *J* = 2.7 Hz, 1H), 1.95 (*ddd*, *J* = 14.1 Hz, *J* = 11.2 Hz, *J* = 3.1 Hz, 1H), 1.33 (*d*, *J* = 6.2 Hz, 3H), **^{13}C NMR**(150 MHz, $CDCl_3$): δ (ppm) 165.8, 135.0, 133.3, 130.2, 129.9, 128.6, 117.1, 97.5, 75.2, 71.0, 70.3, 68.0, 54.9, 29.8, 18.3, **HRMS** (ESI-TOF) m/z $(M + Na)^+$ calcd for $C_{17}H_{22}O_5Na$ 329.1365, found 329.1357, Δppm -2.4.

2-*O*-benzoyl-4-*O*-allyl 3,6-dideoxy-α-L-*arabino*-hexose (47).

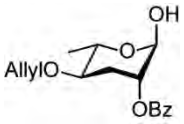

A solution of **93** (5 mg, 16.3 μmol) in acetic acid (180 μl) was treated with a 3 M solution of hydrochloric acid (18 μl, 54 μmol). After stirring the solution for 2 h at 80 °C, the mixture was cooled to room temperature, quenched with $NaHCO_3$ (5 mg) and concentrated under reduced pressure. The resulting residue was purified by flash column chromatography using 20% ethyl acetate in hexane (v/v) as eluent to afford **47** (4 mg, 13.6 μmol, 83%, α/β mixture 3/1) as a colorless oil.

^{1}H NMR (600 MHz, $CDCl_3$) for the dominating α-anomer: δ (ppm) 8.05 (*dd*, *J* = 8.2 Hz, *J* = 1.4 Hz, 2H), 7.59 (*tt*, *J* = 7.2 Hz, *J* = 1.4 Hz, 1H), 7.46 (*dd*, J = 8.2 Hz, *J* = 7.2 Hz, 2H), 5.90 (*dddd*, *J* = 17.4 Hz, *J* = 10.2 Hz, *J* = 5.8 Hz, *J* = 5.6 Hz, 1H), 5.27 (*dddd*, *J* = 17.4 Hz, *J* = 1.7 Hz, *J* = 1.3 Hz, *J* = 1.3 Hz, 1H), 5.21 (*dd*, *J* = 3.2 Hz, *J* = 2.9 Hz, 1H), 5.19 (*br.s*, 1H), 5.17 (*dddd*, *J* = 10.2 Hz, *J* = 1.7 Hz, *J* = 1.1 Hz, *J* = 1.0 Hz, 1H), 4.11 (*dddd*, *J* =12.5 Hz, *J* = 5.6 Hz, *J* = 1.3 Hz,*J* = 1.0 Hz, 1H), 4.04 (*dq*, *J* = 8.8 Hz, *J* = 6.3 Hz, 1H), 3.98 (*dddd*, *J* = 12.5 Hz, *J* = 5.8 Hz, *J* = 1.3 Hz, *J* = 1.1 Hz, 1H), 3.41 (*ddd*, *J* = 11.2 Hz, *J* = 8.8 Hz, *J* = 5.0 Hz, 1H), 2.31 (*ddd*, *J* = 13.8 Hz, *J* = 5.0 Hz, *J* = 2.9 Hz, 1H), 2.05 (*ddd*, *J* = 13.8 Hz, *J* = 11.2 Hz, *J* = 3.2 Hz, 1H), 1.32 (*d*, *J* = 6.3 Hz, 3H), **^{13}C NMR**(150 MHz, $CDCl_3$): δ (ppm) 166.5, 159.8, 149.4, 138.4, 130.4, 128.6, 128.0, 127.9, 120.1, 114.1, 96.8, 75.1, 71.3, 70.7, 68.9, 68.7, 66.3, 55.4, 32.0, 19.1, 18.1, **HR-MS** (ESI-TOF) m/z $(M + Na)^+$ calcd for $C_{16}H_{20}O_5Na$ 315.1208, found 315.1198, Δppm -3.2, $(M_2 + Na)^+$ calcd for $C_{32}H_{40}O_{10}Na$ 607.2519, found 607.2515, Δppm -0.7.

8.6. Synthesis of 2'-*O*-benzoyl-4'-*O*-(4-methoxybenzyloxy)-ascaroside

2-*O*-benzoyl-4-*O*-(4-methoxybenzyl)-3,6-dideoxy-α-L-*arabino*-hexose (94).

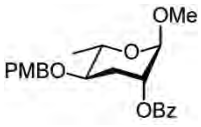

Under N_2 atmosphere, a mixture of **88** (50 mg, 0.19 mmol) and (4-methoxybenzyloxy)-1-methylpyridinium triflate (106 mg, 0.38 mmol) in dichloromethane (633 μl) was treated with camphor-10-sulfonic acid (7 mg, 0.02 mmol). After stirring for 24 h the mixture was concentrated under reduced pressure. The resulting residue was purified by flash column chromatography using 20 % ethyl acetate in hexane as eluent to afford **94** (58 mg, 0.15 mmol, 79%).

^{1}H NMR (600 MHz, $CDCl_3$) δ (ppm) 8.05 (*dd*, *J* = 8.3 Hz, *J* = 1.2 Hz, 2H), 7.59 (*tt*, *J* = 7.4 Hz, *J* = 1.3 Hz, 1H), 7.46 (*dd*, J = 8.3 Hz, *J* = 7.4 Hz, 2H), 7.28 (d, J = 8.8 Hz, 2H), 6.88 (d, J = 8.8 Hz, 2H), 5.15 (ddd, J = 3.1 Hz, J = 2.7 Hz, J = 1.6 Hz, 1H), 4.64 (br.s, 1H), 4.56 (d, J = 11.2 Hz, 1H), 4.42 (d, J = 11.2 Hz, 1H), 3.80 (dq, J = 9.4 Hz, J = 6.3 HZ, 1H), 3.78 (s, 3H), 3.44 (ddd, J = 11.1 Hz, J = 9.4 Hz, J = 4.4 Hz, 1H), 3.41 (s,

3H), 2.32 (ddd, J = 14.1 Hz, J = 4.4 Hz, J = 2.7 Hz, 1H), 1.97 (ddd, J = 14.1 Hz, J = 11.1 Hz, J = 3.1 Hz, 1H), 1.32 (d, J = 6.3 Hz, 3H), **^{13}C NMR**(150 MHz, $CDCl_3$): δ (ppm) 165.8, 159.4, 133.3, 130.0, 129.6, 128.5, 113.9, 97.5, 74.6, 71.0, 70.9, 55.4, 54.9, 29.6, 18.3, **HR-MS** (ESI-TOF) m/z $(M + Na)^+$ calcd for $C_{22}H_{26}O_6Na$ 409.1643 found 409.1627 Δppm 3.9.

8.7. Synthesis of 2'-*O*-benzoyl-4'-*O*-*tert*-butyldimethylsilyl-ascaroside

2-*O*-benzoyl-4-*O*-(4-methoxybenzyl)-3,6-dideoxy-α-L-*arabino*-hexose (95).

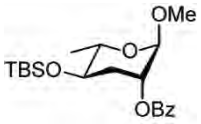

At 0 °C, a solution of **88** (50 mg, 0.19 mmol) in dichloromethane (5 ml) was treated with imidazole (142 mg, 0.95 mmol) followed by *tert*-butyldimethylsilyl chloride (64 mg, 0.95 mmol). After stirring for 48 h at room temperature the mixture was quenched with water (1 ml), dried with Na_2SO_4 and concentrated under reduced pressure. The resulting residue was purified by flash column chromatography using 35% ethyl acetate in hexane *(v/v)* as eluent to afford **95** (66.1 mg, 0.17 mmol, 89%) as a colorless oil.

^{1}H NMR (600 MHz, $CDCl_3$) δ (ppm) 8.04 (*dd*, *J* = 8.4 Hz, *J* = 1.1 Hz, 2H), 7.57 (*ttt*, *J* = 7.5 Hz, *J* = 7.4 Hz, *J* = 1.3 Hz, 1H), 7.45 (*dd*, *J* = 8.4 Hz, *J* = 7.2 Hz, 2H), 5.13 (*ddd*, *J* = 3.1 Hz, *J* = 2.5 Hz, *J* = 1.5 Hz, 1H), 4.64 (*br.s*, 1H), 3.70 (*dq*, *J* = 9.3 Hz, *J* = 5.8 Hz, 1H), 3.67 (*ddd*, *J* = 10.5 Hz, *J* = 9.3 Hz, *J* = 4.4 Hz, 1H), 3.40 (*s*, 3H), 2.17 (*ddd*, *J* = 13.7 Hz, *J* = 4.4 Hz, *J* = 2.5 Hz, 1H), 2.01 (*ddd*, *J* = 13.7 Hz, *J* = 10.5 Hz, *J* = 3.1 Hz, 1H), 1.27 (d, J = 5.8 Hz, 3H), 0.88 (s, 9H), 0.08 (s, 3H), 0.06 (s, 3H), **^{13}C NMR**(150 MHz, $CDCl_3$): δ (ppm) 165.8, 133.3, 130.2, 129.8, 129.5, 97.5, 71.4, 69.5, 69.1, 54.8, 33.7, 25.83, 18.3, -4.1, -4.6, **HR-MS** (ESI-TOF) m/z $(M + Na)^+$ calc for $C_{20}H_{32}O_5NaSi$ 403.1917 found 403.1936 Δppm 4.7.

8.8. Synthesis of 2',4'-di-*O*-benzoyl-caenorhabdose

1-*O*-benzyl-6-deoxy-α-L-*arabino*-hexose (163).

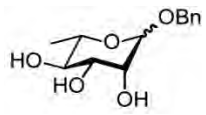

A suspension of L-rhamnose monohydrate **44** (5.0 g, 27.4 mmol) in benzyl alcohol (27 mL) was treated with acetyl chloride (8.6 mL, 121.5 mmol). After stirring overnight at 60 °C the reaction was quenched with K_2CO_3 (10.0 g, 72.4 mmol) and stirred for 1 h. The mixture was diluted with ethyl acetate (55 ml) and the precipitating salt removed by filtration and washed with ethyl acetate (2 x 30 ml). The filtrate was concentrated under reduced pressure and the residue purified by flash column chromatography

on silica gel using a stepwise gradient from 0 to 5% methanol in dichloromethane *(v/v)* as eluent to afford **163** (3.0 g, 11.8 mmol, 43% yield, α/β mixture: 92/8) as a yellow oil.

^{1}H NMR (400 MHz, CD_3OD): δ (ppm) 7.34 (*m*, 5H), 7.29 (*m*, 1H), 4.76 (*d*, *J* = 1.8 Hz, 1H), 4.69 (*d*, *J* = 11.8 Hz, 1H), 4.50 (*d*, *J* = 11.8 Hz, 1H), 3.82 (*dd*, *J* = 3.5 Hz, *J* = 1.7 Hz, 1H), 3.68 (*dd*, *J* = 9.5, *J* = 3.5 Hz, 1H), 3.62 (*m*, 1H), 3.39 (*t*, *J* = 9.5 Hz, 1H), 1.27 (*d*, *J* = 6.3 Hz, 3H), **^{13}C NMR**(100 MHz, CD_3OD): δ (ppm): 139.1, 129.4, 129.0, 128.8, 100.9, 74.0, 72.5, 72.3, 70.04, 70.01, 18.0. NMR identical to data reported in literature [107].

1-*O*-benzyl-6-deoxy-2,3-(*O*-isopropylidene)-α-L-*arabino*-hexose (164).

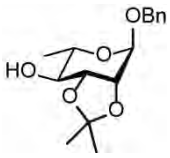

Under N_2 atmosphere a solution of **163** (3.0 g, 11.8 mmol) in dry acetone (50 ml) was treated with 2,2-dimethoxypropane (8 ml, 10.1 mmol) and camphor-10-sulfonic acid (271 mg, 1.18 mmol). After stirring at room temperature for 10 h the reaction was quenched with aqueous 1 M sodium hydroxide solution and concentrated under reduced pressure. The residue was dissolved in dichloromethane and washed with water. The combined organic phases were washed with brine, dried over Na_2SO_4 and concentrated under reduced pressure. The residue was purified by flash column chromatography on silica gel using 35% ethyl acetate in hexane *(v/v)* as eluent to afford **164** (2.2 g, 7.5 mmol, 64% yield) as a white solid.

^{1}H NMR (400 MHz, $CDCl_3$): δ (ppm) 7.34 (*m*, 4H), 5.05 (*s*, 1H), 4.72 (*d*, *J* = 11.7 Hz, 1H), 4.52 (*d*, *J* = 11.7 Hz, 1H), 4.19 (*d*, *J* = 5.7 Hz, 1H), 4.11 (*dd*, *J* = 7.2 Hz, *J* = 5.7 Hz, 1H), 3.74 (*m*, 1H), 3.42 (*dd*, *J* = 9.2 Hz, *J* = 7.2 Hz, 1H), 1.52 (*s*, 3H), 1.35 (*s*, 3H), 1.31 (*d*, *J* = 6.3 Hz, 3H), **^{13}C NMR**(100 MHz, $CDCl_3$): δ (ppm) 137.2, 128.7, 128.4, 128.1, 109.7, 96.5, 78.5, 76.0, 74.7, 69.4, 66.3, 28.1, 26.3, 17.6. NMR identical to data reported in literature[108].

1-*O*-benzyl-6-deoxy-2,3-*O*-(isopropylidene)-4-trifluoromethanesulfonate-α-L-*arabino*-hexose (165).

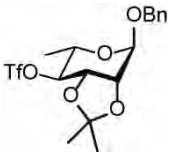

Under N_2 atmosphere a solution of **164** (2.2 g, 7.5 mmol) in dichloromethane (15 mL) at -78 °C was treated dropwise with anhydrous pyridine (1.83 mL, 22.5 mmol) followed by trifluoromethanesulfonic anhydride (1.88 mL, 11.3 mmol). The mixture was stirred at -78 °C for 10 min and then at 0 °C for 2 h, after which it was diluted with dichloromethane (15 mL) and washed with cold 1 M hydrochloric acid

solution (15 mL) and water (15 mL). The organic phase was concentrated under reduced pressure and the residue purified by flash column chromatography on silica gel using 20% ethyl acetate in hexane *(v/v)* as eluent to afford **165** (3.0 g, 7.0 mmol, 93% yield) as an orange oil.

^{1}H NMR (400 MHz, $CDCl_3$): δ (ppm) 7.35 (*m*, 5H), 5.09 (*s*, 1H), 4.70 (*d*, *J* = 11.8 Hz, 1H), 4.56 (*m*, 2H), 4.32 (*dd*, *J* = 7.6 Hz, *J* = 5.5 Hz, 1H), 4.25 (*d*, *J* = 5.4 Hz, 1H), 3.95 (*dq*, *J* = 10.0 Hz, *J* = 6.4 Hz, 1H), 1.54 (*s*, 3H), 1.36 (*s*, 3H), 1.33 (*d*, *J* = 6.3 Hz, 3H), **^{13}C NMR**(100 MHz, $CDCl_3$): δ (ppm) 136.6, 128.8, 128.4, 110.7, 96.1, 89.4, 75.1, 69.8, 63.3, 27.7, 26.4, 17.1. NMR identical to data reported in literature[108].

1-*O*-benzyl-6-deoxy-4-trifluoromethanesulfonate-α-L-*arabino*-hexose (166).

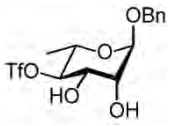

A solution of **165** (3.0 g, 7 mmol) in chloroform (20 mL) was treated with a diluted 1 mM hydrochloric acid solution (0.2 ml). After stirring overnight at 40 °C the mixture was concentrated under reduced pressure and the residue diluted with dichloromethane (20 mL). The solution was washed with water (10 mL), dried over Na_2SO_4, and concentrated under reduced pressure. The residue was purified by flash column chromatography on silica gel using 35% ethyl acetate in hexane *(v/v)* as eluent to afford **166** (900 mg, 2.3 mmol, 33% yield) as a white solid.

^{1}H NMR (400 MHz, $CDCl_3$): δ (ppm) 7.34 (*m*, 5H), 4.89 (s, 1H), 4.69 (*m*, 2H), 4.54 (*d*, *J* = 11.9 Hz, 1H), 4.09 (*m*, 2H), 3.98 (*dq*, *J* = 9.7 Hz, *J* = 6.3 Hz, 1H), 1.36 (*d*, *J* = 6.3 Hz, 3H), **^{13}C NMR** (100 MHz, $CDCl_3$): δ (ppm) 136.7, 128.8, 128.4, 128.2, 98.4, 88.8, 72.1, 69.8, 69.2, 65.4, 17.4. NMR identical to data reported in literature[108].

3,4-anhydro-1-*O*-benzyl-6-dideoxy-α-L-*lyxo*-hexose (167).

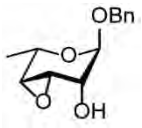

Under N_2 atmosphere a solution of **166** (900 mg, 2.33 mmol) in anhydrous methanol (20 mL) at 0 °C was treated with K_2CO_3 (900 mg, 2.6 mmol). After stirring overnight at room temperature, the mixture was concentrated under reduced pressure. The product was purified by flash column chromatography on silica gel using 25% ethyl acetate in hexane *(v/v)* as eluent to afford **167** (345 mg, 1.46 mmol, 62% yield) as a colorless oil.

^{1}H NMR (400 MHz, $CDCl_3$): δ (ppm) 7.34 (*m*, 4H), 4.70 (*d*, *J* = 11.8 Hz, 1H), 4.64 (*br.s*, 1H) 4.51 (*d*, *J* = 11.8 Hz, 1H), 4.11 (*q*, *J* = 6.5 Hz, 1H), 3.81 (*dd*, *J* = 11.3, *J* = 5.3 Hz, 1H), 3.55 (*t*, *J* = 4.8 Hz, 1H), 3.22 (*d*, *J* = 4.5 Hz, 1H), 2.51 (*d*, *J* = 11.2 Hz, 1H), 1.37 (*d*, *J* = 6.6 Hz, 3H), **^{13}C NMR**(100 MHz, $CDCl_3$): δ (ppm)

137.2, 128.7, 128.2, 128.1, 98.5, 69.5, 63.3, 61.4, 54.9, 51.8, 17.5, HRMS (ESI-TOF) m/z $(M + NH_4)^+$ calcd for $C_{13}H_{20}NO_4$ 254.1387, found 254.1390, m/z $(M + Na)^+$ calcd for $C_{13}H_{16}O_4Na$ 259.0941, found 259.0945.

1-*O*-benzyl-3,6-dideoxy-α-L-*lyxo*-hexose (168).

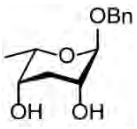

Under N_2 atmosphere, a solution of **167** (345 mg, 1.46 mmol) in dry tetrahydrofuran (8 mL) at 0 °C was treated dropwise with 1.7 M lithium triethylborohydride (Super-Hydride®) solution in tetrahydrofuran (8.3 mL, 14.6 mmol). The reaction was refluxed for 5 h, cooled to room temperature, and quenched with methanol (3 ml). After gas evolution ceased, the solution was poured into ice-cold water (85 mL) and fresh ice was added to the mixture followed by 30% (w/w) aqueous H_2O_2 solution (3.5 mL). The resulting mixture was stirred overnight, concentrated under reduced pressure, and the residue treated with saturated aqueous K_2CO_3 solution (10 ml) and extracted with chloroform (2 x 10 ml). The combined organic phases were dried over Na_2SO_4 and concentrated under reduced pressure. The residue was purified by flash column chromatography on silica gel using 50% ethyl acetate in hexane *(v/v)* as eluent to afford the 1-*O*-benzyl-3,6-dideoxy-α-L-lyxo-hexose **168** (262 mg, 1.10 mmol, 75% yield) as a colorless oil along with 1-*O*-benzyl-4,6-dideoxy-L-*arabino*-hexose **173** (10 mg, 0.04 mmol, 2.7% yield).

^{1}H NMR (400 MHz, $CDCl_3$) of the major isomer **168**: δ (ppm) 7.35 (*m*, 4H), 7.29 (*m*, 1H), 4.81 (*s*, 1H), 4.74 (*d*, *J* = 11.9 Hz, 1H), 4.54 (*d*, *J* = 11.8 Hz, 1H), 3.95 (*qd*, *J* = 6.6 Hz, *J* = 1.3 Hz, 1H), 3.73 (*br.s*, 1H), 3.59 (*br.s*, 1H), 2.03 (*m*, 2H), 1.23 (*d*, *J* = 6.6 Hz, 3H), **^{13}C NMR**(100 MHz, $CDCl_3$): δ (ppm) 137.7, 128.5, 127.9, 127.8, 99.3, 69.1, 68.1, 66.8, 66.4, 31.4, 17.0. NMR identical to data reported in literature[95].

^{1}H NMR (600 MHz, $CDCl_3$) of the minor isomer **173**: δ (ppm) 7.34 (*m*, 5H), 4.93 (*s*, 1H), 4.71 (*d*, *J* = 12.0 Hz, 1H), 4.50 (*d*, *J* = 12.0 Hz, 1H), 4.04 (*ddd*, *J* = 12.7 Hz, *J* =3.6 Hz, *J* =2.9 Hz, 1H), 3.91 (*dqd*, *J* = 12.4 Hz, *J* = 6.3 Hz, *J* = 2.8 Hz, 1H), 3.78 (*br.s*, 1H), 1.77 (*ddd*, *J* = 12.8 Hz, *J* = 3.6 Hz, *J* =2.8 Hz, 1H), 1.52 (*ddd*, *J* = 12.8 Hz, *J* = 12.7 Hz, *J* = 12.4 Hz, 1H), 1.23 (*d*, *J* = 6.3 Hz, 3H)), **^{13}C NMR**(150 MHz, $CDCl_3$): δ (ppm) 137.5, 128.6, 128.0, 99.6, 69.1, 69.0, 65.9, 64.4, 36.6, 21.2.

1-*O*-benzyl-2,4-di-*O*-benzoyl-3,6-dideoxy-α-L-*lyxo*-hexose (169).

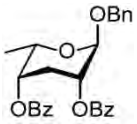

A solution of **168** (154 mg, 646 µmol) in dry pyridine (600 µL) at 0 °C was treated with benzoyl chloride (220 µl, 1.95 mmol). After stirring at 0 °C for 3 h the reaction was quenched with water (1 ml). The organic phase was extracted with hexane (3 x 1 ml), washed with 1.0 M hydrochloric acid (1 ml), dried over Na_2SO_4, and concentrated under reduced pressure. The residue was purified by flash column chromatography on silica gel using dichloromethane as eluent to afford **169** (136 mg, 304 µmol, 47% yield) as a white solid.

^{1}H NMR (400 MHz, $CDCl_3$): δ (ppm) 8.10 (*m*, 2H), 7.90 (*m*, 2H), 7.53 (*m*,1H), 7.43 (*m*, 1H), 7.40 (*m*, 4H), 7.32 (*m*, 3H), 7.15 (*m*, 2H), 5.08 (*s*, 2H), 5.08 (*s*, 1H), 4.79 (*d*, *J* = 11.9 Hz, 1H), 4.65 (*d*, *J* = 11.9 Hz, 1H), 4.27 (*dq*, *J* = 1.2 Hz, *J* = 6.6 Hz, 1H), 2.46 (*m*, 2H), 1.29 (*d*, *J* = 6.6 Hz, 3H), **^{13}C NMR**(100 MHz, $CDCl_3$): δ (ppm) 166.4, 166.0, 137.4, 133.1, 133.0, 133.3, 130.0, 129.9, 128.7, 128.4, 128.2, 128.1, 97.0, 69.7, 68.3, 67.0, 65.2, 27.9, 17.0, HRMS (ESI-TOF) m/z $(M + H)^+$ calcd for $C_{27}H_{27}O_6$ 447.1802, found 477.1805, m/z $(M + NH_4)^+$ calcd for $C_{27}H_{30}NO_6$ 464.2068, found 464.2072.

2,4-di-*O*-benzoyl-3,6-dideoxy-α-L-*lyxo*-hexose (170).

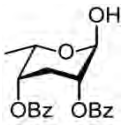

A solution of **169** (134 mg, 300 µmol) in methanol (3 ml) was treated with palladium black (10 mg). After stirring under hydrogen atmosphere (1 atm) for 30 min the mixture was filtered over a thin layer of silica and the catalyst rinsed with ethyl acetate (5 x 3 mL). The filtrate was concentrated under reduced pressure and the residue purified by flash column chromatography on silica gel using 35% ethyl acetate in hexane *(v/v)* as eluent to afford **170** (60.8 mg, 171 µmol, 57% yield, α/β mixture: 7:3) as a white solid.

^{1}H NMR (400 MHz, $CDCl_3$) for the dominating α-anomer: δ (ppm) 8.09 (*m*, 2H), 7.99 (*ddd*, *J* = 7.5 Hz, *J* = 3.9 Hz, *J* = 1.9 Hz, 1H), 7.89 (*m*, 2H), 7.54 (*m*, 1H), 7.44 (*m*, 1H), 7.34 (*td*, *J* = 7.9 Hz, *J* = 1.8 Hz, 2H), 7.24 (*m*, 1H), 7.15 (*m*, 2H) , 5.42 (*s*, 1H), 5.08 (*br.s*, 1H), 5.03 (*br. s*, 2H), 4.51 (*qd*, *J* = 6.6 Hz, *J* = 3.4 Hz, 1H), 2.48 (*m*, 2H), 1.30 (*dd*, *J* = 6.6 Hz, *J* = 1.9 Hz, 3H), **^{13}C NMR**(100 MHz, $CDCl_3$): δ (ppm) 166.4, 166.2, 133.1, 133.1, 130.0, 129.6, 128.5, 128.2, 92.1, 68.3, 67.3, 64.9, 27.3, 17.1, HRMS (ESI-TOF) m/z $(M + NH_4)^+$ calcd for $C_{20}H_{24}NO_6$ 374.1598, found 374.1602, m/z $(M + Na)^+$ calcd for $C_{20}H_{20}O_6Na$ 379.1152, found 379.1147.

8.9. Synthesis of aglycones

8.9.1. Synthesis of (*7R*,*8R*,*2E*)-*threo*-ethyl 7-benzoyloxy-8-hydroxy-2-nonenoate (180).

(*R*)-methyl 2-(4-methoxybenzyloxy)-propanoate (175).

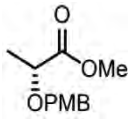

A solution of methyl (*R*)-(+)-lactate **174** (1.0 g, 9.6 mmol) in dichloromethane (2 mL) was treated with 4-methoxybenzyl-2,2,2-trichloroacetimidate (4.8 g, 19 mmol) and camphor-10-sulfonic acid (0.5 g, 2.15 mmol). The mixture was stirred for 5 h at room temperature then quenched with methanol (1 ml) and saturated aqueous $NaHCO_3$ solution (1 ml). The organic phase was separated with dichloromethane (10 ml), washed with brine (2 x 10 ml), dried over Na_2SO_4 and concentrated under reduced pressure. The product was purified by flash column chromatography on silica gel using 10% ethyl acetate in hexane *(v/v)* as eluent to afford **175** (1.18 g, 5.3 mmol 55% yield).

^{1}H NMR (400 MHz, $CDCl_3$): δ (ppm) 7.29 (*d*, *J* = 8.4 Hz, 2H), 6.88 (*d*, *J* = 8.4 Hz, 2H), 4.61 (*d*, *J* = 11.3 Hz, 1H), 4.39 (*d*, *J* = 11.3 Hz, 1H), 4.05 (*q*, *J* = 6.9 Hz, 1H), 3.80 (*s*, 3H), 3.75 (*s*, 3H), 1.42 (*d*, *J* = 6.9 Hz, 3H), **^{13}C NMR**(100 MHz, $CDCl_3$): δ (ppm) 173.9, 159.5, 129.7, 129.7, 113.9, 73.7, 71.8, 55.4, 52.0, 18.8. NMR identical to data reported in literature[11a].

(*R*)-2-(4-methoxybenzyloxy)-propanal (176).

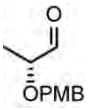

Under N_2 atmosphere a solution of **175** (1.18 g, 5.4 mmol) in dichloromethane (17 mL) at -78 °C was treated dropwise with 1 M diisobutylaluminum hydride (DIBALH) solution in toluene (5.8 mL, 5.8 mmol). After 6 h the reaction was quenched with methanol (0.9 mL) and saturated aqueous potassium sodium tartrate solution (1.8 mL), then stirred for 1 h. The aqueous phase was extracted with dichloromethane (2 x 20 ml), dried over Na_2SO_4, concentrated under reduced pressure and purified by flash column chromatography on silica gel using 9% ethyl acetate in toluene *(v/v)* as eluent to afford **176** (494 mg, 47% yield) as a yellow oil that was directly used for the next step.

^{1}H NMR (400 MHz, $CDCl_3$): δ (ppm) 9.63 (*d*, *J* = 1.8 Hz, 1H), 7.29 (*d*, *J* = 8.7 Hz, 2H), 6.89 (*d*, *J* = 8.7 Hz, 2H), 4.57 (*d*, *J* = 11.4 Hz, 1H), 4.54 (*d*, *J* = 11.4 Hz, 1H), 3.87 (*dq*, *J* = 1.8 Hz, *J* = 7.0 Hz, 1H), 3.80 (*s*, 3H), 1.31 (*d*, *J* = 7.0 Hz, 3H), **^{13}C NMR**(100 MHz, $CDCl_3$): δ (ppm) 203.7, 159.7, 129.8, 129.5, 114.1, 79.3, 71.9, 55.4, 15.4. NMR identical to data reported in literature[11a].

(*2R,3R*)-*threo*-3-hydroxy-2-(4-methoxybenzyloxy)-7-octene (177).

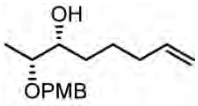

Under N_2 atmosphere at 0 °C, a solution of 4-pentenylmagnesium bromide (5.1 mmol) in diethyl ether (10 ml) (prepared from 5-bromo-1-pentene (767 mg, 5.1 mmol) and magnesium (128 mg, 5.3 mmol) was treated dropwise with **176** (494 mg, 2.5 mmol) in diethyl ether (1.7 ml). After stirring at 0 °C for 1 h the reaction was quenched with NH_4Cl solution (10 ml). The aqueous phase was extracted with ethyl acetate (2 x 10 ml) dried over Na_2SO_4 and concentrated under reduced pressure. The product was purified by flash column chromatography on silica gel using 20% ethyl acetate in hexane *(v/v)* as eluent to afford **177** as a yellow oil (363 mg, 55% yield) with a diastereomeric excess of de >92% as determined by ^{1}H NMR.

^{1}H NMR (400 MHz, $CDCl_3$): δ (ppm) 7.26 (*d*, *J* = 8.6 Hz, 2H), 6.88 (*d*, *J* = 8.6 Hz, 2H), 5.80 (*ddt*, *J* = 16.9, *J* = 10.2 Hz, *J* = 6.7 Hz, 1H), 5.00 (*br.d*, *J* = 17.1 Hz, 1H), 4.95 (*ddt*, *J* = 10.2 Hz, *J* = 2.3 Hz, *J* = 1.2 Hz, 1H), 4.60 (*d*, *J* = 11.2 Hz, 1H), 4.36 (*d*, *J* = 11.1 Hz, 1H), 3.80 (*s*, 3H), 3.41 (*ddd*, *J* = 8.0 Hz, *J* = 6.6 Hz, *J* = 3.1 Hz, 1H), 3.35 (*dq*, *J* = 6.0 Hz, *J* = 6.3 Hz 1H), 2.15 – 1.99 (*m*, 2H), 1.67 – 1.54 (*m*, 1H), 1.54 – 1.36 (*m*, 4H), 1.17 (*d*, *J* = 6.1 Hz, 3H), **^{13}C NMR**(100 MHz, $CDCl_3$): δ (ppm) 159.4, 138.9, 130.6, 129.5, 114.6, 114.0, 78.2, 74.9, 70.8, 55.3, 33.8, 32.4, 24.9, 15.7. NMR identical to data reported in literature[11a].

(*2R,3R*)-*threo*-3-benzoyloxy-2-(4-methoxybenzyloxy)-7-octene (178).

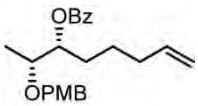

A solution of **177** (363 mg, 1.37 mmol) and dry pyridine (331 µL, 4.11 mmol) in dichloromethane (1 mL) at 0 °C was treated with a solution of benzoyl chloride (320 µL, 2.74 mmol) in dichloromethane (10 mL). After stirring overnight at room temperature, the mixture was diluted with dichloromethane (10 mL), washed with 1 M hydrochloric acid solution (10 mL) and saturated aqueous $NaHCO_3$ solution (10 mL), dried with Na_2SO_4 and concentrated under reduced pressure. The product was purified by flash column chromatography on silica gel using 10% ethyl acetate in hexane *(v/v)* as eluent to afford **178** (435.5 mg, 86% yield) as a colorless oil with a diastereomeric excess of de >99% as determined by ^{1}H NMR.

^{1}H NMR (400 MHz, $CDCl_3$): δ (ppm) 8.09 (*d*, *J* = 7.6 Hz, 2H), 7.59 (*m*, 1H), 7.47 (*m*, 2H), 7.26 (*d*, *J* = 8.5 Hz, 2H), 6.86 (*d*, *J* = 8.5 Hz, 2H), 5.79 (*ddt*, *J* = 17.0 Hz, *J* = 10.3 Hz, *J* = 6.7 Hz, 1H), 5.25 (*m*, 1H), 5.01 (*d*, *J* = 17.1 Hz, 1H), 4.96 (*d*, *J* = 10.3 Hz, 1H), 4.62 (*d*, *J* = 11.5 Hz, 1H), 4.49 (*d*, *J* = 11.5 Hz, 1H), 3.81 (*s*, 3H), 3.74 (*dq*, *J* = 4.9 Hz, *J* = 6.3 Hz, 1H), 2.10 (*m*, 2H), 1.77 (*m*, 2H), 1.46 (*m*, 2H), 1.23 (*d*, *J* = 6.4 Hz, 3H), **^{13}C**

NMR(100 MHz, $CDCl_3$): δ (ppm) 166.4, 159.3, 138.5, 133.0, 130.7, 129.8, 129.4, 129.0, 128.5, 114.9, 113.9, 76.1, 74.6, 70.9, 55.4, 33.7, 29.0, 25.0, 15.5. NMR identical to data reported in literature[11a].

(*7R,8R,2E*)-*threo*-ethyl 7-benzoyloxy-8-(4-methoxybenzyloxy)-2-nonenoate (179).

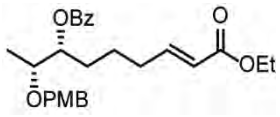

A solution of **178** (435.5 mg, 1.18 mmol) and ethyl acrylate (643 µL, 5.9 mmol) in dichloromethane (35 mL) was treated with Grubb's 2nd generation catalyst (59 mg, 70 µmol) and stirred at 40 °C for 3 h. The solution was cooled to room temperature and then concentrated under reduced pressure. The product was purified by flash column chromatography on silica gel using 20% ethyl acetate in hexane *(v/v)* as eluent to afford **179** (460 mg, 89% yield) as a brown oil.

^{1}H NMR (400 MHz, $CDCl_3$): δ (ppm) 8.07 (*d*, *J* = 7.2 Hz, 2H), 7.57 (*m*, 1H), 7.47 (*m*, 2H), 7.25 (*d*, *J* = 8.6 Hz, 2H), 6.93 (*dt*, *J* = 15.6 Hz, *J* = 7.0 Hz, 1H), 6.86 (*d*, *J* = 8.6 Hz, 2H), 5.82 (*d*, *J* = 15.6 Hz, 1H), 5.24 (*m*, 1H), 4.62 (*d*, *J* = 11.5 Hz, 1H), 4.48 (*d*, *J* = 11.5 Hz, 1H), 4.19 (*q*, *J* = 7.0 Hz, 2H), 3.81 (*s*, 3H), 3.73 (*dq*, *J* = 4.6 Hz, *J* = 6.4 Hz, 1H), 2.23 (*m*, 2H), 1.78 (*m*, 2H), 1.52 (*m*, 2H), 1.30 (*t*, *J* = 6.9 Hz, 3H), 1.23 (*d*, *J* = 6.4 Hz, 3H), **^{13}C NMR**(100 MHz, $CDCl_3$): δ (ppm) 166.7, 166.4, 159.3, 148.6, 133.1, 130.7, 130.4, 129.8, 129.5, 128.5, 121.8, 113.9, 75.8, 74.4, 70.9, 60.3, 55.4, 32.1, 29.1, 24.2, 15.4, 14.4. NMR identical to data reported in literature[11a].

(*7R,8R,2E*)-*threo*-ethyl 7-benzoyloxy-8-hydroxy-2-nonenoate (180).

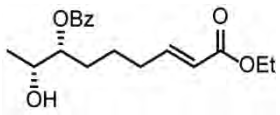

A solution of **179** (480 mg, 1.04 mmol) in dichloromethane (7.5 mL) was treated with water (376 µL) and 2,3-dichloro-5,6-dicyano-1,4-benzoquinone (DDQ) (254 mg, 1.14 mmol). The mixture was stirred for 1 h at room temperature then quenched with water (2 mL). The aqueous phase was extracted with dichloromethane (3 x 5 ml), dried with Na_2SO_4 and concentrated under reduced pressure. The product was purified by flash column chromatography on silica gel using 35% ethyl acetate in hexane *(v/v)* as eluent to afford **180** (290 mg, 87% yield) as an orange oil.

^{1}H NMR (400 MHz, $CDCl_3$): δ (ppm) 8.05 (*m*, 2H), 7.57 (*m*, 1H), 7.45 (*m*, 2H), 6.91 (*dt*, *J* = 15.7 Hz, *J* = 7.0 Hz, 1H), 5.80 (*d*, *J* = 15.7 Hz, 1H), 5.05 (*dt*, *J* = 7.8 Hz, *J* = 5.0 Hz, 1H), 4.16 (*q*, *J* = 7.2 Hz, 2H), 3.94 (*dq*, *J* = 4.8 Hz, *J* = 6.4 Hz, 1H), 2.23 (*m*, 2H), 1.77 (*m*, 2H), 1.55 (*m*, 2H), 1.26 (*t*, *J* = 7.0 Hz, 3H), 1.23 (*d*, *J* = 6.5 Hz, 3H), **^{13}C NMR**(100 MHz, $CDCl_3$) δ (ppm): 166.7, 166.6, 148.4, 133.3, 130.1, 129.8, 128.6, 121.9, 77.9, 69.0, 60.3, 32.0, 30.2, 24.1, 19.6, 14.4. NMR identical to data reported in literature[11a].

8.9.2. Synthesis of (*R*)-7-octen-2-ol (110).

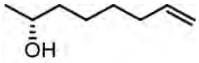

Under N_2 atmosphere a mixture of magnesium (97 mg, 4 mmol) in tetrahydrofuran (6 ml) was treated with 5-bromo-pentene (433 µl, 3.7 mmol). After stirring for 1 h the reaction was cooled to 0 °C, treated with copper(I)iodide (63 mg, 0.33 mmol) and (*R*)-(+)-propylene oxide **108** (230 µl, 3.3 mmol) in tetrahydrofuran (6 ml) was added dropwise. After stirring at room temperature for 1 h the reaction was quenched by addition of saturated ammonium chloride solution, the organic phase washed with saturated ammonium chloride solution, dried over Na_2SO_4, and concentrated under reduced pressure. The resulted residue was purified by flash column chromatography on silica gel using 10% ethyl acetate in hexane *(v/v)* as eluent to afford **110** (262 mg, 2.1 mmol, 64% yield).

^{1}H NMR (400 MHz, $CDCl_3$): δ (ppm) 5.83 (*ddt*, *J* = 17.2 Hz, 10.3 Hz, 6.9 Hz, 1H), 5.02 (*dd*, *J* = 17.2 Hz, 1.9 Hz, 1H) 4.96 (*dd*, *J* = 10.2 Hz, 1.9Hz, 1H), 3.87 – 3.75 (*m*, 1H), 2.14 – 2.04 (*m*, 2H), 1.75 – 1.69 (*m*, 1H), 1.56 – 1.38 (*m*, 4H), 1.21 (*d*, *J* = 6.2 Hz, 3H). NMR identical to data reported in literature[109].

8.10. Synthesis of modular ascarosides

8.10.1 General procedure for the glycosylation

- **Via the trichloroacetimidate route**

A solution of ascarylose or caenorhabdose (1 eq) in dry dichloromethane (75 µl/mmol) was treated with 2eq of trichloroacetonitrile (300 µl/ µmol of ascaroside) and 5 µL 1,8-diazabicyclo (5.4.0) undec-7-ene. After stirring for 30 min, the mixture was concentrated under reduced pressure and the residue quickly purified with a short silica gel flash column chromatography with 10% ethyl acetate in hexane and directly used for the next step. The purified trichloroacetimidate ascaroside in dry dichloromethane (69 µl/mmol) was treated with 1.5 eq. of alcohol in dry dichloromethane (18 µl /mmol) and 5 µL trimethylsilyltriflate at 0 °C. The mixture was stirred from 0 °C to room temperature until completion of the reaction then the mixture was quenched with saturated aqueous $NaHCO_3$ solution and diluted with dichloromethane. The organic phase was dried over Na_2SO_4 and concentrated under reduced pressure. The resulting residue was purified by flash column chromatography on silica gel using 20% ethyl acetate in hexane *(v/v)* as eluent.

- **Via BF_3,OEt_2 route**

Under N_2 atmosphere at 0 °C, a solution of ascarylose (1 eq) in dry dichloromethane (200 µl/mmol) was treated with alcohol (4 µmol/ µmol of ascaroside) followed by borontrifluoride etherate (700 µl/mmol of ascaroside). After stirring for 20 min, the mixture the mixture was quenched with saturated aqueous $NaHCO_3$ solution and diluted with dichloromethane. The organic phase was dried

over Na_2SO_4 and concentrated under reduced pressure. The resulting residue was purified by flash column chromatography on silica gel using 20% ethyl acetate in hexane (*v/v*) as eluent.

Sugar unit	Amount of sugar	Alcohol	Amount of alcohol	Ascaroside
2,4-di-*O*-benzoyl-ascarylose (63)	200 mg, 0.56 mmol	(*R*)-5-hexene-2-ol	90 µl, 0.74 mmol	**200** (125 mg, 0.28 mmol, 50%)
2-*O*-benzoyl-4-*O*-TBDPS-ascarylose (45)	100 mg, 0.20 mmol	(*R*)-5-hexene-2-ol	51 µl, 0.41 mmol	**141** (58.4 mg, 0.10 mmol, 50%)
	200 mg, 0.41 mmol	(2*R,* 5*R*)-2,5-hexan-diol	53 mg, 0.82 mmol	**130** (150 mg, 0.25 mmol, 61%)
	152 mg, 0.31 mmol	(*R*)-7-octen-2-ol	40 mg, 0.62 mmol	**111** (102 mg, 0.17 mmol, 47%)
	1.0 g, 2.0 mmol	(*R*)-3-butyn-2-ol	156 mg, 2.25 mmol	**151** (720 mg, 1.33 mmol, 67%)
2-*O*-benzoyl-4-*O*-benzyl-ascarylose (46)	100 mg, 0.29 mmol	(*R*)-3-butyn-2-ol	41 mg, 0.58 mmol	**210** (68 mg, 0.17 mmol, 59%)[1]
2,4-di-*O*-benzoyl-caenorhabdose (170)	15 mg, 42 µmol	(7*R*,8*R*,2*E*)-*threo*-ethyl 7-benzoyloxy-8-hydroxy-2-nonenoate	12 mg, 42 µmol	**181** (8.8 mg, 0.013 mmol, 32%)

(*8R*)-8-[(2-*O*-benzoyl-4-*O*-*tert*-butyldiphenylsilyl-3,6-dideoxy-α-L-*arabino*-hexopyranosyl)oxy]-1-octene (111).

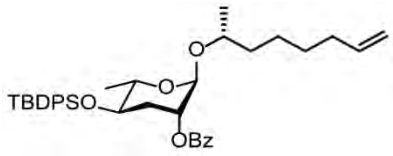

^{1}HNMR (400 MHz, $CDCl_3$): δ (ppm) 7.72 (*d*, *J* = 8.2 Hz, 2H), 7.68 (*d*, *J* = 7.9 Hz, 2H), 7.66 (*d*, *J* = 7.9 Hz, 1H), 7.41 – 7.36 (*m*, 4H), 7.34 – 7.31 (*m*, 3H), 7.31-7.27 (*m*, 2H), 5.86 (*ddt*, *J* = 17.0 Hz, *J* = 10.2 Hz, *J* = 6.7 Hz, 1H), 5.04 (*ddt*, *J* = 17.1 Hz, *J* = 1.7 Hz, *J* = 1.5 Hz, 1H), 4.98 (*dd*, *J* = 10.2 Hz, *J* = 1.7 Hz, 1H), 4.87 (*dd*, *J* = 3.7 Hz, *J* = 2.9 Hz, 1H), 4.74 (*br.s*, 1H), 3.89 (*dq*, *J* = 9.2, *J* = 6.2 Hz, 1H), 3.79 (*dqd*, *J* = 6.4 Hz, *J* = 6.1 Hz, *J* = 5.8 Hz, 1H), 3.65 (*ddd*, *J* = 11.2 Hz, *J* = 9.4 Hz, *J* = 4.5 Hz, 1H), 2.12 (*dtd*, *J* = 7.5 Hz, *J* = 6.7 Hz, *J* = 1.5 Hz, 2H), 2.04 (*ddd*, *J* = 13.9 Hz, *J* = 11.2 Hz, *J* = 2.9 Hz, 1H), 1.87 (*ddd*, *J* = 13.9 Hz, *J* = 4.5 Hz, *J* = 2.9 Hz, 1H), 1.63 (*m*, 1H), 1.51-1.40 (*m*, 4H), 1.48 (*m*, 1H), 1.26 (*d*, *J* = 6.2 Hz, 3H), 1.12 (*d*, *J* = 6.1 Hz, 3H), 1.06 (s, 9H), **^{13}C NMR**(150 MHz, $CDCl_3$): δ (ppm) 165.5, 139.1, 136.1, 136.0, 134.2, 133.4, 133.1, 130.0, 129.9, 129.84, 129.76, 128.30, 127.8, 127.6, 114.6, 93.6, 72.2, 72.0, 70.4, 69.9, 37.2, 34.0, 33.4, 29.0, 27.1, 25.4, 19.5, 19.3, 18.5, **HRMS** (ESI-TOF) m/z $(M + NH_4)^+$ calcd for $C_{37}H_{52}NO_5Si$ 618.3615, found 618.3624, Δ 1.5 ppm.

[1] Via BF_3,OEt_2 route

(*5R*)-5-[(2-*O*-benzoyl-4-*O*-*tert*-butyldiphenylsilyl-3,6-dideoxy-α-L-*arabino*-hexopyranosyl)oxy]-2,5-hexadiol (130).

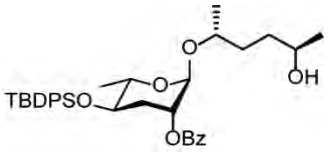

^{1}H NMR (600 MHz, $CDCl_3$): δ (ppm) 7.73 (*d*, *J* = 8.3 Hz, 2H), 7.69 (*d*, *J* = 8.3 Hz, 2H), 7.67 (*d*, *J* = 7.6 Hz, 2H), 7.55 (*t*, *J* = 7.5 Hz, 1H), 7.40 – 7.36 (*m*, 3H), 7.30-7.32 (*m*, 3H), 7.32-7.28 (*m*, 2H), 4.89 (*dd*, *J* = 3.8 Hz, *J* = 3.1 Hz, 1H), 4.78 (*br. s*), 3.90 (*dq*, *J* = 9.4 Hz, *J* = 6.4 Hz, 1H), 3.88 (*m*, 1H), 3.84 (*m*, 1H), 3.67 (*ddd*, *J* = 11.2 Hz, *J* = 9.4 Hz, *J* = 4.2 Hz, 1H), 2.05 (*ddd*, *J* = 13.7 Hz, *J* = 11.2 Hz, *J* = 3.1 Hz, 1H), 1.89 (*ddd*, *J* = 13.7 Hz, *J* = 4.2 Hz, *J* = 3.8 Hz, 1H), 1.74 (*m*, 1H), 1.61 – 1.54 (*m*, 2H), 1.59 (*m*, 1H), 1.28 (*d*, *J* = 6.4 Hz, 3H), 1.26 (*d*, *J* = 6.2 Hz, 3H), 1.16 (*d*, *J* = 6.2 Hz, 3H), 1.07 (*s*, 9H), **^{13}C NMR**(150 MHz, $CDCl_3$) : δ (ppm) 165.5, 134.0, 135.97, 135.89, 134.1, 133.2, 133.1, 129.9, 129.8, 129.7, 128.3, 127.7,127.6, 93.5, 72.2, 71.9, 70.3, 70.0, 67.9, 35.1, 33.3, 33.1, 27.1, 23.7, 19.4, 19.2, 18.4, **HRMS** (ESI-TOF) m/z $(M + NH_4)^+$ calcd for $C_{35}H_{50}NO_6Si$ 608.3407, found 608.3409, Δ 0.3ppm, $(M + Na)^+$ calcd for $C_{35}H_{46}O_6SiNa$ 613.2961 found 613.2966, Δ 0.5 ppm.

(*5R*)-5-[(2-*O*-benzyl-4-*O*-*tert*-butyldiphenylsilyl-3,6-dideoxy-α-L-*arabino*-hexopyranosyl)oxy]-1-hexene (141).

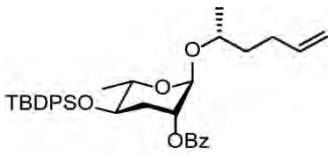

^{1}HNMR (600 MHz, $CDCl_3$): δ (ppm) 7.74-7.71 (*m*, 2H), 7.70-7.67 (*m*, 2H), 7.67-7.64 (*m*, 2H), 7.55 (*tt*, *J* = 8.8 Hz, 1.3 Hz, 1H), 7.40-7.36 (*m*, 3H), 7.34-7.31 (*m*, 3H), 7.31-7.27 (*m*, 2H), 5.86 (*ddt*, *J* = 17.1 Hz, 10.2 Hz, 6.7 Hz, 1H), 5.04 (*ddt*, *J* = 17.1 Hz, 1.9 Hz, 1.6 Hz, 1H), 4.98 (*ddt*, *J* = 10.2 Hz, 1.9 Hz, 1.2 Hz, 1H), 4.87 (*dd*, *J* = 3.7 Hz, 2.9 Hz, 1H), 4.74 (*br s*, 1H), 3.89 (*dq*, *J* = 9.0 Hz, 6.2 Hz, 1H), 3.79 (*m*, 1H), 3.65 (*ddd*, *J* = 11.2 Hz, 9.0 Hz, 4.6 Hz, 1H), 2.15-2.08 (m, 2H), 2.04 (ddd, *J* = 13.7 Hz, 11.2 Hz, 2.9 Hz, 1H), 1.87 (*ddd*, *J* = 13.7 Hz, 4.6 Hz, 3.7 Hz, 1H), 1.50-1.40 (*m*, 2H), 1.26 (*d*, *J* = 6.2 Hz, 3H), 1.12 (*d*, *J* = 6.1 Hz, 3H), **^{13}C NMR**(150 MHz, $CDCl_3$) : δ (ppm) 165.4, 139.0, 135.9, 135.9, 134.1, 133.2, 129.9, 129.74, 129.72, 129.6, 128.2, 127.6, 127.5, 114.5, 93.4, 72.1, 71.9, 70.3, 69.8, 31.0, 33.9, 33.3, 28.8, 27.0, 25.3, 19.3, 19.2, 18.4. NMR identical to data reported in literature[40].

(*3R*)-3-[(2-*O*-benzoyl-4-*O*-*tert*-butyldiphenylsilyl-3,6-dideoxy-α-L-*arabino*-hexopyranosyl)oxy]-1-butyne (151).

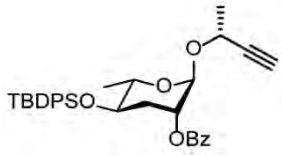

^{1}H NMR (400 MHz, $CDCl_3$): δ (ppm) 7.75-7.71 (*m*, 2H), 7.71-7.65 (*m*, 4H), 7.56 (*m*, 1 H), 7.42-7.26 (*m*, 8H), 4.93 (*dd*, *J* = 3.6 Hz, 3.1 Hz, 1 H), 4.80 (*br.s*, 1 H), 4.43 (*dq*, *J* = 6.7 Hz, *J* = 2.2 Hz, 1H), 4.07 (*dq*, *J* = 9.2 Hz, *J* = 6.2 Hz, 1 H), 3.68 (*ddd*, *J* = 11.2 Hz, 9.2 Hz, 4.4 Hz, 1 H), 2.49 (*d*, *J* = 2.2 Hz, 1 H), 2.09 (*ddd*, *J* = 13.9 Hz, 11.2 Hz, 3.1 Hz, 1 H), 1.89 (*ddd*, *J* = 13.9 Hz, 4.4 Hz, *J* = 3.1 Hz, 1 H), 1.49 (*d*, *J* = 6.7 Hz, 3 H), 1.28 (*d*, *J* = 6.2 Hz, 3 H), 1.06 (*s*, 9 H), **^{13}C NMR**(100 MHz, $CDCl_3$) : δ (ppm) 165.4, 136.1, 136.0, 134.2, 133.4, 133.1, 129.9, 128.3, 127.8, 127.6, 95.8, 84.2, 72.5, 71.4, 70.4, 70.3, 63.8, 33.4, 27.2, 22.2, 19.5, 18.2, HRMS (ESI-TOF) m/z $(M + NH_4)^+$ calcd for $C_{33}H_{42}NO_5Si$ 560.2832, found 560.2831, Δppm -0.2.

(*3R*)-3-[(2-*O*-benzoyl-4-*O*-benzyl-3,6-dideoxy-α-L-*arabino*-hexopyranosyl)oxy]-1-butyne (210).

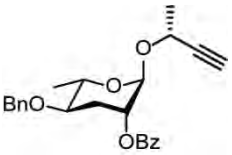

^{1}H NMR (400 MHz, $CDCl_3$): δ (ppm) 8.01 (*dd*, *J* = 8.2 Hz, *J* = 2.0 Hz, 2H), 7.59 (*tt*, *J* = 7.4 Hz, *J* = 2.0 Hz, 1H), 7.45 (*dd*, *J* = 8.2 Hz, *J* = 7.4 Hz, 2H), 7.36-7.29 (*m*, 5H), 5.14 (*ddd*, *J* = 3.2 Hz, *J* = 2.8 Hz, *J* = 1.5 Hz, 1H), 4.90 (*br.s*, 1H), 4.44 (*dq*, *J* = 6.7 Hz, *J* = 2.1 Hz, 1H), 4.08 (*dq*, *J* = 9.5 Hz, *J* = 6.2 Hz, 1H), 3.49 (*ddd*, *J* = 10.8 Hz, *J* = 9.5 Hz, *J* = 5.2 Hz, 1H), 2.43 (*d*, *J* = 2.1 Hz, 1H), 2.35 (*ddd*, *J* = 13.7 Hz, *J* = 5.2 Hz, *J* = 2.8 Hz, 1H), 2.05 (*ddd*, *J* = 13.7 Hz, *J* = 10.8 Hz, *J* = 3.2 Hz, 1H), 1.48 (*d*, *J* = 6.7 Hz, 3H), 1.33 (*d*, *J* = 6.2 Hz, 3H), **^{13}C NMR**(100 MHz, $CDCl_3$) : δ (ppm) 165.6, 138.1, 133.3, 129.8, 128.4, 127.9, 127.8, 95.7, 75.0, 72.4, 71.2, 71.1, 68.7, 63.6, 29.7, 22.0, 17.8, HRMS (ESI-TOF) m/z $(M + Na)^+$ calcd for $C_{24}H_{26}O_5Na$ 417.1674, found 417.1672, Δppm -1.4.

(*5R*)-5-[(2,4-di-*O*-benzoyl-3,6-dideoxy-L-*arabino*-hexopyranosyl)oxy]-1-hexene (200).

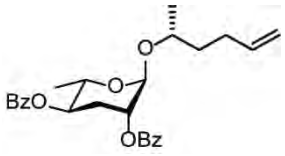

^{1}HNMR (600 MHz, $CDCl_3$): δ (ppm) 8.13-8.09 (*m*, 2H), 8.06-8.02 (*m*, 2H), 7.61-7.56 (*m*, 2H), 7.50-7.43 (*m*, 4H), 5.88 (*ddt*, *J* = 16.9 Hz, *J* = 10.2 Hz, *J* = 6.6 Hz, H), 5.19 (*ddd*, *J* = 11.3 Hz, *J* = 9.8 Hz, *J* = 4.7 Hz, 1H), 5.15 (*ddd*, *J* = 3.4 Hz, *J* = 3.1 Hz, *J* = 1.5 Hz, 1H), 5.09 (*ddt*, *J* = 16.9 Hz, *J* = 1.9 Hz, *J* = 1.7 Hz, 1H), 5.02 (*ddt*, *J* = 10.2 Hz, *J* = 1.9 Hz, *J* = 1.2 Hz, 1H), 4.96 (*br. s*, 1H), 4.12 (*dq*, *J* = 9.8 Hz, *J* = 6.3 Hz, 1H),

3.88 (*m*, 1H), 2.42 (*ddd*, *J* = 13.6 Hz, *J* = 4.7 Hz, *J* = 3.4 Hz, 1H), 2.29-2.15 (*m*, 2H), 2.214 (*ddd*, *J* = 13.6 Hz, *J* = 11.3 Hz, *J* = 3.1 Hz, 1H), 1.76 (*m*, 1H), 1.61 (*m*, 1H), 1.28 (*d*, *J* = 6.3 Hz, 3H), 1.21 (*d*, *J* = 6.1 Hz, 3H), **^{13}C NMR**(150 MHz, $CDCl_3$) : δ (ppm) 165.9, 138.6, 133.41, 133.35, 130.1, 130.01, 129.98, 129.8, 128.6, 114.9, 93.83, 72.1, 71.4, 70.8, 67.2, 36.49, 30.1, 29.9, 19.2, 18.0. NMR identical to data reported in literature[110].

(*7R,8R,2E*)-*threo*-ethyl 7-benzoyloxy-8-[(2,4-di-O-benzoyl-3,6-dideoxy-a-L-*lyxo*-hexopyranosyl)oxy]-2-nonenoate (181).

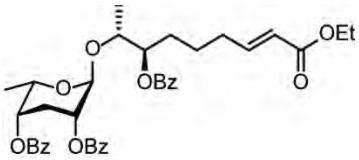

^{1}H NMR (400 MHz, $CDCl_3$): δ (ppm) 8.07 (*m*, 4H), 7.85 (*m*, 2H), 7.60 (*m*, 1H), 7.53 (*m*, 1H), 7.48 (*m*, 2H), 7.42 (*m*, 1H), 7.32 (*m*, 2H), 7.12 (*m*, 2H), 6.94 (*dt*, *J* = 15.6 Hz, *J* = 6.9 Hz, 1H), 5.83 (*dt*, *J* = 15.6 Hz, *J* = 1.5 Hz, 1H), 5.28 (*dt*, *J* = 6.3 Hz, *J* = 6.0 Hz, 1H), 5.10 (*s*, 1H), 4.93 (*dd*, *J* = 3.8 Hz, *J* = 1.9 Hz, 1H), 4.77 (*s*, 1H), 4.18 (*q*, *J* = 7.1 Hz, 2H), 4.06 (*dq*, *J* = 6.2 Hz, *J* = 6.0 Hz, 1H), 2.43 – 2.31 (*m*, 2H), 2.30 – 2.18 (*m*, 3H), 1.79 (*q*, *J* = 7.4 Hz, *J* = 6.9 Hz, 3H), 1.67 – 1.55 (*m*, 3H), 1.27 (*d*, *J* = 6.2 Hz, 3H), 1.28 (*t*, *J* = 7.1 Hz, 3H) 1.17 (*d*, *J* = 6.6 Hz, 3H), **^{13}C NMR**(100 MHz, $CDCl_3$): δ (ppm) 166.7, 166.3, 166.2, 148.3, 133.4, 133.1, 133.0, 130.3, 130.0, 129.9, 129.8, 128.7, 128.4, 128.2, 122.1, 94.2, 75.9, 72.5, 68.2, 67.5, 65.3, 60.4, 32.0, 29.7, 27.7, 24.1, 16.9, 14.9, 14.4, HRMS (ESI-TOF) m/z $(M + H)^+$ calcd for $C_{38}H_{43}O_{10}$ 659.2851, found 658.2873, m/z $(M + NH_4)^+$ calcd for $C_{38}H_{46}NO_{10}$ 676.3116, found 676.3137.

8.10.2. Synthesis of 4'-UC-ascr-C6MK (ucas#2, 35) and 4'-UC-ascr-ΔC9 (ucas#3, 37).

(5*R*)-5-[(2-*O*-benzoyl-4-*O*-*tert*-butyldiphenylsilyl-3,6-dideoxy-α-L-*arabino*-hexopyranosyl)oxy]-hexan-2-one (131).

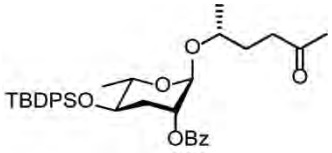

A solution of **130** (150 mg, 0.25 mmol) in dichloromethane (3.6 ml) was treated with molecular sieves (4 Å, 143 mg) followed by pyridinium chlorochromate (214 mg, 1.4 mmol). After stirring for 22 h at room temperature, the solution was diluted with hexane (4 ml) and filtered over a short silica plug using 20% ethyl acetate in hexane *(v/v)* as eluent. The filtrate was concentrated under reduced pressure to afford **131** (125 mg, 0.2 mmol, 80%) as a colorless oil and used for the next step without any further purification.

^{1}H NMR (600 MHz, $CDCl_3$): δ (ppm) 7.72 (*d*, *J* = 8.2 Hz, 2H), 7.68 (*d*, *J* = 7.8 Hz, 2H), 7.66 (*d*, *J* = 7.3 Hz,

2H), 7.55 (*t*, *J* = 7.5 Hz, 1H), 7.40-7.36 (*m*, 3H), 7.35-7.32 (*m*, 3H), 7.32-7.28 (*m*, 2H), 4.87 (*dd*, *J* = 3.8 Hz, *J* = 3.0 Hz, 1H), 4.74 (*br.s*, 1H), 3.82 (*m*, 1H), 3.82 (*dq*, *J* = 9.1 Hz, *J* = 6.3 Hz, 1H), 3.65 (*ddd*, *J* = 11.0 Hz, *J* = 9.1 Hz, *J* = 4.7 Hz, 1H), 2.62 (*t*, *J* = 7.3 Hz, 2H), 2.23 (*s*, 3H), 2.01 (*ddd*, *J* = 14.1 Hz, *J* = 11.0 Hz, *J* = 3.0 Hz, 1H), 1.88 (*ddd*, *J* = 14.1 Hz, *J* = 4.7 Hz, *J* = 3.8 Hz, 1H), 1.88-1.77 (*m*, 2H), 1.27 (*d*, *J* = 6.3 Hz, 3 H), 1.15 (*d*, *J* = 6.1 Hz, 3H), 1.06 (*s*, 9H), **^{13}C NMR**(150 MHz, $CDCl_3$): δ (ppm) 208.8, 165.5, 136.0, 135.9, 134.1, 133.3, 133.1, 129.9, 129.9, 129.8, 129.8, 128.3 127.8, 127.6, 93.3 71.8, 71.2, 70.2, 39.8, 33.3, 30.9, 30.1, 27.1, 19.4, 19.1, 18.5, **HRMS** (ESI-TOF) m/z $(M + NH_4)^+$ calcd for $C_{35}H_{48}NO_6Si$ 606.3251, found 606.3254, Δ 0.5 ppm.

(5*R*)-5-[(4-*O*-*tert*-butyldiphenylsilyl-3,6-dideoxy-α-L-*arabino*-hexopyranosyl)oxy]-2-hexanone (132).

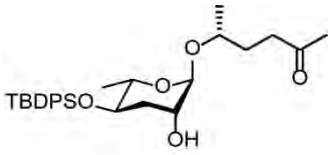

A solution of **131** (125 mg, 0.2 mmol) in 1,4-dioxane (5.3 ml) was treated with a solution of lithium hydroxide monohydrate (18 mg, 0.4 mmol) in water (1.1 ml). After stirring overnight at 60 °C, the mixture was cooled to room temperature, quenched with acetic acid (1 ml) and concentrated under reduced pressure. The resulting residue was purified by flash column chromatography using 35% ethyl acetate in hexane *(v/v)* as eluent to afford **132** (68 mg, 0.14 mmol, 67%) as a colorless oil.
^{1}H NMR (600 MHz, $CDCl_3$): δ (ppm) 7.69 (d, *J* = 7.7 Hz, 2H), 7.66 (d, *J* = 7.8 Hz, 2H), 7.43-7.40 (m, 2H), 7.40-7.35 (m, 4H), 4.57 (br. s, 1H), 3.79 (m, 1H), 3.71 (dq, *J* = 9.4 Hz, *J* = 6.3 Hz, 1 H), 3.66 (ddd, *J* = 10.1 Hz, *J* = 9.4 Hz, *J* = 4.7 Hz, 1H), 3.63 (dd, *J* = 3.9 Hz, *J* = 3.2 Hz, 1H), 2.60 (t, *J* = 7.6 Hz, 2 H), 2.20 (s, 3H), 1.87-1.73 (m, 4H), 1.16 (d, *J* = 6.3 Hz, 3H), 1.11 (d, *J* = 6.2 Hz, 3H), 1.06 (s, 9H), **^{13}C NMR**(150 MHz, $CDCl_3$): δ (ppm) 208.8, 136.0, 134.4, 133.6, 129.9, 129.8, 127.8, 127.6, 96.0, 70.5, 70.4, 69.9, 69.1, 39.8, 35.7. 30.1, 27.1, 19.4, 19.0, 18.2.

(5*R*)-5-[(2-*O*-(4-methoxybenzyloxy)-4-*O*-*tert*-butyldiphenylsilyl-3,6-dideoxy-α-L-*arabino*-hexopyranosyl)oxy]-2-hexanone (133).

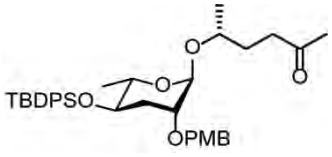

Under N_2 atmosphere, **132** (50 mg, 0.1 mmol) in dichloromethane (300 µl) was treated with 2-(4-methoxybenzyloxy)-4-methylquinoline (57 mg, 0.2 mmol) followed by camphor-10-sulfonic acid (3 mg, 10 µmol). After stirring overnight at room temperature, the reaction was concentrated under

reduced pressure and the resulting residue purified by flash column chromatography using a gradient of 0 to 10% ethyl acetate in hexane *(v/v)* as eluent to afford **133** (46.5 mg, 0.075 mmol, 75%) as a colorless oil.

^{1}H NMR (600 MHz, $CDCl_3$): δ (ppm) 7.74-7.69 (*m*, 4H), 7.46-7.41 (*m*, 2H), 7.41.-7.36 (*m*, 4H), 6.99 (*d*, *J* = 8.7 Hz, 1H), 6.78 (*d*, *J* = 8.7 Hz, 1H), 4.61 (*br.s*, 1H), 4.10 (*d*, *J* = 11.8 Hz, 1H), 3.98 (*d*, *J* = 11.8 Hz, 1H), 3.78 (*s*, 3H), 3.78 (*m*, 1H), 3.76 (*ddd*, *J* = 10.6 Hz, *J* = 8.7 Hz, *J* = 4.6 Hz, 1H), 3.70 (*dq*, *J* = 8.7 Hz, *J* = 6.3 Hz, 1H), 3.28 (*dd*, *J* = 3.9 Hz, *J* = 2.8 Hz, 1H), 2.59 (*dd*, *J* = 7.5 Hz, *J* = 5.2 Hz, 2H), 2.20 (*s*, 3H), 1.81 (*m*, 1H), 1.74 (*m*, 1H), 1.83 (*ddd*, 13.5 Hz, *J* = 4.6 Hz, *J* = 3.9 Hz, 1H), 1.64 (*ddd*, 13.5 Hz, *J* = 10.6 Hz, *J* = 2.8 Hz, 1H), 1.26 (*d*, *J* = 6.3 Hz, 3H), 1.06 (*d*, *J* =6.1 Hz, 3H), 1.06 (*s*, 9H), **^{13}C NMR**(150 MHz, $CDCl_3$): δ (ppm) 208.8, 159.1, 136.1, 136.0, 129.9, 129.7, 129.2, 127.8, 127.7, 113.7, 94.6, 75.0, 70.4, 70.2, 70.2, 69.7, 55.4, 40.0, 32.3, 31.0, 27.1, 19.5, 19.0, 18.4, **HRMS** (ESI-TOF) m/z $(M + NH_4)^+$ calcd for $C_{36}H_{52}NO_6Si$ 622.3564, found 622.3574, Δ 1.6 ppm.

(5*R*)-5-[(2-*O*-(4-methoxybenzyloxy)-3,6-dideoxy-α-L-*arabino*-hexopyranosyl)oxy]-2-hexanone (134).

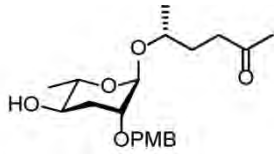

A solution of **133** (45 mg, 74 µmol) in tetrahydrofuran (2 ml) was treated with tetrabutylammonium fluoride solution (1 M in tetrahydrofuran, 0.42 ml, 0.42 mmol). After stirring for 12 h at room temperature the mixture was quenched with water (1 ml). The aqueous phase was extracted with dichloromethane (2 x 4 ml), dried over Na_2SO_4, and then concentrated under reduced pressure. The resulting residue was purified by flash column chromatography using 35% ethyl acetate in hexane *(v/v)* as eluent to afford **134** (13.2 mg, 36 µmol, 51%) as a colorless oil.

^{1}H NMR (600 MHz, $CDCl_3$): δ (ppm) 7.26 (*d*, *J* = 8.7 Hz, 1H), 6.87 (*d*, *J* = 8.7 Hz, 1H), 4.74 (*br. s*, 1H), 4.53 (*d*, *J* = 11.8 Hz, 1H), 4.50 (*d*, *J* = 11.8 Hz, 1H), 3.80 (*s*, 3H), 3.78 (*m*, 1H), 3.62 (*ddd*, *J* = 11.1 Hz, *J* = 9.3 Hz, *J* = 4.4 Hz, 1H), 3.55 (*dq*, *J* = 9.3 Hz, *J* = 6.2 Hz, 1H), 3.49 (*dd*, *J* = 3.8 Hz, *J* = 3.1 Hz, 1H), 2.59-2.46 (*m*, 2H), 2.15 (*s*, 3H), 2.11 (*ddd*, 13.2 Hz, *J* = 4.4 Hz, *J* = 3.8 Hz, 1H), 1.79 (*m*, 1H), 1.73 (*m*, 1H), 1.68 (*ddd*, *J* = 13.2, 11.1, 3.1 Hz, 1H), 1.27 (*d*, *J* = 6.2 Hz, 3H), 1.08 (*d*, *J* = 6.1 Hz, 3H), **^{13}C NMR**(150 MHz, $CDCl_3$): δ (ppm) 208.9, 159.3, 130.4, 129.4, 113.9, 93.9, 75.4, 70.9, 70.3, 70.0, 68.4, 55.4, 40.1, 32.8, 31.1, 30.0, 18.9, 17.8, **HRMS** (ESI-TOF) m/z $(M + Na)^+$ calcd for $C_{20}H_{30}O_6Na$ 389.1930, found 389.1934, Δ -1.5 ppm, $(M + NH_4)^+$ calcd for $C_{20}H_{34}NO_6$ 384.2386 found 384.2378 Δ -0.8 ppm.

(5*R*)-5-[(2-*O*-(4-methoxybenzyloxy)-4-*O*-((*E*)-3-(1-(*tert*-butoxycarbonyl)-1*H*-imidazol-4-yl)-propenoate)-3,6-dideoxy-α-L-*arabino*-hexopyranosyl)oxy]-2-hexanone (135).

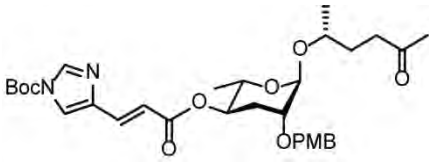

A solution of Nboc-urocanic acid (9.8 mg, 41 µmol) in dichloromethane (1 ml) was treated with 4-dimethylaminopyridine (7.8 mg, 62.8 µmol) followed by dicyclohexylcarbodiimide (13.5 mg, 62.8 µmol). The mixture was stirred for 5 min then **134** (10 mg, 27.3 µmol) in dichloromethane (500 µl). After stirring for 24 h the mixture was diluted with dichloromethane, filtered and treated with water (200 µl). The solution was dried over Na_2SO_4 and concentrated under reduced pressure. The resulting mixture was purified by flash column chromatography using 50% ethyl acetate in hexane *(v/v)* as eluent to afford **135** (15 mg, 25.6 µmol, 94%) as a colorless oil.

^{1}H NMR (600 MHz, $CDCl_3$): δ (ppm) δ 8.10 (*s*, 1H), 7.51 (*d*, *J* = 15.6 Hz, 1H), 7.52 (*s*, 1 H), 7.51 (*d*, *J* = 15.6 Hz, 1H), 7.51 (*s*, 1H), 7.28 (*d*, *J* = 8.6 Hz, 2 H), 6.87 (*d*, *J* = 8.6 Hz, 2 H), 6.64 (*d*, *J* = 15.6 Hz, 1 H), 4.94 (*ddd*, *J* = 10.2 Hz, *J* = 9.7 Hz, 4.5 Hz, 1H), 4.76 (*s*, 1 H), 4.62 (*d*, *J* = 11.8 Hz, 1H), 4.48 (*d*, *J* = 11.8 Hz, 1 H), 3.81 (*dq*, *J* = 9.7 Hz, *J* = 6.3 Hz, 1H), 3.79 (*tq*, *J* = 6.1 Hz, *J* = 5.4 Hz, 1H), 3.79 (*s*, 3 H), 3.50 (*dd*, *J* = 3.7 Hz, *J* = 3.0 Hz, 1H), 2.54 (*m*, 2H), 2.33 (*ddd*, *J* = 13.1 Hz, *J* = 10.2 Hz, *J* =3.0 Hz, 1H), 1.77-1.64 (*m*, 2H), 1.77 (*ddd*, *J* = 13.7 Hz, *J* = 4.5 Hz, *J* = 3.7 Hz, 1H), 1.20 (*d*, *J* = 6.3 Hz, 3H), 1.09(*d*, *J* = 6.1 Hz, 3H), **^{13}C NMR**(150 MHz, $CDCl_3$): δ (ppm) 208.7, 166.3, 159.3, 138.1, 135.0, 130.2, 129.6, 119.2, 118.6, 113.9, 94.6, 86.8, 74.5, 70.7, 70.5, 70.5, 67.4, 55.4, 39.9, 31.0, 30.1, 29.0, 28.0, 26.5, 19.0, 17.9, **HRMS** (ESI-TOF) m/z $(M + Na)^+$ calcd for $C_{31}H_{42}N_2NaO_9$ 609.2788, found 609.2788, Δppm -2.6, $(M + H)^+$ calcd for $C_{31}H_{43}N_2O_9$ 587.2969, found 587.2958, Δppm -1.9.

(5*R*)-5-[4-*O*-((*E*)-3-(1*H*-imidazol-4-yl)-propenoate)-3,6-dideoxy-α-L-*arabino*-hexopyranosyl)oxy]-2-hexanone (35).

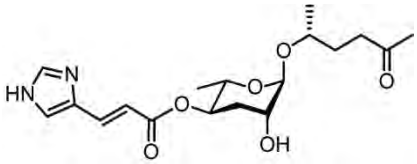

A solution of **135** (5 mg, 8.5 µmol) in dichloromethane (1.5 ml) was treated with trifluoroacetic acid (20 µl). After stirring at room temperature for 1 h the mixture was concentrated under reduced pressure and the resulting residue was purified by flash column chromatography using 10% methanol in dichloromethane *(v/v)* followed to afford the 4'-(*E*)-UA-asc-C6MK **35** (1.3 mg, 3.5 µmol, 42%).

^{1}H NMR (600 MHz, CD_3OD) δ (ppm), 7.78 (*s*, 1 H), 7.61 (*d*, *J* = 15.8 Hz, 1H), 7.45 (*s*, 1H), 6.42 (*br.s*, 1H), 4.96 (*ddd*, *J* = 11.4 Hz, *J* = 9.4 Hz, *J* = 4.8 Hz, 1H), 4.70 (*br.s*, 1H), 3.80 (*m*, 1H), 3.87 (*dq*, *J* = 9.4 Hz, *J* =

6.4 Hz, 1H), 3.74 (*dd*, *J* = 3.8 Hz, *J* = 3.0 Hz, 1H), 2.68-2.59 (*m*, 2H), 2.18 (*s*, 3H), 2.10 (*ddd*, *J* = 13.3 Hz, *J* = 4.8 Hz, *J* = 3.8 Hz, 1H), 1.89 (*ddd*, *J* = 13.3 Hz, *J* = 11.4 Hz, *J* = 3.0 Hz, 1H), 1.85-1.74 (*m*, 2 H),1.16 (*d*, *J* = 6.2 Hz, 3H), 1.17 (*d*, *J* = 6.4 Hz, 3H), **^{13}C NMR**(150 MHz, CD_3OD) δ (ppm) 178.3, 166.6, 137.5, 136.6, 120.3, 120.1, 114.6, 96.3, 70.5, 69.8, 67.9, 67.3, 38.9, 31.8, 30.5, 28.3, 17.6, 16.6 (**Table S 2**), **HRMS** (ESI-TOF) m/z $(M + H)^+$ calcd for $C_{18}H_{27}N_2O_6$ 367.1869, found 367.1861, Δ 0.5 ppm.

(5*R*)-5-[4-*O*-((*Z*)-3-(1*H*-imidazol-4-yl)-propenoate)3,6-dideoxy-α-L-*arabino*-hexopyranosyl)oxy]-2-hexanone (36).

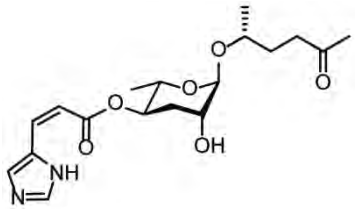

A solution of **35** (0.6 mg, 1.02 µmol) in methanol (600 µl) was irradiated in a quartz NMR tube for 50 min with a 254 nm lamp. The resulting mixture was concentrating under reduced pressure then purified by flash column chromatography using 10% methanol in dichloromethane (*v/v*) as an eluent to afford **36** (0.3 mg, 0.51 µmol, 50%).

^{1}H NMR (600 MHz, CD_3OD) δ (ppm), 7.85 (*s*, 1 H), 7.42 (*s*, 1 H), 6.99 (*d*, *J* = 12.5 Hz, 1 H), 5.76 (*d*, *J* = 12.5 Hz, 1 H), 4.99 (*ddd*, *J* = 11.9 Hz, 10.7 Hz, 6.2 Hz, 1 H), 4.70 (*br.s*, 1 H), 3.86 (*dq*, *J* = 9.3 Hz, *J* = 6.1 Hz, 1 H), 3.83 (*m*, 1 H), 3.75 (*dd*, *J* = 3.4 Hz, *J* = 3.1 Hz, 1 H), 2.64-2.60 (*m*, 2 H), 2.17 (s, 3 H), 2.12 (*ddd*, *J* = 13.9 Hz, *J* = 5.4 Hz, *J* = 3.1 Hz, 1 H), 1.89 (*ddd*, *J* = 13.9 Hz, *J* = 11.9 Hz, *J* = 3.4 Hz, 1 H), 1.85-1.73 (*m*, 2 H), 1.16 (*d*, *J* = 6.1 Hz, 3H), 1.17 (*d*, *J* = 6.1 Hz, 3H), ^{13}C NMR(150 MHz, CD_3OD) δ (ppm) 178.6, 167.2, 132.3, 112.7, 97.2, 71.6, 71.5, 70.0, 68.1, 40.0, 32.6, 31.7, 29.5, 18.7, 17.6, **HRMS** (ESI-TOF) m/z $(M - H)^-$ calcd for $C_{18}H_{25}N_2O_6$ 365.1713, found 365.1712, Δ - 0.3 ppm.

(7*R*)-7-[(4-*O*-*tert*-butyldiphenyl-3,6-dideoxy-α-L-*arabino*-hexopyranosyl)oxy]-1-octene (122).

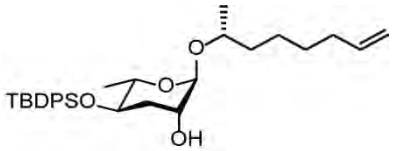

A solution of **111** (100 mg, 0.17 mmol) in 1,4-dioxane (4.2 ml) was treated with a solution of lithium hydroxide monohydrate (14.6 mg, 0.34 mmol) in water (1 ml). After stirring overnight at 60 °C, the mixture was cooled to room temperature, quenched with acetic acid (120 µl) and concentrated under reduced pressure. The resulting residue was purified by flash column chromatography using 10% ethyl acetate in hexane *(v/v)* as eluent to afford **122** (66 mg, 0.13 mmol, 76%) as a colorless oil.

^{1}H NMR (600 MHz, $CDCl_3$): δ (ppm) 7.62 (*d*, *J* = 8.3 Hz, 2H), 7.59 (*d*, *J* = 7.9 Hz, 2H), 7.37-7.33 (*m*, 2H),

7.33-7.28 (*m*, 4H), 5.77 (*ddt*, *J* = 17.0 Hz, *J* = 10.2 Hz, *J* = 6.7 Hz, 1H), 4.96 (*ddt*, *J* = 17.0 Hz, *J* = 1.7 Hz, *J* = 1.5 Hz, 1H), 4.90 (*dd*, *J* = 10.2 Hz, *J* = 1.7 Hz, 1H), 4.52 (*br.s*, 1H), 3.73 (*dq*, *J* = 9.3 Hz, *J* = 6.3 Hz, 1H), 3.70 (*m*, 1H), 3.57 (*ddd*, *J* = 11.0 Hz, *J* = 9.3 Hz, *J* = 4.6 Hz, 1H), 3.55 (*dd*, *J* = 3.8 Hz, *J* = 3.1 Hz, 1H), 2.03 (*dt*, *J* = 6.7 Hz, *J* = 5.6 Hz, 2H), 1.79 (*ddd*, *J* = 13.5 Hz, *J* = 11.0 Hz, *J* = 3.1 Hz, 1H), 1.71 (*ddd*, *J* = 13.5 Hz, *J* = 4.6 Hz, *J* = 3.8 Hz, 1H), 1.52 (*m*, 1H), 1.41-1.31 (*m*, 4H), 1.39 (m, 1H), 1.10 (*d*, *J* = 6.3 Hz, 3H), 1.02 (*d*, *J* = 6.1 Hz, 3H), 0.98 (*s*, 9H), **^{13}C NMR**(150 MHz, $CDCl_3$): δ (ppm) 139.0, 136.1, 129.9, 129.8, 127.8, 127.6, 114.6, 96.2, 71.5, 70.0, 69.4, 35.8, 34.0, 27.1, 25.5, 19.5, 19.2, 18.3, **HRMS** (ESI-TOF) m/z $(M + NH_4^+)^+$ calcd for $C_{30}H_{48}NO_4Si$ 514.3353, found 514.3362, Δ 1.7 ppm.

(7*R*)-7-[(2-*O*-(4-methoxybenzyloxy)-4-*O*-*tert*-butyldiphenyl-3,6-dideoxy-α-L-*arabino*-hexopyranosyl)oxy]-1-octene (123).

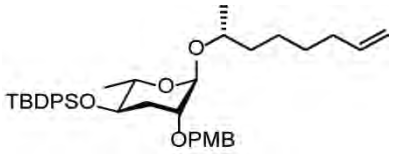

Under N_2 atmosphere, **122** (60 mg, 0.13 mmol) in dichloromethane (350 µl) was treated with 2-(4-methoxybenzyloxy)-4-methylquinoline (67 mg, 0.24 mmol) followed by camphor-10-sulfonic acid (4 mg, 12 µmol). After stirring overnight at room temperature, the reaction was concentrated under reduced pressure and the resulting residue purified by flash column chromatography using a gradient of 0 to 10% ethyl acetate in hexane *(v/v)* as eluent to afford **123** (34 mg, 0.055 mmol, 42%) as a colorless oil.

^{1}H NMR (600 MHz, $CDCl_3$): δ (ppm) 7.74-7.67 (*m*, 4H), 7.45-7.40 (*m*, 2H), 7.40-7.35 (*m*, 4H), 6.98 (*d*, *J* = 8.6 Hz, 2H), 6.77 (*d*, *J* = 8.6 Hz, 2H), 5.84 (*ddt*, *J* = 17.0 Hz, *J* = 10.2 Hz, *J* = 6.7 Hz, 1H), 5.03 (*ddt*, *J* = 17.0 Hz, *J* = 1.7 Hz, *J* = 1.5 Hz, 1H), 4.96 (*dd*, *J* = 10.2 Hz, *J* = 1.7 Hz, 1H), 4.62 (*br.s*, 1 H), 4.09 (*d*, *J* = 11.9 Hz, 1H), 3.97 (*d*, *J* = 11.9 Hz, 1H), 3.78 (*s*, 3H), 3.77 (*dq*, *J* = 9.6 Hz, 6.2 Hz, 1H), 3.76 (*m*, 1H), 3.75 (*ddd*, *J* = 10.5 Hz, *J* = 9.6 Hz, *J* = 4.7 Hz, 1H), 3.27 (*dd*, *J* = 3.9 Hz, *J* = 3.2 Hz, 1H), 2.10 (*dt*, *J* = 6.7 Hz, *J* = 5.8 Hz, 1 H), 1.81 (*ddd*, 13.5 Hz, *J* = 4.7 Hz, *J* = 3.9 Hz, 1H), 1.67 (*ddd*, *J* = 13.5 Hz, *J* = 10.5 Hz, *J* = 3.9 Hz, 1H), 1.56 (*m*, 1H), 1.48-1.37 (*m*, 4H), 1.44 (*m*, 1H), 1.25 (*d*, *J* = 6.2 Hz, 3H), 1.05 (*s*, 9H), 1.04 (*d*, *J* = 6.1 Hz, 3H), **^{13}C NMR**(150 MHz, $CDCl_3$): δ (ppm) 139.1, 136.1, 136.0, 129.9, 129.2, 127.8, 127.6, 114.6, 113.7, 94.7, 75.2, 70.9, 70.3, 70.2, 69.6, 55.4, 37.3, 34.0, 32.3, 31.1, 29.0, 27.1, 25.5, 19.6, 18.5, **HRMS** (ESI-TOF) m/z $(M + NH_4^+)^+$ calcd for $C_{38}H_{56}NO_5Si$ 634.3928, found 634.3930, Δ 0.3 ppm.

(7*R*)-7-[(2-*O*-(4-methoxybenzyloxy)-3,6-dideoxy-α-L-*arabino*-hexopyranosyl)oxy]-1-octene (124).

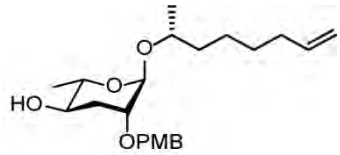

A solution of **123** (20 mg, 33.2 µmol) in tetrahydrofuran (1.7 ml) was treated with tetrabutylammonium fluoride solution (1 M in tetrahydrofuran, 166 µl, 166 µmol). After stirring for 18 h at room temperature the mixture was quenched with water (500 µl). The aqueous phase was extracted with dichloromethane (2 x 2 ml), dried over Na_2SO_4, and then concentrated under reduced pressure. The resulting residue was purified by flash column chromatography using 35% ethyl acetate in hexane *(v/v)* as eluent to afford **124** (8.7 mg, 23.0 µmol, 69%) as a colorless oil.

^{1}H NMR (600 MHz, $CDCl_3$): 7.26 (*d*, *J* = 8.6 Hz, 2H), 6.87 (*d*, *J* = 8.6 Hz, 2H), 5.80 (*ddt*, *J* = 17.1 Hz, *J* = 10.1 Hz, *J* = 6.7 Hz, 1H), 5.00 (*ddd*, *J* = 17.1 Hz, *J* = 2.2 Hz, *J* = 1.7 Hz, 1H), 4.76 (*br.s*, 1H), 4.52 (*s*, 2H), 3.80 (*s*, 3H), 3.77 (*qdd*, *J* = 6.1 Hz, *J* = 5.8 Hz, *J* = 4.8 Hz, 1H), 3.65-3.59 (*m*, 2H), 3.51 (*ddd*, *J* = 3.2 Hz, *J* = 3.2 Hz, *J* = 1.7 Hz, 1H), 2.10 (*ddd*, *J* = 13.0 Hz, *J* = 4.5 Hz, *J* = 3.2 Hz, 1H), 2.08-2.02 (*m*, 2H), 1.72 (*ddd*, *J* = 13.0 Hz, *J* = 10.0 Hz, *J* = 3.2 Hz, 1H), 1.53 (*m*, 1H), 1.43-1.35 (*m*, 2H), 1.4152 (*m*, 1H), 1.4148 (*m*, 1H), 1.33 (*m*, 1H), 1.27 (*d*, *J* = 5.8 Hz, 3H), 1.07 (*d*, *J* = 6.1 Hz, 3H), **^{13}C NMR**(150 MHz, $CDCl_3$): δ (ppm) 159.4, 139.1, 130.5, 129.4, 114.5, 113.9, 94.2, 75.7, 71.3, 70.9, 69.9, 68.6, 55.4, 37.2, 33.9, 33.0, 29.0, 25.4, 19.1.

***Tert*-butyl-(7*R*)-7-[(2-*O*-(4-methoxybenzyloxy)-4-*O*-*tert*-butyldiphenyl-3,6-dideoxy-α-L-*arabino*-hexopyranosyl)oxy]-2-nonenoate (127).**

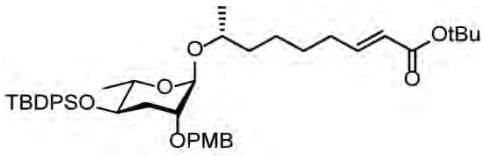

A solution of **123** (34 mg, 55 µmol) and *tert*-butyl acrylate (36 µl, 25 µmol) in dry dichloromethane (2 ml) was treated with Grubb's 2nd generation catalyst (4 mg, 4.7 µmol). The solution was refluxed for 22 h then cooled to room temperature and concentrated under reduced pressure. The given residue was purified by flash column chromatography on silica gel using 10% ethyl acetate in hexane (*v/v*) as eluent to afford **127** (30 mg, 42 µmol, 76%) as a yellow oil.

^{1}H NMR (600 MHz, CDCl3) δ (ppm): 7.74-7.66 (*m*, 4 H), 7.45-7.40 (*m*, 2H), 7.40-7.35 (*m*, 4H), 6.98 (*d*, *J* = 8.7 Hz, 1 H), 6.88 (*dt*, *J* = 15.5 Hz, 6.9 Hz, 1H), 6.77 (*d*, *J* = 8.6 Hz, 1H), 5.76 (dt, *J* = 15.6 Hz, 1.5 Hz, 1H), 4.61 (*br.s* , 1H), 4.10 (*d*, *J* = 11.9 Hz , 1H), 3.97 (*d*, *J* = 11.9 Hz, 1H), 3.78 (*s*, 3H), 3.75 (*ddd*, *J* = 10.6 Hz, *J* = 9.4 Hz, *J* = 4.4 Hz, 1H), 3.749 (*dq*, *J* = 9.4 Hz, *J* = 5.9 Hz, 1H), 3.745 (*m*, 1H), 3.27 (*dd*, *J* = 3.9 Hz, *J* = 3.1 Hz), 2.21 (*dt*, *J* = 6.9 Hz, 5.4 Hz, 2H), 1.81 (*ddd*, *J* = 13.3 Hz, *J* = 4.4 Hz, *J* = 3.9 Hz, 1H), 1.66 (*ddd*, *J* = 13.3

Hz, *J* = 10.6 Hz, *J* = 3.1 Hz, 1H), 1.56 (*m*, 1H), 1.53-1.44 (*m*, 2H), 1.52-1.36 (*m*, 4H), 1.43 (*m*, 1H), 1.25 (d, *J* = 5.9 Hz, 3H), 1.05 (s, 9H), 1.04 (d, *J* = 6.1 Hz, 3H), **^{13}C NMR**(150 MHz, $CDCl_3$): δ (ppm) 166.3, 159.1, 148.1, 136.1, 136.0, 129.9, 129.7, 129.2, 127.8, 127.7, 123.2, 113.7, 94.8, 71.0, 70.3, 70.2, 69.7, 55.4, 37.1, 32.3, 28.3, 28.2 27.1, 25.6, 19.6, 19.1, 18.5, **HRMS** (ESI-TOF) m/z $(M + NH_4^+)^+$ calcd for $C_{43}H_{64}NO_7Si$ 734.4452, found 734.4459, Δ 1 ppm.

***Tert*-butyl-(7*R*)-7-[(2-O-(4-methoxybenzyloxy)-3,6-dideoxy-α-L-*arabino*-hexopyranosyl)oxy]-2-nonenoate (128).**

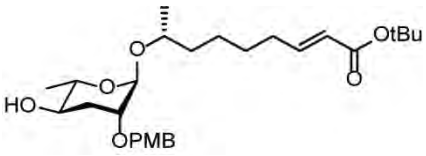

A solution of **127** (30 mg, 45 µmol) in tetrahydrofuran (2 ml) was treated with tetrabutylammonium fluoride solution (1 M in tetrahydrofuran, 0.18 ml, 0.18 mmol). After stirring for 15 h at room temperature the mixture was quenched with water (1 ml). The organic phase was extracted with dichloromethane (2 x 5 ml), dried over Na_2SO_4 and then concentrated under reduced pressure. The resulting residue was purified by flash column chromatography using 35% ethyl acetate in hexane *(v/v)* as eluent to afford **128** (16.7 mg, 35 µmol, 78%) as a colorless oil.

^{1}H NMR (600 MHz, CDCl3): δ (ppm) 7.26 (*d*, *J* = 8.7 Hz, 2H), 6.86 (*d*, *J* = 8.7 Hz, 2H),6.84 (*dt*, *J* = 14.1 Hz, *J* = 6.9Hz, 1H), 5.73 (*dt*, *J* =14.1 Hz, *J* = 1.5Hz, 1H), 4.76 (*br. s*, 1H), 4.53 (d, *J* = 11.9 Hz, 1H), 4.50 (*d*, *J* = 11.9 Hz, 1H), 3.80 (*s*, 3H), 3.77 (*ddq*, *J* = 6.2 Hz, *J* = 6.0 Hz, *J* = 5.3 Hz, 1H), 3.61 (*ddd*, *J* = 11.0 Hz, *J* = 9.5 Hz, *J* = 4.7 Hz, 1H), 3.59 (*dq*, *J* = 9.5 Hz, *J* = 5.8 Hz, 1H), 3.50 (*dd*, *J* = 3.8 Hz, *J* = 3.0 Hz, 1Hz), 2.18 (*dt*, *J* = 6.9 Hz, *J* = 5.1 Hz, 2H), 2.12 (*ddd*, *J* = 13.7 Hz, *J* = 4.7 Hz, *J* = 3.8 Hz, 1 H), 1.69 (*ddd*, *J* = 13.7 Hz, *J* = 11.0 Hz, *J* = 3.0 Hz, 1H), 1.52-1.40 (*m*, 2H), 1.50 (*m*, 1H), 1.47 (*s*, 9H), 1.433 (*m*, 1H), 1.427 (*m*, 1H), 1.36 (*m*, 1H), 1.28 (*d*, *J* = 5.8 Hz, 3H), 1.06 (*d*, *J* = 6.0 Hz, 3H), **^{13}C NMR**(150 MHz, $CDCl_3$): δ (ppm) 166.5, 159.3, 148.1, 129.4, 123.3, 113.9, 94.1, 70.8, 70.8, 70.1, 68.5, 55.4, 37.1, 32.9, 32.0, 28.3, 28.0, 25.2, 19.1, 17.9, **HRMS** (ESI-TOF) m/z $(M + H)^+$ calcd for $C_{27}H_{42}O_7$ 479.3009, found 479.2991, Δ -3.9 ppm.

4-methoxybenzyl-(7*R*)-7-[(2-*O*-(4-methoxybenzyloxy)-3,6-dideoxy-α-L-*arabino*-hexopyranosyl)oxy]-2-nonenoate (125).

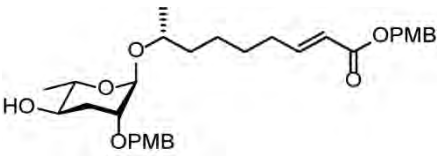

A solution of **124** (7 mg, 18.5 µmol) and 4-methoxy-benzyloxy acrylate (18 mg, 92.4 µmol) in dry dichloromethane (330 µl) was treated with Grubb's 2nd generation catalyst (7 mg, 8 µmol). The

solution was refluxed for 10 h, then cooled to room temperature and concentrated under reduced pressure. The given residue was purified by flash column chromatography on silica gel using 35% ethyl acetate in hexane (v/v) as eluent to afford **125** (8 mg, 14.7 µmol, 79%).

^{1}H NMR (600 MHz, CDCl3) δ (ppm): 7.31 (*d*, *J* = 8.3 Hz, 2H), 7.26 (*d*, *J* = 8.4 Hz, 2H), 6.98 (*dt*, *J* = 14.2 Hz, *J* = 7.1 Hz, 1H), 6.89 (*d*, *J* = 8.3 Hz, 2H), 6.88 (*d*, *J* = 8.4 Hz, 2H), 5.84 (*dt*, *J* = 14.2 Hz, *J* = 1.4 Hz, 1H), 5.10 (*s*, 2H), 4.75 (*br.s*, 1H), 4.53 (*d*, *J* = 11.2 Hz, 1H), 4.51 (*d*, *J* = 11.2 Hz, 1H), 3.81 (*s*, 3H), 3.80 (*s*, 3H), 3.76(*dtd*, *J* = 6.2 Hz, *J* = 6.0 Hz, *J* = 5.0 Hz, 1H), 3.60 (*m*, 1H), 3.58 (*m*, 1H), 3.50 (*ddd*, *J* = 3.0 Hz, *J* = 3.0 Hz, *J* = 1.8 Hz, 1H), 2.23-2.17 (*m*, 2H), 2.11 (*ddd*, *J* = 13.4 Hz, *J* = 4.5 Hz, *J* = 3.0 Hz, 1H), 1.68 (*ddd*, *J* = 13.4 Hz, *J* = 10.8 Hz, *J* = 3.0 Hz, 1H), 1.51 (*m*, 1H), 1.51-1.40 (*m*, 2H), 1.422 (*m*, 1H), 1.418 (*m*, 1H), 1.34 (*m*, 1H), 1.26 (*d*, *J* = 5.6 Hz,) 1.06 (*d*, *J* = 6.0 Hz, 3H), **^{13}C NMR**(150 MHz, $CDCl_3$): δ (ppm) 166.9, 159.8, 159.4, 149.9, 130.5, 130.3, 129.4, 121.4, 114.1, 114.0, 94.1, 75.6, 70.90, 70.86, 70.1, 68.5, 66.1, 55.4, 37.1, 32.9, 32.2, 27.9, 25.2, 19.1, 17.8, **HRMS** (ESI-TOF) m/z $(M + Na)^+$ calcd for $C_{31}H_{42}O_8Na$ 565.2777, found 565.2766, ∆ppm -1.1.

***Tert*-butyl-(7*R*)-7-[(2-*O*-(4-methoxybenzyloxy)-4-*O*-((*E*)-3-(1-(*tert*-butoxycarbonyl)-1*H*-imidazol-4-yl)-propenoate)-3,6-dideoxy-α-L-*arabino*-hexopyranosyl)oxy]-2-nonenoate (129).**

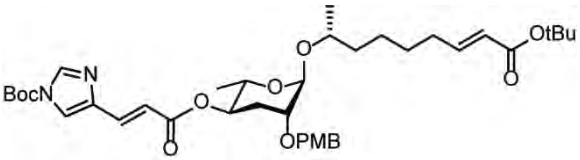

A solution of Nboc-urocanic acid (8.3 mg, 37.5 µmol) in dichloromethane (750 µl) was treated with 4-dimethylaminopyridine (7 mg, 57.5 µmol) followed by 1-(3-dimethylaminopropyl)-3-ethylcarbodiimide hydrochloride (10.9 mg, 57.5 µmol). The mixture was stirred for 5 min then **128** (12 mg, 25 µmol) in dichloromethane (450 µl). After stirring for 24 h water (100 µl) was added to the mixture and the mixture was dried with Na_2SO_4 then concentrated under reduced pressure. The resulting mixture was purified by flash column chromatography using 35% ethyl acetate in hexane *(v/v)* as eluent to afford **129** (11 mg, 15.7 µmol, 63%) as a colorless oil.

^{1}H NMR (600 MHz, CDCl3): δ (ppm) 8.12 (*s*, 1H), 7.52 (*s*, 1H), 7.51 (*d*, *J* = 16.6 Hz, 1H), 7.29 (*d*, *J* = 7.9 Hz, 2H), 6.87 (*d*, *J* = 7.9 Hz, 2H), 6.86 (*dt*, *J* = 15.6 Hz, *J* = 6.5 Hz, 1H), 6.68 (*d*, *J* = 16.6 Hz, 1H), 5.74 (*dt*, *J* = 15.6 Hz, *J* = 1.5 Hz, 1H), 4.94 (*ddd*, *J* = 11.0 Hz, *J* = 9.2 Hz, *J* = 4.9 Hz, 1H), 4.77 (*br.s*, 1H), 4.63 (*d*, *J* = 11.8 Hz, 1H), 4.49 (*d*, *J* = 11.8 Hz, 1H), 3.87 (*dq*, *J* = 9.2 Hz, *J* = 6.3 Hz, 1H), 3.80 (*s*, 3H), 3.78 (*ddt*, *J* = 6.8 Hz, *J* = 6.1 Hz, *J* = 5.3 Hz, 1H), 3.51 (*dd*, *J* = 3.9 Hz, *J* = 2.8 Hz, 1H), 2.32 (*ddd*, *J* = 13.6 Hz, *J* = 4.9 Hz, *J* = 3.9 Hz, 1H), 2.19 (*dt*, *J* = 6.5 Hz, *J* = 6.1 Hz, 2H), 1.63 (*s*, 9H), 1.56 (*m*, 1H), 1.51-1.43 (*m*, 2H), 1.47 (*s*, 3H), 1.45 (*m*, 1H), 1.44 (*m*, 1H), 1.35 (*m*, 1H), 1.19 (*d*, *J* = 6.3 Hz, 3H), 1.08 (*d*, *J* = 6.2 Hz, 1H), **^{13}CNMR** (150 MHz, $CDCl_3$): δ (ppm) 166.3, 166.2, 148.0, 137.9, 129.6, 123.8, 118.5, 113.9, 94.7, 71.4, 70.9, 70.5,

67.3, 55.4, 37.1, 32.2, 29.1, 28.3, 28.2, 28.0, 25.5, 19.1, 17.9, **HRMS** (ESI-TOF) m/z $(M + H)^+$ calcd for $C_{38}H_{55}N_2O_{10}$ 699.3857, found 699.3851, Δ -0.9 ppm.

4-methoxybenzyl-(7*R*)-7-[(2-*O*-(4-methoxybenzyloxy)-4-*O*-((*E*)-3-(1-(*tert*-butoxycarbonyl)-1*H*-imidazol-4-yl)-propenoate)-3,6-dideoxy-α-L-*arabino*-hexopyranosyl)oxy]-2-nonenoate (126).

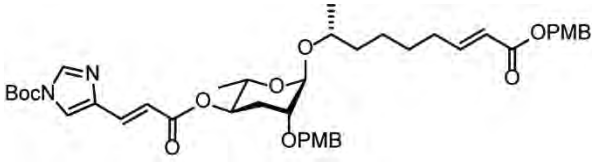

A solution of *N*-boc-urocanic acid (8 mg, 29.5 µmol) in dichloromethane (588 µl) was treated with 4-dimethylaminopyridine (5.2 mg, 44.1 µmol) followed by 1-(3-dimethylaminopropyl)-3-ethylcarbodiimide hydrochloride (8.3 mg, 44.1 µmol). The mixture was stirred for 5 min then **125** (8 mg, 14.7 µmol) in dichloromethane (360 µl) was added. After stirring for 14 h, water (200 µl) was added and the mixture was dried over Na_2SO_4 and then concentrated under reduced pressure. The resulting mixture was purified by flash column chromatography using 35% ethyl acetate in hexane *(v/v)* as eluent to afford **126** (10 mg, 13.4 µmol, 91%) as a colorless oil.

^{1}H NMR (600 MHz, CDCl3): δ (ppm) 8.06 (*s*, 1H), 7.510 (*s*, 1H), 7.507 (*d*, *J* = 15.6 Hz, 1H), 7.30 (*d*, *J* = 8.5 Hz, 2H), 7.29 (*d*, *J* = 8.7 Hz, 2H), 7.00 (*dt*, *J* = 15.7 Hz, *J* = 6.9 Hz, 1H), 6.88 (*d*, *J* = 8.5 Hz, 2H), 6.87 (*d*, *J* = 8.7 Hz, 2H), 6.64 (*d*, *J* = 15,6 Hz, 1H), 5.85 (*d*, *J* = 15.7 Hz, 1H), 5.10 (*s*, 2H), 4.94 (*ddd*, *J* = 11.2 Hz, *J* = 9.3 Hz, *J* = 5.5 Hz, 1H), 4.77 (*br.s*, 1H), 4.63 (*d*, *J* = 11.8 Hz, 1H), 4.49 (*d*, *J* = 11.8 Hz, 1H), 3.86 (*dq*, *J* = 9.3 Hz, *J* = 6.2 Hz, 1H), 3.801 (*s*, 3H), 3.797 (*s*, 3H), 3.77 (*qdd*, *J* = 6.0 Hz, *J* = 6.0 Hz, *J* = 5.3 Hz, 1H), 3.51 (*ddd*, *J* = 3.1 Hz, *J* = 2.6 Hz, *J* = 1.6 Hz, 1H), 2.32 (*ddd*, *J* = 13.6 Hz, *J* = 5.5 Hz, *J* = 3.1 Hz, 1H), 2.21 (*dt*, *J* = 7.2 Hz, *J* = 6.9 Hz, 2H), 1.78 (*ddd*, *J* = 13.6 Hz, *J* = 11.2 Hz, *J* = 2.6 Hz, 1H), 1.69 (*s*, 9H), 1.54 (*m*, 1H), 1.50-1.42 (*m*, 2H), 1.429 (*m*, 1H), 1.434 (*m*, 1H), 1.35 (*m*, 1H), 1.19 (*d*, *J* = 6.2 Hz, 3H), 1.07 (*d*, *J* = 6.0 Hz, 3H), **^{13}CNMR** (150 MHz, $CDCl_3$): δ (ppm) 166.7, 166.4, 159.7, 159.3, 149.8, 139.3, 138.1, 135.2, 130.4, 130.2, 129.6, 128.4, 121.3, 119.1, 118.6, 114.1, 113.9, 94.8, 86.6, 74.7, 71.4, 70.8, 70.5, 67.3, 66.0, 55.4, 37.1, 32.3, 29.1, 28.1, 28.0, 25.5, 19.1, 17.9, **HRMS** (ESI-TOF) m/z $(M + H)^+$ calcd for $C_{42}H_{55}N_2O_{11}$ 763.3806, found 763.3807, Δppm 0.1, $(M + Na)^+$ calcd for $C_{42}H_{54}N_2NaO_9$ 785.3625, found 3622, Δppm -0.4.

(7*R*)-7-[4-*O*-((*E*)-3-(1*H*-imidazol-4-yl)-propenoate)-3,6-dideoxy-α-L-*arabino*-hexopyranosyl)oxy]-2-nonenoic acid (37).

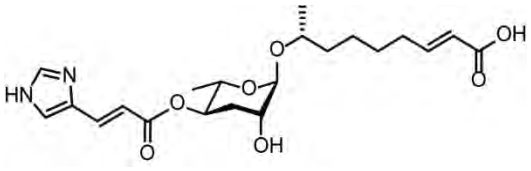

A solution of **126** (8 mg, 10.7 µmol) in dichloromethane (2 ml) was treated with trifluoroacetic acid (20 µl, 258 µmol). After stirring at room temperature for 6 h the mixture was concentrated under reduced pressure and the resulting residue was purified by flash column chromatography using 10% methanol in dichloromethane *(v/v)* as eluant to afford **37** (2.8 mg, 6.6 µmol, 62%).

^{1}H NMR (600 MHz, CD_3OD): δ (ppm), 8.40 (*s*, 1H), 7.69 (*s*, 1H), 7.61 (*d*, *J* = 16.0 Hz, 1H), 6.98 (*dt*, *J* = 15.4 Hz, *J* = 14.0 Hz, 1H), 6.51 (*d*, *J* = 16.0 Hz, 1H), 5.83 (*dt*, *J* = 15.4 Hz, *J* = 5.8 Hz, 1H), 4.97 (*ddd*, *J* = 11.1 Hz, *J* = 9.6 Hz, *J* = 4.5 Hz, 1H), 4.71 (*br.s*, 1H), 3.91 (*dq*, *J* = 9.6 Hz, *J* = 6.3 Hz, 1H), 3.82 (*m*, 1H), 3.75 (*dd*, *J* = 3.2 Hz, *J* = 2.9 Hz, 1H), 2.30-2.25 (*m*, 2H), 2.11 (*ddd*, *J* = 13.1 Hz, *J* = 11.1 Hz, *J* = 3.2 Hz, 1H), 1.89 (*ddd*, *J* = 13.1 Hz, *J* = 4.5 Hz, *J* = 2.9 Hz, 1H), 1.59 (*m*, 1H), 1.58-1.49 (*m*, 2H), 1.531 (*m*, 1H), 1.527 (*m*, 1H), 1.43 (*m*, 1H), 1.16 (*d*, *J* = 6.3 Hz, 3H), 1.15 (*d*, *J* = 6.1 Hz, 3H), **^{13}CNMR** (150 MHz, CD_3OD): δ (ppm) 168.3, 165.7, 150.7, 137.9, 133.2, 132.07, 122.78, 122.61, 122.60, 97.4, 72.7, 71.5, 69.3, 68.1, 37.9, 32.9, 32.8, 28.9, 26.3, 19.2, 17.8, **HRMS** (ESI-TOF) m/z $(M - H)^-$ calcd for $C_{21}H_{29}N_2O_7$ 421.1975, found 421.1978, Δ 0.7 ppm.

(7*R*)-7-[4-*O*-((*Z*)-3-(1*H*-imidazol-4-yl)-propenoate)-3,6-dideoxy-α-L-*arabino*-hexopyranosyl)oxy]-2-nonenoic acid (38).

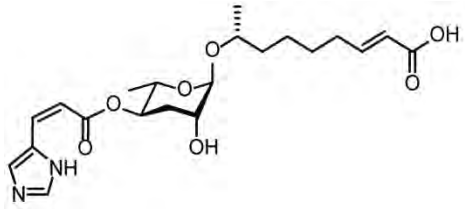

A solution of **37** (1.3 mg, 3.1 µmol) in methanol (600 µl) was irradiated in a quartz NMR tube for 50 min with a 254 nm lamp. The resulting mixture was concentrating under reduced pressure then purified by flash column chromatography using 10% methanol in dichloromethane (*v/v*) as an eluent to afford **38** (825 µg, 2.0 µmol, 65%) along with **37** (275 µg, 0.7 µmol, 23%) as 8/2 mixture.

^{1}H NMR (600 MHz, $CDCl_3$) of the major isomer: δ (ppm) 7.83 (s, 1H), 7.56 (s, 1H), 6.99 (d, J = 12.6 Hz, 1H), 6.73 (dt, J = 16.3 J = 7.2 Hz, 1H), 5.84 (dt, J = 16.3 Hz, J = 2.5 Hz, 1H), 5.79 (d, J = 12.6 Hz, 1H), 4.99 (ddd, J = 11.8 Hz, J = 11.4 Hz, J = 4.7 Hz, 1H), 4.71 (br.s, 1H), 3.90 (dq, J = 9.3 Hz, J = 6.3 Hz, 1H), 3.81 (m, 1H), 3.75 (ddd, J = 3.0 Hz, J = 2.9 Hz, J = 1.3 Hz, 1H), 2.21-2.17 (m, 2H), 2.11 (ddd, J = 13.3 Hz, J = 4.7 Hz, J = 2.9 Hz, 1H), 1.89 (ddd, J = 13.3 Hz, J = 11.4 Hz, J = 3.0 Hz, 1H), 1.56-1.48 (m, 2H), 1.58 (m,

1H), 1.52 (m, 1H), 1.51 (m, 1H), 1.44 (m, 1H), 1.15 (d, J = 6.1 Hz, 3H), 1.17 (d, J =6.3 Hz, 3H); **^{13}CNMR** (150 MHz, CD_3OD): δ (ppm) 167.1, 145.9, 138.5, 133.4, 134.9, 126.9, 113.6, 97.4, 72.6, 71.4, 69.3, 68.0, 37.8, 32.8, 32.7, 29.3, 26.1, 19.2, 17.7, **HRMS** (ESI-TOF) m/z (M - H)$^-$ calcd for $C_{21}H_{29}N_2O_7$ 421.1975, found 421.1986 Δ 2.6 ppm.

8.10.3. Synthesis of 4'-AB-asc-C5 (abas#9, 34)

- **Route A**

(4*R*)-4-[(2-*O*-benzyl-4-*O*-*tert*-butyldiphenylsilyl-3,6-dideoxy-L-*arabino*-hexopyranosyl)oxy]-pentanoic acid (142).

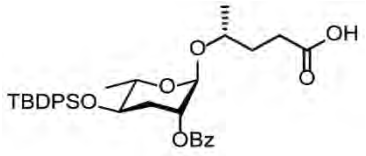

A solution of **141** (149 mg, 0.26 mmol) in dichloromethane (2 ml), acetonitrile (2 ml), and water (1.5 ml) was treated with ruthenium (III) chloride hydrate (5.4 mg, 0.03 mmol) in water (0.5 ml) while stirring vigorously. After 5 min, sodium periodate (278 mg, 1.3 mmol) was added to the mixture. After stirring for 16 h, water (6 ml) was added to the mixture and the organic phase was extracted with dichloromethane (2 x 6 ml). The organic phase was dried with Na_2SO_4 and concentrated under reduced pressure. The resulting residue was purified by flash column chromatography on silica gel using 40% ethyl acetate in hexane *(v/v)* as eluent to afford **142** (107 mg, 0.18 mmol, 70% yield) as a colorless oil. **^{1}HNMR** (400 MHz, $CDCl_3$): δ (ppm) 7.77-7.71 (*m*, 2H), 7.71-7.60 (*m*, 4H), 7.55 (*t*, *J* = 7.8 Hz, 1H), 7.42-7.27 (*m*, 8H), 4.88 (*br.s*, 1H), 4.76 (*br.s*, 1H), 3.92-3.81 (*m*, 2H), 3.67 (*ddd*, *J* = 11.1 Hz, *J* = 9.8 Hz, *J* = 4.3 Hz, 1H), 2.64-2.47 (*m*, 2H), 2.01 (*m*, 1H), 1.95-1.84 (*m*, 3H), 1.28 (*d*, *J* = 6.5 Hz, 3H), 1.17 (*d*, *J* = 6.0 Hz, 3H), 1.07 (*s*, 9H), **^{13}C NMR**(100 MHz, $CDCl_3$): δ (ppm) 179.1, 165.5, 136.1, 136.0, 134.2, 133.4, 133.1, 130.0, 129.9, 129.84, 129.77, 128.3, 127.8, 127.6, 93.5, 71.9, 71.2, 70.31, 70.28, 33.4, 32.0, 27.2, 27.1, 19.5, 19.1, 18.4, 14.3. NMR identical to data reported in literature[40].

(4*R*)-4-[(4-*O*-*tert*-butyldiphenylsilyl-3,6-dideoxy-L-*arabino*-hexopyranosyl)oxy]-pentanoic acid (143).

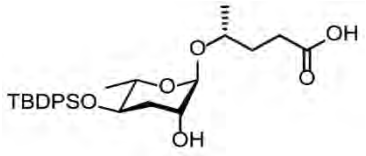

A solution of **142** (107 mg, 0.18 mmol) in 1,4-dioxane (5 ml) was treated with a solution of lithium hydroxide monohydrate (30.2 mg, 0.72 mmol) in water (780 µl). After stirring for 20 h at 60 °C, the mixture was cooled to room temperature, glacial acetic acid (540 µl) was added and the mixture was

concentrated under reduced pressure. The resulting mixture was purified by flash column chromatography on silica gel using 10% ethyl acetate in hexane *(v/v)* as eluent to afford **143** (74 mg, 0.15 mmol, 83% yield).

^{1}HNMR (400 MHz, $CDCl_3$): δ (ppm) 7.72-7.64 (m, 4H), 7.47 (t, J = 7.6 Hz, 1H), 7.44-7.34 (m, 5H), 4.59 (br.s, 1H), 3.85 (m, 1H), 3.75 (dq, J = 6.3 Hz, J = 8.6 Hz, 1H), 3.69-3.59 (m, 2H), 2.61-2.45 (m, 2H), 1.93-1.83 (m, 3H), 1.78 (m, 1H), 1.16 (d, J = 6.3 Hz, 3H), 1.14 (d, J = 6.1 Hz, 3H),1.05 (s, 9H). NMR identical to data reported in literature [40].

Benzyl-(4*R*)-4-[(2-*O*-benzyl-4-*O*-*tert*-butyldiphenylsilyl-3,6-dideoxy-L-*arabino*-hexopyranosyl)oxy]-pentanoate(144).

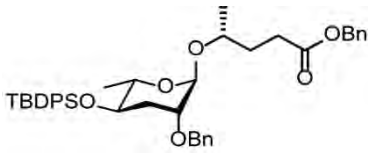

A solution of **143** (52 mg, 0.08 mmol) in dimethylformamide (3 ml) was treated with benzyl bromide (5 ml, 0.66 mmol) and sodium hydride (52 mg, 1.3 mmol). After stirring for 13 h, the solution was cooled to 0 °C, quenched with 1 M hydrochloric acid solution (1 ml) and extracted with ethyl acetate. The organic phase was dried with Na_2SO_4 and concentrated under reduced pressure. The resulting residue was purified by flash column chromatography using 5% ethyl acetate in hexane *(v/v)* as eluent to afford **144** (52.5 mg, 0.017 mmol, 72% yield).

^{1}HNMR (400 MHz, $CDCl_3$): δ (ppm) 7.74-7.67 (m, 4H), 7.42-7.31 (m, 10H), 7.26-7.18 (m, 3H), 7.08-7.04 (m, 2H), 5.18 (d, J = 12.2 Hz, 1H), 5.13 (d, J = 12.2 Hz, 1H), 4.64 (br.s, 1H), 4.14 (d, J = 12.2 Hz, 1H), 4.05 (d, J = 12.2 Hz, 1H), 3.86-3.68 (m, 3H), 3.28 (br.s, 1H), 2.60-2.42 (m, 2H), 1.92-1.76- (m, 3H), 1.65 (ddd, J = 13.5 Hz, J = 10.6 Hz, J = 2.7 Hz, 1H), 1.25 (d, J = 5.8 Hz, 3H), 1.07 (d, J = 6.2 Hz, 3H), 1.05 (s, 9H), **^{13}C NMR**(100 MHz, $CDCl_3$): δ (ppm) 173.6, 138.4, 138.3, 136.2, 136.08, 136.06, 136.04, 136.03, 134.8, 133.9, 129.9, 129.7, 128.7, 128.6, 127.9, 127.8, 127.7, 127.6, 94.5, 75.6, 72.3, 70.5, 70.3, 70.13, 70.10, 69.4, 32.4, 32.3, 30.7, 27.1, 19.5, 18.8, 18.5. NMR identical to data reported in literature[40].

Benzyl-(4*R*)-4-[(2-*O*-benzyl-4-*O*-*tert*-butyldiphenylsilyl-3,6-dideoxy-L-*arabino*-hexopyranosyl)oxy]-pentanoate (145).

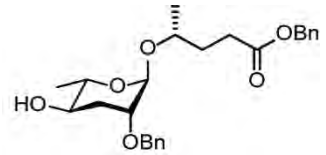

A solution of **144** (52.5 mg, 0.08 mmol) in tetrahydrofuran (2 ml) was treated with a 1 M solution of tetrabutylammonium fluoride in tetrahydrofuran (0.28 ml,0.28 mmol). After stirring overnight at room

temperature, water (1 ml) was added to the mixture and the aqueous phase was extracted with dichloromethane (5 ml). The combined organic phase was dried with Na_2SO_4 and concentrated under reduced pressure. The resulting residue was purified by flash column chromatography on silica gel using 20% ethyl acetate in hexane *(v/v)* as eluent to afford **145** (17 mg, 55 %) as a colorless oil.

^{1}HNMR (400 MHz, $CDCl_3$): δ (ppm) 7.42-7.25 (m, 10H), 5.12 (s, 2H), 4.78 (br.s, 1H), 4.60 (d, J = 12.4 Hz, 1H), 4.56 (d, J = 12.4 Hz, 1H), 3.83 (m, 1H), 3.68-3.52 (m, 2H), 3.50 (br.s, 1H), 2.54-2.39 (m, 2H), 2.12 (dt, J = 13.1 Hz, J = 3.6 Hz, 1H), 1.92-1.77 (m, 2H), 1.69 (ddd, J = 13.4 Hz, J = 10.8 Hz, J = 3.0 Hz, 1H), 1.25 (d, J= 6.0 Hz, 3H), 1.10 (d, J= 6.0 Hz, 3H). NMR identical to data reported in literature[40].

Benzyl-(4*R*)-4-[(2-*O*-benzyl-4-((benzyloxy)carbonyl)amino)benzoyl-3,6-dideoxy-α-L-*arabino*-hexopyranosyl)oxy]-2-pentanoate (146).

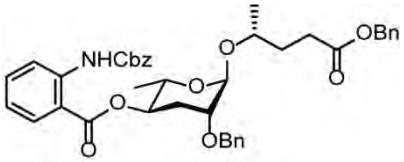

A solution of NCbz-anthranilic acid (21 mg, 0.08 mmol) in dichloromethane (7 ml) was treated with ethylcarbodiimide hydrochloride (15 mg, 0.08 µmol) and 4-dimethylaminopyridin (9.3 mg, 0.08 mmol). The mixture was stirred for 30 min then **145** (17 mg, 0.04 mmol) in dichloromethane (3 ml) was added to the mixture. After stirring for 22 h, the mixture was quenched with water (1 ml), extracted with dichloromethane (2 x 5 ml), dried with Na_2SO_4 and concentrated under reduced pressure. The resulting residue was purified by flash column chromatography using 50% of ethyl acetate in hexane *(v/v)* as eluent to afford **146** (8.5 mg, 0.01 mol, 25%) as a colorless oil.

^{1}HNMR (400 MHz, $CDCl_3$): δ (ppm) 8.47 (dd, J = 8.6 Hz, J = 0.9 Hz, 1H), 7.97 (dd, J = 8.0 Hz, J = 1.7 Hz, 1H), 7.54 (ddd, J = 8.8 Hz, J = 7.3 Hz, J = 1.7 Hz, 1H), 7.47-7.42 (m, 2H), 7.41-7.27, (m, 13H), 7.00 (ddd, J = 8.2 Hz, J = 7.3 Hz, J = 1.1 Hz, 1H), 5.23 (s, 2H), 5.15 (d, J = 12.3 Hz, 1H), 5.10 (d, J = 12.3 Hz, 1H), 5.05 (ddd, J = 10.7 Hz, J = 9.6 Hz, J = 4.6 Hz, 1H), 4.82 (br.s, 1H), 4.70 (d, J = 12.3 Hz, 1H), 4.58 (d, J = 12.3 Hz, 1H), 3.95 (dq, J = 10.7 Hz, J = 6.2 Hz, 1H), 3.86 (m, 1H), 3.54 (ddd, J = 3.7 Hz, J = 2.8 Hz, J = 1.8 Hz, 1H), 2.58-2.41 (m, 2H), 2.35 (ddd, J = 13.0 Hz, J = 4.6 Hz, J = 2.8 Hz, 1H), 1.91-1.84 (m, 2H), 1.85 (ddd, J = 13.0 Hz, J = 10.7 Hz, J = 3.7 Hz, 1H), 1.21 (d, J = 6.2 Hz, 3H), 1.11 (d, J = 6.1 Hz, 3H), **^{13}C NMR**(100 MHz, $CDCl_3$): δ (ppm) 173.4, 167.2, 153.6, 142.1, 138.2, 136.3, 136.1, 134.8, 130.4, 128.74, 128.71, 128.50, 128.46, 128.43, 128.40, 128.37, 121.8, 119.1, 94.5, 75.1, 71.7, 71.2, 70.6, 67.3, 67.1, 66.5, 32.3, 30.7, 29.3, 18.8, 18.0, **HRMS** (ESI-TOF) m/z $(M + H)^+$ calcd for $C_{40}H_{44}NO_9$ 682.3016, found 682.3008, Δppm -1.2 ppm, $(M + NH_4)^+$ calcd for $C_{40}H_{47}N_2O_9$ 699.3282, found 699.3278, Δppm -0.6.

- **Route B**

(3*R*)-3-[(2-*O*-benzoyl-4-*O*-*tert*-butyldiphenylsilyl-3,6-dideoxy-L-*arabino*-hexopyranosyl)oxy]-1-butene (148).

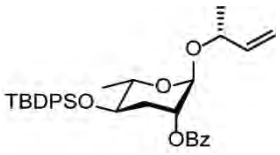

A solution of **151** (304 mg, 0.56 mmol) in ethyl acetate (4 ml) was added to a mixture of Lindlar's catalyst (300 mg) and quinoline (300 µl) in ethyl acetate (4 ml). $H_{2(g)}$ (1 atm) was added to the mixture while stirring vigorously. After stirring for 24 h, the mixture was filtered over a silica plug and the catalyst washed with ethyl acetate (2 x 2 ml). The filtrate was concentrated under reduced pressure and the residue poured into a 10% hydrochloric acid solution (100 µl). The aqueous phase was extracted with dichloromethane, dried over Na_2SO_4 and concentrated under reduced pressure. The resulting residue was purified by column flash chromatography on silica gel using 10% ethyl acetate in hexane *(v/v)* as eluent to afford **148** (301 mg, 0.55 mmol, 98% yield).

^{1}H NMR (400 MHz, $CDCl_3$): δ (ppm) 7.73 (*dd*, *J* = 8.3 Hz, *J* = 1.3 Hz, 2H), 7.66 (*m*, 4H), 7.55 (*tt*, *J* = 7.2 Hz, *J* = 1.4 Hz 1H), 7.38 (*dd*, *J* = 7.7 Hz, *J* = 7.2 Hz, 2H), 7.31 (*m*, 6H), 5.94 (*ddd*, *J* = 17.1 Hz, *J* = 10.5 Hz, *J* = 6.2 Hz, 1 H), 5.25 (*dd*, *J* = 17.3, *J* = 1.4 Hz, 1H), 5.13 (*dd*, *J* = 10.5, *J* = 1.4 Hz, 1H), 4.92 (*dd*, *J* = 3.9 Hz, *J* = 3.0 Hz, 1 H), 4.78 (*s*, 1 H), 4.24 (*dq*, *J* = 6.4 Hz, *J* = 6.2 Hz, 1 H), 3.90 (*dq*, *J* = 9.2, *J* = 6.2 Hz, 1 H), 3.66 (*ddd*, *J* = 11.2 Hz, *J* = 9.2 Hz, *J* = 4.3 Hz, 1 H), 2.07 (*ddd*, *J* = 14.0, *J* = 11.2, *J* = 3.0 Hz, 1 H), 1.88 (*ddd*, *J* = 14 Hz, *J* = 3.9 Hz, 3 Hz, 1 H), 1.26 (*d*, *J* = 6.4 Hz, 3 H), 1.24 (*d*, *J* = 6.3 Hz, 3 H), 1.05 (*s*, 9 H), **^{13}C NMR**(100 MHz, $CDCl_3$): δ (ppm) 165.5, 140.4, 136.1, 136.0, 133.1, 129.9, 128.3, 127.5, 127.6, 114.7, 94.5, 73.9, 71.8, 70.5, 69.9, 33.4, 27.2, 20.0, 19.5, 18.3, **HRMS** (ESI-TOF) m/z $(M + NH_4)^+$ calcd for $C_{33}H_{44}NO_5Si$ 562.2989, found 562.2991, ∆ppm 0.4.

(3*R*)-3-[(4-*O*-*tert*-butyldiphenylsilyl-3,6-dideoxy-L-*arabino*-hexopyranosyl)oxy]-1-butene (150).

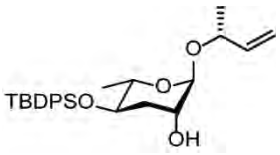

A solution of **148** (147 mg, 0.27 mmol) in 1,4-dioxane (7 ml) was treated with a solution of lithium hydroxide monohydrate (23 g, 0.54 mmol) in water (1.5 ml). The mixture was heated to 60 °C. After stirring for 24 h, the mixture was cooled to room temperature, glacial acetic acid (300 µl) was added and the mixture was concentrated under reduced pressure. The resulting mixture was purified by flash column chromatography on silica gel using 10% ethyl acetate in hexane *(v/v)* as eluent to afford **150** (101 mg, 0.23 mmol, 85% yield).

^{1}H NMR (400 MHz, $CDCl_3$): δ (ppm) 7.67 (*m*, 4H), 7.39 (m, 6 H), 5.92 (*ddd*, *J* = 17.2 Hz, *J* = 10.5 Hz, *J* = 6.0 Hz, 1H), 5.24 (*dd*, *J* = 17.2 Hz, *J* = 1.5 Hz 1 H), 5.12 (*dd*, *J* = 10.5 Hz, *J* = 1.5 Hz, 1 H) 4.62 (s, 1H), 4.23 (*dq*, *J* = 6.3 Hz, *J* = 6.0 Hz, 1 H), 3.81 (*dq*, *J* = 9.0 Hz, *J* = 6.3 Hz, 1H), 3.66 (*dd*, *J* = 3.8 Hz, *J* = 3.0 Hz, 1H), 3.64 (*ddd*, *J* = 10.7 Hz, *J* = 9.1 Hz, *J* = 4.2 Hz, 1 H), 1.88 (*ddd*, *J* = 13.7 Hz, *J* = 10.8 Hz, *J* = 3.1 Hz, 1H), 1.78 (*ddd*, *J* = 13.4 Hz, *J* = 4.2 Hz, *J* = 3.8 Hz, 1H), 1.22 (*d*, *J* = 6.3 Hz, 3H), 1.15 (*d*, *J* = 6.2 Hz, 3H), 1.05 (*s*, 9H), **^{13}C NMR**(100 MHz, $CDCl_3$) δ (ppm) 140.4, 136.1, 133.9, 130.3, 129.9, 129.8, 128.6, 127.8, 127.6, 114.5, 97.1, 73.3, 70.1, 70.1, 69.3, 35.8, 27.1, 20.6, 19.8, 19.5, 18.2, **HRMS** (ESI-TOF) m/z $(M + NH_4)^+$ calcd for $C_{26}H_{40}NO_4Si$ 458.2727, found 458.2731, Δppm 0.9.

(*3R*)-3-[(2-*O*-benzyl-4-*O*-*tert*-butyldiphenylsilyl-3,6-dideoxy-L-*arabino*-hexopyranosyl)oxy]-1-butene (152).

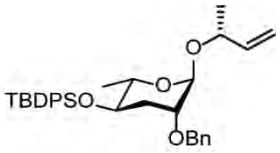

A solution of **150** (85.7 mg, 0.19 mmol) in dry dimethylformamide (3.7 ml) was treated with benzyl bromide (68.4 µl, 0.57 mmol) followed by sodium hydride (29.6 mg, 1.24 mmol). After stirring the solution for 14 h at room temperature, 1 M hydrochloric solution (1.5 ml) was added to the mixture and the aqueous phase was extracted with ethyl acetate (2 x 5 ml). The combined organic phases were dried over Na_2SO_4 and concentrated under reduced pressure. The resulting residue was purified by flash column chromatography on silica gel using 20% ethyl acetate in hexane *(v/v)* as eluent to afford **152** (97.8 mg, 0.18 mmol, 95% yield) as a colorless oil.

^{1}H NMR (400 MHz, $CDCl_3$): δ (ppm) 7.76-7.66 (*m*, 4H), 7.40-7.34 (*m*, 11H), 5.92 (*ddd*, *J* = 17.3, *J* = 10.5, *J* = 5.8 Hz, 1H), 5.22 (*ddd*, *J* = 17.3 Hz, *J* = 1.5 Hz, *J* = 1.5 Hz, 1H), 5.10 (*ddd*, *J* = 10.5, *J* = 1.5 Hz, *J* = 1.5 Hz, 1H), 4.69 (*br.s*, 1H), 4.24 (*qd*, *J* = 6.4 Hz, *J* = 5.8 Hz, 1H), 4.17 (*d*, *J* = 12.2 Hz, 1H), 4.09 (*d*, *J* = 12.2 Hz, 1H), 3.77 (*ddd*, *J* = 10.5 Hz, *J* = 9.2 Hz, *J* = 4.8 Hz, 1H), 3.80 (*dq*, *J* = 9.2 Hz, *J* = 6.1 Hz, 1H), 3.36 (*dd*, *J* = 3.8 Hz, *J* = 3.1 Hz, 1H), 1.84 (*ddd*, *J* = 13.5 Hz, *J* = 4.8 Hz, *J* = 3.8 Hz, 1H), 1.74 (*ddd*, *J* = 13.5, *J* = 10.5, *J* = 3.1 Hz, 1H), 1.24 (*d*, *J* = 6.1 Hz, 3H), 1.19 (*d*, *J* = 6.4 Hz, 3H), 1.06 (*s*, 9H), **^{13}C NMR**(150 MHz, $CDCl_3$): δ (ppm) 140.5, 136.1, 136.0, 128.6, 127.9, 114.3, 95.4, 75.4, 72.5, 70.3, 70.2, 70.1, 32.3, 27.1, 19.5, 18.3, **HRMS** (ESI-TOF) m/z $(M + NH_4)^+$ calcd for $C_{33}H_{46}NO_4Si$ 548.3196, found 548.3202, Δppm 1.1.

(3*R*)-3-[(2-*O*-benzoyl-3,6-dideoxy-L-*arabino*-hexopyranosyl)oxy]-1-butene (149).

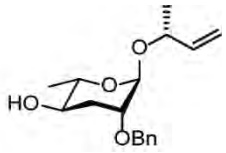

A solution of **152** (97.8 mg, 0.18 mmol) in tetrahydrofuran (5 ml) was treated with a 1 M solution of tetrabutylammonium fluoride in tetrahydrofuran (0.54 ml, 0.54 mmol). After stirring overnight at room temperature, water (1 ml) was added to the mixture and the aqueous phase was extracted with dichloromethane (2 x 5 ml). The combined organic phase was washed with Na_2SO_4 and concentrated under reduced pressure. The resulting residue was purified by flash column chromatography on silica gel using 20% ethyl acetate in hexane *(v/v)* as eluent to afford **149** (32.7 mg, 62%) as a colorless oil.

^{1}H NMR (400 MHz, $CDCl_3$): δ (ppm) 7.37-726 (*m*, 5 H), 5.87 (*ddd*, *J* = 17.2 Hz, *J* = 10.5 Hz, 6.0 Hz, 1H), 5.20 (*ddd*, *J* = 17.3 Hz, *J* = 1.5 Hz, *J* = 1.5 Hz, 1H), 5.07 (*ddd*, *J* = 10.5 Hz, *J* = 1.5 Hz, *J* = 1.5 Hz, 1H), 4.82 (*br.s*, 1H), 4.59 (*s*, 2H), 4.25 (*qd*, *J* = 6.4 Hz, *J* = 6.0 Hz, 1 H), 3.65 (*ddd*, *J* = 10.5 Hz, *J* = 9.5 Hz, *J* = 4.3 Hz, 1H), 3.64 (*dq*, *J* = 9.5 Hz, *J* = 5.9 Hz, 1H), 3.58 (*ddd*, *J* = 3.8 Hz, *J* = 3.2 Hz, *J* = 1.7 Hz, 1 H), 2.14 (*ddd*, *J* = 13.2 Hz, *J* = 4.3 Hz, *J* = 3.7 Hz, 1 H), 1.77 (*ddd*, *J* = 13.2 Hz, *J* = 10.5 Hz, *J* = 3.1 Hz, 1 H), 1.26 (*d*, *J* = 5.9 Hz, 3H), 1.20 (*d*, *J* = 6.4 Hz, 3H), **^{13}C NMR**(100 MHz, $CDCl_3$): δ (ppm) 140.4, 138.4, 128.5, 127.8, 127.8, 114.4, 94.9, 75.9, 72.7, 71.3, 69.9, 68.6,32.9, 19.7, 17.7, **HRMS** (ESI-TOF) m/z $(M + Na)^+$ calcd for $C_{17}H_{24}NaO_4$ 315.1572, found 315.1567, Δppm -1.6.

Benzyl-(4*R*)-4-[(2-*O*-benzyl-3,6-dideoxy-L-*arabino*-hexopyranosyl)oxy]-2-pentenoate (153).

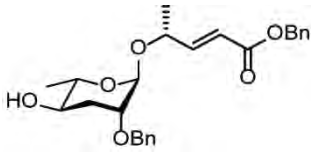

A solution of **149** (32.7 mg, 0.11 mmol) and benzyl acrylate (59 µl, 0.55 mmol) in dry dichloromethane (5 ml) was treated with Grubb's 2nd generation catalyst (8.8 mg, 0.01 mmol). The solution was refluxed overnight then cooled to room temperature and concentrated under reduced pressure. The given residue was purified by flash column chromatography on silica gel using 35% ethyl acetate in hexane *(v/v)* as eluent to afford **153** (30.5 mg, 65%) as a brown oil.

^{1}H NMR (400 MHz, $CDCl_3$): δ (ppm) 7.41-7.27 (*m*, 10H), 6.97 (*dd*, *J* = 15.7 Hz, *J* = 5.3 Hz, 1H), 6.04 (*dd*, *J* = 15.7 Hz, *J* = 1.7 Hz, 1H), 5.20 (*d*, *J* =11.8 Hz, 1H), 5.19 (*d*, *J* = 11.8 Hz, 1H) 4.82 (*s*, 1H), 4.61 (*d*, *J* = 12.1 Hz, 1H), 4.57 (*d*, *J* = 12.0 Hz, 1H), 4.43 (*dq*, *J* = 6.5 Hz, *J* = 5.3 Hz, 1H), 3.64 (*ddd*, *J* = 11.0 Hz, *J* = 9.5 Hz, 4.5 Hz, 1H), 3.59 (*ddt*, *J* = 3.9 Hz, *J* = 3.0 Hz, *J* = 1.7 Hz, 1H), 3.55 (*dq*, *J* = 9.5 Hz, *J* = 6.1 Hz, 1H), 2.17 (*ddd*, *J* = 13.1 Hz, *J* = 4.5 Hz, *J* = 3.9 Hz, 1H), 1.76 (*ddd*, *J* = 13.1 Hz, *J* = 11.0 Hz, *J* = 3.0 Hz, 1H), 1.24 (*d*, *J* = 6.5 Hz, 3H), 1.23 (*d*, *J* = 6.1 Hz, 3H), **^{13}C NMR**(100 MHz, $CDCl_3$): δ (ppm) 166.4, 149.9, 128.7, 128.6,

128.5, 128.4, 127.9, 127.8, 119.8, 94.9, 75.7, 71.3, 70.5, 70.2, 68.4, 66.5, 32.9, 19.1, 17.8, **HRMS** (ESI-TOF) m/z $(M + NH_4)^+$ calcd for $C_{25}H_{34}NO_6$ 444.2386, found 444.2386, Δppm 0.

Benzyl-(2*E*, 4*R*)-4-[(2-*O*-benzyl-4-((benzyloxy)carbonyl)amino)benzoyl-3,6-dideoxy-α-L-*arabino*-hexopyranosyl)oxy]-2-pentenoate (154).

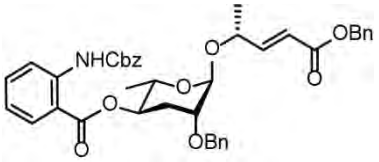

At 0 °C, a solution of **153** (30.5 mg, 72 µmol) in dichloromethane (800 µl) was treated with NCbz-anthranilic acid (39 mg, 288 µmol) and 4-dimethylaminopyridin (24 mg, 36 µmol). The mixture was stirred for 5 min then dicyclohexylcarbodiimide (59 mg, 288 µmol) in dichloromethane (500 µl) was added to the mixture. After stirring for 21 h, the mixture was diluted with dichloromethane (500 µl), filtered and water was added to the mixture. The organic phase was dried with Na_2SO_4 and concentrated under reduced pressure. The resulting residue was purified by flash column chromatography using 10% of ethyl acetate in hexane *(v/v)* as eluent to afford **154** (17 mg, 25 µmol, 35%) as a colorless oil.

^{1}HNMR (400 MHz, $CDCl_3$): δ (ppm) 8.47 (*d*, *J* = 8.5 Hz, 1 H), 7.98 (*dd*, *J* = 8.0 Hz, *J* = 1.6 Hz, 1 H), 7.54 (*ddd*, *J* = 8.0 Hz, *J* = 7.5 Hz, *J* = 1.5 Hz, 1 H), 7.48-7.27 (*m*, 15 H), 7.02 (*ddd*, *J* = 8.5 Hz, *J* = 7.5 Hz, *J* = 1.6 Hz, 1H), 7.00 (*dd*, *J* = 15.9 Hz, *J* = 5.4 Hz, 1H), 6.06 (*dd*, *J* = 15.9, *J* = 1.6 Hz, 1 H), 5.23 (*s*, 2 H), 5.21 (*s*, 2 H), 5.07 (*ddd*, *J* = 10.4 Hz, *J* = 9.5 Hz, *J* = 4.4 Hz, 1 H), 4.85 (*br.s*, 1 H), 4.71 (*d*, *J* = 12.1 Hz, 1 H), 4.59 (*d*, *J* = 12.1 Hz, 1 H), 4.44 (*qd*, *J* = 6.4 Hz, *J* = 5.4 Hz, 1 H), 3.92 (*dq*, *J* = 9.5 Hz, *J* = 6.2 Hz, 1H), 3.62 (*dd*, *J* = 3.7 Hz, *J* = 3.0 Hz, 1 H), 2.38 (*ddd*, *J* = 13.2, *J* = 10.4 Hz, *J* = 3.0 Hz, 1 H), 1.90 (*ddd*, *J* = 13.0, *J* = 4.4 Hz, *J* = 3.7 Hz, 1 H), 1.26 (*d*, *J* = 6.4 Hz, 3 H), 1.18 (*d*, *J* = 6.2 Hz, 3 H), **^{13}CNMR** (100 MHz, $CDCl_3$): δ (ppm) 167.1, 166.3, 153.5, 149.6, 142.0, 137.9, 136.2, 134.7, 130.9, 128.61, 128.57, 128.5, 128.32, 128.26, 127.84, 127.79, 121.6, 119.9, 118.9, 114.6, 95.4, 74.8, 71.4, 71.2, 71.0, 67.2, 67.0, 66.4, 29.3, 19.1, 17.7. **HRMS** (ESI-TOF) m/z $(M + Na)^+$ calcd for $C_{40}H_{41}NO_9Na$ 702.2700 found 702.2679, Δppm 3.0.

(4*R*)-4-[(4-*O*-(2-amino-benzoyl)-3,6-dideoxy-α-L-*arabino*-hexopyranosyl)oxy]-2-pentanoic acid (34).

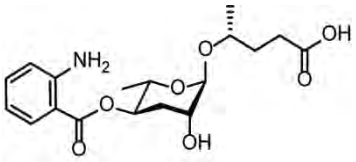

Under N_2 atmosphere, **154** (17 mg, 25 µmol) in methanol (1.5 ml) and ethyl acetate (250 µl) was treated with a suspension 10% palladium on charcoal (25.5 mg) in methanol (2 ml). N_2 was flushed with H_2 (1 atm) and the mixture was stirred at room temperature under H_2 atmosphere. After stirring

for 3 h the mixture was filtered, the catalyst washed with methanol. The filtrate was concentrated under reduced pressure and the given residue purified by semi preparative HPLC. Separation was achieved using gradient elution with 15 to 60% *(v/v)* acetonitrile in water with 0.05% trifluoroacetic acid *(v/v)* over 50 min then 60 to 100% over 20 min at a flow rate of 8 ml/min to afford **34** (3.8 mg, 10.3 µmol, 41%) along with **147** (2 mg, 5 µmol, 21%).

^{1}HNMR (400 MHz, CD_3OD): δ (ppm) 7.77 (*dd*, *J* = 8.2 Hz, *J* = 1.8 Hz, 1H), 7.23 (*ddd*, *J* = 8.4 Hz, *J* = 7.1 Hz, *J* = 1.8 Hz, 1H), 6.74 (*dd*, *J* = 8.4 Hz, *J* = 1.2 Hz, 1H), 6.57 (*ddd*, *J* = 8.2 Hz, *J* = 7.1 Hz, *J* = 1.2 Hz, 1H), 5.07 (*ddd*, *J* = 11.1 Hz, *J* = 9.7 Hz, *J* = 4.8 Hz, 1H), 4.74 (*br.s*, 1 H), 4.00 (*dq*, *J* = 9.7 Hz, *J* = 6.4 Hz, 1H), 3.90 (*m*, 1H), 3.78 (*dd*, *J* = 3.9 Hz *J* =, 3.1 Hz, 1H), 2.55-2.39 (*m*, 1H), 2.17 (*ddd*, *J* = 13.5 Hz, *J* = 4.8 Hz, *J* = 3.9 Hz, 1H), 1.97 (*ddd*, *J* = 13.5 Hz, *J* = 11.1 Hz, *J* = 3.2 Hz, 1H), 1.93-1.77 (*m*, 1H), 1.18 (*d*, *J* = 6.1 Hz, 3H), 1.19 (*d*, *J* = 6.4 Hz, 3H), **^{13}CNMR** (100 MHz, CD_3OD): δ (ppm) 177.5, 168.6, 152.9, 132.0, 111.2, 97.5, 71.7, 71.0, 69.5, 68.7, 33.4, 33.2, 19.0, 18.1 (**Table S 3**) , **HRMS** (ESI-TOF) m/z $(M + H)^+$ calcd for $C_{18}H_{26}NO_7$ 368.1709, found 368.1711, Δppm 0.2, $(M - H)^-$ calcd for $C_{18}H_{24}NO_7$ 366.1553, found 366.1555, Δppm 0.5.

8.10.4. Synthesis of cae-7OH-ΔC9 (caen#1, 39)

(*7R,8R,2E*)-*threo*-8-[(3',6'-dideoxy-α-L-*lyxo*-hexopyranosyl)oxy]-7-hydroxy-2- nonenoic acid (39).

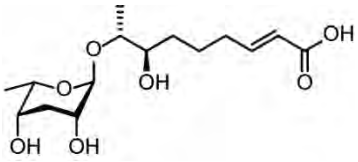

A solution of **181** (7.7 mg, 11.7 µmol) in 1,4-dioxane (1 ml) was treated with a solution of lithium hydroxide monohydrate (9.2 mg, 230 µmol) in water (0.1 ml). After stirring at 60 °C for 7 h, the mixture was cooled to room temperature, treated with glacial acetic acid (40 µl), and concentrated under reduced pressure. The product was purified using semi preparative HPLC. Separation was achieved using gradient elution with 15 to 100% *(v/v)* acetonitrile in water with 0.05% trifluoroacetic acid *(v/v)* over 60 minutes at a flow rate of 8 ml/min to afford **39** (1.7 mg, 5.3 µmol, 45% yield) as a colorless oil showing LC-MS and NMR data identical to the natural product isolated from *C. nigoni.*

^{1}HNMR (400 MHz, CD_3OD): δ (ppm) 6.91 (*dt*, *J* = 15.6 Hz, *J* = 7.0 Hz, 1H), 5.82 (*dt*, *J* = 15.6 Hz, *J* = 1.5 Hz, 1H), 4.78 (*s*, 1H), 3.99 (*qd*, *J* = 6.6 Hz, *J* = 1.0 Hz, 1H), 3.75 (*dq*, *J* = 4.1 Hz, *J* = 6.3 Hz, 1H), 3.58 (*br.s*, 1H), 3.57 (*br.s*, 1H), 3.52 (*m*, 1H), 2.26 (*m*, 1H), 2.06 (*dt*, *J* = 14.3 Hz, *J* = 3.1 Hz, 1H), 1.93 (*ddt*, *J* = 14.3 Hz, *J* = 1.0 Hz, *J* = 3.4 Hz, 1H), 1.70 (*m*, 1H), 1.62 – 1.45 (*m*, 3H), 1.18 (*d*, *J* = 6.6 Hz, 3H), 1.15 (*d*, *J* = 6.3 Hz, 3H), **^{13}C NMR**(100 MHz, CD_3OD): δ (ppm) 170.8, 150.0, 123.7, 98.7, 75.7, 75.0, 69.1, 68.5, 68.2, 33.02, 32.97, 32.3, 25.8, 17.2, 14.8 (**Table S 4**), **HRMS** (ESI-TOF) m/z $(M - H)^-$ calcd for $C_{15}H_{25}O_7$ 317.1606, found 317.1601, m/z $(M_2 - H)^-$ calcd for $C_{30}H_{51}O_{14}$ 635.3284, found 635.3279.

8.11. Synthesis of oligomeric ascr-C5

Benzyl-(4*R*)-4-[4-*O*-*tert*-butyldiphenylsilyl-3,6-dideoxy-α-L-*arabino*-hexopyranosyl)oxy]-2-pentenoate (204).

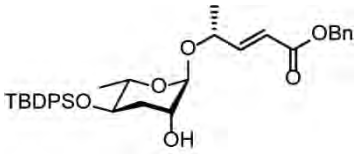

A solution of **150** (200 mg, 0.45 mmol) and benzyl acrylate (0.53 ml, 2.25 mmol) in dry dichloromethane (20 ml) was treated with Grubb's 2nd generation catalyst (36 mg, 0.04 mmol). After refluxing for 16 h, the mixture was cooled to room temperature and concentrated under reduced pressure. The given residue was purified by flash column chromatography on silica gel using 35% ethyl acetate in hexane *(v/v)* as eluent to afford **204** (118.6 mg, 0.28 mmol, 62%) as a brown oil.

^{1}H NMR (600 MHz, $CDCl_3$): δ (ppm) 7.69-7.672 (*m*, 2H), 7.667-7.64 (*m*, 2H),7.43 (*tt*, *J* = 7.4 Hz, *J* = 1.4 Hz, 1H), 7.42-7.32 (*m*, 10H), 7.01 (*dd*, *J* = 15.7 Hz, *J* = 5.1 Hz, 1H), 6.09 (*dd*, *J* = 15.7 Hz, *J* = 1.5 Hz, 1H), 5.23 (*d*, *J* = 12.4 Hz, 1H), 5.21 (*d*, *J* = 12.4 Hz, 1H), 4.62 (*br.s*, 1H), 4.41 (*qdd*, *J* = 6.5 Hz, *J* = 5.1 Hz, *J* = 1.5 Hz, 1H), 3.71 (*dq*, *J* = 9.1 Hz, *J* = 6.2 Hz, 1H), 3.67 (*dd*, *J* = 3.5 Hz, *J* = 3.1 Hz, 1H), 3.63 (*ddd*, *J* = 11.0 Hz, *J* = 9.1 Hz, *J* = 4.7 Hz, 1H), 1.86 (*ddd*, *J* = 13.6 Hz, *J* = 11.0 Hz, *J* = 3.1 Hz, 1H), 1.77 (*ddd*, *J* = 13.6 Hz, *J* = 4.7 Hz, *J* = 3.5 Hz, 1H), 1.26 (*d*, *J* = 6.5 Hz, 3H), 1.13 (*d*, *J* = 6.2 Hz, 3H), **^{13}C NMR**(150 MHz, $CDCl_3$): δ (ppm) 166.5, 149.9, 136.1, 134.4, 133.7, 130.0, 129.8, 128.8, 128.49, 128.45, 127.8, 127.7, 119.8, 96.8, 70.7, 70.4, 69.8, 69.1, 66.5, 35.8, 27.1, 19.4, 19.2, 18.2.

(5*R*)-5-[(3,6-dideoxy-α-L-*arabino*-hexopyranosyl)oxy]-1-hexene (201).

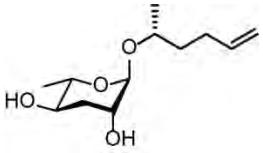

A solution of **200** (124 mg, 0.28 mmol) in 1,4-dioxane (7 ml) was treated with a solution of lithium hydroxide monohydrate (48 mg, 1.12 mmol) in water (1.5 ml). The mixture was heated to 60 °C. After stirring for 16 h, the mixture was cooled to room temperature, glacial acetic acid (400 µl) was added and the mixture was concentrated under reduced pressure. The resulting mixture was purified by flash column chromatography on silica gel using 10% ethyl acetate in hexane *(v/v)* as eluent to afford **201** (62.4 mg, 0.27 mmol, 96% yield) as a colorless oil.

^{1}H NMR (600 MHz, $CDCl_3$): δ (ppm) 5.82 (*ddt*, *J* = 16.8 Hz, *J* = 10.2 Hz, *J* = 6.6 Hz, 1H), 5.03 (*ddt*, *J* = 16.8 Hz, *J* = 1.8 Hz, *J* = 1.6 Hz, 1H), 4.97 (*ddt*, *J* = 10.2 Hz, *J* = 1.8 Hz, *J* = 1.3 Hz, 1H), 4.71 (*br.s*, 1H), 3.82 (*dqd*, *J* = 7.0 Hz, *J* = 6.1 Hz, *J* = 5.6 Hz, 1H), 3.81 (*dd*, *J* = 3.7 Hz, *J* = 3.0 Hz, 1H), 3.69 (*dq*, *J* = 9.3 Hz, *J* = 6.3 Hz,

1H), 3.59 (*ddd*, *J* = 11.1 Hz, *J* = 9.3 Hz, *J* = 4.8 Hz, 1H), 2.19 (*m*, 1H), 2.11 (*m*, 1H), 2.07 (*ddd*, *J* = 13.7 Hz, *J* = 4.8 Hz, *J* = 3.7 Hz, 1H), 1.84 (*ddd*, *J* = 13.7 Hz, *J* = 11.1 Hz, *J* = 3.0 Hz, 1H), 1.67 (*m*, 1H), 1.55 (*m*, 1H), 1.27 (*d*, *J* = 6.3 Hz, 3H), 1.14 (*d*, *J* = 6.1 Hz, 3H), **^{13}CNMR** (150 MHz, $CDCl_3$): δ (ppm) 138.8, 138.5, 114.8, 114.6, 105.4, 96.1, 81.7, 74.1, 71.1, 70.7, 70.0, 69.4, 68.3, 67.6, 36.6, 36.5, 35.3, 30.9, 30.2, 30.1, 19.5, 19.4, 19.0, 17.8.

(5*R*)-5-[(2,4-di-*O*-*tert*-butyldimethylsilyl-3,6-dideoxy-α-L-*arabino*-hexopyranosyl)oxy]-1-hexene (202).

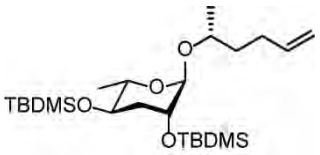

At 0 °C, a solution of **201** (60 mg, 0.26 mmol) in dichloromethane (6 ml) was treated with imidazole (390 mg, 2.6 mmol) followed by *tert*-butyldimethylsilyl chloride (83 mg, 1.3 mmol). After stirring for 48 h at room temperature the mixture was quenched with water (1 ml), dried over Na_2SO_4 and concentrated under reduced pressure. The resulting residue was purified by flash column chromatography using 10% ethyl acetate in hexane *(v/v)* as eluent to afford **202** (90.7 mg, 0.20 mmol, 76%) as a colorless oil.

^{1}H NMR (600 MHz, $CDCl_3$): δ (ppm) 5.83 (*ddt*, *J* = 17.2 Hz, *J* = 10.2 Hz, *J* = 6.6 Hz, 1H), 5.03 (*ddt*, *J* = 17.2 Hz, *J* = 1.8 Hz, *J* = 1.8 Hz, 1H), 4.96 (*ddt*, *J* = 10.2 Hz, *J* = 1.8 Hz, *J* = 1.3 Hz, 1H), 4.55 (*br.s*, 1H), 3.78 (*m*, 1H), 3.77 (*dd*, *J* = 3.7 Hz, *J* = 2.9 Hz, 1H), 3.65 (*ddd*, *J* = 10.4 Hz, *J* = 9.3 Hz, *J* = 5.0 Hz, 1H), 3.60 (*dq*, *J* = 9.3 Hz, *J* = 6.1 Hz, 1H), 2.18 (m, 1H9, 2.11 (*m*, 1H), 1.78 (*ddd*, *J* = 12.9 Hz, *J* = 5.0 Hz, *J* = 3.7 Hz, 1H), 1.77 (*ddd*, *J* = 12.9 Hz, *J* = 10.4 Hz, *J* = 2.9 Hz, 1H), 1.18 (*d*, *J* = 6.1 Hz, 3H), 1.10 (*d*, *J* = 6.1 Hz, 3H), 0.89 (*s*, 9H), 0.88 (*s*, 9H), 0.08-0.03 (*m*, 12H), **^{13}CNMR** (150 MHz, $CDCl_3$): δ (ppm) 138.7, 114.7, 96.6, 70.5, 70.3, 70.2, 68.9, 37.1, 36.6, 30.2, 26.0, 25.9, 19.1, 18.3, 18.20, 18.15, -4.1, -4.5, -4.7, -4.8. **HRMS** (ESI-TOF) m/z $(M + Na)^+$ calcd for $C_{24}H_{50}O_4NaSi_2$ 481.3145 found 481.3164, Δ 3.9 ppm.

(4*R*)-4-[(2,4-di-*O*-*tert*-butyldimethylsilyl-3,6-dideoxy-α-L-*arabino*-hexopyranosyl)oxy]-1-pentanoic acid (203).

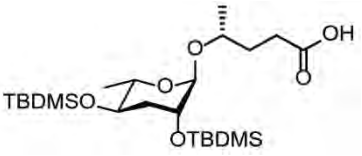

A vigorously stirred solution of **202** (90 mg, 0.2 mmol) in dichloromethane (2 ml), acetonitrile (2 ml) and water (1.5 ml) was treated with ruthenium (III) chloride hydrate (22 mg, 20 μmol) in water (0.5 ml) followed by sodium periodate (207 mg). After stirring for 22 h, water (1ml) was added to the

mixture and the organic phase was extracted with dichloromethane (3 x 2 ml). The organic phase was dried with Na_2SO_4 and concentrated under reduced pressure. The resulting residue was purified by flash column chromatography on silica gel using 35% ethyl acetate in hexane *(v/v)* as eluent to afford **203** (70 mg, 0.15 mmol, 75% yield) as a colorless oil.

^{1}H NMR (600 MHz, $CDCl_3$): δ (ppm) 4.54 (*br.s*, 1H), 3.82 (*m*, 1H), 3.75 (*dd*, *J* = 3.4 Hz, *J* = 2.7 Hz, 1H), 3.64 (*ddd*, *J* = 10.4 Hz, *J* = 9.1 Hz, *J* = 4.4 Hz, 1H), 3.55 (*dq*, *J* = 9.1 Hz, *J* = 6.2 Hz, 1H), 2.51 (*ddd*, *J* = 16.5 Hz, *J* = 8.6 Hz, *J* = 6.4 Hz, 1H), 2.43 (*ddd*, *J* = 16.5 Hz, *J* = 8.6 Hz, *J* = 6.9 Hz, 1H), 1.85-1.77 (*m*, 2H), 1.79 (*ddd*, *J* = 13.1 Hz, *J* = 4.4 Hz, *J* = 3.4 Hz, 1H), 1.74 (*ddd*, *J* = 13.1 Hz, *J* = 10.4 Hz, *J* = 2.7 Hz, 1H), 1.18 (*d*, *J* = 6.2 Hz, 3H), 1.12 (*d*, *J* = 6.1 Hz, 3H), 0.89 (*s*, 9H), 0.88 (*s*, 9H), 0.07-0.02 (*m*, 12H),**^{13}CNMR** (150 MHz, $CDCl_3$): δ (ppm) 179.8, 96.6, 70.6, 70.04, 70.00, 68.8, 37.1, 32.0, 30.5, 26.0, 25.9, 18.9, 18.2, 18.18, 18.1, -4.1, -4.5, -4.76, -4.81. NMR identical to data reported in literature[12b].

(3*R*)-3-[(2-*O*-benzoyl-4-*O*-benzyl-3,6-dideoxy-L-*arabino*-hexopyranosyl)oxy]-1-butene (212).

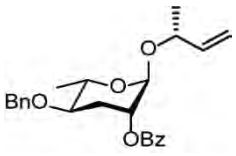

A solution of **211** (31 mg, 79 µmol) in ethyl acetate (1 ml) was added to a mixture of Lindlar's catalyst (30 mg) and quinoline (30 µl) in ethyl acetate (1 ml). $H_{2(g)}$ (1 atm) was added to the mixture while stirring vigorously. After stirring for 14 h, the mixture was filtered over silica plug and the catalyst washed with ethyl acetate (1 ml). The filtrate was concentrated under reduced pressure and the residue poured into a 10% hydrochloric acid solution (100 µl). The aqueous phase was extracted with dichloromethane, dried with Na_2SO_4 and concentrated under reduced pressure. The resulting residue was purified by column flash chromatography on silica gel using 10% ethyl acetate in hexane *(v/v)* as eluent to afford **212** (30 mg, 76 µmol, 96 % yield).

^{1}H NMR (600 MHz, $CDCl_3$): δ (ppm) 8.02 (*dd*, *J* = 8.4 Hz, 1.4 Hz, 2H), 7.59 (*tt*, *J* = 7.5 Hz, *J* = 1.4 Hz, 1H), 7.45 (*dd*, *J* = 8.4 Hz, *J* = 7.5 Hz, 2H), 7.34-7.29 (*m*, 5H), 5.89 (*ddd*, *J* = 17.7 Hz, *J* = 10.5 Hz, *J* = 6.2 Hz, 1H), 5.23 (*ddd*, *J* = 17.7 Hz, *J* = 1.4 Hz, *J* = 1.2 Hz, 1H), 5.15 (*ddd*, *J* = 3.1 Hz, *J* = 2.4 Hz, 1.6 Hz, 1H), 5.08 (*ddd*, *J* = 10.5 Hz, *J* = 1.4 Hz, *J* = 1.2 Hz, 1H), 4.90 (*br.s*, 1H), 4.63 (*d*, *J* = 11.4 Hz, 1H), 4.49 (*d*, *J* = 11.4 Hz, 1H), 4.27 (*qddd*, *J* = 6.4 Hz, *J* = 6.2 Hz, *J* = 1.2 Hz, 1.2 Hz, 1H), 3.91 (*dq*, *J* = 9.3 Hz, *J* = 6.3 Hz, 1H), 3.47 (*ddd*, *J* = 11.2 Hz, *J* = 9.3 Hz, *J* = 4.8 Hz, 1H), 2.34 (*ddd*, *J* = 13.6 Hz, *J* = 4.8 Hz, *J* = 2.4 Hz, 1H), 2.04 (*ddd*, *J* = 13.6 Hz, *J* = 11.2 Hz, *J* = 3.1 Hz, 1H), 1.30 (*d*, *J* = 6.3 Hz, 3H), 1.26 (*d*, *J* = 6.4 Hz, 3H), **^{13}CNMR** (150 MHz, $CDCl_3$): δ (ppm) 165.8, 140.2, 138.2, 133.3, 129.9, 128.5, 128.1, 127.9, 114.7, 94.4, 75.3, 73.7, 71.6, 71.3, 68.3, 29.6, 19.9, 18.1, **HRMS** (ESI-TOF) m/z (M + Na)$^+$ calcd for $C_{24}H_{28}O_5Na$ 419.1834, found 419.1838, Δ 1 ppm.

(3*R*)-3-[(4-*O*-benzyl-3,6-dideoxy-L-*arabino*-hexopyranosyl)oxy]-1-butene (213).

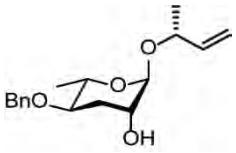

A solution of **212** (59 mg, 0.15 mmol) in 1,4-dioxane (3.7 ml), was treated with lithium hydroxide monohydrate (12.7 mg, 0.30 mmol) in water (0.78 ml). After stirring for 11 h at 60 °C, the solution was cooled to room temperature, quenched with acetic acid (100 µl) and concentrated under reduced pressure. The resulting residue was purified by flash column chromatography using 20% ethyl acetate in hexane *(v/v)* as eluent to afford **213** (39 mg, 0.13 mmol, 87% yield).

^{1}H NMR (600 MHz, $CDCl_3$): δ (ppm) 7.36 – 7.27 (m, 5H), 5.88 (*ddd*, *J* = 17.2 Hz, *J* = 10.4 Hz, *J* = 6.1 Hz, 1H), 5.21 (*ddd*, *J* = 17.2 Hz, *J* = 1.6 Hz, *J* = 1.5 Hz, 1H), 5.07 (*ddd*, *J* = 10.4 Hz, *J* = 1.6 Hz, *J* = 1.3 Hz, 1H), 4.72 (*br.s*, 1H), 4.61 (d, *J* = 11.5 Hz, 1H), 4.47 (*d*, *J* = 11.5 Hz, 1H), 4.25 (*qd*, *J* = 6.4 Hz, *J* = 6.1 Hz, 1), 3.86 (*ddd*, *J* = 3.1 Hz , *J* = 2.9 Hz, *J* = 1.6 Hz, 1H), 3.83 (*dq*, *J* = 9.1 Hz, *J* = 6.3 Hz, 1H), 3.39 (*ddd*, *J* = 11.6 Hz, *J* = 9.1 Hz, 5.0 Hz, 1H), 2.21 (*ddd*, *J* = 13.1 Hz, *J* = 5.0 Hz, *J* = 3.1 Hz, 1H), 1.87 (*ddd*, *J* = 13.1 Hz, *J* = 11.6 Hz, *J* = 2.9 Hz, 1H), 1.25 (*d*, *J* = 6.3 Hz, 3H), 1.23 (*d*, *J* = 6.4 Hz, 3H), **^{13}CNMR** (150 MHz, $CDCl_3$): δ (ppm) 140.2, 138.4, 128.5, 127.9, 127.8, 114.6, 97.0, 75.3, 73.2, 71.2, 69.1, 68.4, 31.9, 19.8, 18.0, **HRMS** (ESI-TOF) m/z $(M + Na)^+$ calcd for $C_{17}H_{24}O_4Na$ 315.1572, found 315.1559, Δ -4.1 ppm.

Benzyloxy-(4*R*)-4-[4-*O*-benzyl-3,6-dideoxy-α-L-*arabino*-hexopyranosyl)oxy]-2-pentenoate (214).

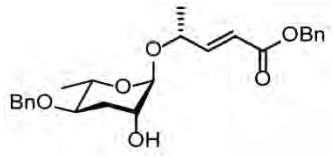

A solution of **213** (55 mg, 0.20 mmol) in dichloromethane (8 ml) was treated with benzyl acrylate (70 µl, µmol) followed by Grubb's 2nd generation catalyst (26 mg, 0.03 mmol) was added. After refluxing for 2 h, the solution was cooled to room temperature then concentrated under reduced pressure. The resulting residue was purified by flash column chromatography using 35% ethyl acetate in hexane *(v/v)* as eluent to afford **214** (44 mg, 0.10 mmol, 50 % yield).

^{1}H NMR (600 MHz, $CDCl_3$): δ (ppm) 7.40-7.27 (*m*, 10H), 6.96 (*dd*, *J* = 15.7 Hz, *J* = 5.2 Hz, 1H), 6.05 (*dd*, *J* = 15.7 Hz, *J* = 1.5 Hz, 1H), 5.20 (d, J = 12.2 Hz, 1H), 5.17 (d, J = 12.2 Hz, 1H), 4.72 (br.s, 1H), 4.61 (d, J = 11.5 HZ, 1H), 4.46 (d, J = 11.5 HZ, 1H), 4.43 (qdd, J = 6.2 Hz, J = 5.2 Hz, J = 1.5 Hz, 1H), 3.88 (ddd, J =3.1 Hz, J= 3.1 Hz, J = 1.7 Hz, 1H), 3.74 (*dq*, *J* = 9.1 Hz, *J* = 6.5 Hz, 1H), 3.39 (*ddd*, *J* = 11.1 Hz, *J* = 9.1 Hz, *J* = 4.4 Hz, 1H), 2.21 (*ddd*, *J* = 13.6 Hz, *J* = 4.4 Hz, *J* = 3.1 Hz, 1H), 1.86 (*ddd*, *J* = 13.6 Hz, *J* = 11.1 Hz, *J* = 3.1 Hz, 1H), 1.27 (*d*, *J* = 6.5 Hz, 3H), 1.23 (*d*, *J* = 6.2 Hz, 3H), **^{13}CNMR** (150 MHz, $CDCl_3$): δ (ppm) 166.4, 149.6, 138.3, 136.0, 128.7, 128.6, 128.4, 127.94, 127.89, 120.0, 96.8, 75.1, 71.3, 70.8, 68.9, 68.7, 66.5,

32.0, 19.2, 18.1, **HRMS** (ESI-TOF) m/z $(M + Na)^+$ calcd for $C_{25}H_{30}O_6Na$ 449.1940, found 449.1930, Δ -2.2 ppm.

(3*R*)-3-[(2,4-di-*O*-benzyl-3,6-dideoxy-L-*arabino*-hexopyranosyl)oxy]-1-butene (215).

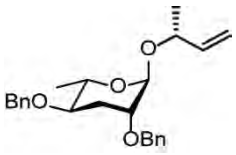

A solution of **212** (15 mg, 38 µmol) in dimethylformamide (1 ml) was treated with benzyl alcohol (12 µl, 114 µmol) and sodium hydride (6 mg, 152 µmol). After stirring for 20 min, benzyl bromide (14 µl, 152 µmol) and sodium hydride (6 mg, 152 µmol) were added to the mixture and the mixture was stirred for 24 h. Then, the solution was cooled to 0 °C, quenched with 1 M hydrochloric acid solution and extracted with ethyl acetate. The organic phase was dried with Na_2SO_4 and concentrated under reduced pressure. The resulting residue was purified by flash column chromatography using 5% ethyl acetate in hexane *(v/v)* as eluent to afford **215** (11 mg, 29 µmol, 76% yield).

^{1}H NMR (600 MHz, $CDCl_3$): δ (ppm) 7.38-7.30 (*m*, 10H), 5.85 (*ddd*, *J* = 17.0 Hz, *J* = 10.5 Hz, *J* = 5.9 Hz, 1H), 5.18 (*ddd*, *J* = 17.0 Hz, *J* = 1.4 Hz, *J* = 1.3 Hz, 1H), 5.04 (*ddd*, *J* = 10.5 Hz, *J* = 1.3 Hz, *J* = 1.3 Hz, 1H), 4.81 (*br.s*, 1H), 4.568 (*d*, *J* = 11.8 Hz, 1H), 4.566 (*s*, 1H), 4.46 (*d*, *J* = 11.8 Hz, 1H), 4.24 (*qddd*, *J* = 6.4 Hz, *J* = 5.9 Hz, *J* = 1.4 Hz, *J* = 1.3 Hz, 1H), 3.78 (*dq*, *J* = 9.2 Hz, *J* = 6.2 Hz, 1H), 3.58 (*ddd*, *J* = 3.0 Hz, *J* = 2.8 Hz, *J* = 1.6 Hz, 1H), 3.45 (*ddd*, *J* = 11.2 Hz, *J* = 9.2 Hz, *J* = 4.9 Hz, 1H), 2.22 (*ddd*, *J* = 13.7 Hz, *J* = 4.9 Hz, *J* = 2.8 Hz, 1H), 1.76 (*ddd*, *J* = 13.7 Hz, *J* = 11.2 Hz, *J* = 3.0 Hz, 1H), 1.26 (*d*, *J* = 6.2 Hz, 3H), 1.18 (*d*, *J* = 6.4 Hz, 3H), **^{13}CNMR** (150 MHz, $CDCl_3$): δ (ppm) 140.3, 138.6, 138.5, 114.4, 94.9, 75.74, 75.70, 72.5, 71.4, 71.3, 68.4. 29.6, 19.6, 18.1, **HRMS** (ESI-TOF) m/z $(M + Na)^+$ calcd for $C_{24}H_{30}O_4Na$ 405.2042, found 405.2035, Δ -1.7 ppm.

Benzyloxy-(4*R*)-4-[2,4-di-*O*-benzyl-3,6-dideoxy-α-L-*arabino*-hexopyranosyl)oxy]-2-pentenoate (216).

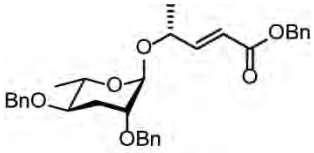

A solution of **215** (5 mg, 13 µmol) in dichloromethane (750 µl) was treated with benzyl acrylate (7 µl, 65 µmol) in dichloromethane (500 µl) followed by Grubb's 2nd generation catalyst (2 mg, 2.4 µmol). After refluxing for 20 h, the solution was cooled to room temperature then concentrated under reduced pressure. The resulting residue was purified by flash column chromatography using 10% ethyl acetate in hexane *(v/v)* as eluent to afford **216** (6 mg, 12 µmol, 92 % yield).

^{1}H NMR (600 MHz, $CDCl_3$): δ (ppm) 7.40-7.27 (*m*, 15H), 6.95 (*dd*, *J* = 15.7 Hz, *J* = 5.1 Hz, 1H), 6.02 (*dd*, *J* = 15.7 Hz, *J* = 1.7 Hz, 1H), 5.20 (*d*, *J* = 12.4 Hz, 1H), 5.16 (*d*, *J* = 12.4 Hz, 1H), 4.80 (*br.s*, 1H), 4.56 (d, *J* = 11.6 Hz, 1H), 4.55 (*s*, 2H), 4.46 (*d*, *J* = 11.6 Hz, 1H), 4.42 (*qdd*, *J* = 6.6 Hz, *J* = 5.1 Hz, *J* = 1.7 Hz, 1H), 3.69 (*dq, J* = 9.4 Hz, *J* = 6.3 Hz, 1H), 3.59 (*ddd*, *J* = 2.9 Hz, *J* = 2.8 Hz, *J* = 1.6 Hz, 1H), 3.44 (*ddd*, *J* = 11.0 Hz, *J* = 9.4 Hz, *J* = 5.4 Hz, 1H), 2.23 (*ddd*, *J* = 13.3 Hz, *J* = 5.4 Hz, *J* = 2.8 Hz, 1H), 1.75 (*ddd*, *J* = 13.3 Hz, *J* = 11.0 Hz, *J* = 2.9 Hz, 1H), 1.24 (*d*, *J* = 6.3 Hz, 3H), 1.23 (*d*, *J* = 6.6 Hz, 3H), **^{13}CNMR** (150 MHz, $CDCl_3$): δ (ppm) 166.4, 149.8, 138.5, 138.4, 136.7, 128.7, 128.54, 128.48, 128.4, 128.0, 127.9, 127.8, 119.8, 94.9, 75.6, 75.5, 71.5, 71.4, 70.3, 68.8, 66.4, 29.6, 19.1, 18.1, **HRMS** (ESI-TOF) m/z $(M + Na)^+$ calcd for $C_{32}H_{36}O_6Na$ 539.2410, found 539.2401, Δ -0.9 ppm.

4-[2,4-di-*O*-benzyl-3,6-dideoxy-α-L-*arabino*-hexopyranosyl)oxy]-2-pentanoic acid (217).

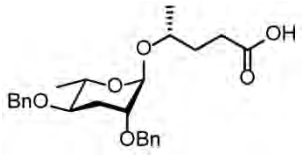

Under N_2 atmosphere, a solution of **216** (14 mg, 27 µmol) in ethanol (1 ml) was treated with palladium on carbon (10%, 10 mg) followed by 1,4-cyclohexadiene (60 µl). After stirring for 24 h the mixture was filtered through a cotton plug and the catalyst rinsed with ethanol and the filtrate concentrated under reduced pressure to give **217** (10 mg, 23 µmol, 85%).

^{1}H NMR (600 MHz, $CDCl_3$): δ (ppm) 7.36-7.26 (m, 10H), 4.77 (br. s, 1H), 4.57 (d, J = 11.6 Hz, 1H), 4.55 (d, J = 12.3 Hz, 1H), 4.53 (d, J = 12.3 Hz, 1H), 4.47 (d, J = 11.6 Hz, 1H), 3.84 (m, 1H), 3.72 (dq, J = 9.3 Hz, J = 6.2 Hz, 1H), 3.53 (ddd, J = 3.0 Hz, J = 2.9 Hz, 1.6 Hz, 1H), 3.44 (ddd, J = 11.0 Hz, J = 9.3 Hz, J = 5.0 Hz, 1H), 2.48 (m, 1H), 2.43 (m, 1H), 2.20 (ddd, J = 13.6 Hz, J = 5.0 Hz, J = 2.9 Hz, 1H), 1.84-1.74 (m, 2H), 1.71 (ddd, J = 13.6 Hz, J = 11.0 Hz, J = 3.0 Hz, 1H), 1.28 (d, J = 6.2 Hz, 3H), 1.10 (d, J = 6.1 Hz, 3H), **^{13}CNMR** (150 MHz, $CDCl_3$): δ (ppm) 178.5, 138.5, 138.4, 128.6, 128.0, 127.8, 94.2, 75.8, 75.6, 71.4, 71.3, 70.1, 68.8, 32.0, 30.3, 29.6, 18.8, 18.2 **HRMS** (ESI-TOF) m/z $(M - H)^-$ calcd for $C_{25}H_{32}O_6$ 427.2121, found 427.2122, Δ 0.2 ppm.

8.11.1. General procedure for the esterification

In a dry flask, a solution of ascaroside (1 eq) in dichloromethane (81 µl/mmol of ascaroside) was treated with 4-dimethylaminopyridine (0.25 mg/ µmol of ascaroside) followed by 1-(3-dimethylaminopropyl)-3-ethylcarbodiimide hydrochloride (0.4 mg/ µmol of ascaroside). The mixture was stirred for 5 min, then 4-TBDPS-asc-ΔC5-OBn (0.9 mg/ µmol of ascaroside) in dichloromethane (43 µl/ mmol of ascaroside) was added. After stirring for 24 h the mixture was diluted with dichloromethane, washed with water, dried with Na_2SO_4 and concentrated under reduced pressure.

The resulting mixture was purified by flash column chromatography on silica gel using 10% ethyl acetate in hexane *(v/v)* as eluent.

Ascaroside	Amount	Oligomer
Silylated monomer 203	30 mg, 62 µmol	**205** (42 mg, 41 µmol, 66%)
Silylated dimer 224	28 mg, 29 µmol	**206** (23.4 mg, 20 µmol, 53%)
Silylated trimer 225	21 mg, 15 µmol	**207** (14 mg, 7 µmol, 47%)
Silylated tetramer 226	5.5 mg, 3.0 µmol	**222** (4.3 mg, 1.7 µmol, 59%)
Benzylated monomer 227	2 mg, 4.7 µmol	**220** (2 mg, 2.4 µmol, 51%)
Benzylated dimer 228	1.2 mg, 1.6 µmol	**223** (700 µg, 0.6 µmol, 38%)

Benzyl (2*E*,4*R*)-4-[[4-*O*-*tert*-butyldiphenylsilyl-3,6-dideoxy-2-*O*-[(4*R*)-4-[(2,4-di-*O*-*tert*-butyldimethylsilyl-3,6-dideoxy-α-L-*arabino*-hexopyranosyl)oxy]-1-oxopentyl]-α-L-*arabino*-hexopyranosyl]oxy]-2-pentenoate (205).

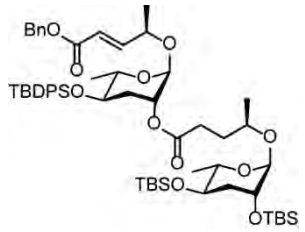

^{1}H NMR (600 MHz, $CDCl_3$) δ (ppm) 7.69-7.65 (*m*, 2 H), 7.65-7.63 (*m*, 2 H), 7.39-7.35 (*m*, 6H), 7.45-7.36 (*m*, 5H), 7.00 (*dd*, *J* = 15.7 Hz, *J* = 5.3 Hz, 1H), 6.07 (*dd*, *J* = 15.7 Hz, *J* = 1.6 Hz, 1H), 5.22 (*s*, 2H), 4.68 (*dd*, *J* = 3.6 Hz, *J* = 3.1 Hz, 1H), 4.62 (*br.s*, 1H), 4.52 (*br.s*, 1H), 4.38 (*qdd*, *J* = 6.5 Hz, *J* = 5.3 Hz, *J* = 1.6 Hz, 1H), 3.76 (*dd*, *J* = 3.5 Hz, *J* = 2.9 Hz, 1H), 3.74 (*dq*, 9.1 Hz, *J* = 6.2 Hz, 1H), 3.73 (*m*, 1H), 3.65 (*ddd*, *J* = 10.5 Hz, *J* = 9.0 Hz, *J* = 4.4 Hz, 1H), 3.54 (*ddd*, *J* = 11.3 Hz, *J* = 9.1 Hz, *J* = 4.4 Hz, 1H), 3.51 (*dq*, *J* = 9.0 Hz, *J* = 6.2 Hz, 1H), 2.26-2.10 (*m*, 2H), 1.88 (*ddd*, *J* = 13.9 Hz, *J* = 11.3 Hz, *J* = 3.1 Hz, 1H), 1.81 (*ddd*, *J* = 14.0 Hz, *J* = 4.4 Hz, *J* = 3.5 Hz, 1H), 1.75 (*ddd*, *J* = 14.0 Hz, *J* = 10.5 Hz, *J* = 2.9 Hz, 1H), 1.71 (*ddd*, *J* = 13.9 Hz, *J* = 4.4 Hz, *J* = 3.8 Hz, 1H), 1.69-1.58 (*m*, 2H), 1.25 (*d*, *J* = 6.5 Hz, 3H), 1.183 (*d*, *J* = 6.2 Hz, 3H), 1.180 (*d*, *J* = 6.2 Hz, 3H), 1.07 (*d*, *J* = 6.1 Hz, 3H), 1.04 (*s*, 9H), 0.90 (*s*, 9H), 0.88 (*s*, 9H), 0.08 -0.04 (*m*, 12 H), **^{13}C NMRC NMR**(150 MHz, $CDCl_3$) δ (ppm) 172.6, 166.5, 149.8, 136.1, 136.0, 129.9, 129.8, 128.7, 128.5, 128.4, 127.8, 127.7, 119.9, 96.3, 94.4, 71.2, 70.9, 70.5, 70.2, 70.1, 70.0, 69.98, 68.9, 66.5, 37.1, 33.1, 32.0, 30.6, 27.1, 26.0, 25.9, 19.5, 19.3, 18.8, 18.4, 18.2, 18.16, -4.1, -4.5, -4.7, -4.8, **HRMS** (ESI-TOF) m/z (M + Na)$^{+}$ calcd for $C_{57}H_{88}O_{11}Si_3Na$ 1055.5532, found 1055.5529, Δ -0.3 ppm.

Benzyl (2*E*, 4*R*)-4-[[4-*O*-*tert*-butyldiphenylsilyl-3,6-dideoxy-2-*O*-[(4*R*)-4-[4-*O*-*tert*-butyldiphenylsilyl-3,6-dideoxy-2-*O*-[(4*R*)-4-[2,4-di-*O*-*tert*-butyldimethylsilyl-3,6-dideoxy- α-L-*arabino*-hexopyranosyl]oxy]-1-oxopentyl]-α-L-*arabino*-hexopyranosyl]oxy]-1-oxopentyl]-α-L-*arabino*-hexopyranosyl]oxy]-2-pentenoate (206).

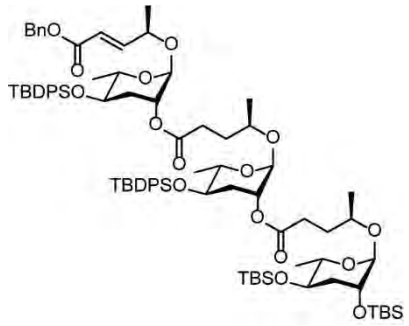

^{1}H NMR (600 MHz, $CDCl_3$) δ (ppm) 7.70-7.63 (*m*, 8H), 7.45-7.39 (*m*, 7H), 7.39-7.31 (*m*, 10H), 7.01 (*dd*, *J* = 15.7 Hz, *J* = 5.3 Hz, 1H), 6.07 (*dd*, *J* = 15.7 Hz, *J* = 1.6 Hz, 1H), 5.22 (*s*, 2H), 4.71 (*dd*, *J* = 3.8 Hz, *J* = 2.9 Hz, 1H), 4.64 (*br.s*, 1H), 4.62 (d, *J* = 3.6 Hz, *J* = 3.1 Hz, 1H), 4.56 (*br.s*, 1H), 4.53 (*br.s*, 1H), 4.38 (*qd*, 6.3 Hz, *J* = 5.3 Hz, 1H), 3.76 (*dd*, *J* = 3.8 Hz, *J* = 3.0 Hz, 1H), 3.76 (*dq*, *J* = 9.3 Hz, *J* = 6.1 Hz, 1H), 3.74 (*dq*, *J* = 9.2 Hz, *J* = 6.2 Hz, 1H), 3.74 (m, 1H), 3.72 (*m*, 1H), 3.65 (*ddd*, *J* = 10.5 Hz, *J* = 9.0 Hz, *J* = 4.4 Hz, 1H), 3.57 (*ddd*, *J* = 11.1 Hz, *J* = 9.3 Hz, 4.5 Hz, 1H), 3.53 (*ddd*, *J* = 11.1 Hz, *J* = 9.2 Hz, *J* = 4.9 Hz, 1H), 3.51 (*dq*, *J* = 9.0 Hz, *J* = 6.1 Hz, 1H), 2.27-2.10 (*m*, 4H), 1.91 (*ddd*, *J* = 14.1 Hz, *J* = 11.1 Hz, *J* = 3.1 Hz, 1H), 1.85 (*ddd*, *J* = 13.8 Hz, *J* = 11.1 Hz, *J* = 3.1 Hz, 1H), 1.81 (*ddd*, *J* = 13.3 Hz, *J* = 10.5 Hz, *J* = 3.0 Hz, 1H), 1.76 (*ddd*, *J* = 13.3 Hz, *J* = 4.4 Hz, *J* = 3.8 Hz, 1H), 1.74 (*ddd*, *J* = 14.1 Hz, *J* = 4.5 Hz, *J* = 3.8 Hz, 1H), 1.73-1.58 (*m*, 4H), 1.72 *(ddd*, *J* = 13.8 Hz, *J* = 4.9 Hz, *J* = 3.6 Hz, 1H), 1.25 (*d*, *J* = 6.3 Hz, 3H), 1.22 (*d*, *J* = 6.2 Hz, 3H),1.20 (*d*, *J* = 6.1 Hz, 3H), 1.18 (*d*, *J* = 6.1 Hz, 3H), **^{13}C NMRC NMR**(150 MHz, $CDCl_3$) δ (ppm) 172.6, 172.5, 149.8, 136.12, 136.11, 135.98, 135.97, 134.24, 134.22, 133.49, 133.48, 129.9, 129.82, 129.80, 128.50, 128.45, 127.8, 127.7, 119.9, 96.5, 94.4, 93.7, 71.3, 71.2, 71.1, 71.0, 70.5, 70.2, 70.14, 70.10, 70.04, 70.00, 68.9, 66.5, 37.1, 33.18, 33.15, 32.1, 31.9, 30.6, 30.4, 29.9, 27.2, 27.1, 25.99, 25.95, 19.5, 19.3, 18.9, 18.8, 18.42, 18.38, 18.22, 18.16, -4.1, -4.5, -4.7, -4.8, **HRMS** (ESI-TOF) m/z $(M + Na)^+$ calcd for $C_{84}H_{124}O_{16}Si_4Na$ 1523.7860, found 1523.7832, Δ -2.1 ppm.

Benzyl (2*E*, 4*R*)-4-[[4-*O*-*tert*-butyldiphenylsilyl-3,6-dideoxy-2-*O*-[(4*R*)-4-[4-*O*-*tert*-butyldiphenylsilyl-3,6-dideoxy-2-*O*-[(4*R*)-4-[4-*O*-*tert*-butyldiphenylsilyl-3,6-dideoxy-2-*O*-[(4R)-4-[(2,4-di-*O*-*tert*-butyldimethylsilyl-3,6-dideoxy- α-L-*arabino*-hexopyranosyl)oxy]-1-oxopentyl]-α-L-*arabino*-hexopyranosyl]oxy]-α-L-*arabino*-hexopyranosyl]oxy]-1-oxopentyl]-α-L-*arabino*-hexopyranosyl]oxy]-1-oxopentyl]-α-L-*arabino*-hexopyranosyl]oxy]-2-pentenoate (207).

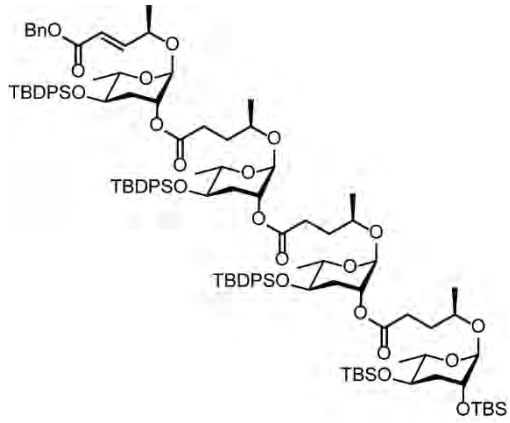

^{1}H NMR (600 MHz, $CDCl_3$) δ (ppm) 7.70-7.63 (*m*, 12H), 7.46-7.39 (*m*, 11H), 7.39-7.32 (*m*, 12H), 7.01 (*dd*, *J* = 15.7 Hz, *J* = 5.3 Hz, 1H), 6.07 (*dd*, *J* = 15.7 Hz, *J* = 1.6 Hz, 1H), 5.23, (*d*, *J* = 12.8 Hz, 1H), 5.21 (*d*, *J* = 12.8 Hz, 1H), 4.71 (*dd*, *J* = 3.9 Hz, *J* = 3.2 Hz, 1H), 4.65 (*dd*, *J* = 3.7 Hz, *J* = 3.3 Hz, 1H), 4.64 (*br.s*, 1H), 4.63 (*dd*, *J* = 3.8 Hz, *J* = 3.2 Hz, 1H), 4.58 (*br.s*, 1H), 4.56 (*br.s*, 1H), 4.53 (*br.s*, 1H), 4.39 (*qdd*, *J* = 6.6 Hz, *J* = 5.3 Hz, *J* = 1.6 Hz, 1H), 3.78-3.717 (*m*, 3H), 3.762-3.69 (*m*, 3H), 3.76 (*dd*, *J* = 3.9 Hz, *J* = 3.1 Hz, 1H), 3.65 (*ddd*, 10.5 Hz, *J* = 9.0 Hz, *J* = 4.5 Hz, 1H), 3.57 (*ddd*, *J* = 11.5 Hz, *J* = 9.7 Hz, *J* = 4.4 Hz, 1H), 3.530 (*ddd*, *J* = 10.3 Hz, *J* = 9.4 Hz, *J* = 4.4 Hz, 1H), 3.523 (*dq*, *J* = 9.0 Hz, *J* = 6.2 Hz, 1H), 3.56 (*m*, 1H), 2.26-2.12 (*m*, 6H), 1.91 (*ddd*, *J* = 14.0 Hz, *J* = 11.5 Hz, *J* = 4.4 Hz, 1H), 1.87 (*ddd*, *J* = 13.7 Hz, *J* = 10.9 Hz, *J* = 3.2 Hz, 1H), 1.86 (*ddd*, *J* = 13.5 Hz, *J* = 10.3 Hz, *J* = 3.1 Hz, 1H), 1.81 (*ddd*, *J* = 12.9 Hz, *J* = 4.5 Hz, *J* = 3.9 Hz, 1H), 1.76 (*ddd*, *J* = 12.9 Hz, *J* = 10.5 Hz, *J* = 3.1 Hz, 1H), 1.747 (*ddd*, *J* = 13.7 Hz, *J* = 4.7 Hz, *J* = 3.8 Hz, 1H), 1.745 (*ddd*, *J* = 14.0 Hz, *J* = 4.4 Hz, *J* = 4.0 Hz, 1H), 1.73-1.59 *(m*, 6H), 1.25 (*d*, *J* = 6.5 Hz, 3H), 1.231 (*d*, *J* = 6.3 Hz, 3H), 1.225 (*d*, *J* = 6.3 Hz, 3H), 1.08 (*d*, *J* = 6.1 Hz, 3H), 1.06 (*d*, *J* = 6.2 Hz, 6H), 1.05 (*s*, 24H), 0.90 (*s*, 9H), 0.89 (*s*, 9H), **^{13}C NMR**(150 MHz, $CDCl_3$): δ (ppm) 172.62, 172.54, 172.49, 149.83, 136.13, 136.10, 136.00, 135.98, 134.24, 133.48, 129.93, 129.82, 128.75, 128.50, 128.45, 127.76, 127.66, 119.89, 96.54, 94.39, 93.69, 93.65, 71.39, 71.34, 71.22, 71.11, 70.96, 70.48, 70.20, 70.14, 70.10, 70.05, 68.89, 66.54, 37.14, 33.21, 33.15, 32.06, 31.91, 30.58, 30.46, 27.17, 27.12, 25.99, 25.92, 19.47, 18.85, 18.83, 18.81, 18.43, 18.38, 18.22, 18.21, 18.16, -4.06, -4.50, -4.73, -4.81, **HRMS** (ESI-TOF) m/z (M + Na)$^{+}$ calcd for $C_{111}H_{160}O_{21}NaSi_5$ 1992.0196, found 1992.0161, Δ -1.8 ppm.

Benzyl(2*E*, 4*R*)-4-[[4-*O*-*tert*-butyldiphenylsilyl-3,6-dideoxy-2-*O*-[(4*R*)-4-[4-*O*-*tert*-butyldiphenylsilyl-3,6-dideoxy-2-*O*-[(4*R*)-4-[4-*O*-*tert*-butyldiphenylsilyl-3,6-dideoxy-2-*O*-[(4R)-4-[4-*O*-*tert*-butyldiphenylsilyl-3,6-dideox-2-*O*-[(4*R*)-4-[(2,4-di-*O*-*tert*-butyldimethylsilyl-3,6-dideoxy-α-L-*arabino*-hexopyranosyl)oxy]-1-oxopentyl]-α-L-*arabino*-hexopyranosyl]oxy]-1-oxypentyl]-α-L-*arabino*-hexopyranosyl]oxy]-1-oxopentenyl]-α-L-*arabino*-hexopyranosyl]oxy]-1-oxopentyl]-α-L-*arabino*-hexopyranosyl]oxy]-pentenoate (222).

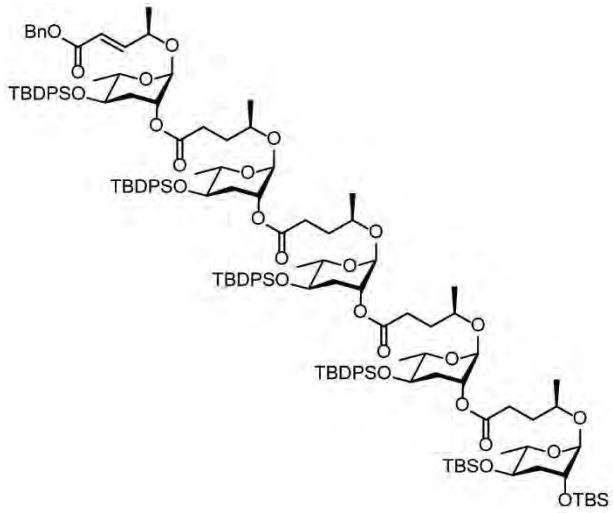

^{1}H NMR (600 MHz, $CDCl_3$) δ (ppm) 7.70-7.63 (*m*, 16H), 7.45-7.39 (*m*, 11H), 7.39-7.33 (*m*, 18H), 7.01 (*dd*, *J* = 15.7 Hz, *J* = 5.5 Hz, 1H), 6.07 (*dd*, *J* = 15.7 Hz, *J* = 1.6 Hz, 1H), 5.22 (*s*, 2H), 4.71 (*dd*, *J* = 3.9 Hz, *J* = 3.2 Hz, 1H), 4.66 (*dd*, *J* = 3.8 Hz, *J* = 3.3 Hz, 2H), 4.64 (*br.s*, 1H), 4.63 (*dd*, *J* = 3.9 Hz, *J* = 3.1 Hz, 1H), 4.58 (*br.s*, 2H), 4.56 (*br.s*, 1H), 4.53 (*br.s*, 1H), 4.39 (*qd*, *J* = 6.3 Hz, *J* = 5.5 Hz, 1H), 3.787-3.717 (*m*, 2H), 3.769-3.694 (*m*, 3H), 3.76 (*dd*, 3.7 Hz, *J* = 3.1 Hz, 1H), 3.754 (*dq*, *J* = 9.2 Hz, *J* = 6.4 Hz, 1H), 3.751 (*dq*, *J* = 9.1 Hz, *J* = 6.1 Hz, 1H), 3.74 (*m*, 1H), 3.65, (*ddd*, *J* = 10.7 Hz, *J* = 9.6Hz, *J* = 4.6 Hz, 1H), 3.596-3.505 (*m*, 2 H), 3.558 (*ddd*, *J* = 11.5 Hz, *J* = 9.2 Hz, *J* = 4.5 Hz, 1H), 3.531 (*ddd*, *J* = 11.4 Hz, *J* = 9.1 Hz, 4.5 Hz, 1H), 3.52 (*dq*, *J* = 9.6 Hz, *J* = 6.2 Hz, 1H), 2.24-2.12 (*m*, 8H), 1.73-1.61 (*m*, 6H), 1.67-1.59 (*m*, 2H), 1.25 (d, *J* = 6.3 Hz, 3H), 1.234 (*d*, *J* = 6.2 Hz, 6H), 1.225 (*d*, *J* = 6.4 Hz, 3H), 1.20 (*d*, *J* = 6.1 Hz, 3H), 1.19 (*d*, *J* = 6.2 Hz, 3H), 1.077 (*d*, *J* = 6.2 Hz, 3H), 1.063 (*d*, *J* = 6.1 Hz, 9H), 1.048 (*s*, 18H), 1.045 (*s*, 18H), 0.90 (*s*, 9H), 0.88 (*s*, 9H), 0.08-0.04 (*m*, 12H), **^{13}C NMR**(150 MHz, $CDCl_3$): δ (ppm) 172.6, 149.8, 136.0, 135.9,135.02, 133.0, 132.5, 129.82, 129.76, 129.6, 128.3, 127.7, 127.6, 119.7, 96.3, 94.1, 93.5, 71.29, 71.27, 71.0, 70.90, 70.87, 70.1, 69.9, 68.9, 36.9, 33.1, 31.8, 31.7, 30.4, 29.6, 27.04, 27.00, 25.87, 25.80, 18.7, 18.3, 18.1, -4.76, **HRMS** (ESI-TOF) m/z $(M + Na)^+$ calcd for $C_{138}H_{196}O_{26}NaSi_6$ 2460.2528, found 2460.2539, Δ 0.4 ppm.

Benzyl (2*E*,4*R*)-4-[[4-*O*-benzyl-3,6-dideoxy-2-*O*-[(4*R*)-4-[(2,4-di-*O*-benzyl-3,6-dideoxy-α-L-*arabino*-hexopyranosyl)oxy]-1-oxopentyl]-α-L-*arabino*-hexopyranosyl]oxy]-2-pentenoate (220).

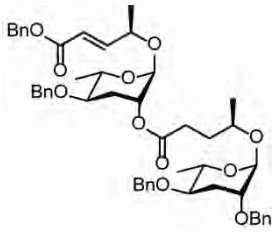

^{1}H NMR (600 MHz, $CDCl_3$) δ (ppm) 7.39-7.26 (*m*, 20H), 6.94 (*dd*, *J* = 15.6 Hz, *J* = 5.5 Hz, 1H), 6.02 (*dd*, *J* = 15.6 Hz, *J* = 1.5 Hz, 1H), 5.19 (*d*, *J* = 12.3 Hz, 1H), 5.16 (*d*, *J* = 12.3 Hz, 1H), 4.89 (*ddd*, *J* = 3.2 Hz, *J* = 2.6 Hz, *J* = 1.4 Hz, 1H), 4.77 (*br.s*, 1H), 4.74 (*br.s*, 1H), 4.59 (*d*, *J* = 11.2 Hz, 1H), 4.57 (*d*, *J* = 11.4 Hz, 1H), 4.56 (*d*, *J* = 12.5 Hz, 1H), 4.54 (*d*, *J* = 12.5 Hz, 1H), 4.46 (*d*, *J* = 11.4 Hz, 1H), 4.45 (*d*, *J* = 11. Hz, 1H), 4.36 (*qd*, *J* = 6.5 Hz, *J* = 5.5 Hz, 1H), 3.82 (*qt*, *J* = 6.1 Hz, *J* = 5.4 Hz, 1H), 3.73 (*dq*, *J* = 9.2 Hz, *J* = 6.2 Hz, 1H), 3.70 (*dq*, *J* = 9.3 Hz, *J* = 6.2 Hz, 1H), 3.54 (*ddd*, *J* = 3.0 Hz, *J* = 2.8 Hz, *J* = 1.5 Hz, 1H), 3.45 (*ddd*, *J* = 11.2 Hz, *J* = 9.2 Hz, *J* = 4.0 Hz, 1H) 3.35 (*ddd*, *J* = 11.4 Hz, *J* = 9.3 Hz, *J* = 5.2 Hz, 1H), 2.48 (*dt*, *J* = 15.9 Hz, *J* = 7.9 Hz, 1H), 2.37 (*dt*, *J* = 15.9 Hz, *J* = 7.9 Hz, 1H), 2.22 (*ddd*, *J* = 13.6 Hz, *J* = 4.0 Hz, J = 2.8 Hz, 1H), 2.21 (ddd, *J* = 13.6 Hz, *J* = 14.1 Hz, *J* = 5.2 Hz, *J* = 2.6 Hz, 1H), 1.89 (*ddd*, *J* = 14.1 Hz, *J* = 11.4 Hz, *J* = 3.2 Hz, 1H), 1.78 (*ddd*, *J* = 7.9 Hz, *J* = 7.9 Hz, *J* = 5.4 Hz, 1H), 1.71 (*ddd*, *J* = 13.6 Hz, *J* = 11.2 Hz, *J* = 3.0 Hz, 1H), 1.29 (*d*, *J* = 6.3 Hz, 3H), 1.25 (*d*, *J* = 6.5 Hz, 3H), 1.23 (*d*, *J* = 6.2 Hz, 3H), 1.10 (*d*, *J* = 6.1 Hz, 3H), **^{13}C NMR**(150 MHz, $CDCl_3$): δ (ppm) 172.9, 166.4, 149.6, 138.5, 138.4, 138.3, 136.1, 128.73, 128.70, 128.6, 128.54, 128.49, 128.4, 128.1, 127.93, 128.88, 128.85, 128.83, 119.9, 94.24, 94.18, 75.9, 75.7, 75.1, 71.5, 71.4, 71.3, 71.2, 70.8, 70.1, 68.8, 68.5, 66.5, 32.2, 30.8, 29.7, 29.5, 19.3, 18.9, 18.3, 18.0, **HRMS** (ESI-TOF) m/z $(M + Na)^+$ calcd for $C_{50}H_{60}O_{11}Na$ 859.4033, found 859.4024, Δ -1 ppm.

Benzyl (2*E*, 4*R*)-4-[[4-*O*-benzyl-3,6-dideoxy-2-*O*-[(4*R*)-4-[4-*O*-benzyl-3,6-dideoxy-2-*O*-[(4*R*)-4-[2,4-di-*O*-benzyl-3,6-dideoxy- α-L-*arabino*-hexopyranosyl]oxy]-1-oxopentyl]-α-L-*arabino*-hexopyranosyl]oxy]-1-oxopentyl]-α-L-*arabino*-hexopyranosyl]oxy]-2-pentenoate (223).

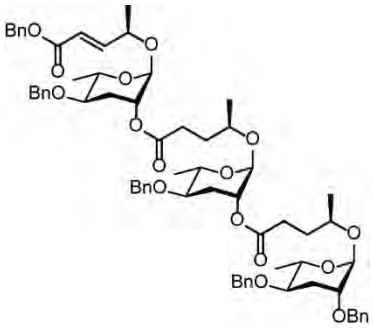

^{1}H NMR (600 MHz, $CDCl_3$) δ (ppm) 7.39-7.26 (m, 25H), 6.94 (dd, J = 15.7 Hz, J = 5.3 Hz, 1H), 6.02 (dd, *J* = 15.7 Hz, *J* = 1.6 Hz, 1H), 5.19 (*d*, *J* = 12.3 Hz, 1H), 5.16 (*d*, *J* = 12.3 Hz, 1H), 4.89 (*ddd*, *J* = 3.2 Hz, *J* = 2.7 Hz, *J* = 1.4 Hz, 1H) , 4.84 (*ddd*, *J* = 2.9 Hz, *J* = 2.7 Hz, *J* = 1.6 Hz, 1H), 4.77, (*br.s*, H), 4.74 (*br.s*, 1H), 4.71 (*br.s*, 1H), 4.60 (*d*, *J* = 11.2 Hz, 1H), 4.59 (*d*, *J* = 11.4 Hz, 1H), 4.57 (*d*, *J* = 11.5 Hz, 1H), 4.56 (*d*, *J* = 12.3 Hz, 1H), 4.54 (*d*, *J* = 12.3 Hz, 1H), 4.46 (*d*, *J* = 11.3 Hz, 1H), 4.45 (*d*, *J* = 11.3 Hz, 2H), 4.37 (*dq*, *J* = 6.6 Hz, *J* = 5.3 Hz, 1H), 3.82 (*m*, 1H), 3.80 (*m*, 1H), 3.77-3.70 (*m*, 2H), 3.71 (*dq*, *J* = 9.2 Hz, *J* = 6.4 Hz, 1H), 3.45 (*ddd*, *J* = 11.1 Hz, *J* = 9.2 Hz, *J* = 4.1 Hz, 1H), 3.36 (*m*, 1H), 3.35 (*m*, 1H), 2.53-2.44 (*m*, 2H), 2.41-2.34 (*m*, 2H), 2.22 (*ddd*, *J* = 13.7 Hz, *J* = 4.1 Hz, *J* = 2.8 Hz, 1H), 2.208 (*ddd*, *J* = 13.8 Hz, *J* = 4.5 Hz, *J* = 2.7 Hz, 1H), 2.206 (*ddd*, *J* = 13.8 Hz, *J* = 4.7 Hz, *J* = 2.7 Hz, 1H), 1.90 (*ddd*, *J* = 13.8 Hz, *J* = 11.2 Hz, *J* = 3.2 Hz, 1H), 1.86 (*ddd*, *J* = 13.8 Hz, *J* = 11.6 Hz, *J* = 2.9 Hz, 1H), 1.83-1.76 (*m*, 4H), 1.71 (*ddd*, *J* = 13.7 Hz, *J* = 11.1 Hz, *J* = 3.1 Hz, 1H), 1.29 (*d*, *J* = 6.4 Hz, 3H), 1.28 (*d*, *J* = 6.3 Hz, 3H), 1.25 (*d*, *J* = 6.6 Hz, 3H), 1.23 (*d*, *J* = 6.3 Hz, 3H), 1.13 (*d*, *J* = 6.1 Hz, 3H), 1.10 (*d*, *J* = 6.1 Hz, 3H), **^{13}C NMR**(150 MHz, $CDCl_3$): δ (ppm) 172.7, 166.0, 149.6, 138.2, 138.0, 136.1, 128.5, 128.2, 127.9, 119.8, 94.11, 94.12, 93.3, 75.8, 75.5, 75.0, 71.3, 71.2, 71.1, 71.0, 70.68, 70.67, 70.0, 66.4, 32.0, 30.6, 29.4, 19.1, 18.7, 18.1, 17.8, **HRMS** (ESI-TOF) m/z $(M + Na)^+$ calcd for $C_{68}H_{84}O_{16}Na$ 1179.5657, found 1179.5636, Δ -1.8 ppm.

8.11.2. General procedure for the hydrogenation of the silylated ascarosides 205-207.

The ascaroside in ethyl acetate (130 µl/ µmol of ascaroside) was added to a suspension of palladium on carbon (10%, 550 µg/ mg of ascaroside) in ethyl acetate (130 µl/ mg of catalyst) then H_2 was added to the mixture. The solution was stirred for 18 h then filtered over cotton and the catalyst rinsed with ethyl acetate. The filtrate was concentrated under reduced pressure and used for the next step without any further purification.

Ascaroside	Amount	Oligomer
Dimer 205	27.8 mg, 26.9 µmol	**224** (25 mg, 26 µmol, 97%)
Trimer 206	23 mg, 15.6 µmol	**225** (22 mg, 16 µmol, 99%)
Tetramer 207	7.0 mg, 3.6 µmol	**226** (5.6 mg, 3.0 µmol, 83%)

(4*R*)-4-[[4-*O*-*tert*-butyldiphenylsilyl-3,6-dideoxy-2-*O*-[(4*R*)-4-[(2,4-di-*O*-*tert*-butyldimethylsilyl-3,6-dideoxy-α-L-*arabino*-hexopyranosyl)oxy]-1-oxopentyl]-α-L-*arabino*-hexopyranosyl]oxy]-pentanoic acid (224)

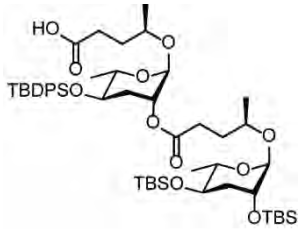

^{1}H NMR (600 MHz, $CDCl_3$) δ (ppm), 7.69-7.66 (*m*, 4H), 7.66-7.64 (*m*, 2H), 7.45-7.40 (*m*, 2H), 7.40-7.34 (*m*, 2H), 4.63 (dd, *J* = 3.5 Hz, *J* = 3.1 Hz, 1H), 4.59 (*br.s*, 1H), 4.53 (*br.s*, 1H), 3.82 (*m*, 1H), 3.78 (*dq*, *J* = 9.2 Hz, *J* = 6.2 Hz, 1H), 3.76 (*dd*, *J* = 3.8 Hz, *J* = 3.0 Hz, 1H), 3.74 (*m*, 1H), 3.65 (*ddd*, *J* = 10.5 Hz, *J* = 9.0 Hz, *J* = 4.4 Hz, 1H), 3.55 (*ddd*, *J* = 10.9 Hz, *J* = 9.2 Hz, *J* = 4.5 Hz, 1H), 3.51 (*dq*, 9.0 Hz, *J* = 6.2 Hz, 1H), 2.58-2.46 (*m*, 1H), 2.24-2.13 (*m*, 2H), 1.92-184 (*m*, 2H), 1.85 (*ddd*, *J* = 13.8 Hz, *J* = 10.9 Hz, *J* = 3.1 Hz, 1H), 1.81 (*ddd*, *J* = 13.8 Hz, *J* = 4.4 Hz, *J* = 3.8 Hz, 1H), 1.76 (*ddd*, *J* = 13.8 Hz, *J* = 10.5 Hz, *J* = 3.0 Hz, 1H), 1.72 (*ddd*, *J* = 13.8 Hz, *J* = 4.5 Hz, *J* = 3.5 Hz, 1H), 1.69-1.59 (*m*, 2H), 1.23 (*d*, *J* = 6.2 Hz, 3H), 1.18 (*d*, *J* = 6.2 Hz, 3H), 1.12 (*d*, *J* = 6.1 Hz, 3H), 1.08 (*d*, *J* = 6.1 Hz, 3H), **^{13}C NMR**(150 MHz, $CDCl_3$): δ (ppm) 178.2, 172.6, 136.1, 136.0, 134.3, 133.5, 129.9, 129.8, 127.7, 96.5, 93.6, 71.3, 70.8, 70.5, 70.2, 70.1, 70.05, 68.9, 37.1, 33.2, 32.1, 19.5, 19.0, 18.8, 18.4, 18.3, 18.2, 18.16, -4.1, -4.5, -4.7, -4.8, **HRMS** (ESI-TOF) m/z $(M - H)^-$ calcd for $C_{50}H_{83}O_{11}Si_3$ 943.5226, found 943.5242, Δ -1.8 ppm.

(4*R*)-4-[[4-*O*-*tert*-butyldiphenylsilyl-3,6-dideoxy-2-*O*-[(4*R*)-4-[4-*O*-*tert*-butyldiphenylsilyl-3,6-dideoxy-2-*O*-[(4*R*)-4-[2,4-di-*O*-*tert*-butyldimethylsilyl-3,6-dideoxy- α-L-*arabino*-hexopyranosyl]oxy]-1-oxopentyl]-α-L-*arabino*-hexopyranosyl]oxy]-1-oxopentyl]-α-L-*arabino*-hexopyranosyl]oxy]-pentanoic acid (225).

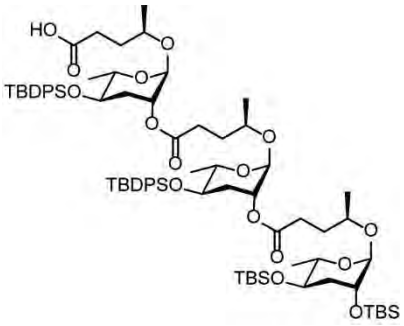

^{1}H NMR (600 MHz, $CDCl_3$) δ (ppm), 7.70-7.63 (*m*, 8H), 7.45-7.40 (*m*, 4H), 7.40-7.34 (*m*, 8H), 4.66 (*dd*, *J* = 3.7 Hz, *J* = 3.3 Hz, 1H), 4.62 (*dd*, *J* = 3.1 Hz, *J* = 3.8 Hz, 1H), 4.61 (*br.s*, 1H), 4.56 (*br.s*, 1H), 4.53 (*br.s*, 1H), 3.83 (*m*, 1H), 3.79 (*dq*, *J* = 9.0 Hz, 6.3 Hz, 1H), 3.75 (*m*, 1H), 3.745 (*dq*, *J* = 9.4 Hz, 6.3 Hz, 1H), 3.73 (*m*, 1H), 3.65 (*ddd*, *J* = 10.5 Hz, *J* = 9.0 Hz, *J* = 4.4 Hz, 1H), 3.58 (*ddd*, *J* = 11.3 Hz, *J* = 9.0 Hz, *J* = 4.6 Hz, 1H), 3.53 (*ddd*, *J* = 11.0 Hz, *J* = 9.4 Hz, *J* = 4.6 Hz, 1H), 3.51 (*dq*, *J* = 9.0 Hz, *J* = 6.3 Hz, 1H), 2.59-2.46 (*m*, 2H), 2.27-2.12 (*m*, 4H), 1.73-1.59 (*m*, 2H), 1.68-1.59 (*m*, 2H), 1.92-1.82 (*m*, 2H), 1.88 (*ddd*, *J* = 13.1 Hz, 11.3 Hz, 3.3 Hz, 1H), 1.85 (*ddd*, *J* = 13.8 Hz, *J* = 11.0 Hz, *J* = 3.1 Hz, 1H), 1.80 (*ddd*, *J* = 13.9 Hz, *J* = 10.5 Hz, *J* = 3.2 Hz, 1H), 1.75 (*ddd*, *J* = 13.9 Hz, *J* = 10.5 Hz, *J* = 3.8 Hz, 1H), 1.74 (*ddd*, *J* = 13.1 Hz, *J* = 11.3 Hz, *J* = 3.7 Hz, 1H), 1.72-1.65 (*m*, 2H), 1.68- 1.61 (*m*, 2H), 1.25 (*d*, *J* = 6.3 Hz, 3H), 1.22 (*d*, *J* = 6.3 Hz, 3H), 1.19 (*d*, *J* = 6.3 Hz, 3H), 1.12(*d, J* = 6.1 Hz, 3H), 1.08 (*d, J* = 6.1 Hz, 3H), 1.07 (d, *J* = 6.0 Hz, 3H), 1.05 (*s*, 9H), 1.04 (*s*, 9H), 0.9 (*s*, 9H), 0.88 (*s*, 9H), 0.07 (*m*, 12 H), **^{13}C NMR**(150 MHz, $CDCl_3$) δ (ppm) 178.2, 172.6, 172.55, 171.4, 136.12, 136.1, 136.0, 129.9, 129.8, 129.81, 127.8, 127.7, 96.5, 93.7, 93.6 71.4, 71.1, 71.09, 70.4, 70.2, 70.14, 70.1, 70.06, 68.9, 37.1, 33.2, 32.1, 31.9, 30.6, 30.5, 30.2, 29.8, 27.2, 27.1, 26.0, 25.9, 19.0, 18.84, 18.82, 18.4, 18.37, 18.2, 18.16, -4.1, -4.5, -4.7, -4.8, **HRMS** (ESI-TOF) m/z (M - H)$^{-}$ calcd for $C_{77}H_{120}O_{16}Si_4$ 1411.7575, found 1411.7581, Δ 0.4 ppm.

(4*R*)-4-[[4-*O*-*tert*-butyldiphenylsilyl-3,6-dideoxy-2-*O*-[(4*R*)-4-[4-*O*-*tert*-butyldiphenylsilyl-3,6-dideoxy-2-*O*-[(4*R*)-4-[4-*O*-*tert*-butyldiphenylsilyl-3,6-dideoxy-2-*O*-[(4*R*)-4-[(2,4-di-*O*-*tert*-butyldimethylsilyl-3,6-dideoxy- α-L-*arabino*-hexopyranosyl)oxy]-1-oxopentyl]-α-L-*arabino*-hexopyranosyl]oxy]-α-L-*arabino*-hexopyranosyl]oxy]-1-oxopentyl]-α-L-*arabino*-hexopyranosyl]oxy]-1-oxopentyl]-α-L-*arabino*-hexopyranosyl]oxy]-pentanoic acid (226).

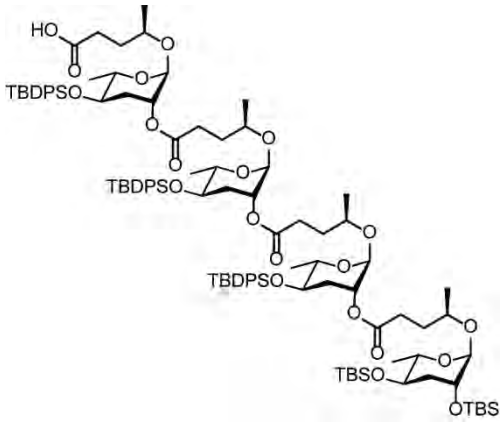

^{1}H NMR (600 MHz, $CDCl_3$) δ (ppm) 7.70-7.64 (*m*, 12H), 7.45-7.40 (*m*, 6H), 7.40-7.34 (*m*, 12H), 4.67-4.64 (*m*, 2H), 4.63 (*dd*, *J* = 3.8 Hz, *J* = 3.2 Hz, 1H), 4.62 (*br.s*, 1H), 4.58 (*br.s*, 1H), 4.56 (*br.s*, 1H), 4.53 (*br.s*, 1H), 3.83 (*m*, 1H), 3.79 (*dq*, *J* = 9.3 Hz, *J* = 6.2 Hz, 1H), 3.77-3.70 (*m*, 3H), 3.76 (*dd*, *J* = 3.6 Hz, *J* = 3.0 Hz, 1H), 3.747 (*dq*, *J* = 9.1 Hz, *J* = 6.2 Hz, 1H), 3.751 (*dq*, *J* = 9.1 Hz, *J* = 6.2 Hz, 1H), 3.65 (*ddd*, *J* = 10.8 Hz, *J* = 9.4 Hz, *J* = 4.3 Hz, 1H), 3.59 (*ddd*, *J* = 10.2 Hz, *J* = 9.2 Hz, *J* = 4.4 Hz, 1H), 3.56 (*ddd*, *J* = 11.0 Hz, *J* = 9.1Hz, *J* = 4.6Hz, 1H), 3.53 (*ddd*, *J* = 10.9 Hz, *J* = 9.1 Hz, *J* = 4.6 Hz, 1H), 3.52 (*dq*, *J* = 9.4 Hz, *J* = 6.2 Hz, 1H), 2.58-2.46 (*m*, 2H), 2.24-2.12 (*m*, 6H), 1.92-1.82 (*m*, 2H), 1.91-1.83 (*m*, 4H), 1.86 (*ddd*, *J* = 13.6 Hz, *J* = 10.9 Hz, *J* = 3.2 Hz, 1H), 1.82 (*ddd*, *J* = 13.5 Hz, *J* = 4.3 Hz, *J* = 3.6 Hz, 1H), 1.76 (*ddd*, *J* = 13.5 Hz, *J* = 10.8 Hz, *J* = 3.0 Hz, 1H), 1.74-1.59 (*m*, 6 H), 1.73 (*ddd*, *J* = 13.6 Hz, *J* = 4.6 Hz, *J* = 3.8 Hz, 1H), 1.25 (*d*, *J* = 6.2 Hz, 3H), 1.234 (*d*, *J* = 6.2 Hz, 3H), 1.225 (*d*, *J* = 6.2 Hz, 3H), 1.19 (*d*, *J* = 6.2 Hz, 3H), 1.13 (*d*, *J* = 6.1 Hz, 3H), 1.08 (*d*, *J* = 6.1 Hz, 3H), 1.064 (*d*, *J* = 6.1 Hz, 3H), 1.062 (*d*, *J* = 6.2 Hz, 3H), 1.054 (*s*, 6H), 1.049 (*s*, 6H), 1.045 (*s*, 6H), 0.90 (*s*, 9H), 0.89 (*s*, 9H), 0.09-0.04 (*s*, 12H), **^{13}C NMR**(150 MHz, $CDCl_3$): δ (ppm) 176.8, 172.62, 172.55, 136.1, 136.0, 135.0, 134.3, 133.6, 133.5, 129.9, 129.82, 129.81, 127.8, 127.7, 96.5, 93.70, 93.67, 93.59, 71.4, 71.1, 70.5, 70.2, 70.11, 70.06, 68.9, 37.1, 32.1, 31.9, 30.6, 30.48, 30.47, 29.92, 29.85, 27.2, 27.1, 26.0, 25.9, 19.49, 19.47, 19.0, 18.9, 18.83, 18.43, 18.38, 18.21, 18.17, 14.4, 1.2, -4.1, -4.5, -4.7, -4.8, **HRMS** (ESI-TOF) m/z $(M - H)^-$ calcd for $C_{104}H_{156}O_{21}Si_5$ 1879.9860, found 1879.9907, Δ -2.5 ppm.

8.11.3. General procedure for the hydrogenation of the benzylated ascarosides 220 and 223

Under N_2 atmosphere, a mixture of ascaroside in ethanol (10 µl/ µmol of ascaroside) and palladium on carbon (10%, 1 µg/ µg of ascaroside) was treated with 1,4-cyclohexadiene (10 µl/ µmol of ascaroside). The solution was stirred for 5 h of the reaction and was then filtered over cotton plug. The filtrate was concentrated under reduced pressure and used for the next step without any further purification.

Ascaroside	Amount	Oligomer
Dimer 220	1.2 mg, 2.1 µmol	**227** (1.2 mg, 1.6 µmol, 76%)
Trimer 223	0.7 mg, 0.6 µmol	**221** (0.5 mg, 0.5 µml, 71%)

(4*R*)-4-[[4-*O*-benzyl-3,6-dideoxy-2-*O*-[(4*R*)-4-[(2,4-di-*O*-benzyl-3,6-dideoxy-α-L-*arabino*-hexopyranosyl)oxy]-1-oxopentyl]-α-L-*arabino*-hexopyranosyl]oxy]-pentanoic acid (227).

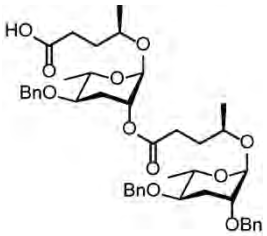

^{1}H NMR (600 MHz, $CDCl_3$) δ (ppm) 7.36-7.26 (*m*, 15H), 4.83 (*ddd*, *J* = 3.3 Hz, *J* = 2.9 Hz, *J* = 1.7 Hz, 1H), 4.77 (*br. s*, 1H), 4.70 (*br.s*, 1H), 4.59 (*d*, *J* = 11.4 Hz, 1H), 4.57 (*d*, *J* = 11.4 Hz, 1H), 4.56 (*d*, *J* = 12.3 Hz, H), 4.53 (*d*, *J* = 12.3 Hz, 1H), 4.47 (*d*, *J* = 11.4 Hz, 1H), 4.46 (*d*, *J* = 11.4 Hz, 1H), 3.85-3.79 (*m*, 2H), 3.77 (*dq*, *J* = 9.2 Hz, *J* = 6.4 Hz, 1H), 3.71 (*dq*, J = 9.5 Hz, *J* = 6.3 Hz, 1H), 3.54 (*ddd*, *J* = 3.1 Hz, *J* = 2.8 Hz, J = 1.7 Hz, 1H), 3.45 (*ddd*, J = 11.0 Hz, *J* = 9.5 Hz, *J* = 4.5 Hz, 1H), 3.34 (*ddd*, *J* = 11.3 Hz, *J* = 9.2 Hz, *J* = 4.6 Hz, 1H), 2.51-2.45 (*m*, 2H), 2.40-2.33 (*m*, 2H), 2.22 (*ddd*, *J* = 13.1 Hz, *J* = 4.5 Hz, *J* = 2.8 Hz, 1H), 2.18 (*ddd*, *J* = 13.5 Hz, *J* = 4.6 Hz, *J* = 2.9 Hz, 1H), 1.86 (*ddd*, *J* = 13.5 Hz, *J* = 11.3 Hz, *J* = 3.3 Hz, 1H), 1.80-1.76 (*m*, 4H), 1.71 (*ddd*, *J* = 13.1 Hz, *J* = 11.0 Hz, *J* = 3.1 Hz, 1H), 1.29 (*d*, *J* = 6.3 Hz, 3H), 1.27 (*d*, *J* = 6.4 Hz, 3H), 1.13 (*d*, *J* = 6.1 Hz, 3H), 1.09 (*d*, *J* = 6.1 Hz, 3H), **^{13}CNMR** (150 MHz, $CDCl_3$) δ (ppm) 176.6, 173.0, 138.53, 138.46, 138.4, 128.6, 128.5, 128.1, 128.0, 127.87, 127.85, 127.84, 94.2, 93.5, 75.9, 75.7, 75.2, 71.5, 71.4, 71.3, 71.2, 70.9, 70.2, 68.8, 68.6, 32.2, 31.9, 30.8, 29.9, 29.7, 29.5, 19.0, 18.9, 18.3, 18.2.

(4*R*)-4-[[4-*O*-benzyl-3,6-dideoxy-2-*O*-[(4*R*)-4-[4-*O*-benzyl-3,6-dideoxy-2-*O*-[(4*R*)-4-[2,4-di-*O*-benzyl-3,6-dideoxy- α-L-*arabino*-hexopyranosyl]oxy]-1-oxopentyl]-α-L-*arabino*-hexopyranosyl]oxy]-1-oxopentyl]-α-L-*arabino*-hexopyranosyl]oxy]-pentanoic acid (221).

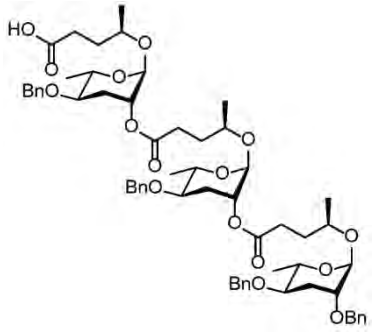

^{1}H NMR (600 MHz, $CDCl_3$) δ (ppm) 7.36-7.28 (*m*, 20H), 4.84 (*br.s*, 2H), 4.77 (*br.s*, 1H), 4.70 (*br.s*, 2H), 4.62 (*d*, *J* = 11.2 Hz, 1H), 4.60 (*d*, *J* = 11.6 Hz, 2H), 4.57 (*d*, *J* = 11.2 Hz, 1H), 4.47 (*d*, *J* = 11.2 Hz, 1H), 4.463 (*d*, *J* =11.2 Hz, 1H), 4.462 (*d*, *J* = 11.2 Hz, 1H), 4.45 (*d*, *J* = 11.2 Hz, 1H), 3.85-3.77 (*m*, 3H), 3.80-3.71 (*m*, 2H), 3.70 (*dq*, *J* = 9.3 Hz, *J* = 6.2 Hz, 1H), 3.54 (*ddd*, *J* = 3.0 Hz, *J* = 2.8 Hz, *J* = 1.7 Hz, 1H), 3.45 (*ddd*, *J* = 11.0 Hz, *J* = 9.3 Hz, *J* = 4.4 Hz, 1H), 3.38-3.32 (*m*, 2H), 2.52-2.43 (*m*, 3H), 2.43-2.33 (*m*, 3H), 2.23-2.17 (*m*, 2H), 2.21 (*ddd*, *J* = 12.8 Hz, *J* = 4.4 Hz, *J* = 2.8 Hz, 1H), 1.89-1.83 (*m*, 2H), 1.87-1.75 (*m*, 6H), 1.71 (*ddd*, *J* = 12.8 Hz, *J* = 11.0 Hz, *J* = 3.0 Hz, 1H), 1.29 (*d*, *J* = 6.2 Hz, 3H), 1.283 (*d*, *J* = 6.2 Hz, 3H), 1,277 (*d*, *J* = 6.2 Hz, 3H), 1.14 (*d*, *J* = 6.1 Hz, 3H), 1.13 (*d*, *J* = 6.0 Hz, 3H), 1.10 (*d*, *J* = 6.1 HZ, 3H), **^{13}CNMR** (150 MHz, $CDCl_3$) δ (ppm) 173.4, 172.2, 138.2, 127.9, 94.0, 93.4, 75.6, 75.3, 75.0, 71.1, 71.3, 70.6, 68.6, 68.3, 31.8, 30.5, 30.2, 29.2, 18.8, 18.0, **HRMS** (ESI-TOF) m/z (M - H)$^-$ calcd for $C_{61}H_{79}O_{16}$ 1067.5368 found 1067.5400 Δppm 3.0.

8.11.4. General procedure for the silyl ethers deprotection

A solution of ascaroside in tetrahydrofuran (100 µl/ µmol of ascaroside) was treated with tetrabutylammonium difluorotriphenylsilicate (8 mg/ µmol of ascaroside). After stirring for 24 h, the mixture was concentrated under reduced pressure. The resulting residue was purified by flash column chromatography on silica gel using a gradient of 35 to 100% ethyl acetate (v/v) in hexane as eluent.

Ascaroside	Amount	Oligomer
Dimer 205	4 mg, 3.9 µmol	**228** (2 mg, 3.5 µmol, 91%)
Trimer 206	4 mg, 2.7 µmol	**229** (2 mg, 2.5 µmol, 93%)
Tetramer 207	3mg, 1.5 µmol	**230** (1.2 mg, 1.2 µmol, 78%)
Pentamer 208	4 mg, 1.6 µmol	**231** (1.3 mg, 1.0 µmol, 65%)

Benzyl(2*E*,4*R*)-4-[[3,6-dideoxy-2-*O*-[(4*R*)-4-[(3,6-dideoxy-α-L-*arabino*-hexopyranosyl)oxy]-1-oxopentyl]-α-L-*arabino*-hexopyranosyl]oxy]-2-pentenoate (228).

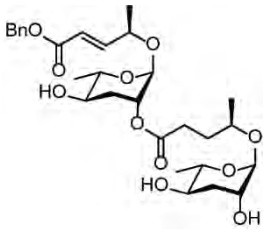

^{1}H NMR (600 MHz, $CDCl_3$) δ (ppm) 7.39-7.32 (*m*, 5H), 6.96 (*dd*, *J* = 15.7 Hz, *J* = 5.3 Hz, 1H), 6.05 (*dd*, *J* = 15.7 Hz, *J* = 1.6 Hz, 1H), 5.21 (*d*, *J* = 12.4 Hz, 1H), 5.18 (*d*, *J* = 12.4 Hz, 1H), 4.90 (*dd*, *J* = 3.6 Hz, *J* = 3.2 Hz, 1H), 4.76 (*br.s*, 1H), 4.70 (*br.s*, 1H), 4.41 (*qdd*, *J* = 6.0 Hz, *J* = 5.3 Hz, *J* = 1.6 Hz, 1H), 3.86 (*m*, 1H), 3.80 (*dd*, *J* = 3.6 Hz, *J* = 3.2 Hz, 1H), 3.61 (*dq*, *J* = 9.6 Hz, *J* = 6.1 Hz, 1H), 3.57 (*ddd*, *J* = 11.0 Hz, *J* = 9.6 Hz, *J* = 4.4 Hz, 1H), 3.57 (*m*, 1H), 3.57 (*m*, 1H), 2.54-2.42 (*m*, 2H), 2.09 (*ddd*, *J* = 13.8 Hz, *J* = 4.2 Hz, *J* = 3.6 Hz, 1H), 2.07 (*ddd*, *J* = 13.8 Hz, *J* = 4.4 Hz, *J* = 3.6 Hz, 1H), 1.93-1.73 (*m*, 1H), 1.92 (*ddd*, *J* = 13.8 Hz, *J* = 10.9 Hz, *J* = 3.2 Hz, 1H), 1.80 (*ddd*, *J* = 13.8 Hz, *J* = 11.0 Hz, *J* = 3.2 Hz, 1H), 1.28 (*d*, *J* = 5.9 Hz, 3H), 1.28 (*d*, *J* = 6.6 Hz, 3H), 1.23 (*d*, *J* = 6.1 Hz, 3H), 1.16 (*d*, *J* = 6.0 Hz, 3H), **^{13}CNMR** (150 MHz, $CDCl_3$) δ (ppm) 172.9, 160.4, 149.5, 128.7, 128.5, 128.45, 120.0, 95.6, 94.1, 71.2, 70.9, 70.4, 70.0, 69.2, 68.2, 68.1, 66.6, 35.3, 32.7, 31.9, 30.4, 29.9, 19.3, 18.8, 17.8, **HR-MS** (ESI-TOF) m/z $(M + Na)^+$ calcd for $C_{29}H_{42}O_{11}Na$ 589.2625 found 589.2648, Δppm 3.9.

Benzyl(2*E*, 4*R*)-4-[[3,6-dideoxy-2-*O*-[(4*R*)-4-[3,6-dideoxy-2-*O*-[(4*R*)-4-[3,6-dideoxy- α-L-*arabino*-hexopyranosyl]oxy]-1-oxopentyl]-α-L-*arabino*-hexopyranosyl]oxy]-1-oxopentyl]-α-L-*arabino*-hexopyranosyl]oxy]-2-pentenoate (229).

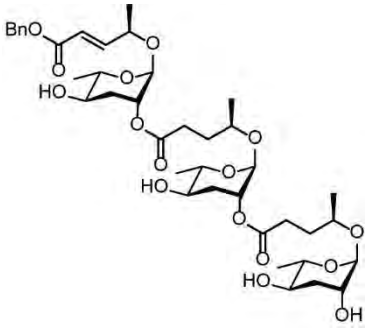

^{1}H NMR (600 MHz, $CDCl_3$) δ (ppm), 7.42-7.37 (*m*, 5H), 6.96 (dd, *J* = 15.7 Hz, 5.3 Hz, 1H), 6.05 (*dd*, *J* = 15.7 Hz, *J* = 1.6 Hz, 1H), 5.21 (*d*, *J* = 12.4 Hz, 1H), 5.18 (d, *J* = 12.4 Hz, 1H), 4.89 (*dd*, *J* = 3.9 Hz, *J* = 3.1 Hz, 1H), 4.83 (*dd*, *J* = 3.8 Hz, *J* = 3.2 Hz, 1H), 4.76 (*br.s*, 1H), 4.75 (*br.s*, 1H), 4.70 (*br.s*, 1H), 4.41 (*qd*, *J* = 6.5 Hz, *J* = 5.3 Hz, 1H), 3.86 (*m*, 1H), 3.80 (*dd*, *J* = 3.6 Hz, *J* = 3.2 Hz, 1H), 3.62 (*dq*, *J* = 9.4 Hz, *J* = 6.1 Hz, 1H), 3.58 (*m*, 1H), 3.52 (*m*, 1H), 2.56-2.50 (*m*, 2H), 2.48-2.41 (*m*, 2H), 2.08 (*ddd*, *J* =13.8 Hz, *J* = 4.7 Hz, *J* = 3.9 Hz, 1H), 2.076 (*ddd*, *J* = 13.3 Hz, *J* = 4.9 Hz, *J* = 3.9 Hz, 1H), 2.07 (*ddd*, *J* = 13.2 Hz, *J* = 4.4 Hz, *J* = 3.6 Hz, 1H), 1.92 (*ddd*, *J* = 13.8 Hz, *J* = 11.3 Hz, *J* = 3.1 Hz, 1H), 1.91-1.85 (*m*, 2H), 1.86 (*ddd*, *J* = 13.3 Hz,

J = 11.0 Hz, *J* = 3.2 Hz, 1H), 1.83-1.75 (*m*, 2H), 1.78 (*ddd*, *J* = 13.2 Hz, *J* = 10.3 Hz, *J* = 3.2 Hz, 1H) 1.284 (*d*, *J* = 6.5 Hz, 3H), 1.28 (*d*, *J* = 5.9 Hz, 3H), 1.27 (*d*, *J* = 6.0 Hz, 3H), 1.22 (*d*, *J* = 6.1 Hz, 3H), 1.165 (*d*, *J* = 6.1 Hz, 3H), 1.164 (*d*, *J* = 6.0 Hz, 3H), **^{13}C NMR**(150 MHz, $CDCl_3$): δ (ppm) 172.8, 166.4, 128.7, 128.5, 128.4, 95.5, 94.2, 71.3, 71.28, 71.1, 70.6, 70.2, 70.0, 69.5, 69.3, 68.2, 68.1, 68.0, 66.5, 35.9, 32.8, 31.9, 31.88, 30.5, 30.3, 19.3, 18.8, 17.8, 17.6, 14.4, **HR-MS** (ESI-TOF) m/z $(M + Na)^+$ calcd for $C_{40}H_{60}O_{16}Na$ 819.3779, found 819.3779, Δ -1.6 ppm, $(M_2 + Na)^+$ calcd for $C_{80}H_{120}O_{32}Na$ 1615.7660, found 1615.7687, Δ 1.7 ppm.

Benzyl(2*E*, 4*R*)-4-[[3,6-dideoxy-2-*O*-[(4*R*)-4-[3,6-dideoxy-2-*O*-[(4*R*)-4-[3,6-dideoxy-2-*O*-[(4*R*)-4-[(3,6-dideoxy- α-L-*arabino*-hexopyranosyl)oxy]-1-oxopentyl]-α-L-*arabino*-hexopyranosyl]oxy]-α-L-*arabino*-hexopyranosyl]oxy]-1-oxopentyl]-α-L-*arabino*-hexopyranosyl]oxy]-1-oxopentyl]-α-L-*arabino*-hexopyranosyl]oxy]-2-pentenoate (230).

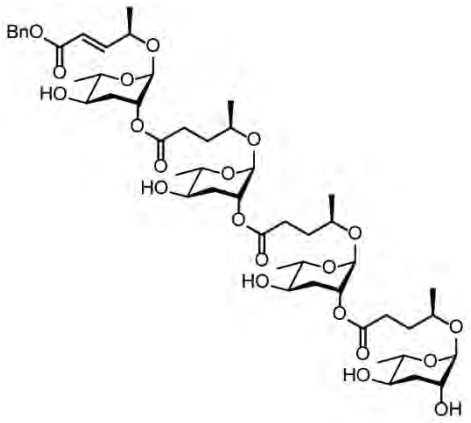

^{1}H NMR (600 MHz, $CDCl_3$) δ (ppm), 7.41-7.30 (*m*, 5H), 6.96 (*dd*, *J* = 15.8 Hz, 5.3 Hz, 1H), 6.05 (*dd*, *J* = 15.8 Hz, 1.6 Hz, 1H), 5.21 (*d*, *J* = 12.3 Hz, 1H), 5.18(*d*, *J* = 12.3 Hz, 1H), 4.90 (*dd*, *J* = 3.7 Hz, *J* = 3.1 Hz, 1H), 4.84 (d*d*, *J* = 3.6 Hz, *J* = 3.3 Hz, 1H), 4.82 (*dd*, *J* = 3.9 Hz, *J* = 3.1 Hz, 1H), 4.76 (*br.s*, 1H), 4.75 (*br.s*, 2H), 4.70 (*br.s*, 1H), 4.41 (*dq*, *J* = 6.4 Hz, *J* = 5.3 Hz, 1H), 3.89-3.82 (*m*, 3H), 3.80 (*dd*, *J* = 3.6 Hz, *J* = 2.8 Hz, 1H), 3.62 (*dq*, *J* = 9.0 Hz, *J* = 6.2 Hz, 1H), 3.60 (*dq*, *J* = 9.3 Hz, *J* = 6.2 Hz, 1H), 3.55 (*ddd*, *J* = 10.8 Hz, *J* = 9.5 Hz, *J* = 4.5 Hz, 1H), 3.55-3.50 (*m*, 3H), 3.53 (*ddd*, *J* = 11.3 Hz, *J* = 9.2 Hz, *J* = 4.4 Hz, 1H), 3.52 (*dq*, *J* = 9.3 Hz, *J* = 6.3 Hz, 1H), 2.59-2.48 (*m*, 3H), 2.48-2.40 (*m*, 3H), 2.09 (*ddd*, *J* = 13.9 Hz, *J* = 4.4 Hz, *J* = 3.7 Hz, 1H), 2.08 (*ddd*, *J* = 13.3 Hz, *J* = 4.2 Hz, *J* = 3.6 Hz, 1H), 2.07 (*ddd*, *J* = 14.0 Hz, *J* = 4.5 Hz, *J* = 3.9 Hz, 1H), 2.06 (*ddd*, *J* = 13.6 Hz, *J* = 4.5 Hz, *J* = 3.6 Hz, 1H), 1.92 (*ddd*, *J* = 13.9 Hz, *J* = 11.3 Hz, *J* = 3.2 Hz, 1H), 1.92-1.84 (*m*, 6H), 1.87 (*ddd*, *J* = 14.0 Hz, *J* = 11.5 Hz, *J* = 3.1 Hz, 1H), 1.84 (*ddd*, *J* = 13.3 Hz, *J* = 11.1 Hz, *J* = 3.3 Hz, 1H), 1.28 (*d*, *J* = 6.4 Hz, 3H), 1.28-1.26 (*m*, 6H), 1.27(*d*, *J* = 6.3 Hz, 3H), 1.22 (*d*, *J* = 6.2 Hz, 3H), 1.17 (*d*, *J* = 6.0 Hz, 3H), 1.166 (*d*, *J* = 6.1 Hz, 3H), 1.16 (*d*, *J* = 6.0 Hz, 3H), **^{13}C NMR**(150 MHz, $CDCl_3$): δ (ppm) 172.6, 166.4, 149.3, 128.4, 128.1, 119.7, 95.3, 94.0, 92.4, 71.1, 71.0, 70.9, 70.2, 70.0, 69.9, 69.7, 69.4, 67.8, 66.3, 35.0, 32.5, 31.5, 30.1, 29.5, 19.1, 18.6, 17.6, 17.5, **HRMS** (ESI-TOF) m/z $(M + Na)^+$ calcd

for $C_{51}H_{78}O_{21}Na$ 1049.4953, found 1049.4949, Δ 1.5 ppm.

Benzyl(2*E*, 4*R*)-4-[[3,6-dideoxy-2-*O*-[(4*R*)-4-[3,6-dideoxy-2-*O*-[(4*R*)-4-[3,6-dideoxy-2-O-[(4*R*)-4-[3,6-dideox-2-*O*-[(4*R*)-4-[(3,6-dideoxy-α-L-*arabino*-hexopyranosyl)oxy]-1-oxopentyl]-α-L-*arabino*-hexopyranosyl]oxy]-1-oxypentyl]-α-L-*arabino*-hexopyranosyl]oxy]-1-oxopentenyl]-α-L-*arabino*-hexopyranosyl]oxy]-1-oxopentyl]-α-L-*arabino*-hexopyranosyl]oxy]-pentenoate (231).

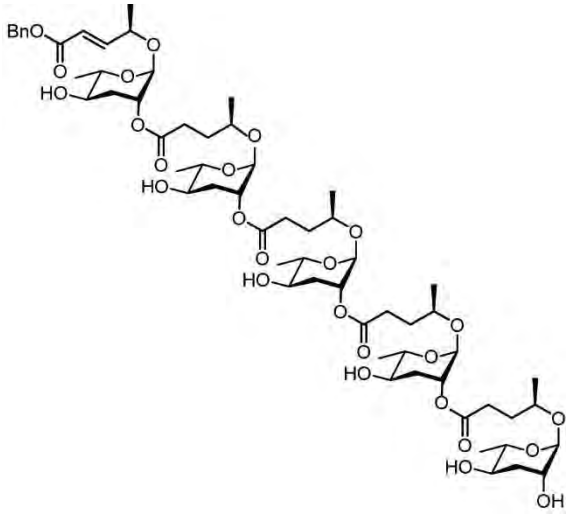

^{1}H NMR (600 MHz, $CDCl_3$) δ (ppm) 7.39-7.32 (*m*, 5H), 6.97 (*dd*, *J* = 15.7 Hz, *J* = 5.3 Hz, 1H), 6.05 (*dd*, *J* = 15.7 Hz, *J* = 1.6 Hz, 1H), 5.20 (*d*, *J* = 12.3 Hz, 1H), 5.18 (*d*, *J* = 12.3 Hz, 1H), 4.90 (*dd*, *J* = 4.1 Hz, *J* = 3.0 Hz, 1H), 4.841 (*dd*, *J* = 3.8 Hz, *J* = 3.0 Hz, 1H), 4.84-4.82 (*m*, 2H), 4.76 (*br.s*, 1H), 4.75 (*br.s*, 1H), 4.74 (*br.s*, 1H), 4.70 (*br.s*, 1H), 4.41 (*qd*, *J* = 6.5 Hz, *J* = 5.3 Hz, 1H), 3.89-3.81 (*m*, 4H), 3.80 (*dd*, *J* = 3.7 Hz, *J* = 3.1 Hz, 1H), 3.62 (*dq*, *J* = 9.1 Hz, *J* = 6.2 Hz, 1H), 3.598 (*dq*, *J* = 9.6 Hz, *J* = 6.2 Hz, 1H), 3.58-3.538 (*m*, 2H), 3.538 (*ddd*, *J* = 10.1 Hz, *J* = 9.5 Hz, *J* = 4.6 Hz, 1H), 3.534-3.478 (*m*, 2H), 3.531 (*ddd*, *J* = 11.5 Hz, *J* = 9.1 Hz, *J* = 4.7 Hz, 1H), 3.525 (*dq*, *J* = 9.5 Hz, *J* = 6.3 Hz, 1H), 3.52 (*ddd*, *J* = 11.4 Hz, *J* = 9.6 Hz, *J* = 4.6 Hz, 1H), 2.60-2.54 (*m*, 2H), 2.53-2.49 (*m*, 2H), 2.47-2.429 (*m*, 2H), 2.427-2.39 (*m*, 2H), 2.085 (*ddd*, *J* = 13.6 Hz, *J* = 4.7 Hz, *J* = 4.1 Hz ,1H), 2.084 (*ddd*, *J* = 13.6 Hz, *J* = 4.6 Hz, *J* = 3.8 Hz ,1H), 2.078 (*ddd*, *J* = 13.5 Hz, *J* = 4.6 Hz, *J* = 3.8 Hz ,1H), 2.058 (*ddd*, *J* = 12.9 Hz, *J* = 4.6 Hz, *J* = 3.7 Hz ,1H), 2.057 (*ddd*, *J* = 13.2 Hz, *J* = 4.6 Hz, *J* = 3.9 Hz ,1H), 1.92 (*ddd*, *J* = 13.6 Hz, *J* = 11.5 Hz, *J* = 3.0 Hz, 1H), 1.905-1.751 (*m*, 8H), 1.89-1.83 (*m*, 2H), 1.85 (*ddd*, 13.5 Hz, *J* = 11.4 Hz, *J* = 3.0 Hz, 1H), 1.78 (*ddd*, *J* = 12.9 Hz, *J* = 10.1 Hz, *J* = 3.1 Hz, 1H), 1.28 (*d*, *J* = 6.5 Hz, 3H), 1.275 (*d*, *J* = 6.2 Hz, 3H),1.272 (*d*, *J* = 6.2 Hz, 3H), 1.270 (*d*, *J* = 6.1 Hz, 3H), 1.269 (*d*, *J* = 6.2 Hz, 3H), 1.22 (*d*, *J* = 6.2 Hz, 3H), 1.168 (*d*, *J* = 6.1 Hz, 3H), 1.16 (*d*, *J* = 6.1 Hz, 3H), **^{13}C NMR**(150 MHz, $CDCl_3$): δ (ppm) 172.61, 172.58, 172.5, 172.3, 166.2, 149.3, 135.8, 128.3, 95.4, 94.2, 92.8, 92.5, 71.1, 71.1, 70.8, 70.1, 69.9, 69.7, 69.0, 67.8, 66.2, 35.2, 32.5, 31.7, 31.5, 30.3, 30.2, 30.0, 29.5, 18.9, 18.6, 17.6.

8.11.5. General procedure for the *O*-debenzylation of ascaroside oligomers

The ascaroside *O*-benzyl ester was added to a suspension of palladium on carbon (10%, 1 mg/mg of ascaroside) in methanol (500 µl/mg of ascaroside) then H_2 (1 atm) was added to the mixture. The solution was stirred for 5 h of the reaction then filtered over a cotton plug and the catalyst rinsed with ethyl acetate. The filtrate was concentrated under reduced pressure and the given residue purified by flash column chromatography using a gradient of 0 to 10% methanol in dichloromethane as eluent.

Ascaroside	Amount	Oligomer
Dimer 228	1.1 mg, 3.5 µmol	**40** (1,1 mg, 1.9 µmol, 79%)
Trimer 229	1.4 mg, 2.4 µmol	**41** (1.4 mg, 1.8 µmol, 78 %)
Benzylated trimer 221	0.5 mg, 0.4 µmol	**41** (0.2 mg, 0.3, µmol, 75 %)
Tetramer 230	2 mg, 1.9 µmol	**42** (0.7 mg, 1 µmol, 53%)

(4*R*)-4-[[3,6-dideoxy-2-*O*-[(4*R*)-4-[(3,6-dideoxy-α-L-*arabino*-hexopyranosyl)oxy]-1-oxopentyl]-α-L-*arabino*-hexopyranosyl]oxy]-2-pentanoic acid , 2'-(asc-C5)-asc-C5, (40).

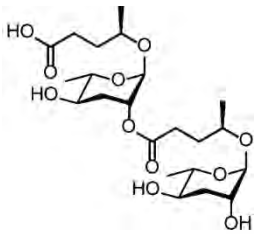

^{1}H NMR (600 MHz, CD_3OD) δ (ppm) 4.79 (*dd*, *J* = 3.7 Hz, 3.1 Hz, 1H), 4.72 (*br.s*, 1H), 4.65 (*br.s*, 1H), 3.85 (*m*, 1H), 3.82 (*m*, 1H), 3.71 (d*dd*, *J* = 3.8 Hz, *J* = 3.1 Hz, *J* = 1.7 Hz, 1H), 3.70 (*dq*, *J* = 9.5 Hz, *J* = 6.6 Hz, 1H), 3.51 (*ddd*, *J* = 11.5 Hz, *J* = 9.5 Hz, *J* = 4.6 Hz, 1H), 3.57 (*dq*, *J* = 9.7 Hz, *J* = 6.2 Hz, 1H), 3.38 (*ddd*, *J* = 11.5 Hz, *J* = 9.5 Hz, *J* = 4.6 Hz, 1H), 2.54-2.45 (*m*, 2H), 2.36 (*dt*, *J* = 14.4 Hz, *J* = 8.1 Hz, 1H), 2.28 (*dt*, *J* = 14.4 Hz, *J* = 7.8 Hz, 1H), 2.01 (*ddd*, *J* = 13.4 Hz, *J* = 4.6 Hz, *J* = 3.7 Hz, 1H), 1.95 (*ddd*, *J* = 13.3 Hz, *J* = 4.6 Hz, *J* = 3.8 Hz, 1H), 1.89 (*ddd*, *J* = 13.4 Hz, *J* = 11.5 Hz, *J* = 3.1 Hz, 1H), 1.89-1.76 (*m*, 2H), 1.84-1.80 (*m*, 2H), 1.76 (*ddd*, *J* = 13.3 Hz, *J* = 11.5 Hz, *J* = 3.1 Hz, 1H), 1.22 (*d*, *J* = 6.6 Hz, 3H), 1.22 (*d*, *J* = 6.2 Hz, 3H), 1.16 (*d*, *J* = 6.3 Hz, 3H), 1.15 (*d*, *J* = 6.3 Hz, 3H), **^{13}C NMR**(150 MHz, CD_3OD) δ (ppm) 179.8, 172.7, 97.0, 94.1, 72.5, 71.2, 70.9, 70.6, 69.6, 68.3, 68.0, 35.6, 34.2, 33.2, 32.0, 31.0, 18.7, 17.7 (**Figure 106**), **HRMS** (ESI-TOF) m/z $(M - H)^-$ calcd for $C_{22}H_{38}O_{11}$ 477.2336, found 477.2335, Δ -0.2 ppm, $(M_2 - H)^-$ calcd for $C_{44}H_{75}O_{22}$ 955.4750, found 955.4745, Δ -0.5 ppm.

(4*R*)-4-[[3,6-dideoxy-2-*O*-[(4*R*)-4-[3,6-dideoxy-2-*O*-[(4*R*)-4-[3,6-dideoxy- α-L-*arabino*-hexopyranosyl]oxy]-1-oxopentyl]-α-L-*arabino*-hexopyranosyl]oxy]-1-oxopentyl]-α-L-*arabino*-hexopyranosyl]oxy]-pentanoic acid, [2'-(asc-C5)]$_2$-asc-C5, (41).

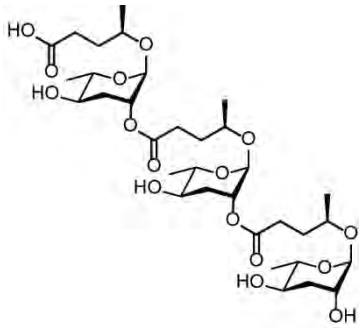

^{1}H NMR (600 MHz, CD_3OD) δ (ppm), 4.79 (*dd*, *J* = 4.1 Hz, 3.2 Hz, 2H), 4.73 (*br.s*, 2H), 4.65 (*br.s*, 1H), 3.845 (*m*, 1H), 3.845 (*m*, 1H), 3.824 (*m*, 1H), 3.72 (*dd*, *J* = 3.7 Hz, *J* = 3.2 Hz, 1H), 3.696 (*dq*, *J* = 9.5 Hz, *J* = 6.2 Hz, 1H), 3.62 (*dq*, *J* = 9.5 Hz, *J* = 6.3 Hz, 1H), 3.57 (*dq*, *J* = 9.7 Hz, *J* = 6.1 Hz, 1H), 3.51 (*ddd*, *J* = 11.1 Hz, *J* = 9.7 Hz, *J* = 4.6 Hz, 1H), 3.42 (*ddd*, *J* = 11.4 Hz, *J* = 9.8 Hz, *J* = 5.1 Hz, 1H), 3.39 (*ddd*, *J* = 11.2 Hz, *J* = 9.5 Hz, *J* = 4.9 Hz, 1H), 2.55-2.45 (*m*, 4H), 2.37 (*dt*, *J* = 15.0 Hz, *J* = 8.2 Hz, 1H), 2.30 (*dt*, *J* = 15.0 Hz, *J* = 7.5 Hz, 1H), 2.023 (*ddd*, *J* = 13.5 Hz, *J* = 5.1 Hz, *J* = 4.1 Hz, 1H), 2.015 (*ddd*, *J* = 12.9 Hz, *J* = 5.1 Hz, *J* = 4.1 Hz, 1H), 1.95 (*ddd*, *J* = 13.3 Hz, *J* = 4.6 Hz, *J* = 3.7 Hz, 1H), 1.89 (*ddd*, *J* = 12.9 Hz, *J* = 11.2 Hz, *J* = 3.2 Hz, 1H), 1.870-1.833 (*m*, 2H), 1.85 (*ddd*, *J* = 13.5 Hz, *J* = 11.4 Hz, *J* = 3.2 Hz, 1H), 1.838-1.796 (*m*, 2H), 1.820-1.763 (*m*, 2H), 1.76 (*ddd*, *J* = 13.3 Hz, *J* = 11.1 Hz, *J* = 3.2 Hz, 1H), 1.234 (*d*, *J* = 6.3 Hz, 3H), 1.229 (*d*, *J* = 6.2 Hz, 3H), 1.227 (*d, J* = 6.1 Hz, 3H), 1.163 (*d*, *J* = 6.3 Hz, 3H), 1.156 (d, *J* = 6.3 Hz, 3H), 1.149 (*d*, *J* = 6.1 Hz, 3H), **^{13}C NMR**(150 MHz, CD_3OD) δ (ppm) 178.7, 172.8, 96.9, 94.2, 72.4, 72.0, 71.3, 71.08, 71.0, 70.6, 69.5, 68.4, 68.1, 67.9, 35.7, 34.1, 33.7, 33.0, 32.8, 30.9, 18.8, 17.7 (**Table S 5**), **HRMS** (ESI-TOF) m/z $(M - H)^-$ calcd for $C_{33}H_{55}O_{16}$ 707.3490, found 707.3498, Δ 1.1 ppm.

(4*R*)-4-[[3,6-dideoxy-2-*O*-[(4*R*)-4-[3,6-dideoxy-2-*O*-[(4*R*)-4-[3,6-dideoxy-2-*O*-[(4*R*)-4-[(3,6-dideoxy-α-L-*arabino*-hexopyranosyl)oxy]-1-oxopentyl]-α-L-*arabino*-hexopyranosyl]oxy]-α-L-*arabino*-hexopyranosyl]oxy]-1-oxopentyl]-α-L-*arabino*-hexopyranosyl]oxy]-1-oxopentyl]-α-L-*arabino*-hexopyranosyl]oxy]-pentanoic acid, [2'-(asc-C5)]$_3$-asc-C5 (42).

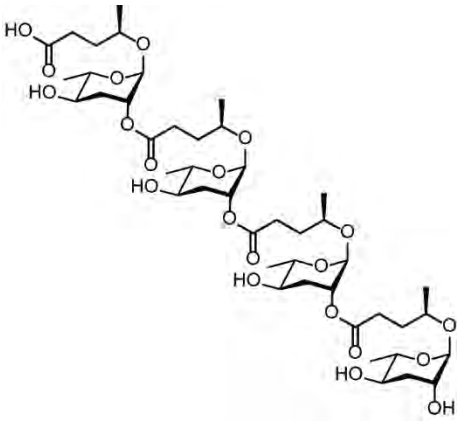

^{1}H NMR (600 MHz, CD_3OD) δ (ppm) 4.79 (*dd*, *J* = 3.9 Hz, *J* = 3.2 Hz, 2H), 4.79 (*dd*, *J* = 3.7 Hz, *J* = 3.1 Hz, 1H), 4.73 (*br.s*, 3H), 4.65 (*br.s*, 1H), 3.854 (*m*, 2H), 3.850 (*m*, 1H), 3.82 (*tq*, *J* = 8.8 Hz, *J* = 6.1 Hz, 1H), 3.72 (*dd*, *J* = 3.9 Hz, *J* = 3.0 Hz, 1H), 3.71 (*dq*, *J* = 9.1 Hz, *J* = 6.2 Hz, 1H), 3.62 (*dq*, *J* = 9.3 Hz, *J* = 6.2 Hz, 2H), 3.57 (*dq*, *J* = 9.3 Hz, *J* = 6.1 Hz, 1H), 3.51 (*ddd*, *J* = 11.2 Hz, *J* = 9.3 Hz, *J* = 4.5 Hz, 1H), 3.42 (*ddd*, *J* = 11.8 Hz, *J* = 9.3 Hz, *J* = 4.7 Hz, 2H), 3.38 (*ddd*, *J* = 11.3 Hz, *J* = 9.1 Hz, *J* = 4.5 Hz, 1H), 2.55-2.45 (*m*, 6H), 2.35 (*dt*, *J* = 14.4 Hz, *J* = 7.3 Hz, 1H), 2.26 (*dt*, *J* = 14.4 Hz, *J* = 6.7 Hz, 1H), 2.02 (*ddd*, *J* = 14.2 Hz, *J* = 4.7 Hz, *J* = 3.9 Hz, 2H), 2.01 (*ddd*, *J* = 13.9 Hz, *J* = 4.5 Hz, *J* = 3.7 Hz, 1H), 1.95 (*ddd*, *J* = 13.3 Hz, *J* = 4.5 Hz, *J* =3.9 Hz, 1H), 1.900 (*ddd*, *J* = 13.9 Hz, *J* = 11.3 Hz, *J* = 3.1 Hz, 1H), 1.895-1.761 (m, 6H), 1.85 (*ddd, J* = 14.2 Hz, *J* = 11.8 Hz, *J* = 3.2 Hz, 2H), 1.82 (*ddt*, *J* = 8.8 Hz, *J* = 7.3 Hz, *J* = 6.7 Hz, 2H), 1.76 (*ddd*, *J* = 13.3 Hz, *J* = 11.2 Hz, *J* = 3.0 Hz, 1H), 1.231 (*d*, *J* = 6.2 Hz, 6H), 1.226 (*d*, *J* = 6.2 Hz, 3H), 1.225 (*d*, *J* = 6.1 Hz, 3H), 1.163 (*d*, *J* = 6.1 Hz, 6H), 1.155 (*d*, *J* = 6.1 Hz, 3H), 1.145 (*d*, *J* = 6.1 Hz, 3H), **^{13}C NMR**(150 MHz, CD_3OD) δ (ppm) 174.33, 172.76, 97.0, 94.1, 72.53, 71.58, 71.00, 70.93, 70.71, 69.63, 68.06, 67.88, 35.64, 33.77, 33.03, 32.52, 30.99, 18.71, 17.74 (**Table S 6**), **HRMS** (ESI-TOF) m/z $(M - H)^-$ calcd for $C_{44}H_{74}O_{21}$ 937.4644, found 937.4654, Δ 1.1 ppm.

(4*R*)-4-[[3,6-dideoxy-2-*O*-[(4*R*)-4-[3,6-dideoxy-2-*O*-[(4*R*)-4-[3,6-dideoxy-2-*O*-[(4*R*)-4-[3,6-dideox-2-*O*-[(4*R*)-4-[(3,6-dideoxy-α-L-*arabino*-hexopyranosyl)oxy]-1-oxopentyl]-α-L-*arabino*-hexopyranosyl]oxy]-1-oxypentyl]-α-L-*arabino*-hexopyranosyl]oxy]-1-oxopentenyl]-α-L-*arabino*-hexopyranosyl]oxy]-1-oxopentyl]-α-L-*arabino*-hexopyranosyl]oxy]-pentanoic acid, [2'-(asc-C5)]$_4$-asc-C5 (43).

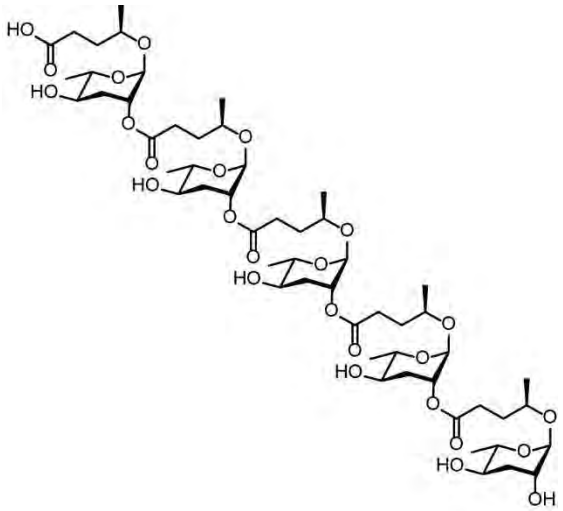

^{1}H NMR (600 MHz, CD_3OD) δ (ppm), 4.79 (*br.s,* 4H), 4.73 (*br.s,* 4H), 4.65 (*br.s*, 1H), 3.88-3.81 (*m*, 5H), 3.72 (*ddd*, *J* = 3.5 Hz, *J* = 3.0 Hz, *J* = 1.6 Hz, 1H), 3.68 (*dq*, *J* = 9.2 Hz, *J* = 6.5 Hz, 1H), 3.62 (*dq*, *J* = 9.1 Hz, *J* = 6.4 Hz, 3H), 3.57 (*dq*, *J* = 9.9 Hz, *J* = 6.5 Hz, 1H), 3.51 (*ddd*, *J* = 11.6 Hz, *J* = 9.9 Hz, *J* = 5.0 Hz, 1H), 3.425 (*ddd*, *J* = 11.6 Hz, *J* = 9.1 Hz, *J* = 4.7 Hz, 3H), 3.416 (*ddd*, *J* = 11.4 Hz, *J* = 9.2 Hz, *J* = 4.7 Hz, 1H), 2.53-2.46 (*m*, 8H), 2.41 (*m*, 1H), 2.36 (*m*, 1H), 2.02 (*ddd*, *J* = 13.8 Hz, *J* = 4.7 Hz, *J* = 3.3 Hz,1H), 2.02 (*ddd*, *J* = 13.2 Hz, *J* = 4.7 Hz, *J* = 3.3 Hz, 3H), 1.95 (*ddd*, *J* = 12.9 Hz, *J* = 5.0 Hz, *J* = 3.0 Hz, 1H), 1.89-1.76 (*m*, 8H), 1.87 (*ddd*, *J* = 13.8 Hz, *J* = 11.4 Hz, *J* = 3.7 Hz, 1H), 1.85 (*ddd*, *J* = 13.2 Hz, *J* = 11.6 Hz, *J* = 3.7 Hz, 3H), 1.84-1.79 (*m*, 2H), 1.76 (*ddd*, *J* = 12.9 Hz, *J* = 11.6 Hz, *J* = 3.5 Hz, 1H), 1.232 (*d*, *J* = 6.4 Hz, 9H), 1.225 (*d*, *J* = 6.5 Hz, 3H), 1.224 (*d*, *J* = 6.5 Hz, 3H), 1.164 (*d*, *J* = 6.1 Hz, 9H), 1.156 (*d*, *J* = 6.0 Hz, 3H), 1.153 (*d*, *J* = 5.9 Hz, 3H) (**Table S 7**), **HRMS** (ESI-TOF) m/z $(M - H)^-$ calcd for $C_{55}H_{92}O_{26}$ 1167.5799, found 1167.5796, Δ -0.3 ppm.

9. Supporting information

Figure S 1: ^{1}H NMR spectra (400 MHz) of the isolated 4'-UC-asc-ΔC9 (37).

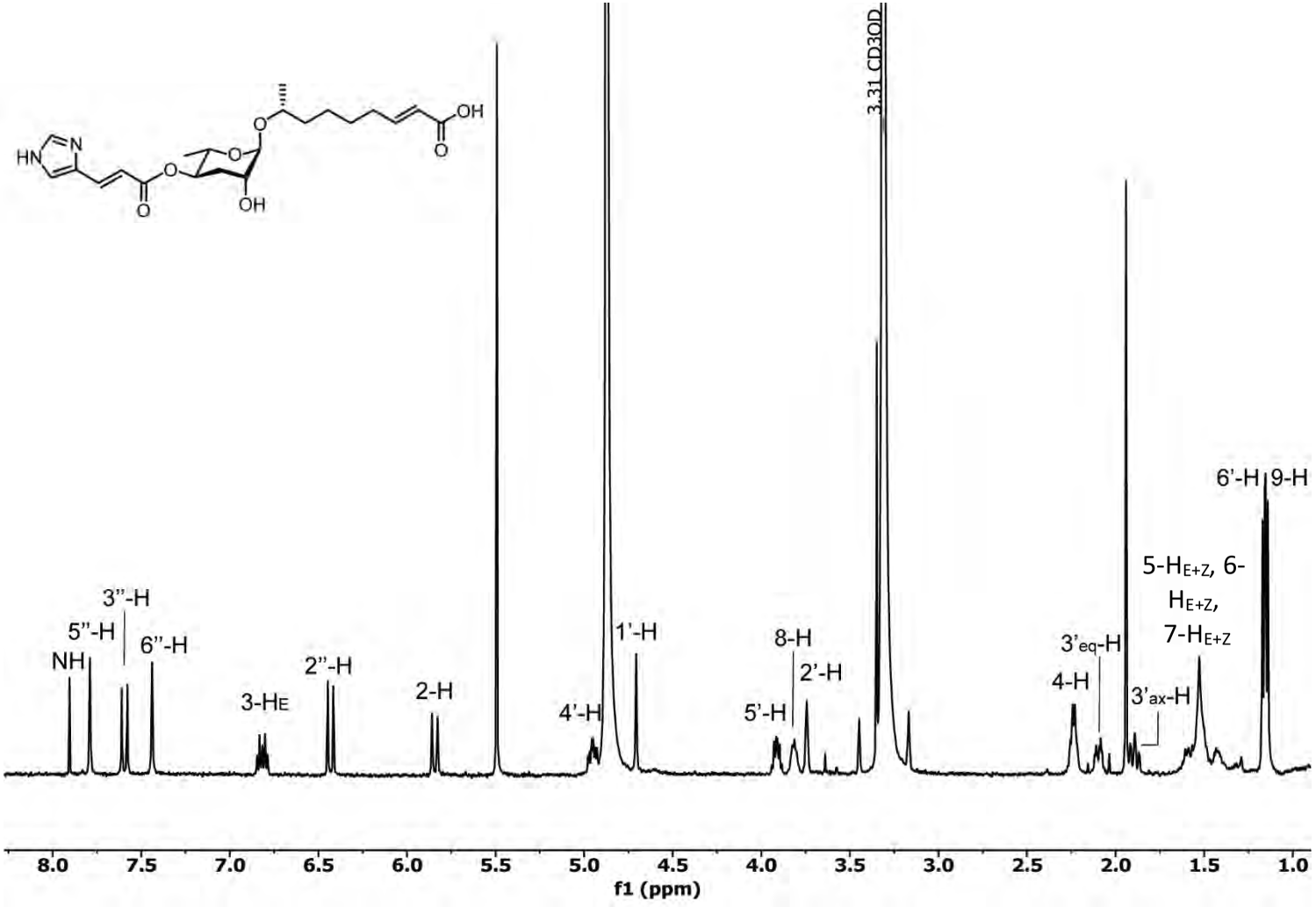

Figure S 2: *dqf*-COSY spectra (400 MHz) of the isolated 4'-UC-asc-ΔC9 (37).

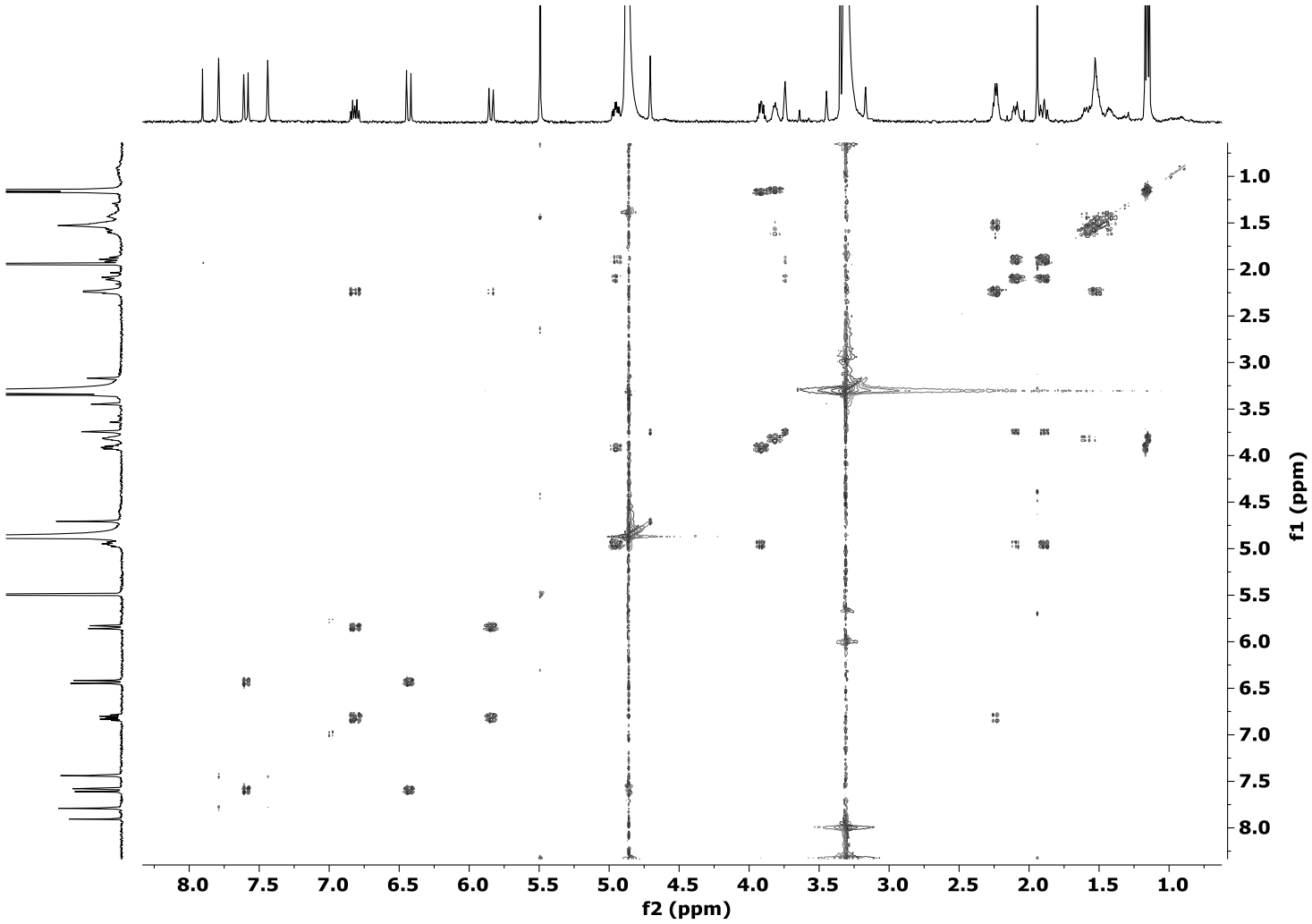

Figure S 3: ^{1}H NMR spectrum (400 MHz) of a mixture of (*E*)-4'-UC-asc-ΔC9 (37) and (*Z*)-4'-UC-asc-ΔC9 (38) enriched from the *C. remanei* exometabolome.

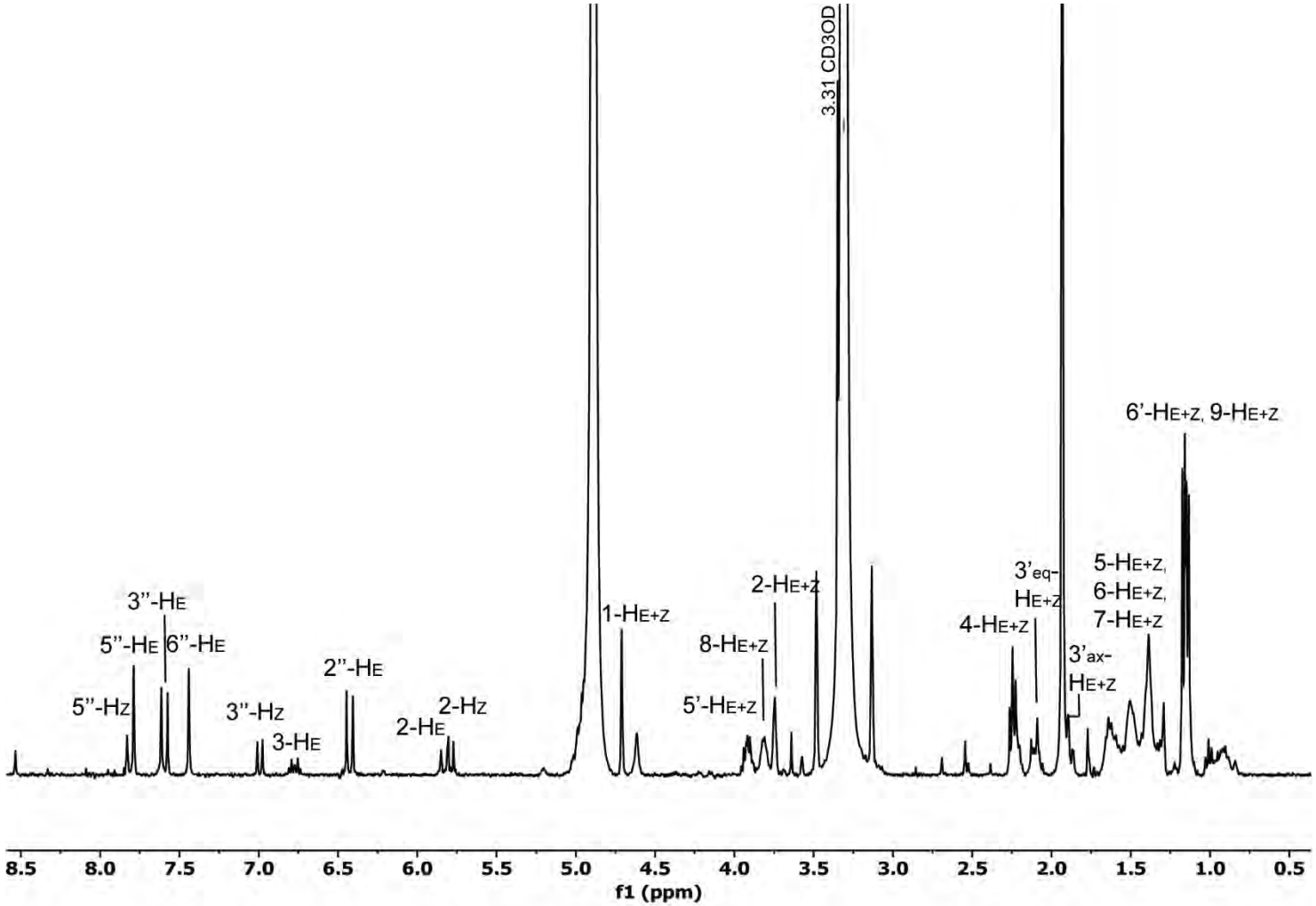

Figure S 4: *dqf*-COSY spectrum (400 MHz) of a mixture of (*E*)-4'-UC-asc-ΔC9 (37) and (*Z*)-4'-UC-asc-ΔC9 (38) enriched from the *C. remanei* exometabolome.

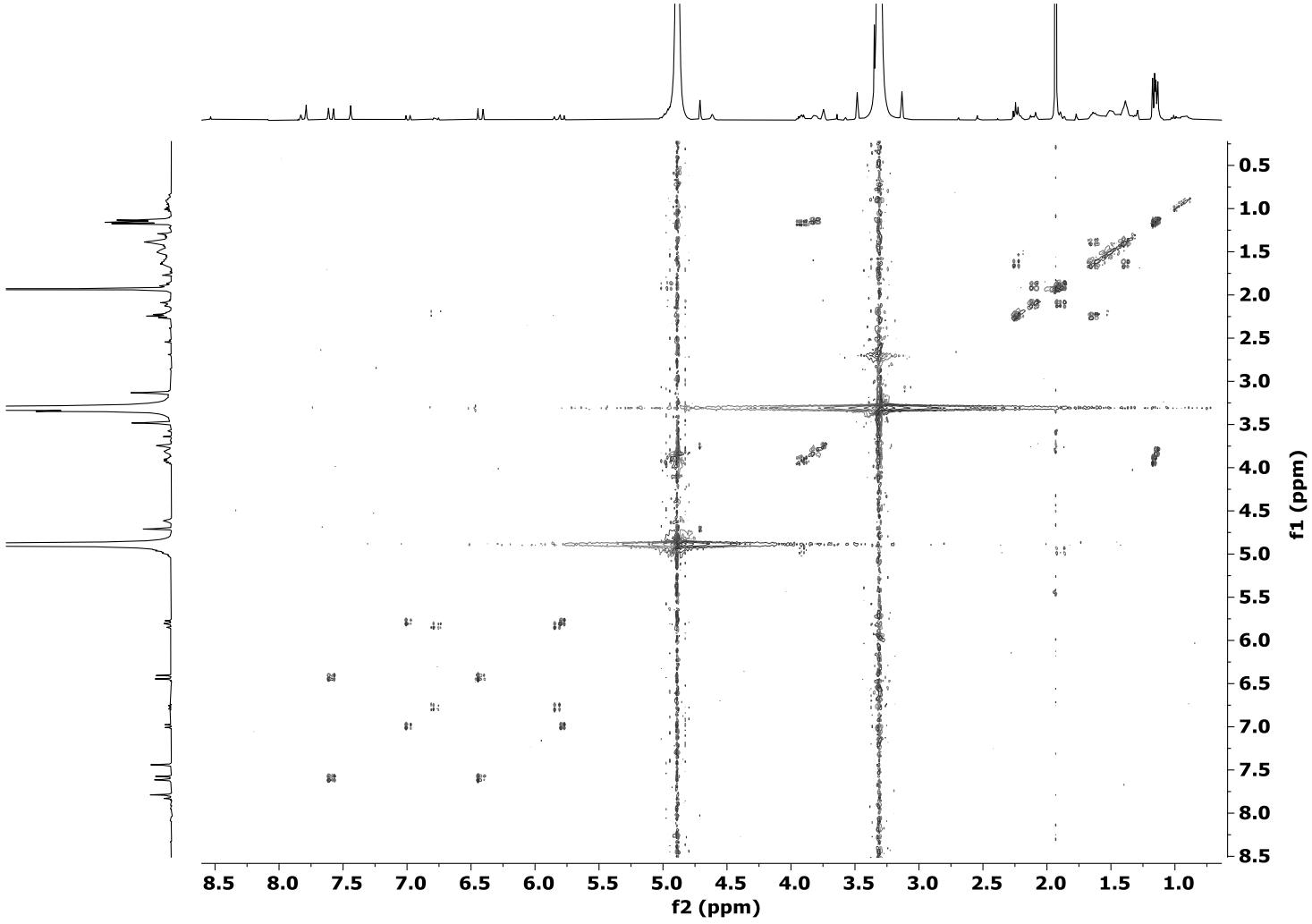

Figure S 5: Comparison of ^{1}H NMR spectra of the enriched mixture of (*Z*) and (*E*)- 4'-UC-asc-ΔC9 (A) the synthetic (B) (*E*)-4'-UC-asc-ΔC9 and the crude synthetic mixture (C) of (*Z*) and (*E*)- 4'-UC-asc-ΔC9.

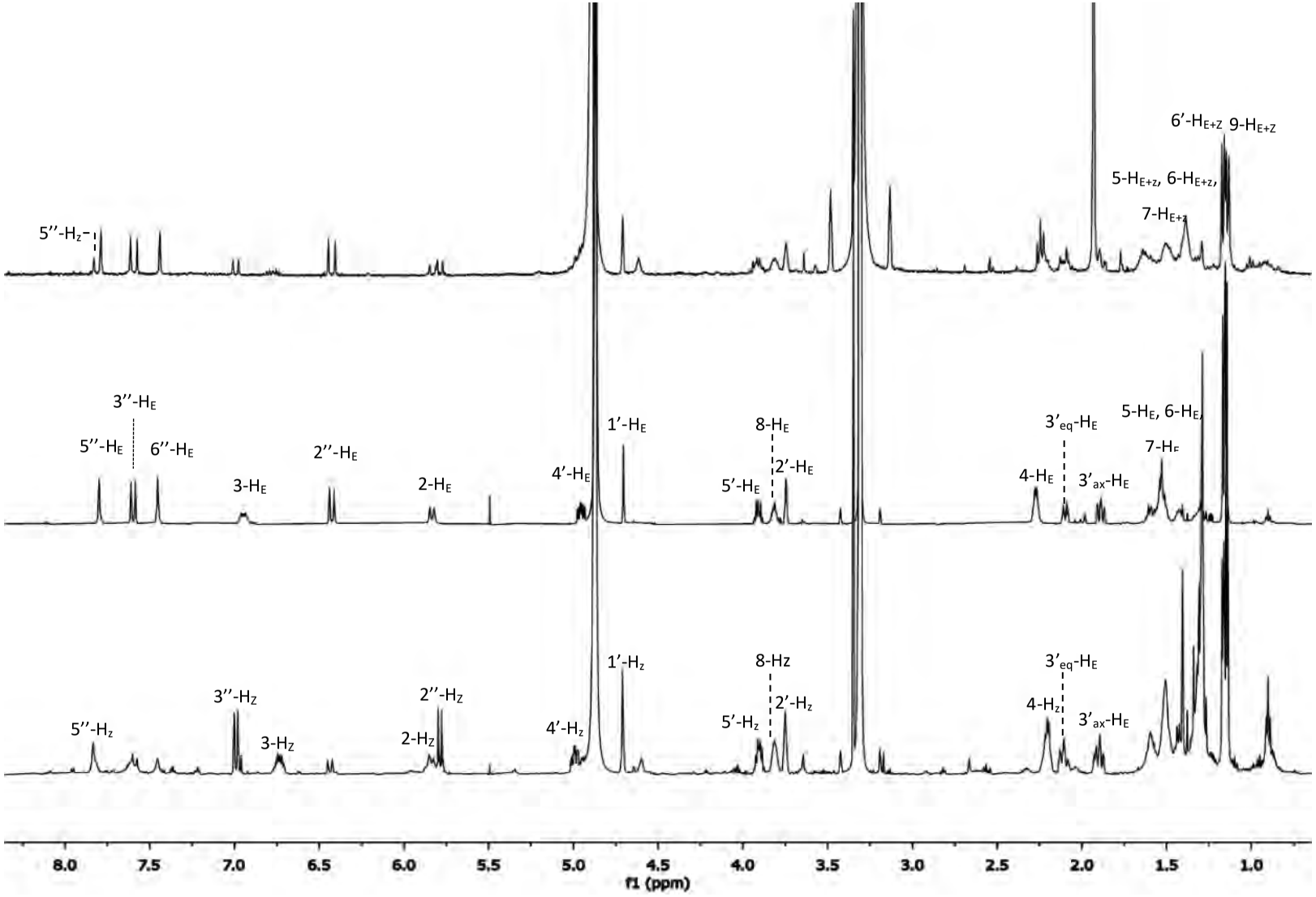

Figure S 6: Production of 4'-UA-asc-ΔC9 (37) in female and male *C. nigoni* and *C. remanei*.

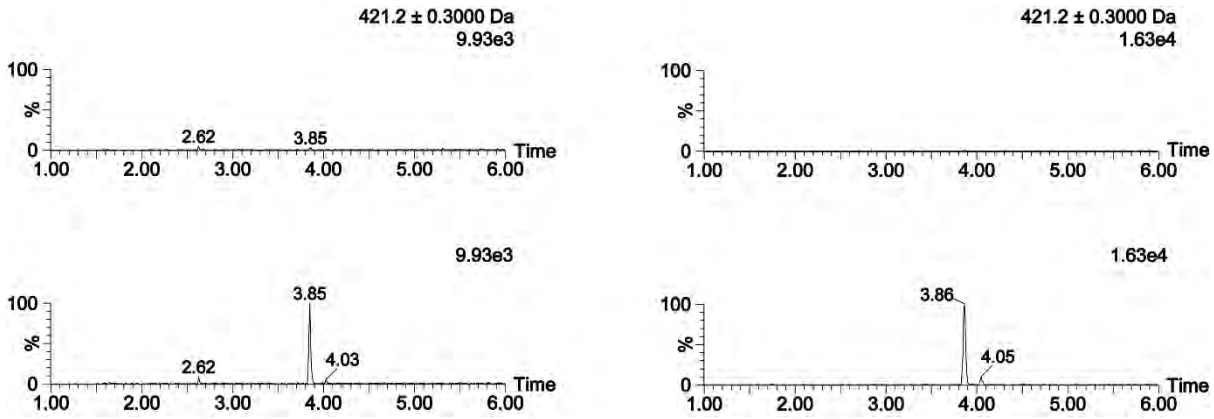

Figure S 7: Comparison of ^{1}H NMR (400 MHz) of the enriched 4'-AB-asc-C5 (34) and the synthetic 4'-(N-methyl-AB)-asc-C5 (147).

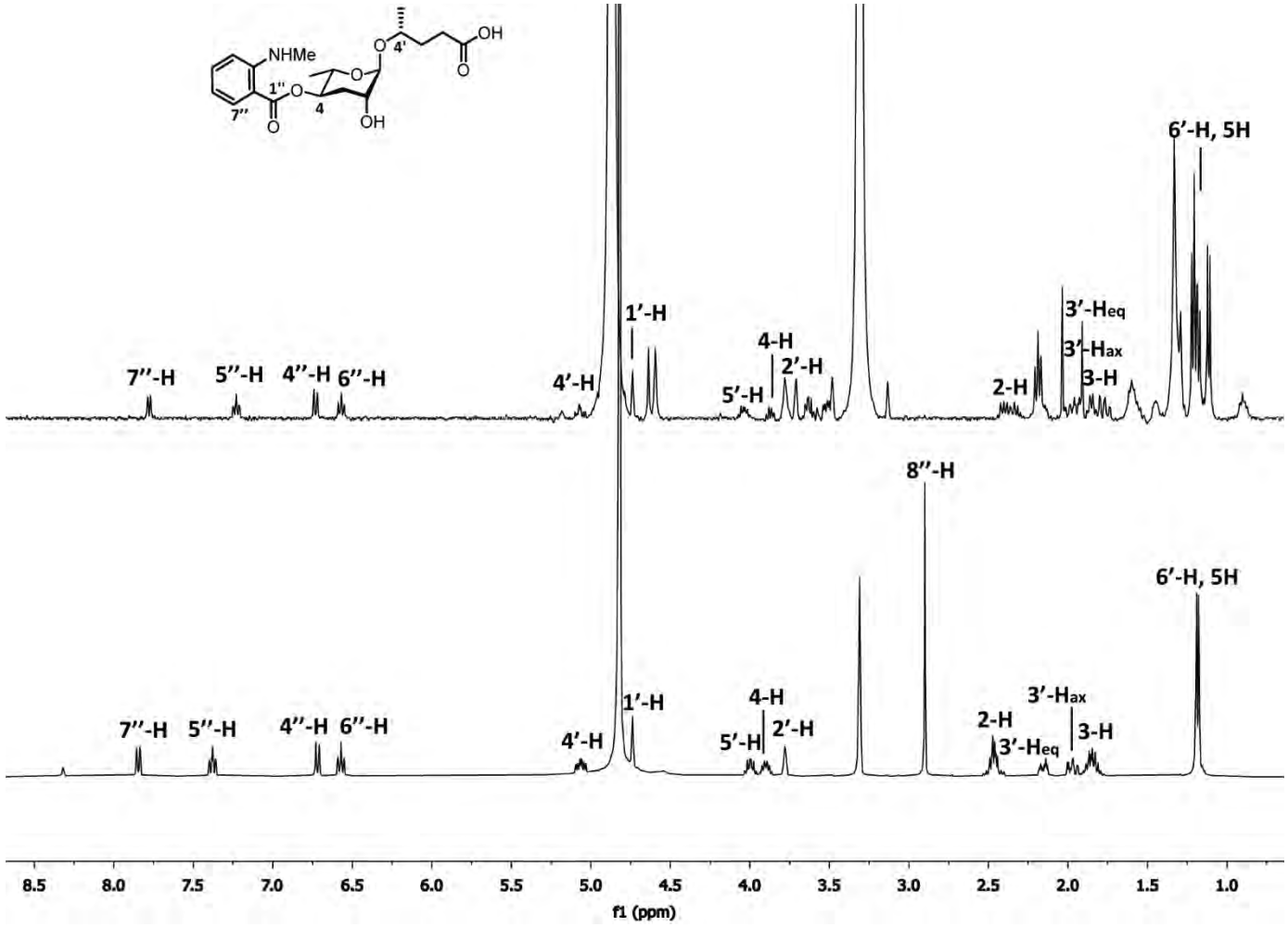

Figure S 8: Comparison of HPLC-ESI-(-)-HR-MS of the enriched 4'-AB-asc-C5 (34) from *C. nigoni* with a 1:1 mixture of the natural and the synthetic 4'-AB-asc-C5 and the synthetic 4'-AB-asc-C5 (34).

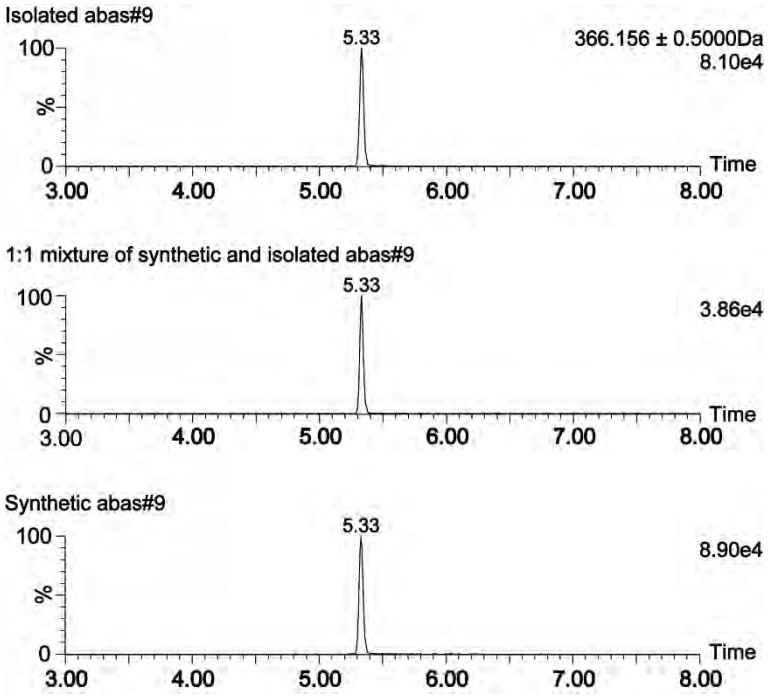

Figure S 9: Comparison of ^{1}H NMR (400 MHz) of the enriched 4'-AB-asc-C5 (34) and the synthetic 4'-AB-asc-C5 (34).

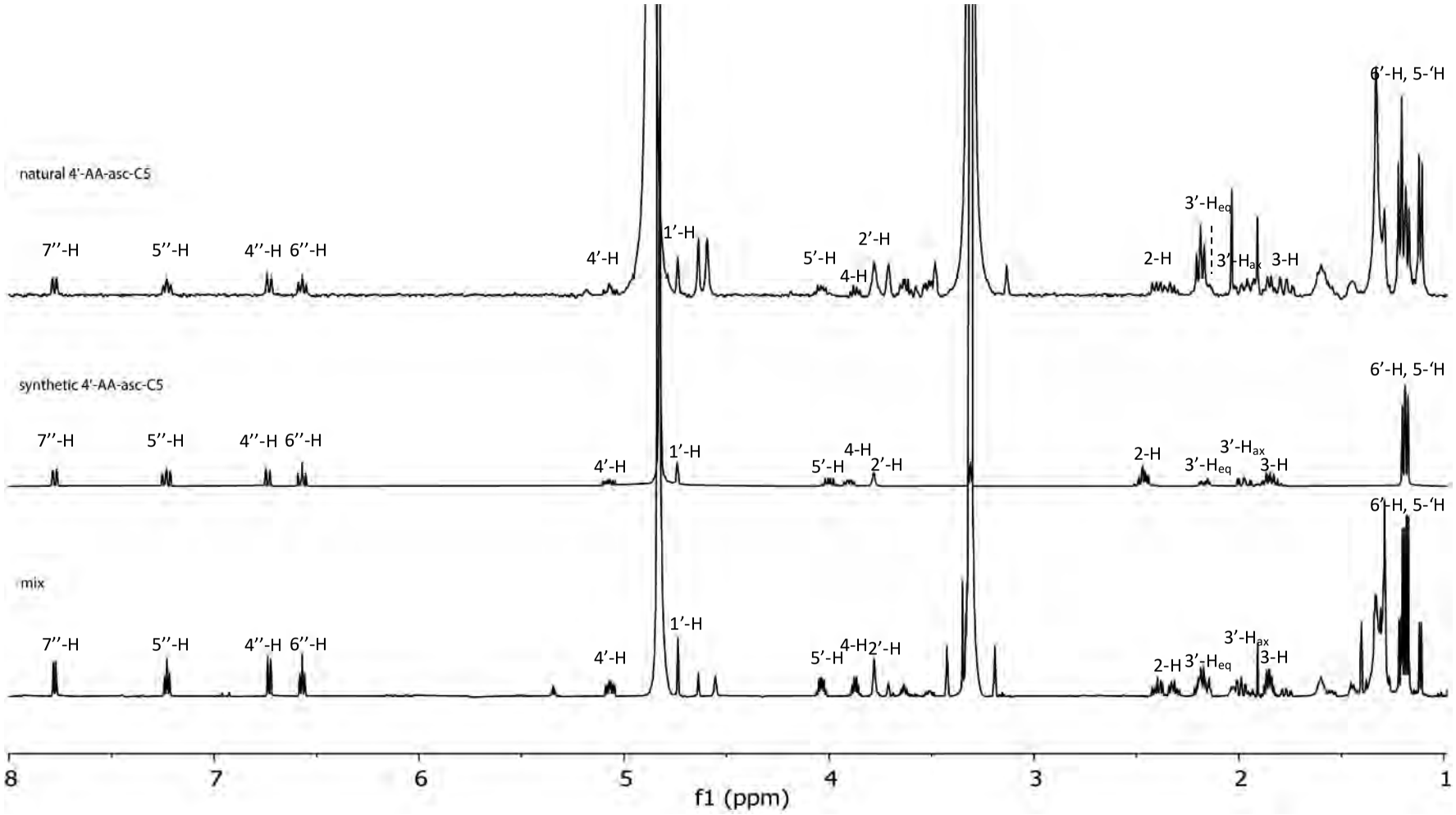

Figure S 10: Comparative analysis of 400 MHz ^{1}H NMR spectra between 4.85 and 3.30 ppm of two consecutive RP-C18 HPLC fractions from *C. nigoni* highlights signals corresponding to asc-C7 (1) and cae-7OH-ΔC9 (39)[92].

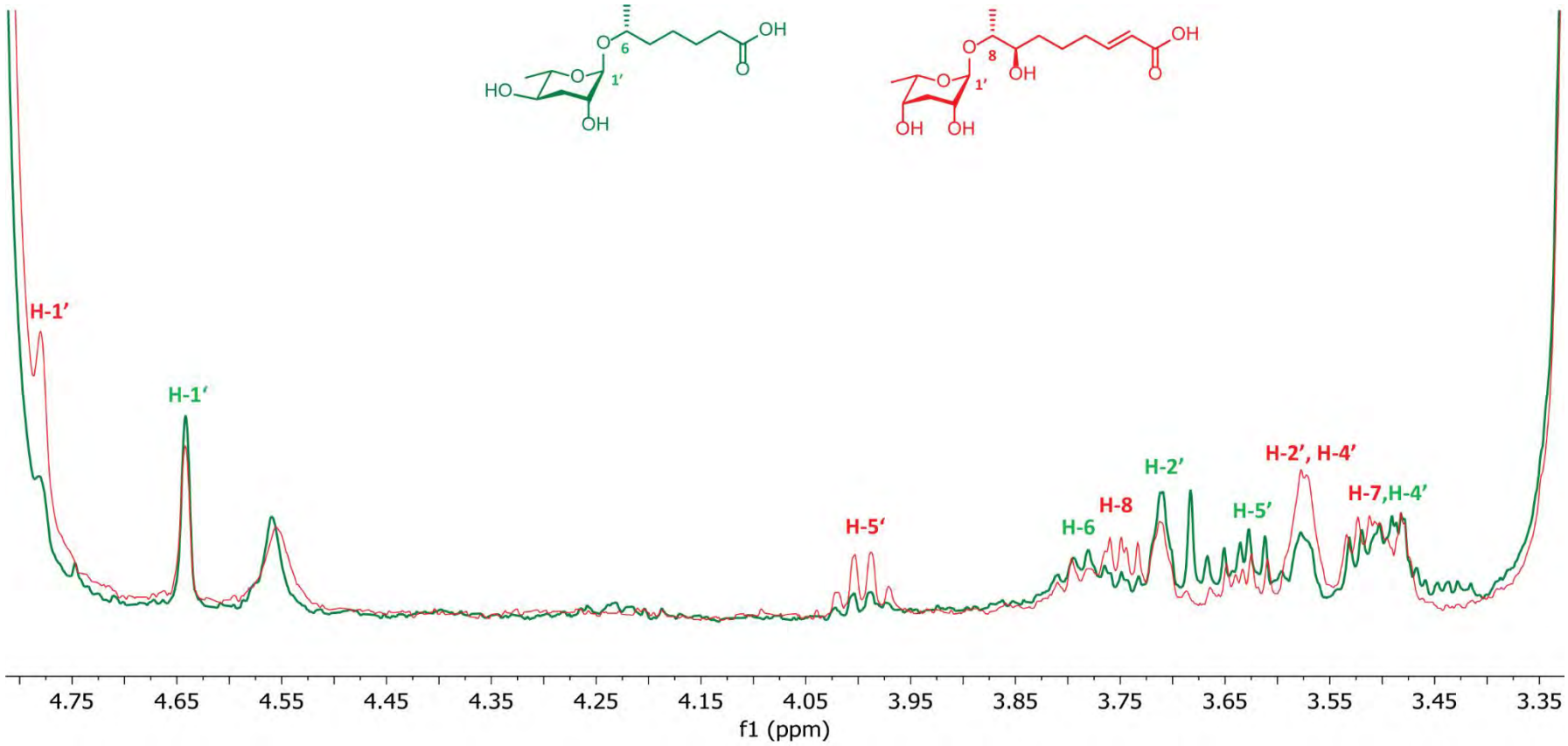

Figure S 11: Comparative analysis of 400 MHz ^{1}H NMR spectra between 2.30 and 1.00 ppm of two consecutive RP-C18 HPLC fractions from *C. nigoni* highlights signals corresponding to asc-C7 (1) and cae-7OH-ΔC9 (39)[92].

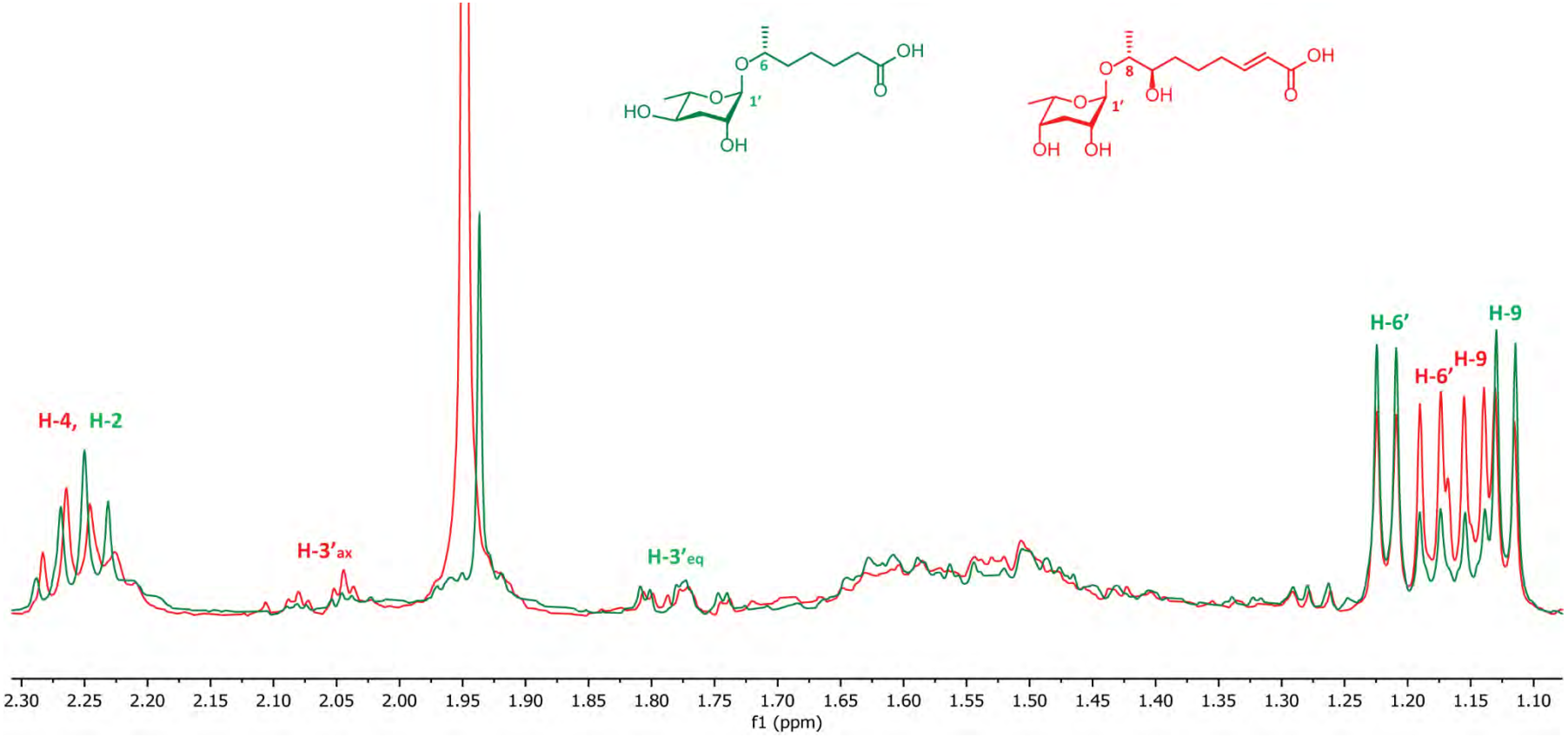

Figure S 12: Sections of the *dqf*-COSY spectrum of a mixture of asc-C7 (1) and cae-7OH-ΔC9 (39) isolated from *C. nigoni*[92].

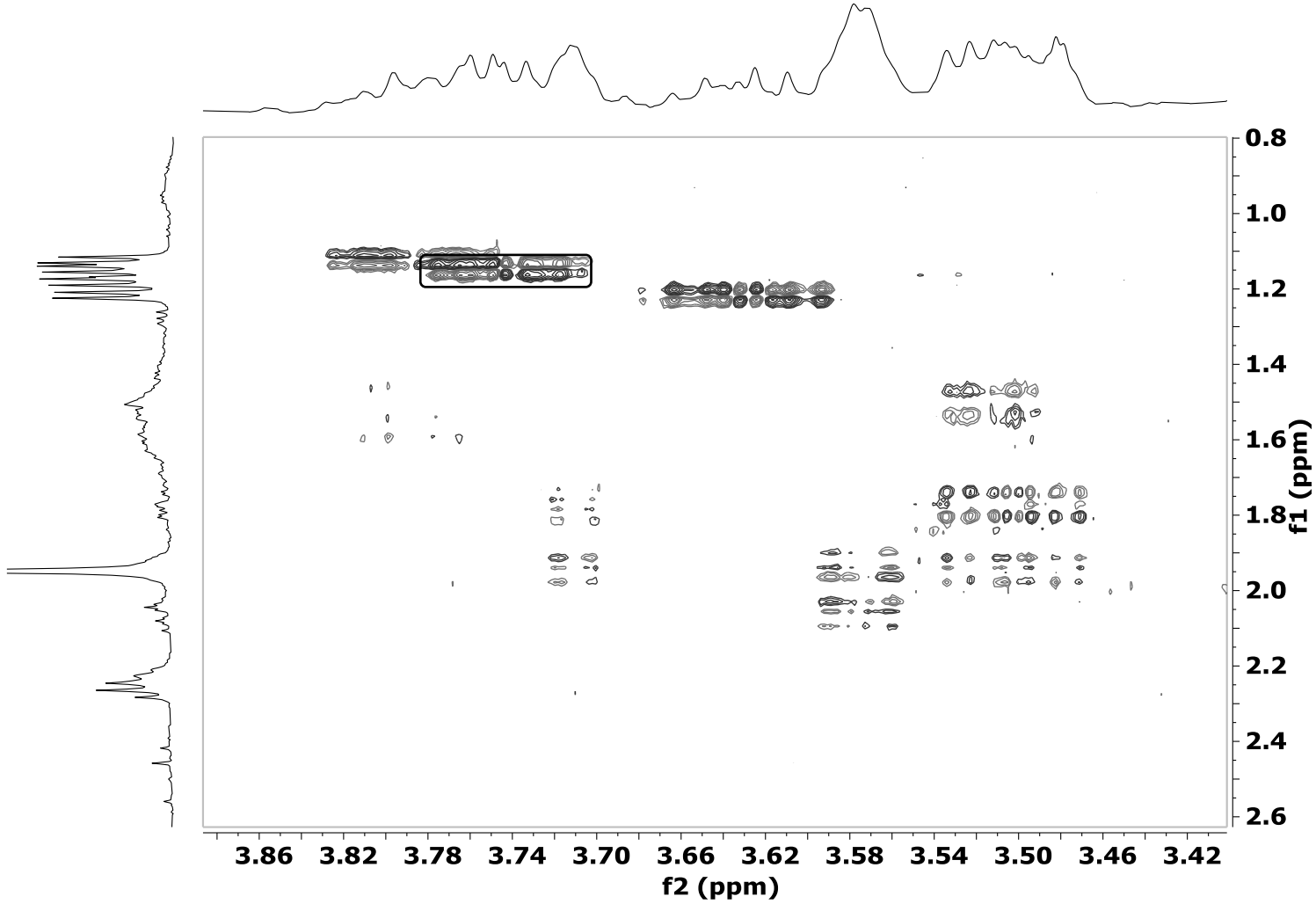

Figure S 13: Sections of the *dqf*-COSY spectrum of a mixture of asc-C7 (1) and cae-7OH-ΔC9 (39) isolated from *C. nigoni*[92].

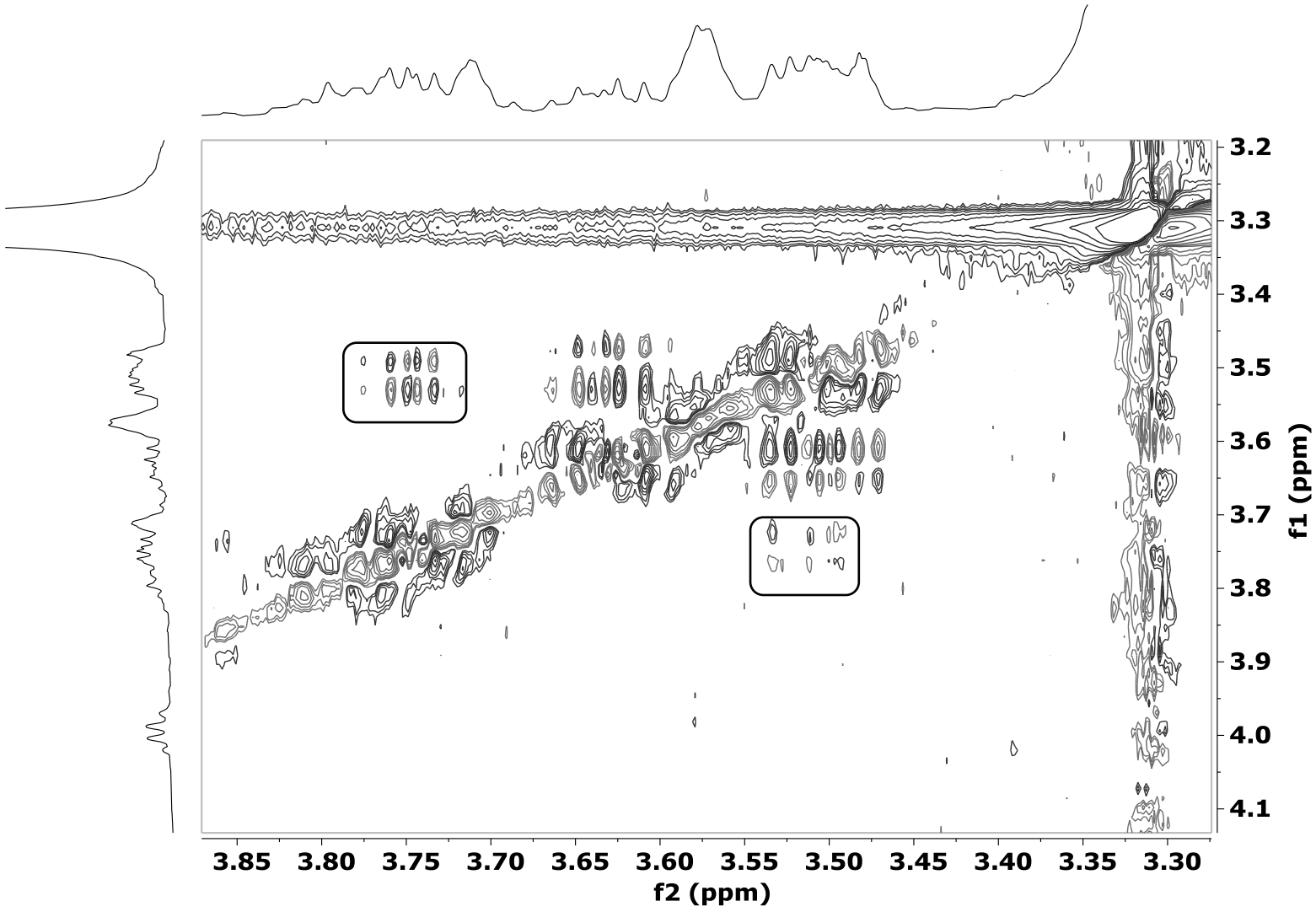

Figure S 14: Comparative analysis of 400 MHz dqf-COSY spectra of (A) natural cae-7OH-ΔC9 (39) isolated from *C. nigoni*; (B) synthetic *threo*-asc-7OH-ΔC9 (17) identified in *C. nigoni*, and (C) synthetic *erythro*-asc-7OH-ΔC9 (162) (in CD_3OD) indicates the *threo*-configuration of natural 39[92].

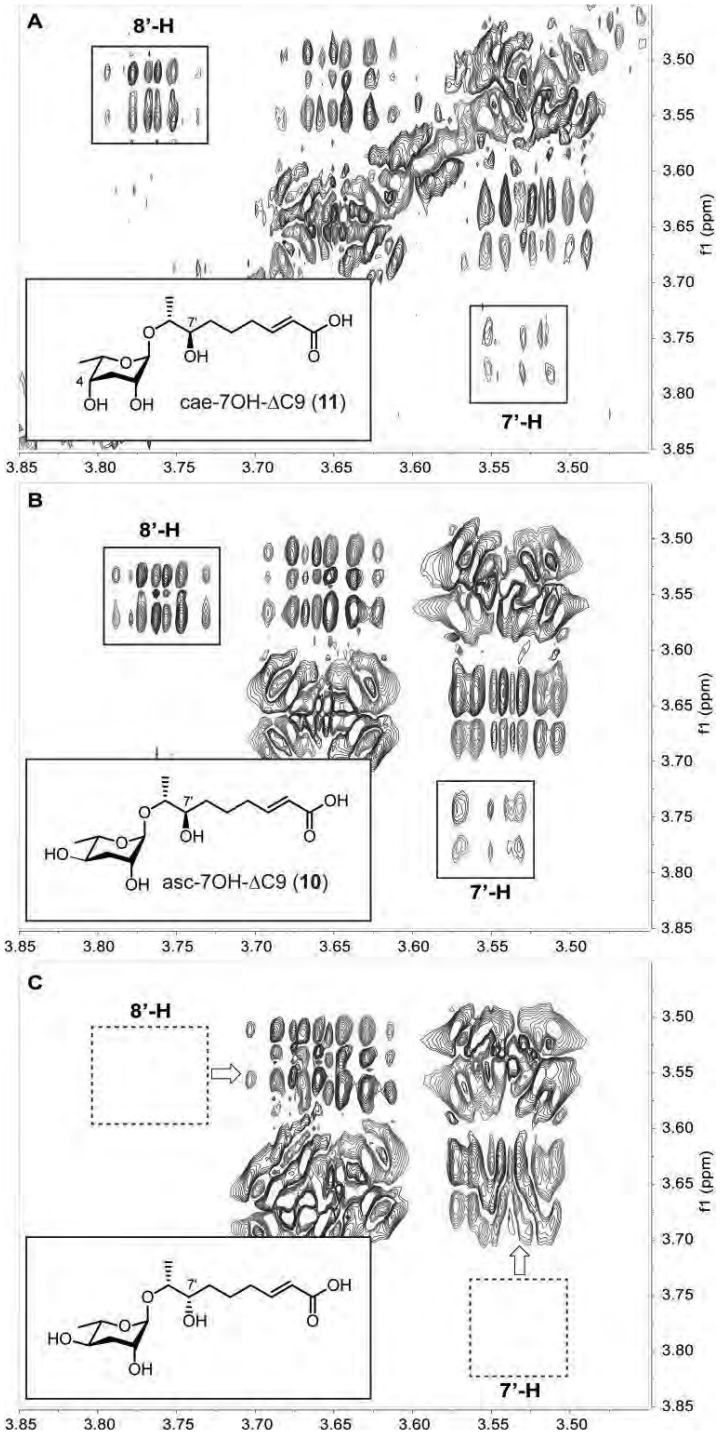

Figure S 15: Comparison of ^{1}H NMR spectra of (A) the 1:1 mixture of natural asc-C7 (1) and cae-7OH-ΔC9 (39) and (B) the synthetic cae-7OH-ΔC9 (39) in CD_3OD.

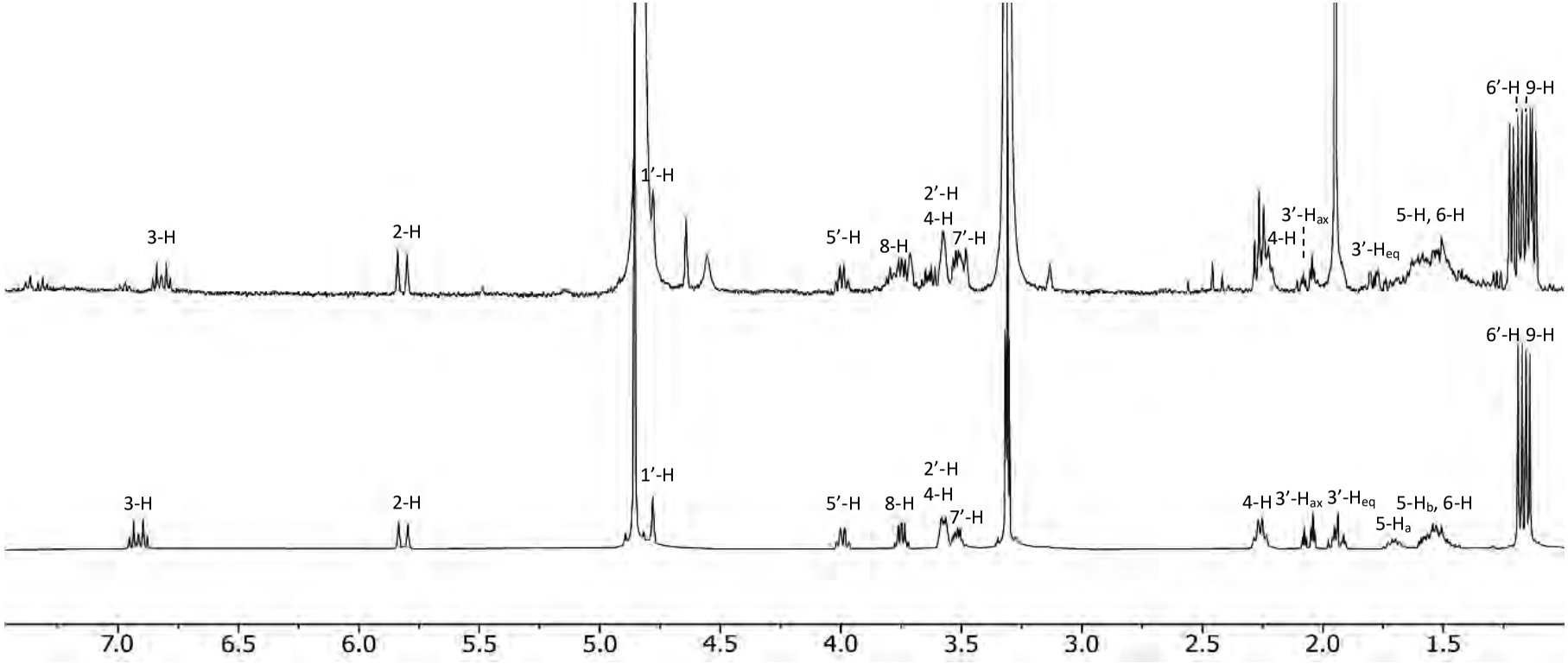

Figure S 16: Comparative HPLC-HR-MS/MS analysis of (A) synthetic asc-7OH-ΔC9 (17) and cae7OH-ΔC9 (39) and (B) the natural products isolated from *C. nigoni*[92].

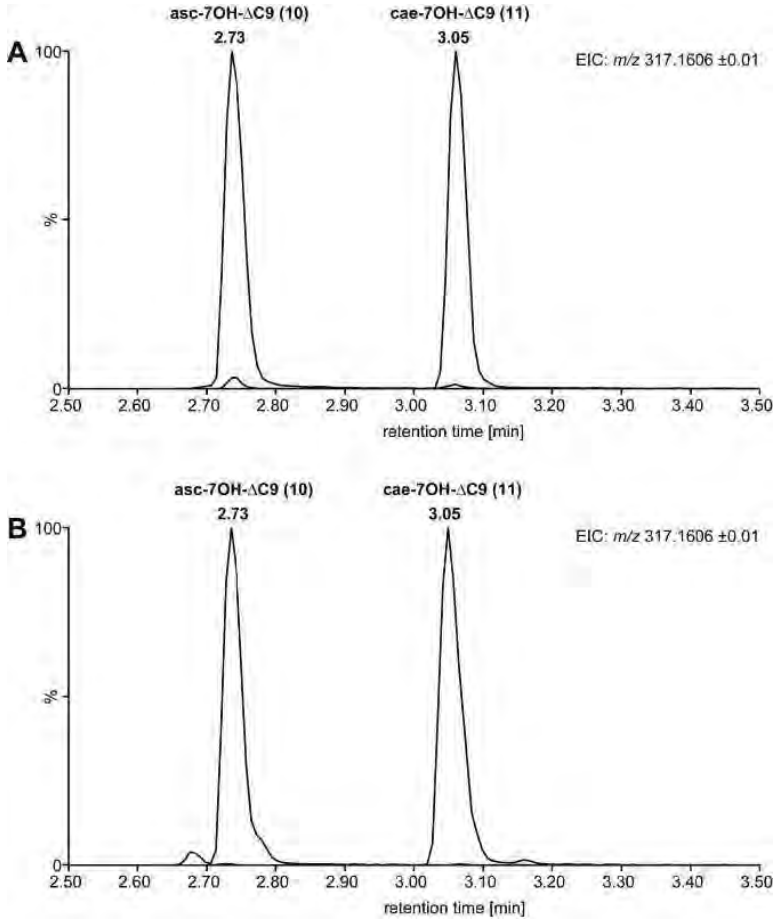

Figure S 17: HPLC-ESI-(-)-MS analysis of SPE fraction of *C. nigoni* exometabolome[92].

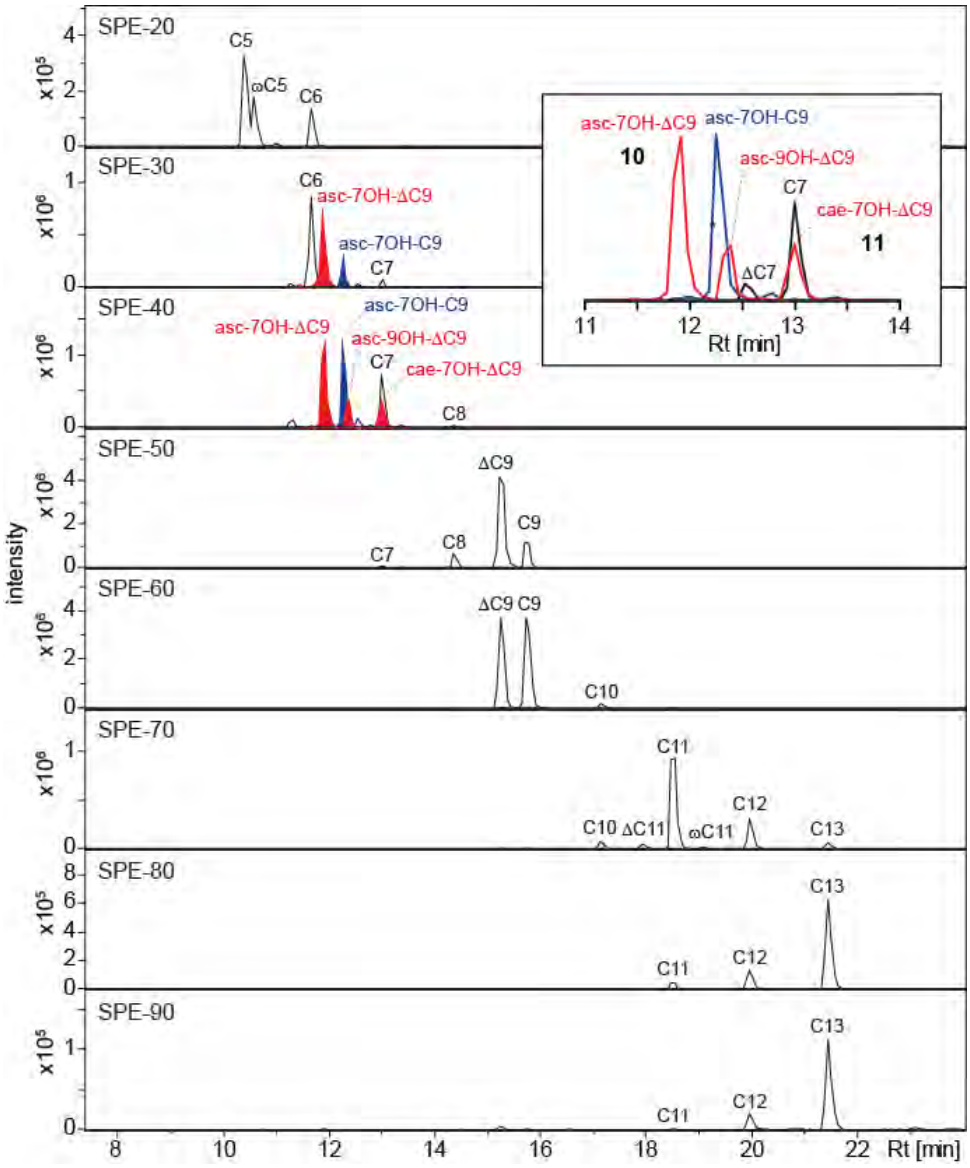

Figure S 18: HPLC-ESI-(-)-HR-MS/MS spectrum of natural and synthetic dimeric asc-C5 (40).

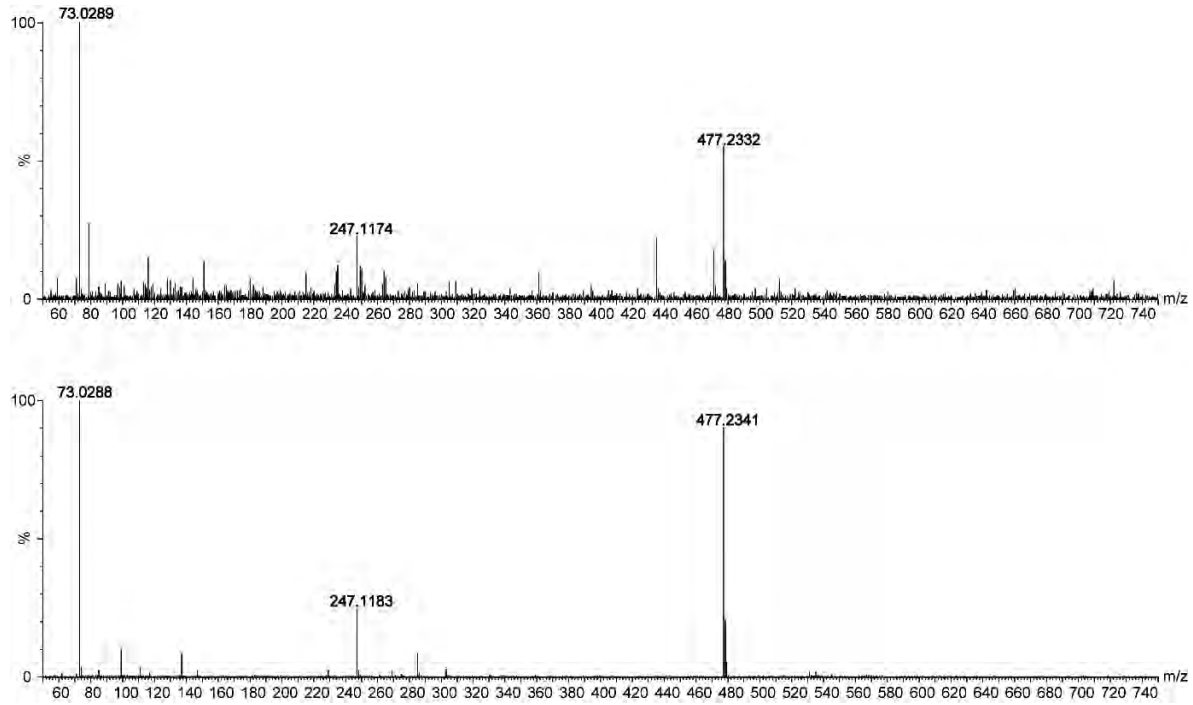

Figure S 19: HPLC-ESI-(-)-HR-MS/MS spectrum of natural and synthetic trimeric asc-C5 (41).

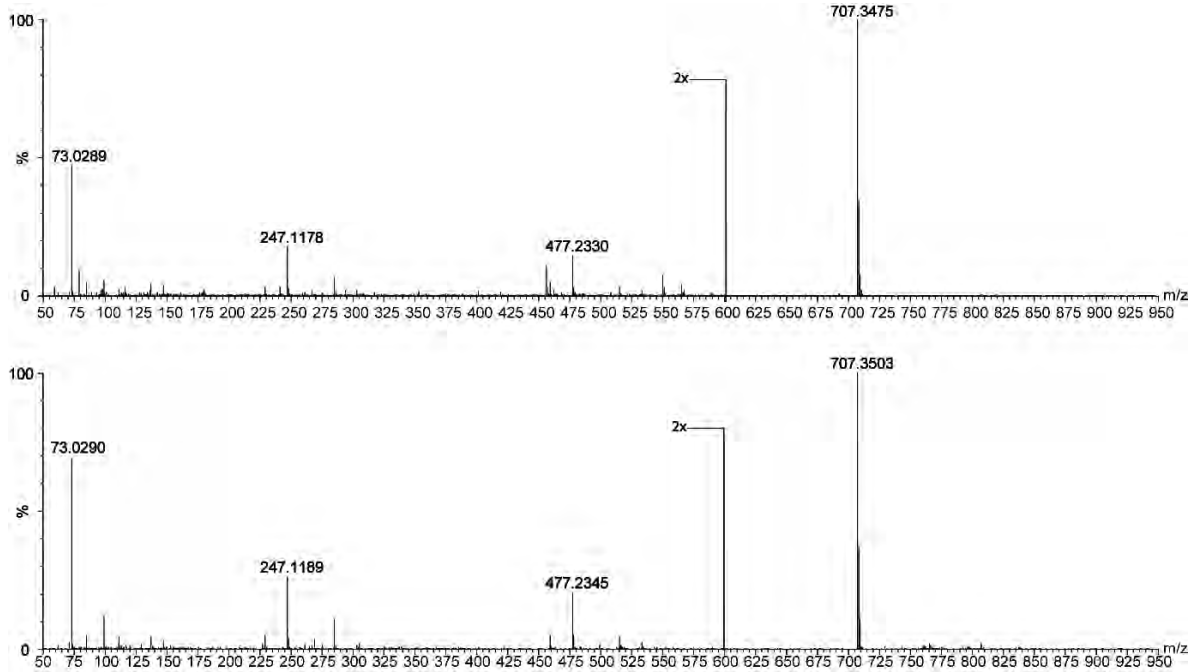

Figure S 20: HPLC-ESI-(-)-HR-MS/MS spectrum of natural and synthetic tetrameric asc-C5 (42).

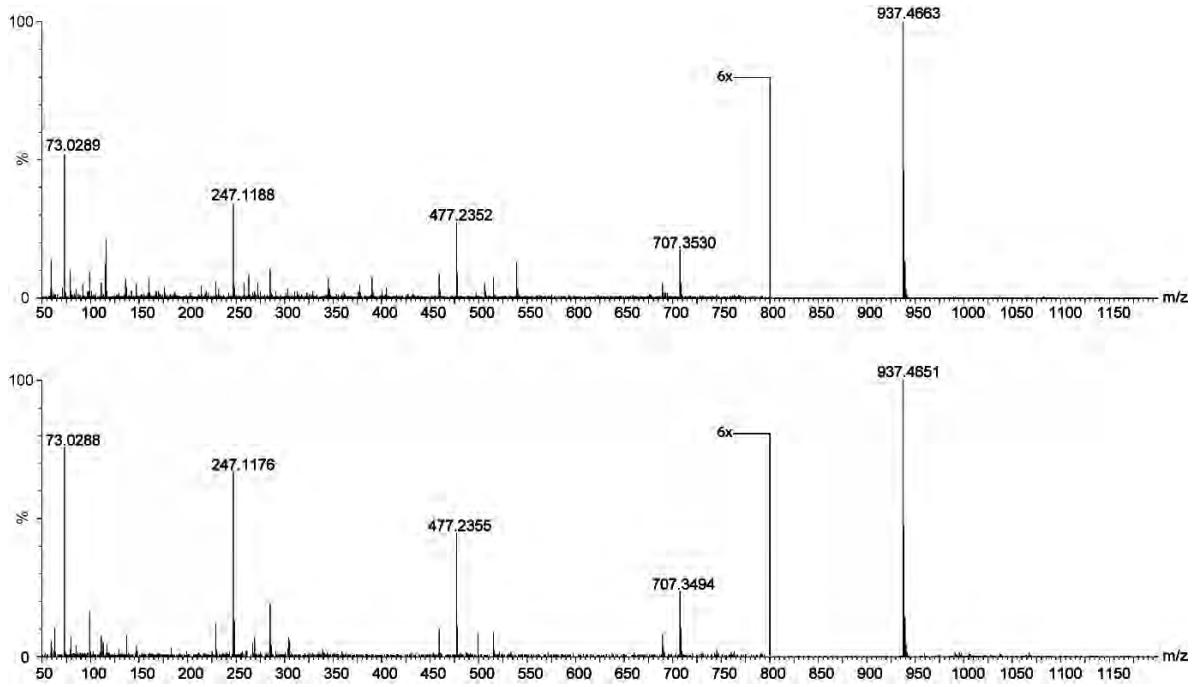

Figure S 21: HPLC-ESI-(-)-HR-MS/MS spectrum of natural and synthetic pentameric asc-C5 (43).

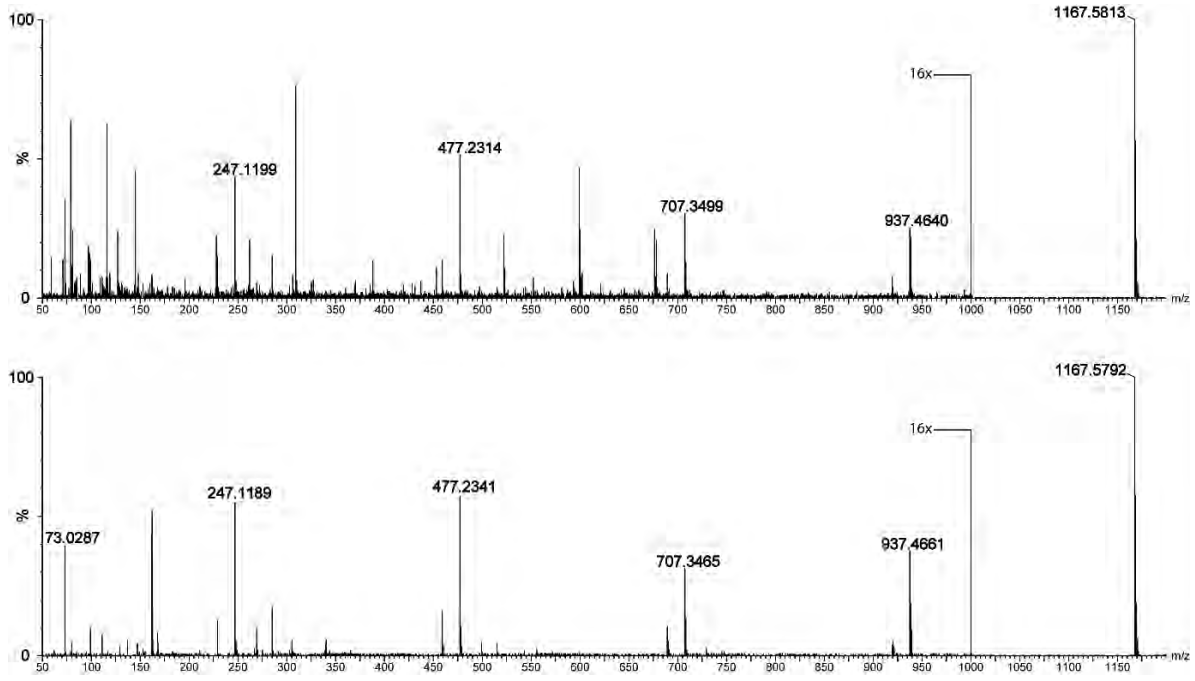

Table S1 : NMR data of the synthetic (*E*)- (37) and (*Z*)-UC-asc-ΔC9 (38).

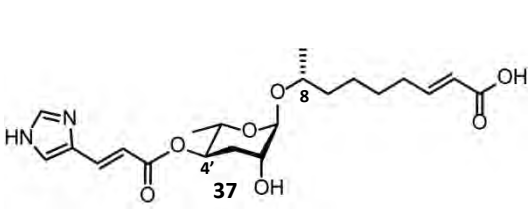

37

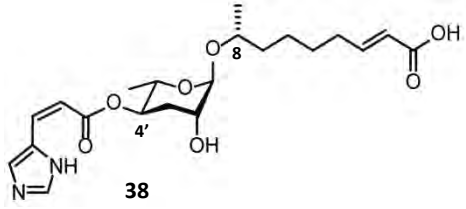

38

	(*E*)-4'-UC-asc-ΔC9 (37)		(*Z*)-UC-asc-ΔC9 (38)	
	^{1}H	^{13}C	^{1}H	^{13}C
1	4.71 br.s	97.3	4.71 br.s	97.4
2	3.75 dd (3.2, 2.9)	69.3	3.75 ddd (3.0, 2.9, 1.3)	69.3
3ax	1.89 ddd (13.1, 11.1, 3.2)	32.8	1.89 ddd (13.3, 11.4, 3.0)	32.7
3eq	2.10 ddd (13.1, 4.5, 2.9)		2.11 ddd (13.3, 4.7, 2.9)	
4	4.96 ddd (11.1, 9.6, 4.5)	71.0	4.99 ddd (11.8, 11.4, 4.7)	71.4
5	3.91 dq (9.6, 6.3)	68.1	3.9 dq (9.3, 6.3)	68.0
6	1.16 d (6.3)	17.7	1.17 d (6.3)	17.7
1'	-	168.9	-	nd
2'	5.83 dt (15.4, 3.0)	126.7	5.84 dt (16.3, 2.5)	126.9
3'	6.95 dt (15.4, 7.0)	146.1	6.73 dt (16.3, 7.2)	145.9
4'	2.30-2.22 m	32.8	2.21-2.17 m	32.8
5'	1.531 m	26.3	1.52 m	26.1
5'	1.43 m		1.44 m	
6'	1.58-1.49 m	29.2	1.56-1.48 m	29.3
7'	1.59 m	37.8	1.58 m	37.8
7'	1.527 m		1.51 m	
8'	3.82 m	72.4	3.81 m	72.6
9'	1.15 d (6.1)	19.1	1.15 d (6.1)	19.2
1''	-	166.8	-	167.1
2''	6.43 d (16.0)	116.1	5.79 d (12.6)	113.6
3''	7.60 d (16.0)	136.0	6.99 d (12.6)	133.4
4''	-	nd	-	nd
5''	7.45 s	nd	7.56 s	134.9
6''	7.79 s	138.9	7.83 s	138.5

Table S 2: NMR data of the synthetic (*E*)- (35) and (*Z*)-UC-asc-ΔC9 (36).

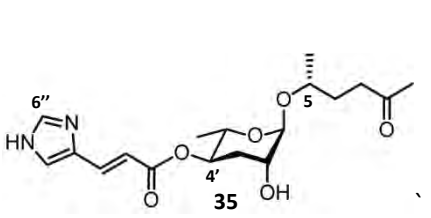

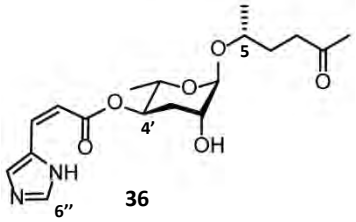

	(*E*)-4'-UC-asc-C6MK (35)		(*Z*)-4'-UC-asc-C6MK (36)	
	^{1}H	^{13}C	^{1}H	^{13}C
1'	4.70 br. s	96.3	4.70 br.s	97.24
2'	3.74 dd (3.8,3.0)	67.9	3.75 dd (3.4, 3.1)	68.98
3'ax	1.89 ddd (13.3, 11.4, 3.0)	31.8	1.89 ddd (13.9, 11.9, 3.4)	32.56
3'eq	2.10 ddd (13.3, 4.8, 3.8)		2.12 ddd (13.9, 6.2, 3.1	
4'	4.96 ddd (11.4, 9.4, 4.8)	69.8	4.99 ddd (11.9, 10.7, 6.2)	71.50
5'	3.87 dq (9.4, 6.4)	67.3	3.86 dq (9.3, 6.1)	68.11
6'	1.17 d (6.4)	16.6	1.17 d (6.1)	17.59
1	2.18 s	28.3	2.17 s	29.46
2	-	178.3	-	178.6
3	2.68-2.59 m	38.9	2.64-2.60 m	40.03
4	1.85-1.74 m	30.5	1.85-1.73 m	31.71
5	3.80 m	70.5	3.83 m	71.61
6	1.16 d (6.2)	17.6	1.16 d (6.1)	18.73
1''	-	166.6	-	167.2
2''	6.42 br. s	114.6	5.76 d (12.5)	112.73
3''	7.61 d	136.6	6.99 d (12.5)	132.31
4''	-	120.3	-	nd
5''	7.45 s	120.1	7.42 s	nd
6''	7.78 s	137.5	7.85s	nd

Table S 3 : NMR data of the synthetic of 4'-AB-asc-C5 (34).

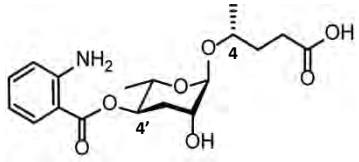

	^{1}H	^{13}C
1'	4.74 br.s	97.5
2'	3.78 dd (3.9, 3.1)	69.5
3'ax	1.97 ddd (13.5, 11.1, 3.2)	33.2
3'eq	2.17 ddd (13.5, 4.8, 3.9)	
4'	5.07 ddd (11.1, 9.7, 4.8)	71.0
5'	4.00 dq (9.7, 6.4)	68.7
6'	1.19 d (6.4)	18.1
1	-	177.5
2	2.55-2.39 m	31.4
3	1.93-1.77 m	33.4
4	3.90 m	71.7
5	1.18 d (6.1)	19.0
1''	-	168.6
2''	-	111.2
3''	7.77	132.0
4''	6.57	116.6
5''	7.23	135.2
6''	6.74	117.8
7''	-	152.9

Table S 4 : NMR data of the synthetic of cae-7OH-ΔC9 (39).

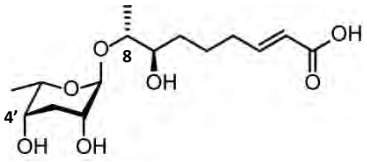

	^{1}H	^{13}C
1'	4.78 s	98.7
2'	3.58 br.s	68.2
3'ax	2.06 dt (14.3, 3.1)	32.3
3'eq	1.93 ddt (14.3, 1.0, 3.4)	
4'	3.57 br.s	69.1
5'	3.99 dq (6.6, 1.0)	68.5
6'	1.18 d (6.6)	17.2
1	-	170.8
2	5.82 dt (15.6, 1.5)	123.7
3	6.91 dt (15.6, 7.0)	150.0
4	2.26 m	33.02
5	1.70 m	25.8
5	1.62-1.45 m	
6	1.62-1.45 m	32.97
7	3.52 m	75.0
8	3.75 qd (6.3, 4.1)	75.7
9	1.15 d (6.3)	14.8

Table S 5: NMR data of the synthetic [2'-(asc-C5)]$_2$-asc-C5 (41) CD_3OD.

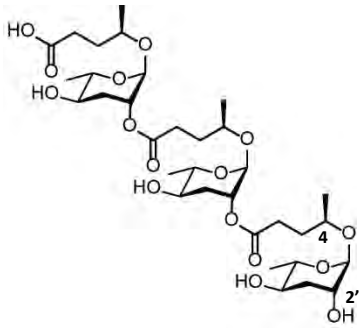

		^1H	^{13}C
Ascarylose A	1'	4.65 br.s	96.9
	2'	3.72 dd (3.7, 3.2)	69.5
	3'ax	1.76 ddd (13.3, 11.1, 3.2)	35.7
	3'eq	1.95 ddd (13.3, 4.6, 3.7)	
	4'	3.51 ddd (11.1, 9.7, 4.6)	67.9
	5'	3.57 dq (9.7, 6.1)	71.08
	6'	1.227 d (6.1)	17.7
Ascarylose B or C	1'	4.73 br.s	94.2
	2'	4.79 dd (4.0, 3.2)	72.4
	3'ax	1.89 ddd (12.9, 11.2, 3.2)	33.0
	3'eq	2.015 ddd (12.9, 5.1, 4.1)	
	4'	3.39 ddd (11.2, 9.5, 4.9)	68.4
	5'	3.696 dq (9.5, 6.2)	70.6
	6'	1.229 d (6.2)	17.7
Ascarylose B or C	1'	4.73 br.s	94.2
	2'	4.79 dd (4.1, 3.2)	72.4
	3'ax	1.85 ddd (13.5, 11.4, 3.2)	33.0
	3'eq	2.023 ddd (13.5, 5.1, 4.1)	
	4'	3.42 ddd (11.4, 9.8, 5.1)	68.1
	5'	3.62 dq (9.5, 6.3)	71.0
	6'	1.234 d (6.3)	17.7
Aglycone A, B or C	1	-	172.8
	2	2.55-2.45 m	30.9
	3	1.870-1.833 m	32.8
	4	3.852 m	71.2
	5	1.163 d (6.3)	18.8
Aglycone A, B or C	1	-	172.8
	2	2.55-2.45 m	30.9
	3	1.820-1.763 m	32.8
	4	3.845 m	71.3
	5	1.156 d (6.3)	18.8
Aglycone A, B or C	1	-	178.7
	2	2.30 dt (15.0, 7.5)	33.7
	2	2.37 dt (15.0, 8.2)	
	3	1.838-1.796 m	34.1
	4	3.824 m	72.0
	5	1.149 d (6.1)	18.8

Table S 6: NMR data of the synthetic [2'-(asc-C5)]$_3$-asc-C5 (42) CD_3OD.

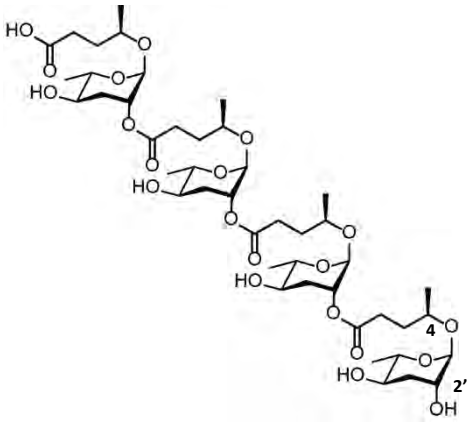

		^1H	^{13}C
Ascarylose A	1'	4.65 br.s	97.0
	2'	3.72 dd (3.9, 3.0)	69.63
	3'ax	1.76 ddd (13.3, 11.2, 3.0)	35.64
	3'eq	1.95 ddd (13.3, 4.5, 3.9)	
	4'	3.51 ddd (11.2, 9.3, 4.5)	67.88
	5'	3.57 dq (9.3, 6.1)	71.00
	6'	1.225 d (6.1)	17.74
Ascarylose B, C or D (1 sugar)	1'	4.73 br.s	94.1
	2'	4.79 dd (3.7, 3.1)	72.53
	3'ax	1.900 ddd (13.9, 11.3, 3.1)	33.03
	3'eq	2.013 ddd (13.9, 4.5, 3.7)	
	4'	3.382 ddd (11.3, 9.1, 4.5)	68.06
	5'	3.709 dq (9.1, 6.2)	70.71
	6'	1.226 d (6.2)	17.74
Ascarylose B, C or D (2 sugars)	1'	4.73 br.s	94.1
	2'	4.79 dd (3.9, 3.2)	72.53
	3'ax	1.851 ddd (14.2, 11.8, 3.2)	33.03
	3'eq	2.021 ddd (14.2, 4.7, 3.9)	
	4'	3.421 ddd (11.8, 9.3, 4.7)	68.06
	5'	3.622 dq (9.3, 6.2)	70.93
	6'	1.231 d (6.2)	17.74
aglycone A, B, C or D (1 aglycone)	1	-	172.76
	2	2.55-2.45 m	30.99
	3	1.895-1.761 m	33.03
	4	3.850 m	71.58
	5	1.155 d (6.1)	18.71
aglycone A, B, C or D (2 aglycones)	1	-	172.76
	2	2.55-2.45 m	30.99
	3	1.895-1.761 m	33.03
	4	3.854 m	71.58
	5	1.163 d (6.1)	18.71
aglycone A, B, C or D (1 aglycone)	1	-	174.33
	2_a	2.347 dt (14.4, 7.3)	32.52
	2_b	2.256 dt (14.4, 6.7)	
	3	1.816 ddt (8.8, 7.3, 6.7)	33.77
	4	3.816 tq (8.8, 6.1)	71.58
	5	1.145 d (6.1)	18.71

Table S 7: ^{1}H NMR data of the synthetic [2'-(asc-C5)]$_4$-asc-C5 (43) in CD_3OD.

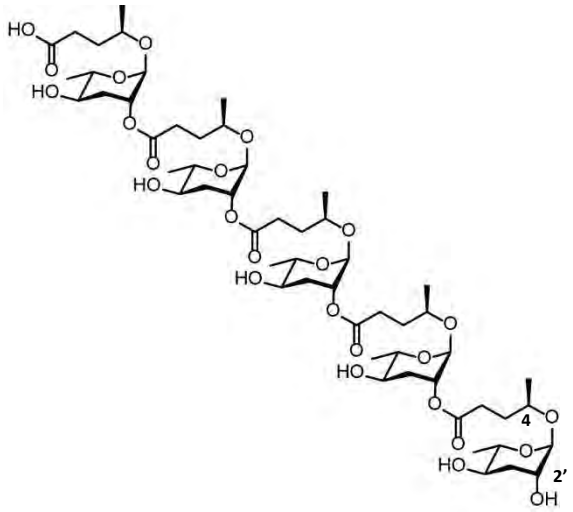

		^{1}H
Ascarylose A	1'	4.65 br.s
	2'	3.72 (*ddd*, *J* = 3.5 Hz, *J* = 3.0 Hz, *J* = 1.6 Hz,1H)
	3'ax	1.76 (*ddd*, *J* = 12.9 Hz, *J* = 11.6 Hz, *J* = 3.5 Hz,1H)
	3'eq	1.95 (*ddd*, *J* = 12.9 Hz, *J* = 5.0 Hz, *J* = 3.0 Hz,1H)
	4'	3.51 (ddd, J = 11.6 Hz, J = 9.9 Hz, J = 5.0 Hz, 1H)
	5'	3.57 (*dq*, *J* = 9.9 Hz, *J* = 6.5 Hz, 1H)
	6'	1.224 (*d*, *J* = 6.5 Hz, 3H)
Ascarylose B, C, D or E (1 sugar)	1'	4.73 *br.s* (4H)
	2'	4.79 *br.s* (4H)
	3'ax	1.872 (*ddd*, *J* = 13.8 Hz, *J* = 11.4 Hz, *J* = 3.7 Hz,1H)
	3'eq	2.021(*ddd*, *J* = 13.8 Hz, *J* = 4.7 Hz, *J* = 3.3 Hz,1H)
	4'	3.416 (ddd, J = 11.4 Hz, J = 9.2 Hz, J = 4.7 Hz, 1H)
	5'	3.678 (*dq*, *J* = 9.2 Hz, *J* = 6.5 Hz, 1H)
	6'	1.225 (*d*, *J* = 6.5 Hz, 3H)
Ascarylose B, C, D or E (3 sugars)	1'	4.73 *br.s* (4H)
	2'	4.79 *br.s* (4H)
	3'ax	1.85 (*ddd*, *J* = 13.2 Hz, *J* = 11.6 Hz, *J* = 3.7 Hz, 3H)
	3'eq	2.02 (*ddd*, *J* = 13.2 Hz, *J* = 4.7 Hz, *J* = 3.3 Hz, 3H)
	4'	3.42 (*ddd*, *J* = 11.6 Hz, *J* = 9.1 Hz, *J* = 4.7 Hz, 3H)
	5'	3.62 (*dq*, *J* = 9.1 Hz, *J* = 6.4 Hz, 3H)
	6'	1.232 (*d*, *J* = 6.4 Hz, 9H)
aglycone A, B, C, D or E (1 aglycone)	1	-
	2	2.53-2.46 (*m*, 8H)
	3	1.89-1.76 (*m*, 8H)
	4	3.88-3.81 (*m*, 5H)
	5	1.156 (*d*, *J* = 6.0 Hz, 3H)
aglycone A, B, C, D or E (3 aglycones)	1	-
	2	2.53-2.46 (*m*, 8H)
	3	1.89-1.76 (*m*, 8H)
	4	3.88-3.81 (*m*, 5 H)
	5	1.164 (*d*, *J* = 6.1 Hz, 9H)
aglycone A, B, C, D or E (1 aglycone)	1	
	2	2.41 (*m*, 1H)
	2	2.36 (*m*, 1H)
	3	1.84-1.79 (*m*, 2H)
	4	3.88-3.81 (*m*, 5H)
	5	1.153 (*d*, *J* = 5.9 Hz, 3H)

NMR Spectra

Figure S 22 : ^{1}H NMR (600 MHz, $CDCl_3$) of 1,2,3,4-tetra-O-benzoyl-6-deoxy- α-L-arabino-hexopyranoside (64).

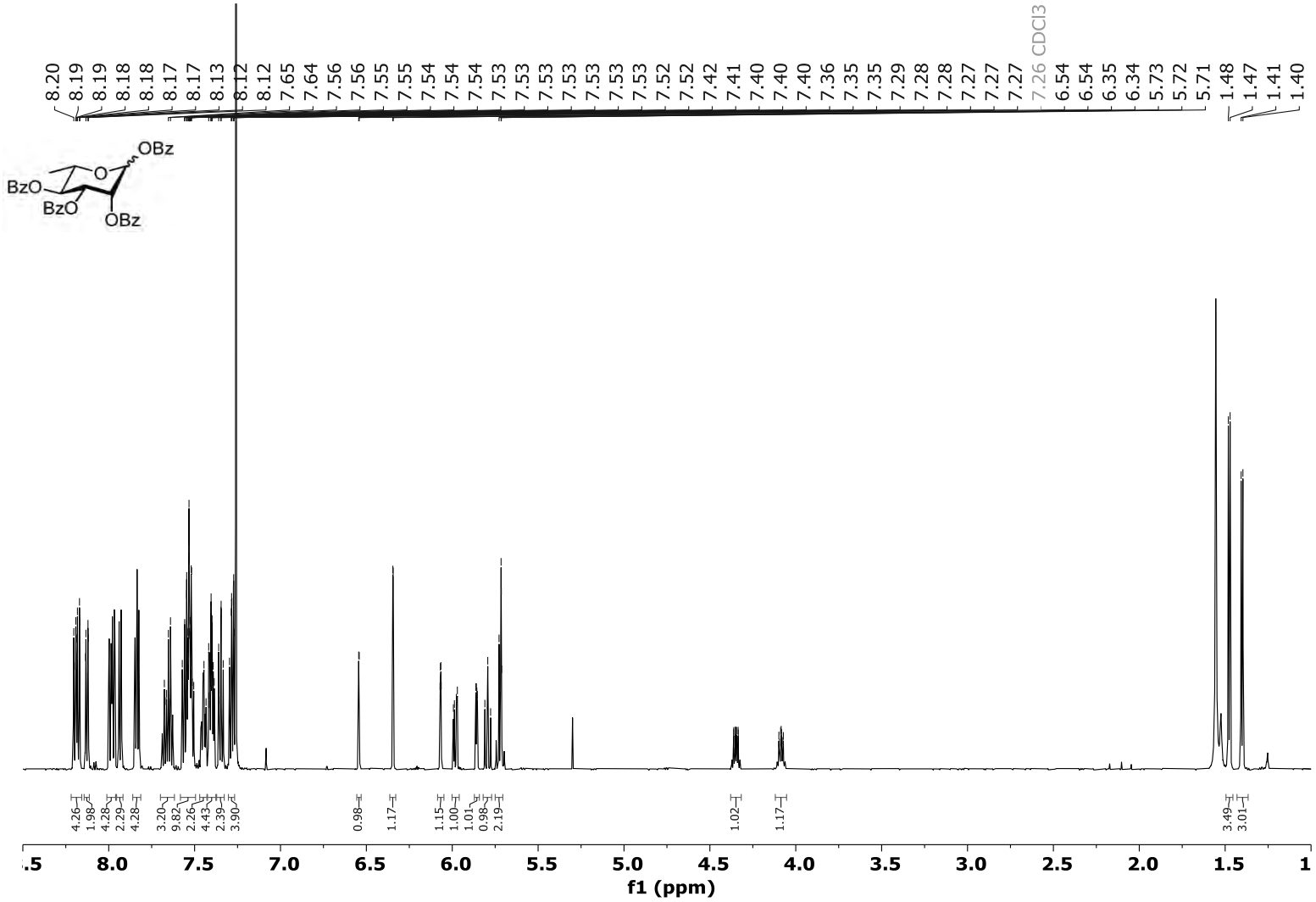

Figure S 23 : ^{1}H NMR (600 MHz, CDCl3) of 2,3,4-tri-*O*-benzoyl-6-deoxy-α-L-*arabino*-hexopyranoside (65).

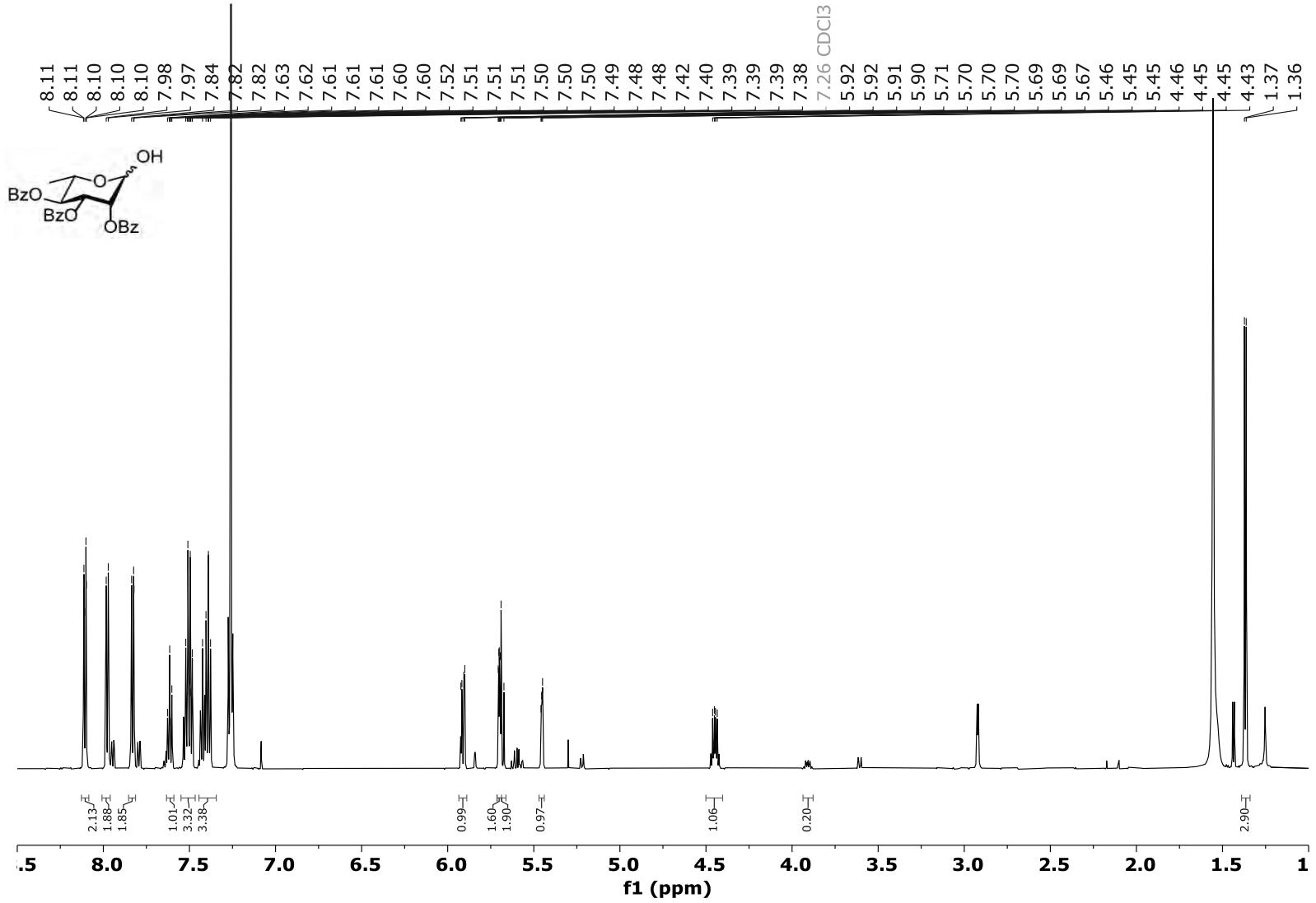

Figure S 24 : ^{1}H NMR (600 MHz, CDCl3) of 2,3,4-tri-*O*-benzoyl-6-deoxy- α-L-*arabino*-hexono-1,5-lactone (66).

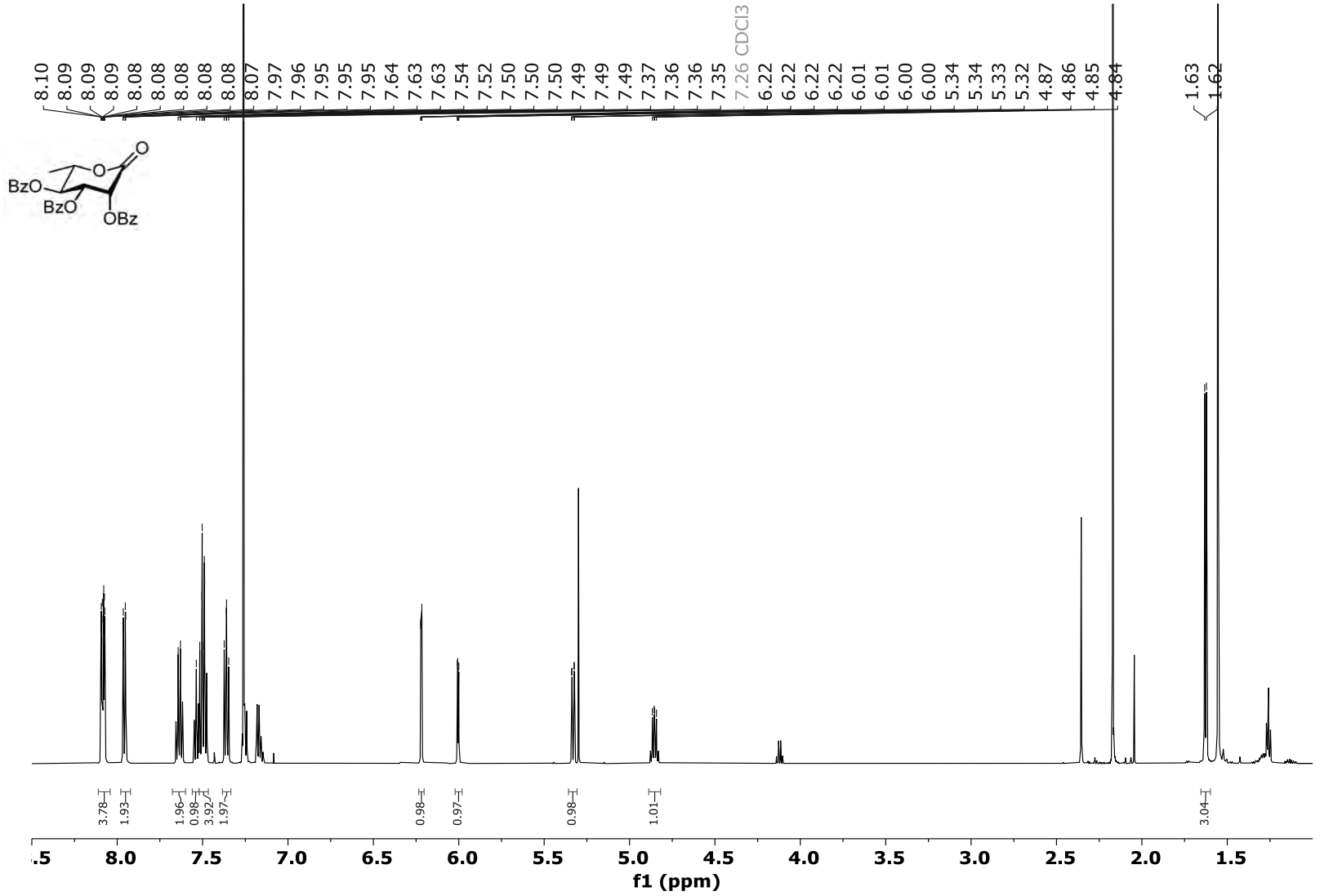

Figure S 25 : ^{1}H NMR (600 MHz, $CDCl_3$) of 2,4-di-*O*-benzoyl-3,6-dideoxy-L-*erythro*-hex-2-enono-1,5-lactone (61).

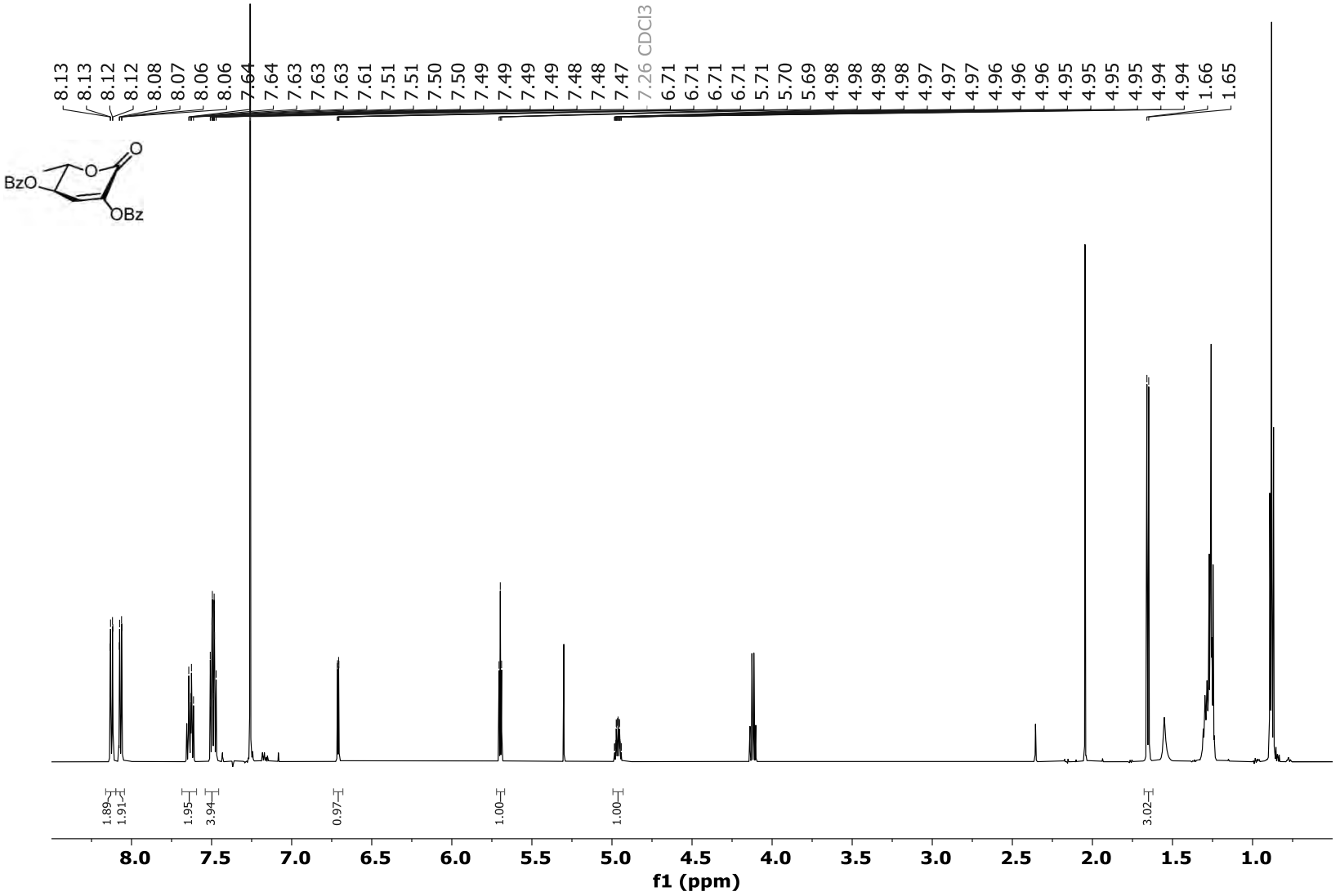

Figure S 26 : ^{1}H NMR (600 MHz, $CDCl_3$) of 2,4-di-*O*-benzoyl-3,6-dideoxy- α-L-*arabino*-hexono-1,5-lactone (62).

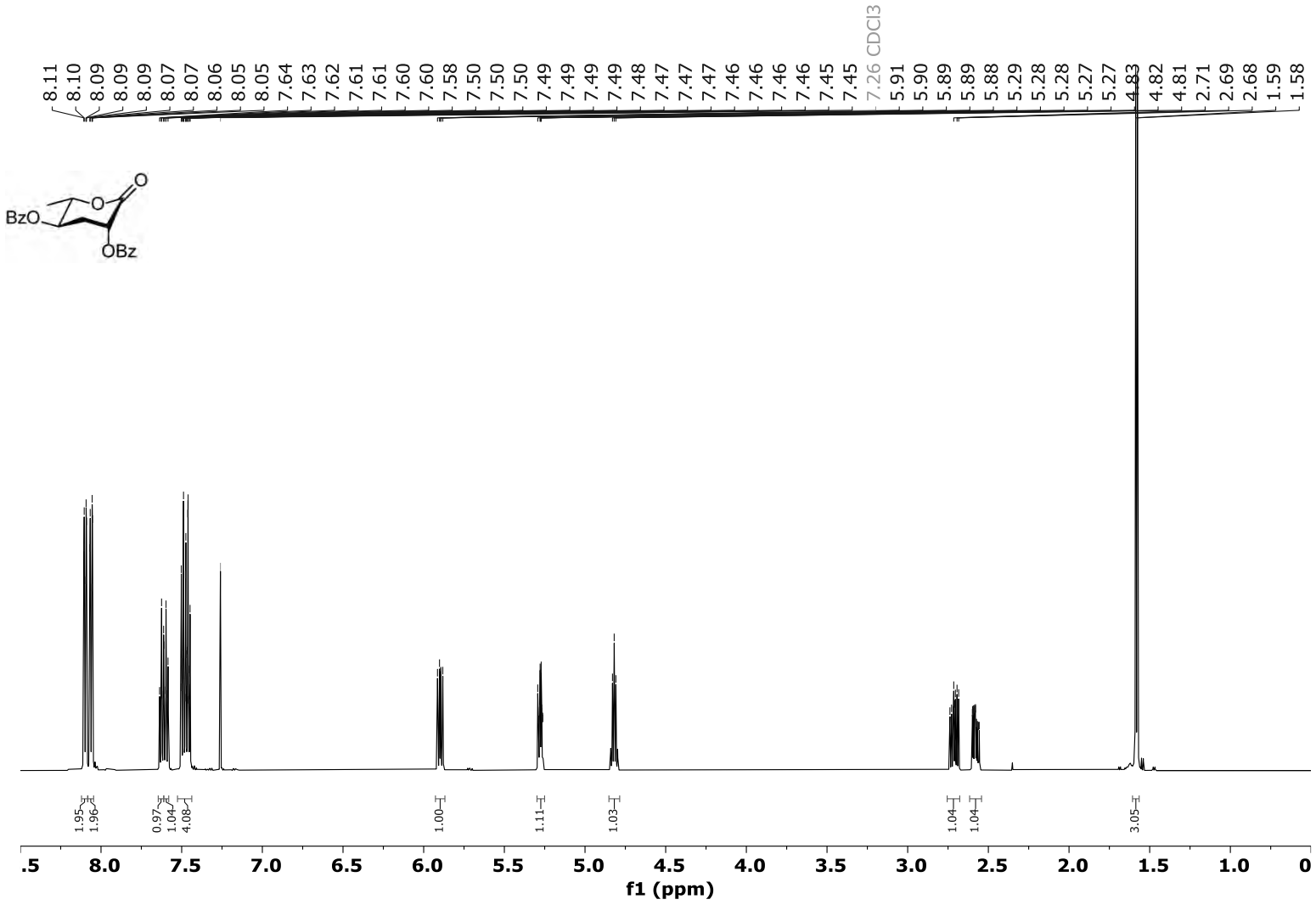

Figure S 27: ^{1}H NMR (600 MHz, CDCl3) of 2,4-di-*O*-benzoyl-3,6-dideoxy- α-L-*arabino*-hexopyranose (63).

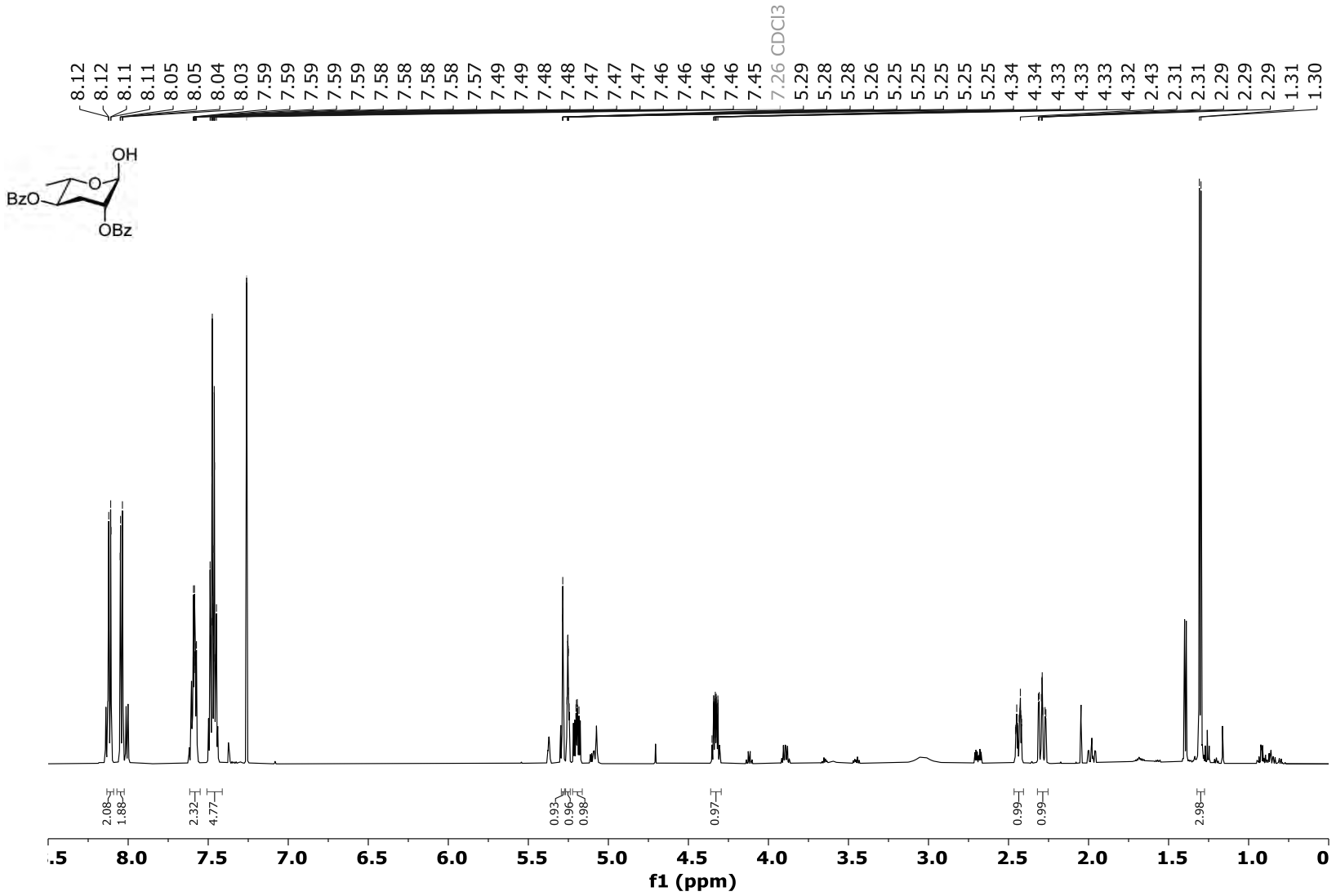

Figure S 28: ^{13}C NMR (150 MHz, $CDCl_3$) of 2,4-di-*O*-benzoyl-3,6-dideoxy- α-L-*arabino*-hexopyranose (63).

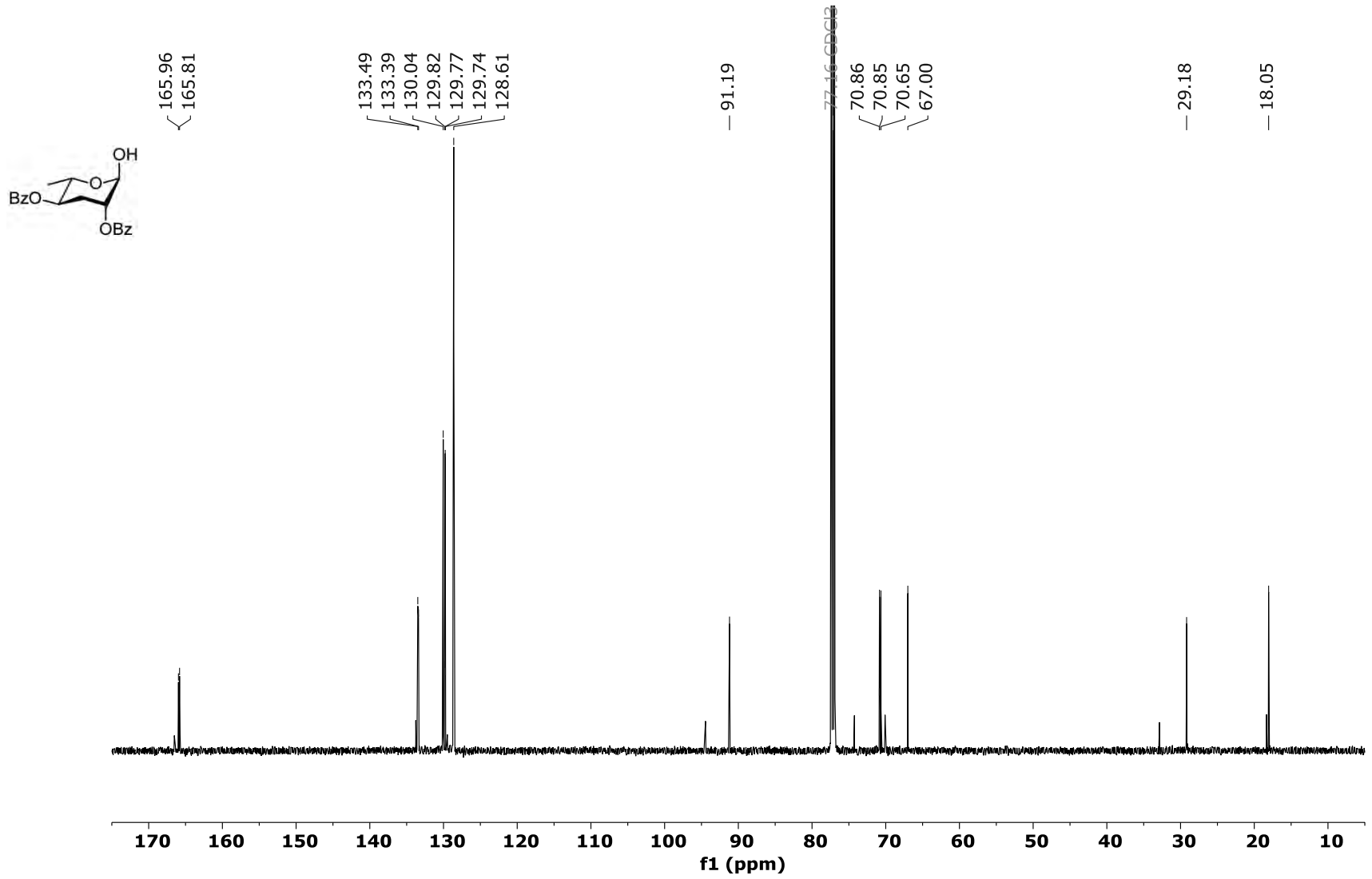

Figure S 29: ^{1}H NMR (400 MHz, CD_3OD) of 1-*O*-methyl-6-deoxy-α-L-*arabino*-hexopyranoside (56).

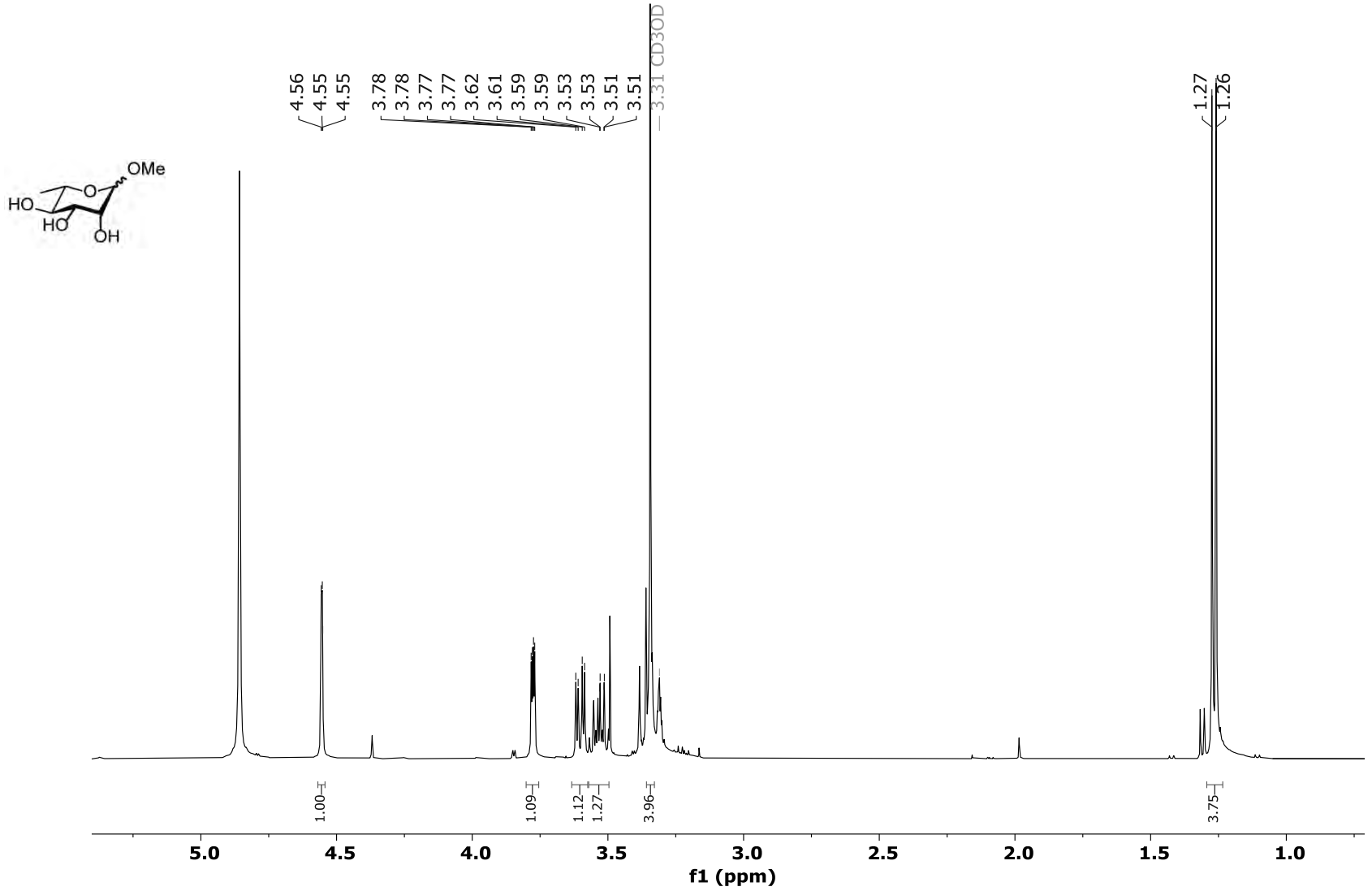

Figure S 30: ^{1}H NMR (600 MHz, $CDCl_3$) of 1-*O*-methyl-3-*O*-phenoxythiocarbonyl-6-deoxy-α-L-*arabino*-hexopyranoside (75).

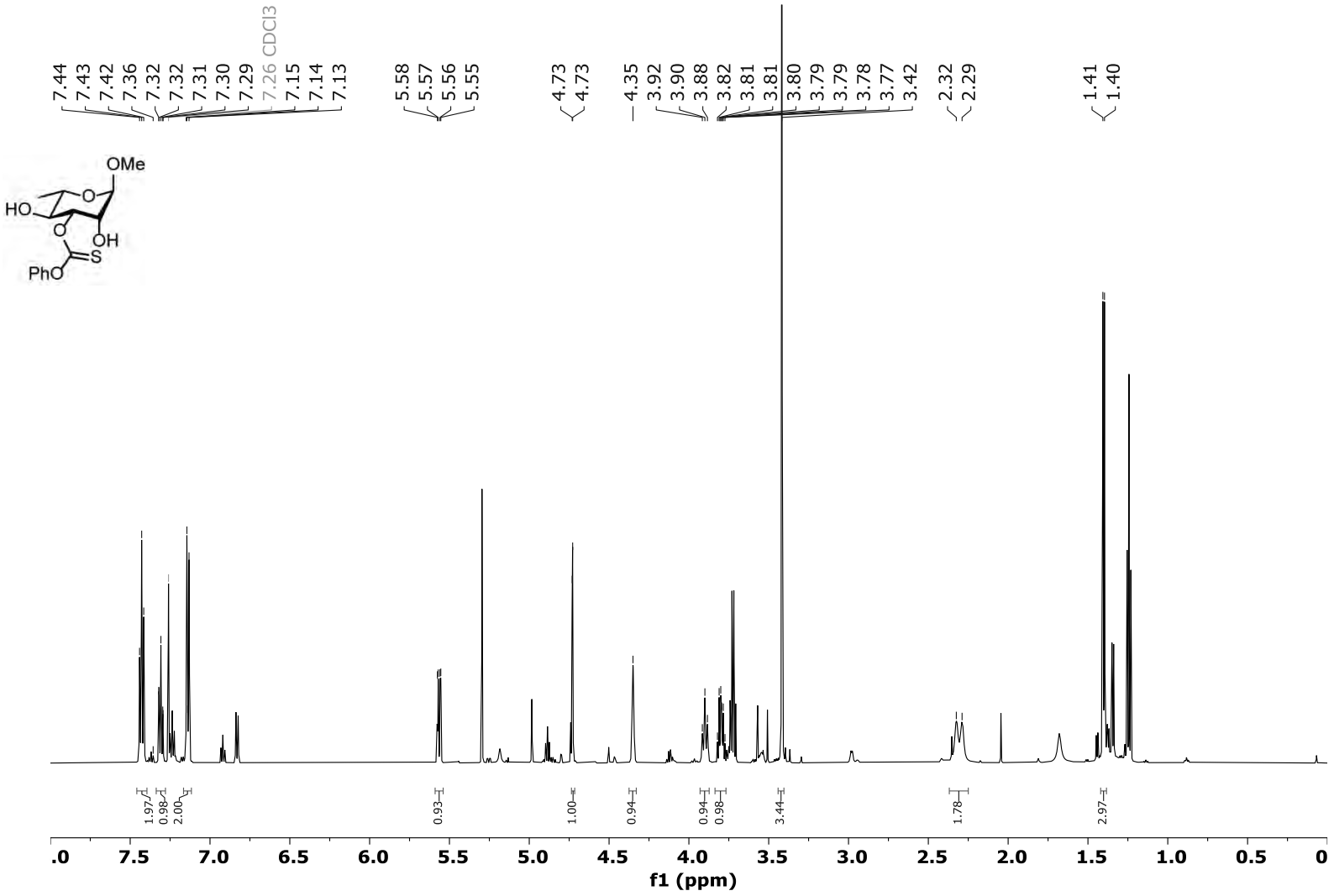

Figure S 31: ^{13}C NMR (150 MHz, CDCl3) of 1-*O*-methyl-3-*O*-phenoxythiocarbonyl-6-deoxy-α-L-*arabino*-hexopyranoside (75).

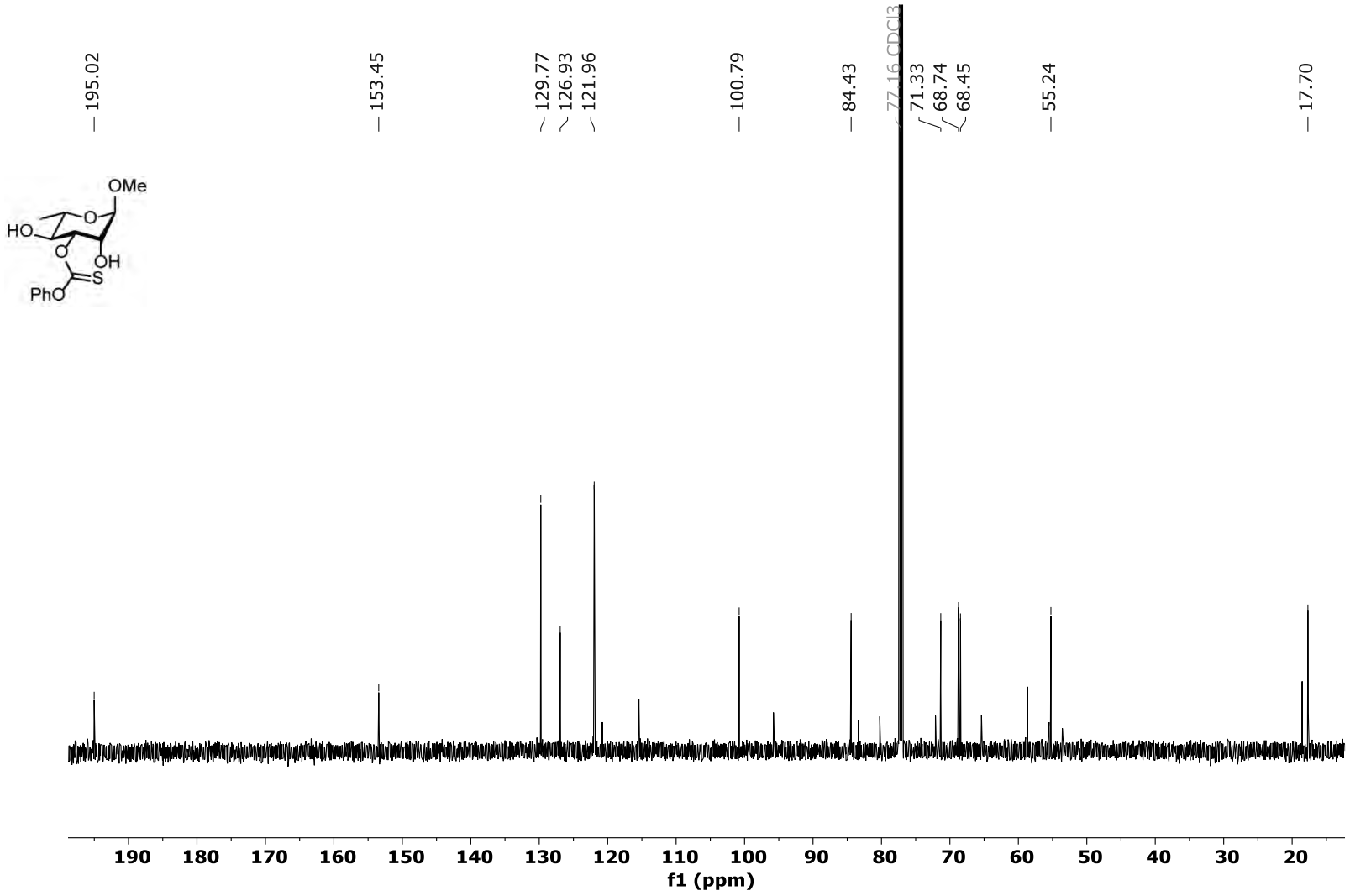

Figure S 32: ^{1}H NMR (600 MHz, $CDCl_3$) of 1-*O*-methyl-2,4-di-*O*-benzoyl-3,6-dideoxy- α-L-*arabino*-hexopyranoside (67).

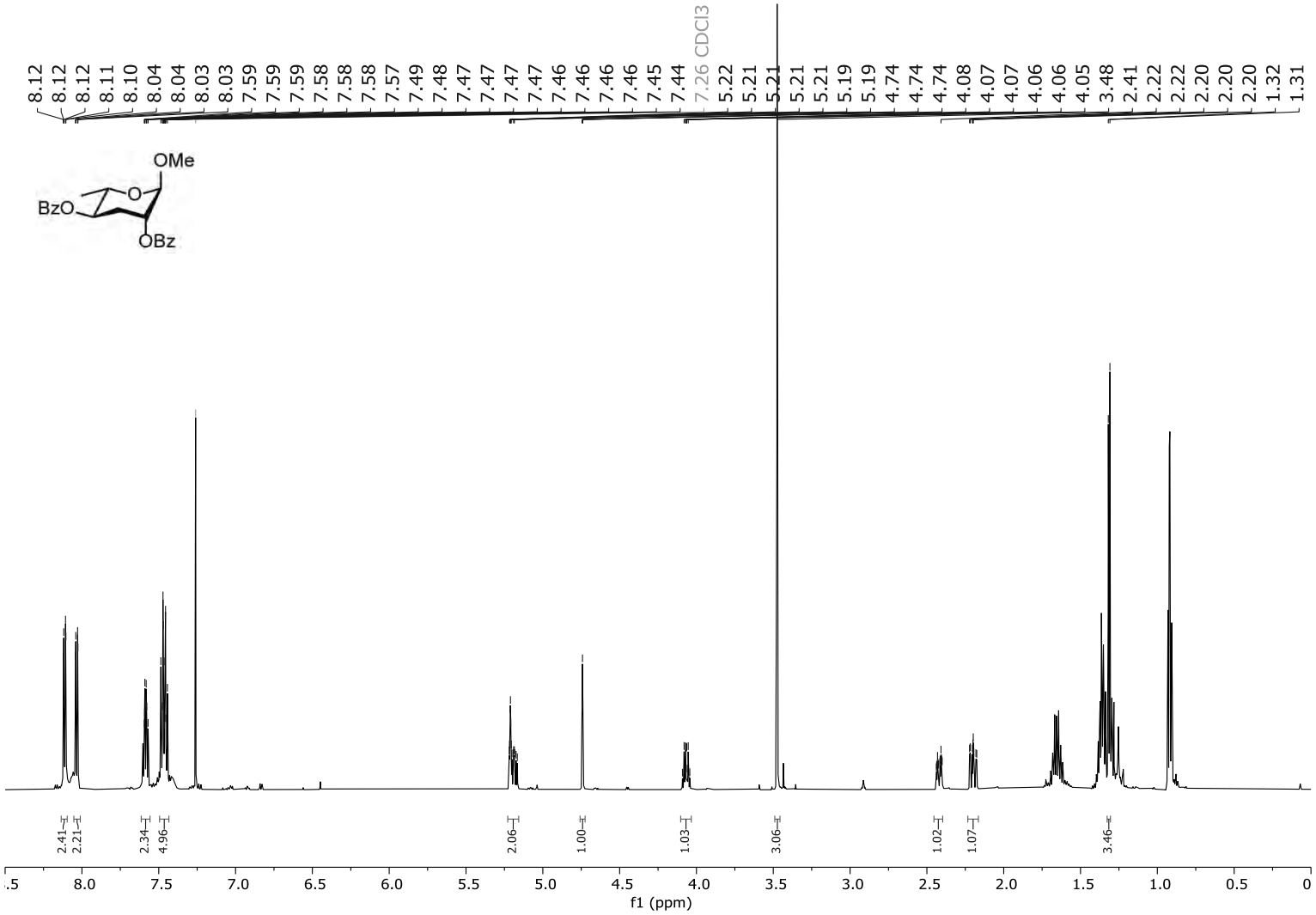

Figure S 33: ^{1}H NMR (400 MHz, $CDCl_3$) of 1-*O*-methyl-*6*-deoxy-2,3-*(O*-isopropylidene*)*-*α*-*L*-arabino-hexopyranoside (76).

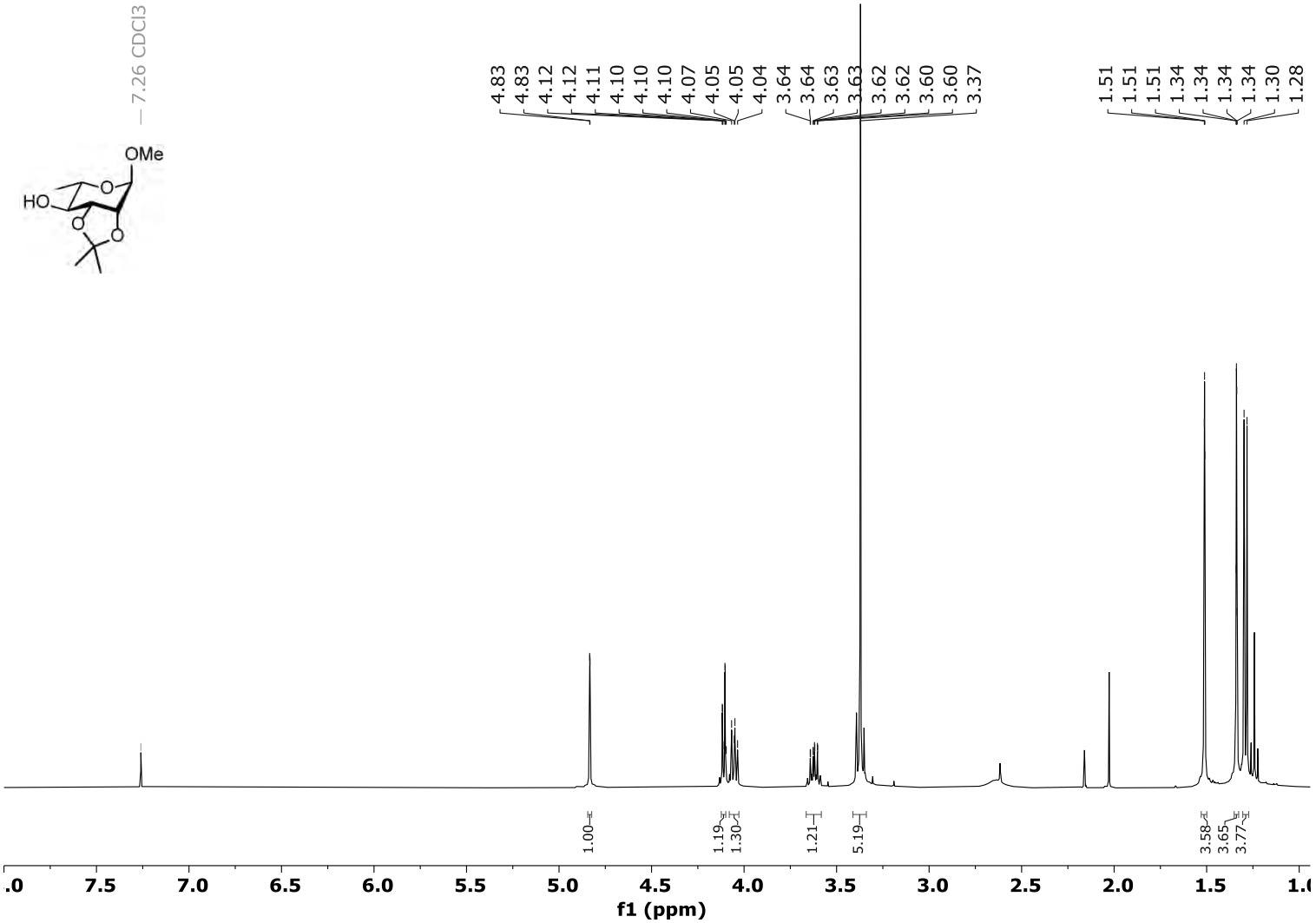

Figure S 34: ^{1}H NMR (400 MHz, $CDCl_3$) of 1-*O*-methyl-6-deoxy-2,3-*O*-(isopropylidene)-4-*tert*-butyldiphenylsilyl-α-L- *arabino*-hexopyranoside (77).

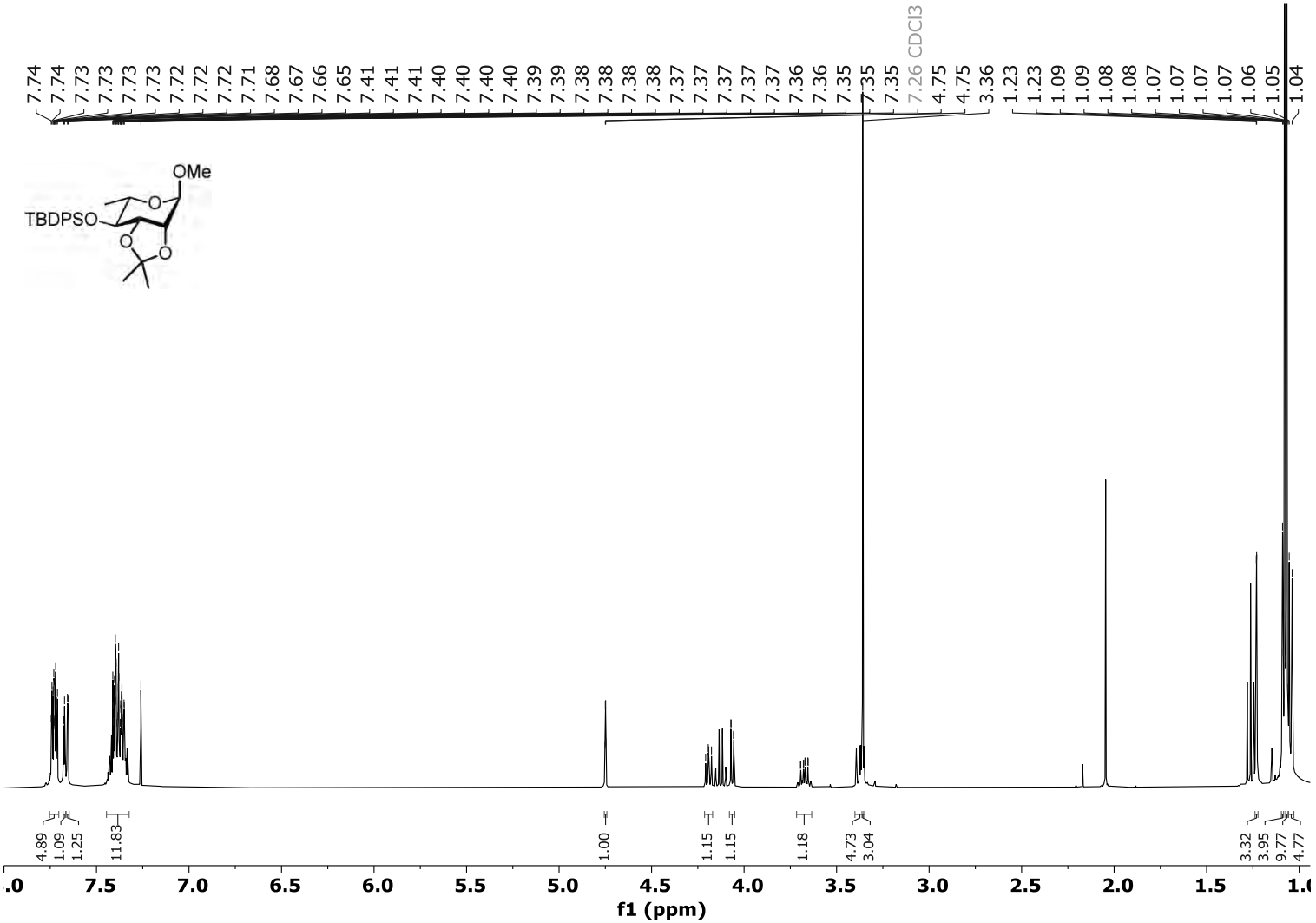

Figure S 35: ^{1}H NMR (400 MHz, $CDCl_3$) of *O*-methyl-6-deoxy-4-*tert*-butyldiphenylsilyl-α-L-*arabino*-hexopyranoside (78).

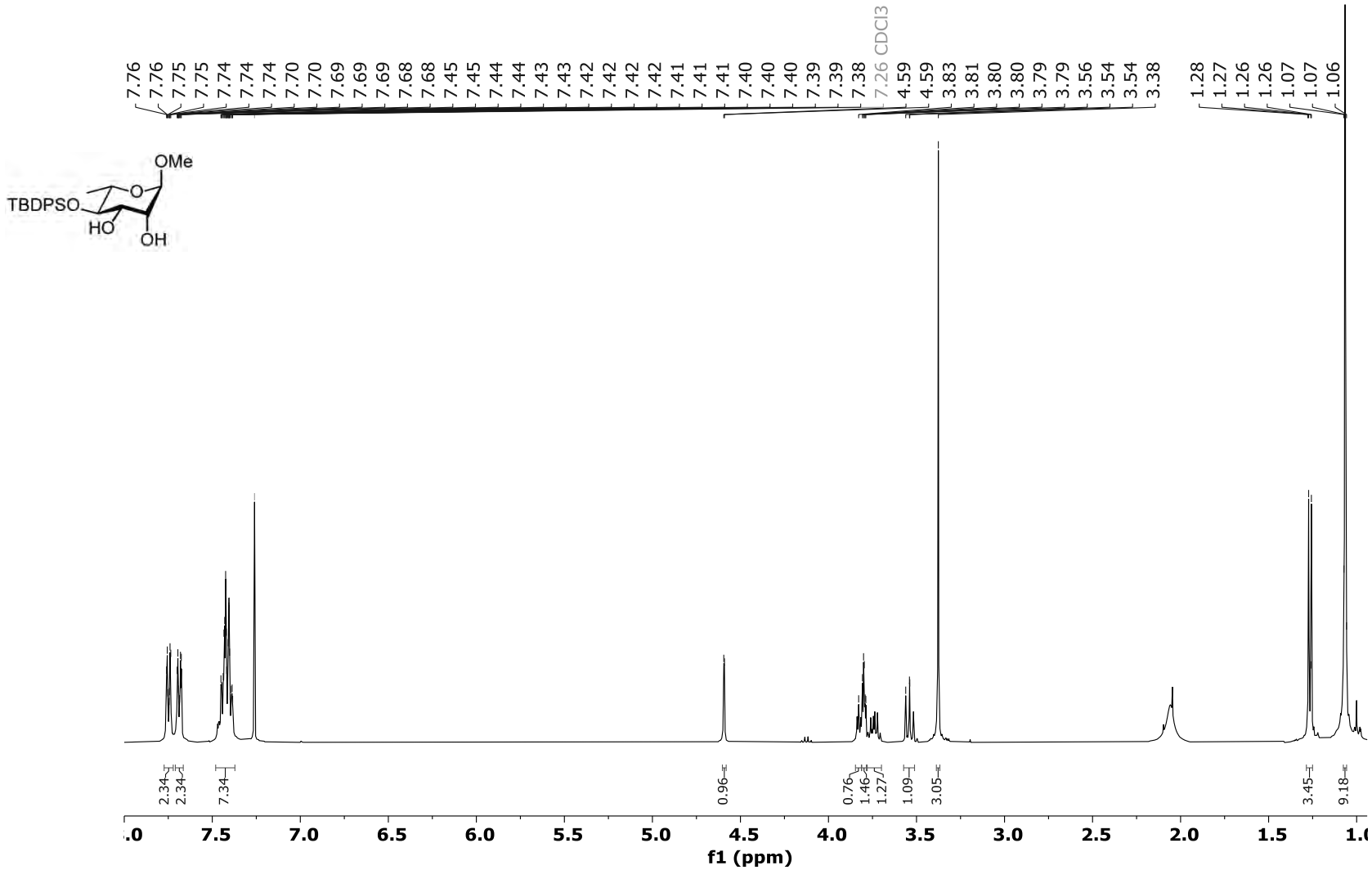

Figure S 36: ^{1}H NMR (400 MHz, $CDCl_3$) 1-*O*-methyl-6-deoxy-2,3-(*O*-sulfite)-4-*tert*-butyldiphenylsilyl-α-L-*arabino*-hexopyranoside (79).

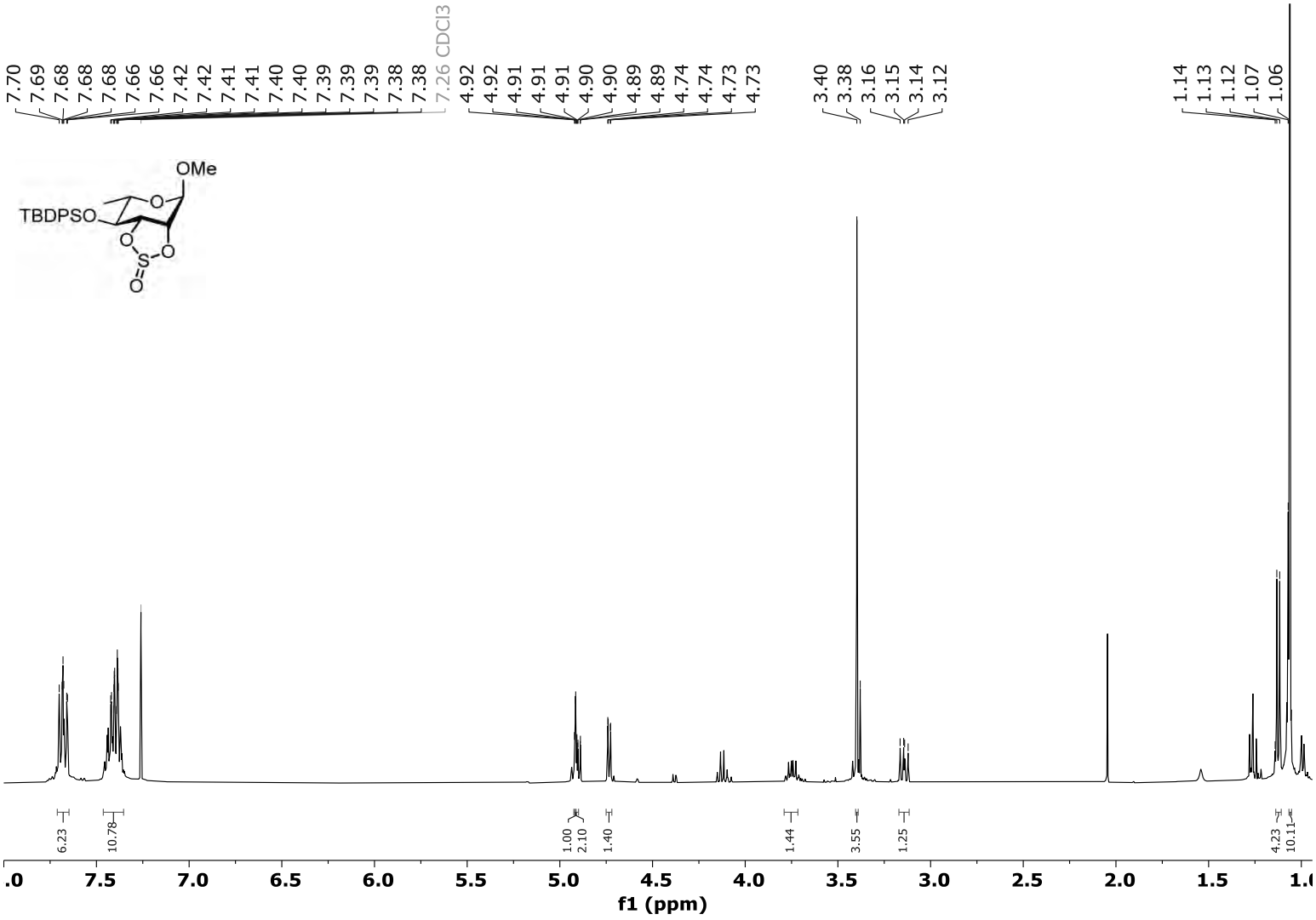

Figure S 37: ^{1}H NMR (400 MHz, $CDCl_3$) 1-O-methyl-6-deoxy-2,3-(*O*-sulfate)-4-tert-butyldiphenylsilyl-α-L-*arabino*-hexopyranoside (80).

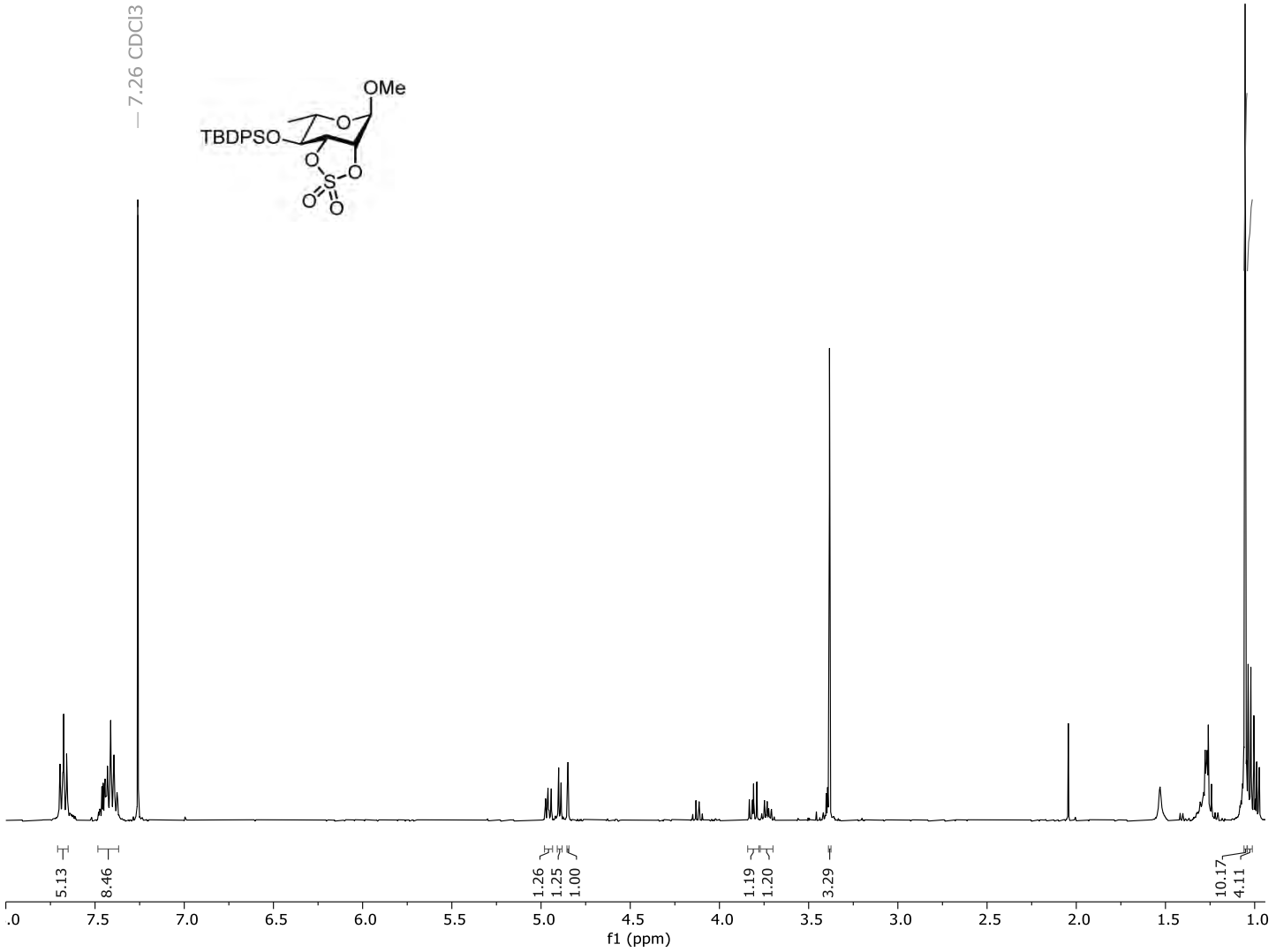

Figure S 38: ^{1}H NMR (400 MHz, $CDCl_3$) of 1-*O*-methyl-4-*O*-*tert*-butyldiphenylsilyl 3,6-dideoxy-α-L-*arabino*-hexopyranose (81).

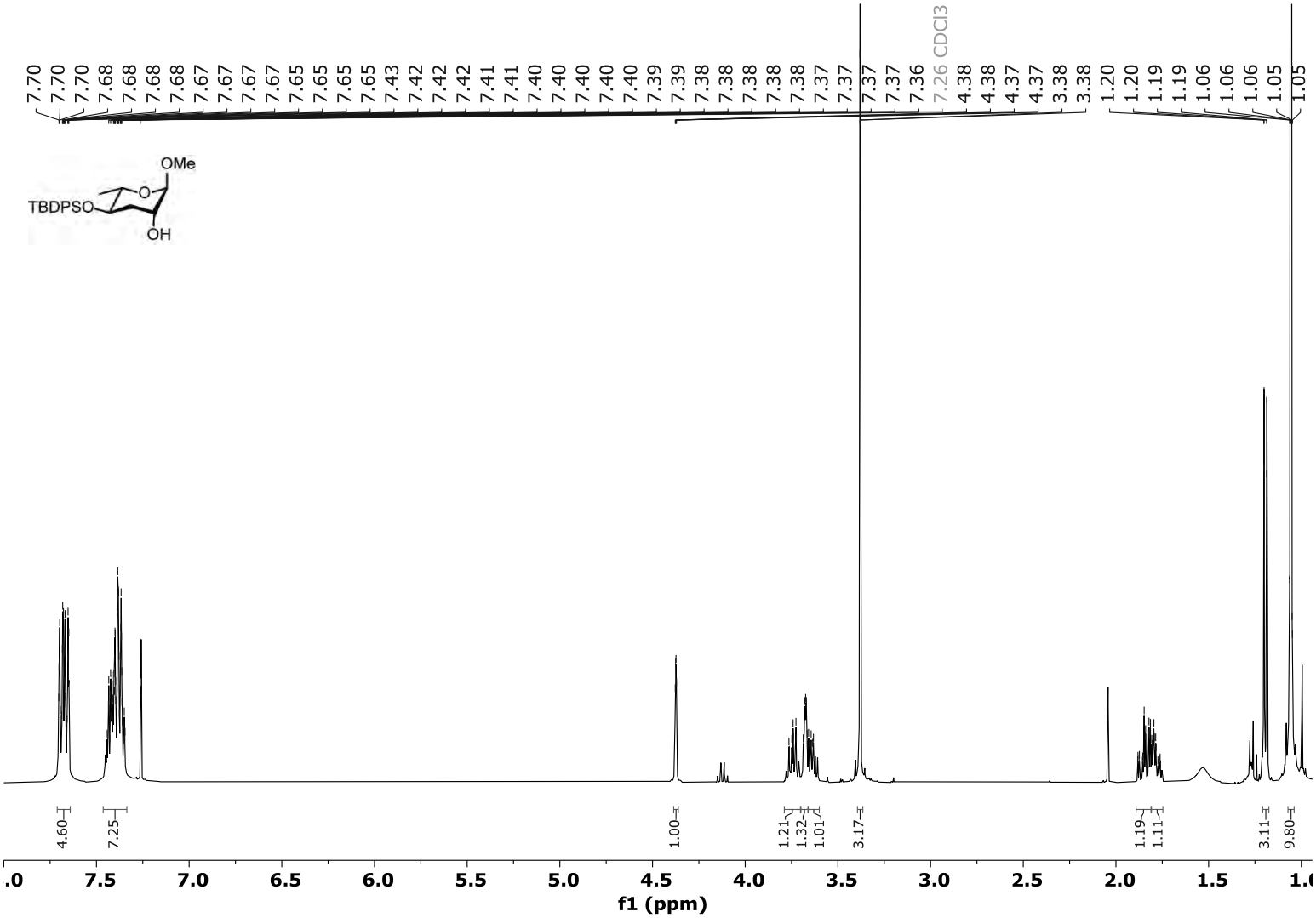

Figure S 39: ^{1}H NMR (400 MHz, $CDCl_3$) of 1-*O*-methyl-2-*O*-benzoyl-4-*O*-*tert*-butyldiphenylsilyl 3,6-dideoxy-α-L-*arabino*-hexopyranose (82).

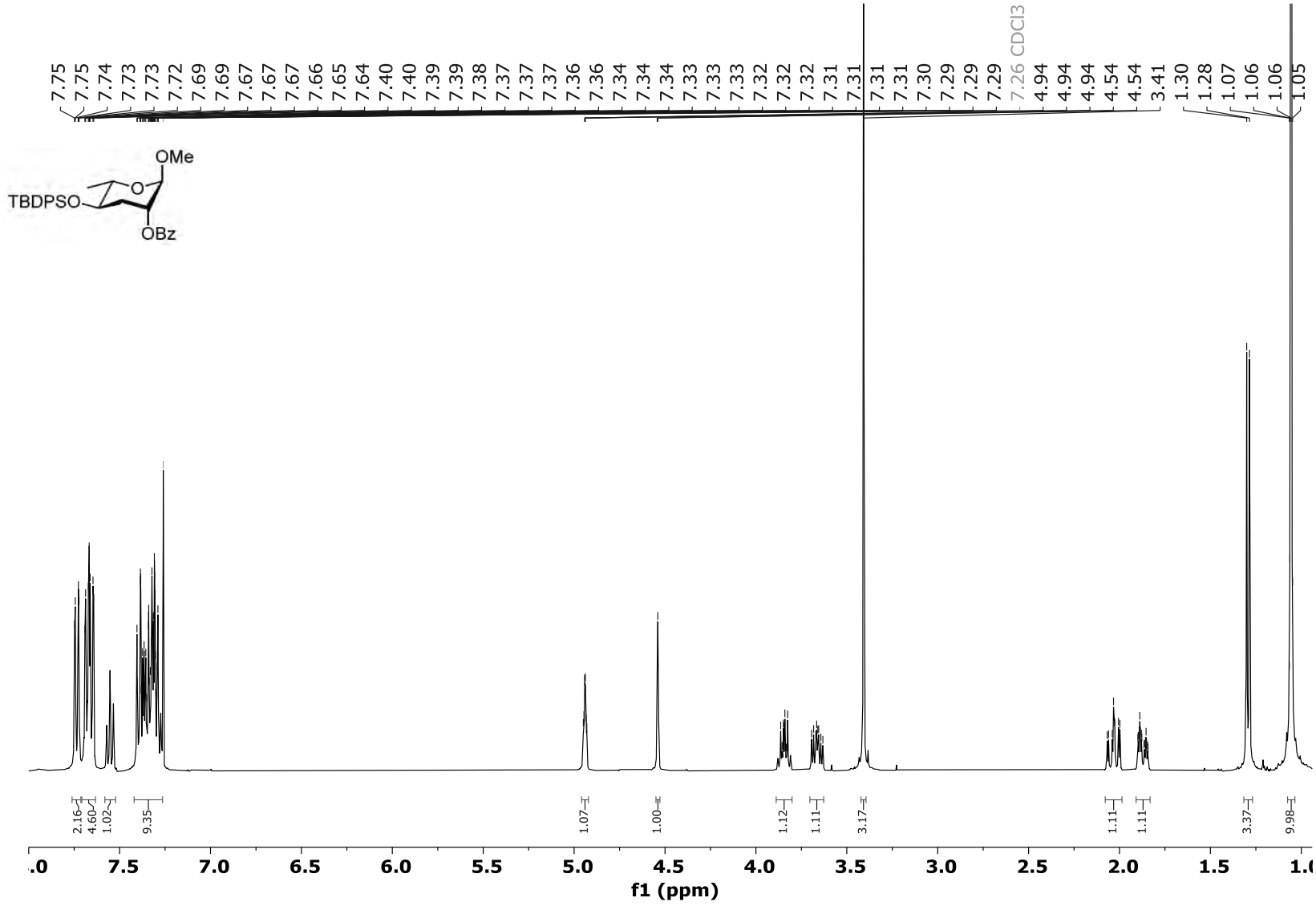

Figure S 40: ^{1}H NMR (400 MHz, $CDCl_3$) of 2-*O*-benzoyl-4-*O*-*tert*-butyldiphenylsilyl-3,6-dideoxy-α-L-*arabino*-hexopyranose (45).

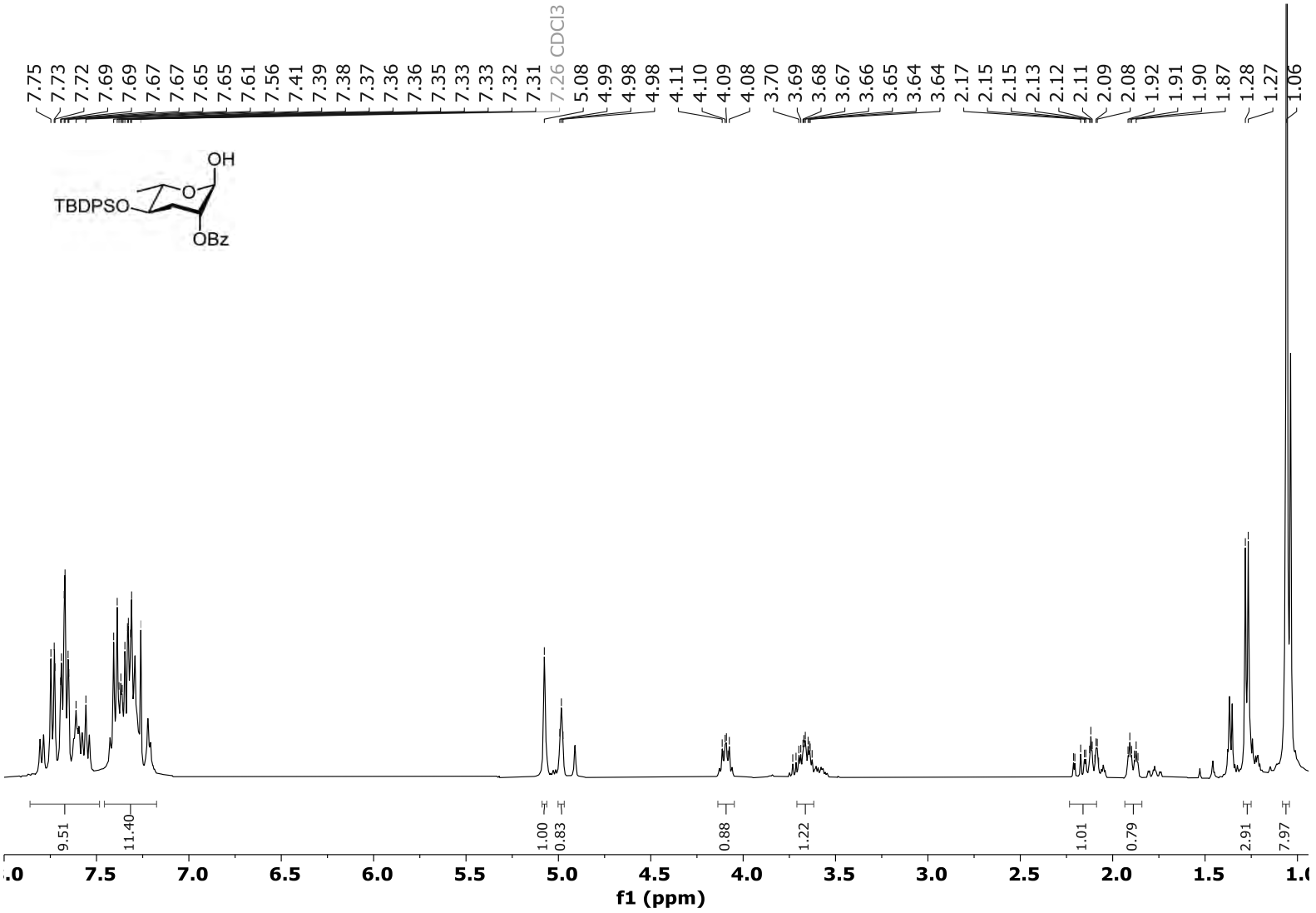

Figure S 41: ^{1}H NMR (600 MHz, $CDCl_3$) 1-*O*-methyl-6-deoxy-2,3-(*O*-benzylidene)-α-L-*arabino*-hexose (57).

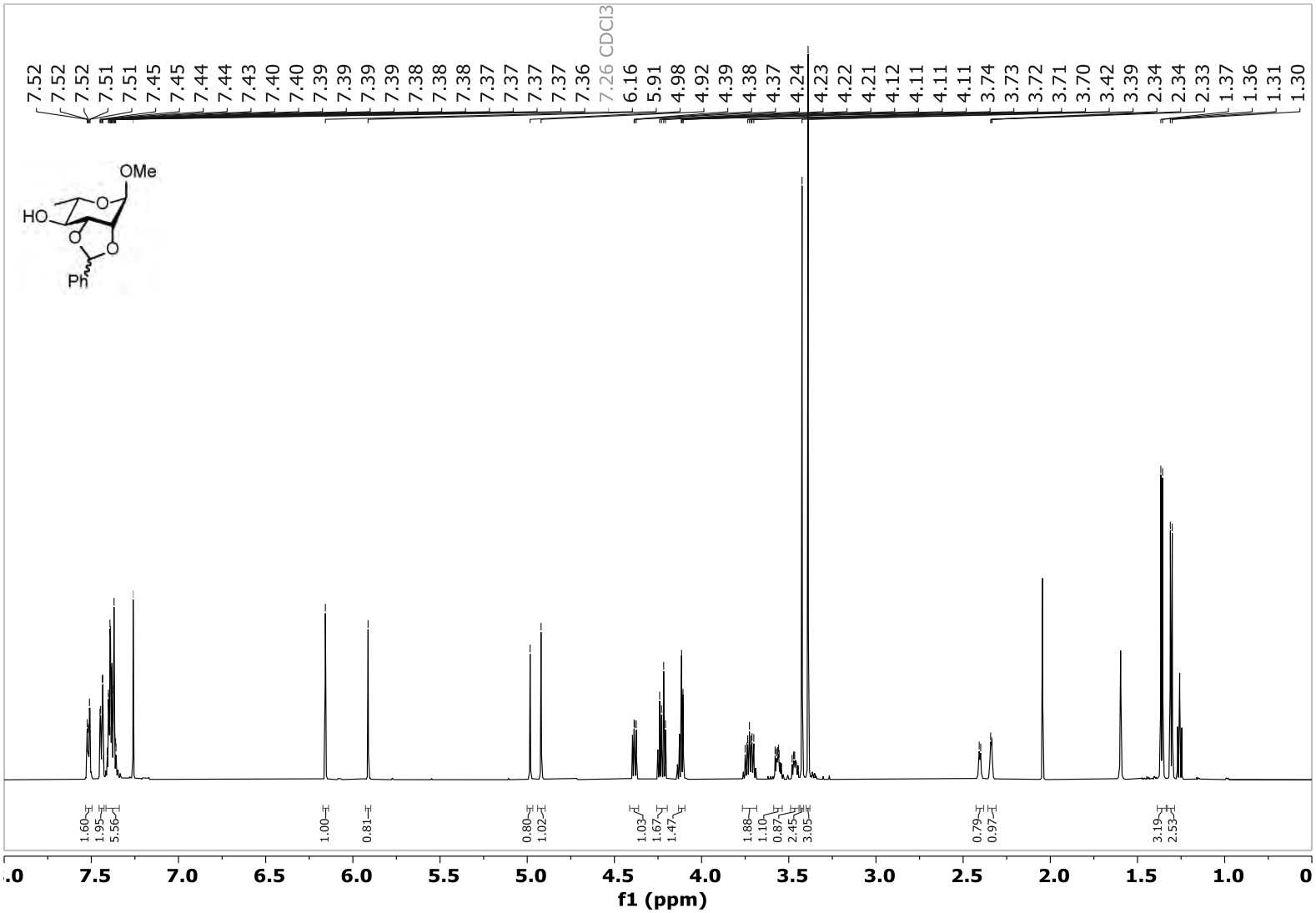

Figure S 42: ^{13}C NMR (150 MHz, $CDCl_3$) of 1-*O*-methyl-6-deoxy-2,3-(*O*-benzylidene)-α-L-*arabino*-hexose (57).

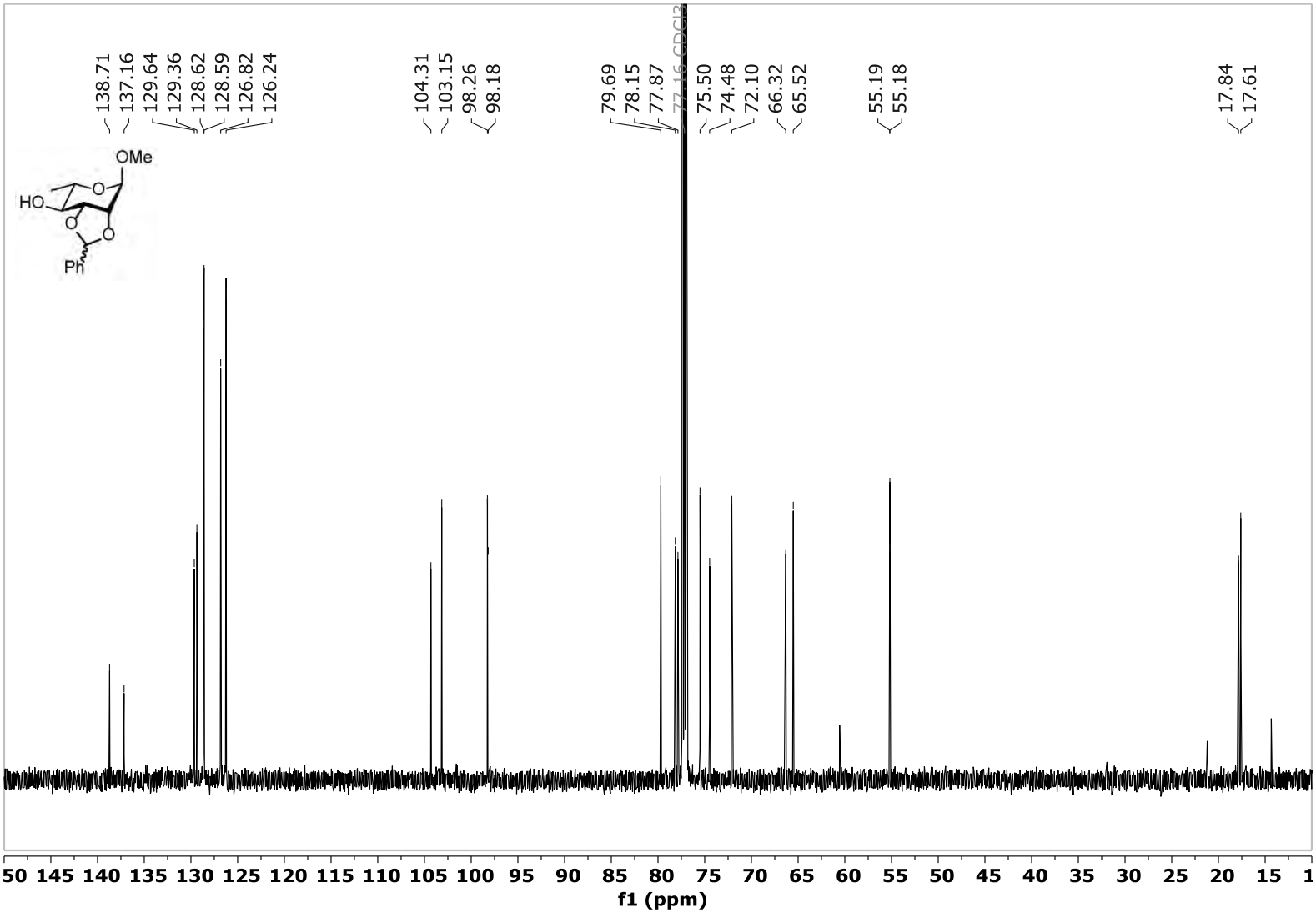

Figure S 43: ***dqf*-COSY (600 MHz, $CDCl_3$) of 1-*O*-methyl-6-deoxy-2,3-(*O*-benzylidene)-α-L-*arabino*-hexose (57).**

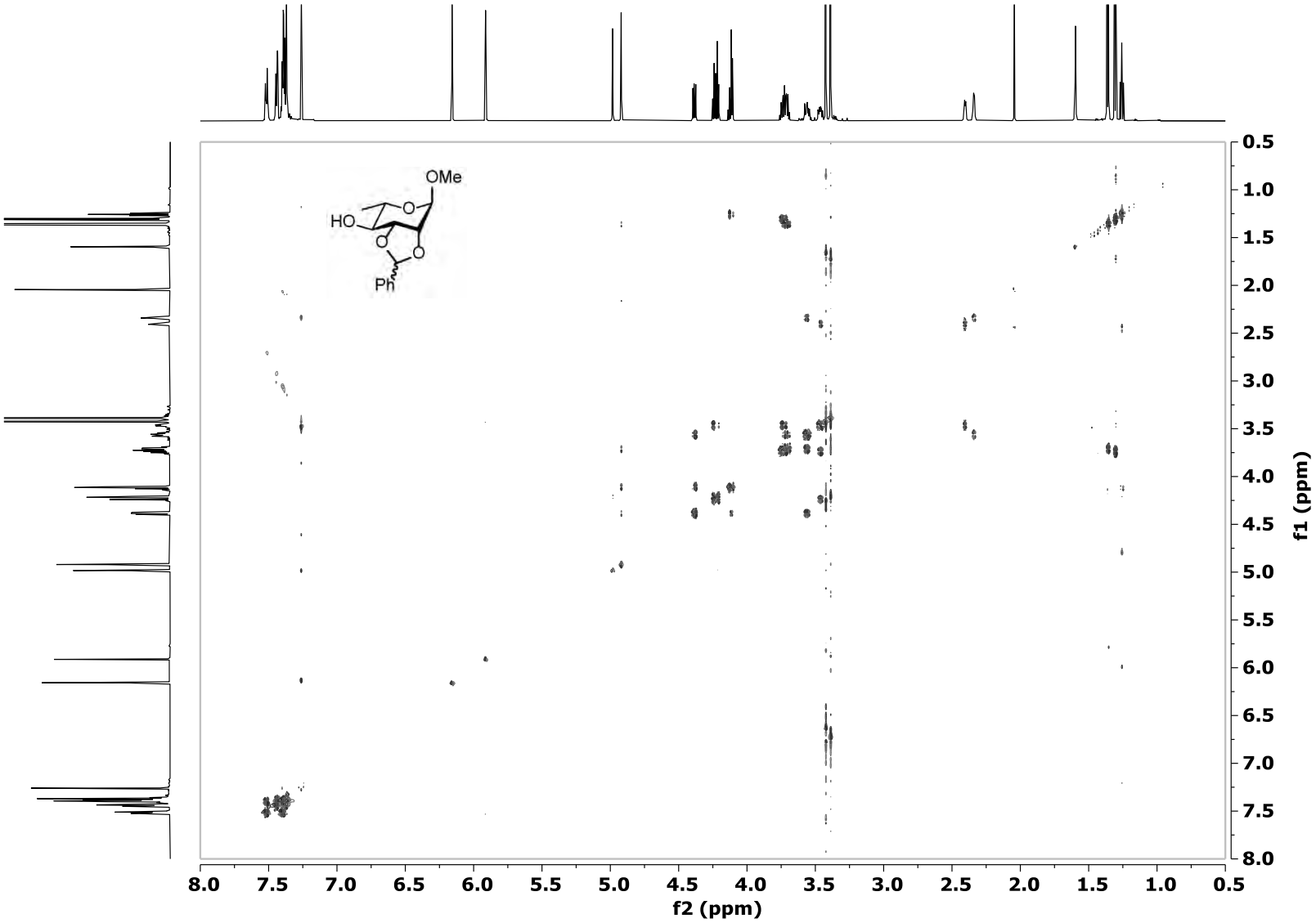

Figure S 44: HSQC (600 MHz, $CDCl_3$) of 1-*O*-methyl-6-deoxy-2,3-(*O*-benzylidene)-α-L-*arabino*-hexose (57).

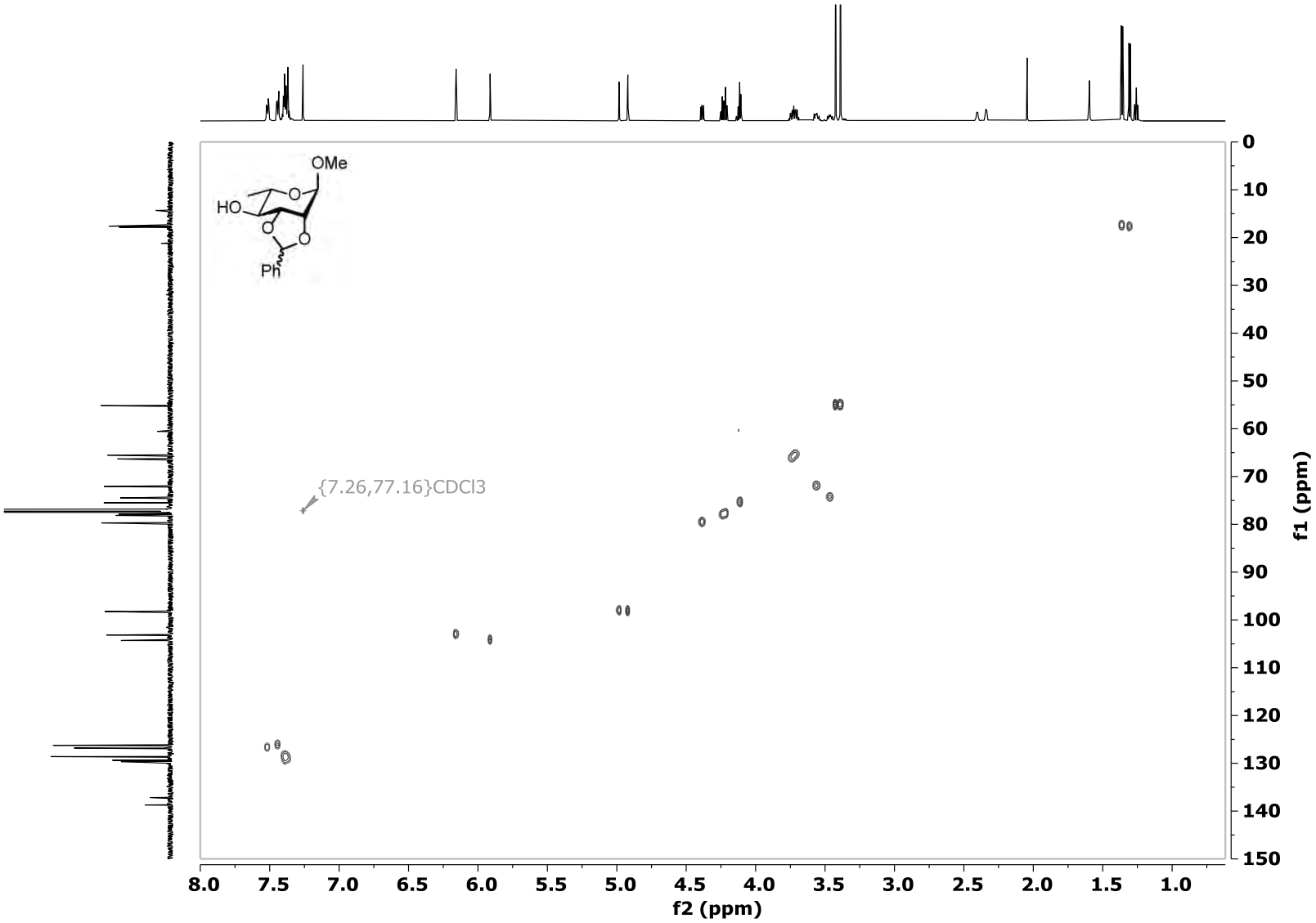

Figure S 45: ^{1}H NMR (600 MHz, $CDCl_3$) of 1-*O*-methyl-2-*O*-benzoyl-3-bromo-3,6-dideoxy-*altro*-hexose (58).

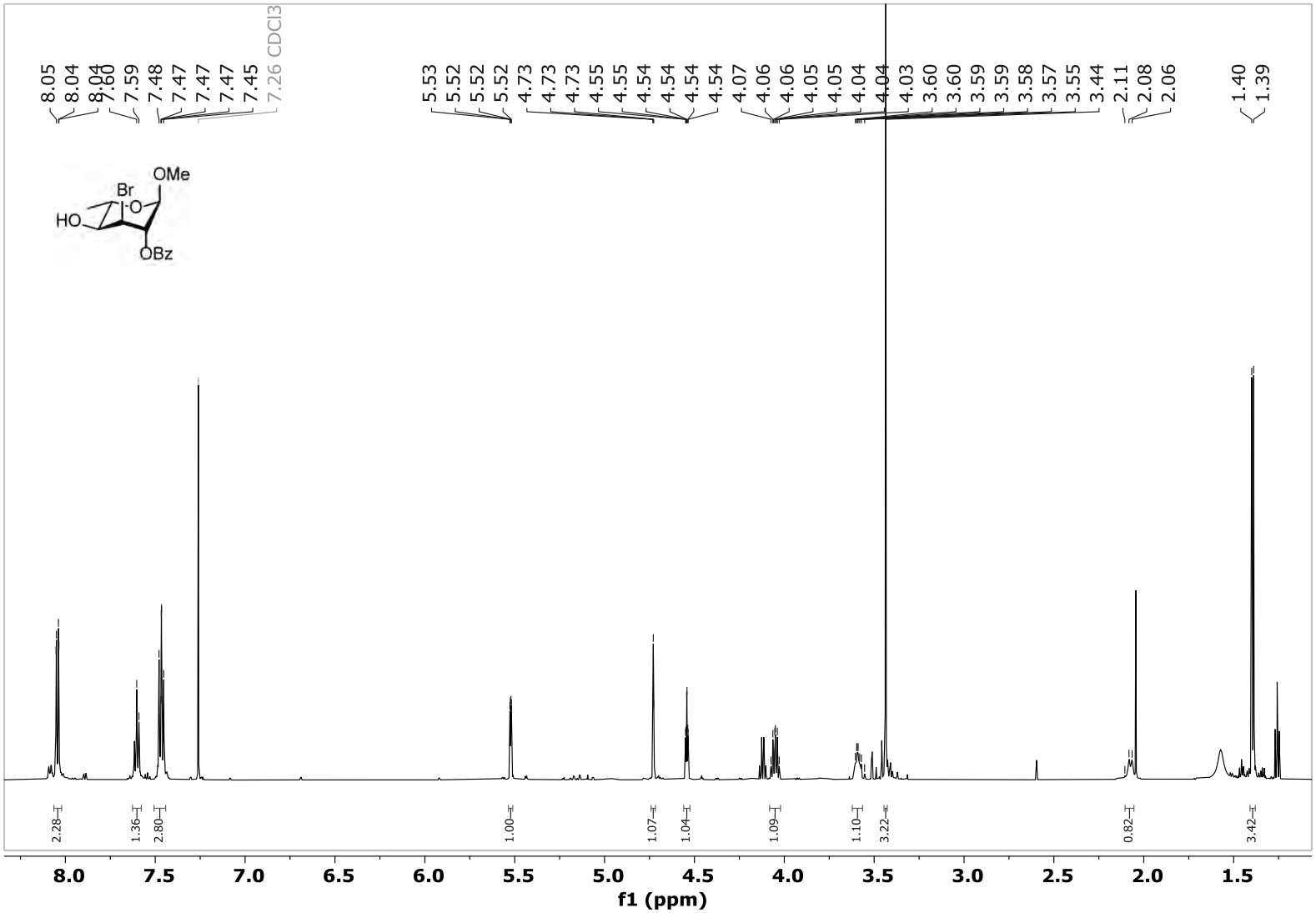

Figure S 46: ^{13}C NMR (150 MHz, $CDCl_3$) of 1-*O*-methyl-2-*O*-benzoyl-3-bromo-3,6-dideoxy-*altro*-hexose (58).

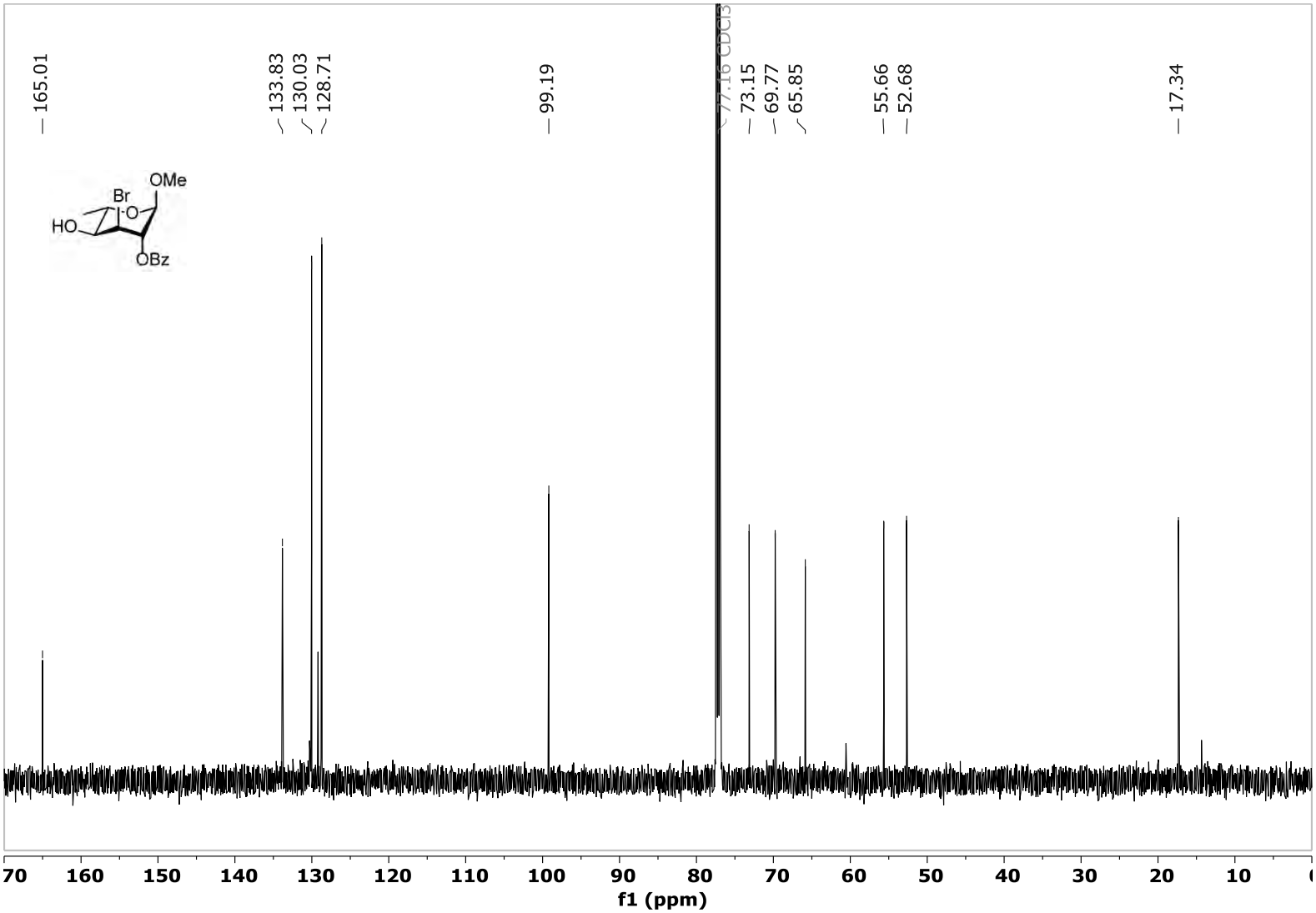

Figure S 47: dqf-COSY (600 MHz, $CDCl_3$) of 1-*O*-methyl-2-*O*-benzoyl-3-bromo-3,6-dideoxy-*altro*-hexose (58).

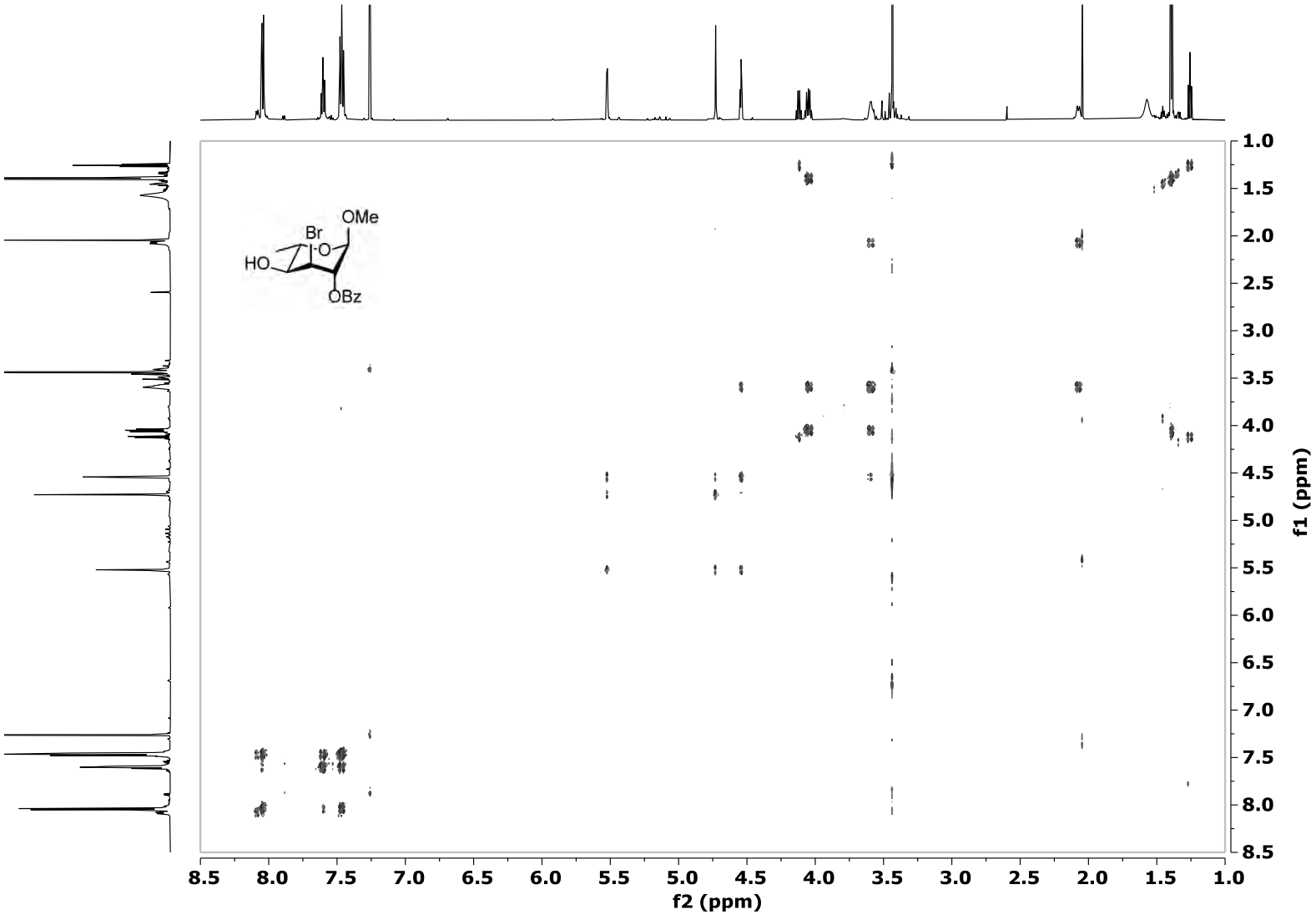

Figure S 48: HSQC of (600 MHz, $CDCl_3$) of 1-*O*-methyl-2-*O*-benzoyl-3-bromo-3,6-dideoxy-*altro*-hexose (58).

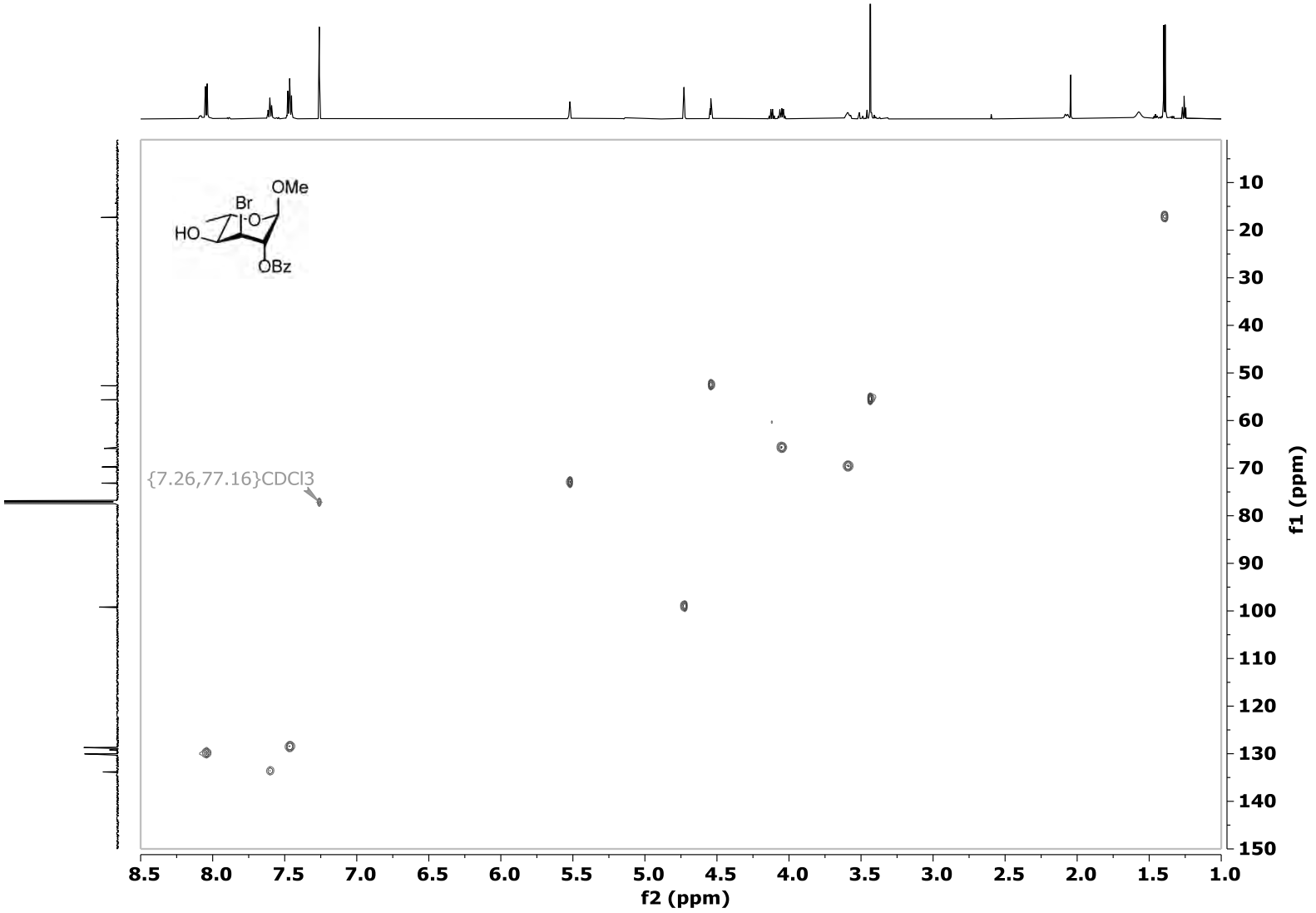

Figure S 49: ^{1}H NMR (600 MHz, $CDCl_3$) of 1-*O*-methyl-2-*O*-benzoyl 3,6-dideoxy-α-L-*arabino*-hexose (88).

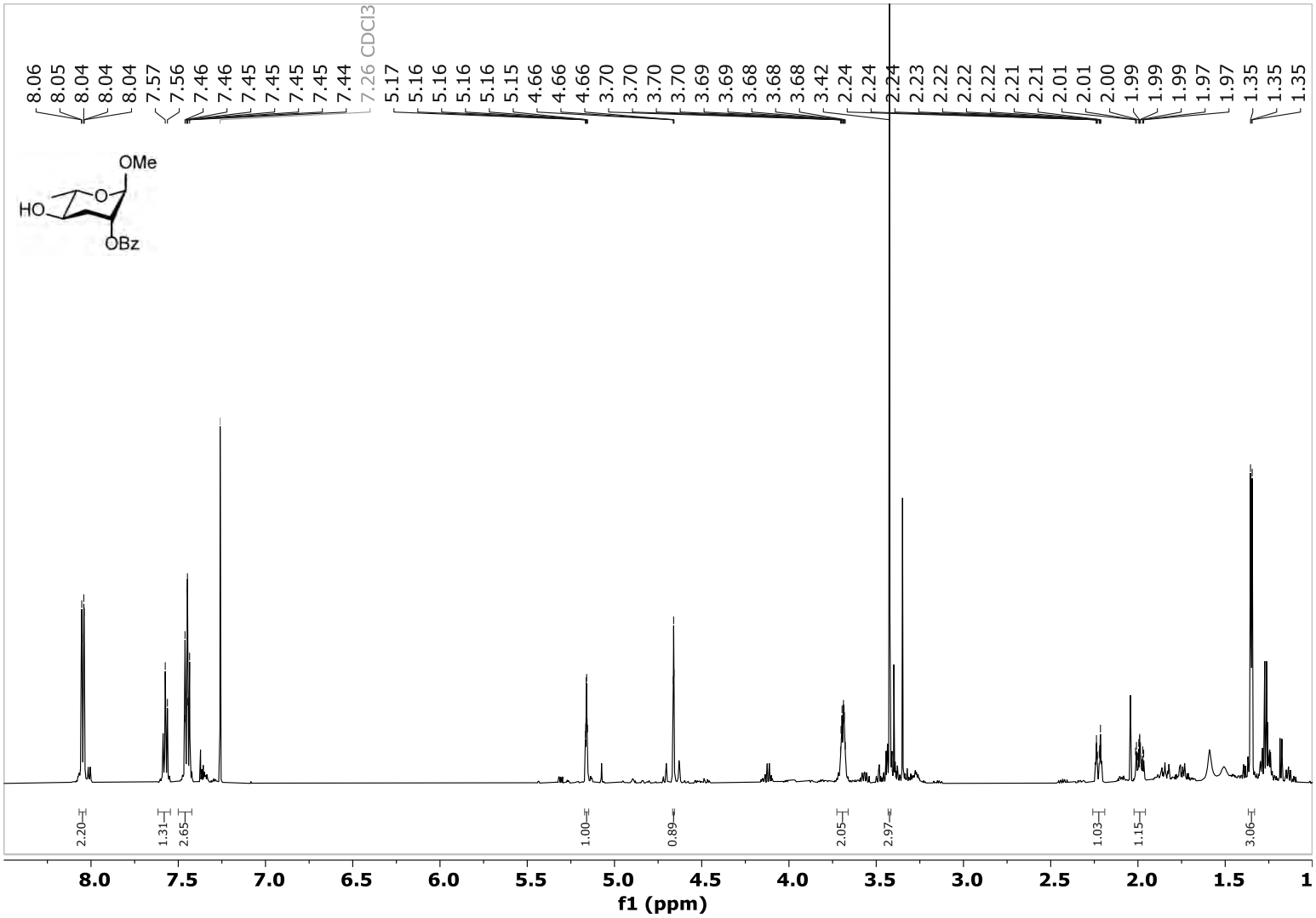

Figure S 50: ^{13}C NMR (150 MHz, $CDCl_3$) of 1-*O*-methyl-2-*O*-benzoyl 3,6-dideoxy-α-L-*arabino*-hexose (88).

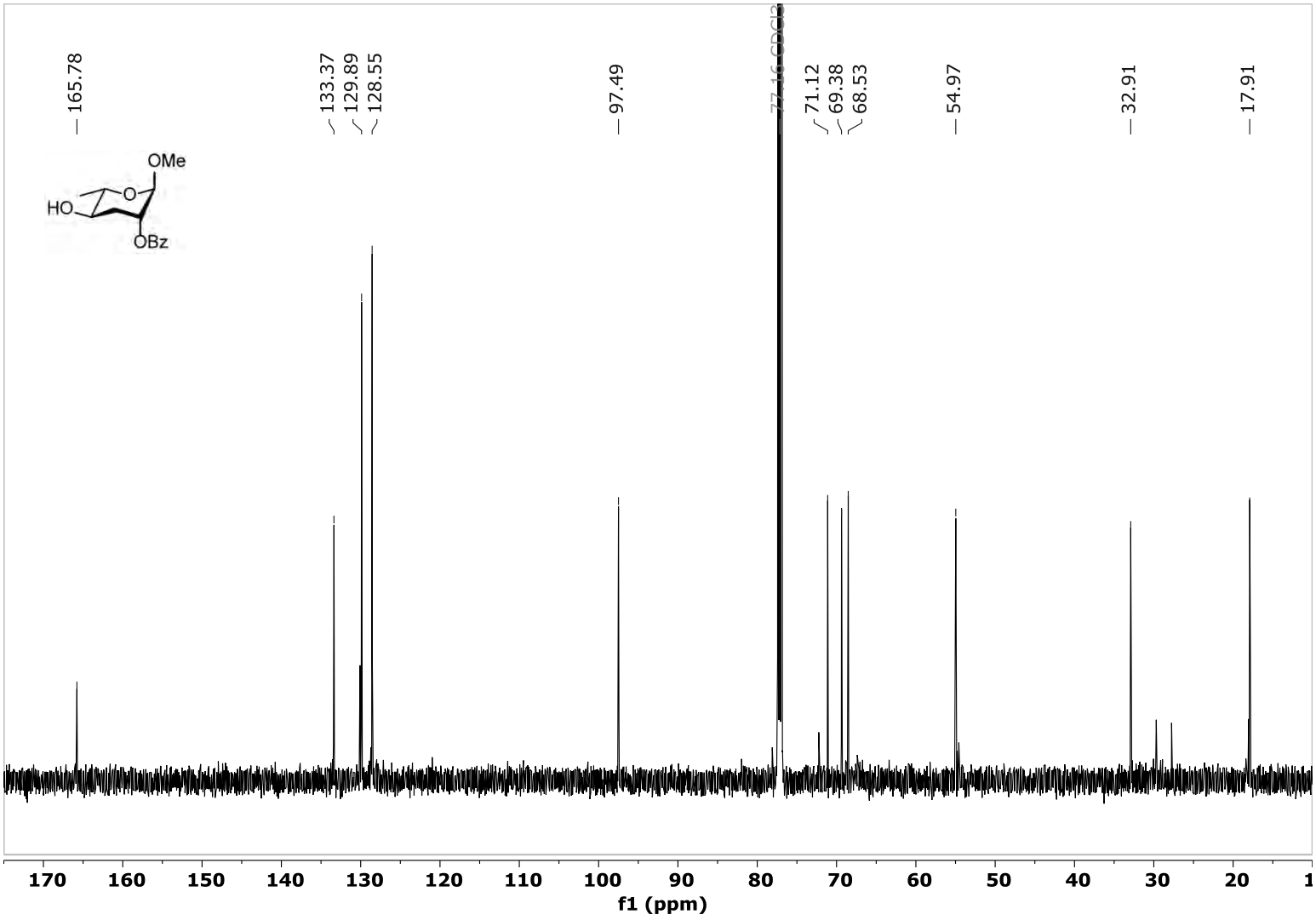

Figure S 51: *daf*-COSY (600 MHz, $CDCl_3$) of 1-*O*-methyl-2-*O*-benzoyl 3,6-dideoxy-α-L-*arabino*-hexose (88).

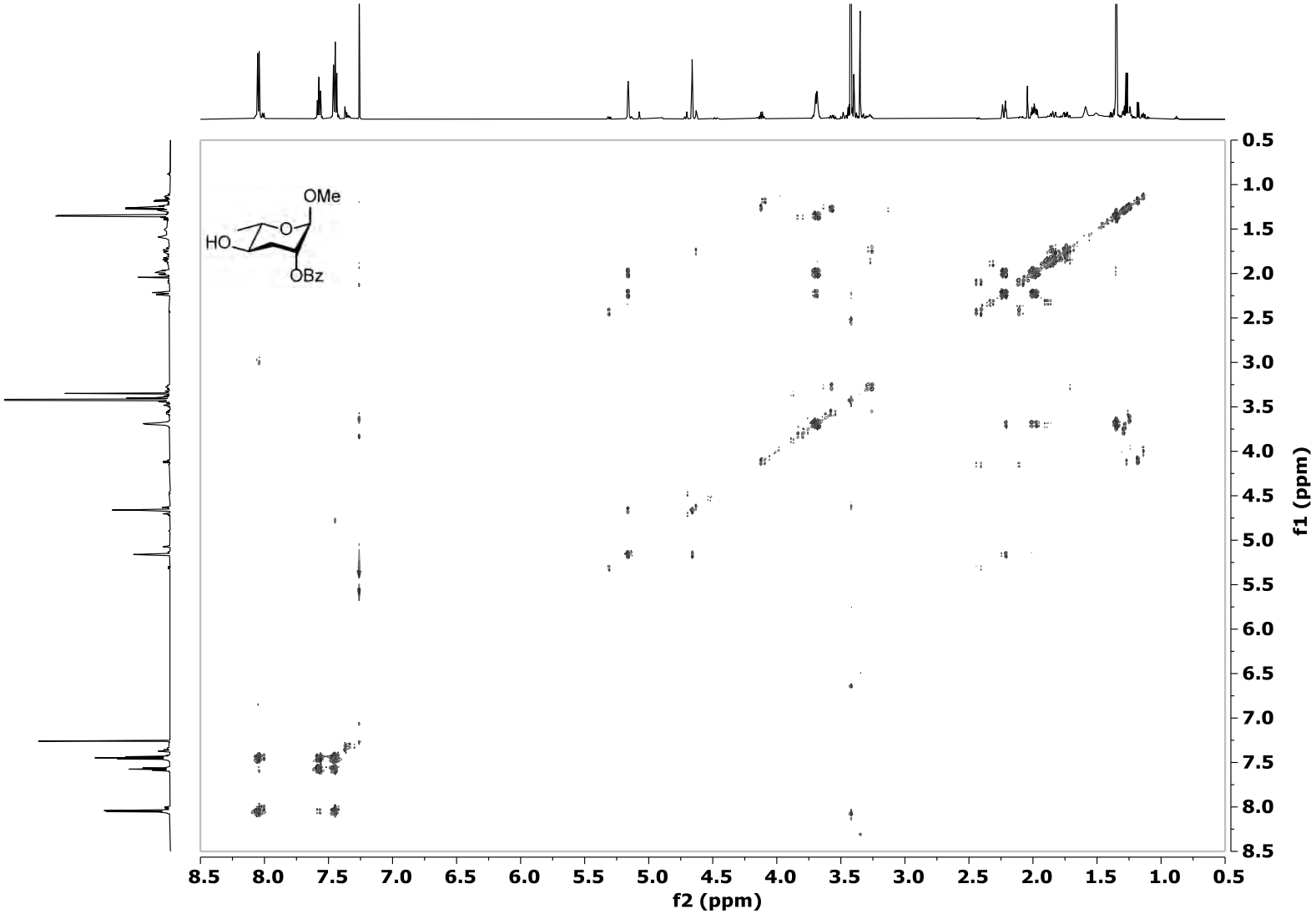

Figure S 52: HSQC (600 MHz, $CDCl_3$) of 1-*O*-methyl-2-*O*-benzoyl 3,6-dideoxy-α-L-*arabino*-hexose (88).

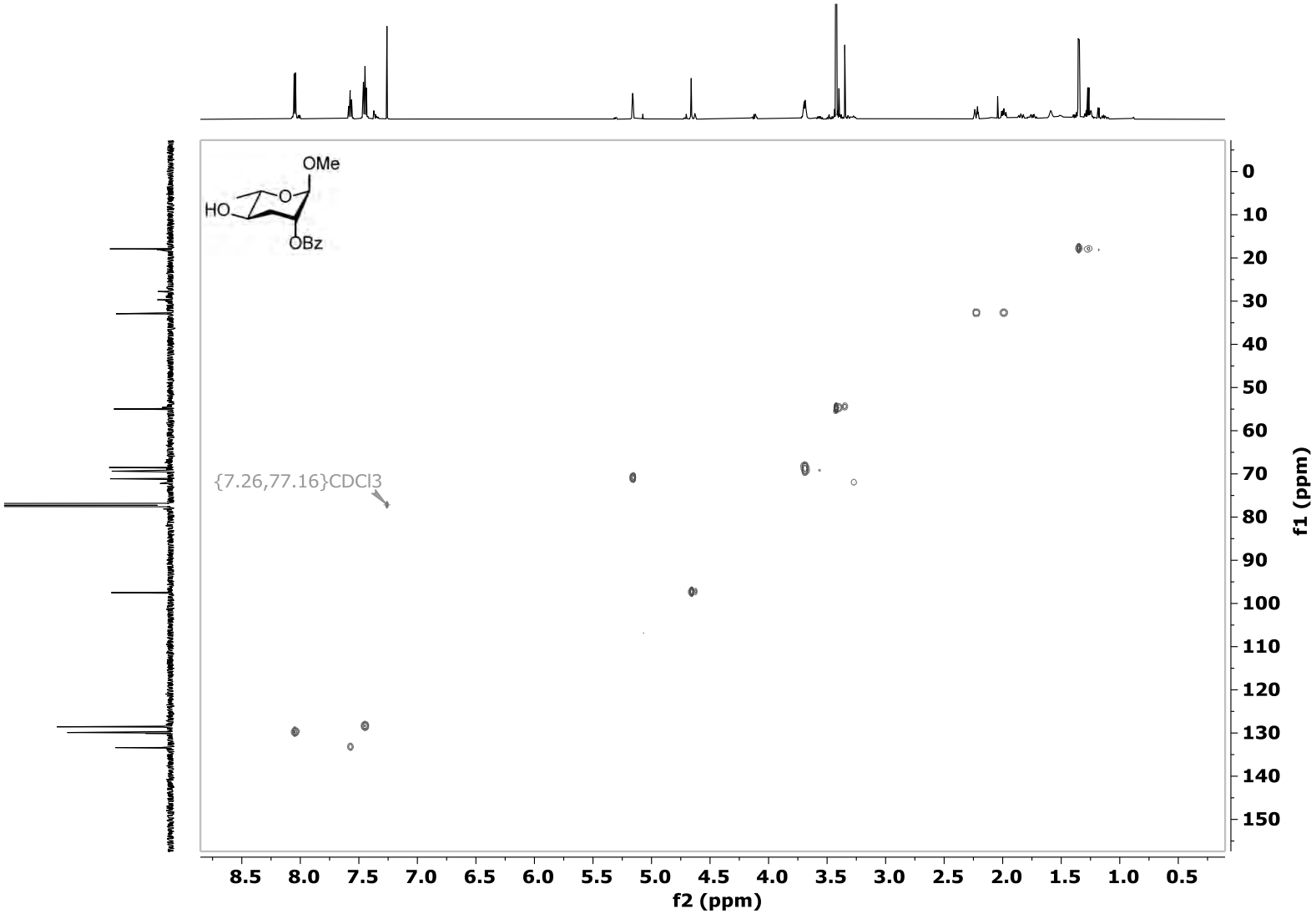

Figure S 53: ^{1}H NMR (600 MHz, $CDCl_3$) of 2-*O*-benzoyl-4-*O*-(4-methoxybenzyl)-3,6-dideoxy-α-L-*arabino*-hexose (95).

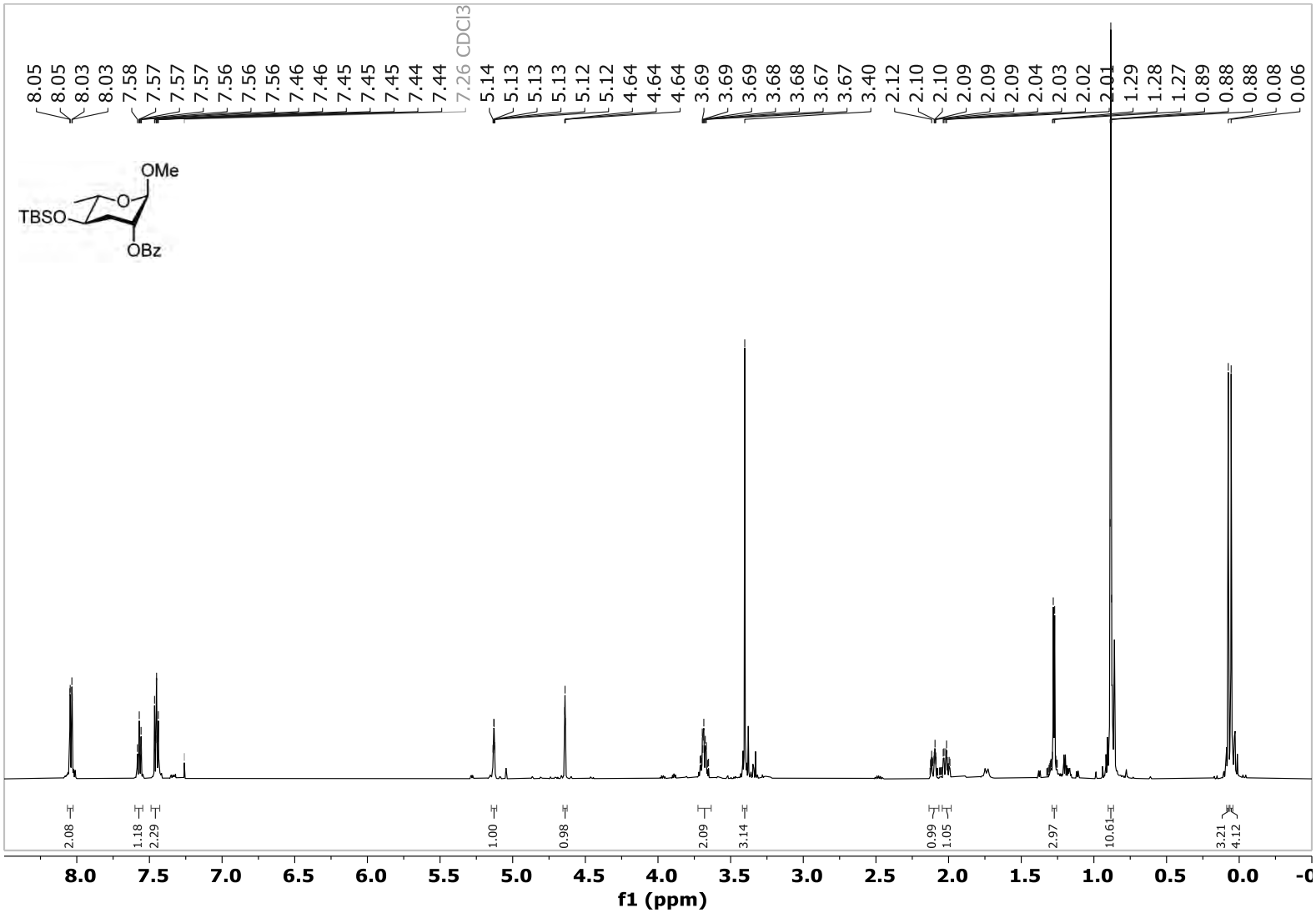

Figure S 54: ^{13}CNMR (150 MHz, $CDCl_3$) of 2-*O*-benzoyl-4-*O*-(4-methoxybenzyl)-3,6-dideoxy-α-L-*arabino*-hexose (95).

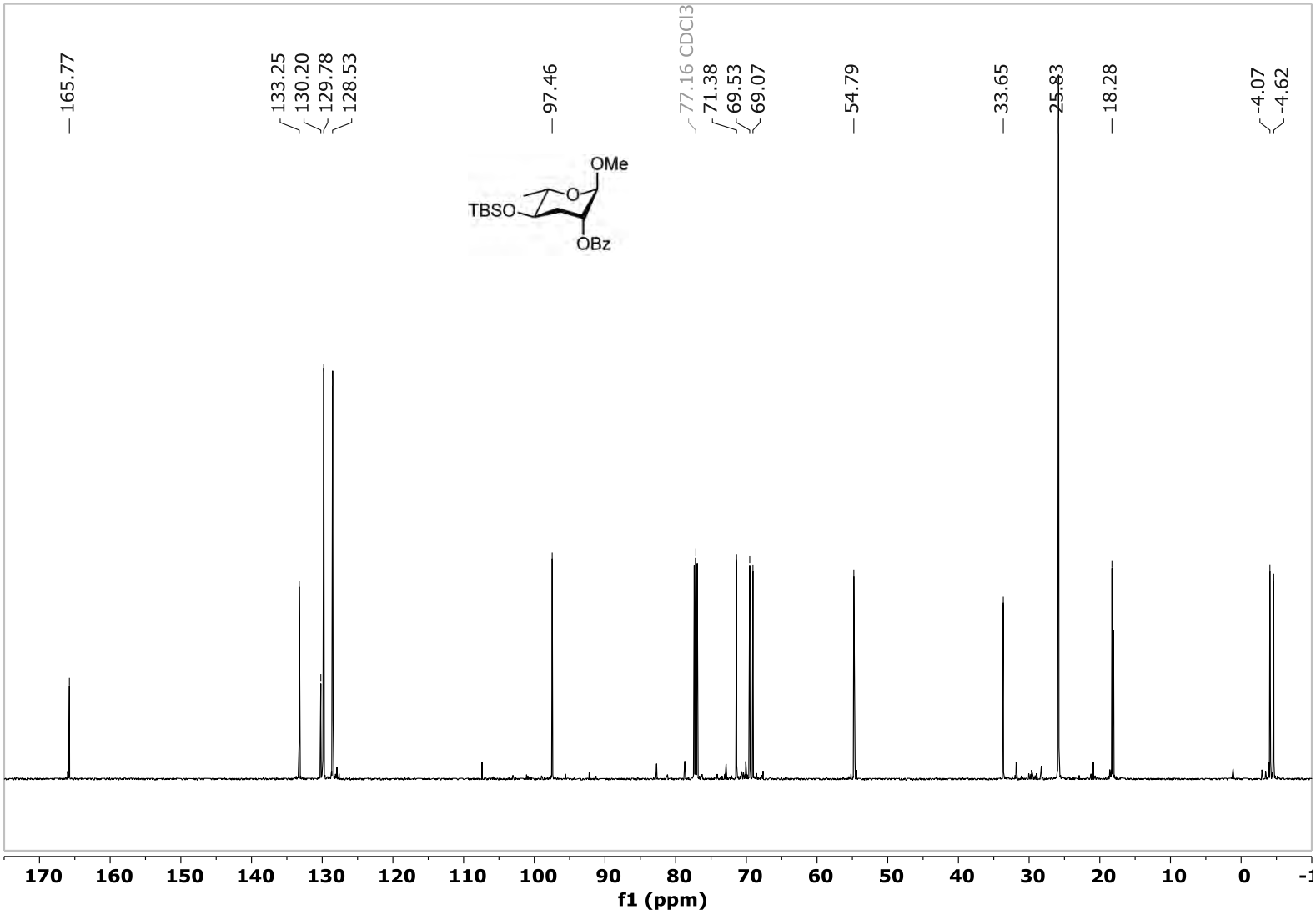

Figure S 55: *dqf*-COSY (600 MHz, $CDCl_3$) of 2-*O*-benzoyl-4-*O*-(4-methoxybenzyl)-3,6-dideoxy-α-L-*arabino*-hexose (95).

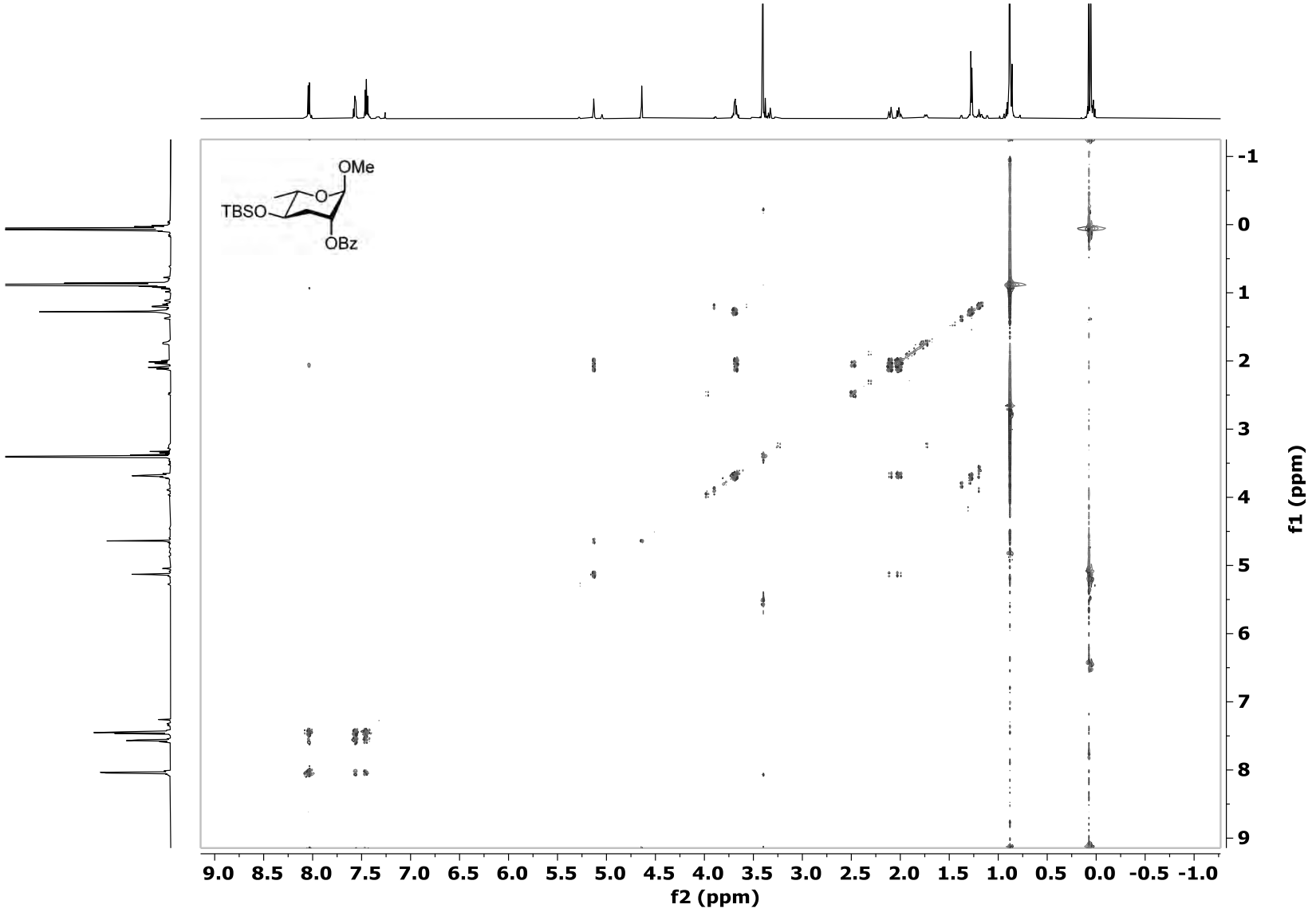

Figure S 56: HSQC (600 MHz, $CDCl_3$) of 2-*O*-benzoyl-4-*O*-(4-methoxybenzyl)-3,6-dideoxy-α-L-*arabino*-hexose (95).

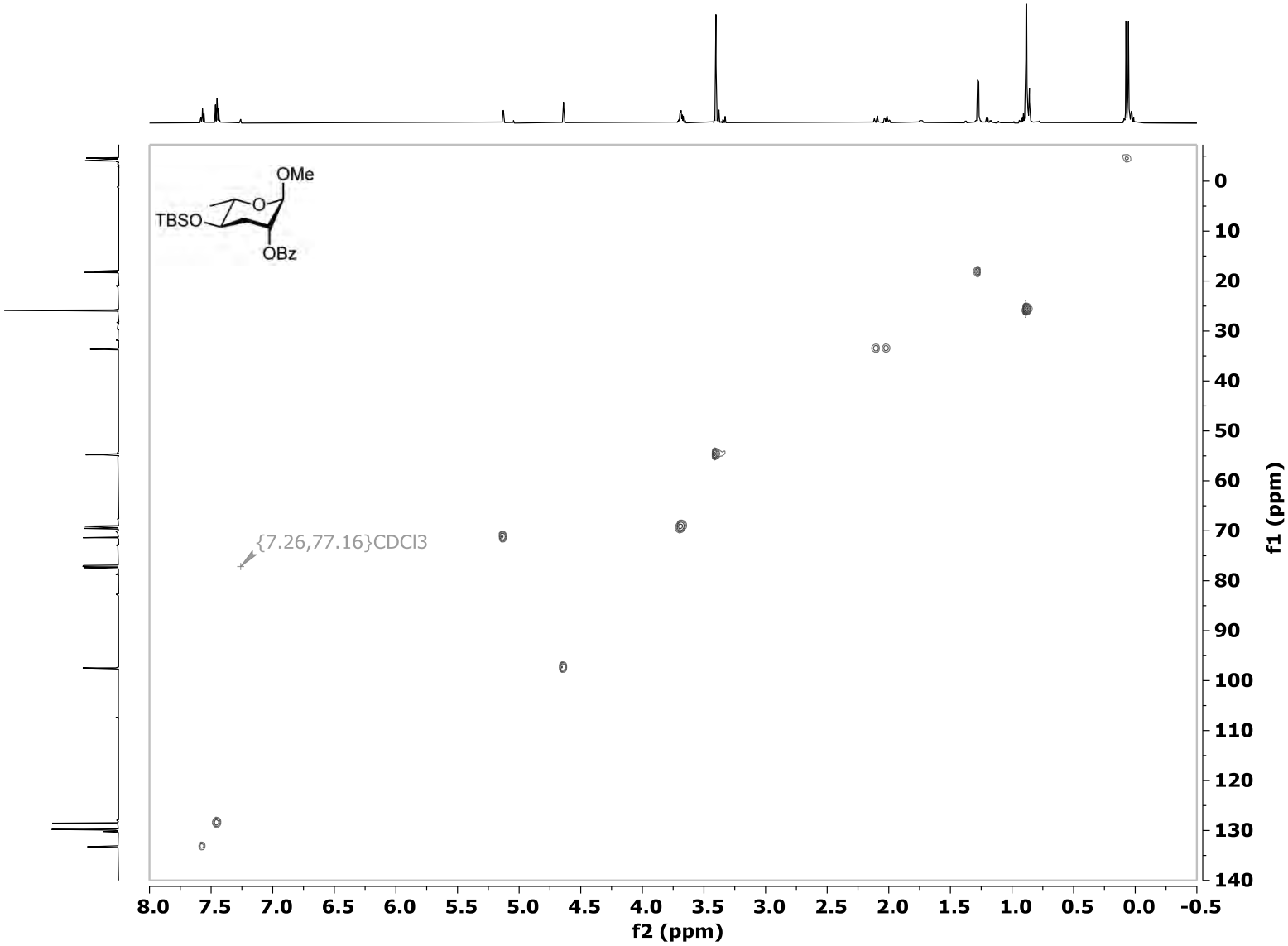

Figure S 57: ^{1}HNMR (600 MHz, $CDCl_3$) of 2-*O*-benzoyl-4-*O*-(4-methoxybenzyl)-3,6-dideoxy-α-L-*arabino*-hexose (94).

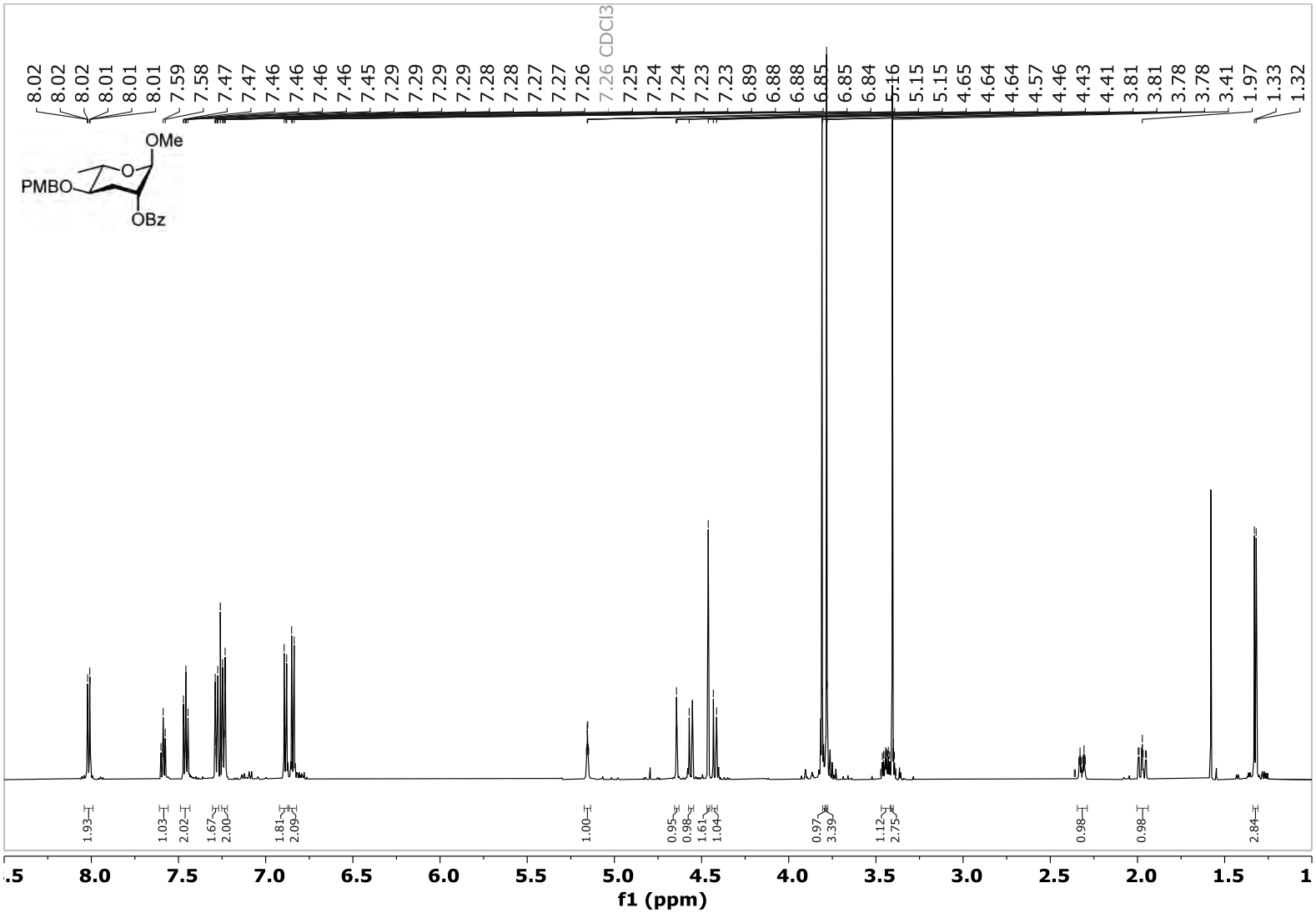

Figure S 58: ^{13}C NMR (150 MHz) 2-*O*-benzoyl-4-*O*-(4-methoxybenzyl)-3,6-dideoxy-α-L-*arabino*-hexose (94).

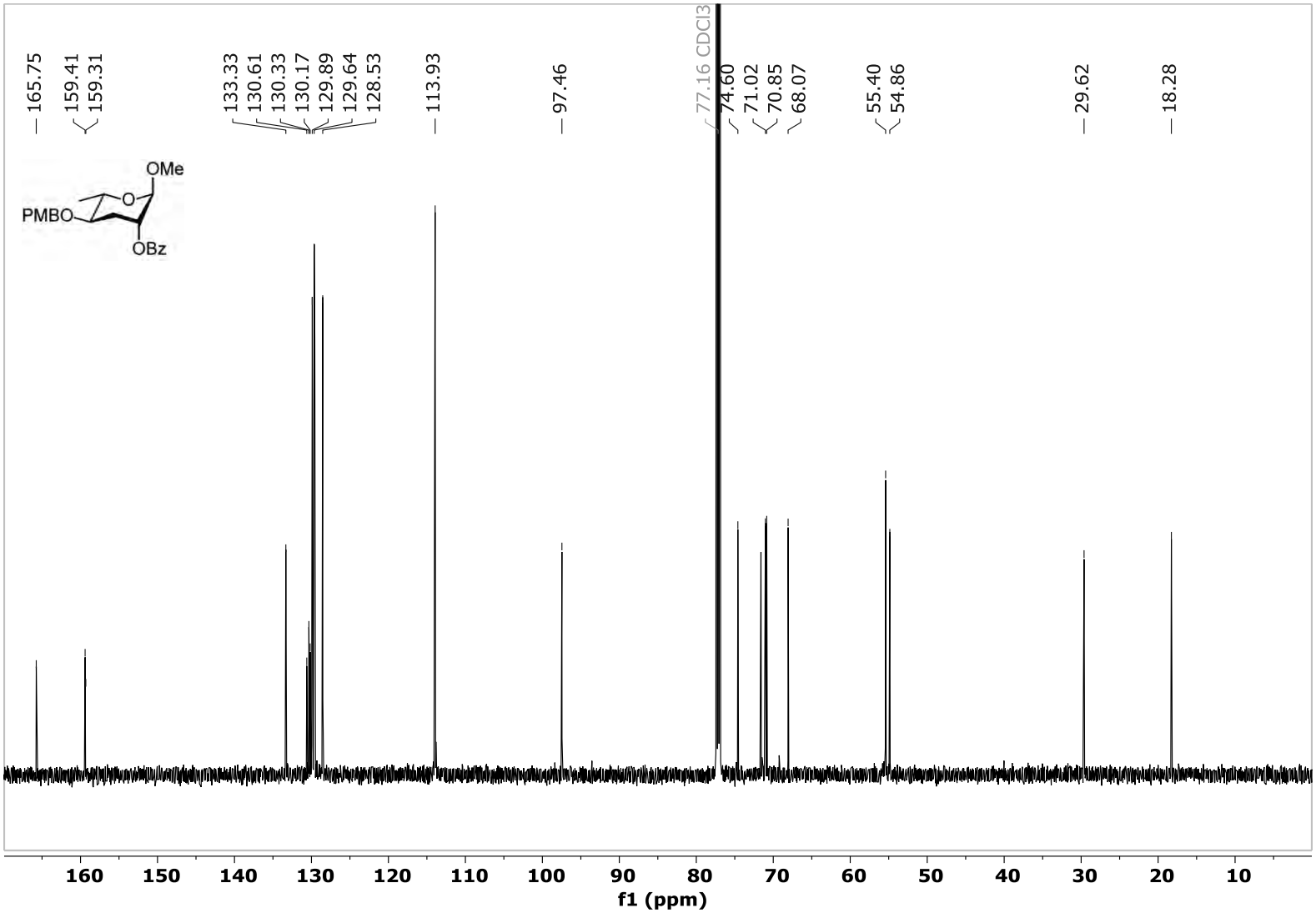

Figure S 59: *dqf*-COSY(600 MHz, $CDCl_3$) of 2-*O*-benzoyl-4-*O*-(4-methoxybenzyl)-3,6-dideoxy-α-L-*arabino*-hexose (94).

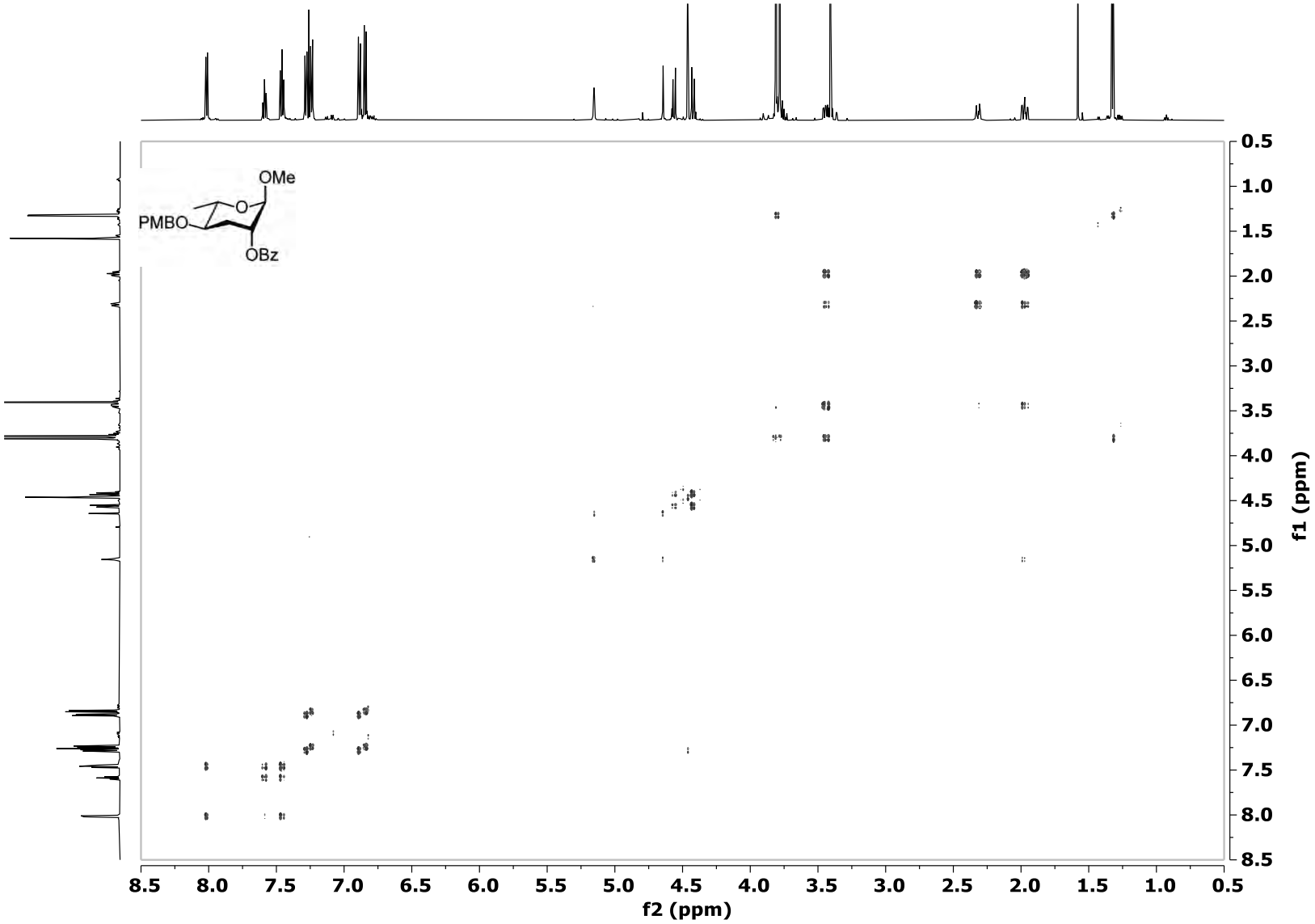

Figure S 60: HSQC (600 MHz, $CDCl_3$) of 2-*O*-benzoyl-4-*O*-(4-methoxybenzyl)-3,6-dideoxy-α-L-*arabino*-hexose (94).

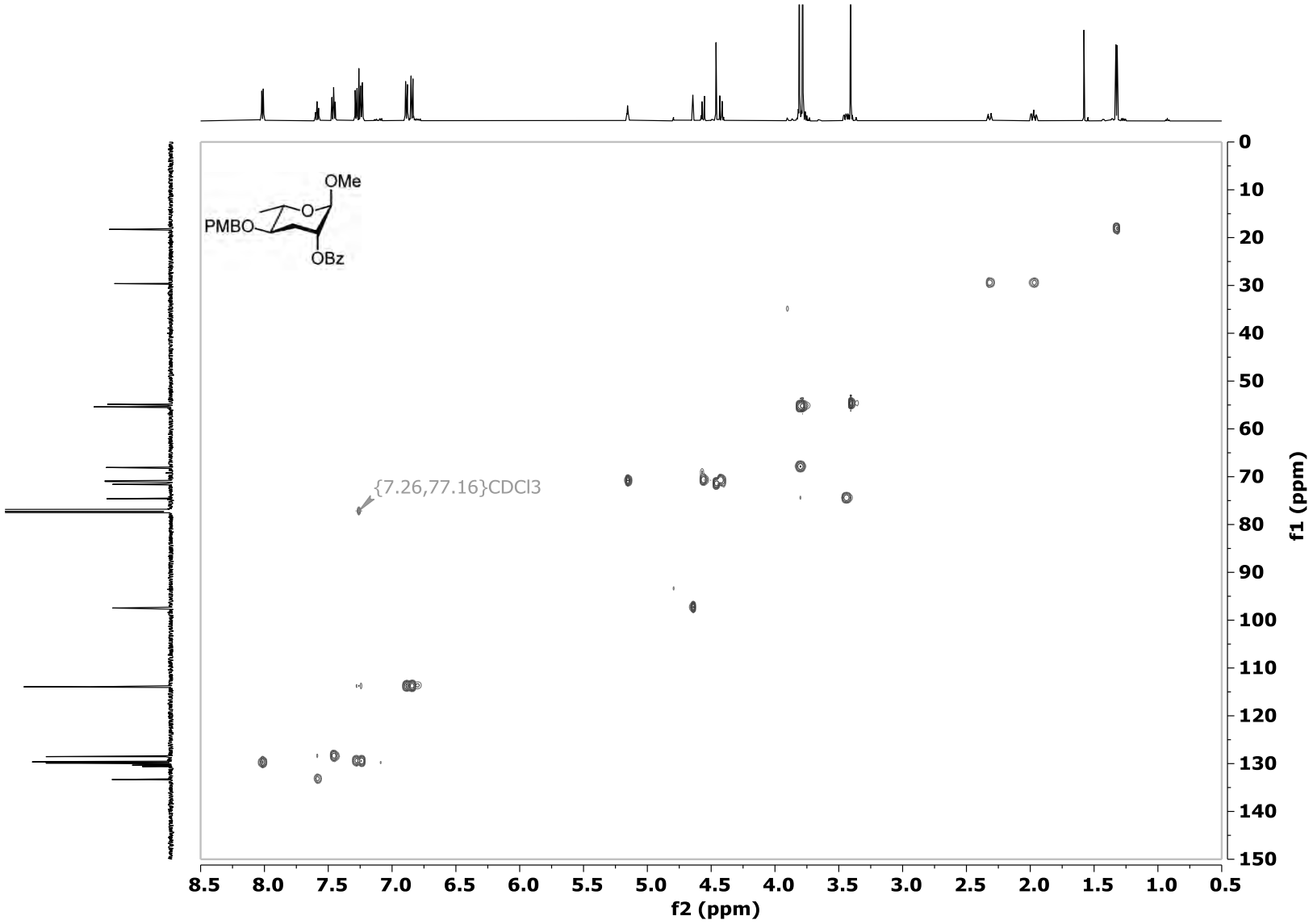

Figure S 61: ^{1}H NMR (600 MHz, $CDCl_3$) of 1-*O*-methyl-2-*O*-benzoyl-4-O-benzyl 3,6-dideoxy-α-L-*arabino*-hexose (92).

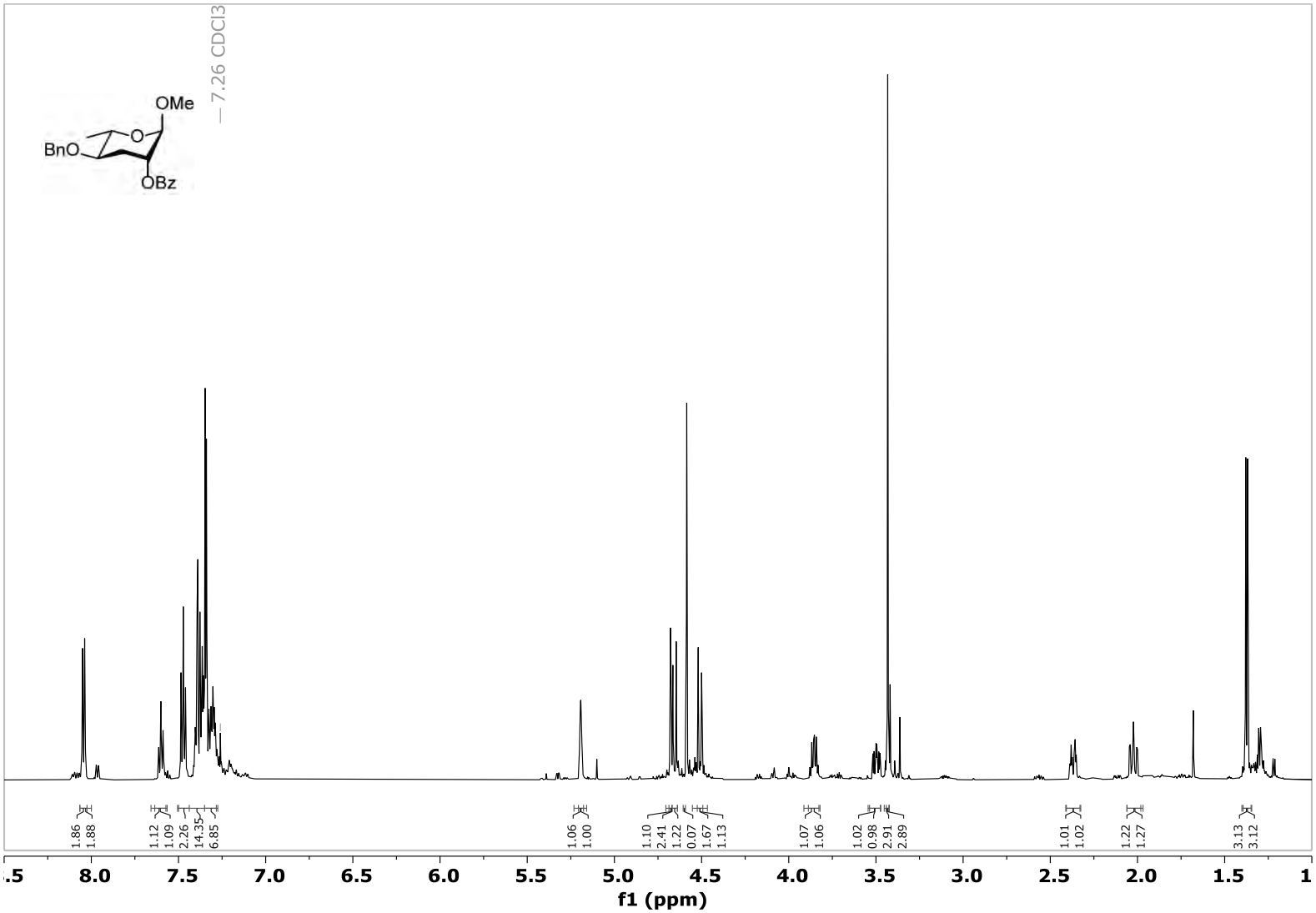

Figure S 62: ^{13}C NMR (150 MHz, $CDCl_3$) of 1-*O*-methyl-2-*O*-benzoyl-4-O-benzyl 3,6-dideoxy-α-L-*arabino*-hexose (92).

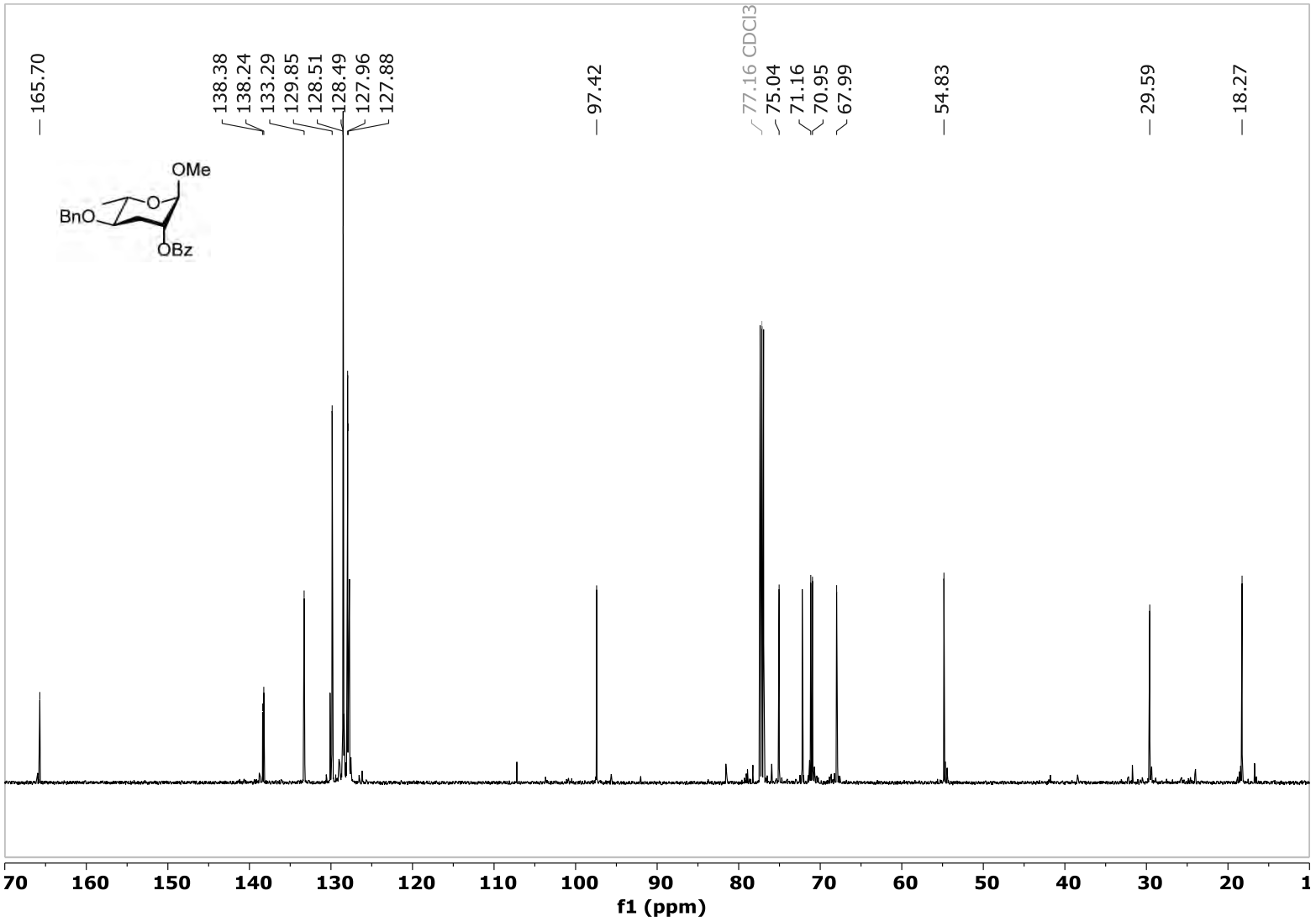

Figure S 63 : *dqf*-COSY (600 MHz, $CDCl_3$) of 1-*O*-methyl-2-*O*-benzoyl-4-*O*-benzyl 3,6-dideoxy-α-L-*arabino*-hexose (92).

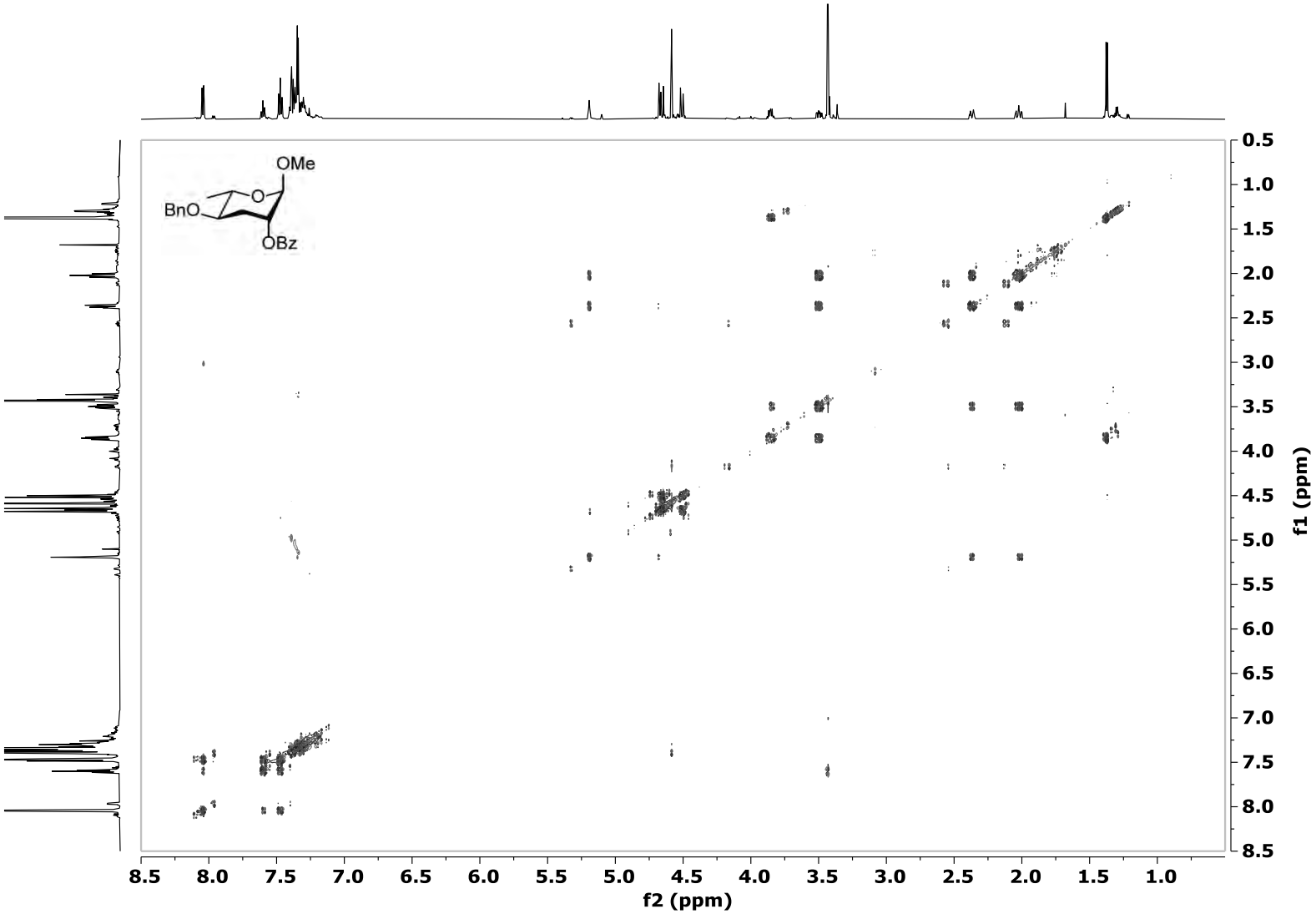

Figure S 64: HSQC (600 MHz, $CDCl_3$) of 1-*O*-methyl-2-*O*-benzoyl-4-*O*-benzyl 3,6-dideoxy-α-L-*arabino*-hexose (92).

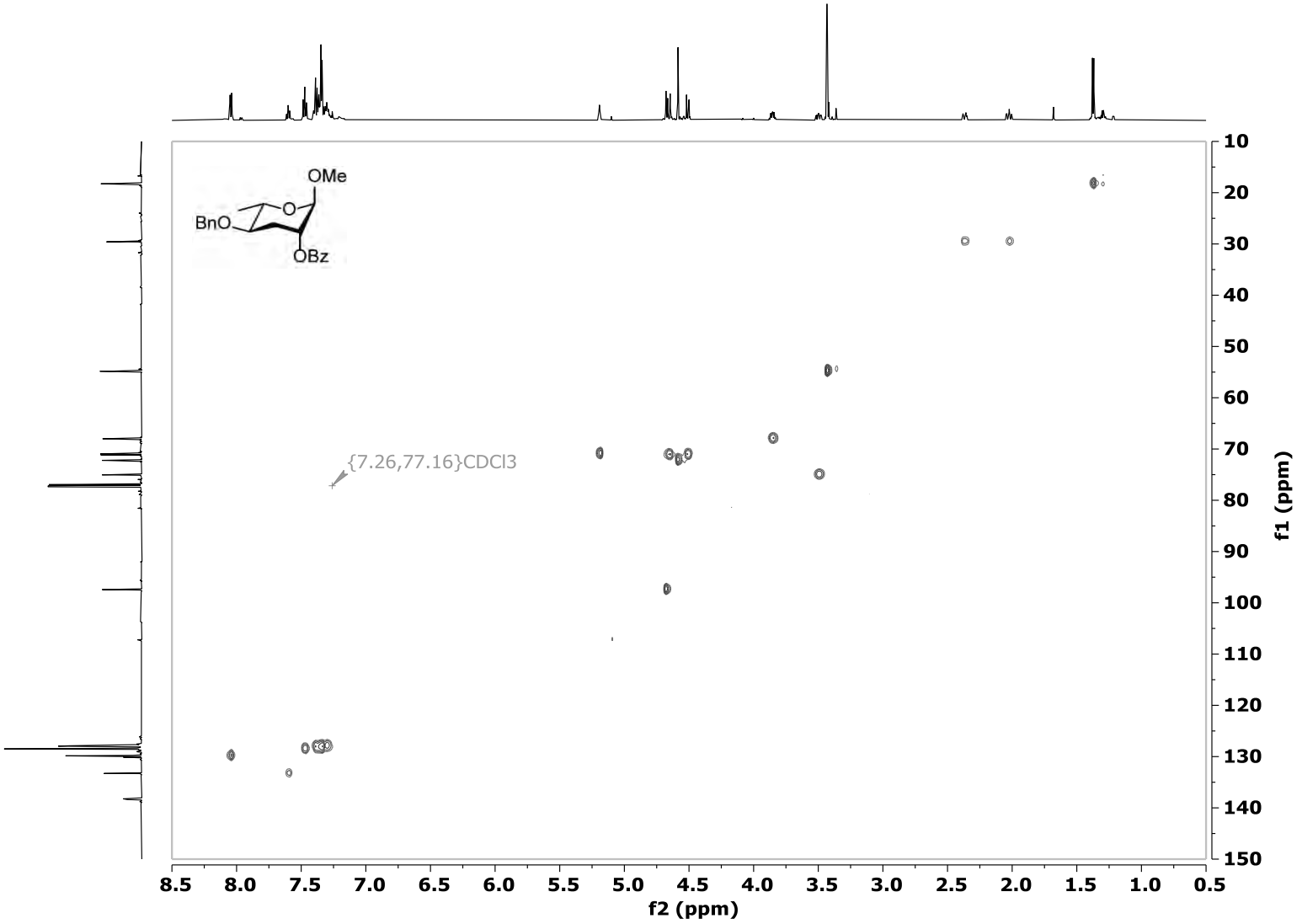

Figure S 65: ^{1}H NMR (600 MHz, $CDCl_3$) of 2-*O*-benzoyl-4-*O*-benzyl 3,6-dideoxy-α-L-*arabino*-hexose (46).

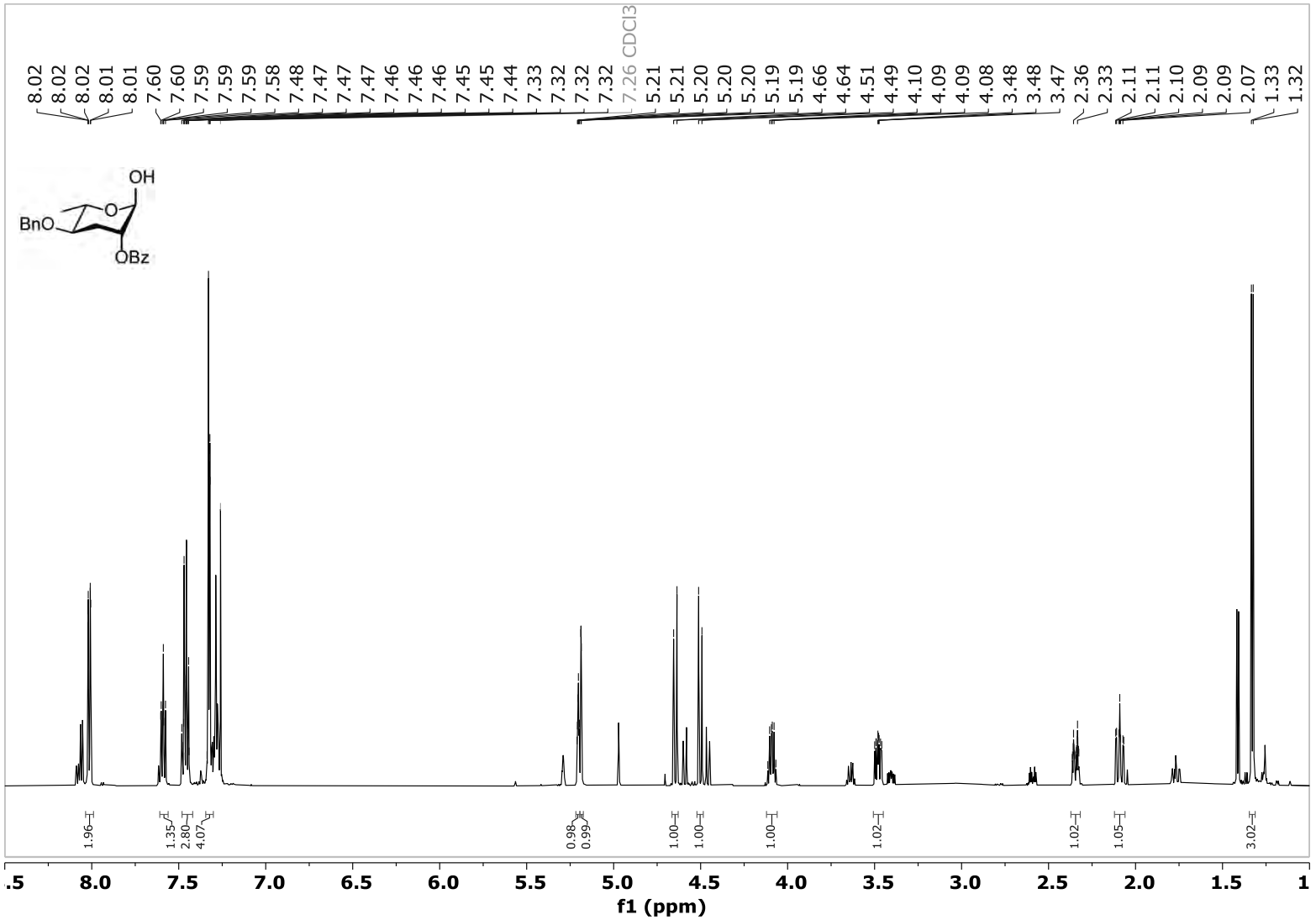

Figure S 66: ^{13}C NMR (150 MHz, $CDCl_3$) of 2-*O*-benzoyl-4-*O*-benzyl 3,6-dideoxy-α-L-*arabino*-hexose (46).

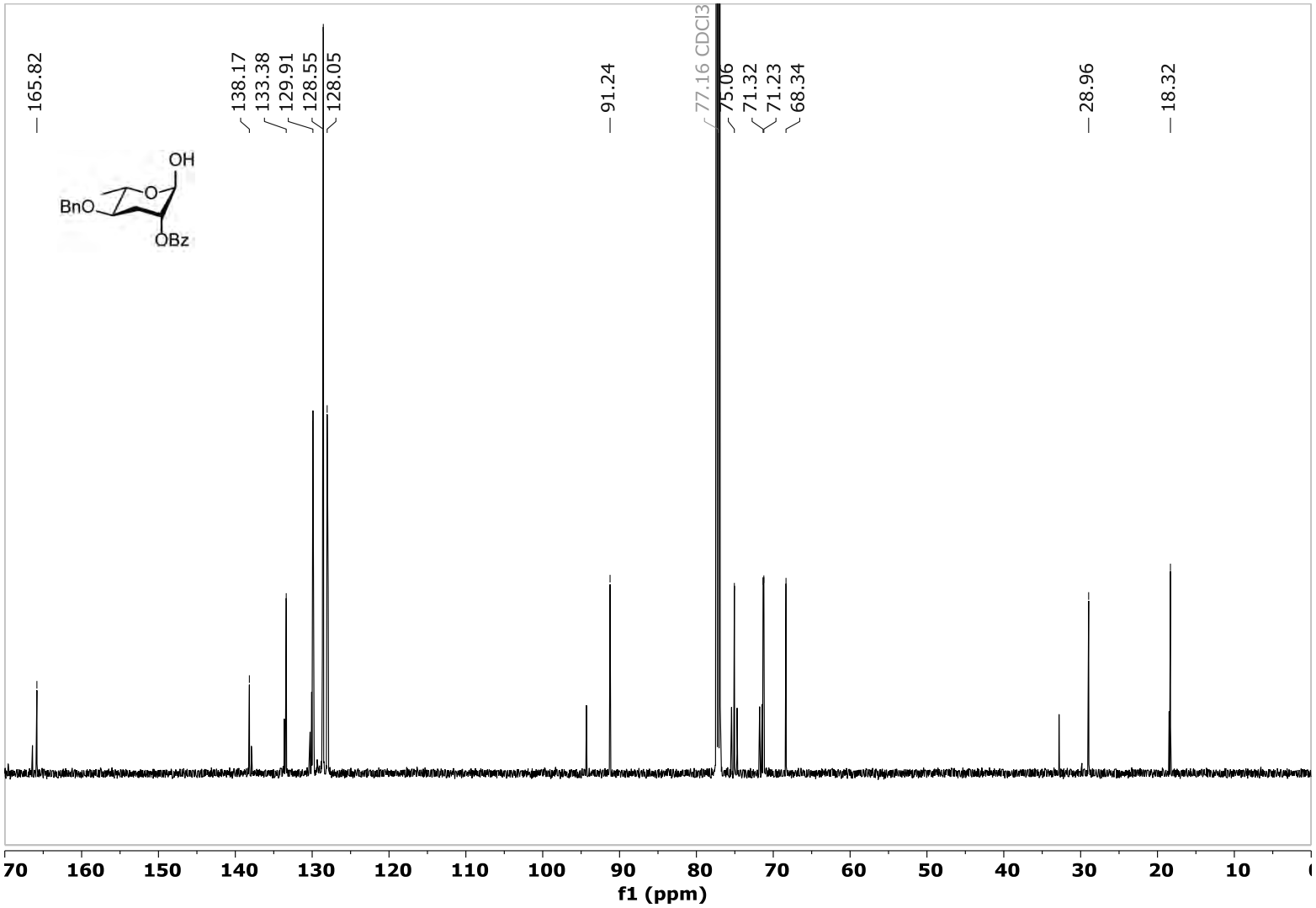

Figure S 67: *dqf*-COSY (600 MHz, $CDCl_3$) of 2-*O*-benzoyl-4-*O*-benzyl 3,6-dideoxy-α-L-*arabino*-hexose (46).

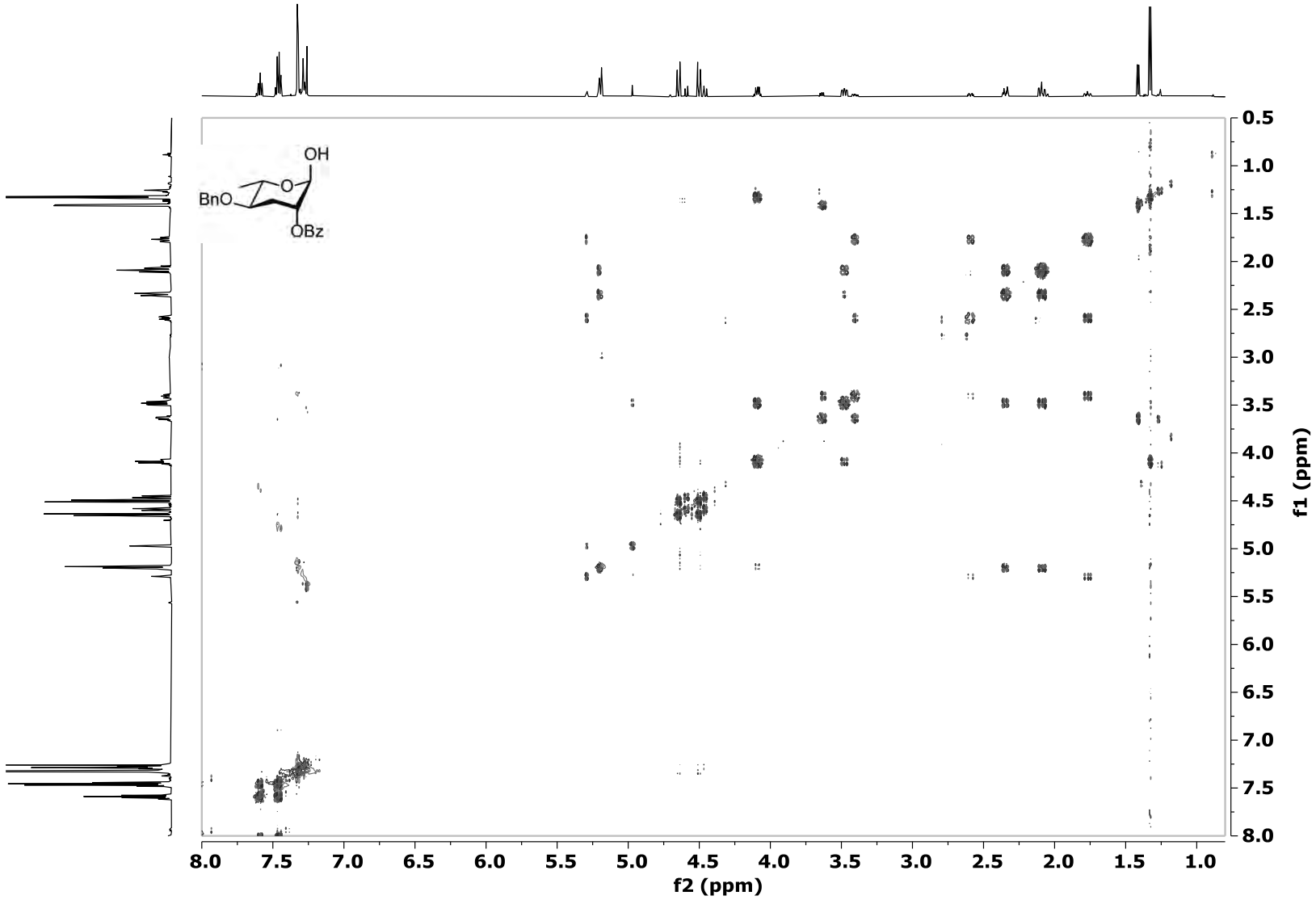

Figure S 68: HSQC (600 MHz, $CDCl_3$) of 2-*O*-benzoyl-4-*O*-benzyl 3,6-dideoxy-α-L-*arabino*-hexose (46).

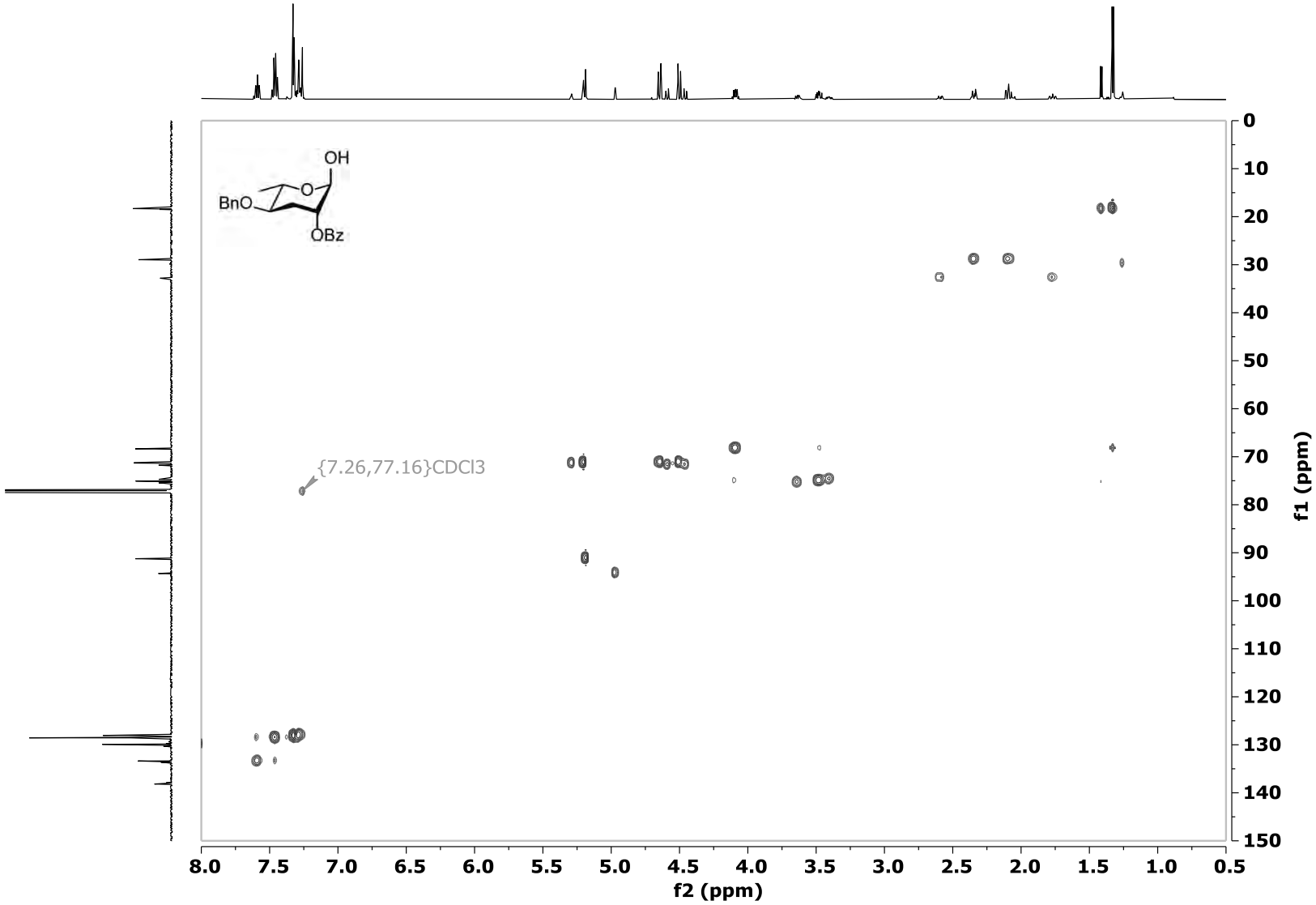

Figure S 69: ^{1}H NMR (600 MHz, $CDCl_3$) of 1-*O*-methyl-2-*O*-benzoyl-4-*O*-allyl 3,6-dideoxy-α-L-*arabino*-hexose (93).

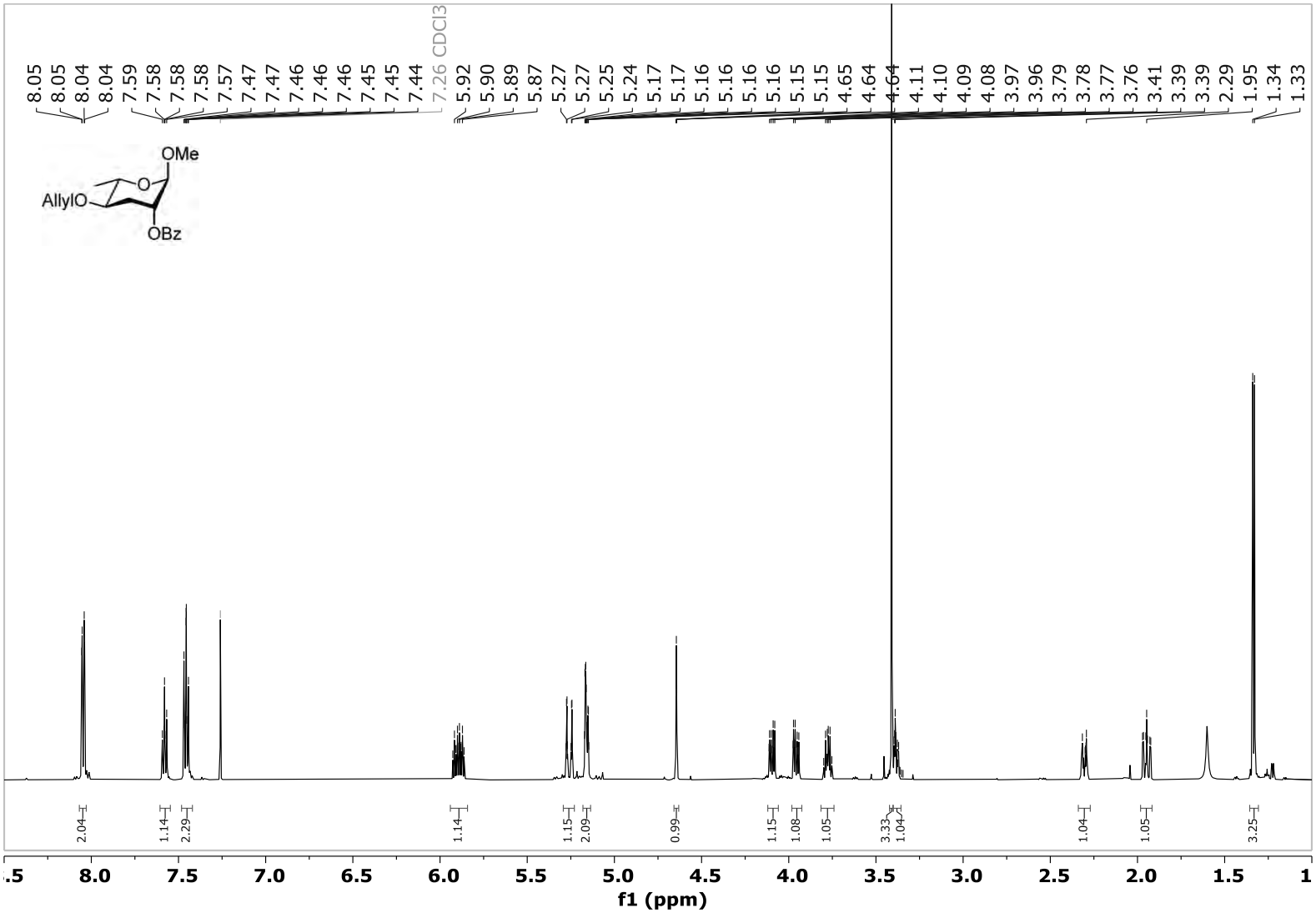

Figure S 70: ^{13}C NMR (150 MHz, $CDCl_3$) of 1-*O*-methyl-2-*O*-benzoyl-4-*O*-allyl 3,6-dideoxy-α-L-*arabino*-hexose (93).

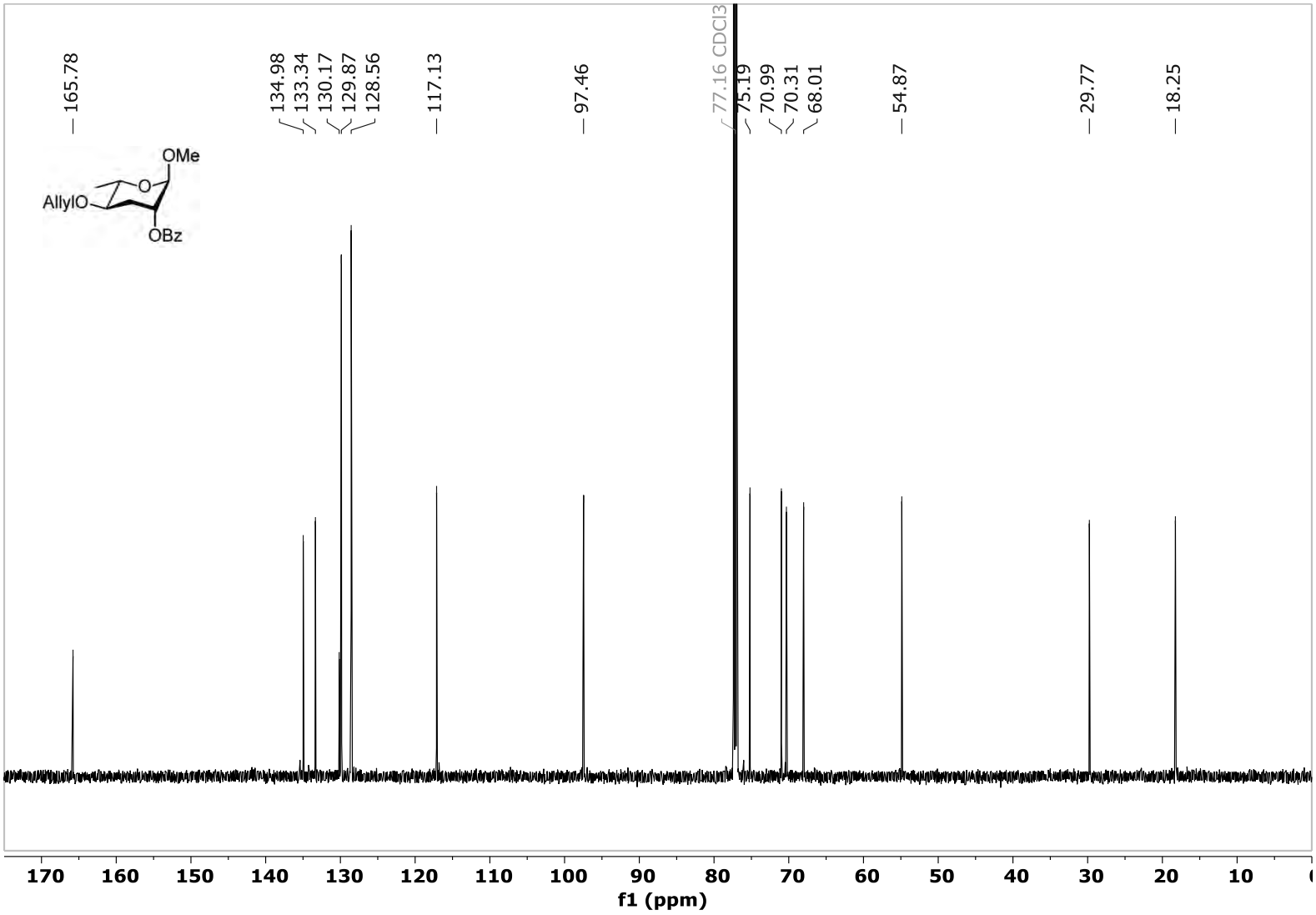

Figure S 71: *dqf*-COSY (600 MHz, $CDCl_3$) of 1-*O*-methyl-2-*O*-benzoyl-4-*O*-allyl 3,6-dideoxy-α-L-*arabino*-hexose (93).

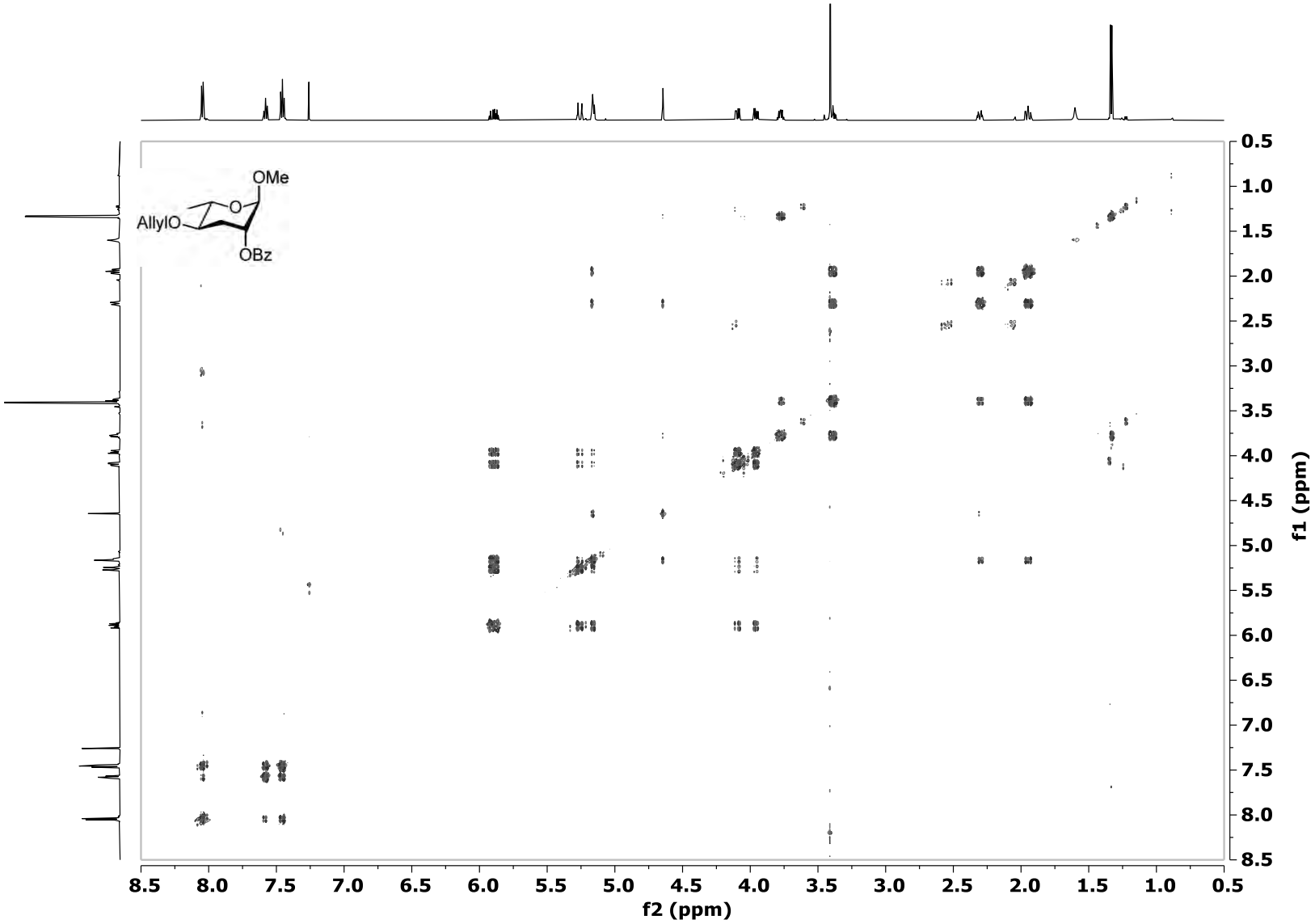

Figure S 72: HSQC (600 MHz, $CDCl_3$) of 1-*O*-methyl-2-O-benzoyl-4-*O*-allyl 3,6-dideoxy-α-L-*arabino*-hexose (93).

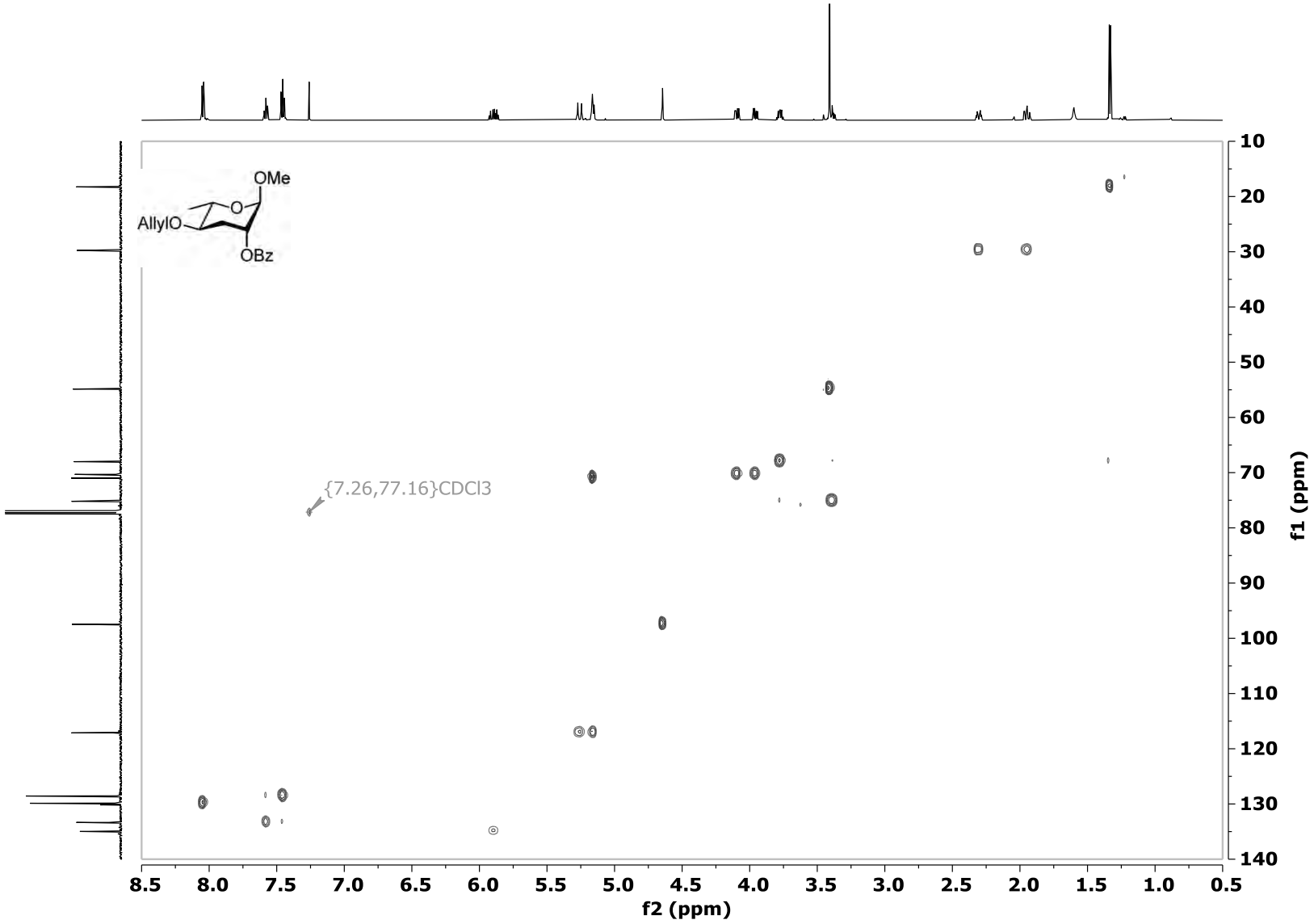

Figure S 73: ^{1}H NMR (600 MHz, $CDCl_3$) of 2-*O*-benzoyl-4-*O*-allyl 3,6-dideoxy-α-L-*arabino*-hexose (47).

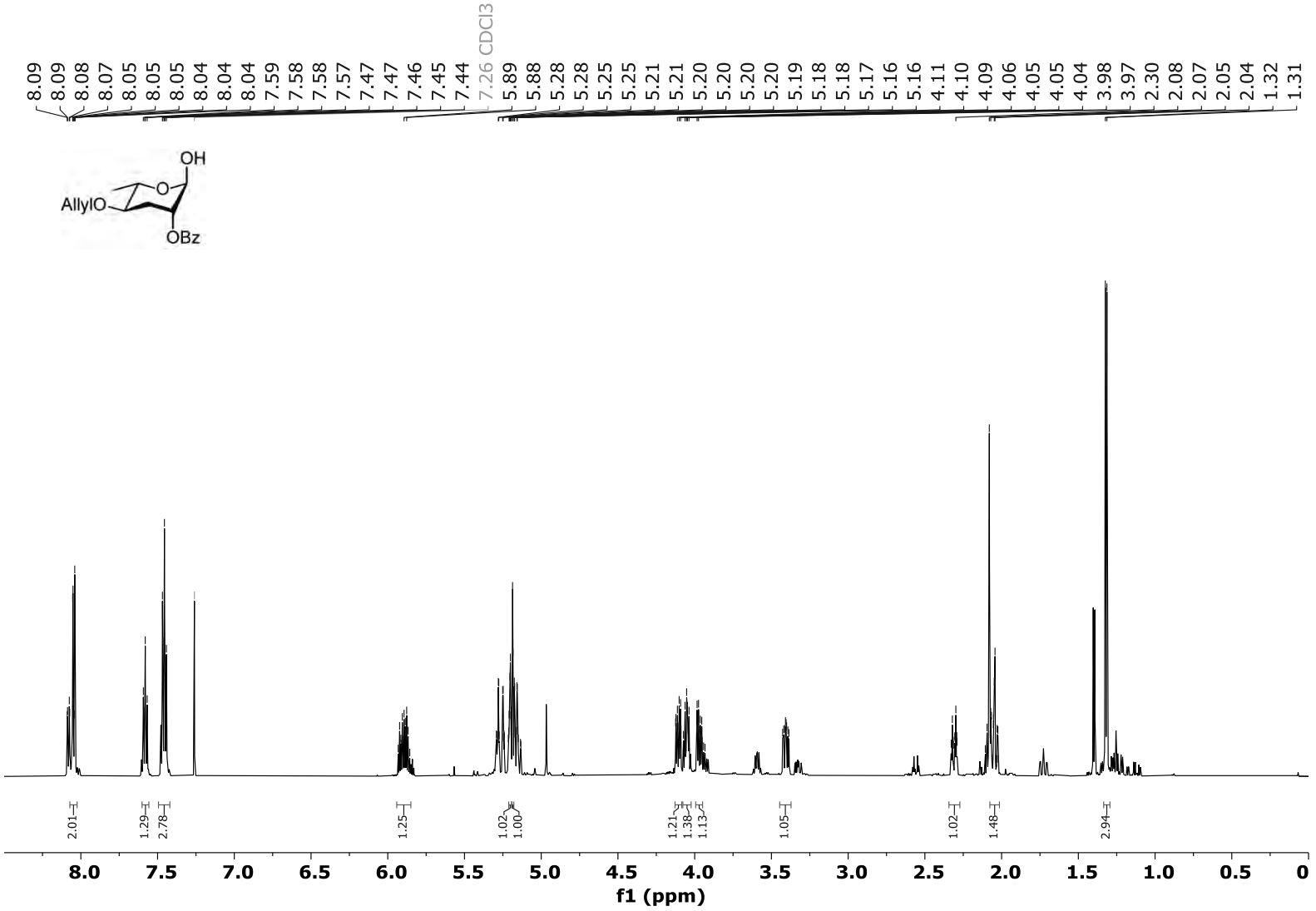

Figure S 74: ^{13}C NMR (150 MHz, $CDCl_3$) of 2-*O*-benzoyl-4-*O*-allyl 3,6-dideoxy-α-L-*arabino*-hexose (47).

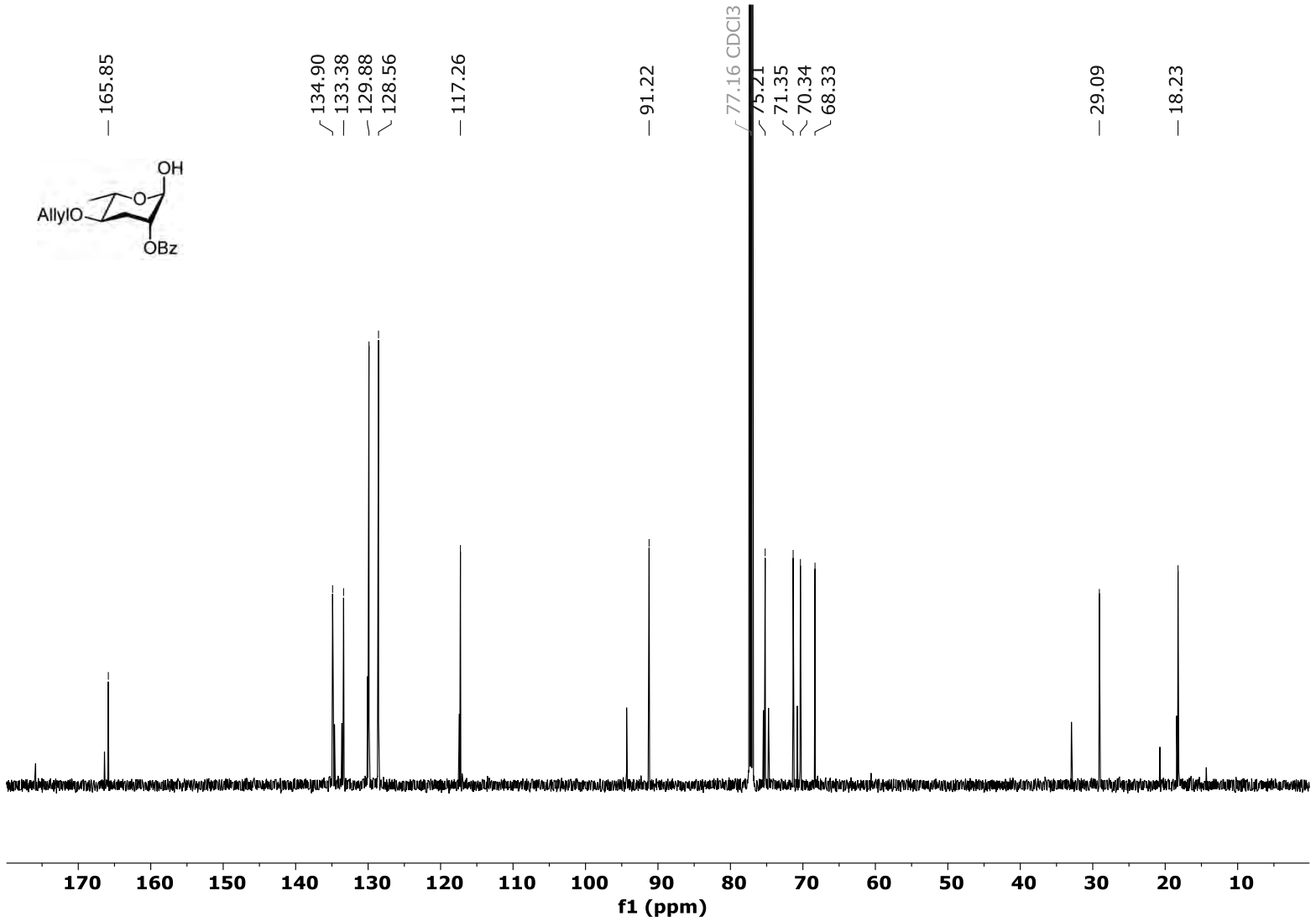

Figure S 75*: dqf*-COSY (600 MHz, $CDCl_3$) of 2-*O*-benzoyl-4-*O*-allyl 3,6-dideoxy-α-L-*arabino*-hexose (47).

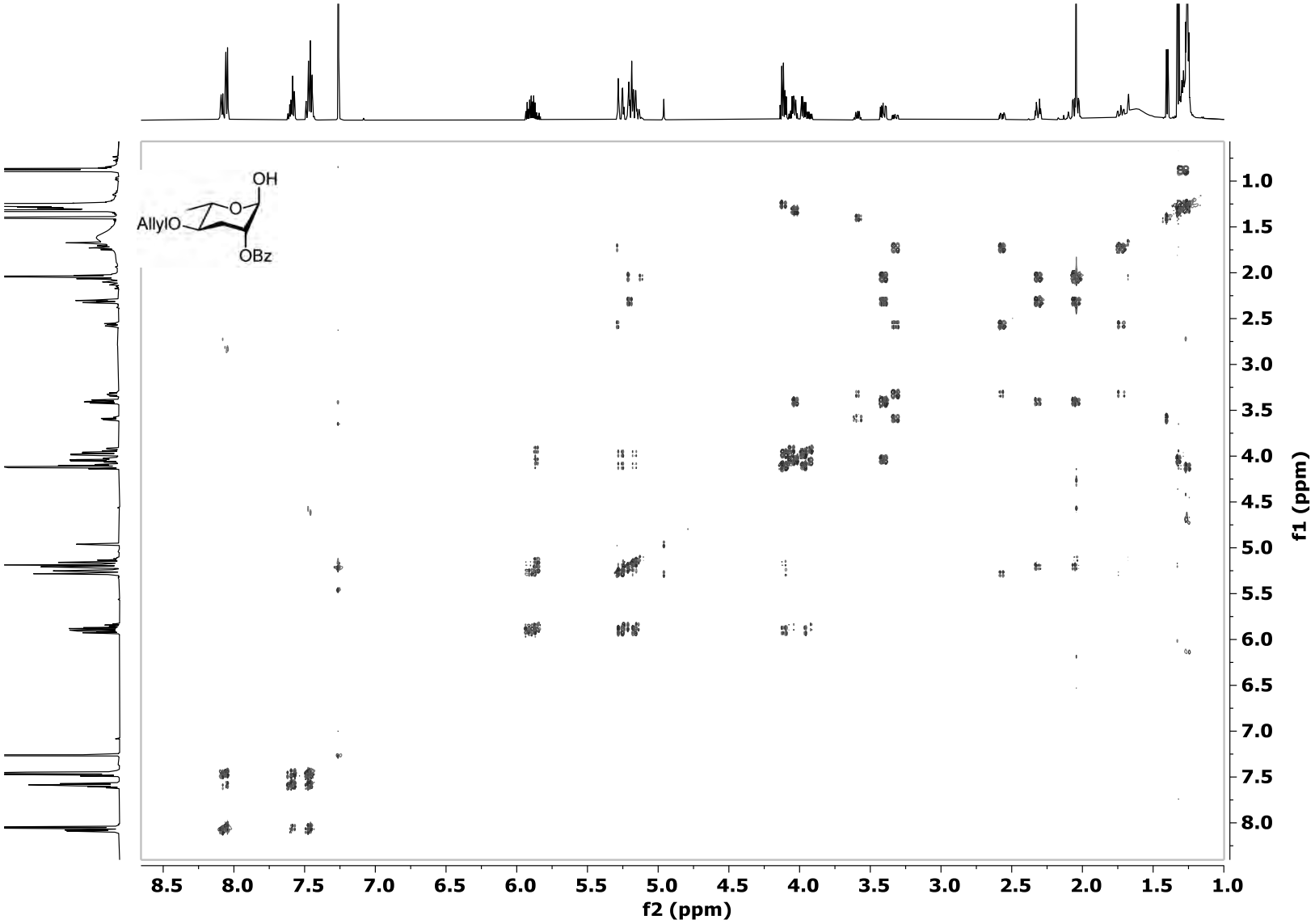

Figure S 76: HSQC (600 MHz, $CDCl_3$) of 2-*O*-benzoyl-4-*O*-allyl 3,6-dideoxy-α-L-*arabino*-hexose (47).

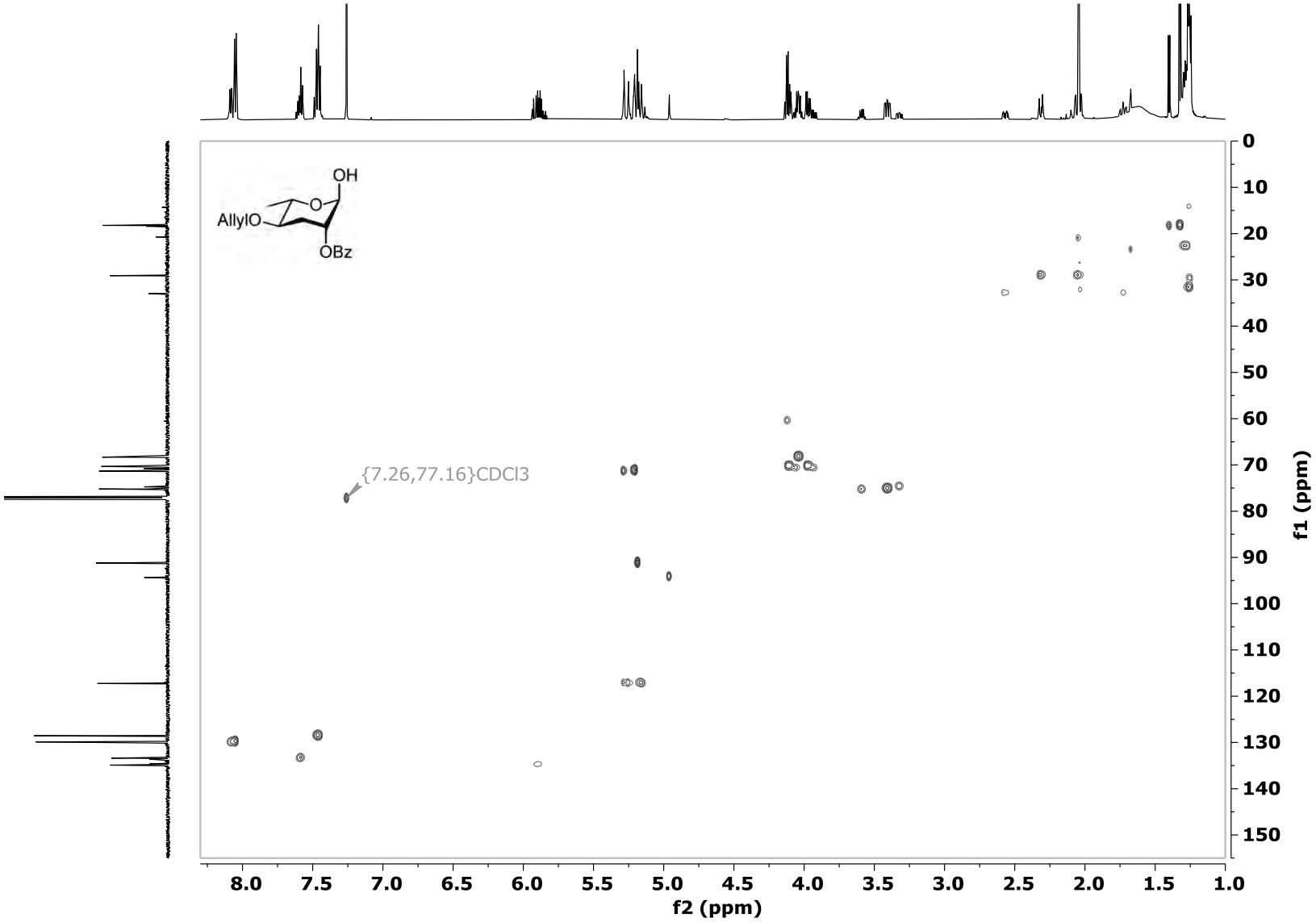

Figure S 77 : ^{1}H NMR (600 MHz, $CDCl_3$) of (8*R*)-8-[(2-*O*-benzoyl-4-O-*tert*-butyldiphenylsilyl-3,6-dideoxy-α-L-*arabino*-hexopyranosyl)oxy]-1-octene (111).

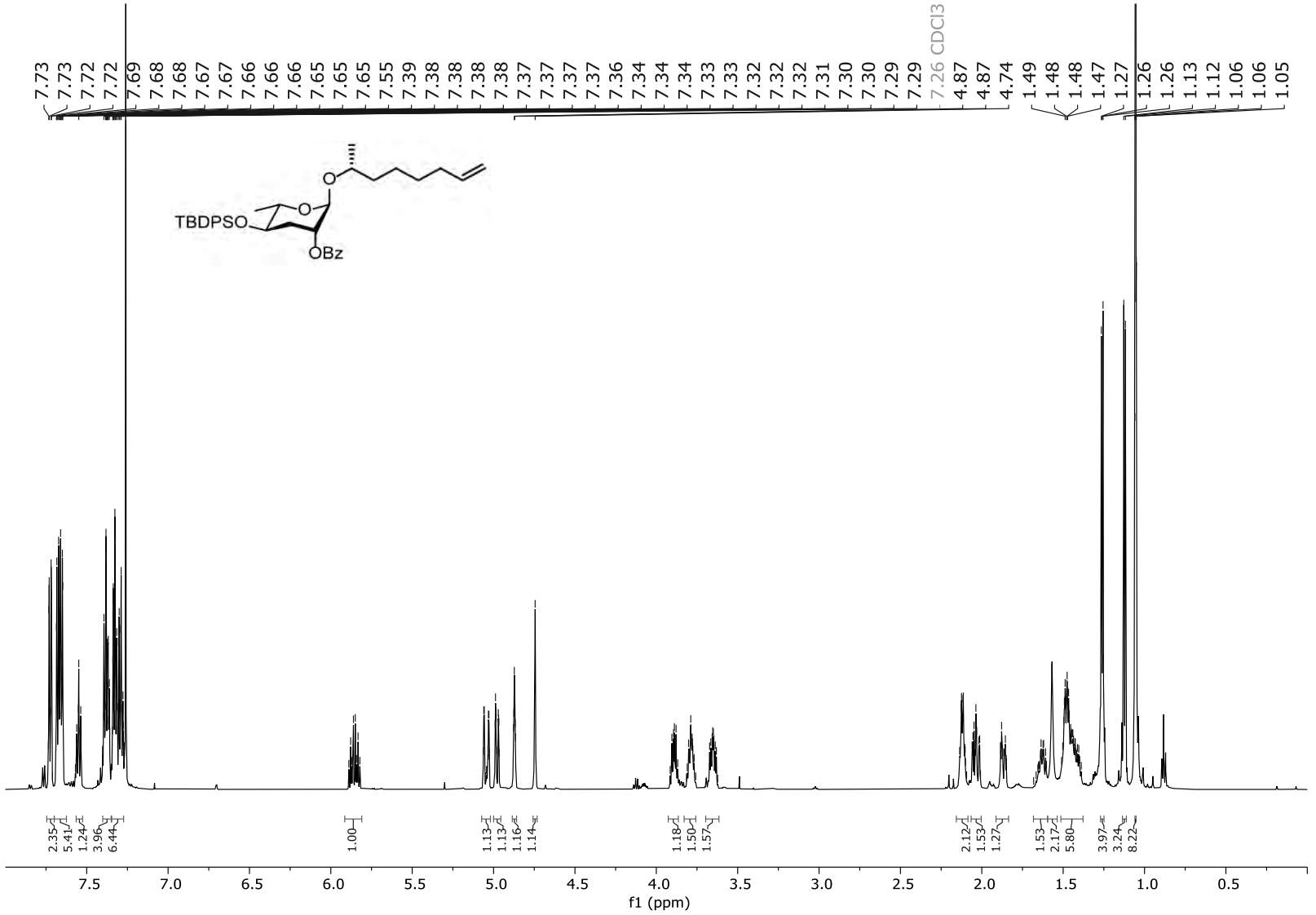

Figure S 78 : ^{13}C NMR (150 MHz, $CDCl_3$) of (8*R*)-8-[(2-*O*-benzoyl-4-*O*-*tert*-butyldiphenylsilyl-3,6-dideoxy-α-L-*arabino*-hexopyranosyl)oxy]-1-octene (111).

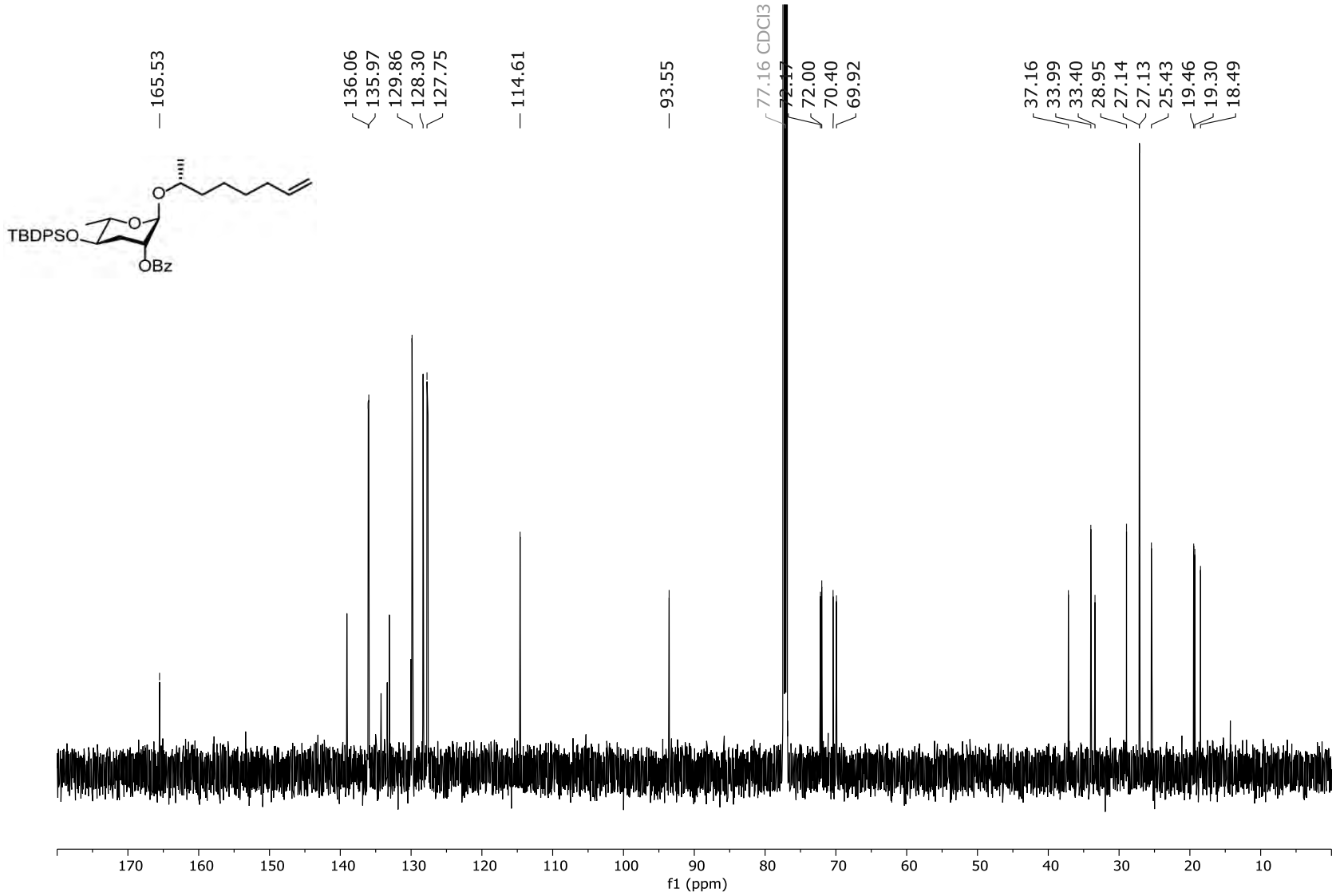

Figure S 79 : *dqf*-COSY (600 MHz, $CDCl_3$) of (8*R*)-8-[(2-*O*-benzoyl-4-*O*-*tert*-butyldiphenylsilyl-3,6-dideoxy-α-L-*arabino*-hexopyranosyl)oxy]-1-octene (111).

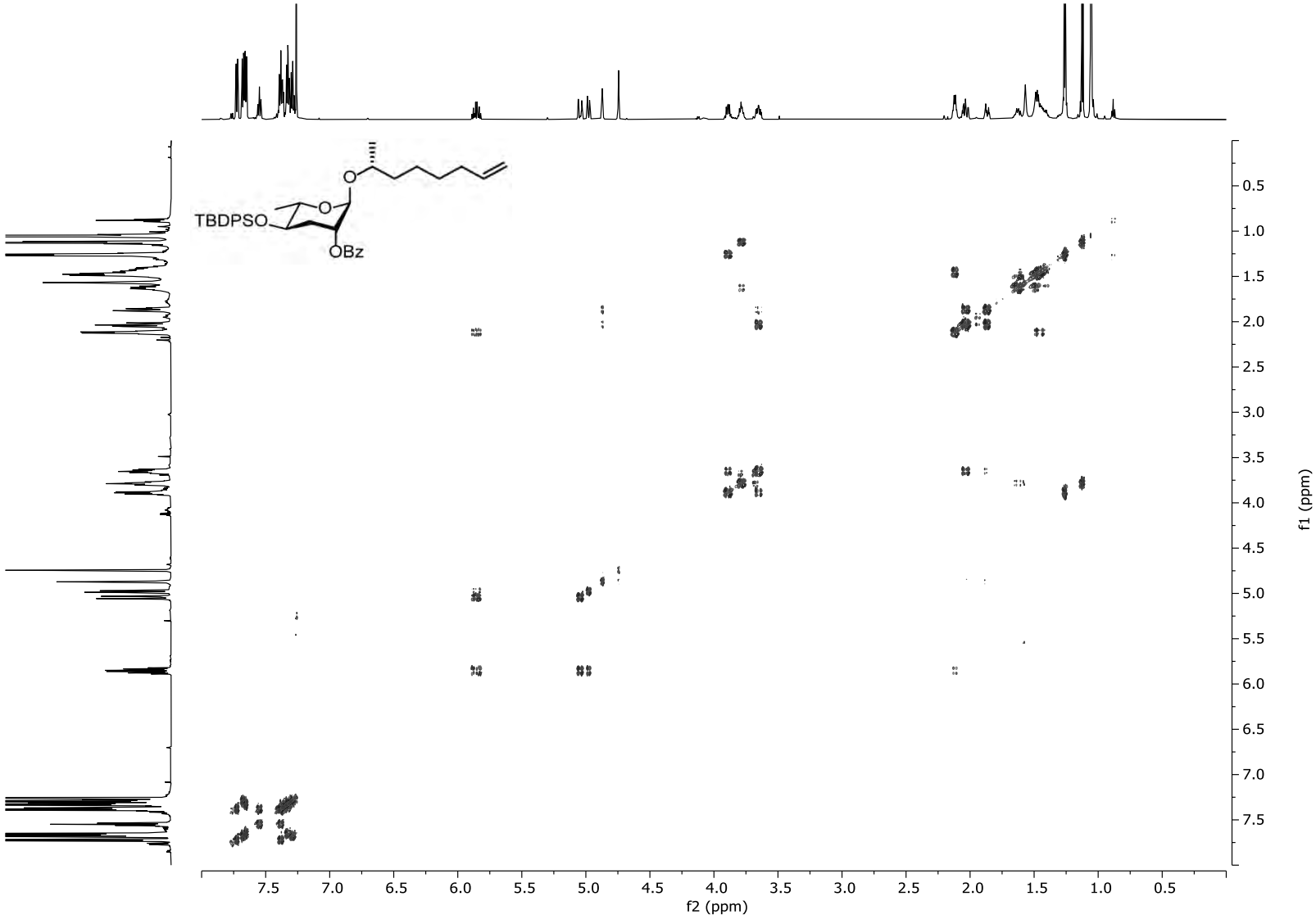

Figure S 80 : HSQC (600 MHz, $CDCl_3$) of (8*R*)-8-[(2-*O*-benzoyl-4-*O*-*tert*-butyldiphenylsilyl-3,6-dideoxy-α-L-*arabino*-hexopyranosyl)oxy]-1-octene (111).

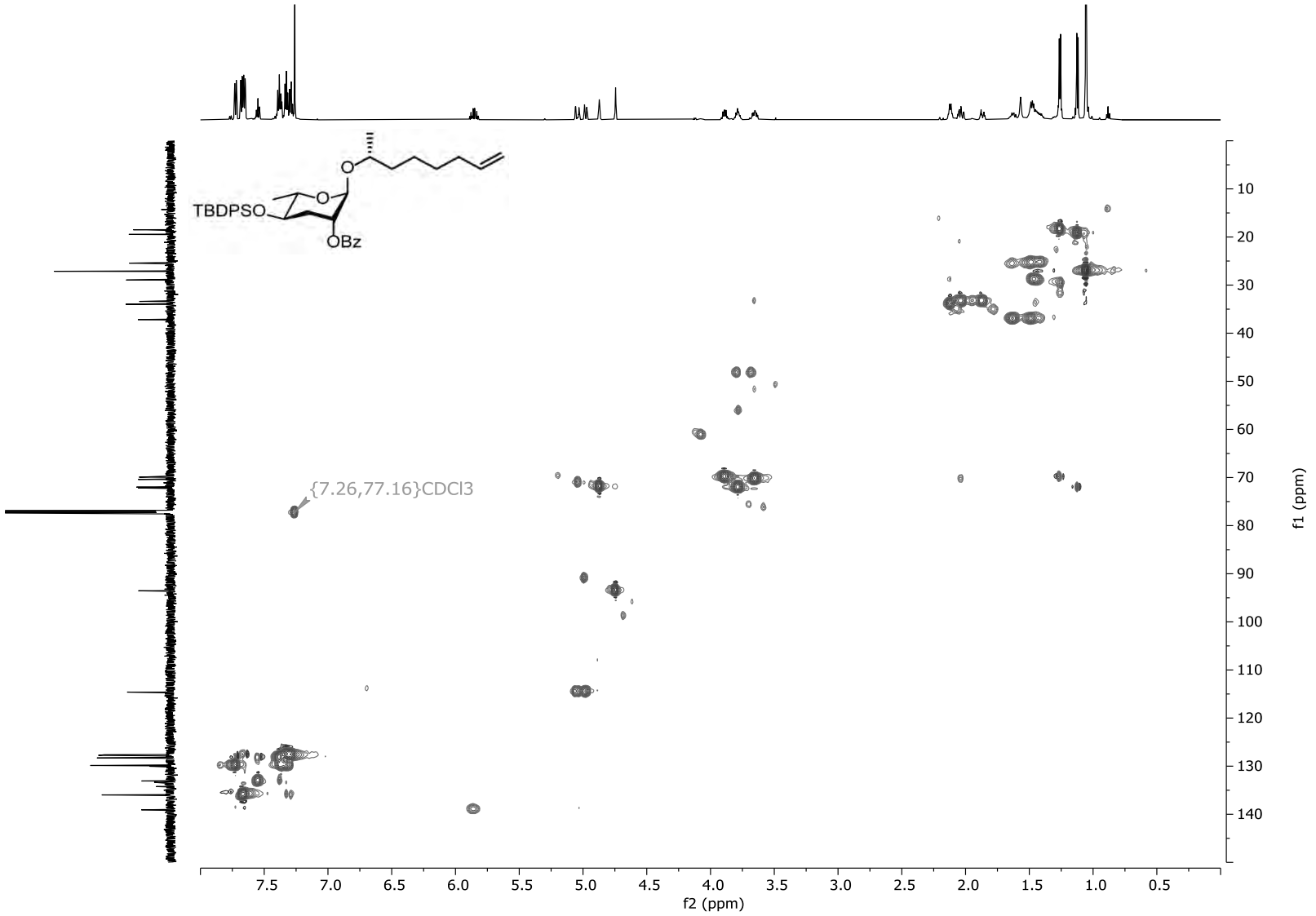

Figure S 81 : ^{1}H NMR (600 MHz, $CDCl_3$) of (7*R*)-7-[(4-*O*-*tert*-butyldiphenyl-3,6-dideoxy-α-L-*arabino*-hexopyranosyl)oxy]-1-octene (122).

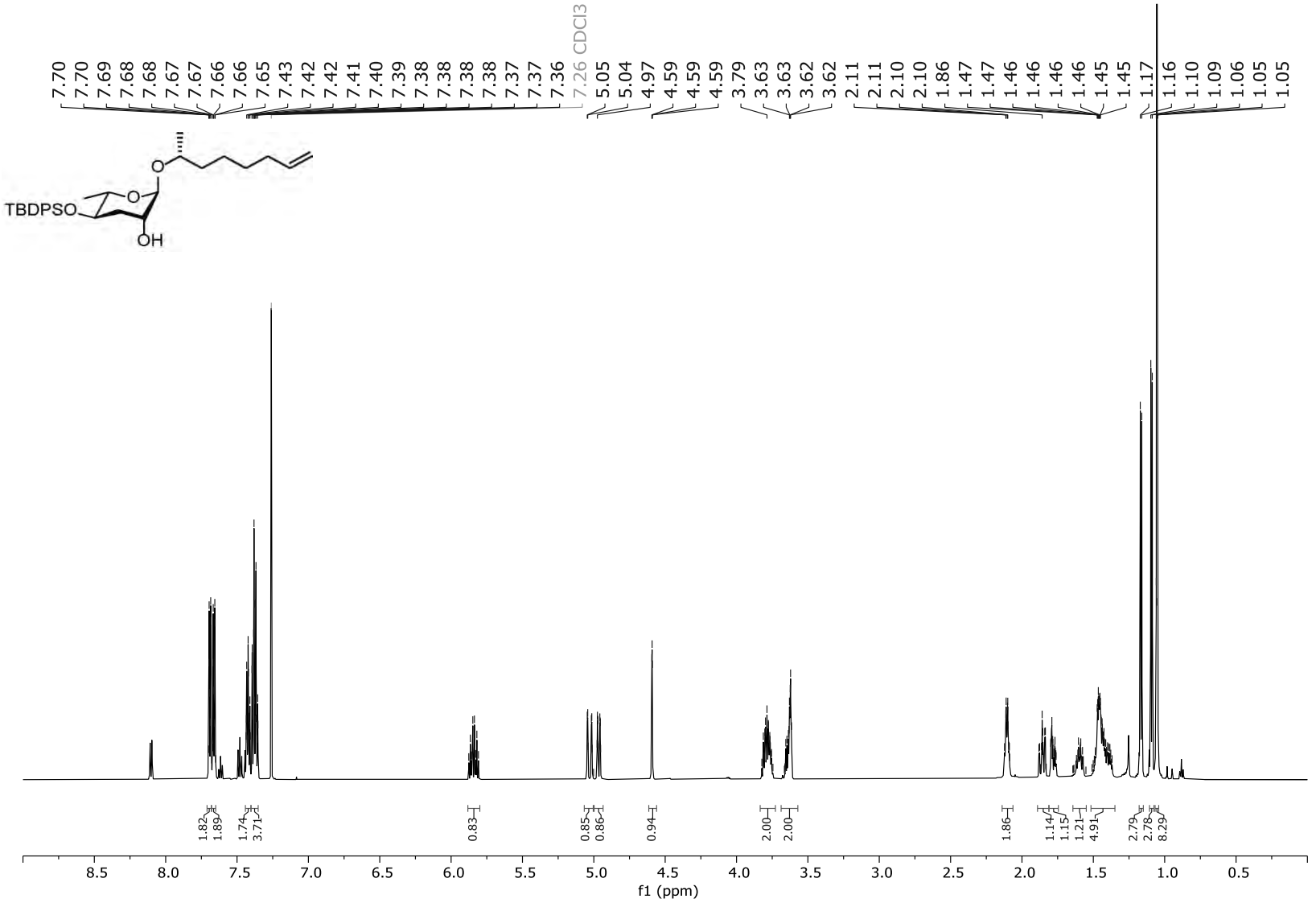

Figure S 82 : ^{13}C NMR (150 MHz, $CDCl_3$) of (7*R*)-7-[(4-*O*-*tert*-butyldiphenyl-3,6-dideoxy-α-L-*arabino*-hexopyranosyl)oxy]-1-octene (122).

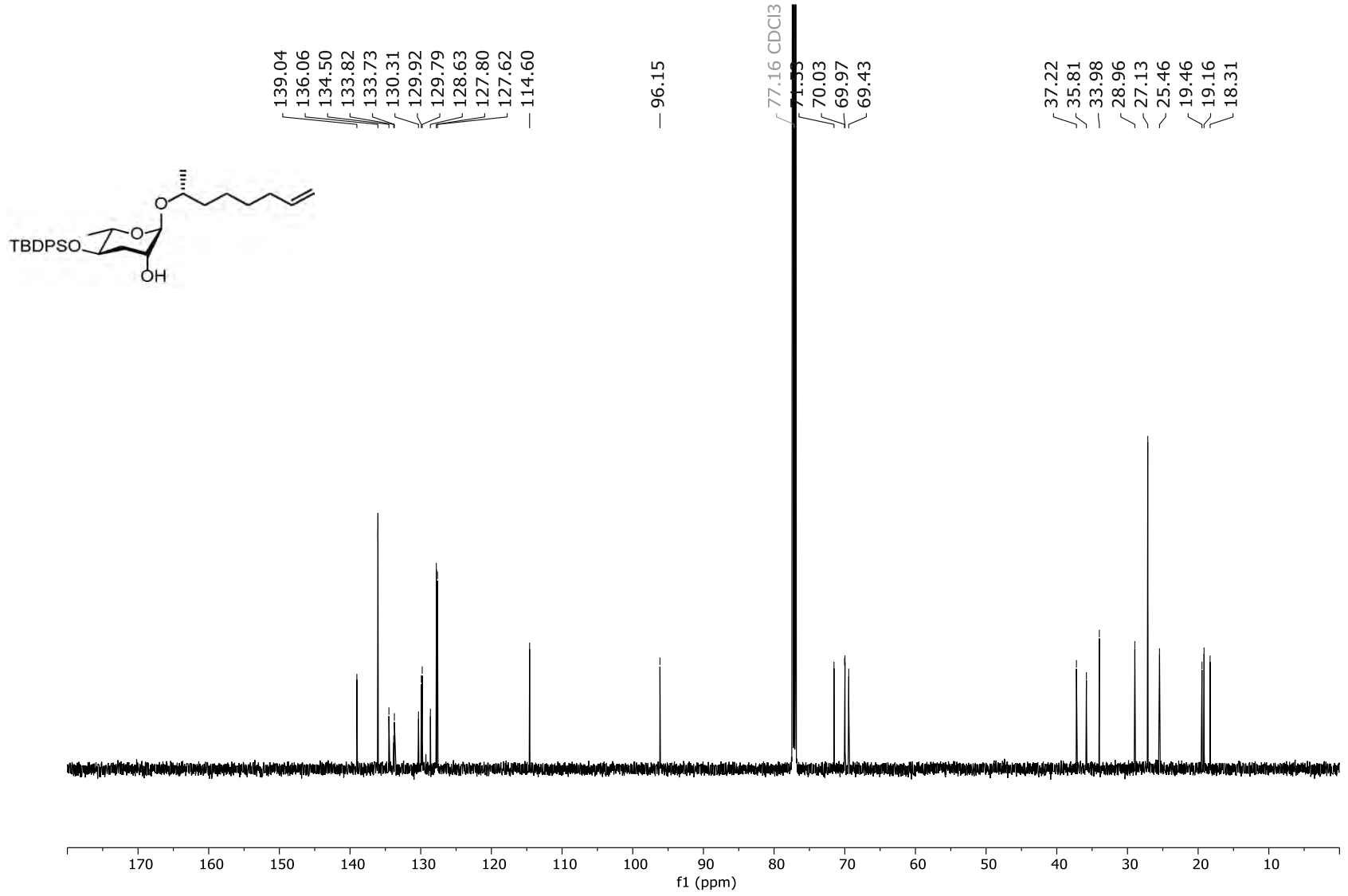

Figure S 83 : *dqf*-COSY (600 MHz, $CDCl_3$) of (7*R*)-7-[(4-*O*-*tert*-butyldiphenyl-3,6-dideoxy-α-L-*arabino*-hexopyranosyl)oxy]-1-octene (122).

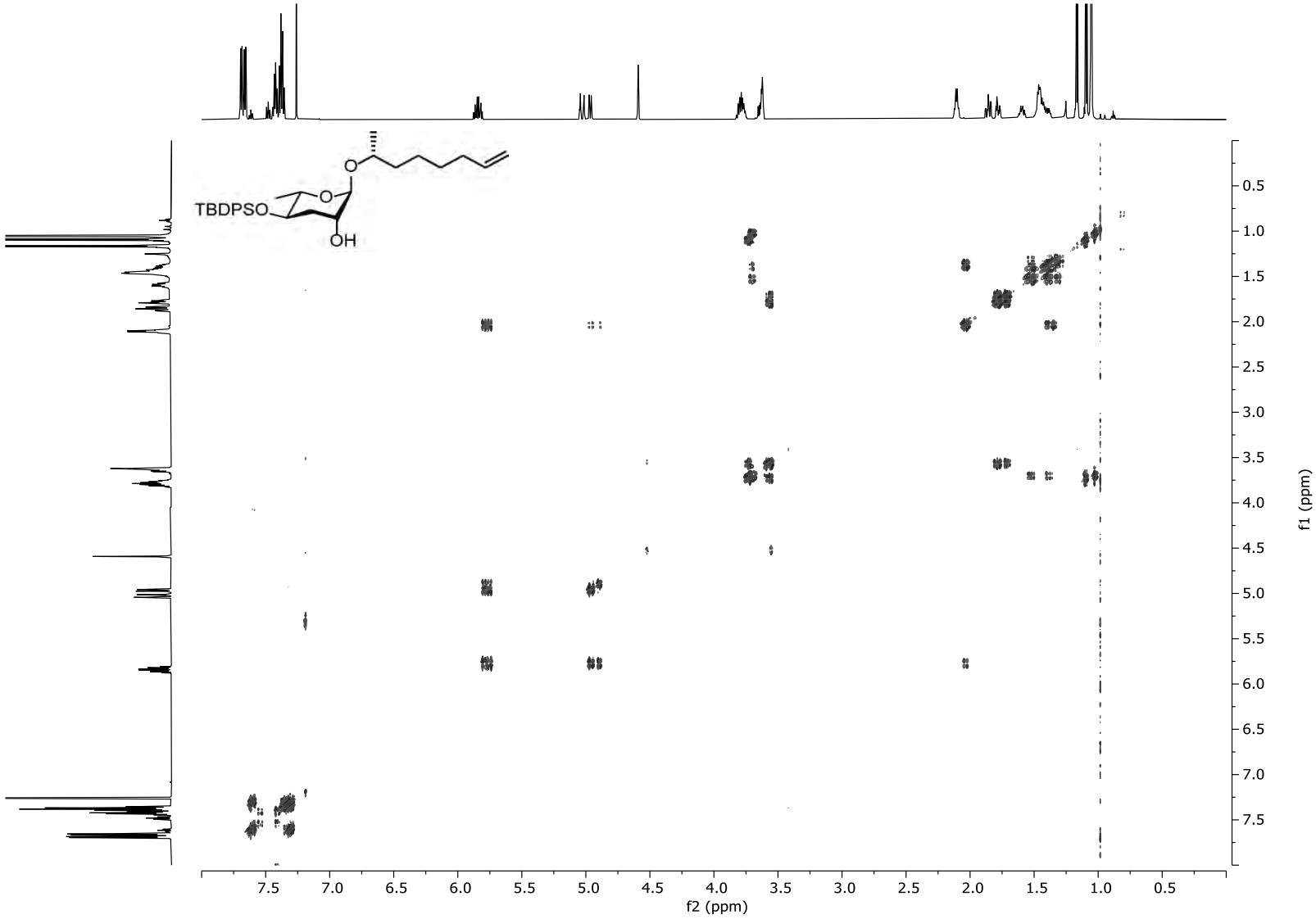

Figure S 84 : HSQC (600 MHz, $CDCl_3$) of (7*R*)-7-[(4-*O*-*tert*-butyldiphenyl-3,6-dideoxy-α-L-*arabino*-hexopyranosyl)oxy]-1-octene (122).

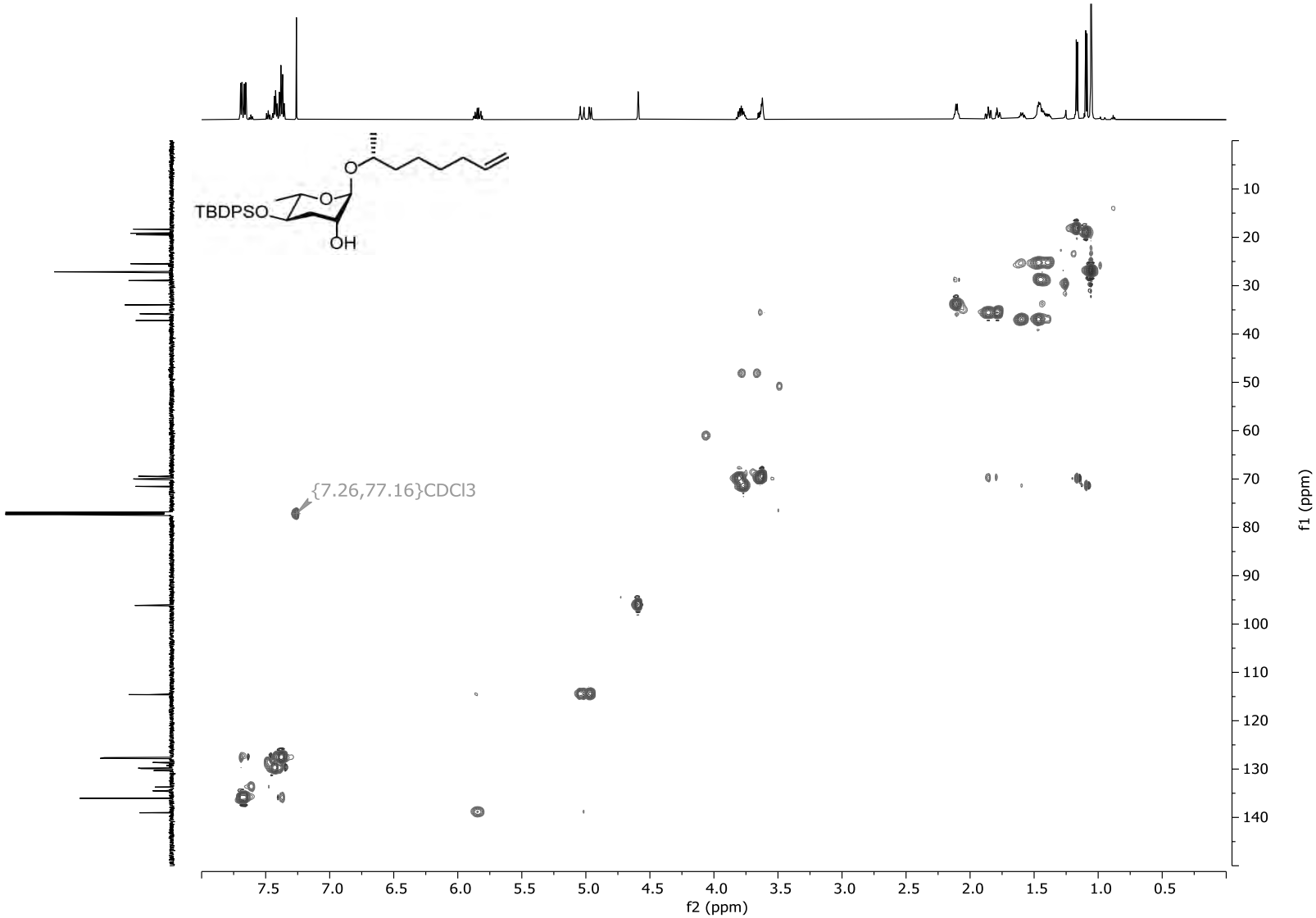

Figure S 85 : ^{1}H NMR (600 MHz, $CDCl_3$) of (7*R*)-7-[(2-O-(4-methoxybenzyloxy)-4-O-*tert*-butyldiphenyl-3,6-dideoxy-α-L-*arabino*-hexopyranosyl)oxy]-1-octene (123).

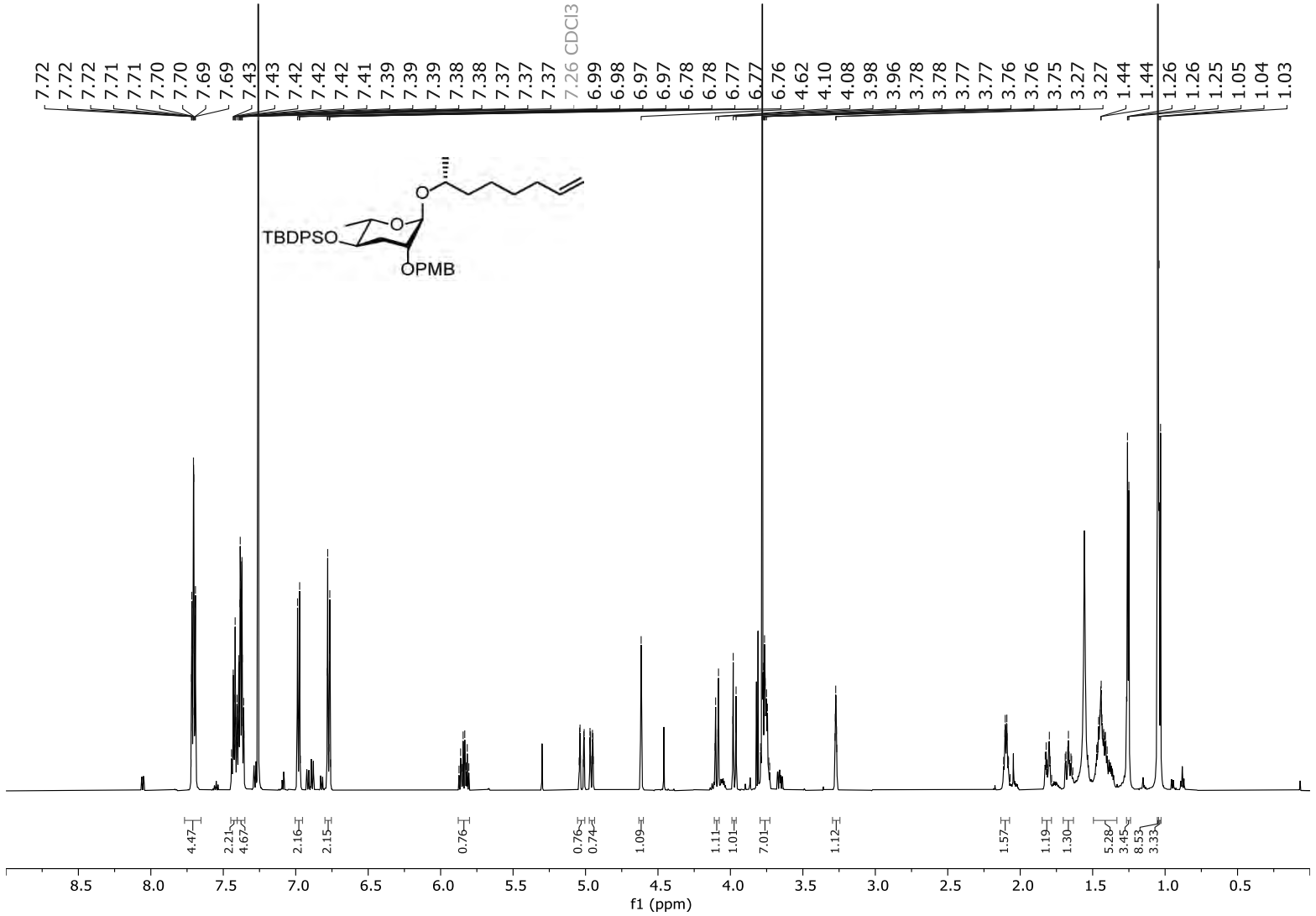

Figure S 86 : ^{13}C NMR (150 MHz, $CDCl_3$) of (7*R*)-7-[(2-*O*-(4-methoxybenzyloxy)-4-*O*-*tert*-butyldiphenyl-3,6-dideoxy-α-L-*arabino*-hexopyranosyl)oxy]-1-octene (123).

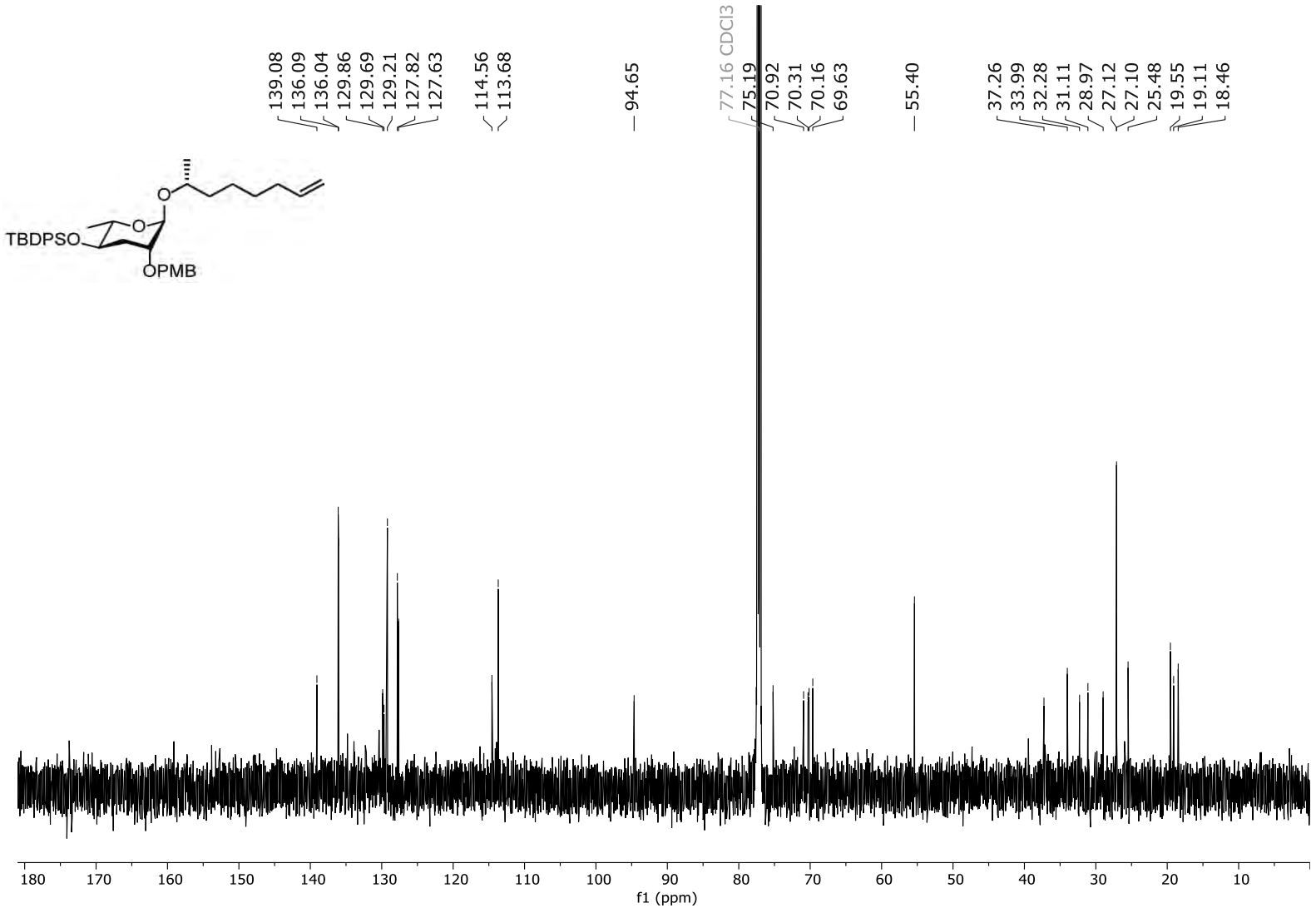

Figure S 87 : *dqf*-COSY (600 MHz, $CDCl_3$) of (7*R*)-7-[(2-O-(4-methoxybenzyloxy)-4-O-*tert*-butyldiphenyl-3,6-dideoxy-α-L-*arabino*-hexopyranosyl)oxy]-1-octene (123).

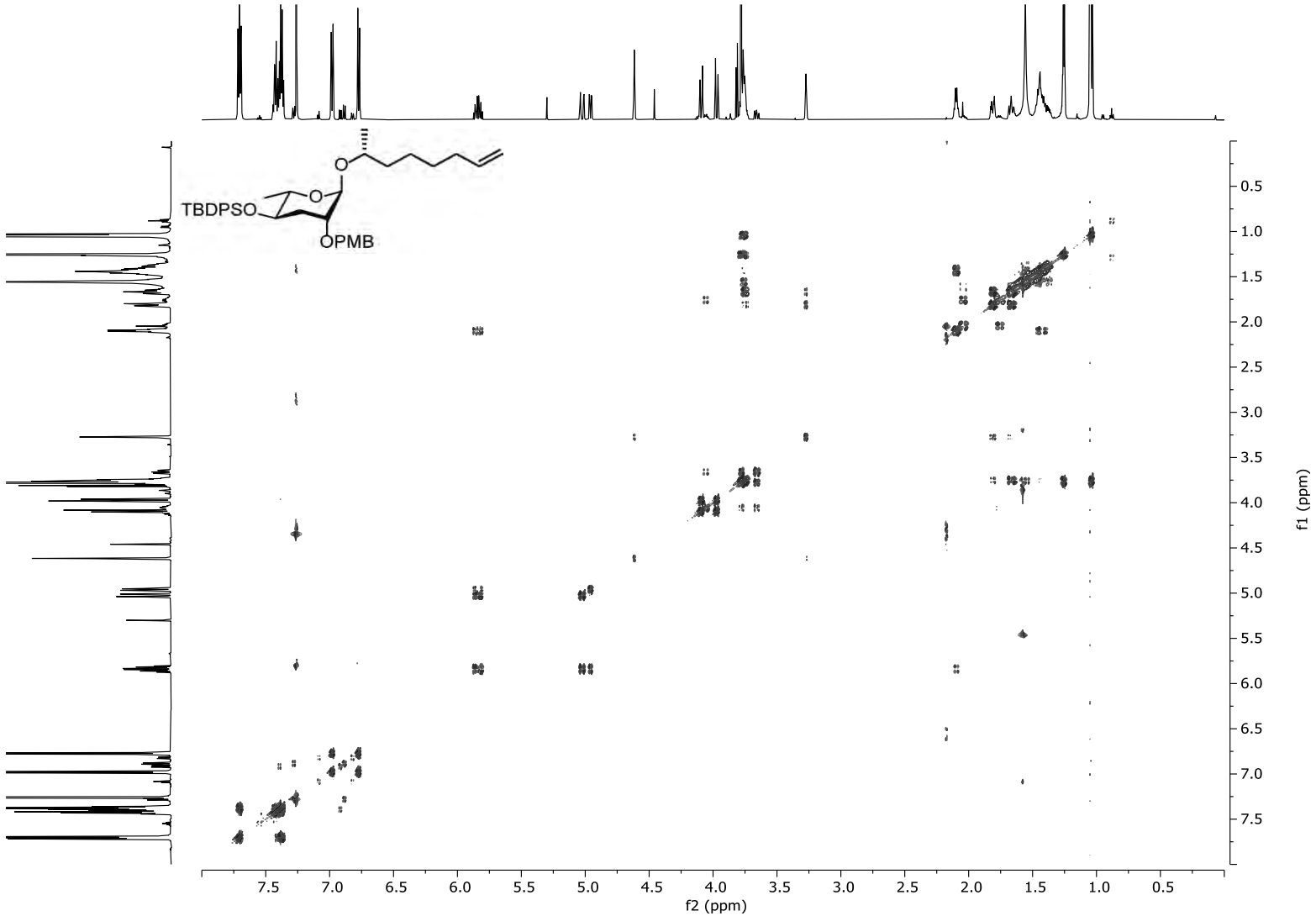

Figure S 88 : HSQC (600 MHz, $CDCl_3$) of (7*R*)-7-[(2-*O*-(4-methoxybenzyloxy)-4-*O*-*tert*-butyldiphenyl-3,6-dideoxy-α-L-*arabino*-hexopyranosyl)oxy]-1-octene (123).

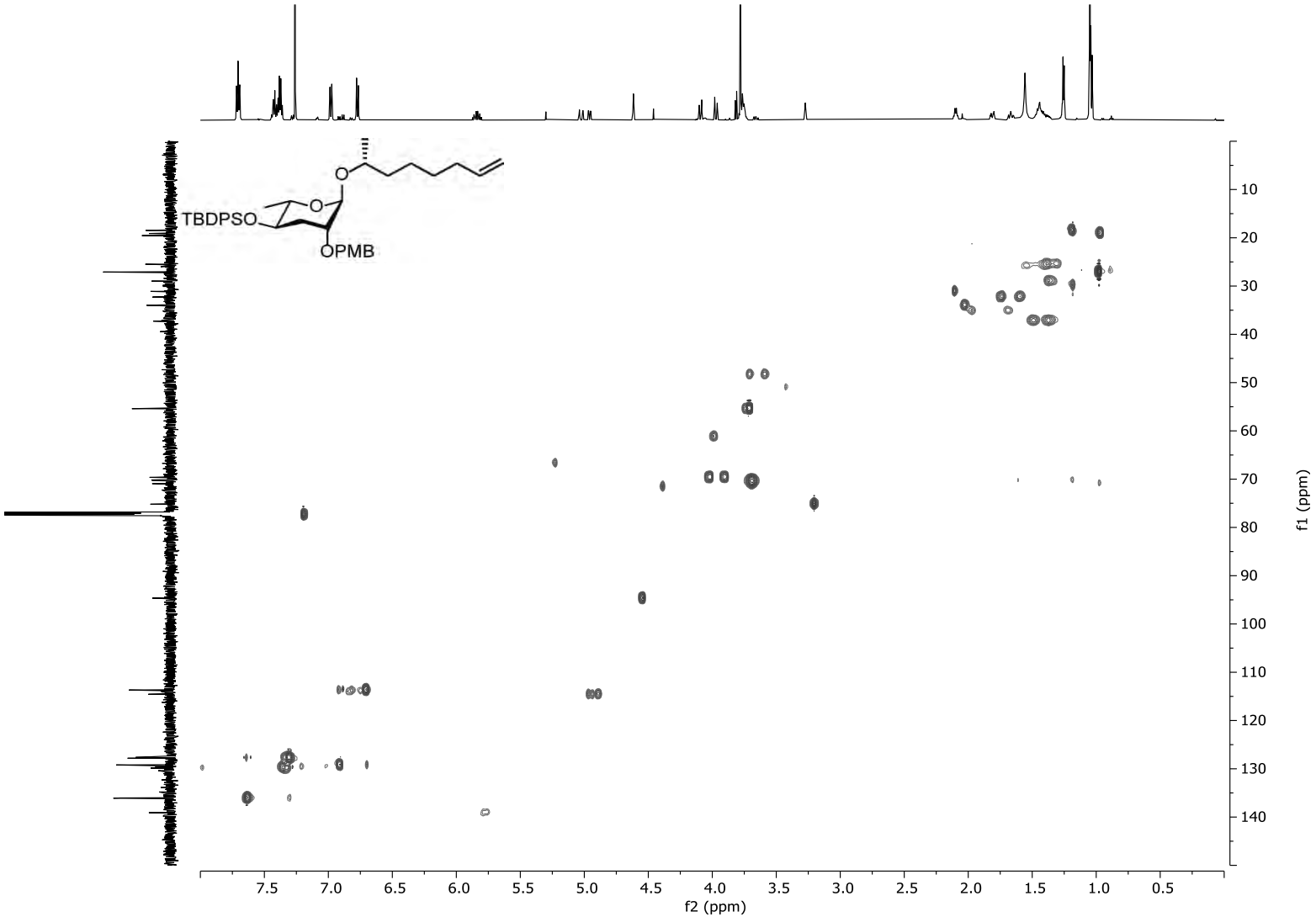

Figure S 89: ^{1}H NMR (600 MHz, $CDCl_3$) of (7*R*)-7-[(2-O-(4-methoxybenzyloxy)-3,6-dideoxy-α-L-*arabino*-hexopyranosyl)oxy]-1-octene (124).

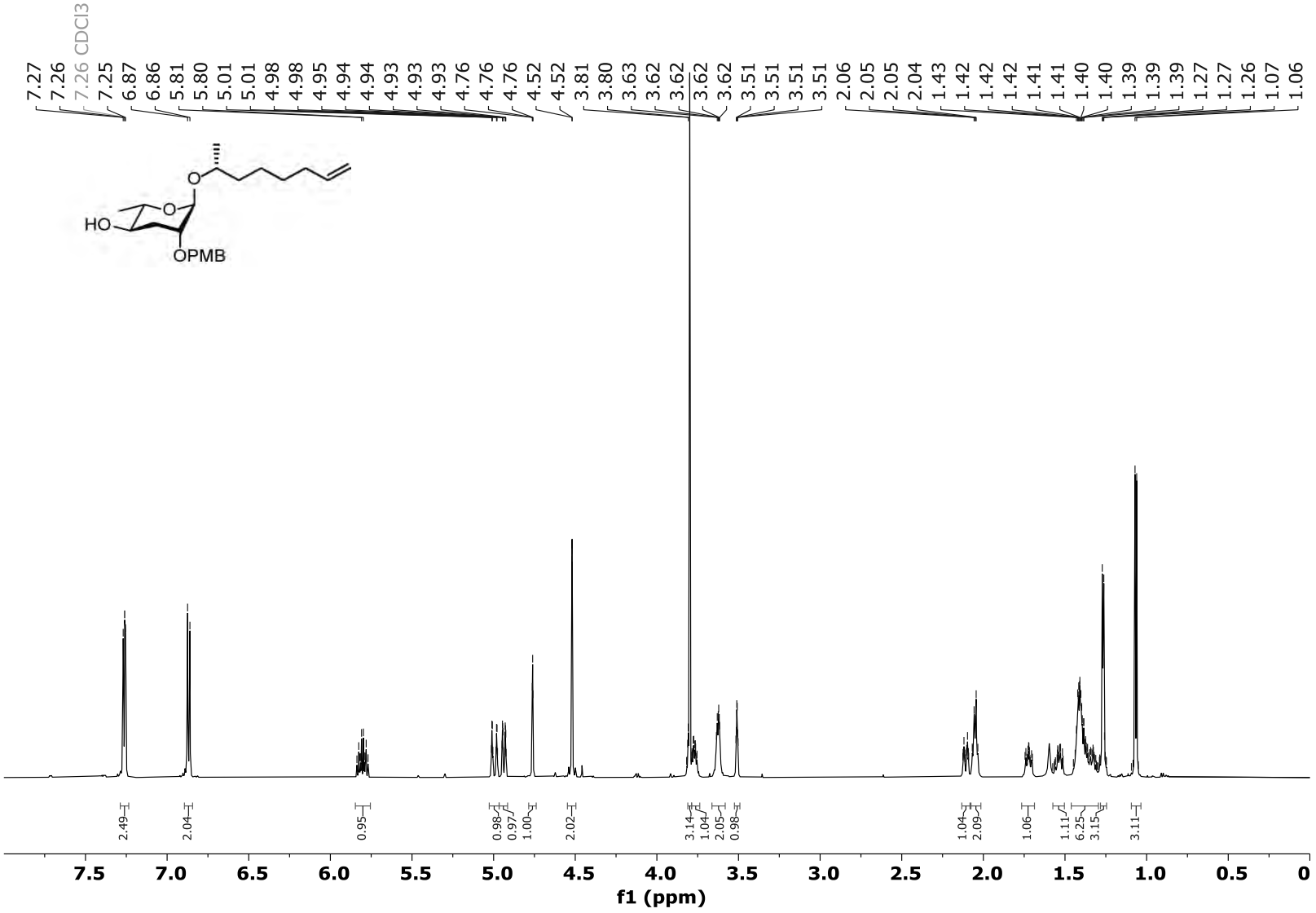

Figure S 90: ^{13}C NMR (150 MHz, $CDCl_3$) of (7*R*)-7-[(2-*O*-(4-methoxybenzyloxy)-3,6-dideoxy-α-L-*arabino*-hexopyranosyl)oxy]-1-octene (124).

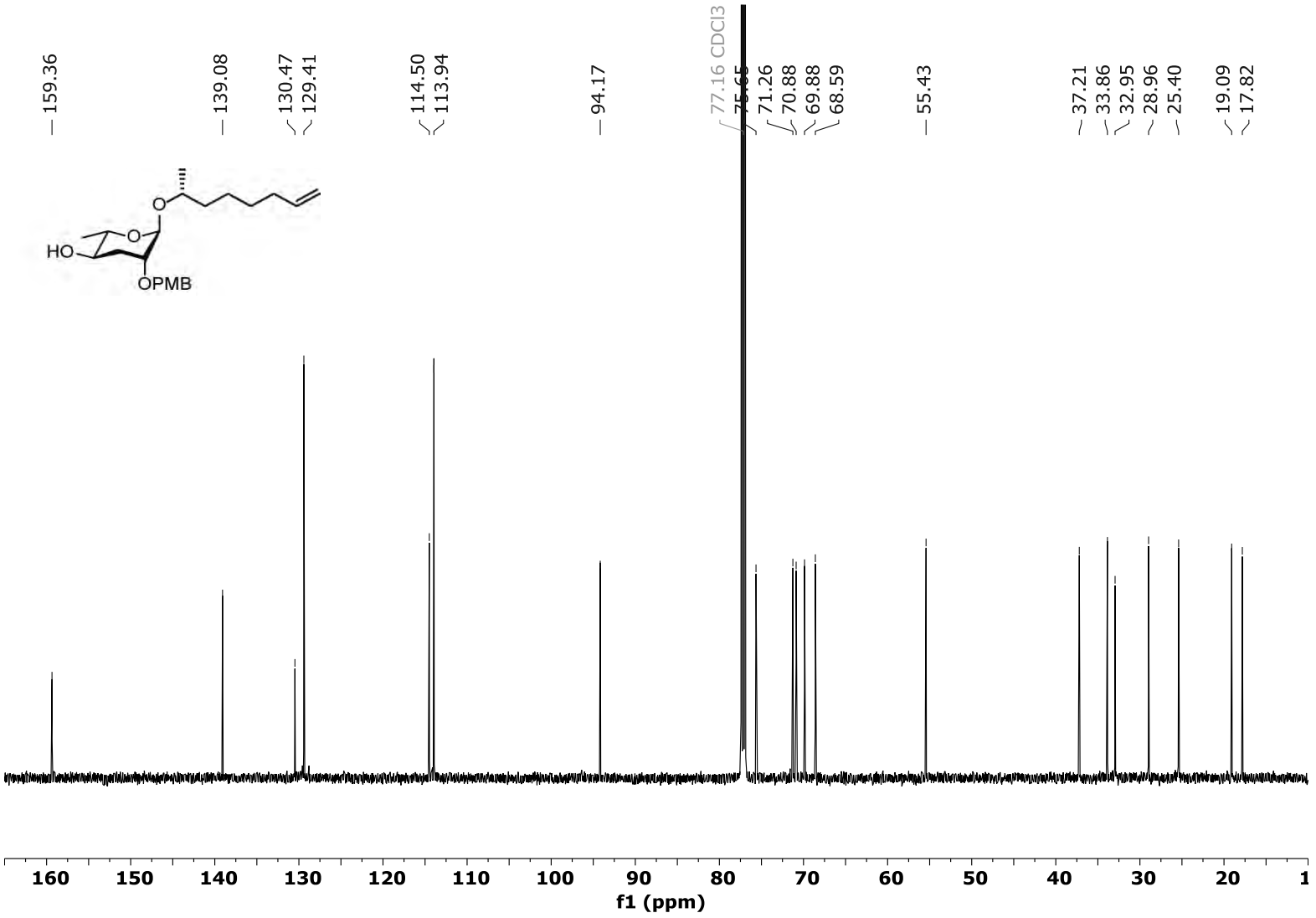

Figure S 91: ***dqf*-COSY (600 MHz, $CDCl_3$) of (7*R*)-7-[(2-O-(4-methoxybenzyloxy)-3,6-dideoxy-α-L-*arabino*-hexopyranosyl)oxy]-1-octene (124).**

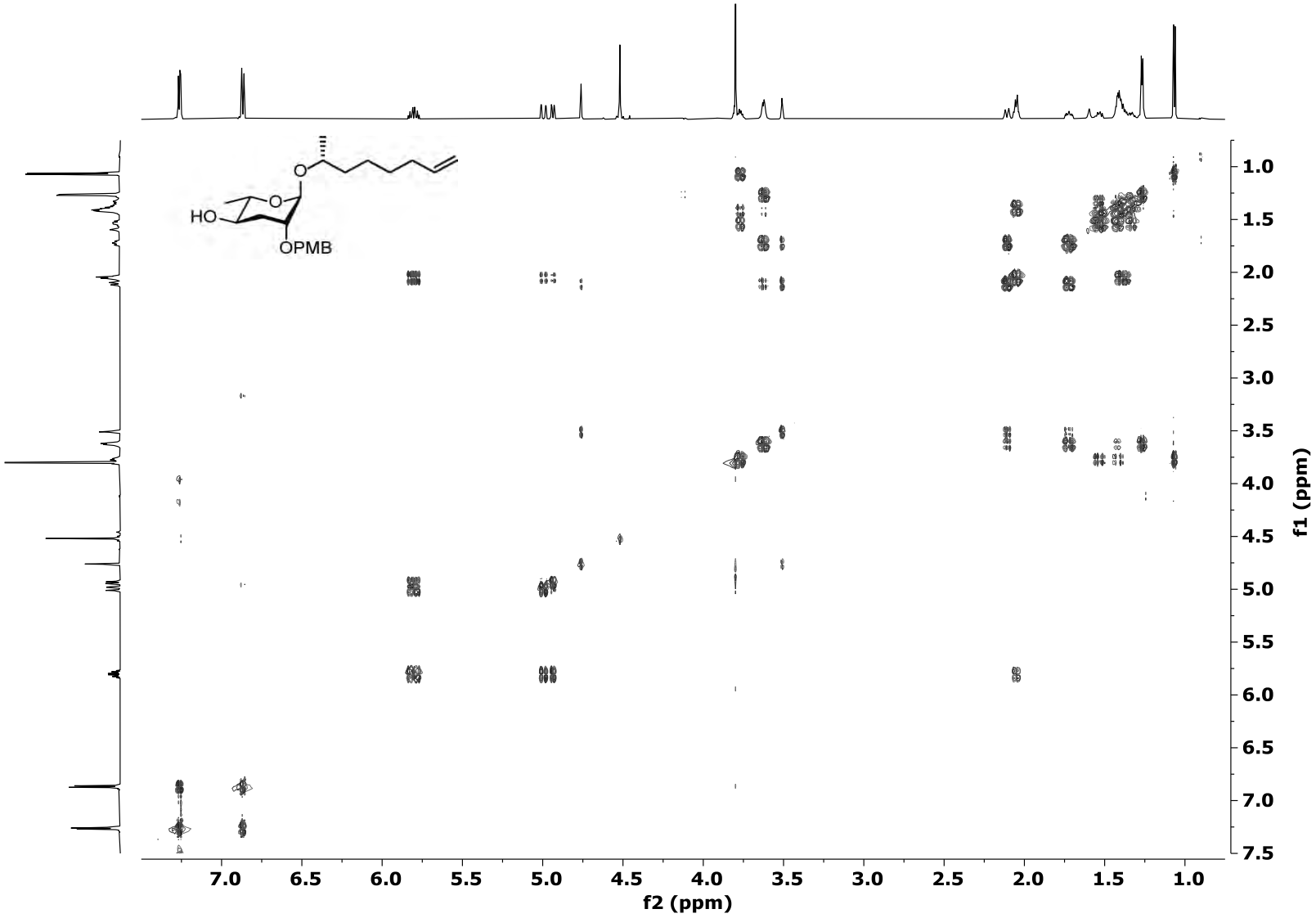

Figure S 92: HSQC (600 MHz, $CDCl_3$) of (7*R*)-7-[(2-*O*-(4-methoxybenzyloxy)-3,6-dideoxy-α-L-*arabino*-hexopyranosyl)oxy]-1-octene (124).

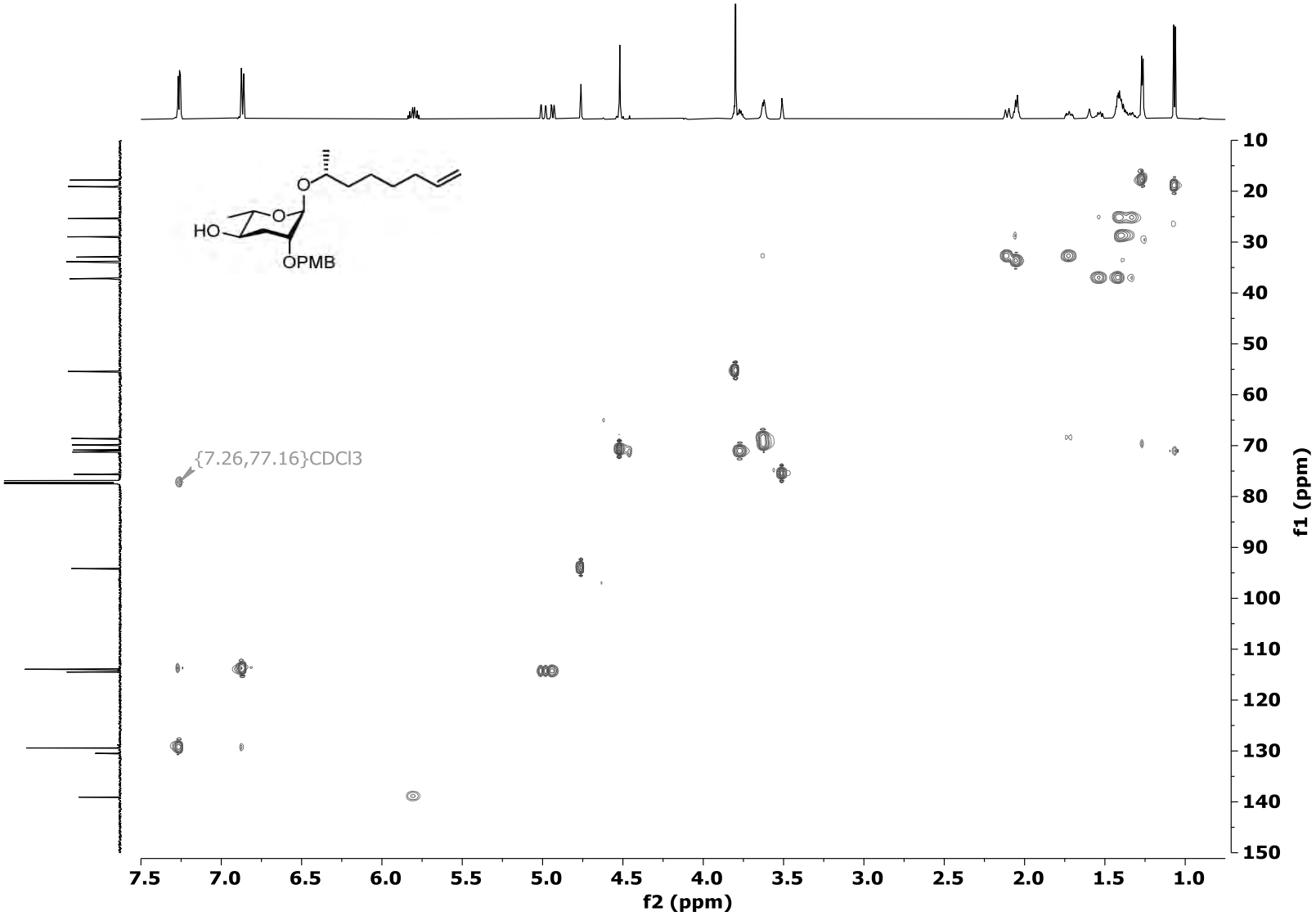

Figure S 93: ^{1}H NMR (600 MHz, $CDCl_3$) of 4-methoxybenzyl-(7*R*)-7-[(2-O-(4-methoxybenzyloxy)-3,6-dideoxy-α-L-*arabino*-hexopyranosyl)oxy]-2-nonenoate (125).

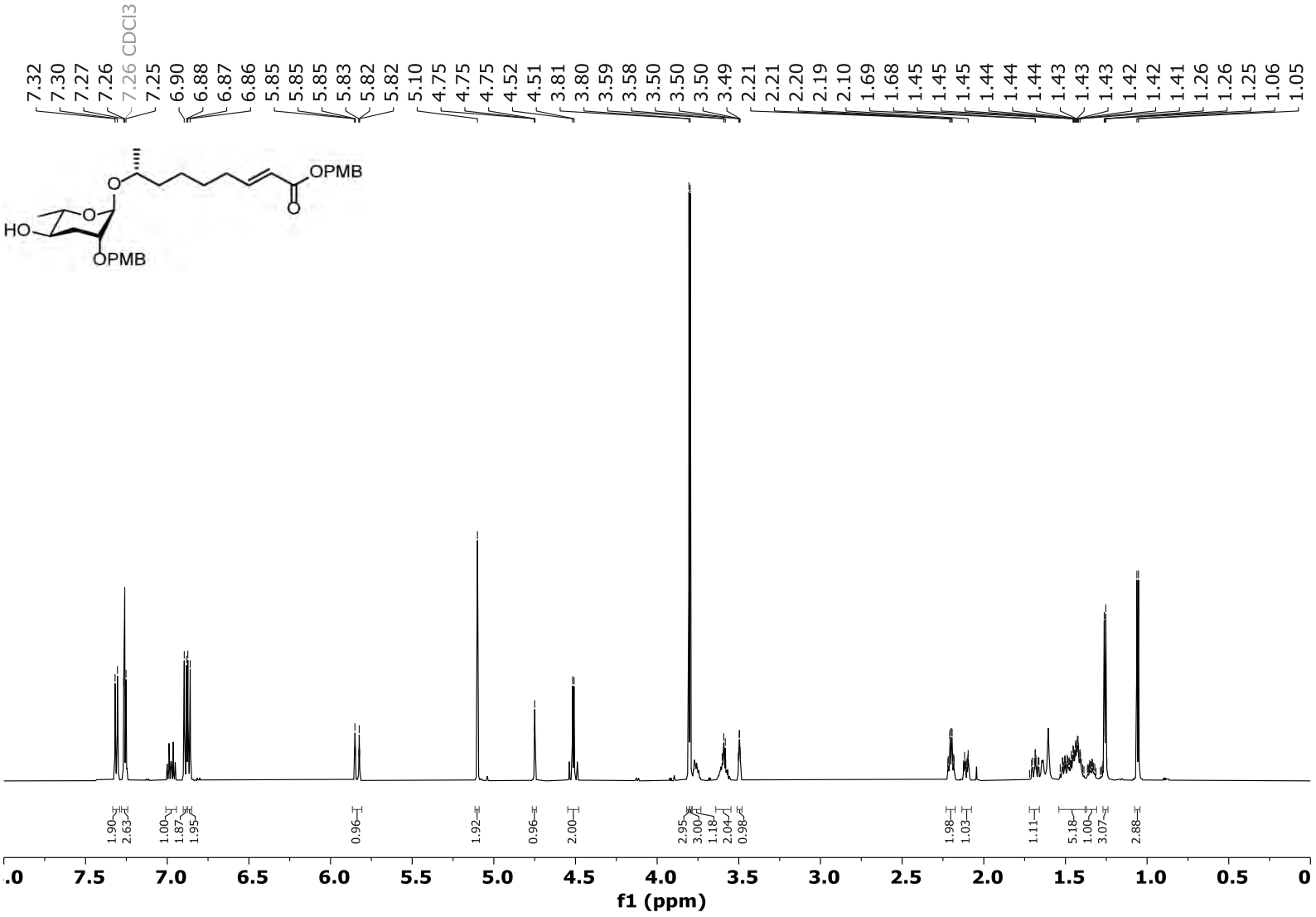

Figure S 94: ^{13}C NMR (150 MHz, $CDCl_3$) of 4-methoxybenzyl-(7*R*)-7-[(2-O-(4-methoxybenzyloxy)-3,6-dideoxy-α-L-*arabino*-hexopyranosyl)oxy]-2-nonenoate (125).

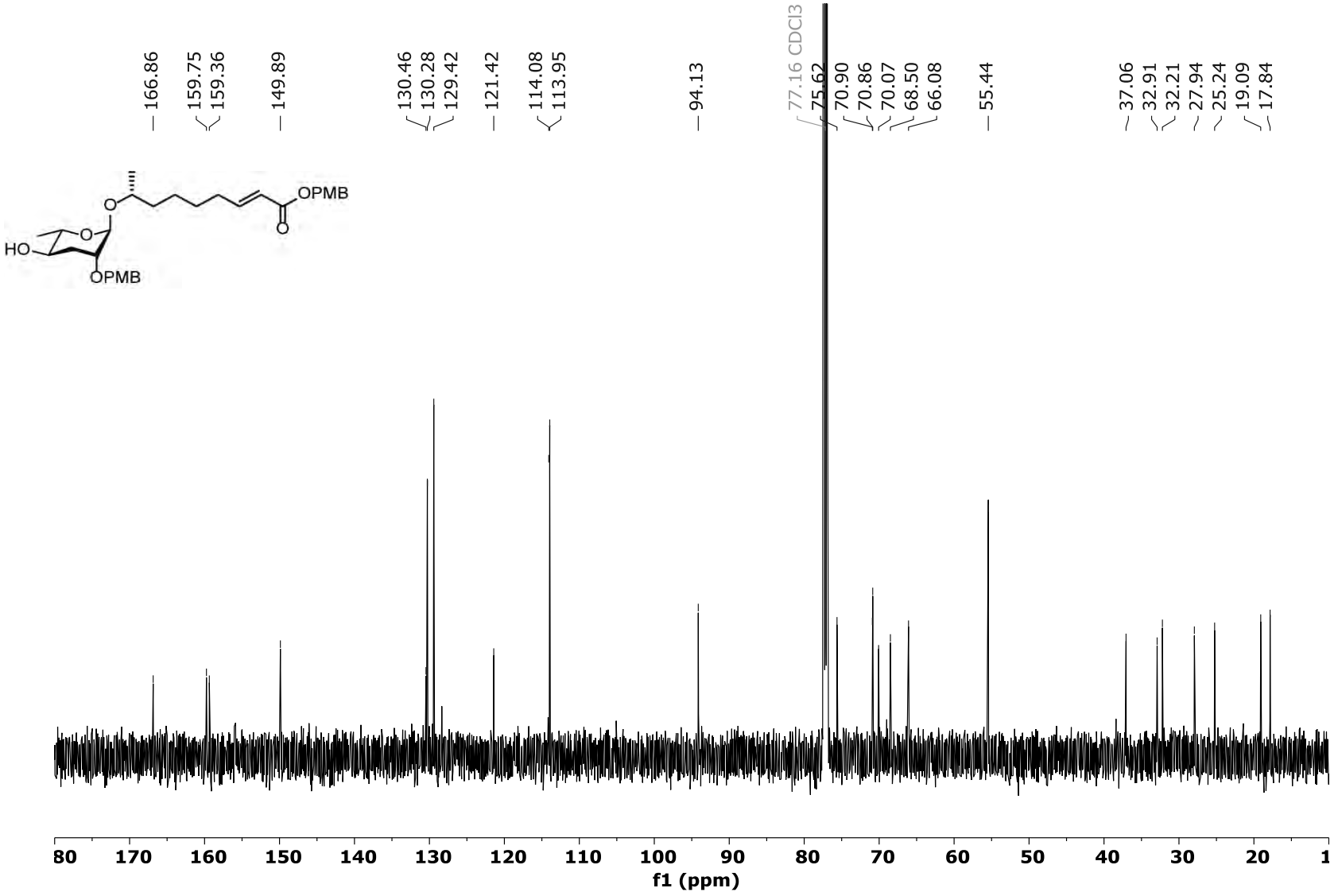

Figure S 95: *dqf*-COSY (600 MHz, $CDCl_3$) of 4-methoxybenzyl-(7*R*)-7-[(2-*O*-(4-methoxybenzyloxy)-3,6-dideoxy-α-L-*arabino*-hexopyranosyl)oxy]-2-nonenoate (125).

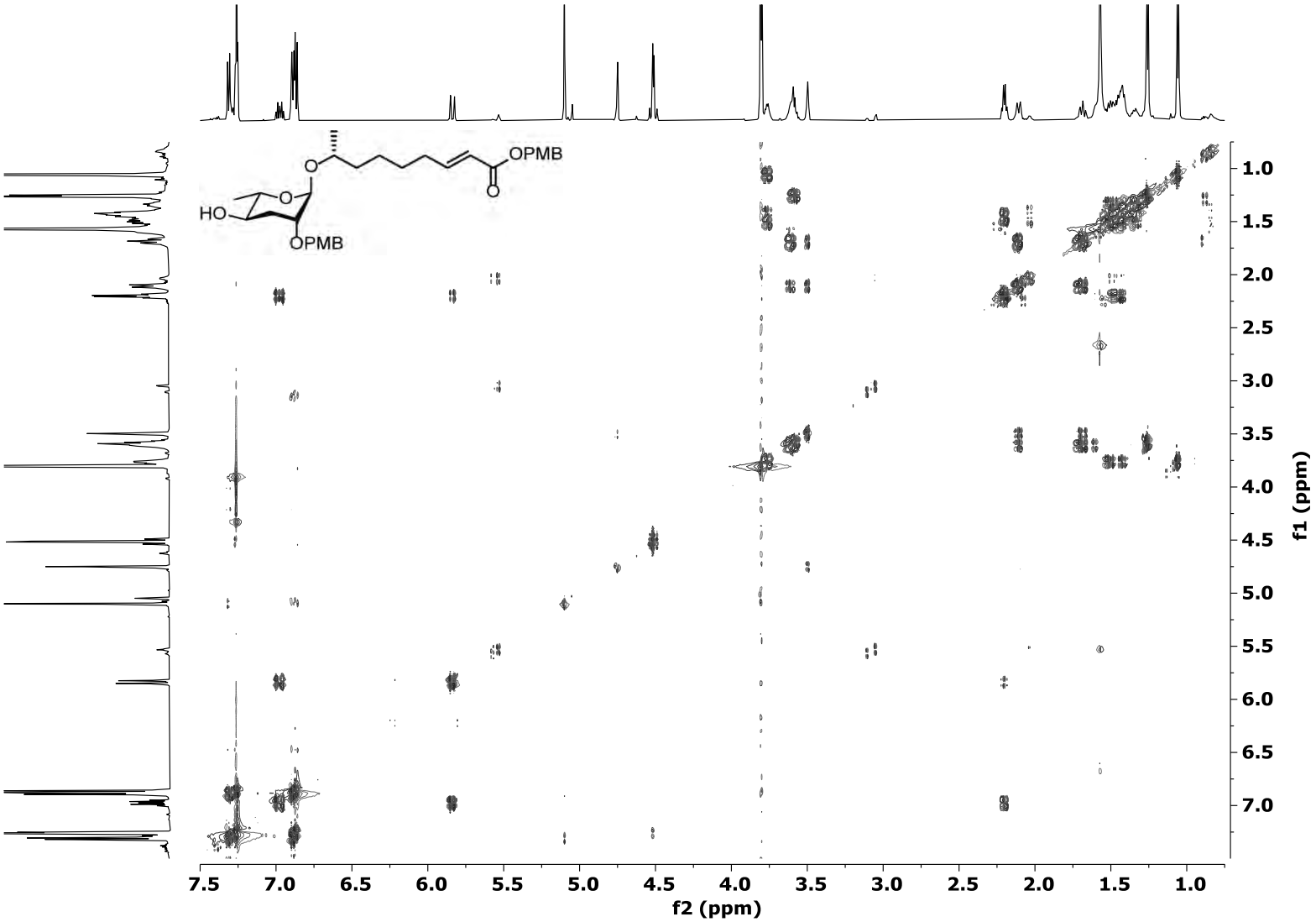

Figure S 96: *dqf*-COSY (600 MHz, $CDCl_3$) of 4-methoxybenzyl-(7*R*)-7-[(2-*O*-(4-methoxybenzyloxy)-3,6-dideoxy-α-L-*arabino*-hexopyranosyl)oxy]-2-nonenoate (125).

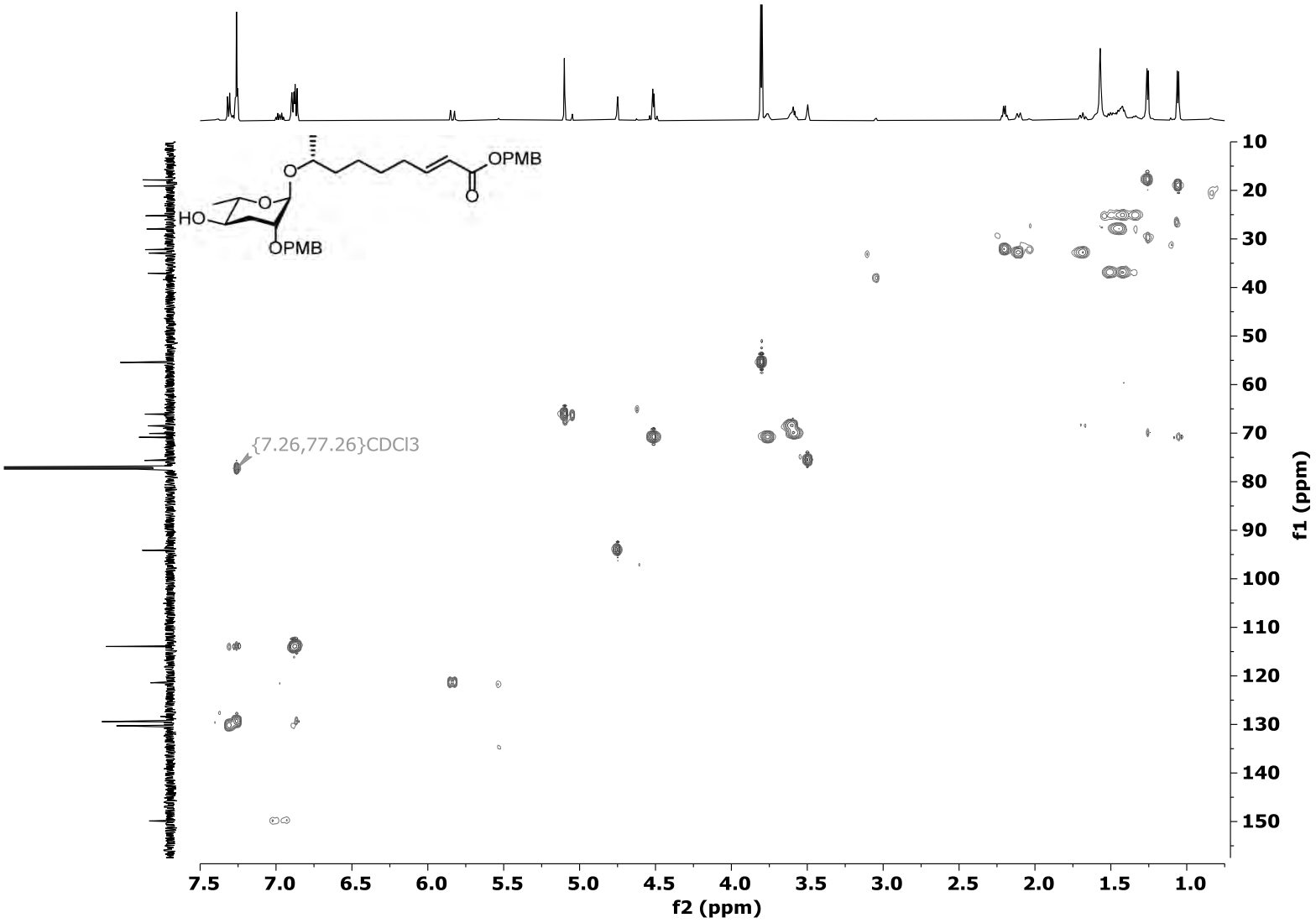

Figure S 97: ^{1}H NMR (600 MHz, $CDCl_3$) of 4-methoxybenzyl-(7*R*)-7-[(2-*O*-(4-methoxybenzyloxy)-4-*O*-((*E*)-3-(1-(*tert*-butoxycarbonyl)-1H-imidazol-4-yl)-propenoate)-3,6-dideoxy-α-L-*arabino*-hexopyranosyl)oxy]-2-nonenoate (126).

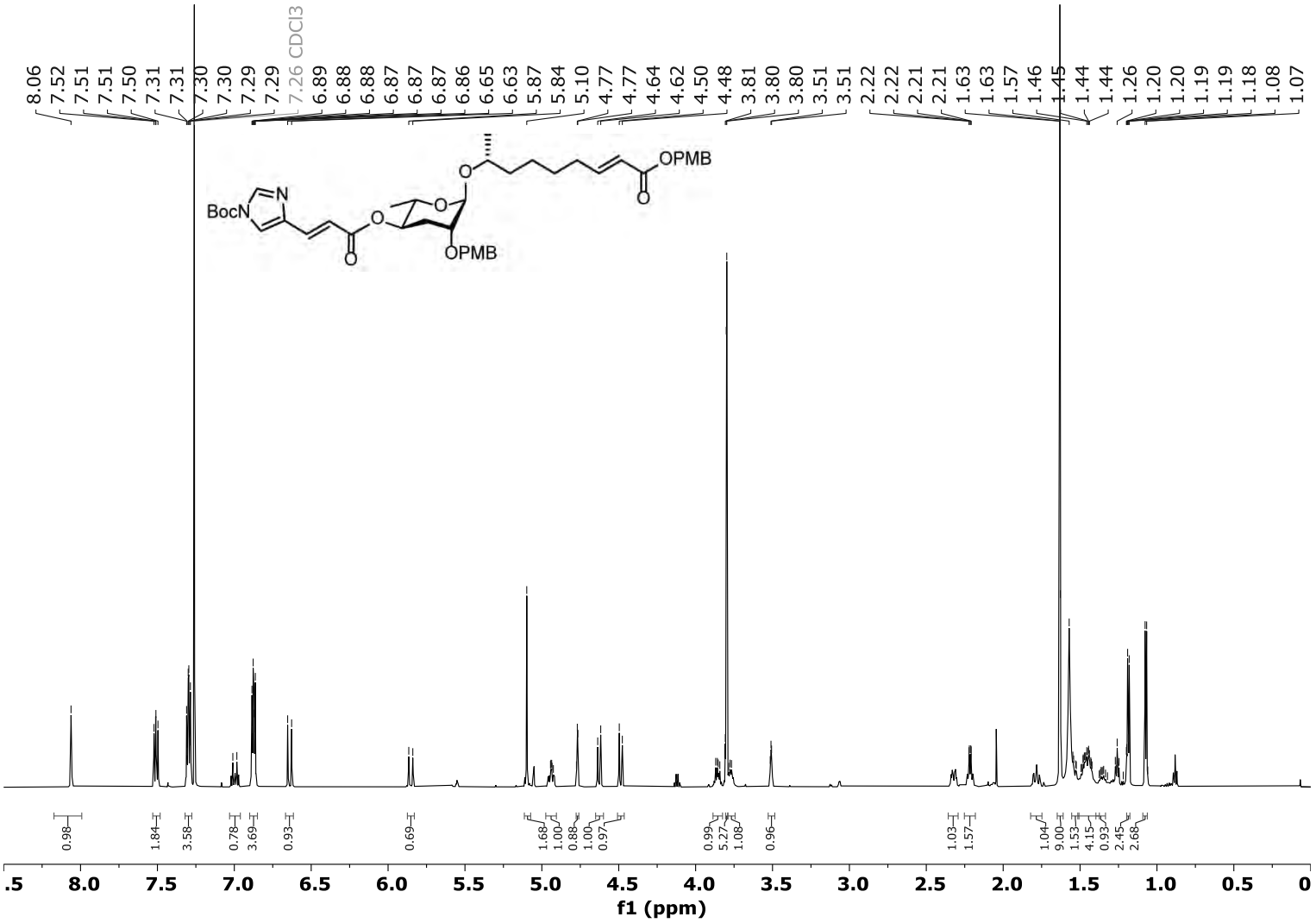

Figure S 98 : ^{13}C NMR (150 MHz, $CDCl_3$) of 4-methoxybenzyl-(7*R*)-7-[(2-*O*-(4-methoxybenzyloxy)-4-*O*-((*E*)-3-(1-(*tert*-butoxycarbonyl)-1H-imidazol-4-yl)-propenoate)-3,6-dideoxy-α-L-*arabino*-hexopyranosyl)oxy]-2-nonenoate (126).

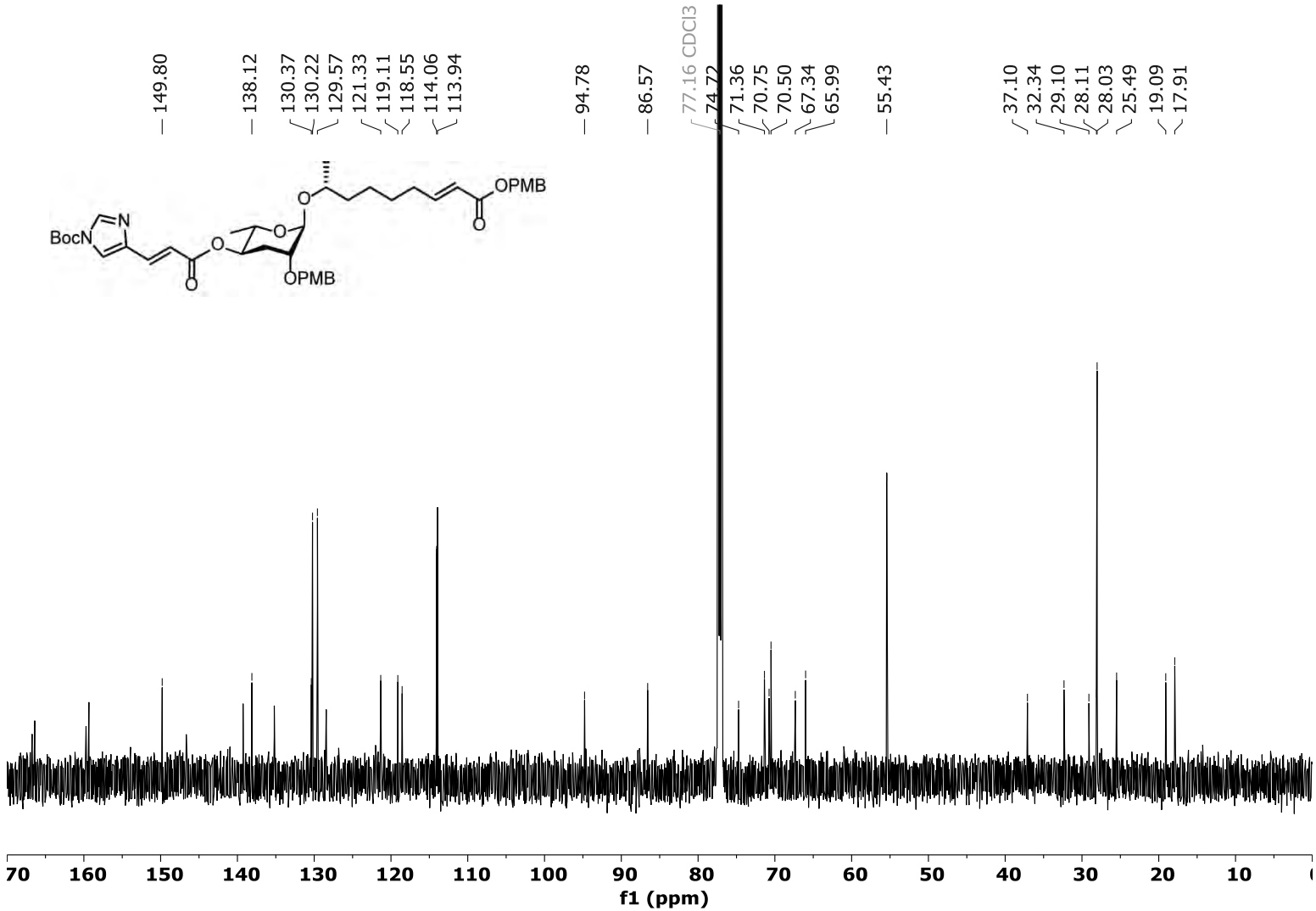

Figure S 99: ***dqf*-COSY(600 MHz, $CDCl_3$) of 4-methoxybenzyl-(7*R*)-7-[(2-*O*-(4-methoxybenzyloxy)-4-*O*-((*E*)-3-(1-(*tert*-butoxycarbonyl)-1H-imidazol-4-yl)-propenoate)-3,6-dideoxy-α-L-*arabino*-hexopyranosyl)oxy]-2-nonenoate (126).**

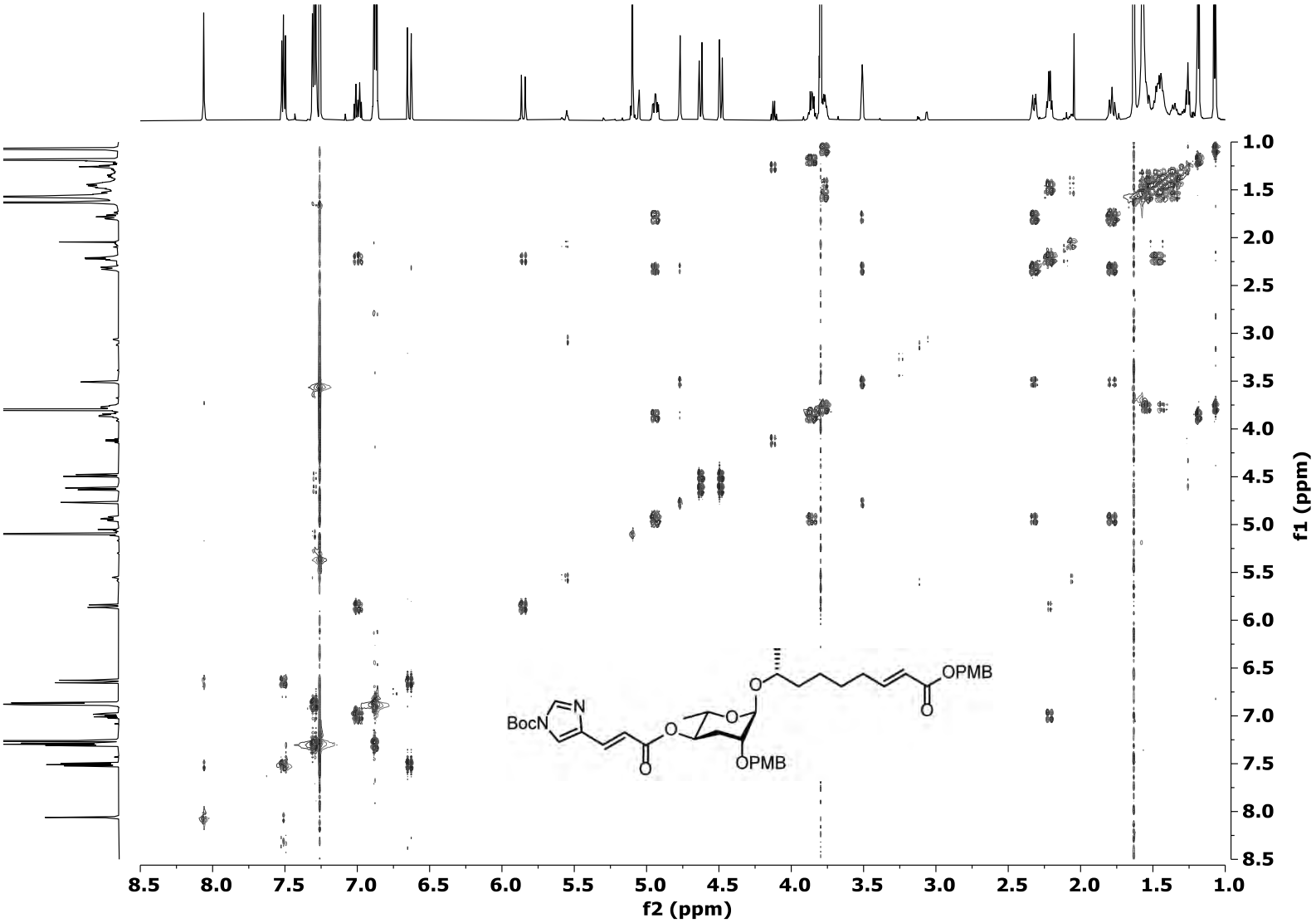

Figure S 100 : HSQC (600 MHz, $CDCl_3$) of 4-methoxybenzyl-(7*R*)-7-[(2-*O*-(4-methoxybenzyloxy)-4-*O*-((*E*)-3-(1-(*tert*-butoxycarbonyl)-1H-imidazol-4-yl)-propenoate)-3,6-dideoxy-α-L-*arabino*-hexopyranosyl)oxy]-2-nonenoate (126).

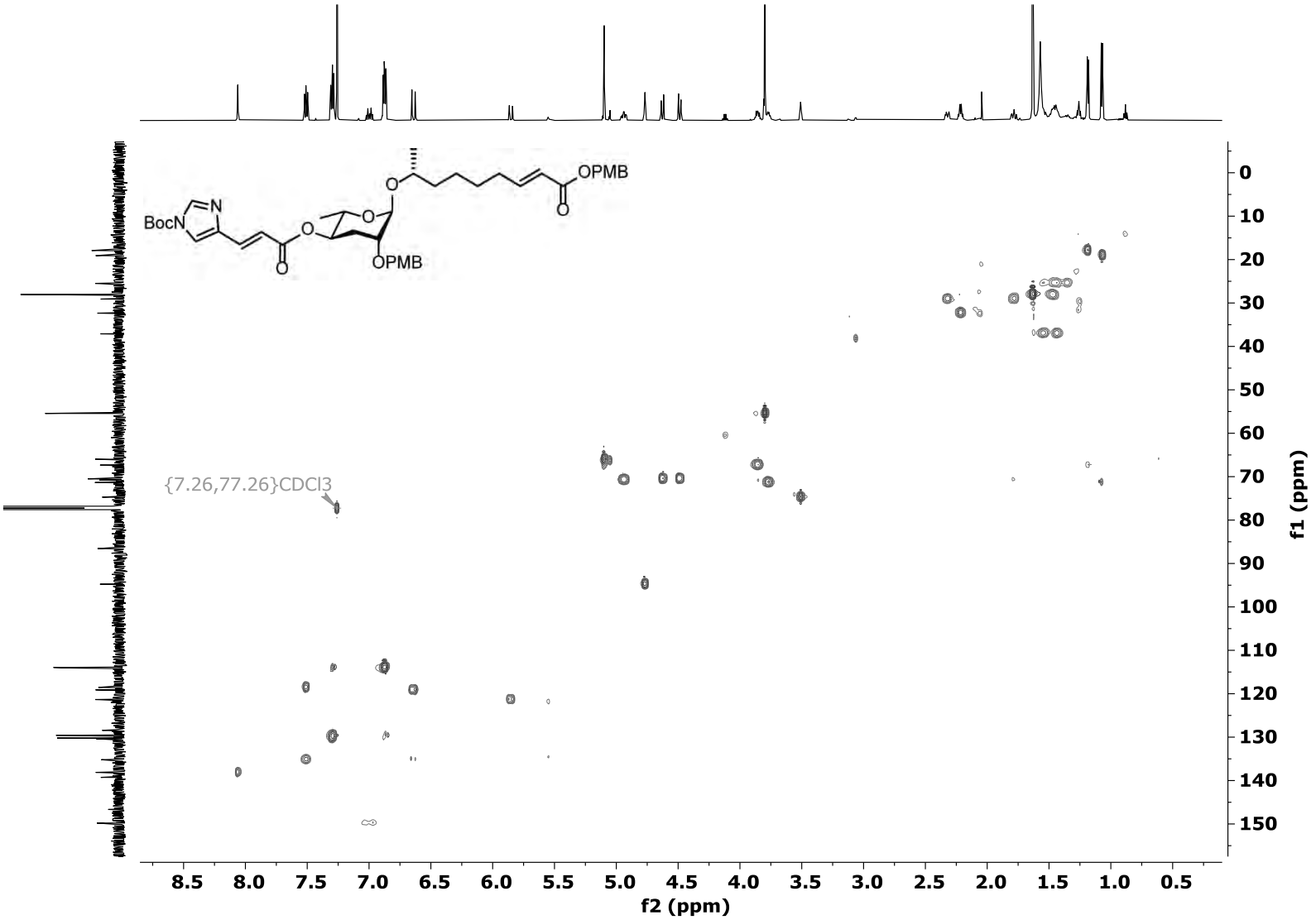

Figure S 101: HMBC (600 MHz, $CDCl_3$) of 4-methoxybenzyl-(7*R*)-7-[(2-*O*-(4-methoxybenzyloxy)-4-*O*-((*E*)-3-(1-(*tert*-butoxycarbonyl)-1*H*-imidazol-4-yl)-propenoate)-3,6-dideoxy-α-L-*arabino*-hexopyranosyl)oxy]-2-nonenoate (126).

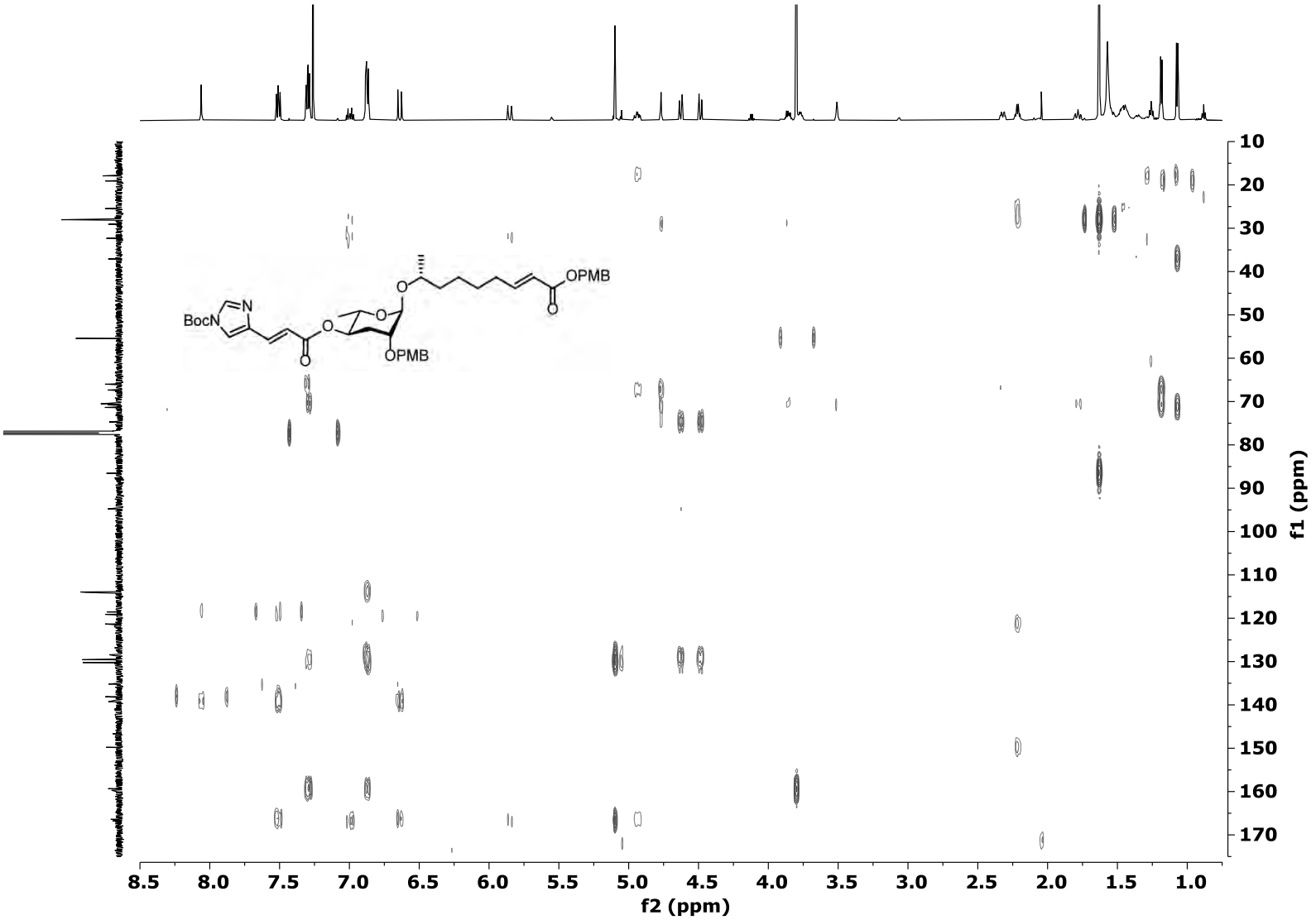

Figure S 102: ^{1}H NMR (600 MHz, $CDCl_3$) of (7*R*)-7-[4-*O*-((*E*)-3-(1*H*-imidazol-4-yl)-propenoate)-3,6-dideoxy-α-L-*arabino*-hexopyranosyl)oxy]-2-nonenoic acid (37).

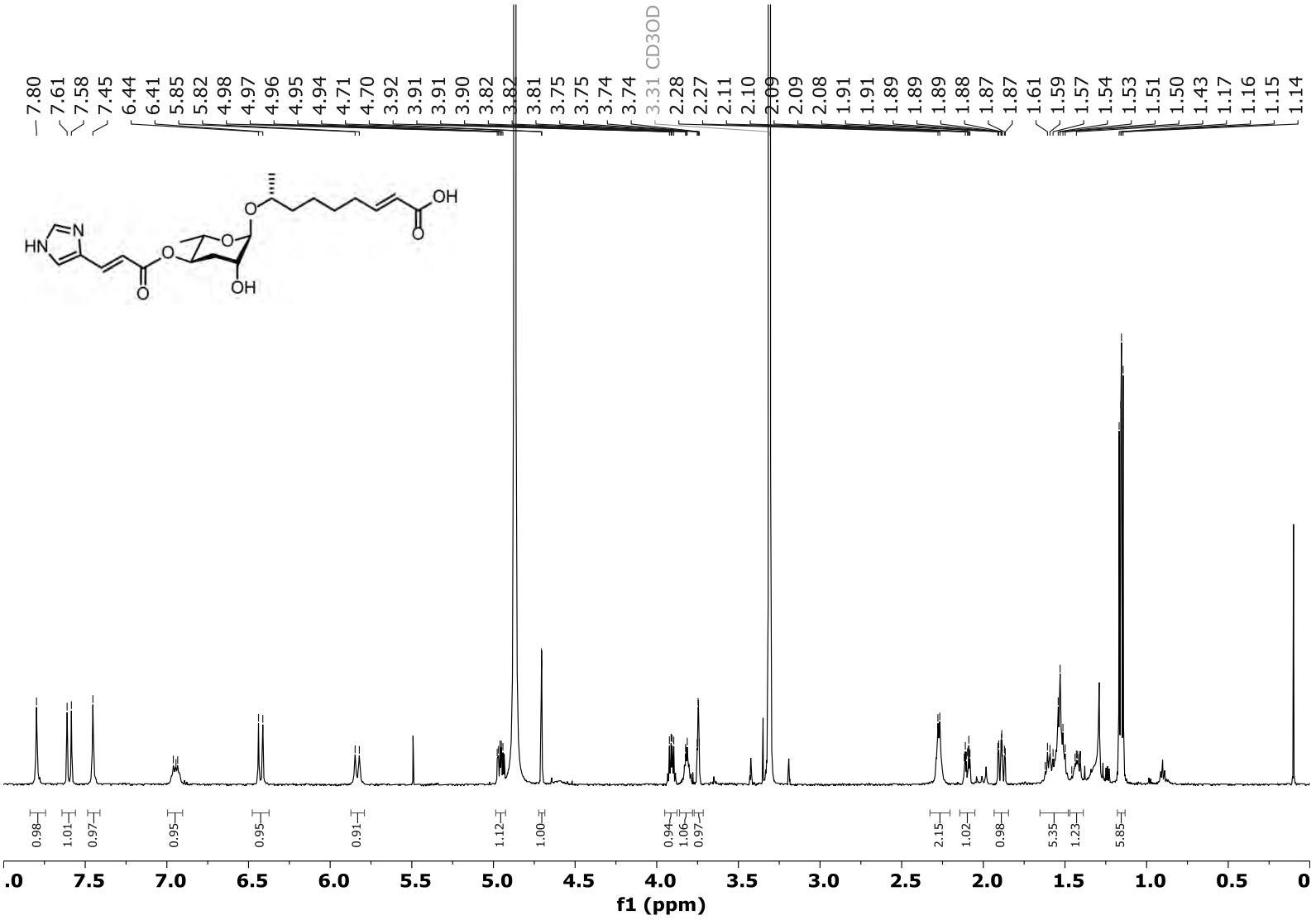

Figure S 103: *dqf*-COSY (600 MHz, $CDCl_3$) of (7*R*)-7-[4-*O*-((*E*)-3-(1*H*-imidazol-4-yl)-propenoate)-3,6-dideoxy-α-L-*arabino*-hexopyranosyl)oxy]-2-nonenoic acid (37).

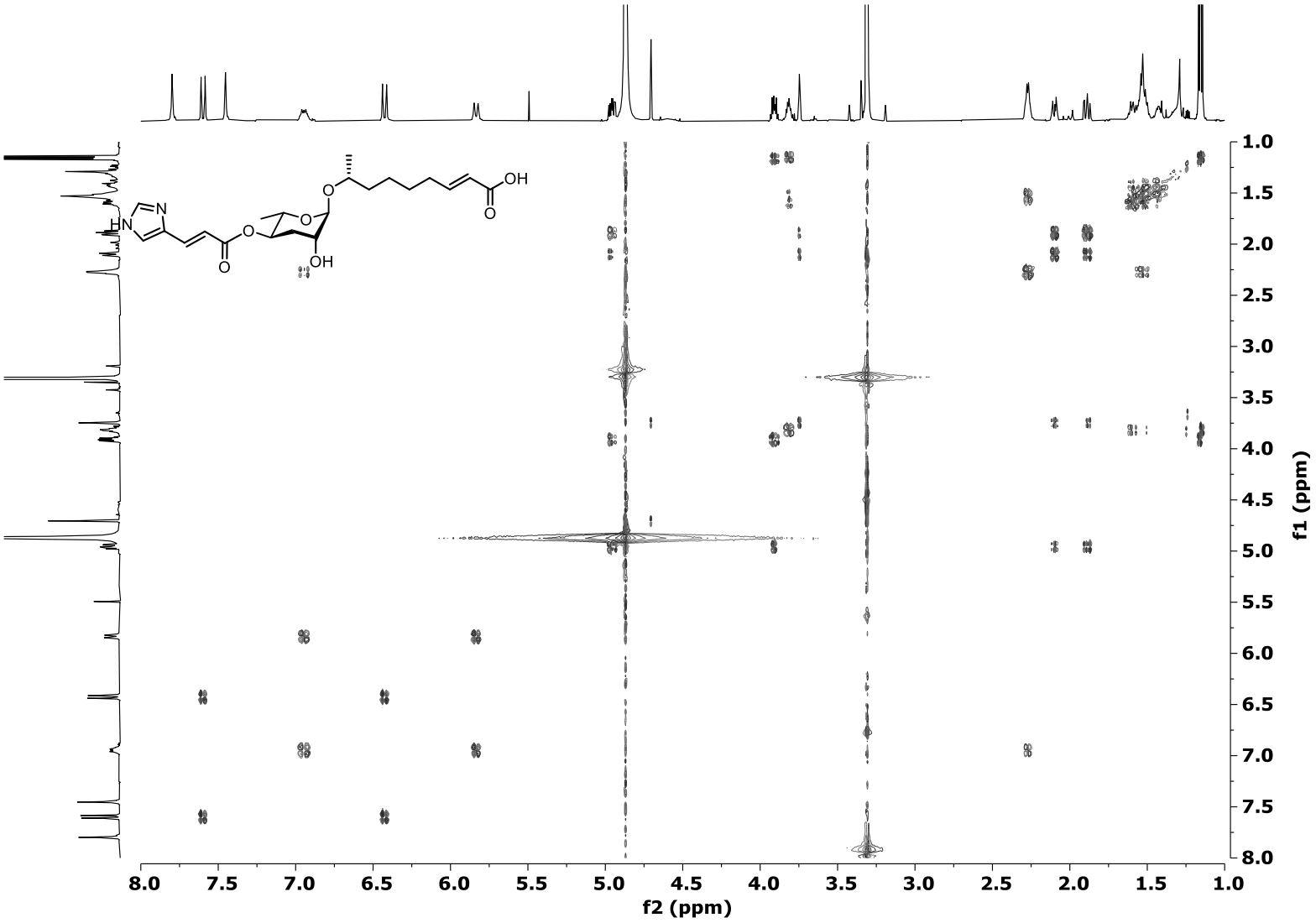

Figure S 104: HSQC (600 MHz, $CDCl_3$) of (7*R*)-7-[4-*O*-((*E*)-3-(1*H*-imidazol-4-yl)-propenoate)-3,6-dideoxy-α-L-*arabino*-hexopyranosyl)oxy]-2-nonenoic acid (37).

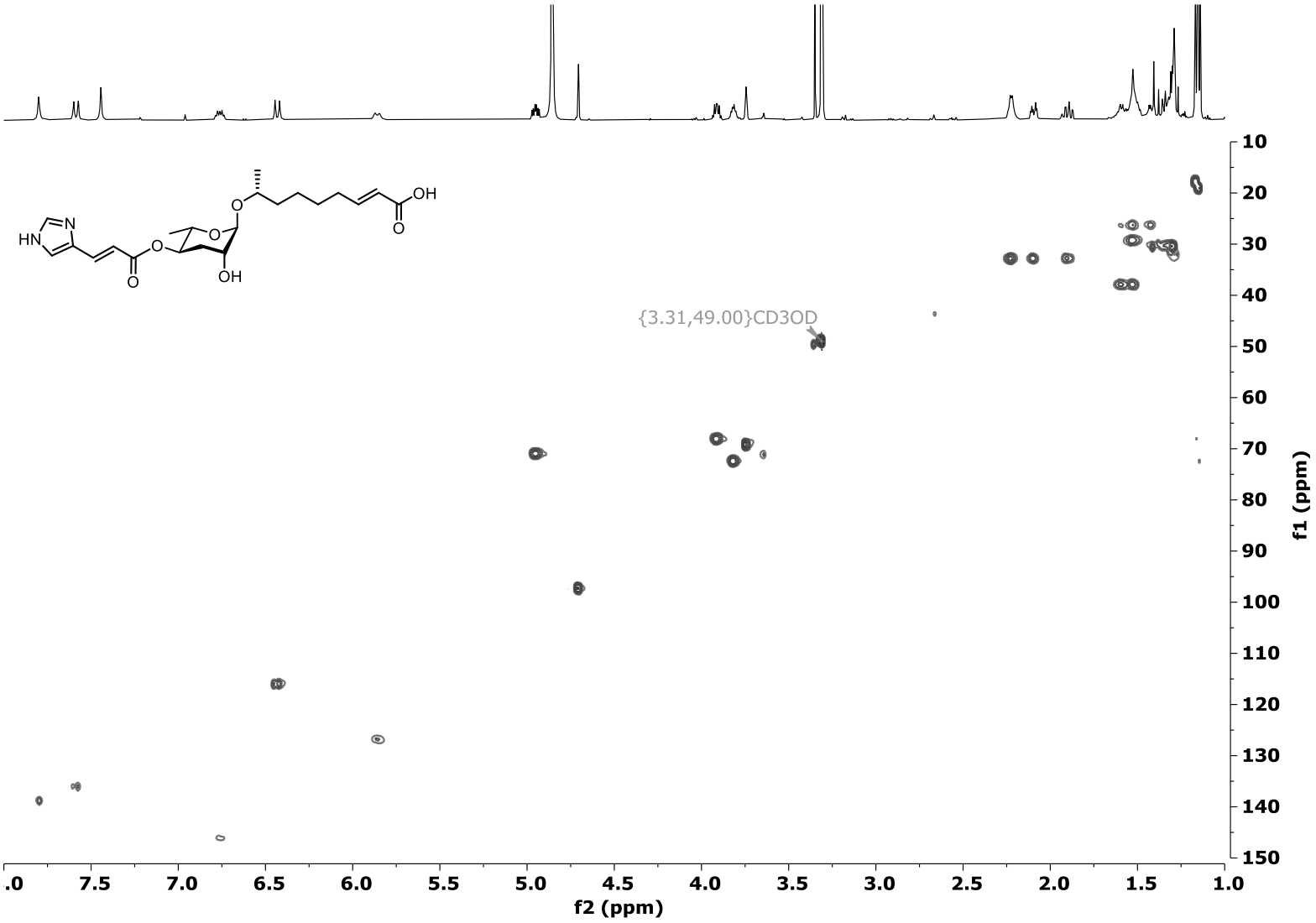

Figure S 105: HMBC (600 MHz, $CDCl_3$) of (7*R*)-7-[4-*O*-((*E*)-3-(1*H*-imidazol-4-yl)-propenoate)-3,6-dideoxy-α-L-*arabino*-hexopyranosyl)oxy]-2-nonenoic acid (37).

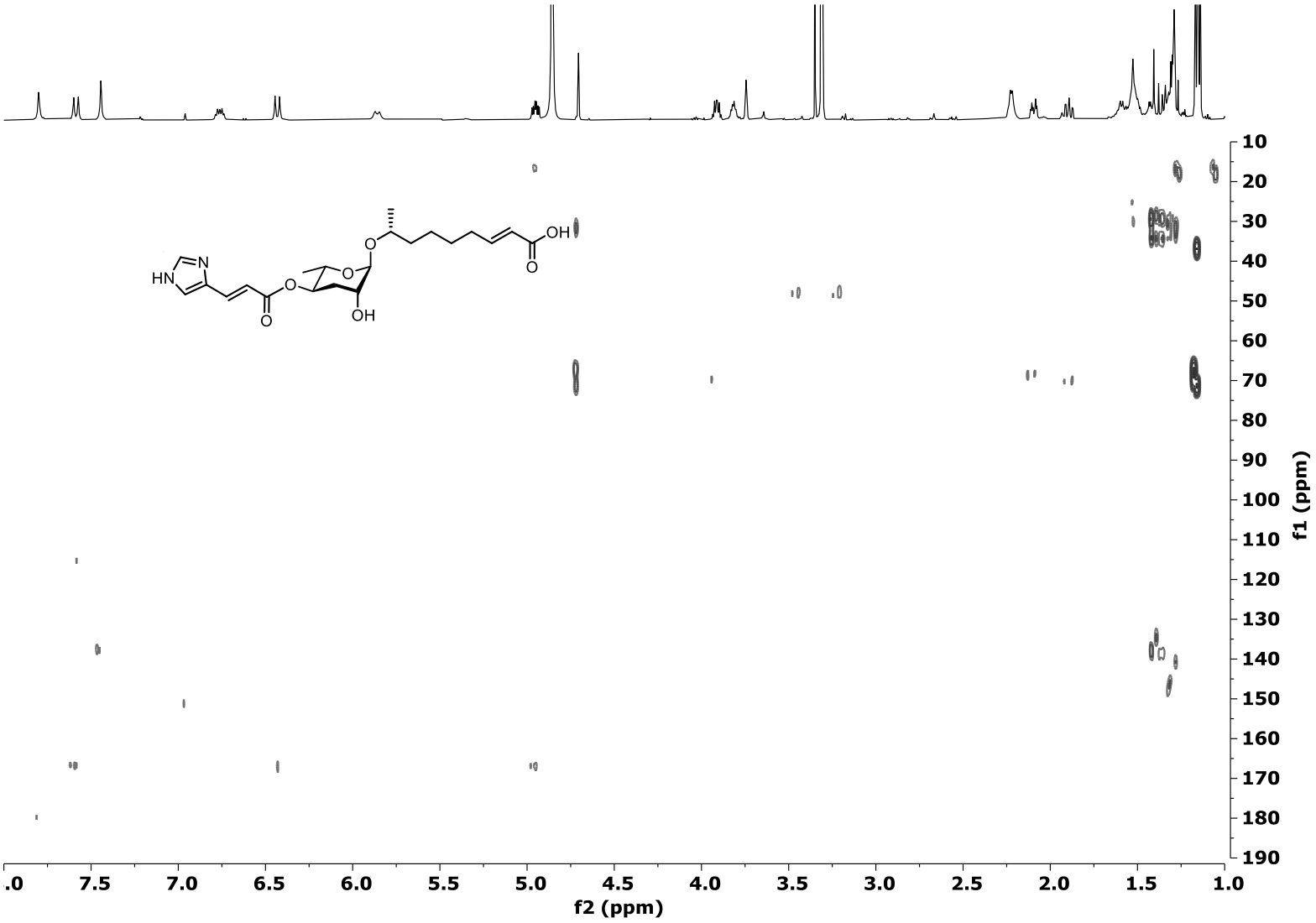

Figure S 106: ^{1}H NMR (600 MHz, $CDCl_3$) of (7*R*)-7-[4-*O*-((*Z*)-3-(1*H*-imidazol-4-yl)-propenoate)-3,6-dideoxy-α-L-*arabino*-hexopyranosyl)oxy]-2-nonenoic acid (38).

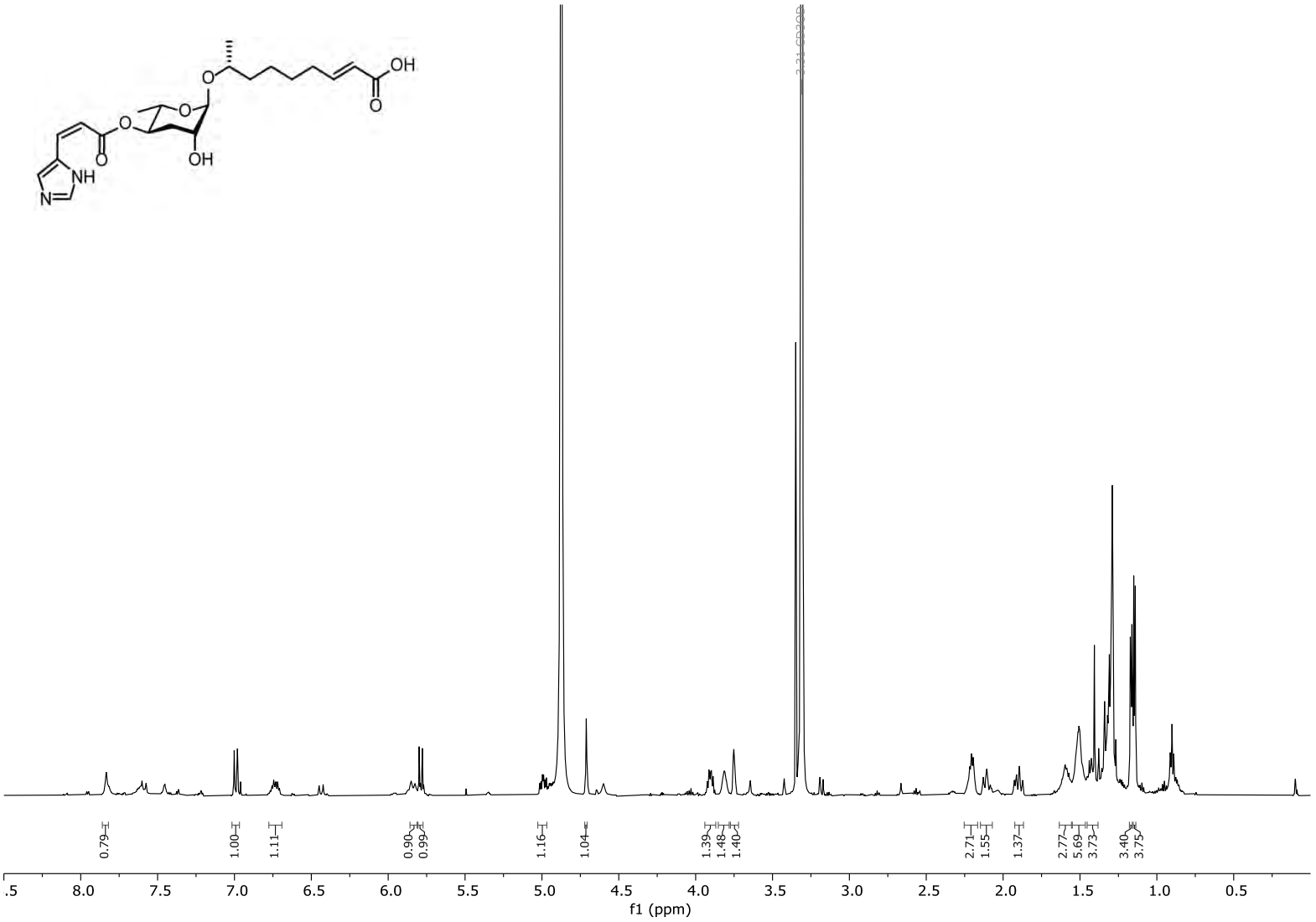

Figure S 107: *dqf*-COSY (600 MHz, $CDCl_3$) of (7*R*)-7-[4-*O*-((*Z*)-3-(1*H*-imidazol-4-yl)-propenoate)-3,6-dideoxy-α-L-*arabino*-hexopyranosyl)oxy]-2-nonenoic acid (38).

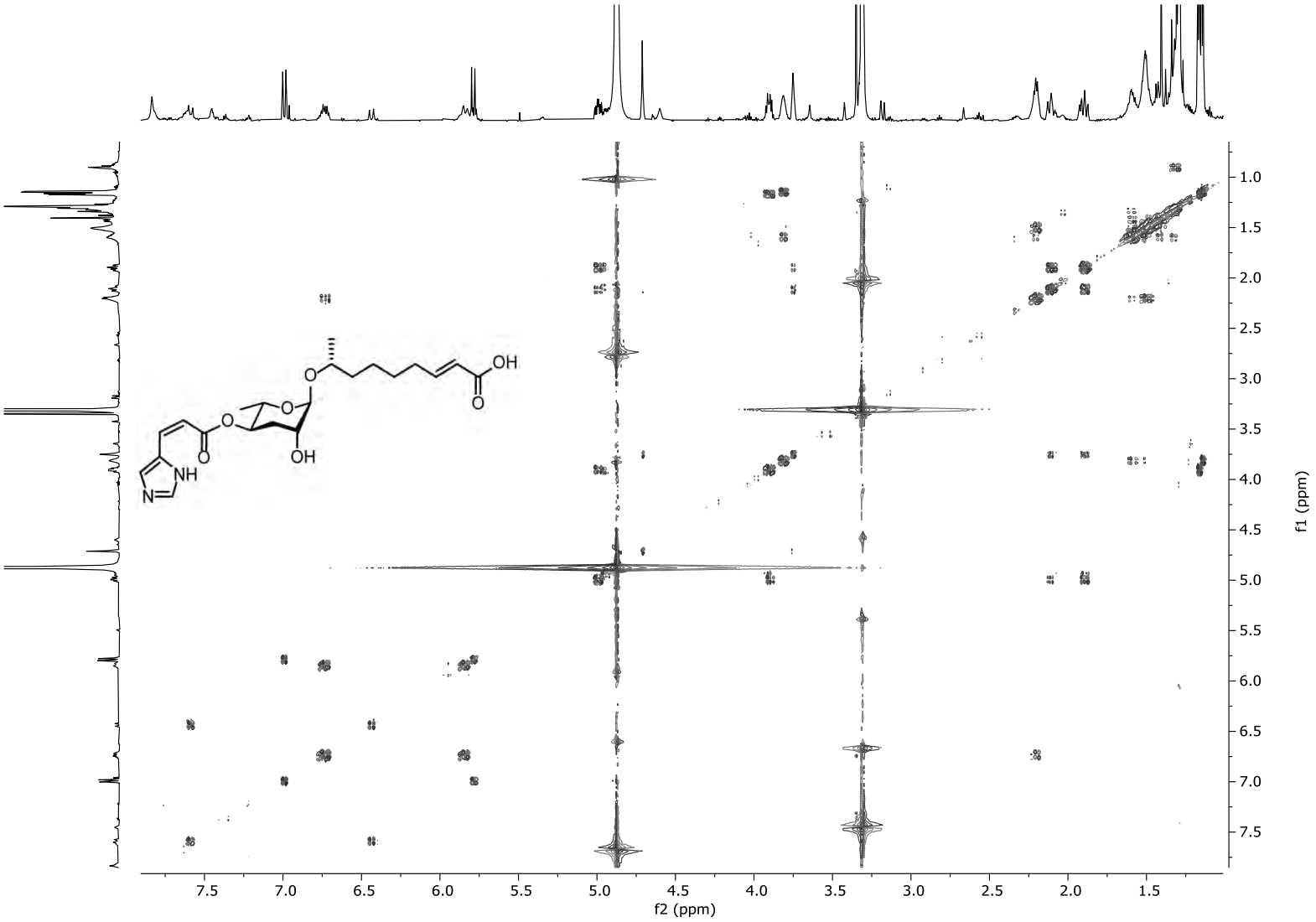

Figure S 108: HSQC (600 MHz, $CDCl_3$) of (7*R*)-7-[4-*O*-((*Z*)-3-(1*H*-imidazol-4-yl)-propenoate)-3,6-dideoxy-α-L-*arabino*-hexopyranosyl)oxy]-2-nonenoic acid (38).

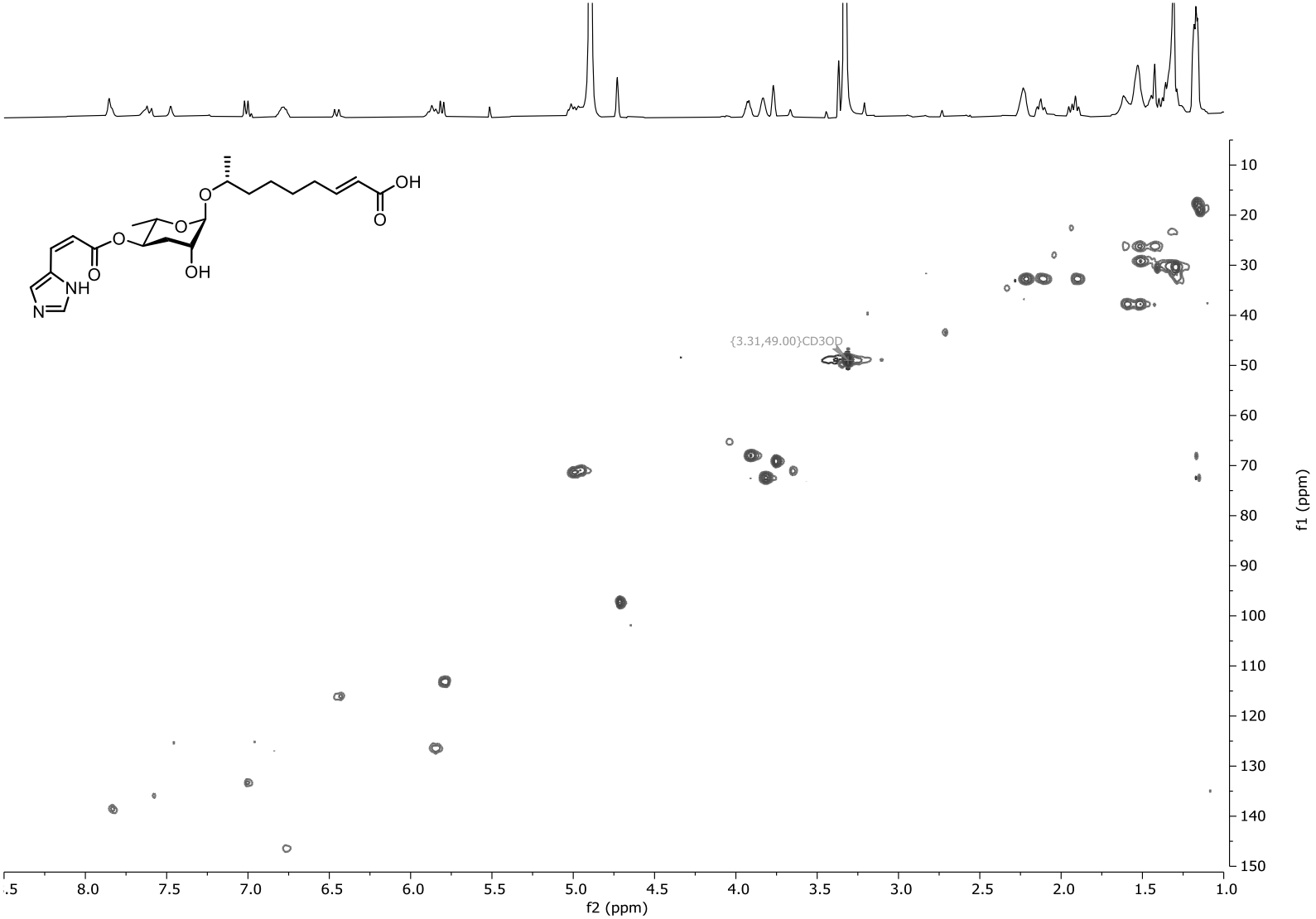

Figure S 109: HMBC (600 MHz, $CDCl_3$) of (7*R*)-7-[4-*O*-((*Z*)-3-(1*H*-imidazol-4-yl)-propenoate)-3,6-dideoxy-α-L-*arabino*-hexopyranosyl)oxy]-2-nonenoic acid (38).

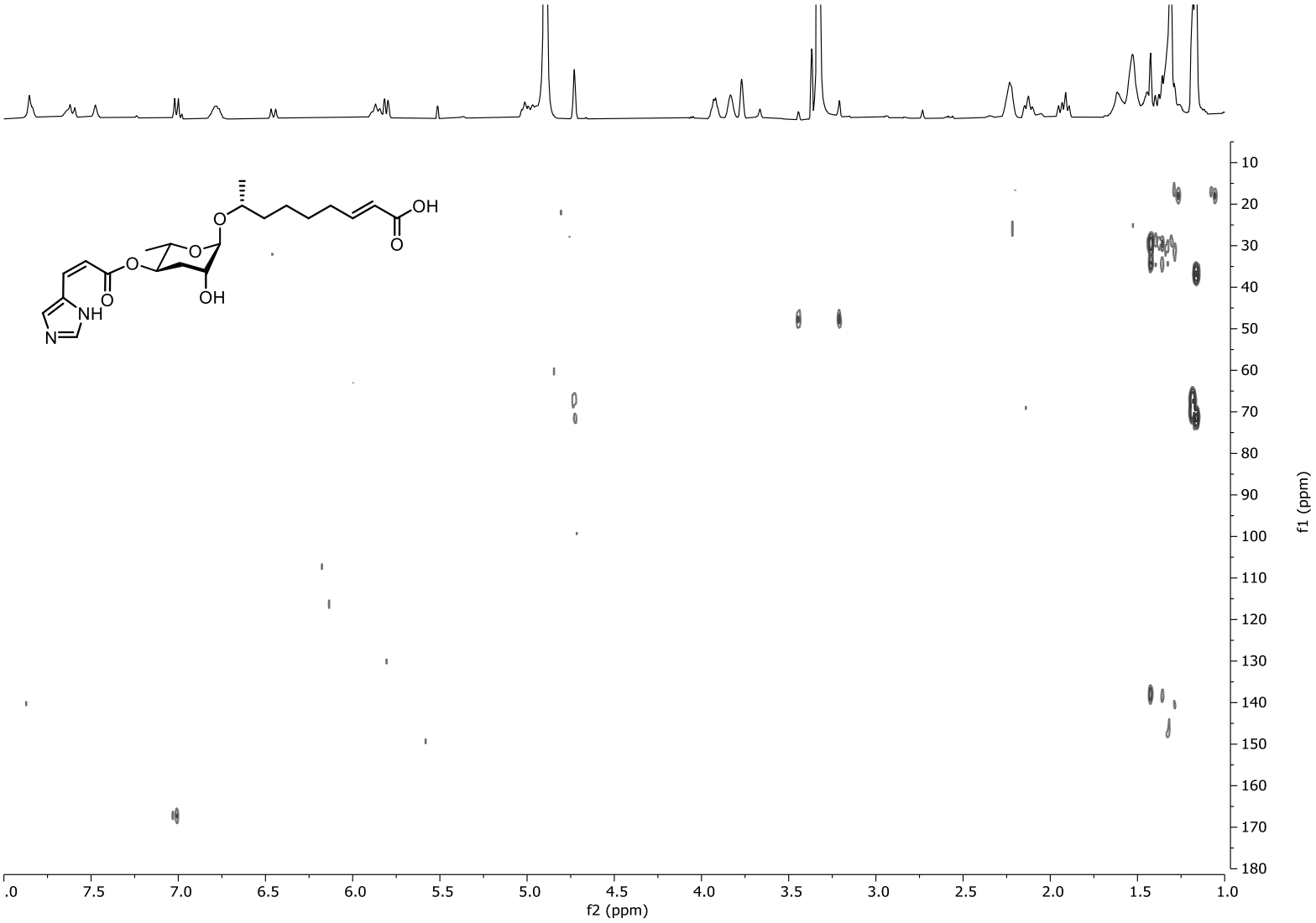

Figure S 110: ^{1}H NMR (600 MHz, $CDCl_3$) of (*5R)*-5-[(2-*O*-benzoyl-4-*O*-*tert*-butyldiphenylsilyl-3,6-dideoxy-α-L-*arabino*-hexopyranosyl)oxy]-2,5-hexadiol (130).

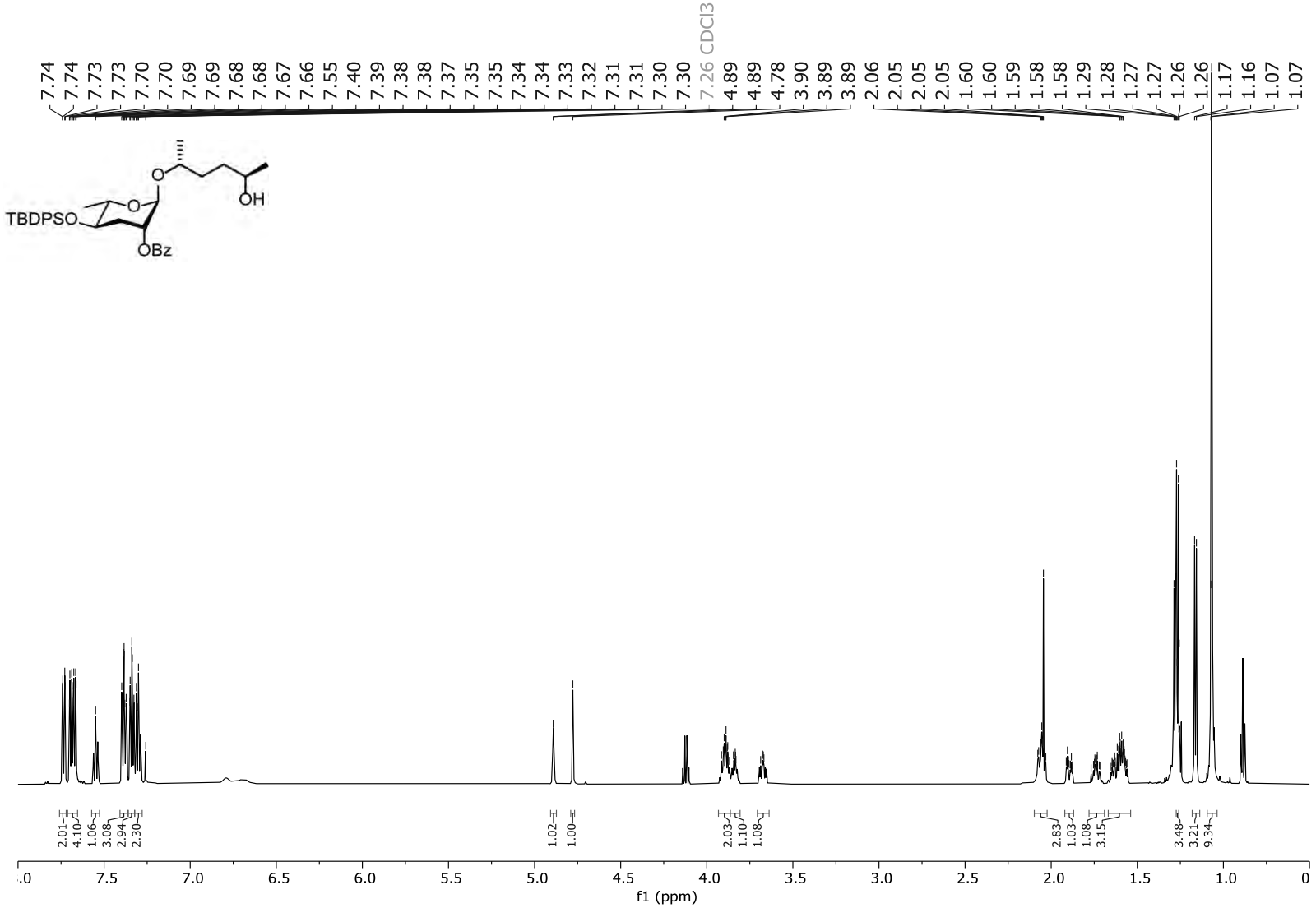

Figure S 111: ^{13}C NMR (150 MHz, $CDCl_3$) of (*5R)*-5-[(2-*O*-benzoyl-4-*O*-*tert*-butyldiphenylsilyl-3,6-dideoxy-α-L-*arabino*-hexopyranosyl)oxy]-2,5-hexadiol (130).

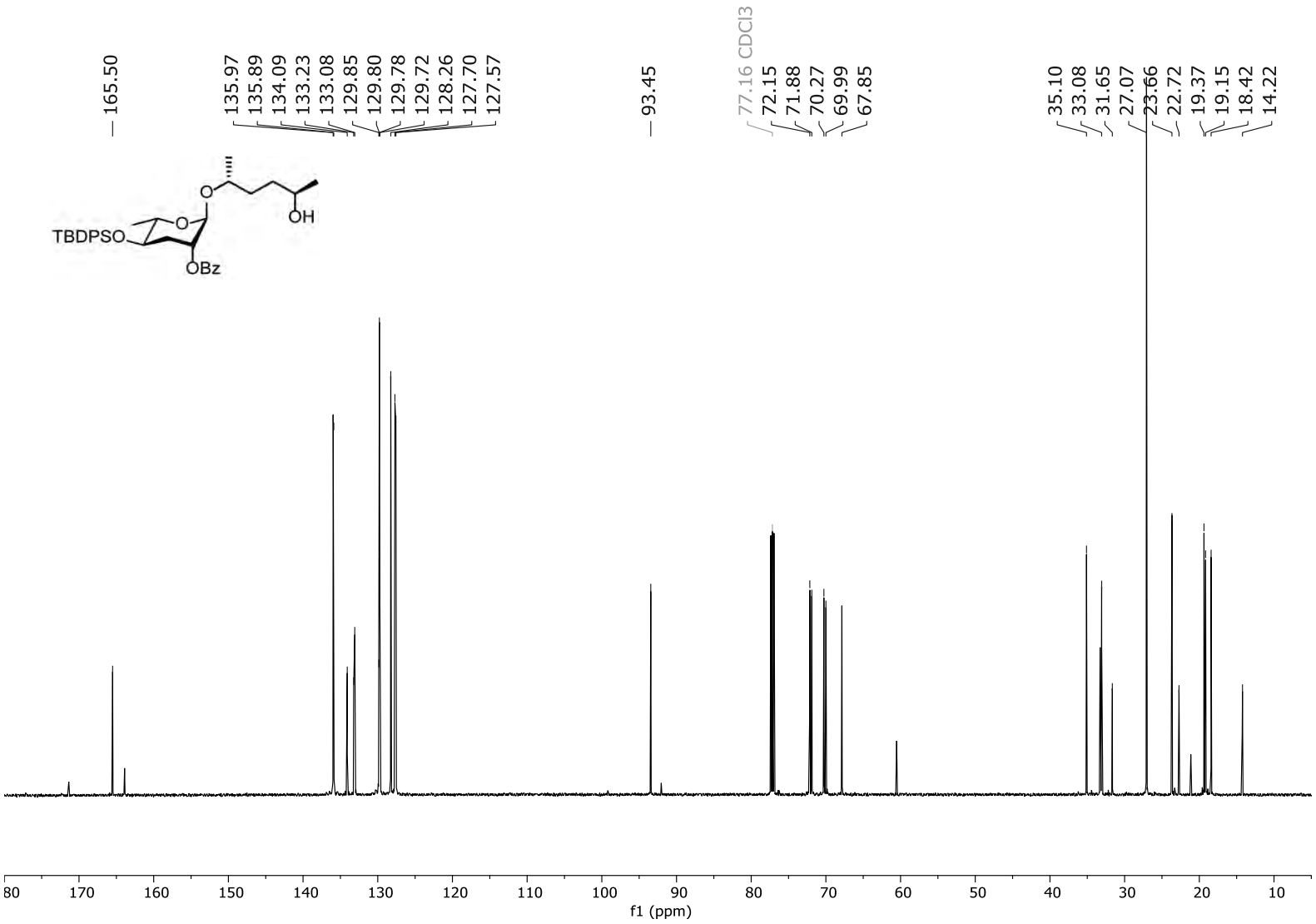

Figure S 112: *dqf*-COSY (600 MHz, $CDCl_3$) of (*5R)*-5-[(2-*O*-benzoyl-4-*O*-*tert*-butyldiphenylsilyl-3,6-dideoxy-α-L-*arabino*-hexopyranosyl)oxy]-2,5-hexadiol (130).

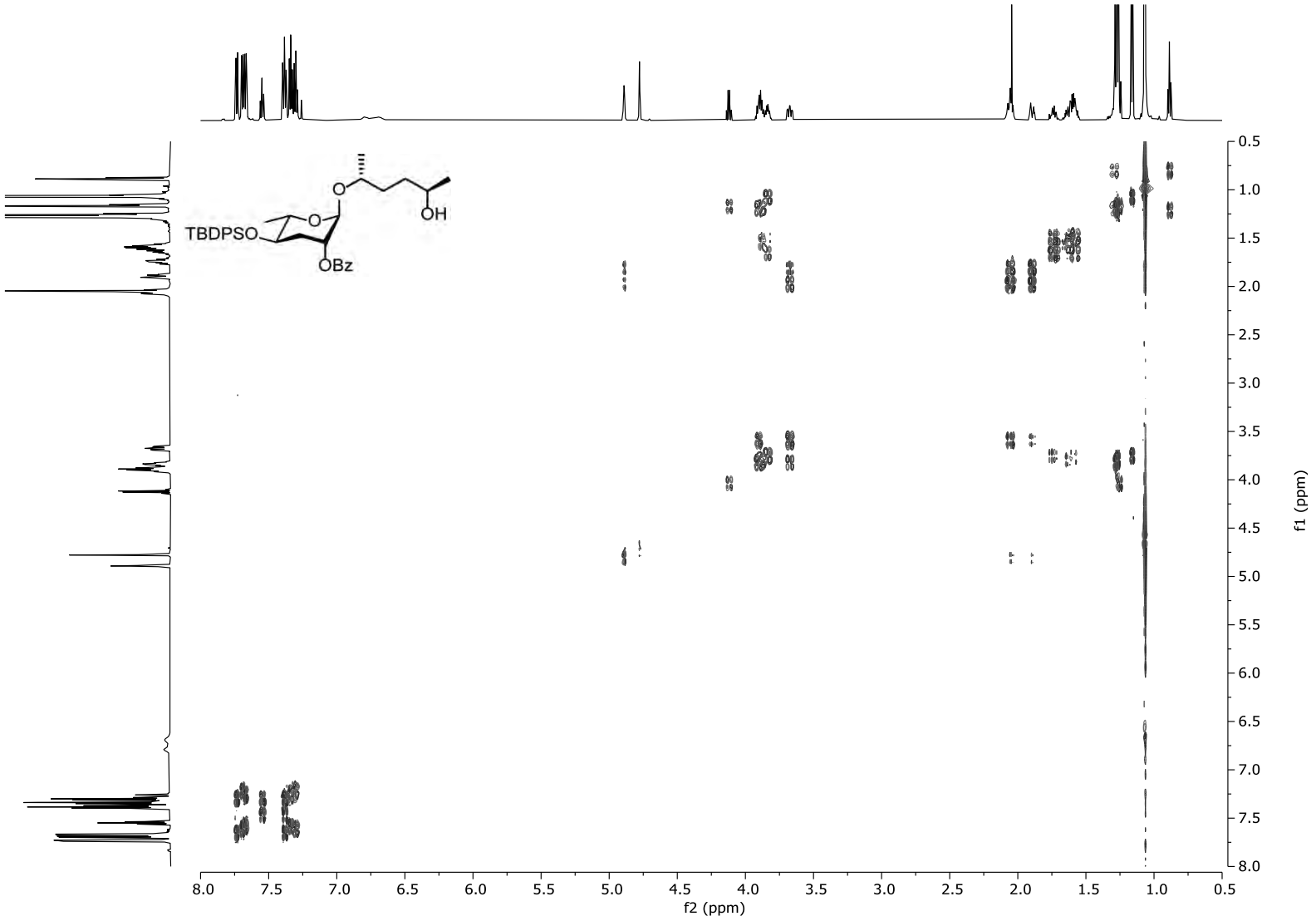

Figure S 113: HSQC (600 MHz, $CDCl_3$) of (*5R)*-5-[(2-*O*-benzoyl-4-*O*-*tert*-butyldiphenylsilyl-3,6-dideoxy-α-L-*arabino*-hexopyranosyl)oxy]-2,5-hexadiol (130).

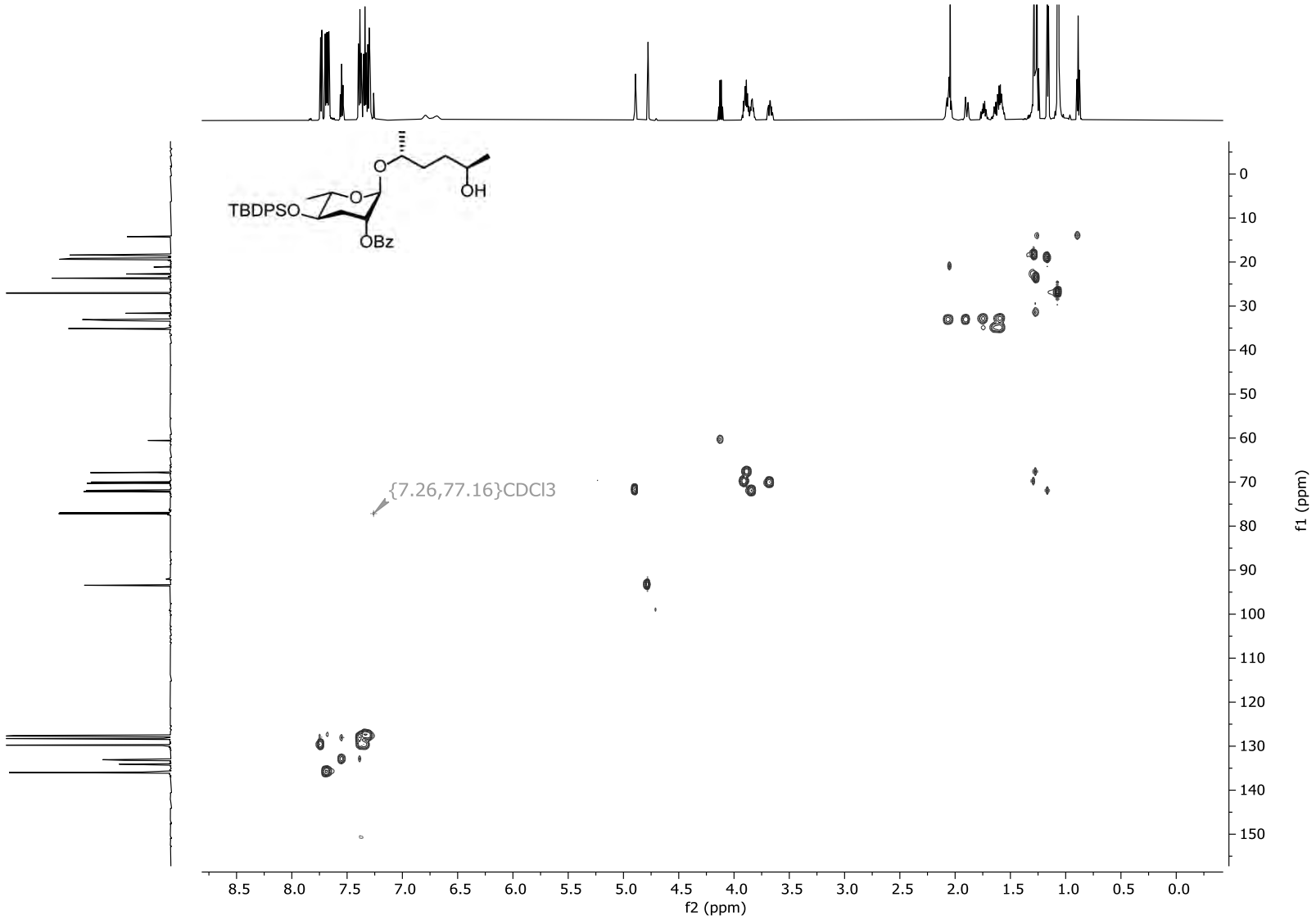

Figure S 114: ^{1}H NMR (600 MHz, $CDCl_3$) of (5*R*)-5-[(2-*O*-benzoyl-4-*O*-*tert*-butyldiphenylsilyl-3,6-dideoxy-α-L-*arabino*-hexopyranosyl)oxy]-hexan-2-one (131).

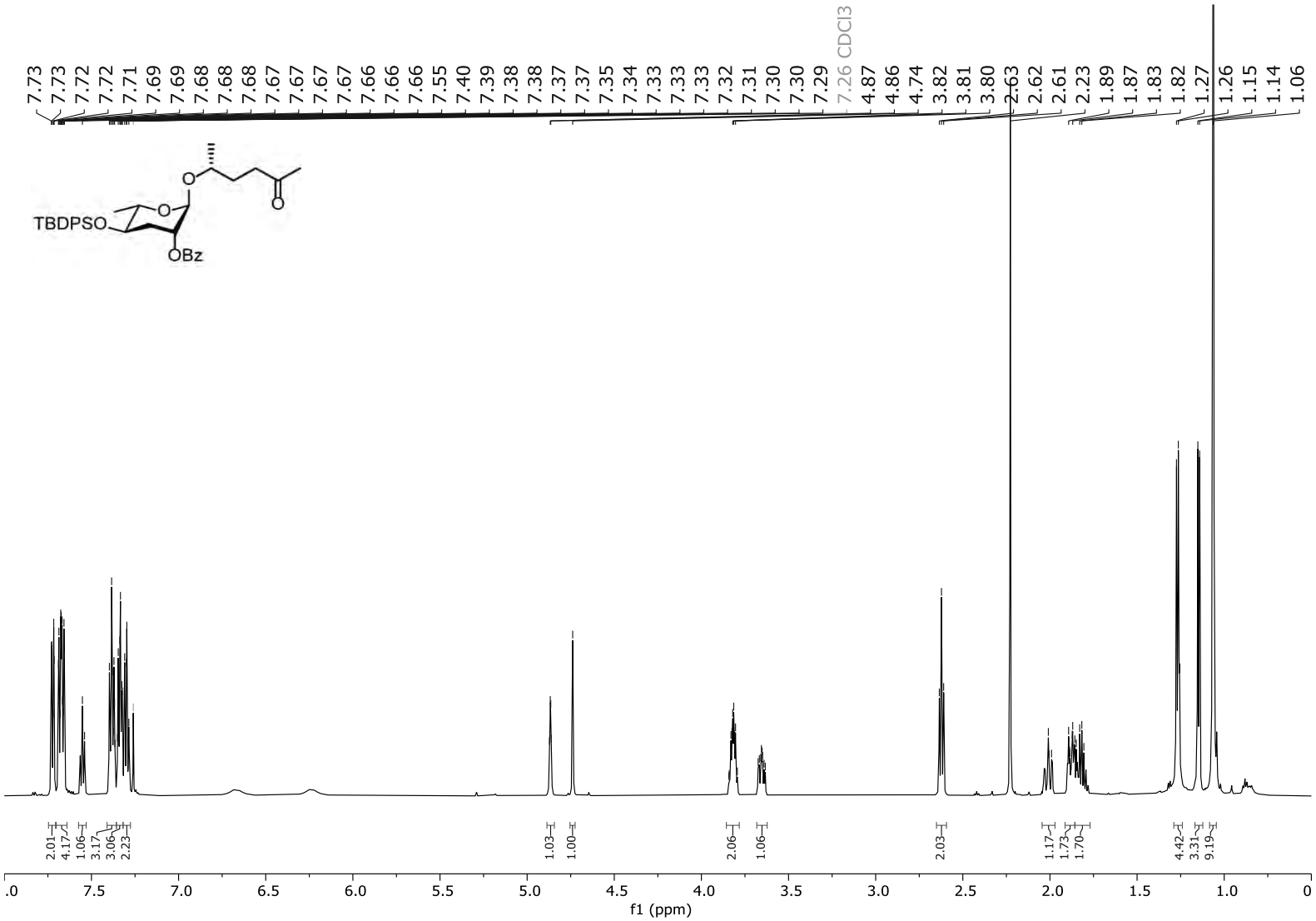

Figure S 115: ^{13}C NMR (150 MHz, $CDCl_3$) of (5*R*)-5-[(2-*O*-benzoyl-4-*O*-*tert*-butyldiphenylsilyl-3,6-dideoxy-α-L-*arabino*-hexopyranosyl)oxy]-hexan-2-one (131).

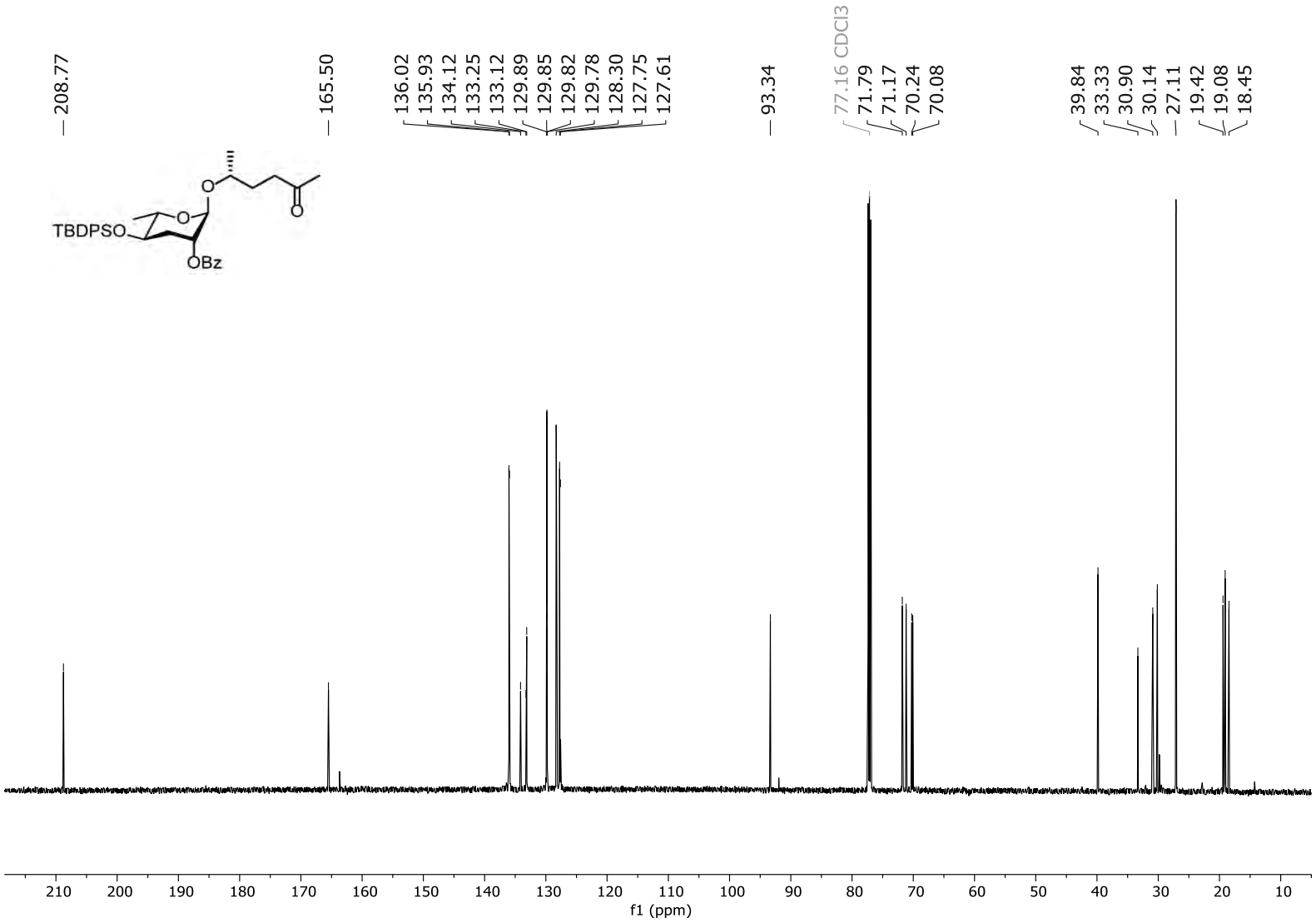

Figure S 116: *dqf*-COSY (600 MHz, CDCl3) of (5*R*)-5-[(2-O-benzoyl-4-O-tert-butyldiphenylsilyl-3,6-dideoxy-α-L-arabino-hexopyranosyl)oxy]-hexan-2-one (131).

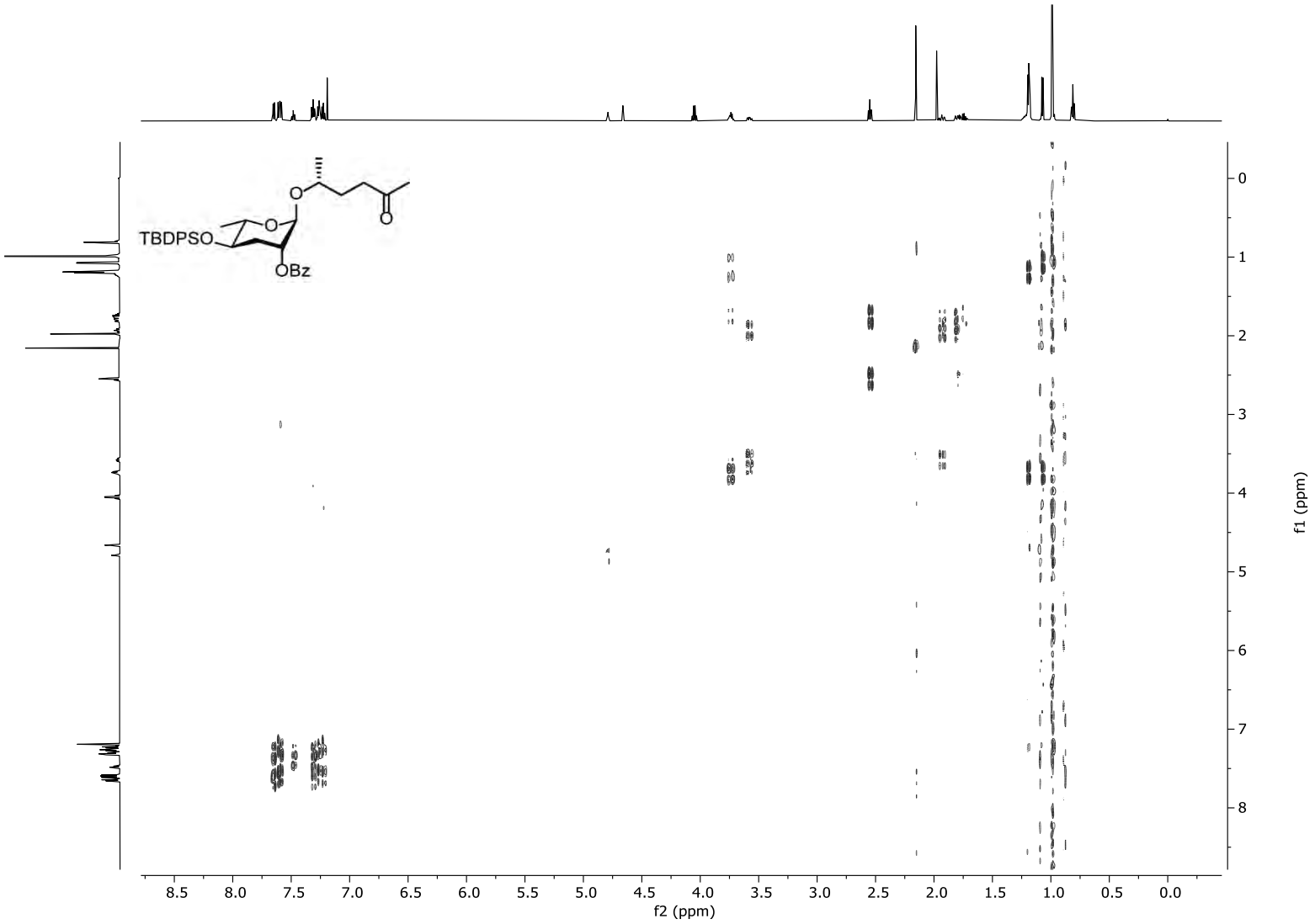

Figure S 117: HSQC (600 MHz, $CDCl_3$) of (5*R*)-5-[(2-*O*-benzoyl-4-*O*-tert-butyldiphenylsilyl-3,6-dideoxy-α-L-arabino-hexopyranosyl)oxy]-hexan-2-one (131).

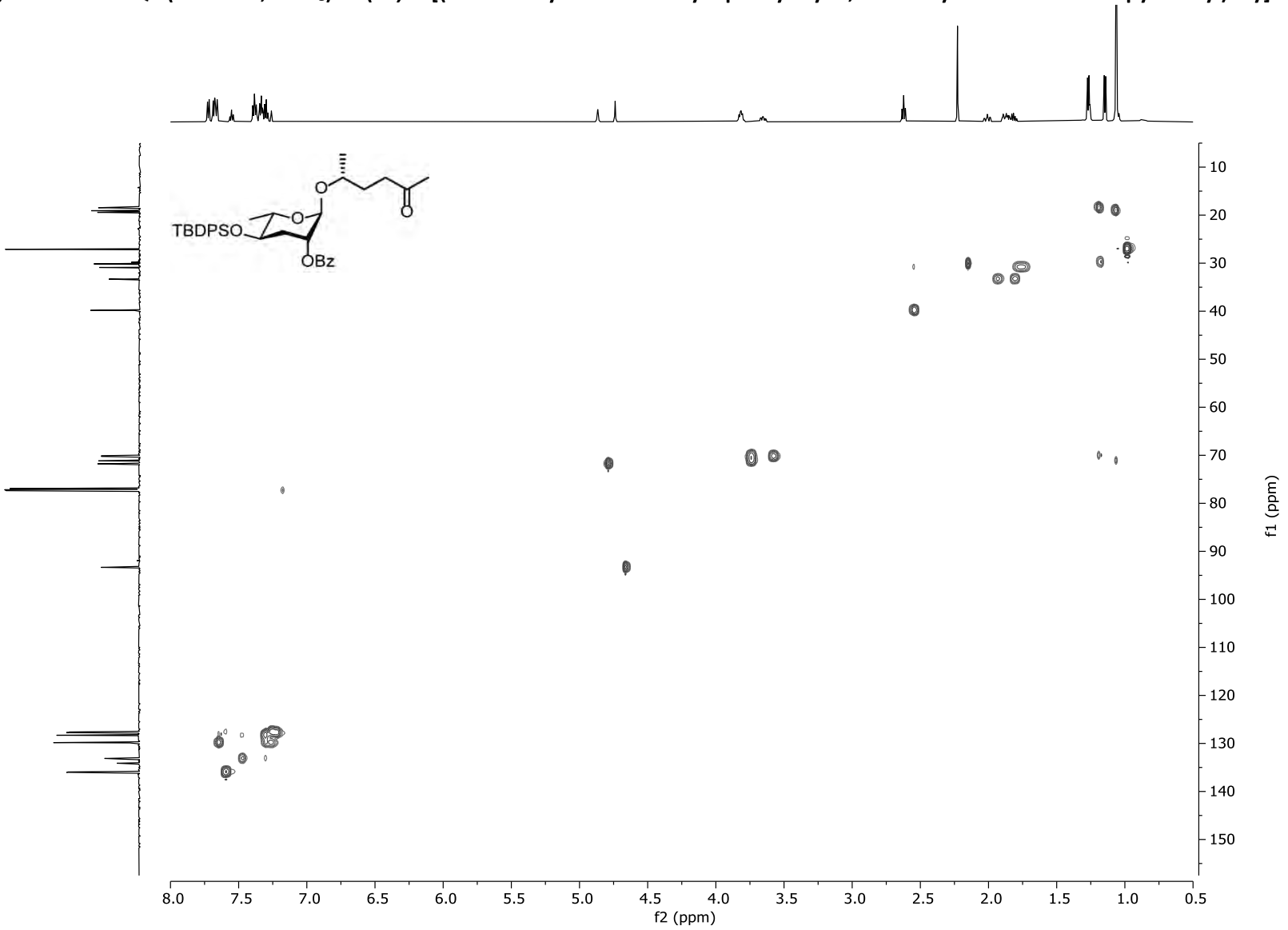

Figure S 118: ^{1}H NMR (600 MHz, $CDCl_3$) of (5*R*)-5-[(4-*O*-*tert*-butyldiphenylsilyl-3,6-dideoxy-α-L-*arabino*-hexopyranosyl)oxy]-2-hexanone (132).

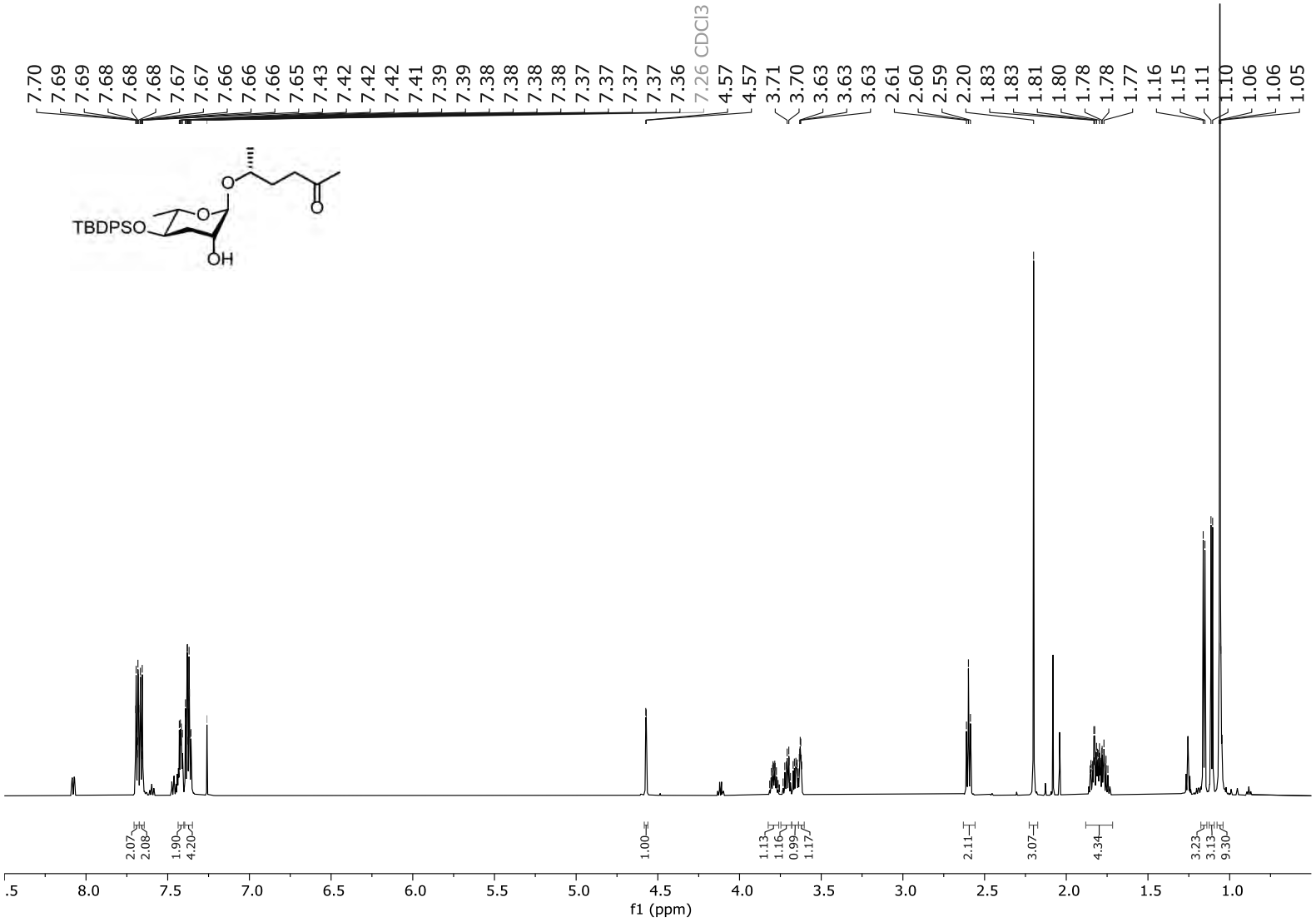

Figure S 119: ^{13}C NMR (150 MHz, $CDCl_3$) of (5*R)*-5-[(4-*O*-*tert*-butyldiphenylsilyl-3,6-dideoxy-α-L-*arabino*-hexopyranosyl)oxy]-2-hexanone (132).

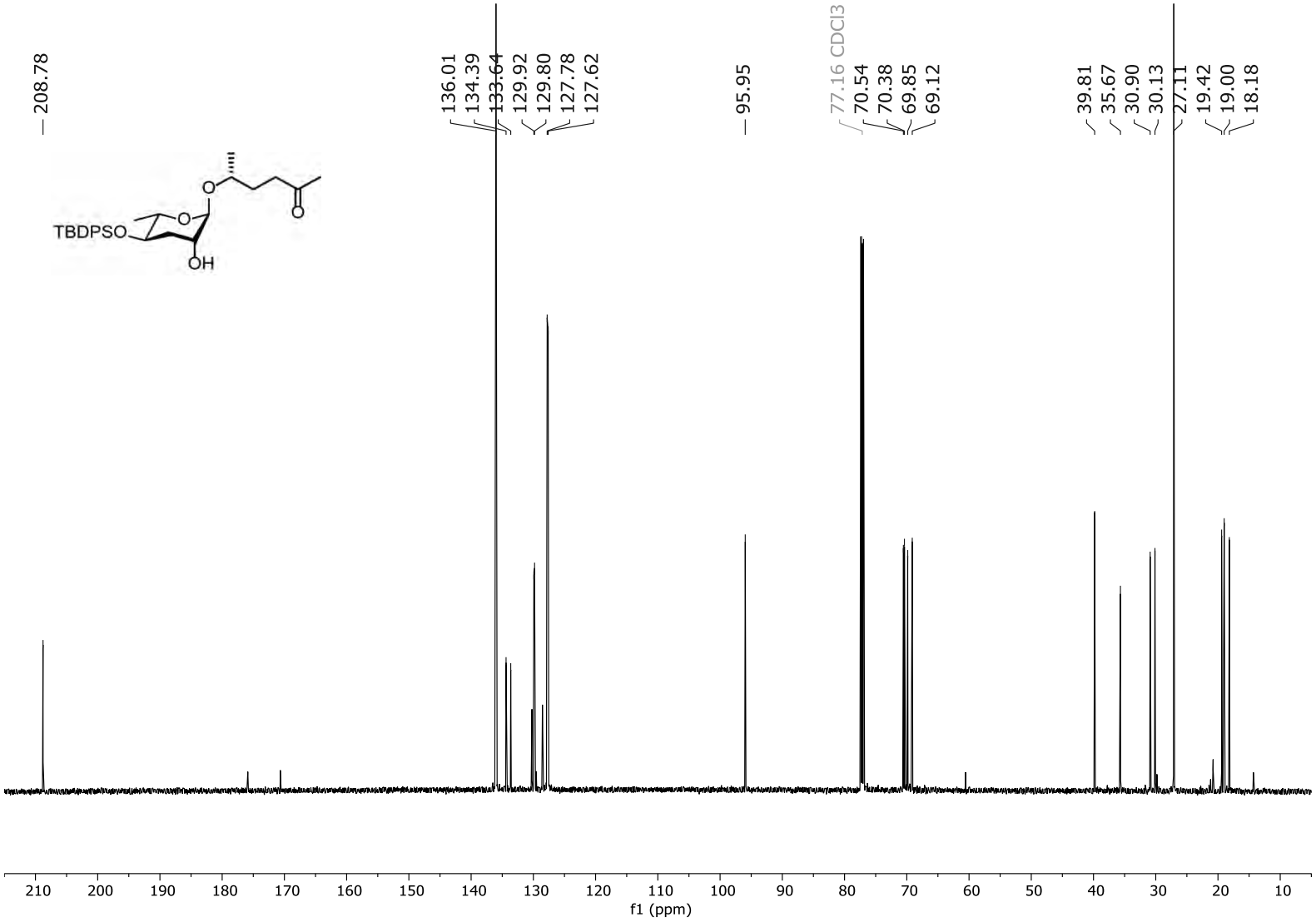

Figure S 120: *dqf*-COSY (600 MHz, CDCl3) of (5*R*)-5-[(4-*O*-*tert*-butyldiphenylsilyl-3,6-dideoxy-α-L-*arabino*-hexopyranosyl)oxy]-2-hexanone (132).

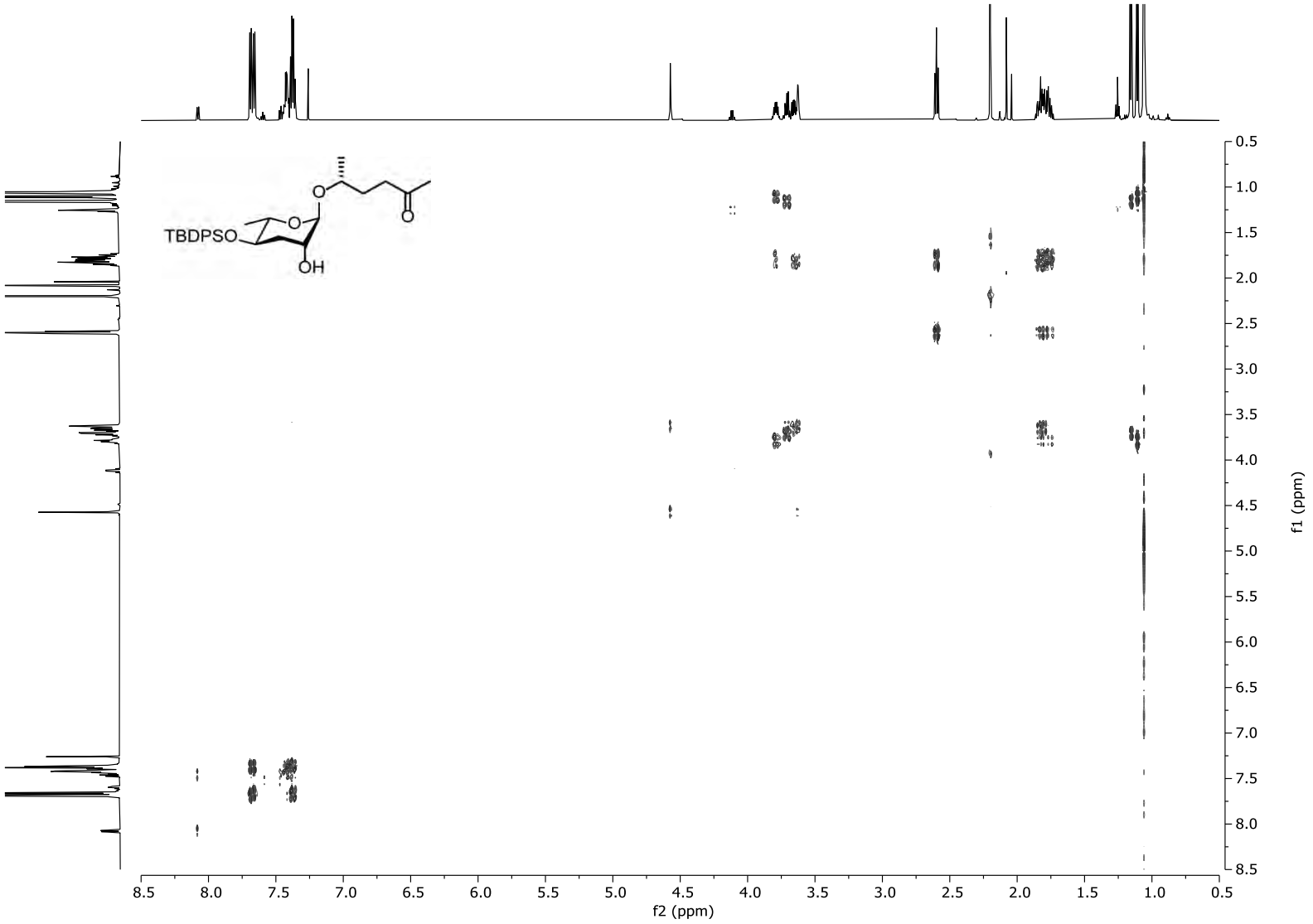

Figure S 121: HSQC (600 MHz, CDCl3) of (5*R*)-5-[(4-*O*-*tert*-butyldiphenylsilyl-3,6-dideoxy-α-L-*arabino*-hexopyranosyl)oxy]-2-hexanone (132).

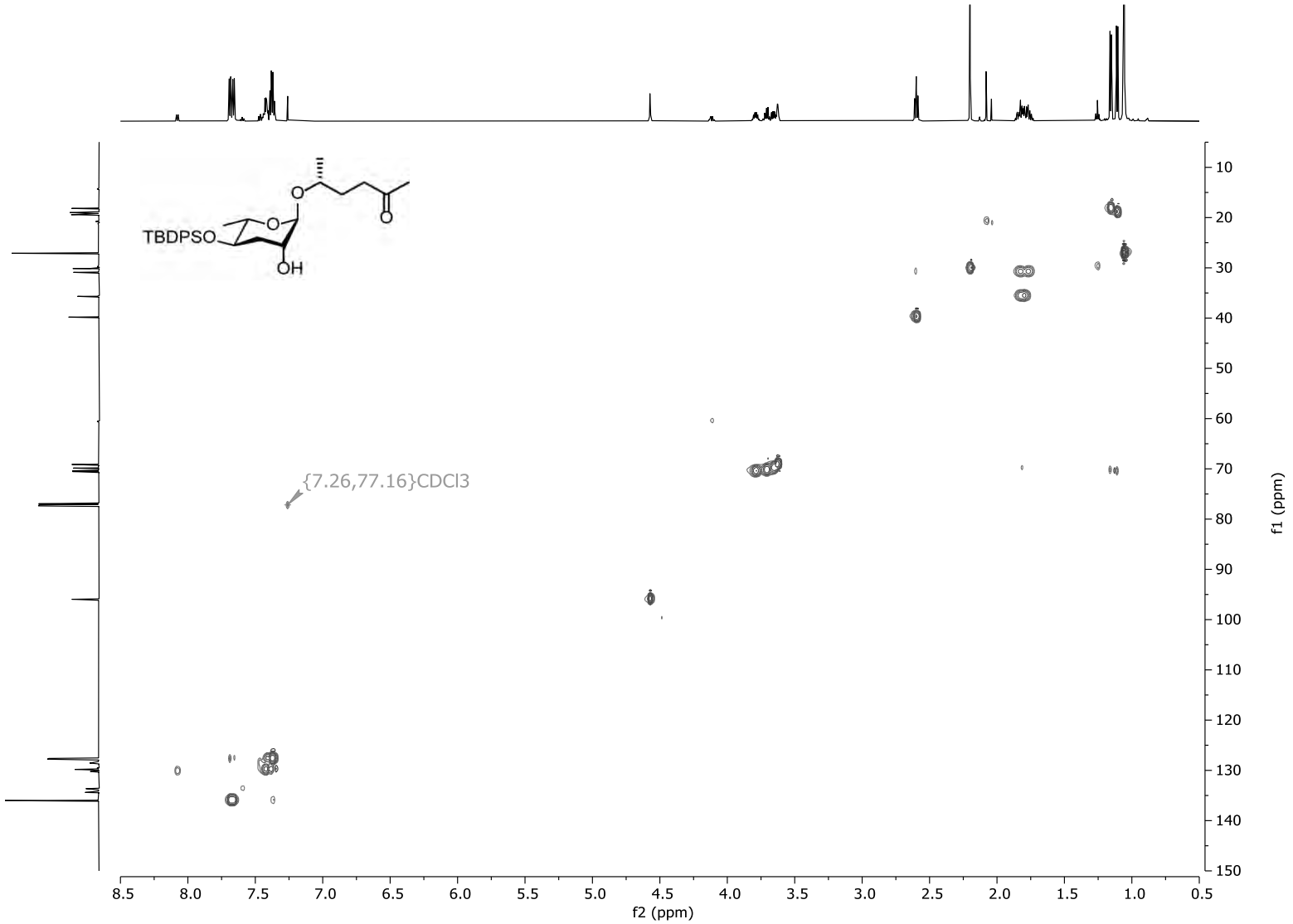

Figure S 122: ^{1}H NMR (600 MHz, $CDCl_3$) of (5*R)*-5-[(2-*O*-(4-methoxybenzyloxy)-4-*O*-*tert*-butyldiphenylsilyl-3,6-dideoxy-α-L-*arabino*-hexopyranosyl)oxy]-2-hexanone (133).